Springer Proceedings in Mathematics & Statistics

Solomon Manukure
Wen-Xiu Ma *Editors*

# Nonlinear and Modern Mathematical Physics

## NMMP-2022, Tallahassee, Florida, USA (Virtual), June 17–19

Springer

**Springer Proceedings in Mathematics & Statistics**

Volume 459

This book series features volumes composed of selected contributions from workshops and conferences in all areas of current research in mathematics and statistics, including data science, operations research and optimization. In addition to an overall evaluation of the interest, scientific quality, and timeliness of each proposal at the hands of the publisher, individual contributions are all refereed to the high quality standards of leading journals in the field. Thus, this series provides the research community with well-edited, authoritative reports on developments in the most exciting areas of mathematical and statistical research today.

Solomon Manukure · Wen-Xiu Ma
Editors

# Nonlinear and Modern Mathematical Physics

## NMMP-2022, Tallahassee, Florida, USA (Virtual), June 17–19

Springer

*Editors*
Solomon Manukure
Department of Mathematics
Florida A&M University
Tallahassee, FL, USA

Wen-Xiu Ma
Department of Mathematics and Statistics
University of South Florida
Tampa, FL, USA

ISSN 2194-1009 ISSN 2194-1017 (electronic)
Springer Proceedings in Mathematics & Statistics
ISBN 978-3-031-59538-7 ISBN 978-3-031-59539-4 (eBook)
https://doi.org/10.1007/978-3-031-59539-4

Mathematics Subject Classification: 35-06, 35C08, 35Q53, 35Q55, 37K40, 35Q51, 34M55, 17B80, 37J35, 37J70, 37K10, 37J06, 34M50



This Springer imprint is published by the registered company Springer Nature Switzerland AG
The registered company address is: Gewerbestrasse 11, 6330 Cham, Switzerland

Paper in this product is recyclable.

# Committees

## Organizing Committee

Solomon Manukure (Chair), Florida A&M University, USA
Ajith Gunaratne (Co-chiar), Florida A&M University, USA
Emmanuel Appiah, Prairie View A&M University, USA
Sarada Bandara, Florida A&M University, USA
Abhinandan Chowdhury, Savannah State University, USA
Mozhgan Entekhabi, Florida A&M University, USA
Aseel Farhat, Florida State University, USA
Cong Hoang, Florida A&M University, USA
Xing Lü, Beijing Jiaotong University, China
Stefani Mancas, Embry–Riddle Aeronautical University, USA
Anh Khoa Vo, Florida A&M University, USA

## Scientific Committee

Wen-Xiu Ma (Chair), University of South Florida, USA
Alejandro Aceves, Southern Methodist University, USA
Cewen Cao, Zhengzhou University, China
Baofeng Feng, University of Texas Rio Grande Valley, USA
Benno Fuchssteiner, University of Paderborn, Germany
Molin Ge, Nankai University, China
Xianguo Geng, Zhengzhou University, China
Boling Guo, IAPCM, China
Jarmo Hietarinta, University of Turku, Finland
Hesheng Hu, Fudan University, China
Mourad E. H. Ismail, University of Central Florida, USA
Nalini Joshi, University of Sydney, Australia

Kenji Kajiwara, Kyushu University, Japan
C. M. Khalique, North-West University, South Africa
Adem Kilicman, University Putra Malaysia, Malaysia
Yuji Kodama, Ohio State University, USA
Boris G. Konopelchenko, Universita del Salento, Italy
Mikhail Kovalyov Sungkyunkwan, University, South Korea
Chun-Ku Kuo, Air Force Academy, Kaohsiung, Taiwan
Jyh-Hao Lee, Academia Sinica, Taiwan
Decio Levi, Roma Tre University, Italy
Xing-biao Hu, Chinese Academy of Sciences, China
Qingping Liu, China University of Mining and Technology, China
Zhangju Liu, Beijing University, China
Sen-Yue Lou, East China Normal University, Ningbo University, China
Fazal Mahomed, University of the Witwatersrand, South Africa
Yoshimasa Nakamura, Kyoto University, Japan
Asli Pekcan, Hacettepe University, Turkey
Sarah Post, University of Hawaii, USA
Zhijun Qiao, University of Texas Rio Grande Valley, USA
Orlando Ragnisco, Roma Tre University, Italy
Colin Rogers, Hong Kong Polytechnic University, Hong Kong
H. O. Roshid, University of Science and Technology, Bangladesh
Aly Seadawy, Taibah University, Saudi Arabia
Roman Smirnov, Dalhousie University, Canada
Yong-Li Sun, Beijing University of Chemical Technology, China
Alexander Tovbis, University of Central Florida, USA
Pavel Winternitz, University of Montreal, Canada
Tiecheng Xia, Shanghai University, China
Jianke Yang, University of Vermont, USA
Xuelin Yong, North China Electric Power University, China
Dajun Zhang, Shanghai University, China
Yi Zhang, Zhejiang Normal University, China
Youjin Zhang, Tsinghua University, China
Zuonong Zhu, Shanghai Jiao Tong University, China

# Speakers

## Plenary Speakers

Alejandro Aceves, Southern Methodist University, USA
Stephen Anco, Brock University, Canada
Gino Biondini, SUNY, USA
Baofeng Feng, University of Texas Rio Grande Valley, USA
Willy Hereman, Colorado School of Mines, USA
Chaudry M. Khalique, North-West University, South Africa
Wen-Xiu Ma, University of South Florida, USA
Ziad H. Musslimani, Florida State University, USA
Zhijun Qiao, University of Texas Rio Grande Valley, USA
Svetlana Roudenko, Florida International University, USA

## Invited Speakers

Alle Adjiri, University of South Florida, USA
Ahmed Ahmed, University of South Florida, USA
Mohammed R. Ali, Benha University, Egypt
Eric Bonnetier, Université Grenoble Alpes, France
Vinodh Chellamuthu, Utah Tech University, USA
Abhinandan Chowdhury, Savannah State University, USA
Anton Dzhamay, University of Northern Colorado, USA
Thao Thuan Vu Ho, University of Milan-Bicocca, Italy
Melike Kaplan, Kastamonu University, Turkey
Sachin Kumar, University of Delhi, India
Chunxia Li, Capital Normal University, China
Sitai Li, Xiamen University, China
Xing Lü, Beijing Jiatong University, China

Hongcai Ma, Donghua University, China
Solomon Manukure, Florida A&M University, USA
Ian Marquette, University of Queensland, Australia
Ratbay Myrzakulov, Ratbay Myrzakulov Eurasian International Centre for Theoretical Physics, Kazakhstan
Loc Nguyen, University of North Carolina at Charlotte, USA
Abba Ramadan, University of Alabama, USA
Yong-Li Sun, Beijing University of Chemical Technology, China
Quoc Bao Tang, University of Graz, Austria
Deng-Shan Wang, Beijing Normal University, China
Fudong Wang, University of Central Florida, USA
Kai Yang, Florida International University, USA
Da-jun Zhang, Shanghai University, China
Guoping Zhang, Morgan State University, USA
Jie-Fang Zhang, Communication University of China, China
Lei Zhang, University of Florida, USA
Qing Zhang, Northwestern Polytechnical University, China
Yi Zhang, Zhejiang Normal University, China
Shijun Zheng, Georgia Southern University, USA
Yuan Zhou, Shanghai International Studies University, China

# Preface

The 6th International Virtual Workshop on Nonlinear and Modern Mathematical Physics (NMMP2022) took place virtually from June 17 to 19, 2022, hosted by Florida Agricultural and Mechanical University. This workshop is part of a series of conferences organized periodically, starting with the inaugural workshop held in China from July 15 to 21, 2009. Subsequent events took place in Tampa at the University of South Florida from March 9 to 11, 2013, at the African Institute for Mathematical Sciences in Cape Town, South Africa from April 9 to 11, 2015, in Kuala Lumpur, Malaysia, from May 4 to 8, 2017, and the 5th edition, which was successfully conducted in Honolulu, Hawaii, from May 20 to 24, 2019.

The 6th edition of the NMMP workshop served as a dynamic forum, bringing together scholars and researchers from various institutions worldwide. Florida A&M University led the organization, with support from the University of South Florida, Florida State University, Embry-Riddle Aeronautical University, Savannah State University, Prairie View A&M University, and Beijing Jiaotong University. The focus of the workshop was on recent advances and prevailing trends in nonlinear science, with a specific emphasis on nonlinear partial differential equations and their applications. Featuring 42 distinguished speakers, the three day event attracted over 300 participants globally, fostering collaboration and knowledge exchange in the field.

This book, a compilation of papers from both speakers and participants of NMMP2022, aims to showcase new ideas and discoveries in the field of partial differential equations (PDEs), integrable systems, and related areas in mathematical physics. In the dynamic landscape of mathematical physics, the exploration of nonlinear phenomena takes center stage, and this compendium, titled "Nonlinear and Modern Mathematical Physics," endeavors to encapsulate the forefront of research and discourse in this field. As customary, each contribution in the book has undergone standard double-blind refereeing.

Nonlinearity, with its intriguing and often unpredictable nature, has emerged as a central theme in contemporary mathematical physics. From the theoretical realms of chaos theory to the practical applications in fluid dynamics, the study of nonlinear phenomena has opened up new avenues of exploration and understanding. One

remarkable example of this is the discovery of solitons, which has had a profound impact on mathematical physics, reshaping our understanding of nonlinear dynamics and leaving a lasting imprint on various scientific disciplines. The introduction of solitons has not only revolutionized our conceptual framework but has also brought forth powerful mathematical methods. Techniques such as the inverse scattering transform and Hirota's method have been developed, offering sophisticated tools to solve a wide range of nonlinear equations across diverse fields. These methods have not only expanded our analytical capabilities but have also facilitated deeper insights into the behavior of nonlinear systems.

This compilation of works boldly explores the forefront of advancements in nonlinear theories, offering a comprehensive examination of the richness and diversity inherent in this dynamic field. The contributors, by delving into the intricacies of nonlinear dynamics, illuminate the multifaceted nature of nonlinear phenomena. Their collective efforts shed light on the profound implications and versatile applications of nonlinear theories across various scientific domains. This volume serves as a testament to the far-reaching impact and ongoing exploration within the captivating realm of nonlinear mathematical physics.

As editors, our aim is to curate a collection that not only reflects the current state of nonlinear mathematical physics but also serves as an intellectual catalyst for future explorations. The breadth and depth of topics covered herein cater to both seasoned researchers navigating the cutting edge and aspiring scholars embarking on their journey into this captivating realm. May this compilation serve as both a testament to the vibrant state of nonlinear mathematical physics and an inspiration for those who embark on the quest to unravel the mysteries that lie beyond the linear veil.

Tallahassee, USA Solomon Manukure
Tampa, USA Wen-Xiu Ma

# Acknowledgments

The editors extend their sincere gratitude to the contributors who have enriched this volume with their expertise and insights. Their dedication to pushing the boundaries of knowledge is evident in the quality and diversity of the content presented.

The editors also express their gratitude for the financial support provided by *Mathematics*, an open-access journal by MDPI, for the plenary speakers during the conference.

Much appreciation also goes to the reviewers for their invaluable contributions to the peer review process. Their expertise and thorough evaluations have played a crucial role in ensuring the quality and rigor of the content presented in this volume. The editors extend their sincere appreciation for the time and effort invested by these esteemed reviewers.

# Contents

# A Hamiltonian Set-Up for 4-Layer Density Stratified Euler Fluids


**R. Camassa, G. Falqui, G. Ortenzi, M. Pedroni, and T. T. Vu Ho**

**Abstract** By means of the Hamiltonian approach to two-dimensional wave motions in heterogeneous fluids proposed by Benjamin [1] we derive a natural Hamiltonian structure for ideal fluids, density stratified in four homogenous layers, constrained in a channel of fixed total height and infinite lateral length. We derive the Hamiltonian and the equations of motion in the dispersionless long-wave limit, restricting ourselves to the so-called Boussinesq approximation. The existence of special symmetric solutions, which generalise to the four-layer case the ones obtained in [11] for the three-layer case, is examined.

R. Camassa
Carolina Center for Interdisciplinary Applied Mathematics, Department of Mathematics, University of North Carolina at Chapel Hill, Chapel Hill, NC 27599, USA
e-mail: camassa@amath.unc.edu

G. Falqui · G. Ortenzi · T. T. Vu Ho
Department of Mathematics and Applications, University of Milano-Bicocca, Via Roberto Cozzi 55, 20125 Milano, Italy
e-mail: gregorio.falqui@unimib.it

G. Ortenzi
e-mail: giovanni.ortenzi@unito.it

G. Falqui
SISSA, via Bonomea 265, 34136 Trieste, Italy

G. Falqui · G. Ortenzi · M. Pedroni · T. T. Vu Ho
INFN, Sezione di Milano-Bicocca, Piazza della Scienza 3, 20126 Milano, Italy
e-mail: marco.pedroni@unibg.it

G. Ortenzi
Dipartimento di Matematica “Giuseppe Peano”, Università di Torino, 10123 Torino, Italy

M. Pedroni
Dipartimento di Ingegneria Gestionale, dell’Informazione e della Produzione, Università di Bergamo, Viale Marconi 5, 24044 Dalmine, BG, Italy

T. T. Vu Ho (✉)
School of Mathematics, Monash University, Melbourne, VIC 3800, Australia
e-mail: thuanvu.vuho@monash.edu



S. Manukure and W.-X. Ma (eds.), *Nonlinear and Modern Mathematical Physics*, Springer Proceedings in Mathematics & Statistics 459,
https://doi.org/10.1007/978-3-031-59539-4_1

**Keywords** Hamiltonian structures · Stratified fluids · Boussinesq approximation

## 1 Introduction

Density stratification in incompressible fluids is an important aspect of fluid dynamics, and plays an important role in variety of phenomena occurring in both the ocean and the atmosphere. In particular, displacement of fluid parcels from their neutral buoyancy position within a density stratified flow can result in internal wave motion. Effective one-dimensional models (in particular, their quasi-linear limit) were introduced to study these phenomena, and were the subject of a number of investigations (see, e.g., [6–10, 13, 14, 16] and references therein). Although most of the theoretical and numerical results that can be found in the literature are focussed on the 2-layer case, multiply-layered fluid configurations appear as effective models of physical phenomena, e.g., in the atmosphere or in mountain lakes. The extension to the $n > 2$ layers case can also be seen as a refined approximation to the real-world continuous stratification of incompressible fluids.

The focus of the present paper is on the dynamics of an ideal (incompressible, inviscid) stably stratified fluid consisting of 4 layers of constant density $\rho_1 < \rho_2 < \rho_3 < \rho_4$, confined in a channel of fixed height $h$ (see Fig. 1 for a schematic of our setup), and, in particular, on its Hamiltonian setting. This will be obtained by a suitable reduction of the Hamiltonian structure introduced by Benjamin [1] in the study of general density stratifications for Euler fluids in 2 dimensions.

We shall follow the approach set forth in our recent paper [4], where the 3-layer case was considered by extending to the multiple layer case a technique introduced in [3]. In particular, after having discussed in details the construction of the Hamiltonian operator for an effective 1D model, we shall consider the so-called Boussinesq limit of the system, and explicitly determine its Hamiltonian structure and Hamiltonian functional, as well as point out the existence of special symmetric solutions.

Our mathematical model is based on some simplifying hypotheses. At first, we assume that an inviscid model suffices to capture the essential features of the dynamics since the scales associated with internal waves are large, and consequently the Reynolds number is typically high ($>10^5$). Although in the ocean and the atmosphere (as well as in laboratory experiments) the density stratification arises as a consequence of diffusing quantities such as temperature and salinity, we can neglect diffusion and mixing since the time scales associated with diffusion processes are far larger than the time scale of internal wave propagation. Finally, we use the rigid lid assumption for the upper surface since the scales associated with internal wave-motion are greatly exceeding the scales of the surface waves (see, e.g., [17] for further details on these assumptions).

The Hamiltonian 4-layer model herewith discussed is a natural extension of the 2 and 3-layer model. Indeed, when two adjacent densities are equal (and as a consequence the relative interface becomes meaningless) we fully recover the dynamics

of the 3 layer model (see, e.g., [4, 11]). Similarly, the 3-layer model reduces to the ordinary 2-layer model when two mass densities coincide.

The layout of the paper is the following. In Sect. 2 we briefly review the Hamiltonian representation for 2-dimensional incompressible Euler fluids of [1]. Section 3 is devoted to a detailed presentation of our Hamiltonian reduction scheme, which endows the dynamics of the set of 4-layer stratified fluids with a natural Hamiltonian structure. In Sect. 4 we compute the reduced Hamiltonian and the ensuing equations of motion, confining ourselves to the case of the so-called Boussinesq approximation. In Sect. 5 a class of special evolutions, selected by a symmetry of the Hamiltonian, is found and briefly examined.

## 2 The 2D Benjamin Model for Heterogeneous Fluids in a Channel

Benjamin [1] proposed and discussed a set-up for the Hamiltonian formulation of an incompressible stratified Euler system in 2 spatial dimensions, which we hereafter summarize for the reader's convenience.

The Euler equations for a perfect inviscid and incompressible but heterogeneous fluid in 2D, subject to gravity $-g\mathbf{k}$, are usually written for the the density $\rho(x, z)$ and the velocity field $\mathbf{u} = (u, w)$ as

$$\frac{D\rho}{Dt} = 0, \qquad \nabla \cdot \mathbf{u} = 0, \qquad \rho \frac{D\mathbf{u}}{Dt} + \nabla p + \rho g \mathbf{k} = 0 \tag{1}$$

together with appropriate boundary conditions, where, as usual, $D/Dt = \partial/\partial t + \mathbf{u} \cdot \nabla$ is the material derivative.

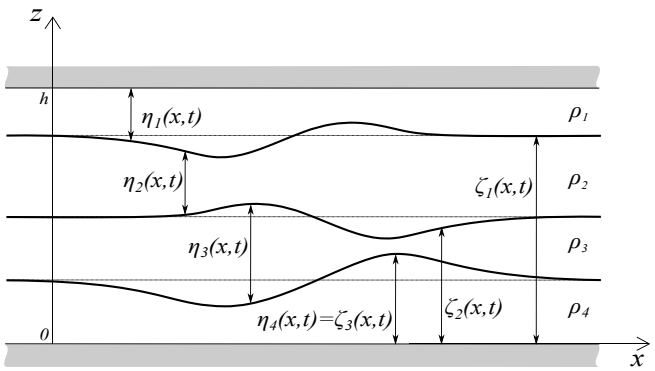


**Fig. 1** Four-layer rigid lid setup and relevant notation: $\zeta_i$ are the surface heights and $\eta_i$ are the layer thicknesses

Benjamin's contribution was to consider, as basic variables for the evolution of such a fluid, the density $\rho$ together with the "weighted vorticity" $\Sigma$ defined by

$$\Sigma = \nabla \times (\rho \mathbf{u}) = (\rho w)_x - (\rho u)_z. \tag{2}$$

The equations of motion for these two fields, ensuing from the Euler equations for incompressible fluids, are

$$\begin{aligned} &\rho_t + u\rho_x + w\rho_z = 0 \\ &\Sigma_t + u\Sigma_x + w\Sigma_z + \rho_x\big(gz - \tfrac{1}{2}(u^2+w^2)\big)_z + \tfrac{1}{2}\rho_z\big(u^2+w^2\big)_x = 0\,. \end{aligned} \tag{3}$$

They can be written in the form

$$\rho_t = -\left[\rho, \frac{\delta H}{\delta \Sigma}\right], \qquad \Sigma_t = -\left[\rho, \frac{\delta H}{\delta \rho}\right] - \left[\Sigma, \frac{\delta H}{\delta \Sigma}\right], \tag{4}$$

where, by definition, the bracket is $[A, B] \equiv A_x B_z - A_z B_x$, and the functional

$$H = \int_{\mathcal{D}} \rho \left(\frac{1}{2}|\mathbf{u}|^2 + gz\right) \mathrm{d}x\, \mathrm{d}z \tag{5}$$

is simply given by the sum of the kinetic and potential energy, $\mathcal{D}$ being the fluid domain. The most relevant feature of this coordinate choice is that $(\rho, \Sigma)$ are physical, directly measurable, variables. Their use, though confined to the 2D case with the above definitions, allows one to avoid the introduction of Clebsch variables (and the corresponding subtleties associated with gauge invariance and limitations of the Clebsch potentials) which are often used in the Hamiltonian formulation of both 2D and the general $3D$ case (see, e.g., [18]).

As shown by Benjamin, Eq. (4) are a Hamiltonian system with respect to a Lie-theoretic Hamiltonian structure, that is, they can be written as

$$\rho_t = \{\rho, H\}, \qquad \Sigma_t = \{\Sigma, H\},$$

for the Poisson bracket defined by the Hamiltonian operator

$$J_B = -\begin{pmatrix} 0 & \rho_x\partial_z - \rho_z\partial_x \\ \rho_x\partial_z - \rho_z\partial_x & \Sigma_x\partial_z - \Sigma_z\partial_x \end{pmatrix}. \tag{6}$$

## 3 The Hamiltonian Reduction Process

As mentioned in the Introduction, we shall consider special stratified fluid configurations, consisting of a fluid with $n = 4$ layers of constant density $\rho_1 < \rho_2 < \rho_3 < \rho_4$ and respective thicknesses $\eta_1, \eta_2, \eta_3, \eta_4$, confined in a channel of fixed height $h$. We

define, as in Fig. 1, the locations of the interfaces at $z = \zeta_k$, $k = 1, 2, 3$, related to the thickness $\eta_j$ by

$$\zeta_3 = \eta_4, \quad \zeta_2 = \eta_4 + \eta_3, \quad \zeta_1 = \eta_4 + \eta_3 + \eta_2. \tag{7}$$

The velocity components in each layer are denoted by $(u_i(x, z), w_i(x, z))$, $i = 1, \ldots, 4$. By means of the Heaviside $\theta$ and Dirac $\delta$ generalized functions, a four-layer fluid configuration can be described within Benjamin's setting as follows. First, the $2D$ density and velocity variables can be written as

$$\begin{aligned}
\rho(x, z) &= \rho_4 + (\rho_3 - \rho_4)\theta(z - \zeta_3) + (\rho_2 - \rho_3)\theta(z - \zeta_2) + (\rho_1 - \rho_2)\theta(z - \zeta_1) \\
u(x, z) &= u_4 + (u_3 - u_4)\theta(z - \zeta_3) + (u_2 - u_3)\theta(z - \zeta_2) + (u_1 - u_2)\theta(z - \zeta_1) \\
w(x, z) &= w_4 + (w_3 - w_4)\theta(z - \zeta_3) + (w_2 - w_3)\theta(z - \zeta_2) + (w_1 - w_2)\theta(z - \zeta_1)\,.
\end{aligned} \tag{8}$$

Thus, the density-weighted vorticity $\Sigma = (\rho w)_x - (\rho u)_z$ can be computed as

$$\begin{aligned}
\Sigma = &\sum_{j=1}^{3} \left(\rho_{j+1}\Omega_{j+1} - \rho_j \Omega_j\right) \theta(z - \zeta_j) + \rho_4 \Omega_4 \\
&+ \sum_{j=1}^{3} \left((\rho_{j+1}u_{j+1} - \rho_j u_j) + (\rho_{j+1}w_{j+1} - \rho_j w_j)\zeta_{j_x}\right) \delta(z - \zeta_j)\,,
\end{aligned} \tag{9}$$

where $\Omega_i = w_{i\,x} - u_{i\,z}$ for $i = 1, \ldots, 4$ are the bulk vorticities.

Next, we assume the bulk motion in each layer to be irrotational, so that $\Omega_i = 0$ for all $i = 1, \ldots, 4$. Thus the density weighted vorticity is explicitly given by

$$\begin{aligned}
\Sigma = &\left((\rho_4 u_4 - \rho_3 u_3) + (\rho_4 w_4 - \rho_3 w_3)\zeta_{3_x}\right) \delta(z - \zeta_3) \\
&+ \left((\rho_3 u_3 - \rho_2 u_2) + (\rho_3 w_3 - \rho_2 w_2)\zeta_{2_x}\right) \delta(z - \zeta_2) \\
&+ \left((\rho_2 u_2 - \rho_1 u_1) + (\rho_2 w_2 - \rho_1 w_1)\zeta_{1x}\right) \delta(z - \zeta_1)\,.
\end{aligned} \tag{10}$$

A further assumption we make right from the outset is that of the long-wave asymptotics, with small parameter $\epsilon = h/L \ll 1$, $L$ being a typical horizontal scale of the motion such as wavelength. This assumption implies (see, e.g., [8] for further details) that at the leading order as $\epsilon \to 0$ we have

$$u_i \sim \overline{u}_i\,, \qquad w_i \sim 0\,,$$

i.e., we can neglect the vertical velocities $w_i$ and trade the horizontal velocities $u_i$ with their layer-averaged counterparts,

$$\overline{u}_i = \frac{1}{\eta_i} \int_{\zeta_i}^{\zeta_{i-1}} u(x, z)\mathrm{d}z, \text{ where } \zeta_0 \equiv h, \ \zeta_4 \equiv 0\,. \tag{11}$$

Hence, from (10) and recalling the first of (8), we obtain

$$\begin{aligned}\rho(x,z) &= \rho(x,z) = \rho_4 + \sum_{i=1}^{3}(\rho_i - \rho_{i+1})\,\theta(z-\zeta_i)\\ \Sigma(x,z) &= \sum_{i=1}^{3}\sigma_i\,\delta(z-\zeta_i)\,,\end{aligned} \tag{12}$$

where, hereafter,

$$\sigma_i \equiv \rho_{i+1}\overline{u}_{i+1} - \rho_i\overline{u}_i \tag{13}$$

is the horizontal averaged momentum shear. We remark that field configurations of the form (12) can be regarded as defining a submanifold, which will be denoted by $\mathcal{I}$, of Benjamin's Poisson manifold $\mathcal{M}$ described in Sect. 2.

The $x$ and $z$-derivative of the Benjamin's variables given by Eq. (12) are generalized functions supported at the interfaces $\{z=\zeta_1\}\cup\{z=\zeta_2\}\cup\{z=\zeta_3\}$, and are computed as

$$\begin{aligned}\rho_x &= -\,\Sigma_{i=1}^{3}(\rho_i - \rho_{i+1})\delta(z-\zeta_i)\zeta_{ix}\\ \rho_z &= \Sigma_{i=1}^{3}(\rho_i - \rho_{i+1})\delta(z-\zeta_i)\,,\end{aligned} \tag{14}$$

and

$$\begin{aligned}\Sigma_x &= -\,\Sigma_{i=1}^{3}\sigma_i\zeta_{ix}\delta'(z-\zeta_i) + \Sigma_{i=1}^{3}\sigma_{ix}\delta(z-\zeta_i)\\ \Sigma_z &= \Sigma_{i=1}^{3}\sigma_i\delta'(z-\zeta_i)\,.\end{aligned} \tag{15}$$

To invert the map (12) we choose to integrate along the vertical direction $z$. To this end, we define the two intermediate isopycnals

$$\overline{\zeta}_{12} = \frac{\zeta_1+\zeta_2}{2}, \qquad \overline{\zeta}_{23} = \frac{\zeta_2+\zeta_3}{2}\,. \tag{16}$$

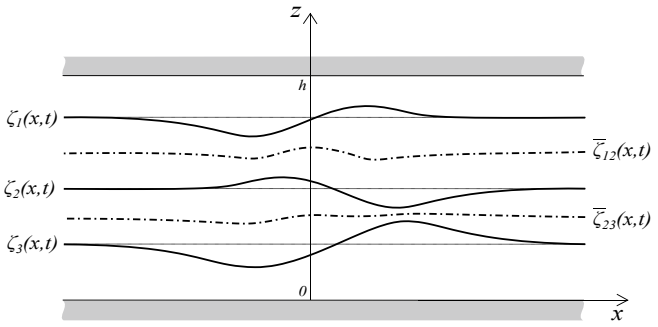


**Fig. 2** Choice of the isopycnals: $\zeta_i$ are the surface heights and $\overline{\zeta}_{12}$, $\overline{\zeta}_{23}$ the intermediate isopycnals

Remarking that $\overline{\zeta}_{12}$ lies in the $\rho_2$-layer and $\overline{\zeta}_{23}$ in the $\rho_3$-layer (see Fig. 2), by means of this choice we can introduce on $\mathcal{I}$ the "projection" $\pi$ by

$$\begin{aligned}&\pi\left(\rho(x,z),\Sigma(x,z)\right)\equiv(\xi_1,\xi_2,\xi_3,\tau_1,\tau_2,\tau_3)\\&=\begin{pmatrix}\int_0^h(\rho(x,z)-\rho_4)\,\mathrm{d}z,\int_0^{\overline{\zeta}_{12}}(\rho(x,z)-\rho_4)\,\mathrm{d}z,\int_0^{\overline{\zeta}_{23}}(\rho(x,z)-\rho_4)\,\mathrm{d}z,\\ \int_0^h\Sigma(x,z)\mathrm{d}z,\int_0^{\overline{\zeta}_{12}}\Sigma(x,z)\mathrm{d}z,\int_0^{\overline{\zeta}_{23}}\Sigma(x,z)\mathrm{d}z\end{pmatrix}\end{aligned}\tag{17}$$

which maps Benjamin's manifold of $2D$ fluid configurations to the space of effective $1D$ fields $\mathcal{S}$, parameterized by the six quantities $(\zeta_k,\sigma_k)$. A straightforward computation shows that the relations

$$\begin{aligned}\xi_1&=(h-\zeta_1)(\rho_1-\rho_2)+(h-\zeta_2)(\rho_2-\rho_3)+(h-\zeta_3)(\rho_3-\rho_4)\\ \xi_2&=\frac{\rho_2-\rho_3}{2}(\zeta_1-\zeta_2)+\frac{\rho_3-\rho_4}{2}(\zeta_1+\zeta_2-2\zeta_3)\\ \xi_3&=\frac{1}{2}(\rho_3-\rho_4)(\zeta_2-\zeta_3)\\ \tau_1&=\sigma_1+\sigma_2+\sigma_3,\quad \tau_2=\sigma_1+\sigma_2,\quad \tau_3=\sigma_3\end{aligned}\tag{18}$$

hold.

To obtain a Hamiltonian structure on the manifold $\mathcal{S}$ by reducing Benjamin's parent structure (6), we have to perform, as per the Hamiltonian reduction scheme of [15], the following steps:

1. Starting from a 1-form on the manifold $\mathcal{S}$, represented by the 6-tuple

$$(\alpha_S^1,\alpha_S^2,\alpha_S^3,\alpha_S^4,\alpha_S^5,\alpha_S^6)\,,$$

we construct its lift to $\mathcal{I}$, that is, a 1-form $\boldsymbol{\beta}_M=(\beta_\rho,\beta_\Sigma)$ satisfying the relation

$$\int_{-\infty}^{+\infty}\int_0^h(\beta_\rho\dot{\rho}+\beta_\Sigma\dot{\Sigma})\,\mathrm{d}x\,\mathrm{d}z=\int_{-\infty}^{+\infty}\sum_{k=1}^{6}\alpha_S^k\cdot\left(\pi_*(\dot{\rho},\dot{\Sigma})\right)^k\,\mathrm{d}x\ ,\tag{19}$$

where $\pi_*$ is the tangent map to (17) and $(\dot{\rho},\dot{\Sigma})$ are generic infinitesimal variations of $(\rho,\Sigma)$ in the tangent space to $\mathcal{I}$.
2. We apply Benjamin's operator (6) to the lifted one form $\boldsymbol{\beta}_M$ to get the vector field

$$\begin{pmatrix}\dot{\rho}\\ \dot{\Sigma}\end{pmatrix}=\begin{pmatrix}Y_M^{(1)}\\ Y_M^{(2)}\end{pmatrix}=J_B\cdot\begin{pmatrix}\beta_\rho\\ \beta_\Sigma\end{pmatrix}.\tag{20}$$

3. We project the vector $(Y_M^{(1)},Y_M^{(2)})$ under $\pi_*$ and obtain a vector field on $\mathcal{S}$. The latter depends linearly on $\{\alpha_S^{(i)}\}_{i=1,\dots,6}$, and defines the reduced Poisson operator $P$ on $\mathcal{S}$.

As in the three layer case of [4] this construction essentially works as in the two-layer case considered in [3], provided one subtle point is taken into account. Thanks to the relations (12) and the definition of $\pi$, we have that, for tangent vectors $(\dot\rho, \dot\Sigma)$,

$$\pi_*\begin{pmatrix}\dot\rho\\ \dot\Sigma\end{pmatrix} = \begin{pmatrix} \int_0^h \dot\rho\,\mathrm{d}z \\ \int_0^{\zeta_{23}} \dot\rho\,\mathrm{d}z + \dot{\overline{\zeta}}_{23}\,(\rho(x,\overline{\zeta}_{23}) - \rho_4) \\ \int_0^{\zeta_{12}} \dot\rho\,\mathrm{d}z + \dot{\overline{\zeta}}_{12}\,(\rho(x,\overline{\zeta}_{12}) - \rho_4) \\ \int_0^h \dot\Sigma\,\mathrm{d}z \\ \int_0^{\zeta_{23}} \dot\Sigma\,\mathrm{d}z + \dot{\overline{\zeta}}_{23}\,\Sigma(x,\overline{\zeta}_{23}) \\ \int_0^{\zeta_{12}} \dot\Sigma\,\mathrm{d}z + \dot{\overline{\zeta}}_{12}\,\Sigma(x,\overline{\zeta}_{12}) \end{pmatrix}. \tag{21}$$

Note that in this formula we have an explicit dependence on the variations $\dot{\overline{\zeta}}_{12}$ and $\dot{\overline{\zeta}}_{23}$. To express these quantities in terms of $\dot\rho$, which is needed to perform the abovementioned steps of the Poisson reduction, we can use the analogue of relations (14), that is

$$\dot\rho = \Sigma_{i=1}^3(\rho_{i+1} - \rho_i)\dot\zeta_i\delta(z-\zeta_i)\,. \tag{22}$$

Integrating this with respect to $z$ on the relevant intervals $[0, h]$, $[0, \overline{\zeta}_{12}]$ and $[0, \overline{\zeta}_{23}]$ yields

$$\begin{aligned}
\int_0^h \dot\rho\,\mathrm{d}z &= (\rho_4-\rho_3)\dot\zeta_3 + (\rho_3-\rho_2)\dot\zeta_2 + (\rho_2-\rho_1)\dot\zeta_1\,,\\
\int_0^{\overline{\zeta}_{12}} \dot\rho\,\mathrm{d}z &= (\rho_4-\rho_3)\dot\zeta_3 + (\rho_3-\rho_2)\dot\zeta_2\,,\\
\int_0^{\overline{\zeta}_{23}} \dot\rho\,\mathrm{d}z &= (\rho_4-\rho_3)\dot\zeta_3\,.
\end{aligned} \tag{23}$$

Solving the linear system (23) with respect to the $\dot\zeta_k$'s, we can obtain $\dot{\overline{\zeta}}_{12}$ and $\dot{\overline{\zeta}}_{23}$ in terms of integrals of $\dot\rho$ along $z$, and thus trade Eq. (21) for

$$\pi_*\begin{pmatrix}\dot\rho\\ \dot\Sigma\end{pmatrix} = \begin{pmatrix} \int_0^h \dot\rho\,\mathrm{d}z \\ c_1\int_0^h \dot\rho\,\mathrm{d}z + (1+c_3-c_2)\int_0^{\overline{\zeta}_{12}}\dot\rho\mathrm{d}z - c_3\int_0^{\overline{\zeta}_{23}}\dot\rho\mathrm{d}z \\ c_2\int_0^{\overline{\zeta}_{12}}\dot\rho\mathrm{d}z + \left(\frac{1}{2}-c_2\right)\int_0^{\overline{\zeta}_{23}}\dot\rho\mathrm{d}z \\ \int_0^h \dot\Sigma\,\mathrm{d}z \\ \int_0^{\zeta_{12}} \dot\Sigma\,\mathrm{d}z \\ \int_0^{\zeta_{23}} \dot\Sigma\,\mathrm{d}z \end{pmatrix}, \tag{24}$$

where, for the sake of compactness, we use the notation

$$c_1 = \frac{1}{2}\frac{\rho_2-\rho_4}{\rho_2-\rho_1}, \qquad c_2 = \frac{1}{2}\frac{\rho_3-\rho_4}{\rho_3-\rho_2}, \qquad c_3 = \frac{1}{2}\frac{\rho_2-\rho_4}{\rho_3-\rho_2}\,. \tag{25}$$

We now have at our disposal all the elements to perform the Poisson reduction process.

**Step 1:** The construction of the lifted 1-form $(\beta_\rho, \beta_\Sigma)$ satisfying (19), i.e.,

$$\int_{-\infty}^{+\infty}\int_0^h (\dot\rho\,\beta_\rho + \dot\Sigma\,\beta_\Sigma)\,\mathrm{d}x\,\mathrm{d}z = \int_{-\infty}^{+\infty} \Sigma_{k=1}^6 \alpha_S^k \pi_\star(\dot\rho,\dot\Sigma)^k \mathrm{d}x\,, \tag{26}$$

yields

$$\begin{aligned}\beta_\rho &= \alpha_S^1 + \big(c_1 + (1+c_3-c_1)\theta(\overline{\zeta}_{12}-z) - c_3\theta(\overline{\zeta}_{23}-z)\big)\,\alpha_S^2 + \\ &\quad \left(c_2\theta(\overline{\zeta}_{12}-z) + (\frac{1}{2}-c_2)\theta(\overline{\zeta}_{23}-z)\right)\alpha_S^3 \\ \beta_\Sigma &= \alpha_S^4 + \theta(\overline{\zeta}_{12}-z)\,\alpha_S^5 + \theta(\overline{\zeta}_{23}-z)\alpha_S^6\,.\end{aligned} \tag{27}$$

In this equation, Heaviside $\theta$'s appear and enable the computation of integrals from the bottom to the chosen isopycnals $\overline{\zeta}_{12}$ and $\overline{\zeta}_{12}$ along the full channel $[0, h]$.
**Step 2:** The computation of the vector fields $(Y_M^1, Y_M^2)$ from the relation

$$\begin{pmatrix} Y_M^{(1)} \\ Y_M^{(2)}\end{pmatrix} = J_B\cdot\begin{pmatrix}\beta_\rho\\ \beta_\Sigma\end{pmatrix} = \begin{pmatrix} 0 & \rho_x\partial_z - \rho_z\partial_x \\ \rho_x\partial_z - \rho_z\partial_x & \Sigma_x\partial_z - \Sigma_z\partial_x\end{pmatrix}\cdot\begin{pmatrix}\beta_\rho\\ \beta_\Sigma\end{pmatrix} \tag{28}$$

is greatly simplified by the specific dependence of the lifted 1-form $(\beta_\rho, \beta_\Sigma)$ of (27) on $z$ and and on the crucial fact that the inequalities

$$\zeta_3 < \frac{\zeta_3+\zeta_2}{2} = \overline{\zeta}_{23} < \zeta_2 < \overline{\zeta}_{12} = \frac{\zeta_1+\zeta_2}{2} < \zeta_1$$

hold in the strict sense, so that the terms $\rho_x\partial_z$ and $\Sigma_x\partial_z$ when acting on $(\beta_\rho, \beta_\Sigma)$ generate products of Dirac $\delta$'s supported at different points, which vanish *qua* generalized functions. Moreover,

$$\begin{aligned}\Sigma_z\cdot\partial_x(\beta_\Sigma) &= (\Sigma_{i=1}^3\sigma_i\delta'(z-\zeta_i))\left(\alpha_S^4 + \theta(\overline{\zeta}_{12}-z)\,\alpha_S^5 + \theta(\overline{\zeta}_{23}-z)\alpha_S^6\right)_x \\ &= (\Sigma_{i=1}^3\sigma_i\delta'(z-\zeta_i))\left(\alpha_{S,x}^4 + \theta(\overline{\zeta}_{12}-z)\,\alpha_{S,x}^5 + \theta(\overline{\zeta}_{23}-z)\alpha_{S,x}^6\right) \\ &\quad + (\Sigma_{i=1}^3\sigma_i\delta'(z-\zeta_i))\left(\delta(\overline{\zeta}_{12}-z)\overline{\zeta}_{12,x}\alpha_S^5 + \delta(\overline{\zeta}_{23}-z)\overline{\zeta}_{23,x}\alpha_S^6\right) \\ &= (\Sigma_{i=1}^3\sigma_i\delta'(z-\zeta_i))\left(\alpha_{S,x}^4 + \theta(\overline{\zeta}_{12}-z)\,\alpha_{S,x}^5 + \theta(\overline{\zeta}_{23}-z)\alpha_{S,x}^6\right)\,,\end{aligned} \tag{29}$$

still due to the above observation about the supports of the Dirac $\delta$'s. Denoting by $\Delta^{(2)}$ this term, we can write (28) as

$$Y_M^{(1)} = -\rho_z(\beta_\Sigma)_x, \quad Y_M^{(2)} = -\rho_z(\beta_\rho)_x - \Delta^{(2)}\,. \tag{30}$$

We obtain

$$
\begin{aligned}
Y_M^{(1)} = &\left(\sum_{k=1}^{3}(\rho_k - \rho_{k+1})\delta(z-\zeta_k)\right)\alpha^4_{S,x} \\
&+ \left(\sum_{k=2}^{3}(\rho_k - \rho_{k+1})\delta(z-\zeta_k)\right)\alpha^5_{S,x} + (\rho_3-\rho_4)\delta(z-\zeta_3)\alpha^6_{S,x}\,,
\end{aligned}
\tag{31}
$$

as well as the more complicated formula for $Y_M^{(2)}$,

$$
Y_M^{(2)} = (\sum_{i=1}^{3}(\rho_i - \rho_{i+1})\delta(z-\zeta_i))\,(\alpha^1_{S,x} + K_2\alpha^2_{S,x} + K_3\alpha^3_{S,x}) - \Delta^{(2)}\,, \tag{32}
$$

where

$$
\begin{aligned}
K_2 &= c_1 + (1 + c_3 - c_1)\theta(\overline{\zeta}_{12} - z) - c_3\theta(\overline{\zeta}_{23} - z) \\
K_3 &= c_2\theta(\overline{\zeta}_{12} - z) + \left(\frac{1}{2} - c_2\right)\theta(\overline{\zeta}_{23} - z)\,.
\end{aligned}
\tag{33}
$$

**Step 3:** The computation of the push-forward under the map $\pi_*$ of the vector field $(Y_M^{(1)}, Y_M^{(2)})$, to obtain the six-component vector field $(\dot{\xi}_k, \dot{\tau}_k)$ on $\mathcal{S}$ is a direct but tedious task. Thanks to the explicit expressions (25) and (33), substituting in (24) and noticing that, due to the presence of the $z$-derivatives of the Dirac $\delta$, $\Delta^{(2)}$ is in the kernel of $\pi_*$, yields

$$
\begin{aligned}
\dot{\xi}_1 &= \alpha^4_{S,x}(\rho_1-\rho_4) + \alpha^5_{S,x}(\rho_2-\rho_4) + \alpha^6_{S,x}(\rho_3-\rho_4) \\
\dot{\xi}_2 &= \frac{1}{2}(\rho_2-\rho_4)\alpha^5_{S,x} + (\rho_3-\rho_4)\alpha^6_{S,x} \\
\dot{\xi}_3 &= \frac{1}{2}(\rho_3-\rho_4)\alpha^6_{S,x} \\
\dot{\sigma}_1 &= (\rho_1-\rho_4)\alpha^1_{S,x} \\
\dot{\sigma}_2 &= (\rho_2-\rho_4)\alpha^1_{S,x} + \frac{1}{2}(\rho_2-\rho_4)\alpha^2_{S,x} \\
\dot{\sigma}_3 &= (\rho_3-\rho_4)\alpha^1_{S,x} + (\rho_3-\rho_4)\alpha^2_{S,x} + \frac{1}{2}(\rho_3-\rho_4)\alpha^3_{S,x}\,.
\end{aligned}
\tag{34}
$$

Thus, the Poisson tensor $P$ on the manifold $\mathcal{S}$ in the coordinates $(\xi_1, \xi_2, \xi_3, \tau_1, \tau_2, \tau_3)$ becomes

$$
P = \begin{pmatrix} 0 & A \\ A^T & 0 \end{pmatrix}\partial_x\,, \text{ where } A = \begin{pmatrix} \rho_1-\rho_4 & \rho_2-\rho_4 & \rho_3-\rho_4 \\ 0 & \dfrac{\rho_2-\rho_4}{2} & \rho_3-\rho_4 \\ 0 & 0 & \dfrac{\rho_3-\rho_4}{2} \end{pmatrix}.
$$

Recalling relations (18), a straightforward computation shows that in the coordinates $(\zeta_1, \zeta_2, \zeta_3, \sigma_1, \sigma_2, \sigma_3)$ the reduced Poisson operator acquires the particularly simple form

$$P = \begin{pmatrix} 0 & 0 & 0 & -1 & 0 & 0 \\ 0 & 0 & 0 & 0 & -1 & 0 \\ 0 & 0 & 0 & 0 & 0 & -1 \\ -1 & 0 & 0 & 0 & 0 & 0 \\ 0 & -1 & 0 & 0 & 0 & 0 \\ 0 & 0 & -1 & 0 & 0 & 0 \end{pmatrix} \partial_x \,. \tag{35}$$

**Remark 1** According to the terminology favored by the Russian school, for Hamiltonian quasi-linear systems of PDEs the coordinates $(\xi_l, \tau_l)$ and, *a fortiori*, the coordinates $(\zeta_l, \sigma_l)$, are "flat" coordinates for the system. In view of the particularly simple form of the Poisson tensor (35), the latter set could be called a system of flat *Darboux* coordinates.

**Remark 2** In [4] we conjectured that in the $n$-layered case, with a stratification given by densities $\rho_1 < \rho_2 < \cdots < \rho_n$ and interfaces $\zeta_1 > \zeta_2 > \cdots > \zeta_{n-1}$, a procedure yielding a natural Hamiltonian formulation for the averaged problem was to consider intervals

$$I_1 = [0, h],\ I_2 = \left[0, \frac{\zeta_1 + \zeta_2}{2}\right], I_3 = \left[0, \frac{\zeta_2 + \zeta_3}{2}\right], \ \ldots\ , \ I_n = \left[0, \frac{\zeta_{n-2} + \zeta_{n-1}}{2}\right]. \tag{36}$$

We explicitly proved it here for $n = 4$, together with the conjecture that the quantities

$$(\zeta_1, \zeta_2, \zeta_3, \sigma_1, \sigma_2, \sigma_3), \tag{37}$$

where $\sigma_k = \rho_{k+1}\overline{u}_{k+1} - \rho_k \overline{u}_k$, are flat Darboux coordinates for the reduced Poisson structure.

## 4 The Reduced Hamiltonian Under the Boussinesq Approximation

The energy of the $2D$ fluid in the channel is just the sum of the kinetic and potential energy,

$$H = \int_{-\infty}^{+\infty} \int_0^h \frac{\rho}{2} \left(u^2 + w^2\right) \mathrm{d}x\, \mathrm{d}z + \int_{-\infty}^{+\infty} \int_0^h g(\rho - \rho_0) z \, \mathrm{d}x\, \mathrm{d}z \,, \tag{38}$$

where $\rho_0$ is the reference density fixed by the far field constant values of the layers' thicknesses. In our case we have $\rho_0 = \sum_{i=1}^4 \rho_i \eta_i^{(\infty)}$, where $\eta_i^{(\infty)}$ are the asymptotic values of the $\eta_i$'s as $|x| \to \infty$.

The potential energy is thus readily reduced, using the first of (8), to

$$U = \int_{-\infty}^{+\infty} \frac{1}{2} \left( g\,(\rho_2 - \rho_1)\,{\zeta_1}^2 + g\,(\rho_3 - \rho_2)\,{\zeta_2}^2 + g\,(\rho_4 - \rho_3)\,\zeta_3^2 \right) \mathrm{d}x + U_\Delta\,, \tag{39}$$

where $U_\Delta$ contains constant and linear in the $\zeta_k$'s terms, which ensure the convergence of the integral, but that do not affect the equations of motion in view of the form (35) of the Poisson tensor.

To obtain the reduced kinetic energy density, we use the fact that at order $O(\epsilon^2)$ we can disregard the vertical velocity $w$, and trade the horizontal velocities with their layer-averaged means. Thus the $x$-density is computed as

$$\begin{aligned} \mathcal{T} &= \frac{1}{2} \left( \int_0^{\zeta_3} \rho_4 \overline{u}_4^2 \,\mathrm{d}z + \int_{\zeta_3}^{\zeta_2} \rho_3 \overline{u}_3^2 \,\mathrm{d}z + \int_{\zeta_2}^{\zeta_1} \rho_2 \overline{u}_2^2 \,\mathrm{d}z + \int_{\zeta_1}^{h} \rho_1 \overline{u}_1^2 \,\mathrm{d}z \right) \\ &= \frac{1}{2} \left( \rho_4 \zeta_3 \overline{u}_4^2 + \rho_3 (\zeta_2 - \zeta_3) \overline{u}_3^2 + \rho_2 (\zeta_1 - \zeta_2) \overline{u}_2^2 + \rho_1 (h - \zeta_1) \overline{u}_1^2 \right) . \end{aligned} \tag{40}$$

The so-called Boussinesq approximation consists of the double scaling limit

$$\rho_i \to \bar{\rho},\ \ i = 1, \ldots, 4, \quad g \to \infty \text{ with } g(\rho_{j+1} - \rho_j) \text{ finite}, \ \ j = 1, 2, 3, \tag{41}$$

where

$$\bar{\rho} = \frac{1}{4} \sum_{i=1}^{4} \rho_i$$

denotes the average density. This approximation then consists of neglecting density differences in the inertia terms of stratified Euler fluids, while retaining these differences in the buoyancy terms, owing to the relative magnitude of gravity forces with respect to those from inertia. This results in the Boussinesq energy density

$$\begin{aligned} \mathcal{E} = &\frac{\bar{\rho}}{2} \left( \zeta_3 \overline{u}_4^2 + (\zeta_2 - \zeta_3) \overline{u}_3^2 + (\zeta_1 - \zeta_2) \overline{u}_2^2 + (h - \zeta_1) \overline{u}_1^2 \right) \\ &+ \frac{1}{2} \left( g\,(\rho_2 - \rho_1)\,\zeta_1^2 + g\,(\rho_3 - \rho_2)\,\zeta_2^2 + g\,(\rho_4 - \rho_3)\,\zeta_3^2 \right) . \end{aligned} \tag{42}$$

To express this energy in terms of the Hamiltonian variables $(\zeta_i, \sigma_i)$, $i = 1, 2, 3$, we use the dynamical constraint

$$(h - \zeta_1) \overline{u}_1 + (\zeta_1 - \zeta_2) \overline{u}_2 + (\zeta_2 - \zeta_3) \overline{u}_3 + \zeta_3 \overline{u}_4 = 0\,, \tag{43}$$

as well as the definitions (13) that, in the Boussinesq approximation, are turned into

$$\sigma_k = \bar{\rho} (\overline{u}_{k+1} - \overline{u}_k)\,. \tag{44}$$

We get

$$\begin{aligned}
\overline{u}_1 &= -\frac{\zeta_1\sigma_1 + \zeta_2\sigma_2 + \zeta_3\sigma_3}{h\bar{\rho}}, \\
\overline{u}_2 &= -\frac{\zeta_1\sigma_1 + \zeta_2\sigma_2 + \zeta_3\sigma_3 - h\sigma_1}{h\bar{\rho}}, \\
\overline{u}_3 &= -\frac{\zeta_1\sigma_1 + \zeta_2\sigma_2 + \zeta_3\sigma_3 - h\sigma_1 - h\sigma_2}{h\bar{\rho}}, \\
\overline{u}_4 &= -\frac{\zeta_1\sigma_1 + \zeta_2\sigma_2 + \zeta_3\sigma_3 - h\sigma_1 - h\sigma_2 - h\sigma_3}{h\bar{\rho}}\,.
\end{aligned} \tag{45}$$

Hence, from (42), the Hamiltonian functional acquires its final form in the Boussinesq approximation as

$$\begin{aligned}
H_B = \int_{\mathbb{R}} \Bigg( & \frac{1}{2\,h\bar{\rho}} \left(\sigma_1^2\zeta_1\,(h-\zeta_1) + \sigma_2^2\,(h-\zeta_2)\,\zeta_2 + \sigma_3^2\,(h-\zeta_3)\,\zeta_3 + \right. \\
& 2\sigma_1\sigma_2\zeta_2\,(h-\zeta_1) + 2\sigma_1\sigma_3\zeta_3\,(h-\zeta_1) + 2\sigma_2\sigma_3\zeta_3\,(h-\zeta_2)) + \\
& \left. \frac{g}{2}\left((\rho_2-\rho_1)\zeta_1^2 + (\rho_3-\rho_2)\zeta_2^2 + (\rho_4-\rho_3)\zeta_3^2\right)\right) \mathrm{d}x\,.
\end{aligned} \tag{46}$$

Thanks to the simple form of the Poisson tensor (35), the ensuing equations of motion can be written as the conservation laws

$$\begin{aligned}
&\zeta_{1t} + \left(\frac{\sigma_1\zeta_1\,(h-\zeta_1)}{h\rho} + \frac{\sigma_3\zeta_3\,(h-\zeta_1)}{h\rho} + \frac{\sigma_2\zeta_2\,(h-\zeta_1)}{h\rho}\right)_x = 0 \\
&\zeta_{2t} + \left(\frac{\sigma_2\,(h-\zeta_2)\,\zeta_2}{h\rho} + \frac{\sigma_3\,(h-\zeta_2)\,\zeta_3}{h\rho} + \frac{\sigma_1\zeta_2\,(h-\zeta_1)}{h\rho}\right)_x = 0 \\
&\zeta_{3t} + \left(\frac{\sigma_3\,(h-\zeta_3)\,\zeta_3}{h\rho} + \frac{\sigma_2\,(h-\zeta_2)\,\zeta_3}{h\rho} + \frac{\sigma_1\zeta_3\,(h-\zeta_1)}{h\rho}\right)_x = 0 \\
&\sigma_{1t} + \left(\frac{(h-2\zeta_1)\,\sigma_1^2}{2h\rho} - \frac{\sigma_1\sigma_2\zeta_2}{h\rho} - \frac{\sigma_1\sigma_3\zeta_3}{h\rho} + g\,(\rho_2-\rho_1)\,\zeta_1\right)_x = 0 \\
&\sigma_{2t} + \left(\frac{(h-2\zeta_2)\,\sigma_2^2}{2h\rho} - \frac{\sigma_2\sigma_3\zeta_3}{h\rho} + \frac{\sigma_1\sigma_2\,(h-\zeta_1)}{h\rho} + g\,(\rho_3-\rho_2)\,\zeta_2\right)_x = 0 \\
&\sigma_{3t} + \left(\frac{(h-2\zeta_3)\,\sigma_3^2}{2h\rho} + \frac{\sigma_2\sigma_3\,(h-\zeta_2)}{h\rho} + \frac{\sigma_1\sigma_3\,(h-\zeta_1)}{h\rho} + g\,(\rho_4-\rho_3)\,\zeta_3\right)_x = 0\,.
\end{aligned} \tag{47}$$

The Hamiltonian formalism easily shows the existence of the eight conserved quantities

$$\begin{aligned}
&Z_j = \int_{-\infty}^{+\infty} \zeta_j\,\mathrm{d}x, \qquad S_j = \int_{-\infty}^{+\infty} \sigma_j\,\mathrm{d}x, \quad j = 1,2,3\,, \\
&K = \int_{-\infty}^{+\infty} \sum_{k=1}^{3} \zeta_k\sigma_k\,\mathrm{d}x \quad \text{and } H_B \text{ given by (4.9).}
\end{aligned} \tag{48}$$

**Remark 3** The first six quantities are Casimir functionals for the Darboux Poisson tensor (35), while the seventh one, $K$, is the generator of $x$-translations. Note that, formulas (45) imply that the total linear momenta of the individual layers are conserved quantities. This is consistent with the fact that the dispersionless limit of the $N$-layer equations are conservation laws for the averaged momenta, and no pressure imbalances can arise in the Boussinesq approximation [2].

**Remark 4** The steps leading to the computation of the effective Hamiltonian (46) can be performed also by dropping the assumptions (41) of the Boussinesq approximation. In this case, the kinetic energy acquires a non trivial rational dependence on the density differences $\rho_i - \rho_{i+1}$, and the equations of motion become much more complicated (as already seen in the 2 and 3-layer cases). However, they are still Hamiltonian equations of motion that preserve, together with their Hamiltonian, the quantities $Z_j,\ S_j,\ j = 1, 2, 3$ and the generator of $x$-translations $K$ of Eq. (48). Note that, as shown in [2] and further discussed in [4], once beyond the Boussinesq approximation pressure imbalances can appear. Hence the individual layer momenta are no longer conserved quantities and $K$ does not even coincide with the total horizontal momentum.

## 5 Symmetric Solutions

Symmetric solutions of the three-layer configurations were ingeniously found in [11] by a direct inspection of the equations of motion (written in velocity – thickness coordinates). They exist provided a certain relation is enforced on the density differences of the individual layers, and were interpreted in [4] as the fixed point of a suitable canonical involution of the phase space of the 3-layer model.

Here we shall adopt the latter point of view, and identify an involution of the phase space of the 4-layer model above that leads to the existence of a family of symmetric solutions. First, we focus on the kinetic energy part of the Boussinesq model (46),

$$\begin{aligned}\mathcal{T}_B = \frac{1}{2\,h\bar{\rho}}\Big(&\sigma_1^2\zeta_1\,(h-\zeta_1) + \sigma_2^2\,(h-\zeta_2)\,\zeta_2 + \sigma_3^2\,(h-\zeta_3)\,\zeta_3 + \\ &2\sigma_1\sigma_2\zeta_2\,(h-\zeta_1) + 2\sigma_1\sigma_3\zeta_3\,(h-\zeta_1) + 2\sigma_2\sigma_3\,(h-\zeta_2)\,\zeta_3\Big).\end{aligned} \tag{49}$$

This expression is clearly invariant under the involutive map

$$\zeta_1 \to h-\zeta_3,\quad \zeta_2 \to h-\zeta_2,\quad \zeta_3 \to h-\zeta_1,\quad \sigma_1 \to -\sigma_3,\quad \sigma_2 \to -\sigma_2,\quad \sigma_3 \to -\sigma_1\,. \tag{50}$$

If we assume that the densities $\rho_k$ fulfill the relations

$$\rho_4 - \rho_3 = \rho_2 - \rho_1 \equiv \rho_\Delta\,, \tag{51}$$

the Hamiltonian density (46) is invariant as well, up to the addition of linear terms in the $\zeta$'s, that is, up to constant terms and Casimir densities of the Poisson tensor $P$ of (35) which do not affect the equations of motion. A straightforward computation shows that the Poisson tensor (35) is left invariant by the above involution. Hence, the manifold $\mathcal{F}$ of fixed points of the involution (50) is invariant under the Hamiltonian flow (47).

The above statement can be cast in a more geometrical light. Suppose that we are given a Poisson manifold $(M, P)$ with Hamilton equations written generically as

$$z_t = P\, dH\,, \tag{52}$$

and suppose that $z \to \varphi(z)$ is an involution preserving $P$, i.e.,

(i) $\varphi \circ \varphi = \mathrm{Id}$
(ii) $\varphi_*\, P\, \varphi^* = P$, where $\varphi_*$ is the (Fréchet) derivative of $\varphi$, and $\varphi^*$ is its pull-back (from the linear algebra perspective, the adjoint map).

Then

$$\varphi(z)_t = \varphi_* z_t = \varphi_* P\, dH = \varphi_* P \varphi^* \varphi^* dH = P \varphi^* dH = P d\varphi^* H\,. \tag{53}$$

Hence, if $z$ satisfies $\varphi(z) = z$ we have $\varphi(z)_t - z_t = 0$ so that initial data fixed by the involution $\varphi$ remain on the invariant submanifold during the time evolution. In our case, the invariant manifold can be explicitly described as the submanifold of $\mathcal{S}$ characterized by the constraints (see Fig. 3)

$$\zeta_1 + \zeta_3 - h = 0\,, \quad \zeta_2 - \frac{h}{2} = 0\,, \quad \sigma_1 + \sigma_3 = 0\,, \quad \sigma_2 = 0\,, \tag{54}$$

and is parametrized by two of the remaining variables, for instance the two quantities

$$\sigma \equiv \sigma_3\,, \quad \zeta \equiv \zeta_3. \tag{55}$$

The reduced equations of motion on $\mathcal{F}$ in these variables are

$$\begin{cases} \zeta_t - \dfrac{2(\zeta^2\sigma)_x}{h\bar{\rho}} + \dfrac{(\zeta\sigma)_x}{\bar{\rho}} = 0 \\ \sigma_t + \dfrac{1}{2}\dfrac{((h-4\zeta)\sigma^2)_x}{h\bar{\rho}} + 2g\rho_\Delta \zeta\zeta_x = 0 \end{cases}, \tag{56}$$

while the restriction of the Hamiltonian (46) is

$$H_{\mathcal{F}} = \int_{\mathbb{R}} \left( \frac{\zeta\,(h-2\zeta)\,\sigma^2}{h\bar{\rho}} + g\rho_\Delta \zeta^2 \right) \mathrm{d}x\,. \tag{57}$$

One can readily check that Eq. (56) are the Hamiltonian equations of motion.

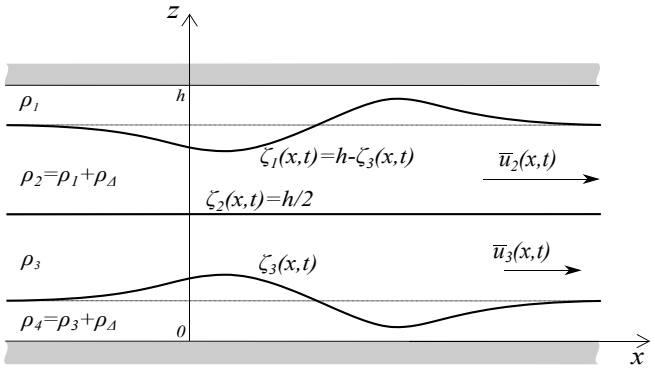


**Fig. 3** Example of a symmetric solution

$$\begin{pmatrix} \zeta_t \\ \sigma_t \end{pmatrix} = P_{\mathcal{F}} \begin{pmatrix} \delta_\zeta H_{\mathcal{F}} \\ \delta_\sigma H_{\mathcal{F}} \end{pmatrix} \text{ with } P_{\mathcal{F}} = \begin{pmatrix} 0 & -\frac{1}{2}\partial_x \\ -\frac{1}{2}\partial_x & 0 \end{pmatrix} . \tag{58}$$

The appearance of the factor $1/2$ in the expression of $P_{\mathcal{F}}$ is readily explained within Dirac's theory of constrained Hamiltonian systems. Indeed, if we consider the constraints (54), we notice that, renaming the constraint densities as

$$\Phi_1 = \zeta_1 + \zeta_3 - h\,, \quad \Phi_2 = \zeta_2 - h/2\,, \quad \Phi_3 = \sigma_1 + \sigma_3\,, \quad \Phi_4 = \sigma_2\,, \tag{59}$$

the sixtuple $(\zeta = \zeta_3, \sigma = \sigma_3, \Phi_1, \ldots, \Phi_4)$ is clearly a set of coordinates. The Poisson tensor in these coordinates is given by the block matrix

$$P = -\partial_x \begin{pmatrix} A & B^T \\ B & C \end{pmatrix} , \tag{60}$$

with

$$A = \begin{pmatrix} 0\,1 \\ 1\,0 \end{pmatrix}, \quad B = \begin{pmatrix} 0\,1 \\ 0\,0 \\ 1\,0 \\ 0\,0 \end{pmatrix}, \quad C = \begin{pmatrix} 0\,0\,2\,0 \\ 0\,0\,0\,1 \\ 2\,0\,0\,0 \\ 0\,1\,0\,0 \end{pmatrix} . \tag{61}$$

In this formalism, Dirac's formula [12] for the $2 \times 2$ reduced tensor $P^D$ with respect to the pair of coordinates $(\zeta, \sigma)$ on the constrained manifold is

$$P^D = \left(A - B^T \cdot C^{-1} \cdot B\right) \partial_x\,, \tag{62}$$

by which we recover the tensor $P_{\mathcal{F}}$ of (58).

As a final remark, we notice that the symmetric solutions might appear somewhat trivial, especially in view of the constraint that fixes the intermediate height $\zeta_2$ to be at the middle of the channel. However, one should remark that the additional requirement (51) on the densities reads $\rho_3 = \rho_4 - \rho_2 + \rho_1$. Thus in general $\rho_3 \neq \rho_2$ and, in the non-Boussinesq case, the constraint $\sigma_2 = \rho_3\overline{u}_3 - \rho_2\overline{u}_2 = 0$ generates a velocity shear along the flat interface $\zeta_2$.

## 6 Conclusions and Discussion

Building on our previous paper [4], we have considered the reduction of a natural Hamiltonian structure from the space of $2D$ general stratified configurations for an Euler incompressible, non-homogeneous fluid, to an effective $1D$ model of a four-layered sharply stratified fluid, in the long-wave dispersionless approximation. We have applied a general scheme for reducing Hamiltonian structures and constructed a set of natural Darboux coordinates on the reduced space of sharply stratified configurations. We then constructed an effective Hamiltonian in the Boussinesq approximation setting, which basically retains density differences only in the buoyancy terms. We finally pointed out the existence of a special family of symmetric solutions to the effective equations of motion which generalize their 3-layer counterpart and can serve to illustrate the expected differences and analogies between the general cases of odd and even number of layers. Symmetric solutions in the 3-layer case were introduced in [11] as a natural setting for the so-called mode 2 internal waves, that is, internal waves with out-of-phase pycnocline displacements. We have geometrically shown that four layer stratifications can support a similar family of waves, with the notable peculiarity that such "opposite" disturbances in the pycnocline displacement happen in the first and fourth layer only. While the middle interface $\zeta_2$ is forced to be flat and at the middle of the channel, velocity shears along this interface are not ruled out. Analytical and numerical properties of these 4-layers solutions (e.g., stability and well-posedness) are currently under investigation and will be communicated elsewhere.

**Acknowledgements** TTVH would like to thank the organizers of the NMMP-2022 Workshop held virtually in Tallahassee, June 17–19, 2022, for the opportunity to present results related with the topic of this paper, as well as the UNC Mathematics Department and CCIAM for hosting her visit in the Spring 2022. This project has received funding from the European Union's Horizon 2020 research and innovation programme under the Marie Skłodowska-Curie grant no 778010 *IPaDEGAN*. We also gratefully acknowledge the auspices of the GNFM Section of INdAM, under which part of this work was carried out, and the support of the project MMNLP (Mathematical Methods in Non Linear Physics) of INFN. RC thanks the support by the National Science Foundation under grants RTG DMS-0943851, CMG ARC-1025523, DMS-1009750, DMS-1517879, DMS-1910824, and by the Office of Naval Research under grants N00014-18-1-2490 and DURIP N00014-12-1-0749. RC & MP thank the Department of Mathematics and Applications of the University of Milano-Bicocca for its hospitality.

## References


1. Benjamin, T.B., On the Boussinesq model for two-dimensional wave motions in heterogeneous fluids, *J. Fluid Mech.* **165** (1986), 445–474.
2. Camassa, R., Chen, S., Falqui, G., Ortenzi, G., and Pedroni, M., An inertia 'paradox' for incompressible stratified Euler fluids, *J. Fluid Mech.* **695** (2012), 330–340.
3. Camassa, R., Falqui, G., and Ortenzi, G., Two-layer interfacial flows beyond the Boussinesq approximation: a Hamiltonian approach, *Nonlinearity* **30** (2017), 466–491.
4. Camassa, R., Falqui, G., Ortenzi, G., Pedroni, M., and Vu Ho, T. T., Hamiltonian aspects of 3-layer stratified fluids, *J. Nonlinear Sci.* **31**:70 (2021).
5. Camassa, R., Falqui, G., Ortenzi, G., Pedroni, M., and Vu Ho, T.T., Simple two-layer dispersive models in the Hamiltonian reduction formalism, *Nonlinearity* **36** (2023), 4523–4552. arXiv:2306.09154.
6. Chesnokov, A.A., El, G.A., Gavrilyuk, S.L., and Pavlov, M.V., Stability of shear shallow water flows with free surface, *SIAM J. Appl. Math.* **77** (2017), 1068–1087.
7. Choi, W., and Camassa, R., Weakly nonlinear internal waves in a two-fluid system, *J. Fluid Mech.* **313** (1996), 83–103.
8. Choi, W., and Camassa, R., Fully nonlinear internal waves in a two-fluid system, *J. Fluid Mech.* **396** (1999), 1–36.
9. Chumakova, L., Menzaque, F.E., Milewski, P.A., Rosales, R.R., Tabak, E.G., and Turner, C.V., Shear instability for stratified hydrostatic flows, *Comm. Pure Appl. Math.* **62** (2009), 183–197.
10. Chumakova, L., Menzaque, F.E., Milewski, P.A., Rosales, R.R., Tabak, E.G., and Turner, C.V., Stability properties and nonlinear mappings of two and three-layer stratified flows, *Stud. Appl. Math.* **122** (2009), 123–137.
11. de Melo Viríssimo, F., and Milewski, P., Three-layer flows in the shallow water limit, *Stud Appl. Math.* **142** (2019), 487–512.
12. Dirac, P.A.M., Generalized Hamiltonian dynamics, *Canad. J. Math.* **2** (1950), 129–148.
13. Duchêne, V., Israwi, S., and Talhouk, R., A new class of two-layer Green-Naghdi systems with improved frequency dispersion, *Stud. Appl. Math.* **137** (2016), 356–415.
14. Lvov, Y.V., and Tabak, E., Hamiltonian Formalism and the Garrett-Munk Spectrum of Internal Waves in the Ocean, *Phys. Rev. Lett.* **87** (2001), 168501.
15. Marsden, J. E., and Ratiu, T., Reduction of Poisson manifolds, *Lett. Math. Phys.* **11** (1986), 161–169.
16. Ovsyannikov, L.V., Two-layer "shallow water" model, *J. Appl. Mech. Tech. Phys.* **20** (1979), 127–135.
17. Vlasenko, V., Stashchuk, N., and Hutter, K., *Baroclinic Tides: Theoretical Modeling and Observational Evidence*, (2005) CUP, Cambridge (UK), 351 pages.
18. Zakharov, V.E., Musher, S.L., Rubenchik, A.M., Hamiltonian approach to the description of non-linear plasma phenomena, *Phys. Rep.* **129** (1985), 285–366.

# Long Wave Propagation in Canals with Spatially Varying Cross-Sections and Currents


**Semyon Churilov and Yury Stepanyants**

**Abstract** Two aspects of wave propagation in inhomogeneous media moving with a spatially varying speed are considered. Firstly, we analyze the mutual transformation of co- and counter-current propagating waves. In sub-critical flows with the current velocity $U$ less than the local wave speed relative to the medium $c$, this process is known as a reflection. In super-critical flows with $U > c$, the process manifests as a simultaneous amplification of positive- and negative-energy waves. The most interesting phenomena in such a case are the wave transformation in currents that transit from sub- to super-critical regime and vice versa. Secondly, we find and examine such inhomogeneous flows that allow an independent propagation of co- and counter-current waves, so-called reflectionless flows. In the latter case, wave energy can be transmitted most efficiently in space which can have both positive and negative effects depending on the particular situation.

**Keywords** Shallow water flow · Wave-current interaction · Reflectionless wave propagation · Wave scattering · Negative energy waves

## 1 Introduction

The theory of wave propagation in inhomogeneous and moving media has a long story (see, for example, [4–6, 15]). An interplay of Doppler effect and spatial non-homogeneity makes the problem rich in physical content and practically important.

S. Churilov
Institute of Solar-Terrestrial Physics of the Siberian Branch of the Russian Academy of Sciences, Irkutsk-33 PO Box 291, 664033, Russia

Y. Stepanyants (✉)
School of Mathematics, Physics, and Computing, University of Southern Queensland, 487–535 West St., Toowoomba, QLD 4350, Australia
e-mail: yury.stepanyants@usq.edu.au

Department of Applied Mathematics, Nizhny Novgorod State Technical University n.a. R.E. Alekseev, Nizhny Novgorod 603950, Russia



S. Manukure and W.-X. Ma (eds.), *Nonlinear and Modern Mathematical Physics*, Springer Proceedings in Mathematics & Statistics 459,
https://doi.org/10.1007/978-3-031-59539-4_2

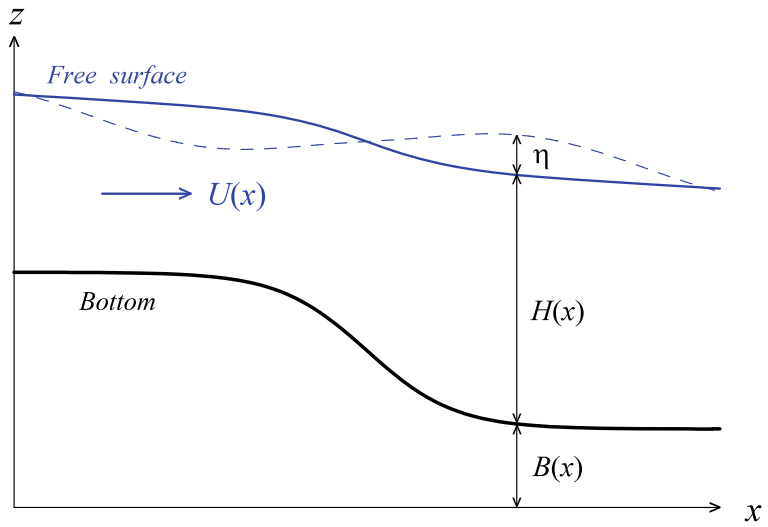


**Fig. 1** Sketch of the flow configuration in the vertical plane. The perturbed upper boundary is drawn in dashes

Many studies have been devoted to the investigation into various aspects of this immense topic, mainly based on approximate methods, such as geometric optics [17, 27] and the WKB [1, 20]. In this review, we consider two classes of wave problems that require the development of exact solutions whereas approximate methods play only an auxiliary role. Exact solutions can be obtained as usual for reasonably simplified problem statements that are still of physical meaning.

Let us consider in linear approximation a one-dimensional problem of wave propagation in a stationary current assuming that all parameters of a medium, including the current velocity $U$, depend only on the $x$-coordinate (see Fig. 1). If an incident wave propagates in such a medium in one direction, for example, from left to right then, due to the inhomogeneities, almost inevitably another reflected wave arises, traveling in the opposite direction, from right to left. The aforementioned approximate methods usually do not allow one to calculate the mutual transformation of these waves, while this process is interesting both per se and in its consequences.

In the space where the background flow is subcritical, i.e. where its speed $U(x)$ is less than the speed of wave propagation relative to the medium, $c(x)$, the mutual wave transformation generally leads to the decrease of incident wave energy. However, there are such configurations of the background flow in which waves reflected from its different parts add out of phase and diminish each other; this dramatically reduces the total wave reflection. A more interesting phenomenon arises in the wave transformation in supercritical flows, where $U > c$. In such a case, a wave traveling against the current has a negative energy (for details on this concept, see, for example, [14, 23]), and a kind of positive feedback can occur when the amplitudes of both waves grow together whereas the total energy conserves (growing positive energy of

an incident wave is compensated by growing (in absolute value) negative energy of a reflected wave). As a result, the incident wave of positive energy passing through the supercritical region leaves it significantly enhanced, while the negative energy wave (NEW) absorbs in the transition zone.

Another circle of problems opposite in its physical content is connected with the interesting phenomenon when waves can propagate in an inhomogeneous medium with a certain flow configuration without reflection. In such cases, both waves can travel in opposite directions independently of each other despite the medium inhomogeneity and movement. Similar situations occur, for example, when a wave scatters on a hump or well of a finite-length $l$ at a specific relationship between its length and wavelength. This effect is well-known in quantum mechanics [19] and in the water-wave theory (see, e.g., [13]). The search for conditions of such reflectionless wave propagation is also based on exact solutions of model equations describing the medium and current configurations.

The problem of the existence of waves propagating without large energy losses in an inhomogeneous moving medium is extremely important for explaining the propagation of waves over long distances, such as tsunami waves, storm surges and tidal bores in the ocean, acoustic waves in the atmosphere, and plasma waves in astrophysics. Knowledge of conditions for non-reflective wave propagation allows one to undertake measures to protect coasts against unwanted highly energetic wave impacts.

As the basic physical model of wave processes under this study, we consider the propagation of surface gravity waves on a shallow water current with the depth $H$ and speed $U$ both dependent on $x$. We begin with the problem formulation and derivation of the governing equations. Then, we apply the equations derived to two classes of problems outlined above.

Firstly, we consider the flows transiting from subcritical regime to supercritical one and (or) vice versa and analyze the solutions in the vicinity of critical points where $U(x) = c(x)$. On this basis, we describe in detail the wave propagation along sub- and super-critical parts of the flow and transition through the critical points, and then calculate the transformation coefficients.

Secondly, we use the wave equation in two alternative forms to obtain the conditions for wave propagation without reflection and analyse them in detail. We show that there are three classes of non-reflecting flows, examine their general properties and illustrate the results by particular solutions. We conclude this chapter with a discussion of the results obtained and their practical applications.

## 2 Problem Statement and Governing Equations

Let us consider the propagation of surface waves on a shallow water flow with the velocity $U(x)$ in a duct with the width $W(x)$ and bottom profile $z_B = B(x)$ gradually varying along the direction of the flow as shown in Fig. 1 (note that the water surface is not horizontal in the presence of spatially inhomogeneous flow).

In a stationary flow, the current velocity $U(x)$ is related to the canal parameters by the flux conservation law,

$$\Phi = U(x)H(x)W(x) = \text{const}, \tag{1}$$

and the Bernoulli equation

$$\frac{1}{2}\,U^2(x) + g\Big[H(x) + B(x)\Big] = \text{const}, \tag{2}$$

where $g$ is the acceleration due to gravity. It is easy to see that by appropriately choosing profiles $B(x)$ and $W(x)$ one can provide the desired (and independent) variation along the duct of the flow velocity $U(x)$ and the speed of long waves $c(x) = \sqrt{gH(x)}$; this velocities are assumed to be positive everywhere.

In the shallow-water theory (see, e.g., [18]), the linearized Euler equation has the form

$$\frac{\partial \tilde{u}}{\partial t} + \frac{\partial (U\tilde{u})}{\partial x} = -g\frac{\partial \eta}{\partial x}, \tag{3}$$

where $\tilde{u}(x,t)$ is the perturbation of the longitudinal component of fluid velocity, and $\eta(x,t)$ is the deviation of a free surface from the equilibrium state. Then the mass balance equation is

$$\frac{\partial S}{\partial t} + \frac{\partial}{\partial x}\Big[S(U+\tilde{u})\Big] = 0, \tag{4}$$

where $S(x,t) = [H(x) + \eta(x,t)]W(x)$ is a part of the duct cross-section occupied by water. Linearizing this equation with respect to small perturbations $\eta$ and $\tilde{u}$ and taking into account Eq. (1) with $\Phi \neq 0$, we obtain

$$\frac{\partial \eta}{\partial t} + \frac{1}{W}\,\frac{\partial}{\partial x}\Big[W(U\,\eta + H\,\tilde{u})\Big] \equiv \frac{\partial \eta}{\partial t} + HU\frac{\partial}{\partial x}\left(\frac{\eta}{H} + \frac{\tilde{u}}{U}\right) = 0. \tag{5}$$

Let us introduce the functions $\varphi(x,t)$ and $\phi(x,t)$ such that

$$\tilde{u} = \partial\varphi/\partial x \qquad \text{and} \qquad W(x)\eta = \partial\phi/\partial x, \tag{6}$$

and integrate Eqs. (3) and (5) in $x$. We obtain

$$\frac{\partial \varphi}{\partial t} + U(x)\,\frac{\partial \varphi}{\partial x} + \frac{1}{W(x)}\,\frac{\partial \phi}{\partial x} = 0, \qquad \frac{\partial \phi}{\partial t} + U(x)\,\frac{\partial \phi}{\partial x} + W(x)H(x)\,\frac{\partial \varphi}{\partial x} = 0. \tag{7}$$

Equations describing the characteristics of this system,

$$\frac{\mathrm{d}x}{\mathrm{d}t} = U(x) \pm c(x), \tag{8}$$

show that it is hyperbolic for any flow. Eliminating $\phi$ from Eq. (7) yields the wave equation

$$\left(\frac{\partial}{\partial t}+U\frac{\partial}{\partial x}-2U\frac{c'}{c}\right)\left(\frac{\partial\varphi}{\partial t}+U\frac{\partial\varphi}{\partial x}\right)=c^2U\frac{\partial}{\partial x}\left(\frac{1}{U}\frac{\partial\varphi}{\partial x}\right), \tag{9}$$

where the prime denotes the derivative with respect to $x$. For an elementary monochromatic wave with frequency $\omega$, $\varphi=\tilde{\varphi}(x)\mathrm{e}^{-\mathrm{i}\omega t}$, this equation transforms to

$$(c^2-U^2)\frac{\mathrm{d}^2\tilde{\varphi}}{\mathrm{d}x^2}+\left[2U^2\frac{c'}{c}-(c^2+U^2)\frac{U'}{U}+2\mathrm{i}\omega U\right]\frac{\mathrm{d}\tilde{\varphi}}{\mathrm{d}x}+\left(\omega^2-2\mathrm{i}\omega U\frac{c'}{c}\right)\tilde{\varphi}=0. \tag{10}$$

Following [2], we seek an exact solution to Eq. (10) in the form resembling a JWKB solution:

$$\begin{aligned}\tilde{\varphi}(x)&=B(x)\left[\exp\left(\mathrm{i}\omega\int\frac{\mathrm{d}x}{c(x)+U(x)}\right)+R(x)\exp\left(-\mathrm{i}\omega\int\frac{\mathrm{d}x}{c(x)-U(x)}\right)\right]\\&\equiv B\left[e_+ + Re_-\right],\end{aligned} \tag{11}$$

where functions $B(x)$ and $R(x)$ can be interpreted, to a certain extent, as, respectively, the complex amplitude of a co-current propagating wave and the relative amplitude of the counter-current propagating wave (i.e., "the local reflection coefficient"); $e_\pm$ denote the corresponding exponential functions. Note that the second term in the square brackets is singular at the critical points, where $U(x)=c(x)$. From the physical point of view, the singularities are caused by the blocking of the wave propagating against the current, so that its phase velocity and wavelength tend to zero at the critical point. Therefore, crossing through the critical point requires special attention and will be discussed in Sect. 3.2.

Using the method of variation of constants (see, e.g., [3]) we arrive at the equations

$$\frac{\mathrm{d}B}{\mathrm{d}x}=b(x)\left(1-R(x)\mathrm{e}^{-\mathrm{i}\Psi(x)}\right)B(x), \tag{12}$$

$$\frac{\mathrm{d}R}{\mathrm{d}x}=-b(x)\left(\mathrm{e}^{\mathrm{i}\Psi(x)}-R^2(x)\mathrm{e}^{-\mathrm{i}\Psi(x)}\right), \tag{13}$$

where (see Eq. (11))

$$\begin{aligned}b(x)&=\frac{1}{2}\left(\frac{c'}{c}+\frac{U'}{U}\right)\equiv\frac{\mathrm{d}\ln a(x)}{\mathrm{d}x},\quad a(x)=\left[c(x)U(x)\right]^{1/2},\\\mathrm{e}^{\mathrm{i}\Psi(x)}&=\frac{e_+(x)}{e_-(x)},\quad \Psi(x)=\omega\int\alpha(x)\mathrm{d}x,\\\alpha(x)&=\frac{1}{c(x)+U(x)}+\frac{1}{c(x)-U(x)}.\end{aligned} \tag{14}$$

The system of equations (12) and (13) has a number of useful properties that make the analysis of wave propagation simpler and more intuitive. Firstly, it is clear that if in some flow region function $a(x) = \text{const}$, then both $B(x) = \text{const}$ and $R(x) = \text{const}$, i.e., waves in this region *do not experience reflection* despite that $c$ and $U$ depend on $x$. Secondly, the problem is reduced to the nonlinear first-order ODE—the Riccati equation (13). After finding a solution to this equation, the amplitude equation for $B(x)$ (12) is immediately integrated:

$$B(x) = B_0\, a(x) \exp\Big[-\int \mathrm{d}x\, b(x)\, R(x) \mathrm{e}^{-\mathrm{i}\Psi(x)}\Big], \quad B_0 = \text{const}. \tag{15}$$

Thirdly, it is easy to see that in the flow regions that do not contain critical points (where $U(x) = c(x)$) Eqs. (12) and (13) have the first integral:

$$\mathcal{E} = \frac{|B(x)|^2}{a^2(x)} \Big[1 - |R(x)|^2\Big] = \text{const}, \tag{16}$$

This equation can be treated as the conservation of wave action which is equivalent in our case to the conservation of the pseudo-energy [14, 21]. According to this law, the amplitude of the incident wave $|B(x)|$ can be expressed in terms of the transformation coefficient $|R(x)|^2$ and the "geometric factor" of the flow $a(x)$.

For the further consideration, it is convenient to introduce the normalized amplitude that does not depend on the geometric factor, $D(x) = B(x)/a(x)$, and the normalized coefficient $r(x) = R(x)\mathrm{e}^{-\mathrm{i}\,\Psi(x)}$ (recall that $R(x)$ is a complex-valued function). These functions satisfy the following equations (see Eqs. (12)–(14)):

$$\frac{\mathrm{d}D}{\mathrm{d}x} = -b(x)\, r(x)\, D(x), \tag{17}$$

$$\frac{\mathrm{d}r}{\mathrm{d}x} = -b(x)\Big[1 - r^2(x)\Big] - \mathrm{i}\,\omega\,\alpha(x)\, r(x). \tag{18}$$

Then, Eqs. (11), (15), and (16) take the form:

$$\tilde{\varphi}(x) = B(x)\Big[1 + r(x)\Big] \exp\left(\mathrm{i}\omega \int \frac{\mathrm{d}x}{c(x) + U(x)}\right), \tag{19}$$

$$B(x) = B_0\, a(x) \exp\Big[-\int \mathrm{d}x\, b(x)\, r(x)\Big], \tag{20}$$

$$\mathcal{E} = \frac{|B(x)|^2}{a^2(x)} \Big[1 - |r(x)|^2\Big] \equiv |D(x)|^2 \Big[1 - |r(x)|^2\Big] = \text{const}. \tag{21}$$

It should be noted that if at some point of the flow $|r(x)| < 1$, then this inequality holds throughout the entire flow due to the conservation law (21) (the same is true for $|r(x)| > 1$).

In some cases it is convenient to express $r(x)$ in terms of the module and argument, $r(x) = |r(x)|\,\mathrm{e}^{\mathrm{i}\,\theta(x)}$ (recall that $|r(x)| \equiv |R(x)|$); then for these quantities we have the equations:

$$\frac{\mathrm{d}|r|}{\mathrm{d}x} = -b(x)\Big[1 - |r(x)|^2\Big]\cos\theta(x), \tag{22}$$

$$|r(x)|\,\frac{\mathrm{d}\theta}{\mathrm{d}x} = b(x)\Big[1 + |r(x)|^2\Big]\sin\theta(x) - \omega\alpha(x)|r(x)|. \tag{23}$$

## 3 Solution in the Vicinity of a Critical Point

### 3.1 The Asymptotic Expansion

Let $x = x_0$ be a regular critical point. This means that in its neighbourhood $U(x)$ and $c(x)$ are smooth functions such that $U(x_0) = c(x_0) \equiv c_0$ and the difference $\sigma = U'(x_0) - c'(x_0)$ is of the order of unity. Let us introduce a parameter $0 < \varepsilon \ll 1$, put $x - x_0 = \varepsilon\xi$, and use the notation $f_0 = f(x_0)$ for any function $f(x)$. Expanding functions $c(x)$ and $U(x)$ in the Taylor series in the vicinity of $x = x_0$ and replacing $x$ with $\xi$ in Eq. (18), we obtain:

$$\xi\frac{\mathrm{d}r}{\mathrm{d}\xi} = \frac{\mathrm{i}\omega}{\sigma}\,r + \varepsilon\xi\left[\frac{c_0' + U_0'}{2c_0}\Big(r^2 - 1\Big) - \frac{\mathrm{i}\omega}{2}\left(\frac{1}{c_0} - \frac{c_0'' - U_0''}{\sigma^2}\right)r\right] + \varepsilon^2\xi^2 S + \ldots, \tag{24}$$

where

$$S = \frac{1}{2}\left[\left(\frac{c_0'' + U_0''}{c_0} - \frac{{c_0'}^2 + {U_0'}^2}{c_0^2}\right)\Big(r^2 - 1\Big)\right.$$

$$\left. + \frac{\mathrm{i}\,\omega}{2}\left(\frac{c_0' + U_0'}{c_0^2} + \frac{2}{3}\,\frac{c_0''' - U_0'''}{\sigma^2} + \frac{(c_0'' - U_0'')^2}{\sigma^3}\right)r\right].$$

Let us look for a solution to this equation in the form $r = r^{(0)} + \varepsilon r^{(1)} + \varepsilon^2 r^{(2)} + \ldots$ and introduce a notation $\beta = \omega/\sigma$. In the zero order on the parameter $\varepsilon$, we obtain:

$$\xi\frac{\mathrm{d}r^{(0)}}{\mathrm{d}\xi} = \mathrm{i}\beta\,r^{(0)}, \qquad r^{(0)} = \tilde{B}_0\xi^{\mathrm{i}\beta}, \quad \tilde{B}_0 = \mathrm{const}. \tag{25}$$

In the first order on this parameter, $O(\varepsilon)$, the equation is:

$$\xi\frac{\mathrm{d}r^{(1)}}{\mathrm{d}\xi} = \mathrm{i}\beta\,r^{(1)} + \xi\left[\frac{c_0' + U_0'}{2c_0}\Big(\tilde{B}_0^2\xi^{2\mathrm{i}\beta} - 1\Big) - \frac{\mathrm{i}\omega}{2}\left(\frac{1}{c_0} - \frac{c_0'' - U_0''}{\sigma^2}\right)\tilde{B}_0\xi^{\mathrm{i}\beta}\right]. \tag{26}$$

A solution to this equation can be readily derived:

$$r^{(1)} = \xi\Big(B_{10} + B_{11}\xi^{\mathrm{i}\beta} + B_{12}\xi^{2\mathrm{i}\beta}\Big), \tag{27}$$

where

$$B_{10} = -\frac{c_0'+U_0'}{2c_0(1-\mathrm{i}\beta)}, \quad B_{11} = -\frac{\mathrm{i}\omega}{2}\left(\frac{1}{c_0} - \frac{c_0''-U_0''}{\sigma^2}\right)\tilde{B}_0, \quad B_{12} = \frac{c_0'+U_0'}{2c_0(1+\mathrm{i}\beta)}\,\tilde{B}_0^2 \tag{28}$$

In the second order on the parameter $\varepsilon$, $O(\varepsilon^2)$, the equation is:

$$\begin{aligned}\xi\frac{\mathrm{d}r^{(2)}}{\mathrm{d}\xi} = \mathrm{i}\beta\, r^{(2)} + \xi\left[\frac{c_0'+U_0'}{c_0}r^{(0)} - \frac{\mathrm{i}\omega}{2}\left(\frac{1}{c_0} - \frac{c_0''-U_0''}{\sigma^2}\right)\right]r^{(1)} \\ + \frac{\xi^2}{2}\left[\left(\frac{c_0''+U_0''}{c_0} - \frac{{c_0'}^2+{U_0'}^2}{c_0^2}\right)\left({r^{(0)}}^2 - 1\right)\right. \\ \left. + \frac{\mathrm{i}\omega}{2}\left(\frac{c_0'+U_0'}{c_0^2} + \frac{2}{3}\,\frac{c_0'''-U_0'''}{\sigma^2} + \frac{(c_0''-U_0'')^2}{\sigma^3}\right)r^{(0)}\right].\end{aligned} \tag{29}$$

The solution to this equation we present in the form:

$$r^{(2)} = \xi^2\Big(B_{20} + B_{21}\xi^{\mathrm{i}\beta} + B_{22}\xi^{2\mathrm{i}\beta} + B_{23}\xi^{3\mathrm{i}\beta}\Big), \tag{30}$$

where

$$\begin{aligned}B_{20} &= -\frac{1}{2(2-\mathrm{i}\beta)}\left[\frac{c_0''+U_0''}{c_0} - \frac{{c_0'}^2+{U_0'}^2}{c_0^2} + \mathrm{i}\omega\left(\frac{1}{c_0} - \frac{c_0''-U_0''}{\sigma^2}\right)B_{10}\right], \\ B_{21} &= \left[\frac{c_0'+U_0'}{2c_0}\,B_{10} + \frac{\mathrm{i}\omega}{8}\left(\frac{c_0'+U_0'}{c_0^2} + \frac{2}{3}\,\frac{c_0'''-U_0'''}{\sigma^2} + \frac{(c_0''-U_0'')^2}{\sigma^3}\right)\right]\tilde{B}_0 \\ &\quad - \frac{\mathrm{i}\omega}{4}\left(\frac{1}{c_0} - \frac{c_0''-U_0''}{\sigma^2}\right)B_{11}, \\ B_{22} &= \frac{1}{2(2+\mathrm{i}\beta)}\left[\left(\frac{c_0''+U_0''}{c_0} - \frac{{c_0'}^2+{U_0'}^2}{c_0^2}\right)\tilde{B}_0^2 + 2\,\frac{c_0'+U_0'}{c_0}\,\tilde{B}_0 B_{11}\right. \\ &\quad \left. - \frac{\mathrm{i}\omega}{2}\left(\frac{1}{c_0} - \frac{c_0''-U_0''}{\sigma^2}\right)B_{12}\right], \\ B_{23} &= \frac{c_0'+U_0'}{2c_0(1+\mathrm{i}\beta)}\,\tilde{B}_0^2 B_{12}.\end{aligned} \tag{31}$$

The solution obtained consists of two parts. One of them is the sum of a slowly varying terms that vanish at the critical point; this part of the solution is represented by the Taylor series:

$$r_{sl}(x) = B_{10}(x - x_0) + B_{20}(x - x_0)^2 + \ldots. \tag{32}$$

Another part of the solution contains the terms with the coefficients $\tilde{B}_0$ and $B_{nm}$ ($m \geq 1$); these terms are strongly oscillating when $x \to x_0$ (see Eqs. (25), (27), and (30)). Note that $B_{nm} \sim (\tilde{B}_0)^m$ and stress that $B_{nm}$ depend on $B_{i0}$, but $B_{i0}$ does not depend on $B_{nm}$ with $m \geq 1$ (this property holds in the higher orders of expansion too). Therefore, the slowly varying part of the solution is entirely determined by the local behavior of functions $c(x)$ and $U(x)$ in the vicinity of the critical point and *does not depend* on the fast oscillating contribution. The latter is determined by both the boundary conditions and behavior of functions $c(x)$ and $U(x)$ to the right or to the left of the point $x_0$. Note, by the way, that $\tilde{B}_0$ and the entire quickly oscillating contribution can be different at the left and right sides of $x_0$, therefore, the found solution is reasonable to represent in the form:

$$r(x) = r_{sl}(x) + \tilde{B}_0^{(\pm)}|x - x_0|^{\mathrm{i}\beta}\Big[1 + O(x - x_0)\Big], \tag{33}$$

where the signs plus and minus pertain to the regions where $x > x_0$ and $x < x_0$, respectively.

The integrals in the Eqs. (19) and (20) converge for $x \to x_0 \pm 0$, and the asymptotic expansions for $B(x)$ and $\tilde{\varphi}(x)$ can be written as:

$$B(x) = c_0 B_0^{(\pm)}\left[1 + \frac{c_0' + U_0'}{2c_0}(x - x_0)\left(1 - \frac{\tilde{B}_0^{(\pm)}}{1 + \mathrm{i}\beta}|x - x_0|^{\mathrm{i}\beta}\right) + O(|x - x_0|^2)\right], \tag{34}$$

$$\tilde{\varphi}(x) = c_0 B_0^{(\pm)}\Big[1 + \tilde{B}_0^{(\pm)}|x - x_0|^{\mathrm{i}\beta} + O(|x - x_0|)\Big]\mathrm{e}^{\mathrm{i}\Psi_+}, \quad \Psi_+ = \omega\int^{x_0}\frac{\mathrm{d}x}{c + U}. \tag{35}$$

## 3.2 Transition Through the Critical Point

As the next step, we need to understand how these solutions can be continued through the critical point. This problem was originally studied for a simplified flow model with a piecewise-linear velocity profile $U(x)$ and $c(x) = \text{const}$ [8], and then the results obtained were generalized to arbitrary smooth profiles of $c(x)$ and $U(x)$ [9].

Equation (35) contains only the principal expansion terms. The first term in the square brackets refers to the co-current propagating wave, and the second term (that is rapidly oscillating) refers to the counter-current propagating wave. As shown in [8, 9], for the correct matching solutions through the critical point, it is necessary to take into account a small viscosity of the medium. The final result is as follows.

If the current passes from the subcritical regime into the supercritical, then

$$B_0^{(+)} = B_0^{(-)}, \qquad \tilde{B}_0^{(+)} = \tilde{B}_0^{(-)} = 0. \tag{36}$$

In other words, co-current traveling waves "do not feel" that the point is critical. The absence of counter-current running waves is due to the fact that on both sides of the critical point, they propagate out of this point and therefore, cannot reach it. Hence, for such a transition we have (see Eqs. (32), (33), (21), and (22)):

$$r(x_0) = 0 \quad \text{and} \quad \mathcal{E}(x_0 + 0) = \mathcal{E}(x_0 - 0). \tag{37}$$

Therefore, we conclude that if $b(x_0) \neq 0$ in Eqs. (22) and (23), then functions $r(x)$ and $\cos\theta$ change their signs in the course of transition through the critical point, i.e. $\theta(x_0 + 0) = \theta(x_0 - 0) \pm \pi$.

On the contrary, in the course of the transition from the supercritical to the subcritical regime, the counter-current propagating waves run to the critical point from both sides and, approaching it with a decreasing wavelength, are completely absorbed in its viscous neighborhood. Their relative amplitudes $\tilde{B}_0^{(+)}$ and $\tilde{B}_0^{(-)}$ depend on their propagation prehistory in the *different* flow regions and therefore, are not related to each other, whereas $B_0^{(+)} = B_0^{(-)}$. The energy flux in the course of the transition through the critical point is not generally conserved,

$$\mathcal{E}(x_0 - 0) = \frac{|B_0^{(-)}|^2}{a^2(x_0)}\left(1 - |\tilde{B}_0^{(-)}|^2\right) \neq \mathcal{E}(x_0 + 0) = \frac{|B_0^{(+)}|^2}{a^2(x_0)}\left(1 - |\tilde{B}_0^{(+)}|^2\right),$$

it can either decrease or increase (see [8, 9]) since the waves absorbed have both positive and negative energy.

Thus, co-current propagating waves do freely transit through critical points of both kinds with no change in their amplitude. By contrast, counter-current propagating waves can not transit through any critical point because they are either unable to reach it or absorbed in its neighborhood. In the next three sections, we consider flows with two critical points in order to highlight the features of wave propagation in ducts with alternating sub- and supercritical parts. In particular, we give special attention to transmitting properties of these parts.

## 4 Wave Propagation in a Sub–Super–Subcritical Flow

### *4.1 The Flow Model and Preliminary Analysis*

Consider a current on the left ($-\infty < x < x_1$) and right ($x_2 < x < +\infty$) ends of which the flow is subcritical, $0 < U(x) < c(x)$, and within the middle part, for $x_1 < x < x_2$,—supercritical, $U(x) > c(x)$, as shown in Fig. 2. Such flows were studied

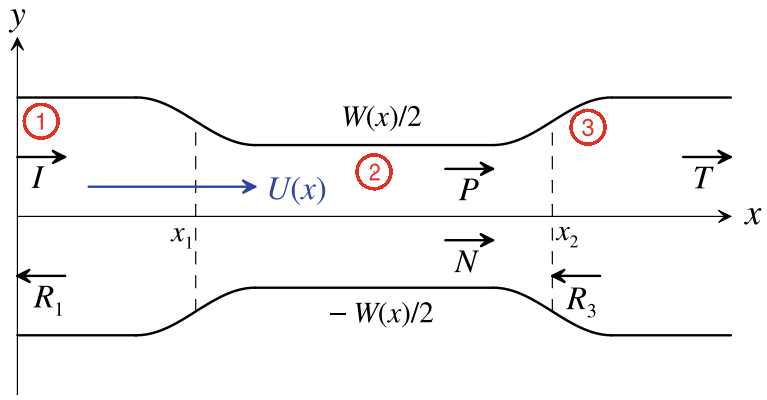


**Fig. 2** (color online) Sketch of the flow with two critical points, view from the top. Arrows indicate the flow direction, incident ($I$), transmitted ($T$), and reflected ($R_1$ and $R_3$) waves in subcritical domains 1 and 3, as well as positive ($P$) and negative ($N$) energy waves in the supercritical domain 2

in Ref. [9] as a hydrodynamic model for a wormhole directed from the black to the white hole. Here $x_1$ and $x_2$ are the critical points such that $U(x_1) = c(x_1) \equiv c_1$ and $U(x_2) = c(x_2) \equiv c_2$. We assume that in both critical points the differences of slopes, $\sigma_{1,2} \equiv U'(x_{1,2}) - c'(x_{1,2})$, are not small (see Fig. 3) and use in this Section the dimensionless variables

$$\tilde{x} = \frac{x}{\Lambda}, \qquad \tilde{U}(\tilde{x}) = \frac{U(x)}{c_1}, \qquad \tilde{c}(\tilde{x}) = \frac{c(x)}{c_1}, \qquad \tilde{\omega} = \frac{\omega}{\sigma_1}, \qquad \Lambda = \frac{c_1}{\sigma_1}. \tag{38}$$

In what follows, tildes will be omitted for brevity.

Let us assume that a plane wave of frequency $\omega$ arrives from the left. Its propagation will be described in terms of functions $D(x)$ and $r(x)$. At the critical point $x = x_1$ and when $x \to +\infty$ there is no wave traveling upstream, therefore solution to Eq. (18) must satisfy the boundary conditions:

$$r(x_1) = 0, \qquad r(+\infty) = 0. \tag{39}$$

Therefore, we can conclude that, firstly, in the entire flow $|r(x)| < 1$ (as it follows from the conservation law (21)) and, secondly, the Eq. (18) should be integrated into the upstream direction in the subcritical areas and downstream—on the supercritical section $x_1 \le x < x_2$.

Further, suppose that for $x \to \pm\infty$ functions $c(x)$ and $U(x)$ tend to their nonzero limiting values, and let $D(-\infty) = 1$. Then from Eq. (20) and the matching conditions (36), $B_0^{(+)} = B_0^{(-)}$, we find the amplitude of the downstream propagating wave as the function of $x$:

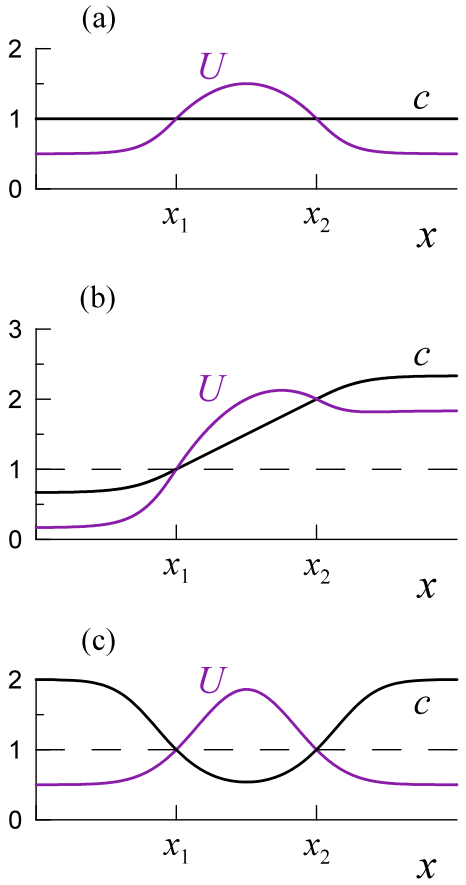


**Fig. 3** (color online) The flow models with two critical points: **a**—flow (66), $\mathcal{M} = 1.5$; **b**—flow (69), $c_2 = 2c_1 = 2$, $d = 1$; **c**—reflectionless flow with $a^2(x) \equiv c(x)U(x) = 1$

$$D(x) = \exp\left[-\int_{-\infty}^{x} b(x')\, r(x')\, \mathrm{d}x'\right], \quad -\infty < x < \infty. \tag{40}$$

Then we can define the transmission ratio $K(x) \equiv |D(x)|$ and present it as:

$$K(x) = \exp\left[-\int_{-\infty}^{x} \mathrm{d}x'\, b(x') \mathrm{Re}\left(r(x')\right)\right] \equiv \exp\left[-\int_{-\infty}^{x} \mathrm{d}x'\, b(x') |r(x')| \cos\theta(x')\right]. \tag{41}$$

As can be seen from Eqs. (22) and (41), the reflection coefficient $|r(x)|$ and transmission ratio $K(x)$ both increase or decrease simultaneously depending on the sign of the product $b(x)\cos\theta(x)$. Finally, in those regions where $b(x) = 0$, i.e. $a(x) =$ const, they are constant too and, as already noted, waves running in the opposite directions do not interact, but the phase difference between them $\theta(x)$ changes due

to the difference in the directions of propagation and difference in the wavelengths (i.e., because $\alpha(x) \neq 0$—see Eq. (23)).

In accordance with the flow structure and conservation law (21), one can distinguish three stages for the downstream propagating wave. In the interval $x < x_1$, the transmission ratio $K(x)$ decreases from unity to $K(x_1) = \sqrt{1 - |r(-\infty)|^2}$. In the supercritical interval, amplitude increases, and $K(x_2) = K(x_1)/\sqrt{1 - |r(x_2 - 0)|^2}$, and in the last interval, $x > x_2$, $K(x)$ decreases again to $K(+\infty) = K(x_2)$ $\sqrt{1 - |r(x_2 + 0)|^2}$ (recall that in the general case $|r(x_2 - 0)| \neq |r(x_2 + 0)|$, therefore the increase and subsequent decrease of $K$ are independent). In addition, $K(x)$ can vary non-monotonically in any of these three intervals. As a result, in each interval of the flow, its integral transmission ratios are presented by the formulae:

$$K_1 = \sqrt{1 - |r(-\infty)|^2} \leq 1, \quad K_2 = \left[1 - |r(x_2 - 0)|^2\right]^{-1/2} \geq 1,$$
$$K_3 = \sqrt{1 - |r(x_2 + 0)|^2} \leq 1, \tag{42}$$

and the total transmission ratio (the transmission coefficient) is $T \equiv K(+\infty) = K_1 \cdot K_2 \cdot K_3$. It can be increased by (i) reducing the transformation of the co-current propagating wave into reflected waves in the subcritical intervals of the flow and (ii) increasing its transformation into the NEW in the supercritical interval.

The first condition can be fulfilled at once for all frequencies if in the subcritical regions $b(x) \equiv 0$ (i.e. $c(x)U(x) \equiv$const) and waves propagate without reflection; then $K_1 = K_3 = 1$. Note that this condition does not prevent the change of the Mach number $\mathcal{M}(x) \equiv U(x)/c(x)$ along the flow, (see, e.g., Fig. 3c). Another way to do it is based on the effect similar to that of anti-reflective coating in the optics. Its principle is that waves reflected from the different flow intervals add up in anti-phase and extinguish each other. As can be seen from Eq. (22), the quenching is complete if:

$$r(-\infty) = \int_{-\infty}^{x_1} b(x)\left[1 - |r(x)|^2\right] \cos\theta(x)\, \mathrm{d}x = 0, \tag{43}$$

$$r(x_2 + 0) = \int_{x_2}^{\infty} b(x)\left[1 - |r(x)|^2\right] \cos\theta(x)\, \mathrm{d}x = 0. \tag{44}$$

Since in those intervals where $b(x) = 0$, function $\theta(x)$ continues to vary, the fulfillment of Eqs. (43) and (44) can be ensured by variation of $\theta(x)$ due to "inserts" with $b(x) = 0$ of the required length in the proper intervals of the flow. But since for $b = 0$ $\mathrm{d}\theta/\mathrm{d}x \sim \omega$ (see Eq. (23)), the choice of the positions of such inserts and especially their lengths significantly depend on the wave frequency.

As for the second condition, we shall see below that both the selection of inserts and the difference in the speeds of wave propagation at the ends of the supercritical

interval (no matter $c_1 < c_2$ or $c_1 > c_2$) can make $K_2$ greater, but the increase in wave frequency prevents to this.

To simplify further analysis, let us strengthen the previously formulated condition of fast convergence of $c(x)$ and $U(x)$ to their limiting values when $x \to \pm\infty$, assuming that $c$ and $U$ are constants and, respectively, $b(x) = 0$ for $x < x_- < x_1$ and $x > x_+ > x_2$. Below we perform the analysis for two limiting cases, when $\omega \ll 1$ and $\omega \gg 1$.

## 4.2 The Low-Frequency Limit, $\omega \ll 1$

Setting $\omega = 0$ in Eq. (18), we get

$$\frac{\mathrm{d}r_0}{\mathrm{d}x} = -\frac{a'(x)}{a(x)}\left(1 - r_0^2\right) \implies r_0(x) = \frac{R_0 - a^2(x)}{R_0 + a^2(x)}, \quad R_0 = c_i U_i \frac{1 + r_{0i}}{1 - r_{0i}}, \tag{45}$$

where $c_i, U_i$, and $r_{0i}$ are the values of $c(x), U(x), r_0(x)$ in some starting point $x = x_i$, and $R_0$ is a constant of integration that depends on the initial conditions in the point $x = x_i$. If $x_i$ coincides with the first critical point $x_1$, then $r_{0i} = 0$, $R_0 = 1$ and

$$r_0(x) = \frac{1 - a^2(x)}{1 + a^2(x)} \equiv \frac{1 - c(x)U(x)}{1 + c(x)U(x)} = 1 - \frac{2c(x)U(x)}{1 + c(x)U(x)}. \tag{46}$$

Next, we look for a solution in the form: $r(x) = r_0(x) + \omega\, r_1(x) + \omega^2 r_2(x) + \ldots$. In the lowest order on the frequency, $O(\omega)$, we have:

$$\frac{\mathrm{d}r_1}{\mathrm{d}x} = 2\,\frac{a'(x)}{a(x)}\, r_0(x) r_1(x) - \mathrm{i}\alpha(x) r_0(x).$$

Integrating this equation with the initial condition $r_1(x_i) = 0$ and using Eq. (45), we get:

$$r_1(x) = -\frac{2\mathrm{i}a^2(x)}{[R_0 + a^2(x)]^2} \int_{x_i}^{x} \frac{\mathrm{d}\xi\, r_0(\xi)}{U(\xi)}\, \frac{[R_0 + a^2(\xi)]^2}{c^2(\xi) - U^2(\xi)}\,. \tag{47}$$

In the next order on the frequency, $O(\omega^2)$, we have the following equation:

$$\frac{\mathrm{d}r_2}{\mathrm{d}x} = \frac{a'(x)}{a(x)}\Big[2r_0(x)r_2(x) + r_1^2(x)\Big] - \mathrm{i}\alpha(x) r_1(x).$$

Its solution subject to the initial condition $r_2(x_i) = 0$ is:

$$r_2(x) = -\frac{4a^2(x)}{[R_0 + a^2(x)]^3} \int_{x_i}^{x} \frac{\mathrm{d}\xi}{U(\xi)} \frac{R_0 a^2(x) + a^4(\xi)}{c^2(\xi) - U^2(\xi)} \int_{x_i}^{\xi} \frac{\mathrm{d}\eta\, r_0(\eta)}{U(\eta)} \frac{[R_0 + a^2(\eta)]^2}{c^2(\eta) - U^2(\eta)}. \tag{48}$$

The integral in the right-hand side of Eq. (47) can be evaluated in the vicinity of the point $x_2$; when $x \to x_2$ we have:

$$I(x) = \int_{x_i}^{x} \frac{\mathrm{d}\xi\, r_0(\xi)}{U(\xi)} \frac{[R_0 + a^2(\xi)]^2}{c^2(\xi) - U^2(\xi)} = I_{1i} - \frac{R_0^2 - c_2^4}{2\sigma_2 c_2^2} \ln|x - x_2| + O(|x - x_2|),$$

where $I_{1i} = \text{const}$, $\sigma_2 = U_2' - c_2'$. The integral converges if $r_0(x_2) = 0$ (i.e. if $R_0 = c_2^2$), otherwise it logarithmically diverges.

Similarly one can evaluate the integral on the right-hand side of Eq. (48):

$$\int_{x_i}^{x} \frac{\mathrm{d}\xi}{U(\xi)} \frac{R_0 a^2(x) + a^4(\xi)}{c^2(\xi) - U^2(\xi)} \int_{x_i}^{\xi} \frac{\mathrm{d}\eta\, r_0(\eta)}{U(\eta)} \frac{[R_0 + a^2(\eta)]^2}{c^2(\eta) - U^2(\eta)}$$

$$= I_{2i} - \frac{R_0 + c_2^2}{2\sigma_2} \left[ I_{1i} \ln|x - x_2| - \frac{R_0^2 - c_2^4}{4\sigma_2 c_2^2} \ln^2|x - x_2| \right] + O(|x - x_2|),$$

where $I_{2i} = \text{const}$. Therefore, when $x \to x_2$, the solution is:

$$r(x) = \frac{R_0 - c_2^2}{R_0 + c_2^2} \left[ 1 + \frac{\mathrm{i}\omega}{\sigma_2} \ln|x - x_2| - \frac{\omega^2}{2\sigma_2^2} \ln^2|x - x_2| + \ldots \right]$$

$$- \frac{2\mathrm{i}\omega c_2^2 I_{1i}}{(R_0 + c_2^2)^2} \left[ 1 + \frac{\mathrm{i}\omega}{\sigma_2} \ln|x - x_2| + \ldots \right] - \frac{4\omega^2 c_2^2 I_{2i}}{(R_0 + c_2^2)^3} + O(|x - x_2|). \tag{49}$$

On the other hand, setting in Eq. (33) $x_0 = x_2$ and $\sigma = \sigma_2$, we obtain for $|x - x_2| \ll 1$ and $\omega|\ln|x - x_2|| \ll 1$:

$$r(x) = r_{sl}(x) + B_0^{(\pm)} |x - x_2|^{\mathrm{i}\omega/\sigma_2} \Big[ 1 + O(|x - x_2|) \Big] =$$

$$r_{sl}(x) + B_0^{(\pm)} \left[ 1 + \frac{\mathrm{i}\omega}{\sigma_2} \ln|x - x_2| - \frac{\omega^2}{2\sigma_2^2} \ln^2|x - x_2| + \ldots \right] \Big[ 1 + O(|x - x_2|) \Big].$$

Matching of this solution with solution (49) shows that when $x \to x_2 \pm 0$ the solution should be as this:

$$r(x) = r_{sl}(x) + \left[ \frac{R_0^{(\pm)} - c_2^2}{R_0^{(\pm)} + c_2^2} - \frac{2\mathrm{i}\omega c_2^2 I_{1i}^{(\pm)}}{(R_0^{(\pm)} + c_2^2)^2} + O(\omega^2) \right] |x - x_2|^{\mathrm{i}\omega/\sigma_2} \Big[ 1 + O(|x - x_2|) \Big], \tag{50}$$

where $r_{sl}(x)$ is determined by the series (32) with $x_0 = x_2$. It was taken into account that $R_0$ and $I_{1i}$ can be different on the left and right of the point $x_2$, because according to the boundary conditions (39), they are calculated through the integration of Eq. (18) in the different flow regions. Therefore, if $r_0(x_2 \pm 0) \neq 0$ (i.e., $R_0^{(\pm)} \neq c_2^2$), then the reflection coefficient and transmission ratios are:

$$|r(x)| \to \left| \frac{R_0^{(\pm)} - c_2^2}{R_0^{(\pm)} + c_2^2} \right| = O(1),$$

$$K_2 \approx \left[ 1 - \left| \frac{R_0^{(-)} - c_2^2}{R_0^{(-)} + c_2^2} \right|^2 \right]^{-1/2}, \quad K_3 \approx \left[ 1 - \left| \frac{R_0^{(+)} - c_2^2}{R_0^{(+)} + c_2^2} \right|^2 \right]^{1/2}.$$

Otherwise, $|r(x)|$ is of the order of $O(\omega^2)$.

It should be emphasized that for $x \to x_2 \pm 0$, the quantity

$$r_0(x_2 \pm 0) = \frac{R_0^{(\pm)} - c_2^2}{R_0^{(\pm)} + c_2^2}$$

determined by Eq. (45) does not describe the limiting value of $r(x)$ (or its main part), but, as seen from Eq. (50), *the amplitude of the rapidly oscillating part of the solution*. Note that oscillations are concentrated in the exponentially narrow neighborhood of the point $x_2$,

$$|x - x_2| = O(\mathrm{e}^{-1/\omega}). \tag{51}$$

This allows us, firstly, to consider $r_0(x_2 \pm 0)$ as the main part of the intermediate asymptotic of the solution, and, secondly, greatly complicates the detection of oscillations in the numerical solution even in the case of not very small $\omega$ (see Sect. 6 and Fig. 5).

Based on these results, we will consider wave propagation within each section of the flow. Let's start from the left interval, $-\infty < x < x_1$, where $U(x) < c(x)$. Given that $b(x) \neq 0$ only in the interval $X = (x_-, x_1)$, we consider two options. The first option is that $x_1 - x_- = O(1)$ and $b(x) = O(1)$ in the entire interval $X$. Then, taking into account the boundary condition (39), we obtain (see Eqs. (46), (22), and (42)):

$$r_- \equiv r(x_-) = \frac{1 - a_-^2}{1 + a_-^2} + O(\omega) \quad \text{and} \quad K_1 = 1 - \left( \frac{1 - a_-^2}{1 + a_-^2} \right)^2 + O(\omega), \quad a_- = a(x_-). \tag{52}$$

Within the context of the analog gravity, subcritical flows simulate the "ordinary" space-time, with the quite natural constancy of the wave velocity, $c \equiv 1$. Then $a_-^2 = U(-\infty) < 1$ and there is necessarily a reflected wave; the transmission rate is $K_1 < 1$. The reflectionless propagation with $a_- = 1$ is possible only in a more complex

model, where $c(x) > 1$ for $x \to -\infty$ and decreases to 1 as we approach the critical point $x_1$ (black-hole horizon)—see, for example, Fig. 3c.

In the second option, the interval $X$ contains two intervals of the length $O(1)$ each, $X_1 = (x_-, x_a)$ and $X_2 = (x_b, x_1)$, with $b(x) = O(1)$. These intervals are separated by the insert $X_0 = (x_a, x_b)$ with $b(x) \equiv 0$. Then, Eq. (46) gives $r_0(x_b) = (1 - a_0^2)/(1 + a_0^2)$, where $a_0 = a(x_a) = a(x_b)$. As $b \equiv 0$ within the insert, $|r(x)| =$ const, and only the phase difference of waves $\theta(x)$ varies with $x$; however, this variation affects the transmission rate. Indeed, in the case of the 'phase inverting insert', when

$$\theta(x_a) - \theta(x_b) = \omega \int_{x_a}^{x_b} \alpha(x)\mathrm{d}x = (2n+1)\pi, \tag{53}$$

where $n$ is natural, $r_0(x_a) = -r_0(x_b)$, so that in accordance with Eq. (45), $R_0 = a_0^4$ and

$$r_0(x_-) = \frac{a_0^4 - a_-^2}{a_0^4 + a_-^2}, \qquad K_1 = \left[1 - \left(\frac{a_0^4 - a_-^2}{a_0^4 + a_-^2}\right)^2\right]^{1/2}. \tag{54}$$

(Note that because the flow is uniform when $x < x_-$, therefore $r_{-\infty} = r_-$.) As a result, the waves reflected in the intervals $X_1$ and $X_2$ cancel out each other upon the condition $a_0^2 = a_-$, which can be easily implemented even in traditional flow models with $c \equiv 1$ (see Fig. 3a), if in the insert section $U(x) = U_a = U_b = \sqrt{U(-\infty)}$ (in this case, $U(-\infty) < U_a < 1$). This equality sets the position of the anti-reflective insert; its length is determined by Eq. (53) and is very long, since it is proportional to $\omega^{-1}$.

In conclusion, we note that wave propagation in the interval $x_2 < x < \infty$ does not differ qualitatively from that just described. Indeed, since $b(x) = 0$ for $x > x_+$, then $a_+ \equiv a(x_+) = a(+\infty)$ and integration of Eq. (18) starts at $x = x_+$ with $r(x_+) = r(+\infty) = 0$. If $x_+ - x_2 = O(1)$ and $b(x) = O(1)$, then

$$r_0(x_2 + 0) = \frac{a_+^2 - a_2^2}{a_+^2 + a_2^2}, \qquad K_3 = \left[1 - \left(\frac{a_+^2 - a_2^2}{a_+^2 + a_2^2}\right)^2\right]^{1/2} + O(\omega), \tag{55}$$

and the condition of suppression of the reflected wave, $a_+ = a_2$, is satisfied if $c(+\infty) > c_2$, i.e. requires an increase in the wave speed downstream from the critical point $x_2$ (see Fig. 3c). But it is possible to suppress the reflected wave using the above-described 'anti-reflective optics effect', i.e. with the help of inverting insert with $b(x) = 0$ in such point $x = x_a$ where $a^2(x_a) = a_2 a_+$.

Let us now turn to the region $x_1 < x < x_2$ where the flow is supercritical. If $x_2 - x_1 = O(1)$ and $b(x) = O(1)$, then Eq. (46) gives:

$$r_0(x_2-0)=\frac{1-c_2^2}{1+c_2^2},\qquad K_2=\left[1-\left(\frac{1-c_2^2}{1+c_2^2}\right)^2\right]^{-1/2}+O(\omega)=\frac{1+c_2^2}{2c_2}+O(\omega). \tag{56}$$

In the case when the wave speeds at the ends of the region are the same ($c_2=c_1=1$), $r_0(x_2-0)=0$, and $K_2=1+O(\omega^2)$ differs almost not from one. Again, one can significantly increase the transmission ratio using an inverting insert. Indeed, since $a_1=a_2=1$, there is a point $x=x_m$ at which $a(x)$ reaches its extreme (maximum or minimum) value, say, $a_m$. Here $b(x)$ changes sign, and the growth of $|r(x)|^2$ is replaced by a decrease, which leads to a decrease in the amplitudes of waves of both positive and negative energy. Changing at this point (more precisely, on the inverting insert with $b=0$) the sign of $\cos\theta$ (and with it the $r$ sign), we will continue to grow $|r(x)|^2$,

$$r_0(x_m-0)=\frac{1-a_m^2}{1+a_m^2}\;\longrightarrow\; r_0(x_m+0)=-r_0(x_m-0)\;\longrightarrow\; r_0(x_2-0)=\frac{a_m^4-1}{a_m^4+1}, \tag{57}$$

and amplitudes of both waves. As the result, $K_2\approx(a_m^4+1)/(2a_m^2)>1$, and to a greater extent, the more strongly $a_m$ differs from 1 (to either way, since $K_2(a_m)\approx K_2(a_m^{-1})$).

If $c_2\neq 1$, then $K_2>1$ and without an inverting insert, and, in addition, $K_2(c_2)=K_2(c_2^{-1})$ up to $O(\omega)$. In other words, the amplification of a wave of positive energy due to its transformation into a NEW is promoted by both a decrease and an increase in the speed of waves in the supercritical section of the flow.

### 4.3 The High-Frequency Limit, $\omega\gg 1$

Let us turn now to waves with $\omega\gg 1$. This limiting case can be still consistent with the shallow-water approximation because, in the dimensional variables, the inequalities $\omega/\sigma_1=O(k\Lambda)\gg 1$ and $kH\ll 1$ are consistent when $\Lambda\gg H$. As follows from the analysis carried out in Sect. 3, in the vicinity of the critical point $x_1$, the function $r(x)$ is defined by the series (32) with coefficients having the order of $O(\omega^{-1})$. Therefore, it is natural to assume that the solution to Eq. (18) has the same order. Setting $r(x)=\mathrm{i}P(x)/\omega$ where $|P|=O(1)$, but $|\mathrm{d}P/\mathrm{d}x|=O(\omega)$, we get the equation:

$$\frac{1}{\omega}\frac{\mathrm{d}P}{\mathrm{d}x}=-\mathrm{i}\alpha(x)P+\mathrm{i}b(x)\left(1+\frac{P^2}{\omega^2}\right).$$

Neglecting the term $O(\omega^{-2})$ in this equation, we arrive at the linear non-homogeneous equation whose solution subject to the boundary conditions (39) is:

$$P(x) = \mathrm{i}\omega \exp\Big[-\mathrm{i}\omega\Psi(x)\Big]\int\limits_{x_0}^{x} \mathrm{d}\xi\, b(\xi) \exp\Big[\mathrm{i}\omega\Psi(\xi)\Big], \qquad \Psi(x) = \int \alpha(x)\mathrm{d}x, \quad (58)$$

and $x_0 = x_1$ when $x < x_2$ and $x_0 = x_+$ when $x > x_2$.

In Eq. (58), when calculating the integral of a rapidly oscillating function, we take into account that $\mathrm{d}\Psi/\mathrm{d}x = \alpha(x)$ has no zeros on the real axis and therefore, there are no stationary phase points, but $\alpha(x)$ has poles at $x = x_{1,2}$. Hence, the main contribution to the integral comes from a neighborhood of the upper limit of integration (see, for example, [22]), then we have:

$$\int\limits_{x_0}^{x} \mathrm{d}\xi\, b(\xi) \exp\Big[\mathrm{i}\omega\Psi(\xi)\Big] \sim \frac{b(x)\exp\Big[\mathrm{i}\omega\Psi(x)\Big]}{\mathrm{i}\omega\alpha(x)} = O(\omega^{-1}). \quad (59)$$

We see that indeed $P(x) = O(1)$ in general. However, $P(x) = o(1)$ when $x \to x_2 \pm 0$ because of presence of $\alpha(x)$ in the denominator. Thus, in the high-frequency limit $K_1$ differs from unity by $O(\omega^{-2})$ whereas $K_2$ and $K_3$ differ from unity even less, only by $o(\omega^{-2})$. Therefore, both the wave reflections in the subcritical regions of the flow and wave amplification in the supercritical region diminish.

## 5 Wave Propagation in a Super–Sub–Supercritical Flow

Let us consider now a duct with a supercritical flow ($U(x) > c(x)$) in the outer domains, left: ($-\infty < x < x_1$), and right: ($x_2 < x < +\infty$), and subcritical in the inner domain ($x_1 < x < x_2$). In this Section we make scaling in the same way as in Eq. (38), namely, with the use of flow parameters at the critical point $x = x_2$ corresponding to the transition from sub- to super-critical flow. As a result, in dimensionless variables,

$$U_2 = c_2 = 1, \qquad \sigma_2 = U_2' - c_2' = 1. \quad (60)$$

In this case, the physical statement of the problem is not so evident as for the sub-super-subcritical flow considered in Sect. 4. First of all, it is hard to determine what is the incident wave. Indeed, the left part of the flow is supercritical, and the waves, both with positive and negative energies, entering the duct from the left end, propagate to the critical point $x_1$ interacting with each other in such a way that the total energy flux $\mathcal{E}$ determined by Eq. (21) is conserved, whereas the amplitudes of both waves change. Because only a finite domain to the left of the point $x_1$ is accessible for observation, in any point of it we see a superposition of both waves and have no possibility to recognize which of these two waves arrives from the left infinity. Of course, if $\mathcal{E} > 0$, the positive energy wave does unambiguously present at

left infinity but the negative energy wave can present there as well, and the amplitudes of both waves remain unknown.

However, we know that in the neighborhood of the critical point $x_1$ any NEW is completely absorbed (see Sect. 3.2). Therefore, it seems that the only reasonable statement of the problem in this case is to set the amplitude of the co-current propagating wave at either end of the subcritical domain and ignore the prehistory of wave propagation in the left supercritical domain $x < x_1$. Technically, it is more convenient to set the amplitude of the co-current propagating wave at $x = x_2$, because both the reflected wave and NEW vanish in this point. Assume that the co-current propagating wave arriving from the domain where $x < x_1$ has the amplitude $D(x_2) = 1$. Then, in the domain $x_1 < x < \infty$ (cf. Eqs (40) and (41)) we have:

$$D(x) = \exp\left[-\int_{x_2}^{x} b(x')\, r(x')\, \mathrm{d}x'\right], \tag{61}$$

$$K(x) = \exp\left[-\int_{x_2}^{x} b(x')\mathrm{Re}\left(r(x')\right) \mathrm{d}x'\right] \equiv \exp\left[-\int_{x_2}^{x} b(x')|r(x')|\cos\theta(x')\, \mathrm{d}x'\right], \tag{62}$$

and the integral transmission ratios of sub- and supercritical domains are (cf. Eq. (42)):

$$K_2 = \sqrt{1 - |r(x_1)|^2} \le 1, \quad K_3 = \left[1 - |r(+\infty)|^2\right]^{-1/2} \ge 1, \quad K(+\infty) = K_2 \cdot K_3. \tag{63}$$

It should be borne in mind that the oscillating component of $r(x)$ develops with the distance from $x_2$ rather than from $x_1$.

Scaling as per Eq. (60) yields $a_2^2 \equiv c_2 U_2 = 1$, therefore, the scattering of low frequency waves in the subcritical domain is approximately described by Eq. (46). Then, the transmission ratio in this domain is:

$$K_2 = \sqrt{1 - \left(\frac{1 - c_1^2}{1 + c_1^2}\right)^2} + O(\omega) = \frac{2c_1}{1 + c_1^2} + O(\omega). \tag{64}$$

From this formula, it follows (bearing in mind a small contribution of the last term $O(\omega)$) that $K_2$ is only slightly less than unity if the wave velocities in the ending points of the domain are the same, $c_1 = c_2 = 1$, but $K_2$ decreases when $c_1$ deviates from $c_2$ in the either side. It should be also noted that $K_2(c_1) \approx K_2(1/c_1)$.

In the high-frequency limit, one can demonstrate by analogy with Sect. 4.2 that $K_2 \to 1 - 0$ for any $c_1$. As a consequence of this, when $c_1 = 1$, $K_2(\omega)$ goes to unity in both limiting cases, when $\omega \to 0$ or $\omega \to \infty$, and inside this frequency range, it has at least one minimum. If $c_1 \neq 1$, then $K_2(\omega)$ grows from $K_2(0) < 1$ up to 1, but

not necessarily monotonically (this will be confirmed below through the numerical calculations shown in Fig. 16).

In the right outer domain $x > x_2$, the transformation of a positive-energy low-frequency wave into a NEW is described by the same Eq. (46), and the transmission ratio is:

$$K_3 = \left[1 - \left(\frac{a^2(+\infty) - 1}{a^2(+\infty) + 1}\right)^2\right]^{-1/2} + O(\omega) = \frac{a^2(+\infty) + 1}{2a(+\infty)} + O(\omega) \qquad (65)$$

Asymptotically $K_3 \sim a(+\infty)/2$ increases with $a(+\infty) \equiv [c(+\infty)U(+\infty)]^{1/2}$. However, when the frequency increases $K_3$ approaches unity from the top.

## 6 Numerical Calculations and Some Remarks

### 6.1 Sub–Super–Subcritical Flows

The analysis presented above shows that the most interesting scenarios of wave propagation occurs in the middle (supercritical) flow region where a positive energy wave is amplified due to the coupling with the NEW; then the transmission coefficient can be noticeably greater than one. Numerical calculations were performed mainly for this region. Recall that at the far end of the region where $x_2 - x \sim \exp(-\omega^{-1})$, the function $r(x)$ rapidly oscillates; therefore, the spatial resolution of the oscillating solution in the numerical calculations can be performed without extra complications only for not too low $\omega$. Below we consider separately two particular cases when the wave speed is (i) the same at the ending points of the supercritical interval and (ii) when it is different.

**Currents with the equal velocities at the ending points** Bearing in mind the conditions (38), we take for calculations a simple flow model with $c_1 = c_2 = 1$ (see Fig. 3a):

$$c(x) \equiv 1, \qquad U(x) = 1 + x(2d - x)/(2d), \quad x_1 = 0, \quad x_2 = 2d. \qquad (66)$$

For such a flow, the Mach number attains its maximum, $\mathcal{M} = 1 + d/2$, at the midpoint of the supercritical interval, $x_m = d$, and function $b(x)$ changes its sign. As was discussed in Sect. 4, the wave amplification can be increased with the use of a properly chosen phase-shifting insert. In our calculations, such an insert begins in the point $x_m$ and is simulated by changing of the phase $\theta = \arg(r)$ by the required value $\Delta\theta$. As a result, function $\theta(x)$ becomes discontinuous in the point $x_m$. Note that in the limit $\omega \to 0$, the most effective insert is inverting one, with $\Delta\theta = \pm\pi$; we have considered this above. However, when the frequency increases, the phase $\theta$ changes more and more significantly in that region where $b(x) \neq 0$, therefore the optimal phase shift that maximizes the transmission ratio $K_2$, depends on the frequency.

**Table 1** Data for the optimal phase shift versus frequency used in the numerical calculations

| $\omega$ | 0.2 | 0.3 | 0.5 | 1 | 3 | 5 | 8 |
|---|---|---|---|---|---|---|---|
| $\Delta\theta$ | 2.688 | 2.443 | 1.990 | 0.977 | −1.187 | −2.234 | −3.002 |

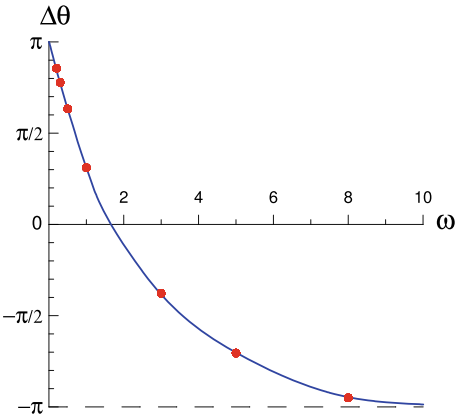


**Fig. 4** (color online) The optimal phase shift as a function of frequency. Dots show the values used in the numerical calculations and presented in Table 1

Specific values of $\Delta\theta(\omega)$ used in our calculations for the flow with $\mathcal{M} = 4$ ($d = 6$) are given in Table 1 and shown in Fig. 4.

Figure 5 shows the reflection coefficient $|r(x)|$ that describes the transformation of the co-current propagating wave into the NEW, as well as $\theta(x) \equiv \arg(r)$ for the frequencies $\omega \leq 1$, both with the optimal phase-shifting insert (OI), and without it (NI). The upper part of Fig. 5 shows that even when the frequency is not very small, the "zero" approximation $|r_0(x)|$ as defined by the Eq. (45) (and with phase inversion, if any) describes pretty well the behavior of the function $|r(x)|$, except for the neighborhood of the point $x = x_2 = 2d$ in the NI version when there is no insert. The difference between the curves is caused by missing in $r_0(x)$, but accumulated in $r(x)$ (due to $\omega \neq 0$) a rapidly oscillating component, although its amplitude is significantly less than in the OI version. For $\omega = 1$, the downstream change in $\theta$ manifests faster, therefore $|r(x)|$ and $|r_0(x)|$ differ notably throughout the entire supercritical region, in both versions of the flow, with the insert (OI-version) and without the insert (NI-version). Note that when $x \to x_2 = 2d$, the reflection coefficients (which are equal here to the amplitudes of fast oscillations of the functions $r(x)$) corresponding to the different flow versions, approach each other (cf. lines 1 and 2 in Fig. 5) and slightly decrease compared with what was for $\omega = 0.3$ in the OI-version. Moreover, we draw attention to the fluctuation of $|r(x)|$ near the point $x_2$, which became noticeable as the result of the expansion of the region of oscillations.

Figure 6 shows the reflection coefficient $|r(x)|$ and function $\theta(x)$ for $\omega > 1$ for both flow models, OI (with insert) and NI (no insert). Here the region of oscillations is even wider, and oscillations of $|r(x)|$ are seen in a notably greater range of $x$. When $x \to x_2$, these oscillations, as expected, decay, and $|r(x)|$ approaches a finite limit

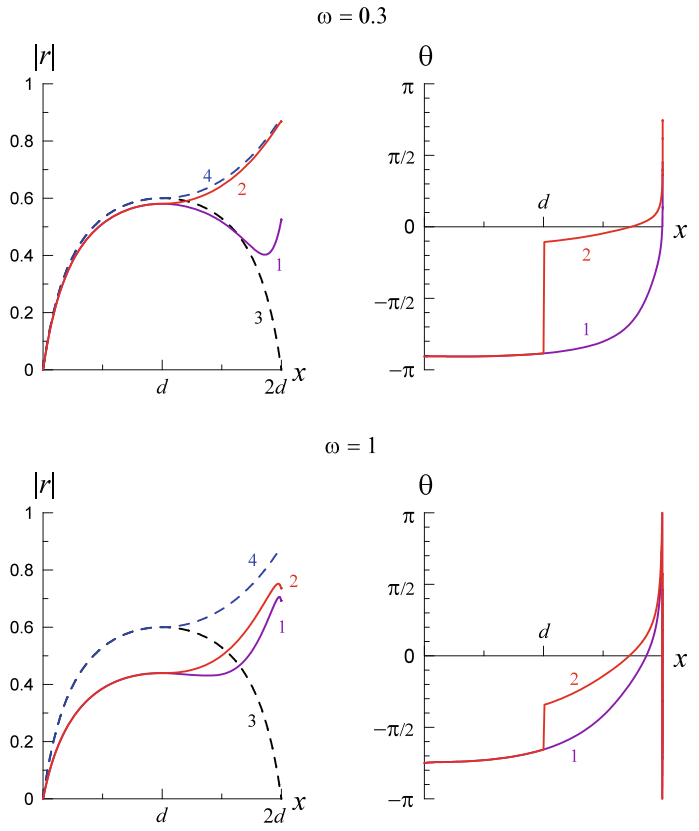


**Fig. 5** (color online) The reflection coefficient (left panels) and function $\theta(x)$ (right panels) as functions of $x$ for three values of frequency $\omega \leq 1$ in the flow model (66) with $\mathcal{M} = 4$: line 1—NI; line 2—OI. Dashed lines correspond to the reference case with $\omega = 0$ and $\Delta\theta = \pi$: line 3—NI; line 4—OI. Function $\theta(x)$ has a jump at the point $x_m$ within the OI model due to the phase shifting insert

which is equal to the amplitude of oscillations of the function $r(x)$. Comparison of graphs for $\omega = 1,\ 3,\ 8$ confirms the conclusion made at the end of Sect. 4 that $|r(x)|$ decreases as $\omega^{-1}$, and even faster in the vicinity of $x_2$.

In the course of propagation from $x_1$ to $x_2$, waves of positive and negative energies interact such that the total energy flux (21) conserves. As a result, their amplitudes synchronously increase or decrease in accordance with the change in their phase difference. Quantitative measure of wave interaction is the gain of the positive energy wave:

$$Q(x) = \left(1 - |r(x)|^2\right)^{-1}; \tag{67}$$

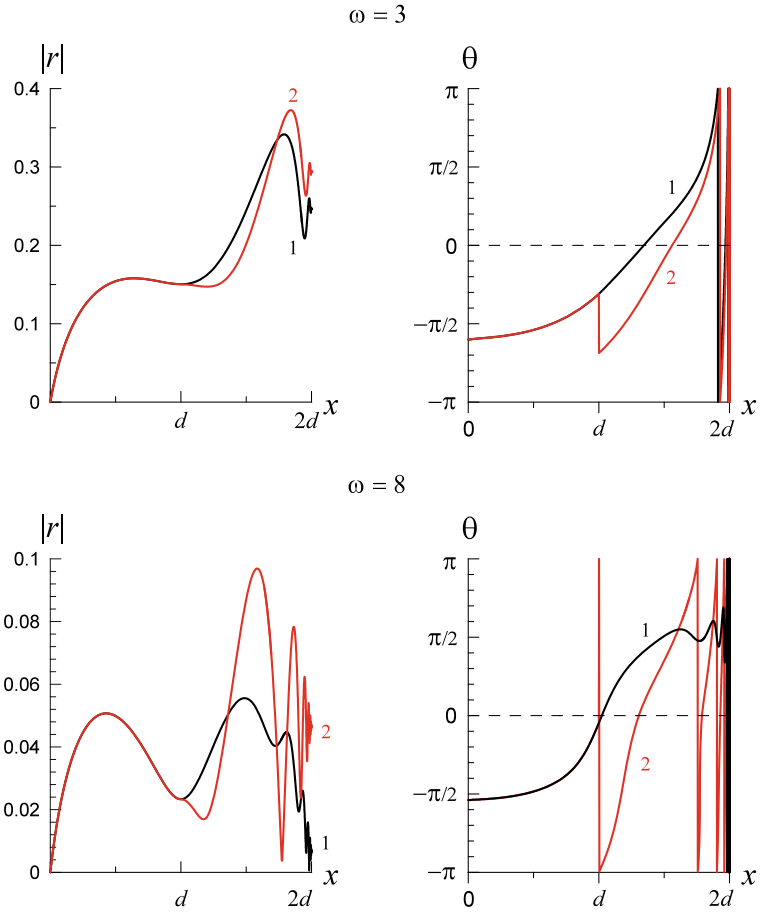


**Fig. 6** (color online) The reflection coefficient (left panels) and function $\theta(x)$ (right panel) as functions of $x$ for two values of the frequency $\omega > 1$ in the flow model (66) with $\mathcal{M} = 4$: line 1—NI; line 2—OI. Function $\theta(x)$ has a jump at the point $x_m$ within the OI model due to the phase shifting insert

this quantity is shown in Fig. 7. According to Eq. (22), the growth is replaced by the decrease when the sign of either $b(x)$ or $\cos\theta$ changes.

At low frequencies ($\omega < 1$) in the OI model of the flow, the change of the $b(x)$ sign is compensated to a large extent by the phase jump, therefore $Q(x)$ grows monotonically and begins to slightly oscillate only near the point $x_2$ (see curves 3). As the frequency increases, $\theta(x)$ varies more and more rapidly, and $Q(x)$ acquires more and more distinct oscillatory character whereas its value becomes closer and closer to unity. Figure 8 shows the dependence of the transmission ratio $K_2$ of the supercritical domain on the frequency $\omega$ for the NI (line 1) and OI (line 2) models. As one can see from the comparison of lines 1 and 2, both models, with the optimal phase-

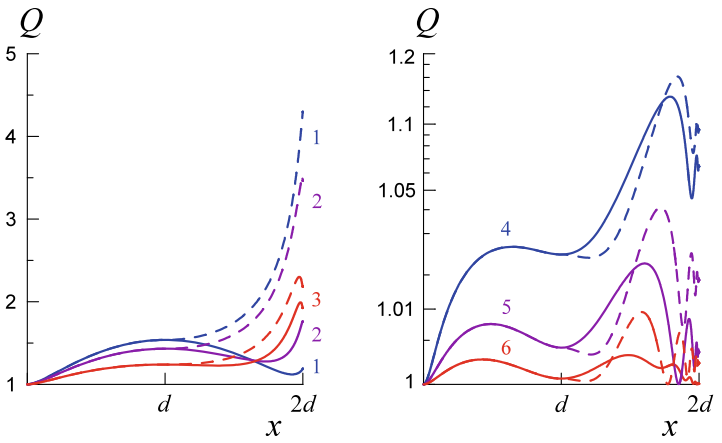


**Fig. 7** (color online) The gain coefficient as the function of $x$ for the several particular frequencies: 1—$\omega = 0.2$, 2—$\omega = 0.5$, 3—$\omega = 1$, 4—$\omega = 3$, 5—$\omega = 5$, 6—$\omega = 8$. Solid lines pertain to the NI model, dashed lines—to the OI model

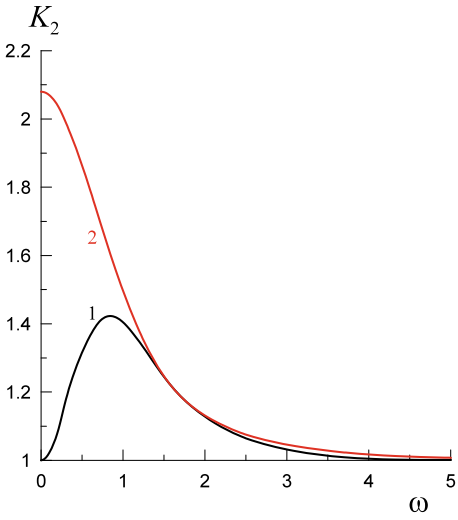


**Fig. 8** (color online) The transmission ratio $K_2$ as functions of frequency $\omega$ for the NI (line 1) and OI (line 2) models

shifting insert (OI) and without it (NI), provide approximately the same transmission ratio for $\omega > 1$, whereas they differ in the low-frequency domain. Whereas the OI model provides monotonic increase of $K_2$ when $\omega \to 0$, in the NI model, $K_2$ has a maximum at $\omega = 1$, and then goes to zero when $\omega \to 0$. Even in the NI model without any insert, the transmission ratio is notably greater than one, which can provide the laser effect of wave amplification in the "active zone". The amplitude gain in the supercritical domain may be drastically reduced by wave reflection in the left and right subcritical domains. To gain a better insight into the effect of domain

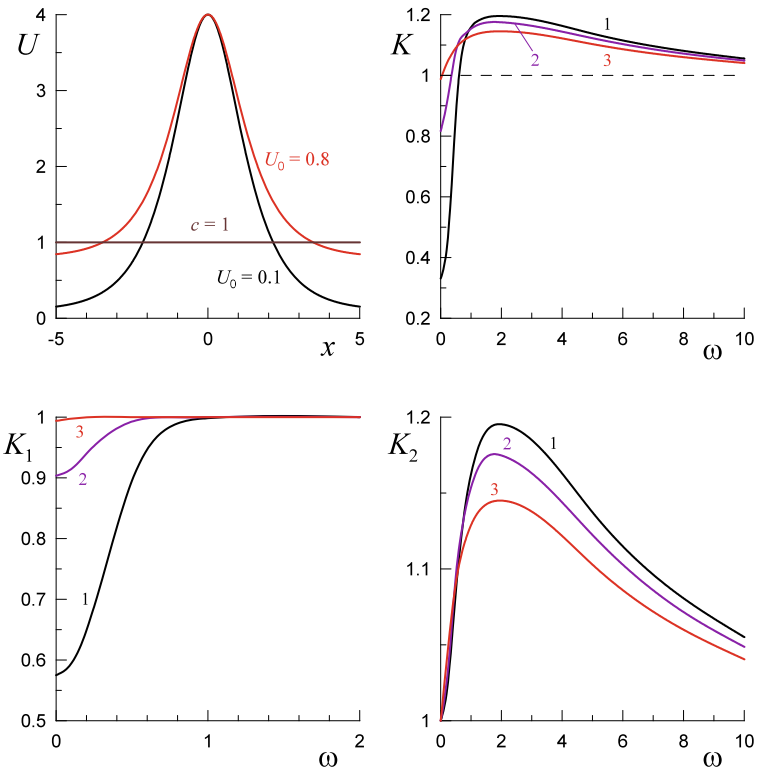


**Fig. 9** (color online) Top panels: left—velocity profiles (68) for $U_0 = 0.1$ and $U_0 = 0.8$, and right—the total transmission ratio $K = K_1 K_2 K_3$ as a function of frequency $\omega$. Bottom panels: left—transmission ratios of the left ($K_1$) domain and right—for the middle ($K_2$) domain as functions of frequency $\omega$; 1—$U_0 = 0.1$, 2—$U_0 = 0.4$, 3—$U_0 = 0.8$

competition, we have calculated the wave transmission through all three domains in the bell-shaped velocity profile (see Fig. 3a) with following dependences:

$$c(x) \equiv 1, \quad \text{and} \quad U(x) = U_0 + (\mathcal{M} - U_0)\,\mathrm{sech}\, x. \tag{68}$$

Calculations were performed for the fixed Mach number $\mathcal{M} = 4$ and with various velocities at the infinity $U_0 \in (0,\ 1)$. The results obtained are presented in Fig. 9.

As one can see, the supercritical flow with any $U_0$ acts as a broadband amplifier (see the top right panel in Fig. 9). This can be explained as follows: the wave reflection plays a noticeable role only at low frequencies, whereas the transmission ratio $K_2$ responsible for the wave amplification decreases with $\omega$ rather slowly. It should be noted in passing that due to the flow symmetry, the transmission ratios in the subcritical domains of the flow are equal, $K_1 = K_3$, so that the total transmission ratio is $K = K_1^2 K_2$. And finally, when comparing $K_2(\omega)$ shown in Fig. 9 with that presented in Fig. 8 by curve 1, it should be born in mind that in calculations presented

in Fig. 9 the scaling (38) was not fulfilled. Due to this, the dimensionless frequencies of the maximal amplification are different.

**Currents with the different velocities at the ending points** In this section, we consider currents in which wave velocity $c(x)$ monotonically increases or decreases downstream from $c_1 = 1$ to $c_2$. For calculations, we take a modification of the flow model (66) without a phase-shifting insert (see Fig. 3b),

$$c(x) = 1 + \frac{c_2 - 1}{2d}\, x, \qquad U(x) = c(x) + \frac{x(2d - x)}{2d}, \quad x_1 = 0, \quad x_2 = 2d. \tag{69}$$

In such a flow, the maximum Mach number is attained at $x = 2d/(1 + \sqrt{c_2})$:

$$\mathcal{M} = 1 + \frac{2d}{(1 + \sqrt{c_2})^2}\,, \tag{70}$$

so that for the given Mach number we have:

$$d = \frac{\mathcal{M} - 1}{2}\left(1 + \sqrt{c_2}\right)^2. \tag{71}$$

Let us assume that in the entire region function $a^2(x) = c(x)U(x)$ varies monotonically, and $b(x)$ does not change its sign. This limits the range of the flow parameters, so that

$$d \le |c_2 - 1|, \qquad 1 < \mathcal{M} \le \begin{cases} 3 - \dfrac{4}{1 + \sqrt{c_2}}\,, & \text{if} \quad c_2 > 1, \\ \dfrac{4}{1 + \sqrt{c_2}} - 1\,, & \text{if} \quad c_2 < 1. \end{cases} \tag{72}$$

The parameters $c_2$ and $\mathcal{M}$ used for calculations are shown in Table 2. For a given $c_2$, the Mach number $\mathcal{M}$ was chosen close to the maximum value, and then the parameter $d$ was calculated using Eq. (71).

For the flows with the increasing velocity $c(x)$, Fig. 10 shows the dependence $|r(x)|$ for different $c_2$ and $\omega$. It is clearly seen that the transformation into the NEW increases with an increase of $c_2$, but falls abruptly when the frequency grows. This is also exhibited by the graphs of the gain coefficient $Q$ for the same set of parameters, see Fig. 11.

Similar relations for the flows with the decreasing function $c(x)$ are shown in Figs. 12 and 13. They demonstrate the strengthening of the wave transformation

**Table 2** The Mach numbers used in numerical calculations with the different values of $c_2$

| $c_2$ | 2 | 3 | 5 | 9 | 2/3 | 0.5 | 1/3 | 1/6 | 0.1 |
|---|---|---|---|---|---|---|---|---|---|
| $\mathcal{M}$ | 1.3 | 1.5 | 1.6 | 2 | 1.2 | 1.3 | 1.5 | 1.8 | 2 |

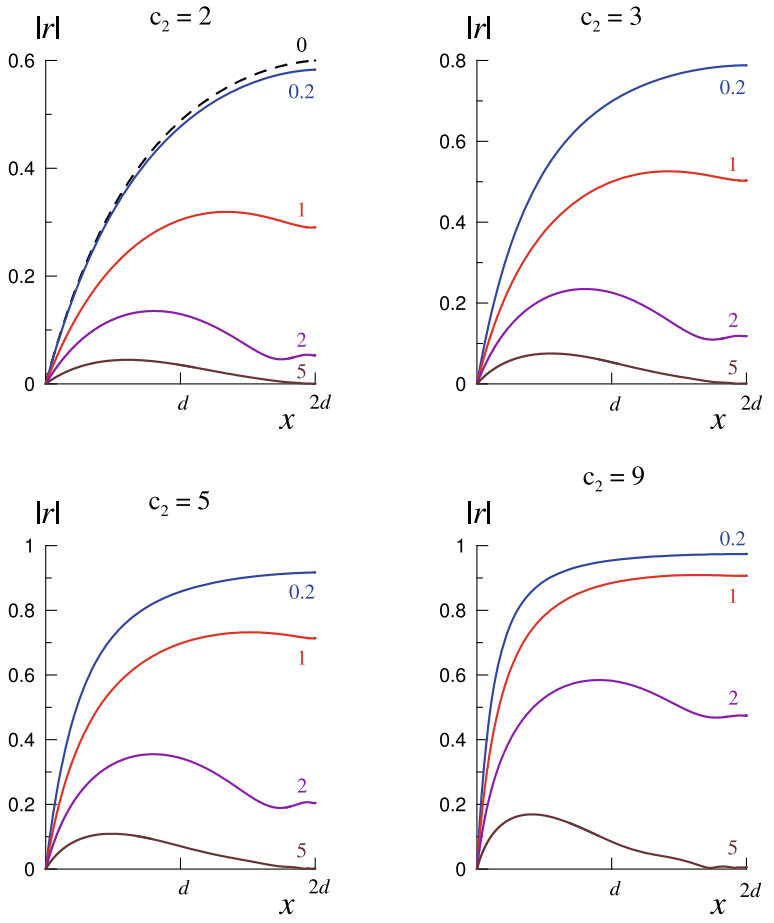


**Fig. 10** (color online) Dependence of $|r(x)|$ in the flows with increasing wave velocity $c(x)$ for different values of $c_2$ and frequencies shown by the numbers next to the curves. Dotted line pertains to $\omega = 0$

with the decrease of the ending value $c_2$ and its sharp weakening with the increase of $\omega$. The oscillatory nature of the transformation near $x_2$ is seen even more clearly than for $c_2 > 1$.

Figure 14 shows the transmission ratio $K_2$ of the inner domain as function of frequency $\omega$ for the different values of $c_2 > 1$ (left panel) and $c_2 < 1$ (right panel). As one can see from the figure, the transmission ratio in both panels monotonically decreases from some maximal value $K_2(\omega = 0)$, which depends on $c_2$, to zero.

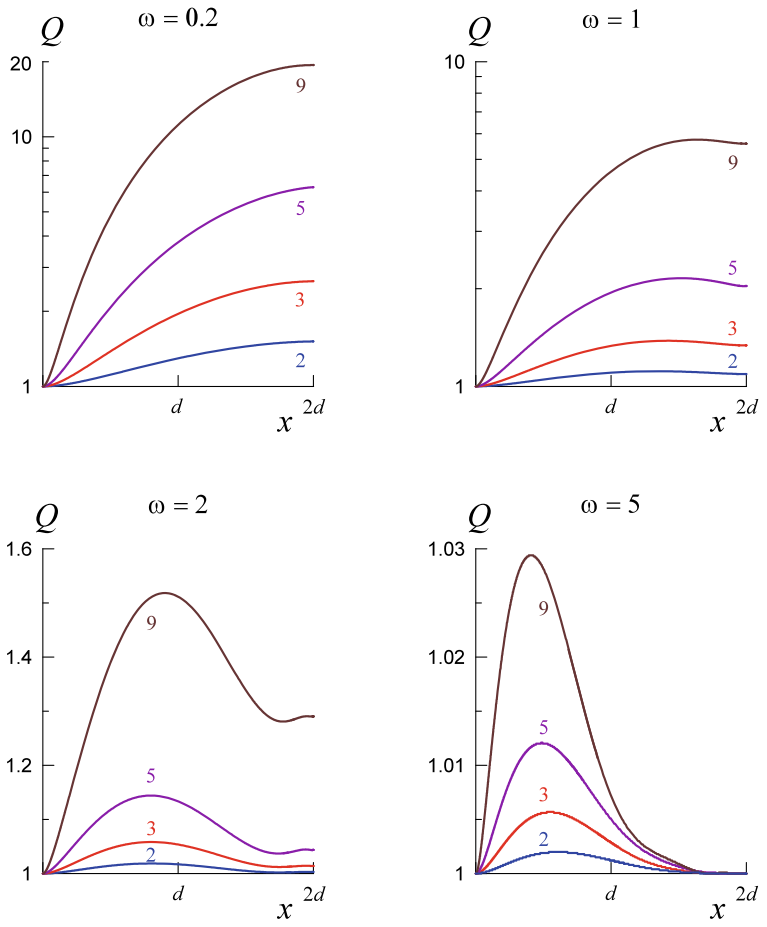


**Fig. 11** (color online) The gain coefficient in the flows with increasing wave velocity $c(x)$ for the different frequencies and ending values of $c_2$ shown by numbers next to the curves

## *6.2 Super–Sub–Supercritical Flows*

For this type of flow, the inner domain, $x_1 < x < x_2$, is subcritical and the corresponding transmission ratio is less than one, $K_2(\omega) \leq 1$. The frequency dependence of $K_2$ is determined by the particular profiles $c(x)$ and $U(x)$ (see Sect. 4.3). For the numerical calculations, we chose a family of flows with the linear $c(x)$ and quadratic $U(x)$ profiles (cf. Eqs. (66) and (69)),

$$c(x) = 1 + \frac{(c_1 - 1)(2d - x)}{2d}, \qquad U(x) = c(x) - \frac{x(2d - x)}{2d}. \tag{73}$$

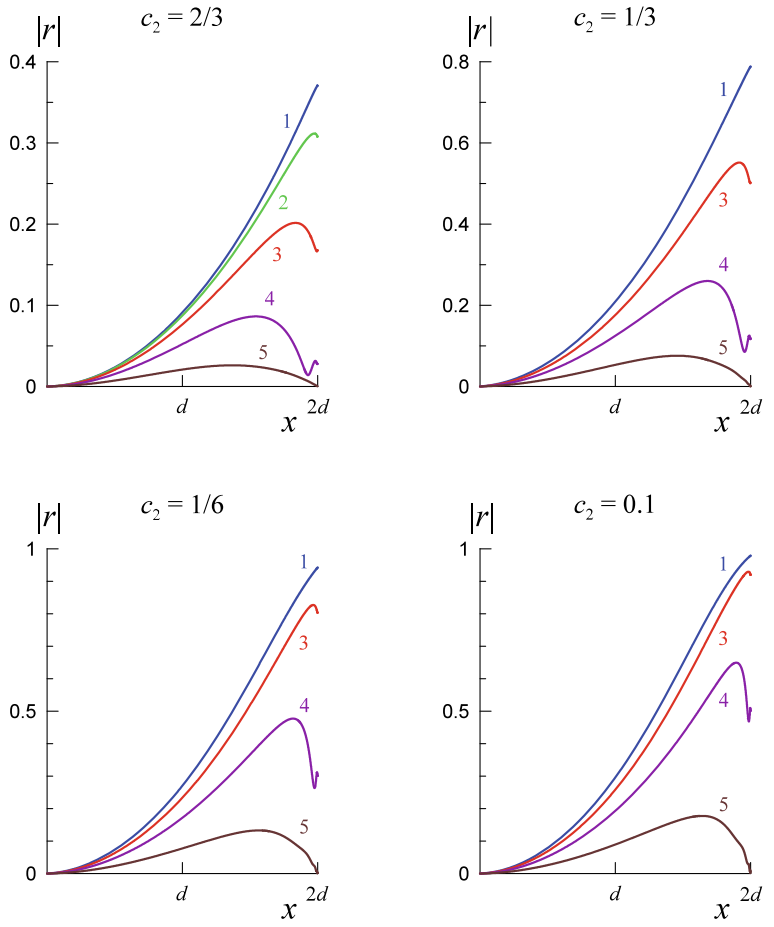


**Fig. 12** (color online) Dependence of $|r(x)|$ in the flows with the decreasing wave velocity $c(x)$ for the different values of $c_2$ and frequencies: 1—$\omega = 0.2$, 2—$\omega = 0.5$, 3—$\omega = 1$, 4—$\omega = 2$, 5 – $\omega = 5$

Here $c_1 = c(0)$, and $d$ is chosen such that $U(x) > 0$ in the entire interval $x_1 = 0 \le x \le x_2 = 2d$.

If $c_1 = c_2 = 1$, then $c(x) \equiv 1$, and $a^2(x) = c(x)U(x) \equiv U(x)$. In this case, the transmission ratio $K_2(\omega) \to 1$ when the frequency goes either to zero or to infinity, and its minimum decreases with the decreasing of $U_{min} = (1 - d/2)$ (see Fig. 15). If, however, $c_1 \neq 1$, then $K_2(0) < 1$ (see Eq. (64)) and $K_2(\omega)$ increases to 1 (not necessarily monotonically) when frequency grows (see right panel in Fig. 16).

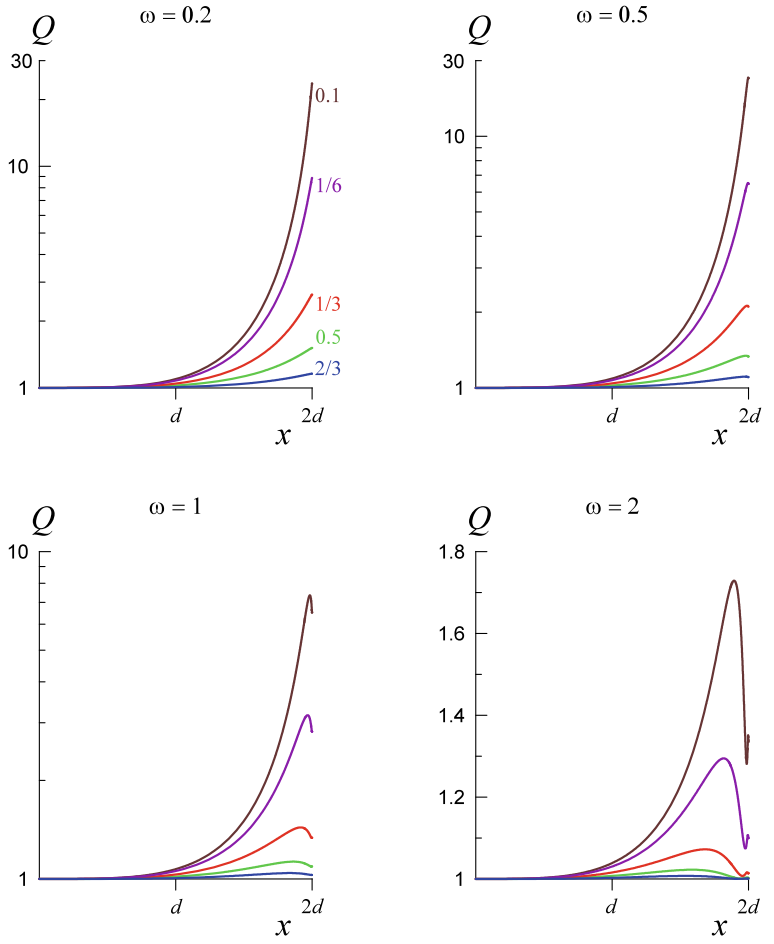


**Fig. 13** (color online) The gain coefficient in the flows with decreasing wave velocity $c(x)$ for the different frequencies and ending values of $c_2$ shown by numbers next to the curves in the upper left panel

The positive energy wave is amplified after passing into the supercritical domain $x > x_2$ due to the interaction with the NEW [14], therefore, the transmission ratio $K_3 \geq 1$. For the calculations, we choose $c(x)$ and $U(x)$ in such that the scaling (60) is satisfied and the finite limits exist when $x \to +\infty$. In particular, if $c(x) \equiv 1$, than we take

$$U(x) = 1 + D\tanh(x/D), \quad x_2 = 0. \tag{74}$$

The results of calculations for $D = 1$ ($U_{max} = 2$) and $D = 3$ ($U_{max} = 4$) are shown in Fig. 17.

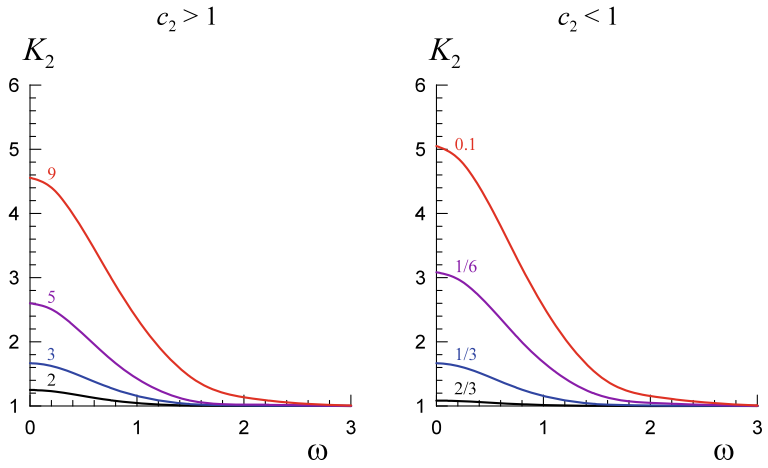


**Fig. 14** (color online) The transmission ratio $K_2$ of the inner domain as a function of frequency $\omega$ for different values of $c_2 > 1$ (left panel) and $c_2 < 1$ (right panel). Numbers next to curves show the values of $c_2$

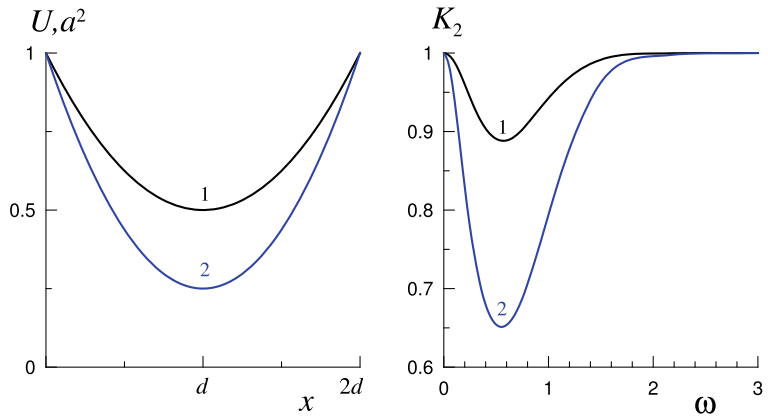


**Fig. 15** (color online) Graphics of the flow as per Eq. (73) with $c_1 \equiv 1$. Left panel: the flow velocity $U(x) \equiv \Pi(x)$ as the function of $x$. Right panel: the frequency dependence of the transmission ratio $K_2(\omega)$. Lines 1 are plotted for $d = 1$ with $U_{min} = 0.5$; lines 2—for $d = 1.5$ with $U_{min} = 0.25$

In the more interesting case when $c(x)$ and $U(x)$ grow simultaneously with $x$ (and $U(x) \geq c(x)$ everywhere), the calculations were carried out for current and wave speed in the following forms, respectively:

$$U(x) = 1 + A_U \tanh\left(\frac{x}{D_U}\right), \quad c(x) = 1 + A_c \tanh\left(\frac{x}{D_c}\right), \tag{75}$$

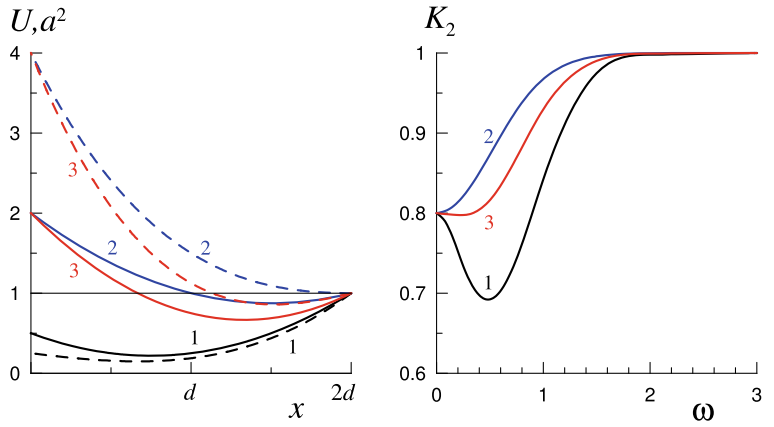


**Fig. 16** (color online) Graphics of the flow as per Eq. (73) with $c_1 \neq 1$. Left panel: the flow velocity $U(x)$ (solid lines) and $\Pi(x)$ (dashed lines) as functions of $x$. Right panel: the frequency dependence of the transmission ratio $K_2(\omega)$. Lines 1 are plotted for $c_1 = 0.5, d = 1$; lines 2—for $c_1 = 2, d = 1$; lines 3—for $c_1 = 2, d = 1.5$

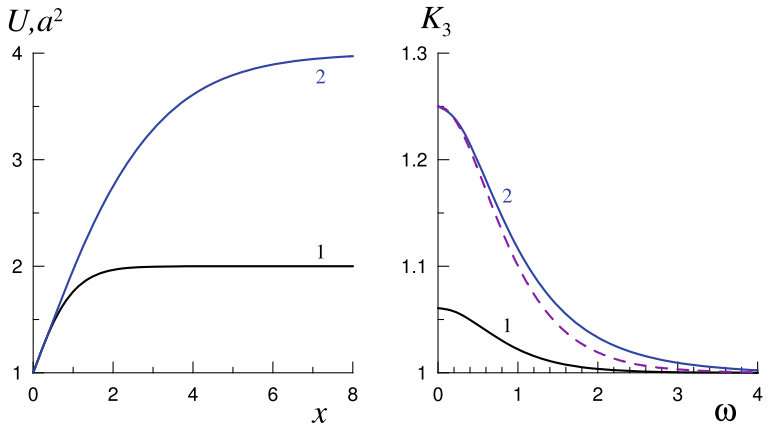


**Fig. 17** (color online) The flow (74), $c(x) \equiv 1$. Left panel: flow velocity $U \equiv a^2$ versus $x$. Right panel: frequency dependence of the transmission ratio $K_3$. 1—$D = 1$ ($U_{max} = 2$), 2—$D = 3$ ($U_{max} = 4$). For comparison, the dashed line presents curve 2 plotted in the right panel of Fig. 18

with the various combinations of parameters satisfying the condition:

$$\frac{A_U}{D_U} - \frac{A_c}{D_c} = 1,$$

which follows from the scaling (60). Figure 18 presents the results of calculations for the three cases:

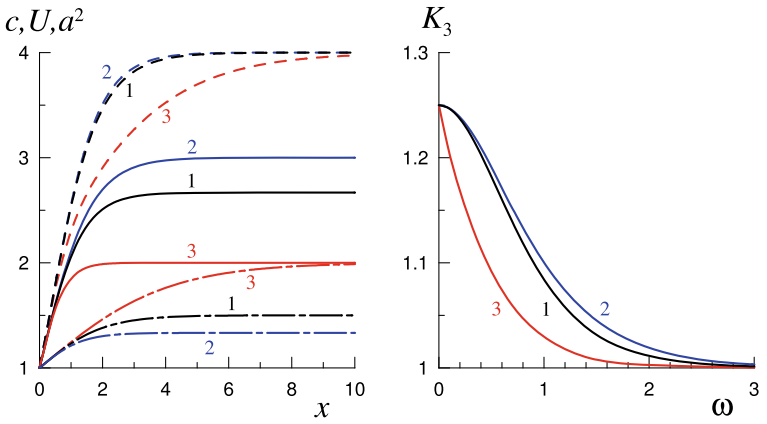


**Fig. 18** (color online) Left panel: $U(x)$ (solid lines), $a^2(x)$ (dashes), and $c(x)$ (dash-dotted lines) graphs. Right panel: frequency dependence of the transmission ratio $K_3$. The numbers next to curves indicate the number of a Case in Eq. (76)

$$\begin{aligned} &\text{Case 1}: A_U = \frac{5}{3},\ D_U = \frac{4}{3},\ A_c = 0.5,\ D_c = 2,\\ &\text{Case 2}: A_U = 2,\ D_U = 1.6,\ A_c = \frac{1}{3},\ D_c = \frac{4}{3},\\ &\text{Case 3}: A_U = 1,\ D_U = 0.8,\ A_c = 1,\ D_c = 4. \end{aligned} \tag{76}$$

As one can see from Fig. 18, the dependence $K_3(\omega)$ in the Case 3 notably deviates from the dependences $K_3(\omega)$ in the Cases 1 and 2. There are two distinction peculiarities in the Case 3. Firstly, the characteristic width of variation of the wave speed, $D_c$, significantly exceeds (5 times) that of current variation $D_U$. Secondly, $U(+\infty) = c(+\infty)$, that is there is a third critical point at infinity. The former distinction feature seems, however, not very important since even if $c(x) \equiv 1$, $K_3$ depends on $\omega$ in nearly the same way as in Cases 1 and 2 (cf. line 2 and dashed line in the right panel of Fig. 17). On the contrary, the presence of an additional (albeit infinitely remote) critical point has a profound impact on the behavior of function $r(x)$ which determines the progress of the wave transformation.

Figure 19 demonstrates the absolute value and argument of $r(x)$ for Case 2 and Case 3; it allows us to compare the wave propagation in these two cases with greater detail. It is clearly seen that in the Case 3 the oscillations of $r(x)$ begin to develop noticeably at a much smaller distance from the critical point $x_2 = 0$, and this results in lesser values and more pronounced oscillatory character of $|r(x)|$. Moreover, when $x$ increases, the oscillation period in the Case 3 decreases whereas in Case 2 it approaches a constant value.

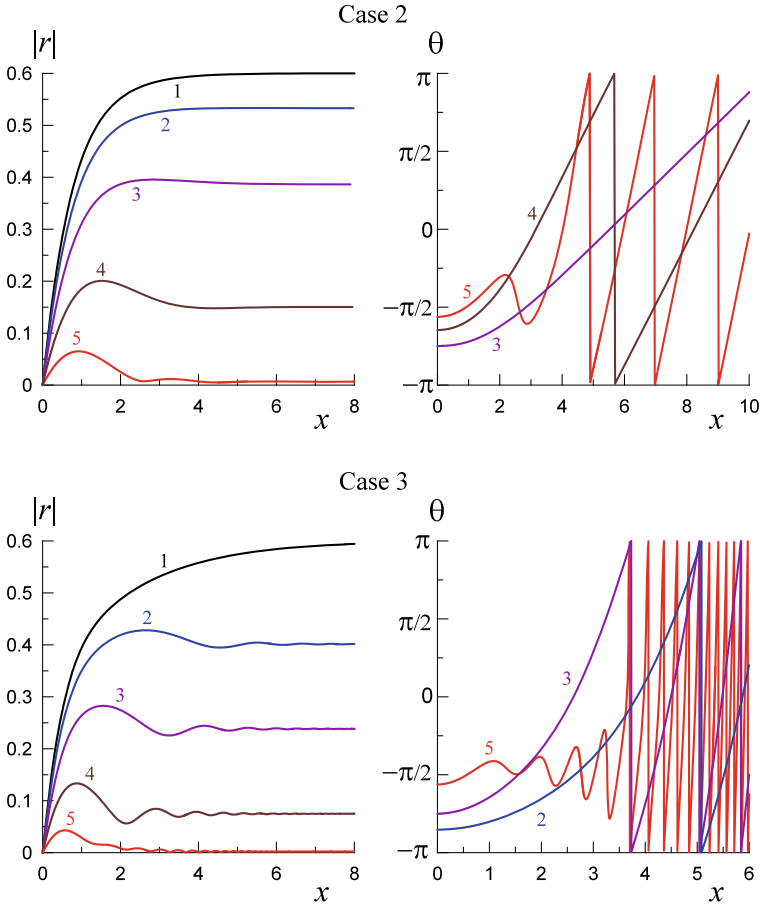


**Fig. 19** (color online) The absolute value and argument of the function $r(x)$ for the Case 2 (top) and Case 3 (bottom). Different numbered curves pertain to different frequencies: 1—$\omega = 0$, 2—$\omega = 0.5$, 3—$\omega = 1$, 4—$\omega = 2$, 5—$\omega = 5$

## *6.3 Some Remarks*

We have carried out the analysis of simple harmonic wave propagation in quite general stationary flows inhomogeneous in the streamwise direction, with emphasis on currents with critical points separating sub- and supercritical flow regimes. Note that in contrast to Ref. [26] where the propagation of *dispersive* gravity-capillary waves was studied, in our paper devoted to *non-dispersive* purely gravity long waves, each of the currents is traversable only in the co-current direction, from left to right in the considered geometry. The reason is that the counter-current waves can not transit through critical points (see Sect. 3.2).

To describe the wave propagation, we have derived the wave equation (9) and reduced it (for a single harmonic) to the set of two first-order ODEs (17) and (18). Solutions to this set of equations have been investigated analytically to describe the transition through the critical points and to determine the conditions of the optimal wave amplification. Our analytical study together with numerical calculations provides results that can be of interest to the interpretation of wave amplification in natural estuaries (rivers, canals, and straits) or laboratory tanks. In addition, this should shed light on the intriguing (and somewhat exotic) problem of wave propagation through wormholes if they exist in nature indeed.

The performed analysis has highlighted a very significant influence of the "geometric factor" $a(x)$ on the wave propagation. So, in the sub-super-subcritical flows, the reflection coefficient in the subcritical regions depends mainly on the behavior of function $a(x)$ rather than on the Mach number at the infinity, $\mathcal{M}_{\pm\infty} = U/c$ . In addition to that, amplification of positive energy waves in the supercritical region is also determined mainly by the difference in the values of $a(x)$ at the ending points of the 'active' (supercritical) region. With regard to this, we recall that at low frequencies, the gain does not depend on which of the speeds is greater, $c_1$ or $c_2$ but is determined entirely by their ratio.

In a super-sub-supercritical flow, the $a(x)$ behavior has a profound impact on the wave propagation as well. However, the frequency dependence of the transmission ratio $K_3$ of its final (supercritical) domain is highly sensitive to that does the Mach number tends to unity at the infinity or not (see Fig. 18).

Finally, with the proviso that $a(x) = \text{const}$ the waves propagate without reflection and transformation regardless of the frequency. In what follows we shall derive and examine other conditions for $a(x)$ which provide the reflectionless (RL) wave propagation as well.

## 7 Surface Wave Propagation Without Reflection: Equations for $a(x)$

To find all conditions of RL propagation for surface waves of arbitrary frequency on inhomogeneous flows (see Fig. 1), let us return to Eqs. (7) and eliminate $\varphi(x,t)$. We arrive at the equation

$$\left(\frac{\partial}{\partial t} + U\frac{\partial}{\partial x} + 2U'\right)\left(\frac{\partial \phi}{\partial t} + U\frac{\partial \phi}{\partial x}\right) = c^2 W \frac{\partial}{\partial x}\left(\frac{1}{W}\frac{\partial \phi}{\partial x}\right), \tag{77}$$

which is complementary to Eq. (9). Then, we represent

$$\varphi(x,t) = A_1(x)\psi(x,t) \quad \text{and} \quad \phi(x,t) = A_2(x)\chi(x,t),$$

substitute into Eqs. (9) and (77), and obtain

$$\frac{\partial^2\psi}{\partial t^2} + (U^2 - c^2)\,\frac{\partial^2\psi}{\partial x^2} + 2U\,\frac{\partial^2\psi}{\partial t\partial x} + 2U\left(\frac{A_1'}{A_1} - \frac{c'}{c}\right)\frac{\partial\psi}{\partial t} + \left[2(U^2 - c^2)\,\frac{A_1'}{A_1} + (U^2 + c^2)\,\frac{U'}{U} - 2U^2\frac{c'}{c}\right]\frac{\partial\psi}{\partial x} + T_1(x)\psi = 0, \tag{78}$$

where

$$A_1(x)\,T_1(x) = (U^2 - c^2)A_1'' + A_1'\Big[(U^2 + c^2)(\ln U)' - 2U^2(\ln c)'\Big],$$

and

$$\frac{\partial^2\chi}{\partial t^2} + (U^2 - c^2)\,\frac{\partial^2\chi}{\partial x^2} + 2U\,\frac{\partial^2\chi}{\partial t\partial x} + 2\left(U\,\frac{A_2'}{A_2} + U'\right)\frac{\partial\chi}{\partial t} + \left[2(U^2 - c^2)\,\frac{A_2'}{A_2} - c^2\,\frac{U'}{U} + 3UU' - 2cc'\right]\frac{\partial\chi}{\partial x} + T_2(x)\chi = 0, \tag{79}$$

where

$$A_2(x)\,T_2(x) = (U^2 - c^2)A_2'' + \Big[3UU' - c^2(\ln U)' - 2cc'\Big]A_2'.$$

One can see (for more details, see [10, 11]) that $T_1(x) \equiv 0$ if

$$\frac{\mathrm{d}A_1}{\mathrm{d}x} = \frac{\mathcal{B}\,c^2(x)U(x)}{c^2(x) - U^2(x)}, \quad \mathcal{B} = \text{const}, \tag{80}$$

and $T_2(x) \equiv 0$ when

$$\frac{\mathrm{d}A_2}{\mathrm{d}x} = \frac{\mathcal{C}}{U(x)\Big[U^2(x) - c^2(x)\Big]}, \qquad \mathcal{C} = \text{const}. \tag{81}$$

As the next step, we consider the model equation

$$\left(\frac{\partial}{\partial t} + w_1(x)\,\frac{\partial}{\partial x} + G(x)\right)\left(\frac{\partial}{\partial t} + w_2(x)\,\frac{\partial}{\partial x}\right)\mathcal{F}(x,t) = 0, \tag{82}$$

where $w_1(x)$, $w_2(x)$, and $G(x)$ are as yet undefined functions. One of its solutions describes a traveling wave,

$$\mathcal{F}(x,t) = \mathcal{F}_1\left(t - \int\frac{\mathrm{d}x}{w_2(x)}\right),$$

where $\mathcal{F}_1(X)$ is an arbitrary function. Expansion of Eq. (82) leads to

$$\frac{\partial^2 \mathcal{F}}{\partial t^2} + w_1 w_2 \frac{\partial^2 \mathcal{F}}{\partial x^2} + \Big(w_1 + w_2\Big)\frac{\partial^2 \mathcal{F}}{\partial t \partial x} + G\,\frac{\partial \mathcal{F}}{\partial t} + \Big[w_1 w_2' + G\,w_2\Big]\frac{\partial \mathcal{F}}{\partial x} = 0. \tag{83}$$

Let us compare this equation with Eq. (78) provided that $T_1(x) \equiv 0$ and Eq. (80) holds. The equations are identical if

$$w_1 w_2 = U^2 - c^2, \qquad w_1 + w_2 = 2U, \qquad G = 2U\left(\frac{A_1'}{A_1} - \frac{c'}{c}\right), \tag{84}$$

and

$$w_1 w_2' + G\,w_2 = 2\Big(U^2 - c^2\Big)\frac{A_1'}{A_1} - 2U^2\,\frac{c'}{c} + \Big(U^2 + c^2\Big)\frac{U'}{U}\,. \tag{85}$$

The first two Eqs. (84) show that either $w_1 = U - c$ and $w_2 = U + c$, or $w_1 = U + c$ and $w_2 = U - c$. In both these cases Eq. (85) provides (cf. with Eq. (14)) $A_1(x) = \Big[c(x)\,U(x)\Big]^{1/2} \equiv a(x)$, and Eq. (80) takes the form

$$\frac{\mathrm{d}a}{\mathrm{d}x} = \frac{\mathcal{B}\,c^2(x)U(x)}{c^2(x) - U^2(x)}\,. \tag{86}$$

Similar calculations demonstrate that Eq. (83) is identical to Eq. (79) with $T_2(x) \equiv 0$ for the same $(w_1, w_2)$ pairs (i.e., for $w_1 = U - c$, $w_2 = U + c$ or $w_1 = U + c$, $w_2 = U - c$) and $A_2(x) = a^{-1}(x)$. Substituting the last relation into Eq. (81) yields

$$\frac{\mathrm{d}a}{\mathrm{d}x} = \frac{\mathcal{C}\,c(x)}{c^2(x) - U^2(x)}\,. \tag{87}$$

As a result, we see that Eq. (78) with $T_1 \equiv 0$ can be presented in two equivalent forms:

$$\begin{aligned}&\left\{\frac{\partial}{\partial t} + \Big[U(x) - c(x)\Big]\frac{\partial}{\partial x} + U(x)\left(\frac{U'(x)}{U(x)} - \frac{c'(x)}{c(x)}\right)\right\}\\ &\qquad\times\left(\frac{\partial}{\partial t} + \Big[U(x) + c(x)\Big]\frac{\partial}{\partial x}\right)\psi \equiv\\ &\left\{\frac{\partial}{\partial t} + \Big[U(x) + c(x)\Big]\frac{\partial}{\partial x} + U(x)\left(\frac{U'(x)}{U(x)} - \frac{c'(x)}{c(x)}\right)\right\}\\ &\qquad\times\left(\frac{\partial}{\partial t} + \Big[U(x) - c(x)\Big]\frac{\partial}{\partial x}\right)\psi = 0.\end{aligned} \tag{88}$$

The general solution to this equation is a superposition of two waves of arbitrary form which propagate along the characteristics (8),

$$\psi(x,t) = \psi_1\left(t - \int \frac{\mathrm{d}x}{U(x)+c(x)}\right) + \psi_2\left(t - \int \frac{\mathrm{d}x}{U(x)-c(x)}\right).$$

The independent propagation of each of these waves in an inhomogeneous medium is provided by Eq. (86) specifying the necessary relation between $c(x)$ and $U(x)$. Similarly, when $T_2 \equiv 0$, $\chi(x,t)$ obeys Eq. (88) as well and can be represented as a sum of two waves of arbitrary form,

$$\chi(x,t) = \chi_1\left(t - \int \frac{\mathrm{d}x}{U(x)+c(x)}\right) + \chi_2\left(t - \int \frac{\mathrm{d}x}{U(x)-c(x)}\right),$$

but in this case $c(x)$ and $U(x)$ must be related by Eq. (87).

Thus, we have derived Eqs. (86) and (87) which relate the flow and wave velocities $U(x)$ and $c(x)$ in such a manner that the fulfillment of either of the two ensures RL wave propagation. When corresponding $a(x) = \left[c(x)U(x)\right]^{1/2}$ is found, the perturbed flow velocity $\tilde{u}$ and free surface elevation $\eta$ in the wave are expressed in terms of $\psi$ and $\chi$ as follows (see Eqs. (1), (3), (5), and (6)):

$$\tilde{u} = a(x)\frac{\partial\psi}{\partial x} + a'(x)\psi, \qquad \eta = -\frac{a(x)}{g}\left[\frac{\partial\psi}{\partial t} + U(x)\,\frac{\partial\psi}{\partial x} + \frac{a'(x)}{a(x)}\,U(x)\psi\right], \tag{89}$$

and

$$\tilde{u} = -\frac{U(x)}{a(x)\Phi}\left[\frac{\partial\chi}{\partial t} + U(x)\,\frac{\partial\chi}{\partial x} - \frac{a'(x)}{a(x)}\,U(x)\,\chi\right],$$
$$\eta = \frac{1}{W(x)\,a(x)}\left[\frac{\partial\chi}{\partial x} - \frac{a'(x)}{a(x)}\,\chi\right]. \tag{90}$$

Equations (86) and (87) are very similar, but the properties of the RL velocity profiles that satisfy them notably differ. Only when $\mathcal{B} = \mathcal{C} = 0$, both equations lead to the already known relation $a(x) = \text{const}$, or

$$c(x)\,U(x) = \Pi = \text{const} > 0. \tag{91}$$

An example of the flow belonging to this class of RL flows (let's call it class A) is shown in Fig. 3c. Note that one may interchange $c(x)$ and $U(x)$ profiles in this figure to obtain the other flow of this class. In view of the flux conservation equation (1), the velocity and width of an A-class flow are related to its depth by

$$U(x)\,H^{1/2}(x) = \text{const} \quad \text{and} \quad W(x)\,H^{1/2}(x) = \text{const}, \tag{92}$$

so that $U(x)/W(x) = \text{const}$, that is, the wider the channel, the higher the fluid velocity.

In studies of RL propagation of long surface waves in channels without current, the second relation (92) plays an important role (see, for example, [12, 16, 24, 25]). It distinguishes the so-called self-consistent channels—the only class of channels with regular $W(x)$ and $H(x)$ profiles, in which waves propagate without reflection along the entire $x$-axis. Class A contains RL flows in self-consistent channels with currents, and these flows are also regular. One can set the profile of one of the velocities (for example, $c(x)$) on the entire $x$-axis in the form of an arbitrary continuous positive function and, using Eq. (91), obtain a family of corresponding profiles for another velocity ($U(x)$) "labelled" by the parameter $\Pi$ (as an example, see Fig. 3c).

The class of RL flows controlled by Eq. (86) with $\mathcal{B} \neq 0$ (the B-class of flows) has been studied in detail in [10] and is described in the next section. And Sect. 9 is devoted to the third class of RL flows controlled by equation Eq. (87) with $\mathcal{C} \neq 0$ (the C-class of flows) which was examined in [11].

## 8 B–class RL Flows

### *8.1 General Properties and Some Examples*

Let us note first that Eq. (86) is invariant with respect to the simultaneous replacement $x \to -x$ and $\mathcal{B} \to -\mathcal{B}$. For this reason, we introduce a variable $\xi = \mathcal{B}x$ which remains the same under such a transformation and rewrite Eq. (86) in two forms:

$$\frac{\mathrm{d}a}{\mathrm{d}\xi} = \frac{c^2(\xi)U(\xi)}{c^2(\xi) - U^2(\xi)} \qquad \text{and} \qquad c(\xi)\frac{\mathrm{d}U}{\mathrm{d}\xi} + U(\xi)\frac{\mathrm{d}c}{\mathrm{d}\xi} = \frac{2c^{5/2}(\xi)U^{3/2}(\xi)}{c^2(\xi) - U^2(\xi)}\,. \quad (93)$$

In addition, Eqs. (86) and (93) are invariant with respect to the scaling transformation $U(x) \to U(x)/c_0$, $c(x) \to c(x)/c_0$, where $c_0 = \text{const}$. In what follows, we will choose the appropriate scale $c_0$. Note also that these equations possess the translational symmetry which means that if $c(\xi)$ and $U(\xi)$ satisfy Eq. (93), then $c(\xi + b)$ and $U(\xi + b)$, where $b$ is an arbitrary constant, satisfy this equation too. And finally, it is easily seen that $a(\xi)$ monotonically increases in subcritical ($U < c$) flows and decreases in supercritical ones.

The right-hand side of Eq. (93) is singular for $U = c$, $U = 0$, $c = 0$, as well as for unbounded growth of $U(\xi)$ or $c(\xi)$. To solve the question of whether these singularities are attainable at a finite $\xi$, we rewrite the first Eq. (93) in the form

$$\frac{1}{a(\xi)}\frac{\mathrm{d}a}{\mathrm{d}\xi} = \frac{c^{3/2}(\xi)U^{1/2}(\xi)}{c^2(\xi) - U^2(\xi)}\,. \quad (94)$$

It is easy to see that if $c(\xi)$ is bounded everywhere, that is $0 < c(\xi) \le c_M < \infty$, then the singularities $U = 0$ and $U = \infty$ are attainable only asymptotically, when

$|\xi| \to \infty$. The same is true for $c = 0$ and $c = \infty$ if $U(\xi)$ is bounded everywhere, and only $U = c$ can be reached at a finite $\xi$, in critical point(s).

In distinction to regular critical points in A-class flows (see Sect. 3), the critical points in B-class flows are singular. At such a point, both velocities, $c(\xi)$ and $U(\xi)$, are finite and nonzero, but their derivatives can be singular. Let us examine the neighborhood of a critical point (say, $\xi = 0$) where $U = c$. Assume that the normalization constant $c_0$ is chosen such that $U(0) = c(0) = 1$. Let us set

$$c(\xi) = 1 + s(\xi), \qquad U(\xi) = 1 + v(\xi),$$

where $s(\xi) \to 0$ and $v(\xi) \to 0$ when $\xi \to 0$. Substituting into the second Eq. (93) yields

$$\Big(s - v\Big)\Big(s' + v'\Big) = 1 + 2\,s + v + O(s^2 + v^2),$$

where prime stands for the derivative with respect to $\xi$. From here, we see that $(s - v)$ and $(s + v)$ are power-type functions of $\xi$:

$$(s - v) \sim \xi^{\lambda_1}, \qquad (s + v) \sim \xi^{\lambda_2}, \tag{95}$$

where $\lambda_1 + \lambda_2 = 1$, $\lambda_{1,2} > 0$.

Since $\xi = 0$ is a branching point and $s(\xi)$ and $v(\xi)$ are real functions, the cases $\xi > 0$ and $\xi < 0$ should be considered separately.

**Case A.** If $\lambda_1 = \lambda_2 = 1/2$, then we readily find for $\xi \geq 0$:

$$c(\xi) = 1 + s_+\xi^{1/2} + O(\xi), \qquad U(\xi) = 1 + v_+\xi^{1/2} + O(\xi), \tag{96}$$

where $s_+^2 = v_+^2 + 2$.

For $\xi \leq 0$, we find:

$$c(\xi) = 1 + s_-(-\xi)^{1/2} + O(\xi), \qquad U(\xi) = 1 + v_-(-\xi)^{1/2} + O(\xi), \tag{97}$$

where $s_-^2 = v_-^2 - 2$. Here $s_\pm$ and $v_\pm$ are constants which can have any sign, depending on the branch of the solution (subcritical or supercritical). Moreover, it is not necessary that both velocities have singularities at $\xi = 0$. In particular, in the domain $\xi \geq 0$ the flow velocity can be regular ($v_+ = 0$), while the wave speed can be regular ($s_- = 0$) in the domain where $\xi \leq 0$ .

If $\lambda_1 \neq \lambda_2$ we can present $s(x)$ and $u(x)$ as:

$$s(\xi) = s_{a\pm}|\xi|^{\lambda_1} + s_{b\pm}|\xi|^{\lambda_2} + \ldots, \qquad v(\xi) = v_{a\pm}|\xi|^{\lambda_1} + v_{b\pm}|\xi|^{\lambda_2} + \ldots,$$

where the indices plus (minus) pertain to the regions $\xi \geq 0$ ($\xi \leq 0$).

**Case B.** If $0 < \lambda_1 < \lambda_2$, then from the condition $(s + v) \sim |\xi|^{\lambda_2}$, we obtain:

$$s_{a\pm} + v_{a\pm} = 0, \qquad 2\lambda_2 s_{a\pm}(s_{b\pm} + v_{b\pm}) = \pm 1. \tag{98}$$

**Case C.** When, conversely, $\lambda_1 > \lambda_2 > 0$, from the condition $(s - v) \sim |\xi|^{\lambda_1}$, we obtain:

$$s_{b\pm} = v_{b\pm}, \qquad 2\lambda_2 s_{b\pm}(s_{a\pm} - v_{a\pm}) = \pm 1. \tag{99}$$

Emphasize that in any case at least one of the velocities is singular at the critical point $\xi = 0$. Moreover, both flows, subcritical and supercritical, do exist on the same semiaxis of $\xi$, positive or negative. Since the flow velocities at the critical point do not vanish, the flow exists on the complementary part of $\xi$-axis as well, but ceases to be reflectionless. It would be very interesting to know what happens when the wave passes through a critical point,—its reflection, or (most likely, partial) absorption, or a combination of these,—but this issue requires a separate study.

For further consideration, it is convenient to introduce functions determined by the ratio of the velocities $U(\xi)$ and $c(\xi)$ in each point $\xi$,

$$F(\xi) = \left[\frac{U(\xi)}{c(\xi)}\right]^{1/2} \equiv \left[\frac{U^2(\xi)}{gH(\xi)}\right]^{1/4} \quad \text{and} \quad f(\xi) = \frac{1}{F(\xi)}\,. \tag{100}$$

For the sake of brevity, we will call function $F(\xi)$ the Froude number, and function $f(\xi)$ the reciprocal Froude number. Note that $\mathcal{M} = F^2$, where $\mathcal{M}$ is the Mach number introduced in Sect. 4.1. In terms of $F$ and $f$, Eq. (93) can be written in two equivalent forms:

$$\frac{\mathrm{d}F}{\mathrm{d}\xi} = \frac{F^2(\xi)}{1 - F^4(\xi)} - \frac{F(\xi)}{c(\xi)}\frac{\mathrm{d}c(\xi)}{\mathrm{d}\xi}\,, \tag{101}$$

$$\frac{\mathrm{d}f}{\mathrm{d}\xi} = \frac{f^3(\xi)}{1 - f^4(\xi)} + \frac{f(\xi)}{c(\xi)}\frac{\mathrm{d}c(\xi)}{\mathrm{d}\xi}\,, \tag{102}$$

where $c(\xi)$ is assumed to be given. As a useful illustration, let us consider two examples.

### 8.1.1 Currents of a Constant Depth, $H(x) = \mathrm{const}$

In this case, the wave velocity is also constant, $c(\xi) = c_0$. Setting $c_0 = 1$ and integrating Eq. (101), we arrive at the algebraic equation

$$F^4 + 3(\xi - \xi_0)F + 3 = 0. \tag{103}$$

When $\xi < \xi_* = \xi_0 - 4/3$, it has two positive roots, $F_-(\xi) < 1$ and $F_+(\xi) > 1$ which merge in one double root $F = 1$ at $\xi - \xi_*$. These solutions do exist only for $\xi < \xi_*$ and are singular,

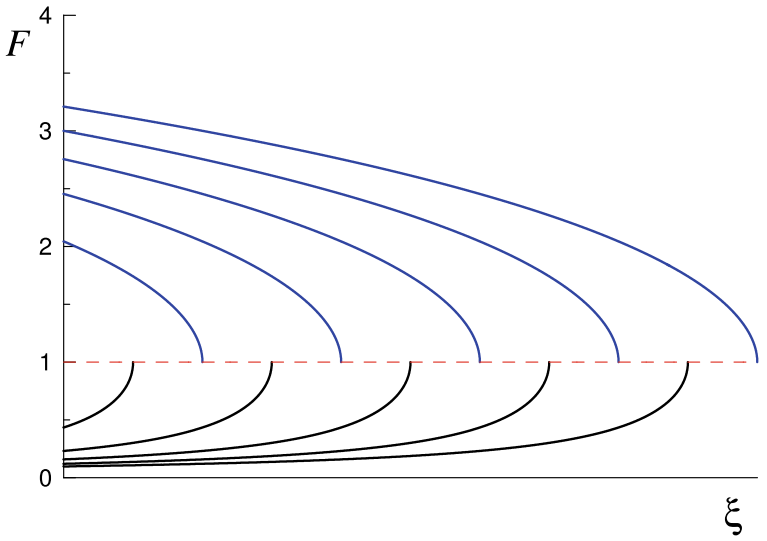


**Fig. 20** (color online) Solutions to Eq. (103) for different values of $\xi_0$ in the subcritical ($F < 1$) and supercritical ($F > 1$) regimes

$$F_{\pm}(\xi) = 1 \pm \left(\frac{\xi_* - \xi}{2}\right)^{1/2} + \frac{\xi_* - \xi}{12} + \ldots, \quad U_{\pm}(\xi) = F_{\pm}^2(\xi) = 1 \pm \left[2(\xi_* - \xi)\right]^{1/2} + \ldots, \tag{104}$$

where plus/minus signs correspond to super/subcritical flow. And for $\xi \to -\infty$ the asymptotic solutions originated for each root are (we are recalling that $a(\xi) = c(\xi)\, F(\xi)$):

$$\begin{aligned} a_-(\xi) = F_-(\xi) \approx (-\xi)^{-1}, \quad a_+(\xi) = F_2(\xi) \approx (-3\xi)^{1/3}, \\ U_-(\xi) = F_-^2(\xi) \approx (-\xi)^{-2}, \quad U_+(\xi) = F_+^2(\xi) \approx (-3\xi)^{2/3}. \end{aligned} \tag{105}$$

Solutions of Eq. (103) are shown in Fig. 20.

### 8.1.2 Flows with the Exponential Variation of Wave Speed $c(\xi)$

Let $c(\xi) = C \exp(\mu\xi)$. Then Eq. (101) takes the form:

$$\frac{\mathrm{d}F}{\mathrm{d}\xi} = \frac{F^2}{1 - F^4} - \mu F. \tag{106}$$

This equation, in contrast to the one considered above, has a null-isocline (NI) $F(\xi) = F_0 = \text{const}$ on which its right-hand side vanishes. The value of $F_0$ is a positive root of the equation

$$F_0^4 + \frac{F_0}{\mu} - 1 = 0. \tag{107}$$

It is evident that for $\mu > 0$, the value of $F_0 < 1$, i.e. corresponds to the subcritical domain, whereas for $\mu < 0$, the value of $F_0 > 1$, which corresponds to the supercritical domain. It can be shown (for more details, see [10]) that the phase trajectories of Eq. (106) are moving apart from NI as $\xi$ increases, see Fig. 21.

As a result, the upper half-plane $(\xi,\ F)$ is split into three strips (separated from each other by the straight lines $F = F_0$ and $F = 1$), in which the behavior of solutions to Eq. (106) is significantly different. If $\mu > 0$, then $0 < F_0 < 1$, and solutions to equation (106) are such as shown in Fig. 21a. In the lower strip, $0 < F < F_0$, any solution $F(\xi)$ decreases monotonically approaching $F_0$ from below when $\xi \to -\infty$ and zero from the top when $\xi \to +\infty$, according to $F \approx F_{m+} \exp(-\mu\xi)$. Respectively, in the same limit we have $a(\xi) \to$ const and

$$W(\xi) \sim U(\xi) \sim F(\xi) \sim H^{-1/2}(\xi) \sim c^{-1}(\xi). \tag{108}$$

In the middle strip, $F_0 < F \le 1$, any solution $F(\xi)$ grows monotonically from $F_0$ when $\xi \to -\infty$ to $F = 1$ at some $\xi_*$. Near this critical point the asymptotic solution is

$$F(\xi) = 1 - \left(\frac{\xi_* - \xi}{2}\right)^{1/2} - \frac{1 - 8\mu}{12}\Big(\xi_* - \xi\Big) + \ldots \tag{109}$$

In the upper strip any solution tends to infinity as $F \approx F_{m-} \exp(-\mu\xi)$ when $\xi \to -\infty$ and decreases with $\xi$ approaching unity, when $\xi$ tends to some $\xi_+$ as per the formula:

$$F(\xi) = 1 + \left(\frac{\xi_+ - \xi}{2}\right)^{1/2} - \frac{1 - 8\mu}{12}\Big(\xi_+ - \xi\Big) + \ldots \tag{110}$$

If $\mu < 0$, then $F_0 > 1$. Solutions to Eq. (106) are shown in Fig. 21b. In the lower strip, $0 < F < 1$, all solutions $F(\xi)$ monotonically increase from $F \approx F_{M-} \exp(-\mu\xi)$ when $\xi \to -\infty$ attaining $F = 1$ at some finite $\xi$ as per dependence similar to described by Eq. (109). In the middle strip, $1 < F < F_0$, solutions $F(\xi)$ monotonically decrease from $F_0$ when $\xi \to -\infty$ to $F = 1$ achieving this value at some finite $\xi$ as per dependence similar to (110). In the upper strip, $F > F_0$, solutions $F(\xi)$ monotonically increase from $F_0$ when $\xi \to -\infty$, to $F \approx F_{M+} \exp(-\mu\xi)$ when $\xi \to +\infty$; the dependences similar to (108) are held in this limit.

It should be noted that in the lower strip for $\mu > 0$ and in the upper strip for $\mu < 0$ solutions are *global*, i.e., they are defined on the entire $\xi$-axis, whereas in other strips, solutions are defined only to the left of some finite point $\xi_*$ which is different for each particular realization.

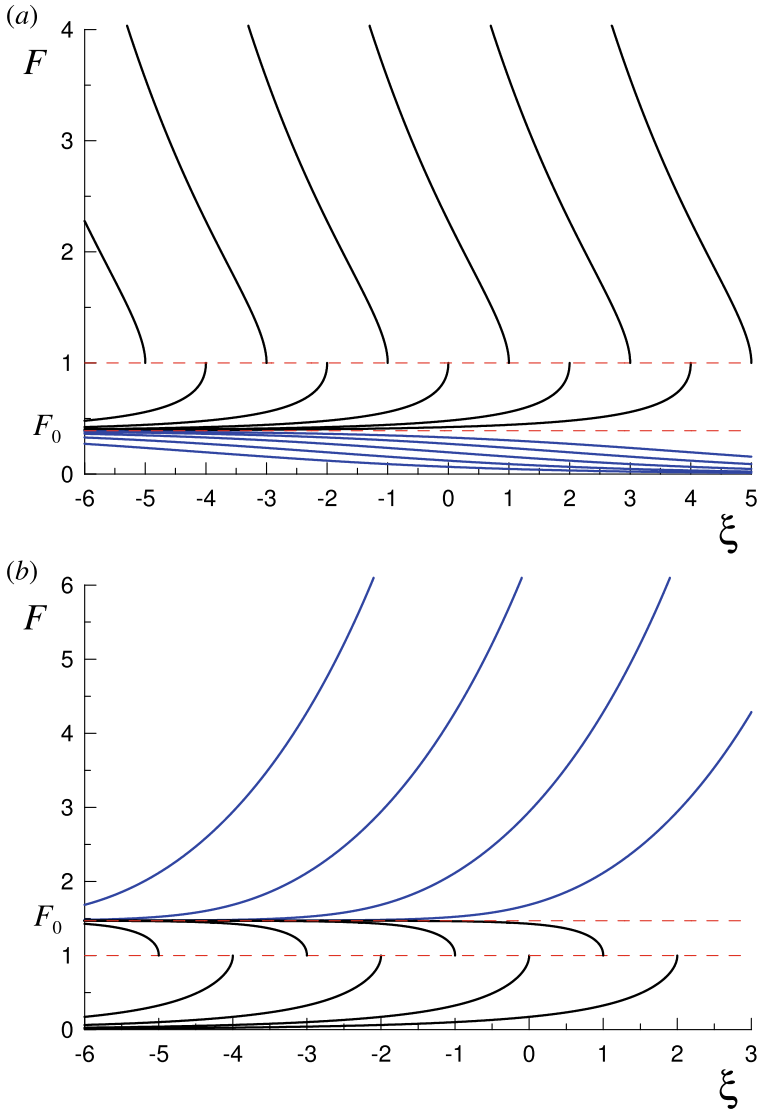


**Fig. 21** (color online) Solutions of Eq. (106) with **a** positive $\mu = 0.4$ ($F_0 = 0.3907$) and **b** negative $\mu = -0.4$ ($F_0 = 1.4705$). Blue lines correspond to global solutions

## 8.2 Global Solutions and Conditions of Their Existence

As follows from the analysis presented above for the specific flow models, in the majority of cases solutions for the RL current profile are valid only on the limited spatial interval, because the profiles of the flow depth, width, or velocity become either singular in certain points, or diverge at the infinity. Therefore, one of the important questions is whether it is possible to find such conditions when solutions for the profiles are globally defined on the entire $x$-axis. Such a problem was solved in the case when there is no current [24]. We provide the solution for the case when the current is taken into account.

Let us recall that in the case of the exponential variation of the wave speed $c(\xi)$ considered above, horizontal NI ($F = F_0 = \text{const}$) is the flow trajectory in itself and serves as the separatrix separating the global trajectories from those that are defined on the bounded $\xi$-interval. Under a non-exponential variation of $c(\xi)$, NI $F = F_0(\xi)$, on which the right-hand side of Eq. (101) vanishes, is still described by Eq. (107) but now $\mu(\xi) \equiv \mathrm{d}\ln c(\xi)/\mathrm{d}\xi \neq \text{const}$. In other words, NI is not horizontal, not a trajectory, and not a separatrix because it does not obey Eq. (101) and is intersected on the $(\xi,\ F)$-plane by some trajectories of Eq. (101). Nevertheless, it is necessary for the existence of global solutions.

In the subcritical domain ($F < 1$) NI exists if $c(\xi)$ increases ($\mu(\xi) > 0$) whereas in the supercritical domain ($F > 1$) decreasing of $c(\xi)$ ($\mu(\xi) < 0$) is required. Let us consider first subcritical flows. If $c(\xi)$ grows so fast that $\mu(\xi)$ increases monotonically, with or without limit (see lines 2 and 1 in Fig. 22a respectively). NI $F = F_0(\xi)$ also increases monotonically starting at $\xi = \xi_m$ (possibly, at $\xi = -\infty$) to some $F_M \leq 1$ when $\xi \to +\infty$ (see line 1 in Fig. 23a).Trajectories representing solutions of Eq. (101) either intersect NI and are global, or lie entirely above it and are bounded from the right by some $\xi = \xi_b$. (Note that NI has a positive derivative, whereas trajectories below it have negative slopes. Therefore, all such trajectories intersect NI when $\xi$ decreases.)

If function $c(\xi)$ grows slower than exponentially, then $\mu(\xi)$ has a maximum (possibly, even more than one, but it does not matter, in principle) and vanishes when $\xi \to +\infty$ (see Fig. 22b). NI $F = F_0(\xi)$ has qualitatively the same shape (see line 1 in Fig. 23b). All trajectories lying above or crossing its right (descending) slope (for example, like line 2 in Fig. 23b) are, obviously, bounded from the right by some $\xi = \xi_b$. The global trajectories such as shown by line 3 in Fig. 23b must lie below $F_0(\xi)$ for sufficiently large $\xi$.

Consider the trajectory passing through the point $(\xi_1,\ F_1)$ in the subcritical domain ($0 < F_1 < 1$). Integrating Eq. (94) with the use of the mean-value theorem provides

$$\frac{1}{a(\xi)} = \frac{1}{a(\xi_1)} - \int_{\xi_1}^{\xi} \frac{\mathrm{d}y}{c(y)[1 - F^4(y)]} = \frac{1}{c(\xi_1)\,F_1} - \frac{1}{1 - F^4(\xi_a)} \int_{\xi_1}^{\xi} \frac{\mathrm{d}y}{c(y)}, \quad (111)$$

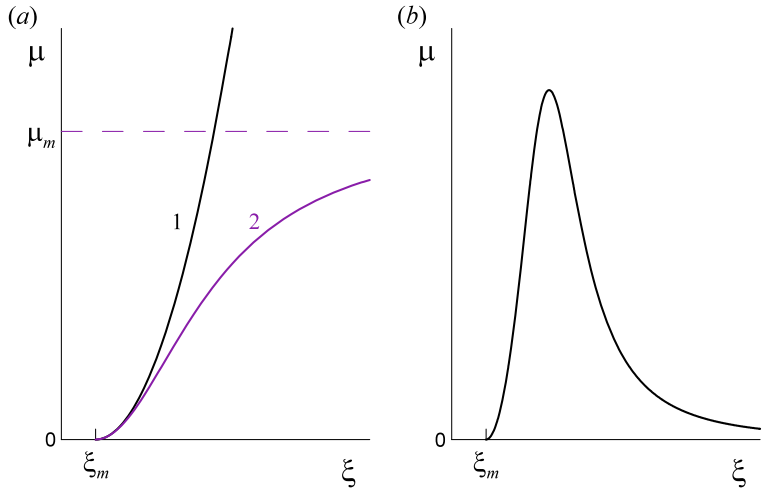


**Fig. 22** (color online) The qualitative dependence of $\mu(\xi)$ for the flows with **a** fast and **b** slow growth of $c(\xi)$

where $\xi_a$ is between $\xi_1$ and $\xi$. It turns out that in the subcritical domain both the existence of global solutions and asymptotic (as $\xi \to \pm\infty$) behavior of $F(\xi)$ depend on the convergence of integrals

$$I_{F\pm}(\xi) = \pm \int_{\xi}^{\pm\infty} \frac{\mathrm{d}y}{c(y)} \tag{112}$$

on the upper limit. Indeed, let $\mu(\xi) \ll 1$ and decreases monotonically for $\xi \geq \xi_1$. Then, according to Eq. (107), $F_0(\xi) \approx \mu(\xi)$ and decreases as well. For $F_1 < F_0(\xi_1)$, the trajectory lies below NI on some interval containing $\xi_1$. If $I_{F+}(\xi_1)$ diverges, the right-hand side of Eq. (111) vanishes at some finite $\xi$ and $F(\xi)$ increases up to $F = 1$, and therefore the trajectory intersects NI. If, however, $c(\xi)$ grows rapidly enough (faster than $\xi$) so that $I_{F+}(\xi_1)$ converges, and if $F_1$ is sufficiently small, the right-hand side of Eq. (111) tends to a finite limiting value $a_{1+}^{-1} > 0$ as $\xi \to +\infty$. Then $a(\xi) = c(\xi)F(\xi) \to a_{1+}$ while $c(\xi)F_0(\xi) \approx \mu(\xi)c(\xi) = c'(\xi) \to +\infty$, and the trajectory is global because it lies below NI when $\xi > \xi_1$. Thus, the convergence of the integral $I_{F+}(\xi)$ for any finite $\xi$ is necessary and sufficient for the existence of global subcritical RL flows of class B. Figure 24 demonstrates a qualitative variation of the global flow parameters along the channel.

In the supercritical domain, NI exists if $\mu(\xi) < 0$, i.e., if the depth $H(\xi)$ and wave speed $c(\xi)$ decrease with $\xi$. In this domain, it is convenient to use the reciprocal Froude number $f(\xi) = 1/F(\xi)$; then $a(\xi) = c(\xi)/f(\xi))$. In this case, all the reasoning presented above remains almost the same. As a result, it is sufficient to replace

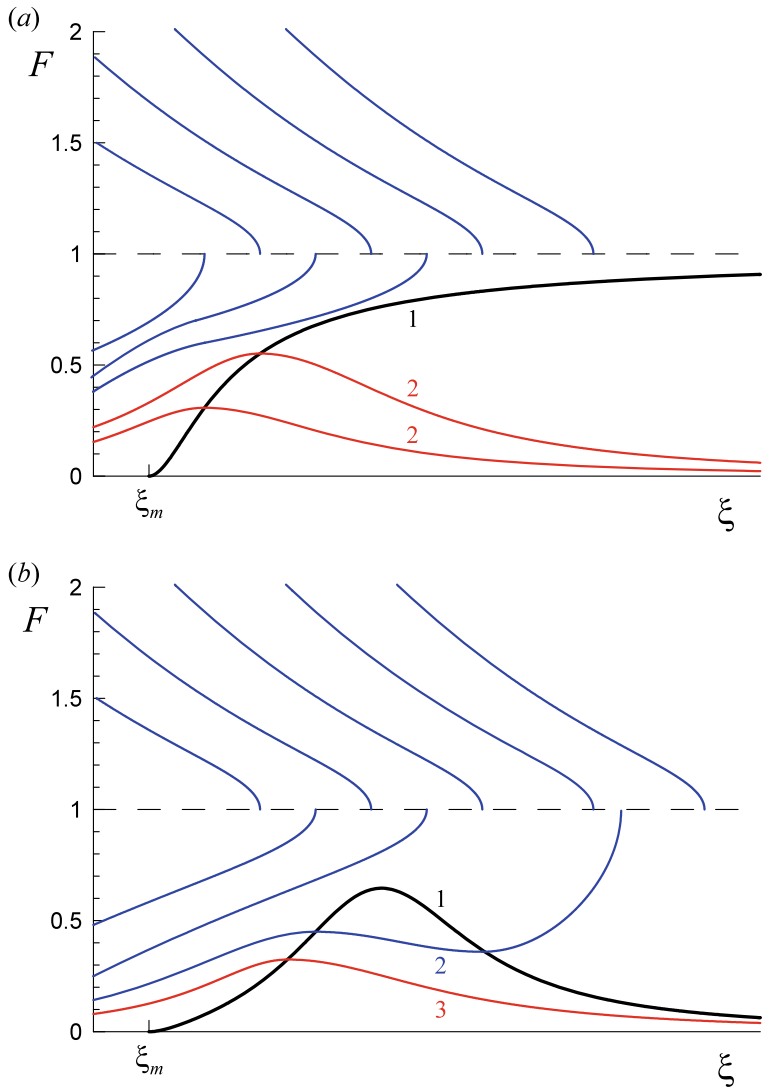


**Fig. 23** (color online) Solutions of Eq. (101) for **a** fast and **b** slow growth of $c(\xi)$. Line 1 corresponds to NI in both frames. Lines 2 in frame **a** illustrate examples of global trajectories; other non-numbered blue lines illustrate bounded solutions that exist for $\xi \le \xi_b$ with the individual value of $\xi_b$ for each line. In frame **b** non-numbered blue lines depict bounded trajectories, line 2 is an $\xi$-bounded trajectory partially passing below NI, and line 3 illustrates a global solution

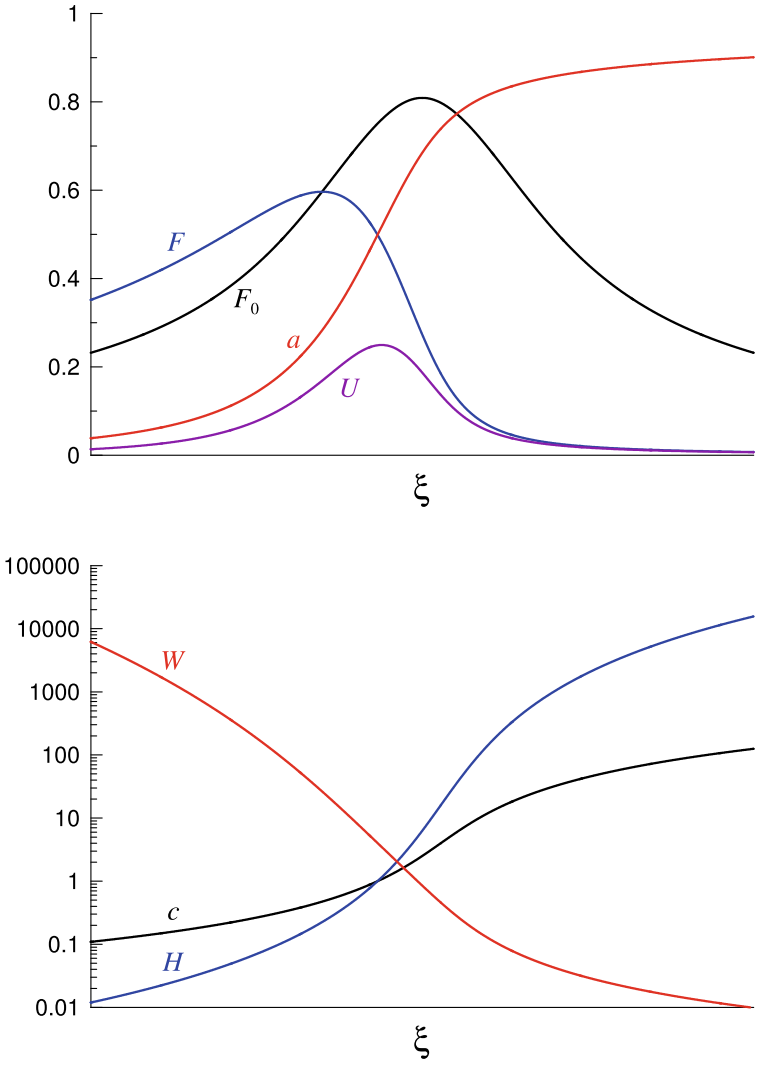


**Fig. 24** (color online) Typical variation of the subcritical global flow parameters along the channel. All variables are normalized to some reference values and presented in dimensionless form

$\mu$ by $|\mu|$ (or by $-\mu$) in Fig. 22 and $F$ by $f$ in Fig. 23 in order to have an idea of the solutions of Eq. (102).

In this domain, NI is described by the algebraic equation

$$f_0^4(\xi) + \frac{f_0^3(\xi)}{|\mu(\xi)|} - 1 = 0, \tag{113}$$

and global solutions exist if the integral $I_{f+}(\xi)$, where

$$I_{f\pm}(\xi) = \pm \int_{\xi}^{\pm\infty} \mathrm{d}y c^3(y), \tag{114}$$

converges for any finite $\xi$, that is, if $c(\xi)$ decreases with $\xi$ faster than $\xi^{-1/3}$. Indeed, let us consider the trajectory passing through the point $(\xi_2,\ f_2)$ and rewrite Eq. (94) in terms of $f(\xi)$:

$$\frac{1}{a(\xi)}\frac{\mathrm{d}a(\xi)}{\mathrm{d}\xi} = -\frac{f^3(\xi)}{1-f^4(\xi)} = -\frac{c^3(\xi)}{a^3(\xi)[1-f^4(\xi)]}$$

Integrating it with the use of the mean-value theorem provides

$$a^3(\xi) = a^3(\xi_2) - 3\int_{\xi_2}^{\xi} \frac{\mathrm{d}y c^3(y)}{1-f^4(y)} = \frac{c^3(\xi_2)}{f_2^3} - \frac{3}{1-f^4(\xi_b)}\int_{\xi_2}^{\xi} \mathrm{d}y c^3(y), \tag{115}$$

where $\xi_b$ is between $\xi_2$ and $\xi$. Suppose that for $\xi \geq \xi_2$ $|\mu(\xi)| \ll 1$ and decreases monotonically. Then Eq. (113) yields $f_0(\xi) \approx |\mu(\xi)|^{1/3} \ll 1$. If $I_{f+}(\xi_2)$ converges, the right-hand side of Eq. (115) tends to a finite limiting value $a_{2+}^3$ as $\xi \to +\infty$, and this value is positive for sufficiently small $f_2$. Therefore, $f^3(\xi) \approx c^3(\xi)/a_{2+}^3 \ll \xi^{-1}$ on the trajectory while $f_0^3(\xi) \approx |\mu(\xi)| = |c'(\xi)|/c(\xi) \gtrsim \xi^{-1}$. Hence, $f(\xi) \ll f_0(\xi)$ and the trajectory is global.

In closing, it should be noted that the conditions for the existence of global sub- and supercritical RL flows are incompatible, therefore, depending on the behavior of $c(\xi)$, there may be either one or the other (or there may not be global flows at all, see Fig. 20).

## 8.3 *Asymptotic Behavior When $\xi \to -\infty$*

Consider the trajectory passing through the point $(\xi_1,\ F_1)$ and use Eq. (111) for $\xi < \xi_1$. Its right-hand side is positive and grows with a decrease in $\xi$. If the integral $I_{F-}(\xi_1)$ converges (see Eq. (112)), $a(\xi) \to a_{F-} = \mathrm{const} > 0$ and relations (108) are fulfilled.

If, conversely, $I_{F-}(\xi_1)$ diverges, let us suppose first that

$$c(\xi) \sim (-\xi)^p,\quad p < 1, \quad \Longrightarrow \quad \mu(\xi) \equiv \frac{c'(\xi)}{c(\xi)} = -\frac{p}{\xi},\quad a^{-1}(\xi) \sim \int^{\xi} \frac{\mathrm{d}y}{c(y)} \sim (-\xi)^{1-p}.$$

The solution to Eq. (101) is $F(\xi) = (p-1)/\xi$. For $\xi \to -\infty$, it has a qualitatively similar behavior at any $p < 1$ including $p < 0$ when $\mu(\xi)$ becomes positive and NI $F_0(\xi) \approx \mu(\xi) = -p/\xi$ emerges. On the contrary, the flow velocity and other flow parameters do significantly depend on $p$:

$$U(\xi) \sim \left(-\xi\right)^{p-2}, \quad W(\xi) \sim \left(-\xi\right)^{2-3p}, \quad H(\xi) \sim \left(-\xi\right)^{2p}, \quad a(\xi) \sim \left(-\xi\right)^{p-1}. \tag{116}$$

In particular, the channel width is constant at $p = 2/3$, expands for $p < 2/3$, and contracts when $p > 2/3$.

To change qualitatively the $F(\xi)$ behavior, $\mu(\xi)$ should be greater. For example, if $\mu(\xi) = b(-\xi)^\beta$ with $-1 < \beta < 0$, then NI $F = F_0(\xi) \approx \mu(\xi)$, and

$$F(\xi) = \mu(\xi) + \frac{1}{F(\xi)}\frac{\mathrm{d}F}{\mathrm{d}\xi} \approx b(-\xi)^\beta - \frac{\beta}{\xi}$$

approaches NI when $\xi \to -\infty$. And in the limiting case $\beta \to 0$ we obtain $F_0(\xi) =$ const and the trajectories $F = F(\xi)$ shown in Fig. 21a.

Similarly, for the supercritical trajectory going through the point $(\xi_2,\ f_2)$ into the $\xi < \xi_2$ domain, Eq. (115) shows that if the integral $I_{f-}(\xi_2)$ converges (see Eq. (114)) then $a(\xi) \to a_{2-} = \text{const} > 0$, and relations (108) are fulfilled. If, conversely, it diverges and $\mu(\xi) = q/\xi$ with $q > -\frac{1}{3}$, then we obtain $f(\xi) = \left[-(q+\frac{1}{3})/\xi\right]^{-1/3}$ and

$$\begin{aligned} U(\xi) &\sim \left(-\xi\right)^{q+2/3}, \quad W(\xi) \sim \left(-\xi\right)^{-(3q+2/3)}, \\ H(\xi) &\sim \left(-\xi\right)^{2q}, \quad a(\xi) \sim \left(-\xi\right)^{q+1/3}. \end{aligned} \tag{117}$$

Finally, when $|\mu(\xi)|$ is greater, $f(\xi)$ approaches NI $f = f_0(\xi)$ as $\xi \to -\infty$.

## 9 C–class RL Flows

### *9.1 The Distinctive Features of C-Class Flows*

The similarities and differences in the behavior of C-class and B-class flows are determined by the similarities and differences between Eqs. (86) and (87). Equation (86) is homogeneous in the velocities $c$ and $U$, and the constant $\mathcal{B}$ has the dimension of inverse length, whereas Eq. (87) does not have this property, and $\mathcal{C}$ has the dimension of acceleration. Therefore, in the C-class the dimensionless variables can be introduced only through the scaling

$$\tilde{\xi} = \mathcal{C}x/c_0^2, \quad \tilde{c} = c/c_0, \quad \tilde{U} = U/c_0, \quad \tilde{a} = a/c_0. \tag{118}$$

Omitting the tildes, we rewrite Eq. (87) in two equivalent forms:

$$\frac{\mathrm{d}a}{\mathrm{d}\xi} = \frac{c(\xi)}{c^2(\xi) - U^2(\xi)} \quad \text{and} \quad \frac{\mathrm{d}(c\,U)}{\mathrm{d}\xi} = \frac{2\,c^{3/2}(\xi)U^{1/2}(\xi)}{c^2(\xi) - U^2(\xi)}\,. \tag{119}$$

The right-hand side of the second Eq. (119) is singular for $U = c$, $U = 0$, $c = 0$ as well as for the unbounded growth of $U(\xi)$ or $c(\xi)$. To understand whether these singularities are attainable at a finite $\xi$, we rewrite the first Eq. (119) in the form

$$\frac{\mathrm{d}}{\mathrm{d}\xi}\,\ln a(\xi) = \frac{c^{1/2}(\xi)}{U^{1/2}(\xi)\Big[c^2(\xi) - U^2(\xi)\Big]}\,. \tag{120}$$

It is easy to see that, if $c(\xi)$ is bounded everywhere, i.e., $0 < c(\xi) < \infty$, then not only can $U = c$ be reached at a finite $\xi$, as in the B-class of flows, but also $U = 0$ can be reached at some other finite point $\xi$, whereas $U = \infty$ can be attained only asymptotically, when $\xi \to -\infty$. Similarly, $c = 0$ and $c = \infty$ are attainable only asymptotically.

It is easily shown that in the neighborhood of the critical point $U = c$ the class-C flows have the same behavior as the B-class ones. But the singularity $U = 0$ at some finite $\xi = \xi_U$ is the distinctive property of the C class. Near this point, we set $c(\xi) = c_U + c'_U(\xi - \xi_U) + \ldots$ and obtain using Eq. (119)

$$\frac{\mathrm{d}}{\mathrm{d}\xi}\Big(cU\Big)^{1/2} = \frac{c}{c^2 - U^2} \approx c^{-1} \implies \Big(cU\Big)^{1/2} = \frac{\xi - \xi_U}{c_U}\left[1 - \frac{c'_U}{2c_U}\,(\xi - \xi_U) + \ldots\right],$$

so that when $\xi \to \xi_U + 0$

$$\begin{aligned} &U(\xi) = \frac{(\xi - \xi_U)^2}{c_U^3}\left[1 - \frac{2c'_U}{c_U}\,(\xi - \xi_U) + \ldots\right], \\ &F(\xi) \sim (\xi - \xi_U), \quad \text{and} \quad W(\xi) \sim (\xi - \xi_U)^{-2}. \end{aligned} \tag{121}$$

For further analysis, it is convenient to rewrite Eq. (119) in terms of the Froude numbers $F(\xi)$ and $f(\xi)$ (see Eq. (100)):

$$c^2(\xi)\,\frac{\mathrm{d}F}{\mathrm{d}\xi} = \frac{1}{1 - F^4(\xi)} - M(\xi)F(\xi), \tag{122}$$

$$c^2(\xi)\,\frac{\mathrm{d}f}{\mathrm{d}\xi} = \frac{f^6(\xi)}{1 - f^4(\xi)} + M(\xi)f(\xi), \tag{123}$$

$$c(\xi)\,\frac{\mathrm{d}a}{\mathrm{d}\xi} = \frac{1}{1 - F^4(\xi)} \quad = \quad \frac{f^4(\xi)}{f^4(\xi) - 1}\,, \tag{124}$$

where

$$M(\xi) = c(\xi)\,\frac{\mathrm{d}c}{\mathrm{d}\xi} \equiv \frac{\mathrm{d}}{\mathrm{d}\xi}\left(\frac{c^2(\xi)}{2}\right) \equiv \frac{g}{2}\,\frac{\mathrm{d}H(\xi)}{\mathrm{d}\xi} \tag{125}$$

is determined by the variation of the flow depth. It is convenient to present solutions of these equations as a set of trajectories (the phase portrait) on the half-plane $(\xi,\ F)$ or $(\xi,\ f)$ (recall that functions $F$ and $f$ are positive).

As a useful illustration, consider flows of constant depth where the wave speed is also constant, $c(\xi) = c_0$. Setting $c_0 = 1$ and integrating Eq. (122), we arrive at the algebraic equation

$$F^5(\xi) - 5F(\xi) + 5(\xi - \xi_0) = 0, \qquad \xi_0 = \text{const}.$$

If $\xi \le \xi_* = \xi_0 + 4/5$, it has two positive roots $F_\pm(\xi)$ which merge into one double root $F = 1$ at $\xi = \xi_*$. In the vicinity of the point $\xi_*$ these solutions are

$$F_\pm(\xi) = 1 \pm \left[\frac{1}{2}\Big(\xi_* - \xi\Big)^{1/2}\right] - \frac{1}{4}\Big(\xi_* - \xi\Big) + \ldots \tag{126}$$

The bigger root, $F_+ > 1$, grows indefinitely when $\xi$ decreases from $\xi_*$ up to minus infinity, whereas the smaller root, $F_- < 1$, changes its sign at $\xi = \xi_0$

$$F_-(\xi) = \xi - \xi_0 + \frac{1}{5}(\xi - \xi_0)^5 + \ldots, \tag{127}$$

so that, for $\xi < \xi_0$ there is only a single positive root.

Thus, in C-class, subcritical flows of constant depth (as opposed to those of B-class) remain RL only within a finite interval of $\xi$, $\xi_0 < \xi < \xi_*$, and supercritical flows are RL on the semi-axis $\xi < \xi_*$ (see Fig. 25 and compare it with Fig. 20). Let us find the conditions under which these restrictions are absent for some part of the trajectories.

## 9.2 Global Trajectories and Asymptotic Behavior

For a subcritical trajectory to be unbounded in $\xi$, i.e. to be global, it must reach neither $F = 1$ when $\xi$ increases, nor $F = 0$ when $\xi$ decreases. Thus, the task is split into two parts. Let us find first the conditions under which a trajectory is not bounded from the right. As in the B-class flows, reaching the value $F = 1$ can only be prevented by the presence of NI separating regions with opposite signs of the right-hand side of Eq. (122). NI is described by the equation

$$G(F_0) = F_0^5(\xi) - F_0(\xi) = -M^{-1}(\xi), \tag{128}$$

which has two positive roots, $0 < F_{0_-}(\xi) \le F_{0_+}(\xi) < 1$ if (see Fig. 26a)

$$M(\xi) \ge M_c = \frac{5^{5/4}}{4} \approx 1.8692. \tag{129}$$

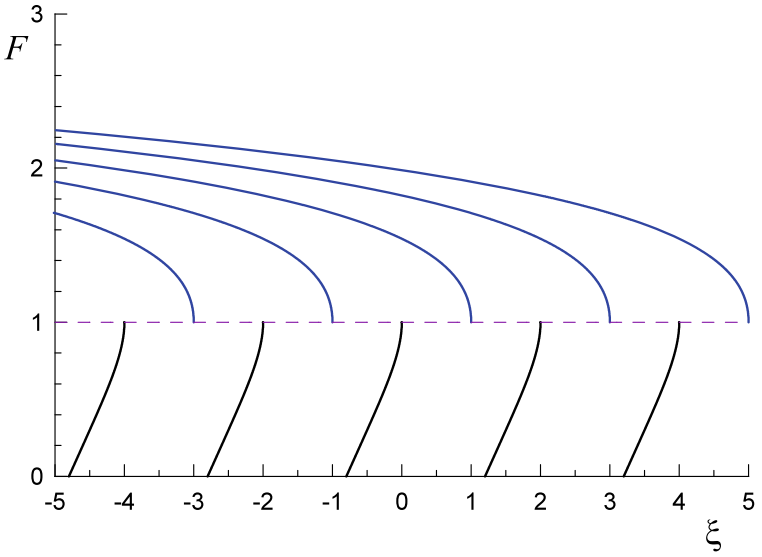


**Fig. 25** (color online) Phase portrait of C-class flows of constant depth in subcritical ($F < 1$) and supercritical ($F > 1$) domains

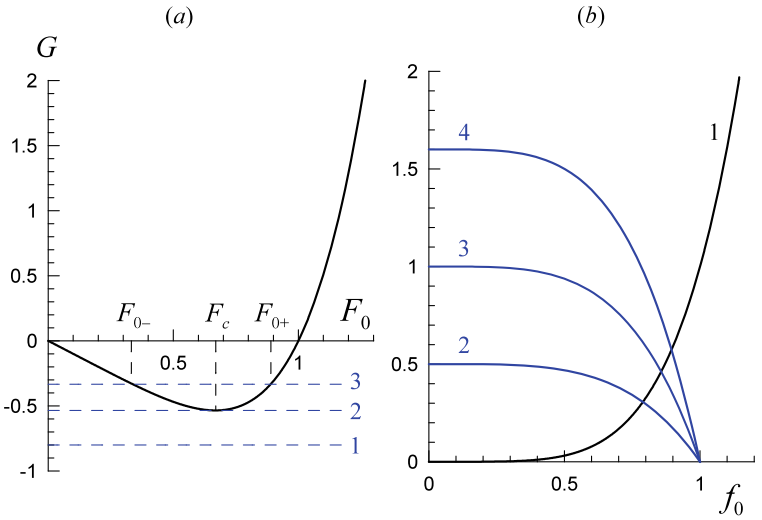


**Fig. 26** (color online) Roots of equations for null isoclines: **a** Eq. (128): dashed lines 1—$M = 1.25$, 2—$M = M_c$ and 3—$M = 3$; **b** Eq. (136): the left-hand side (curve 1) and the right-hand side for $M = -0.5$ (curve 2), $M = -1$ (curve 3), and $M = -1.6$ (curve 4)

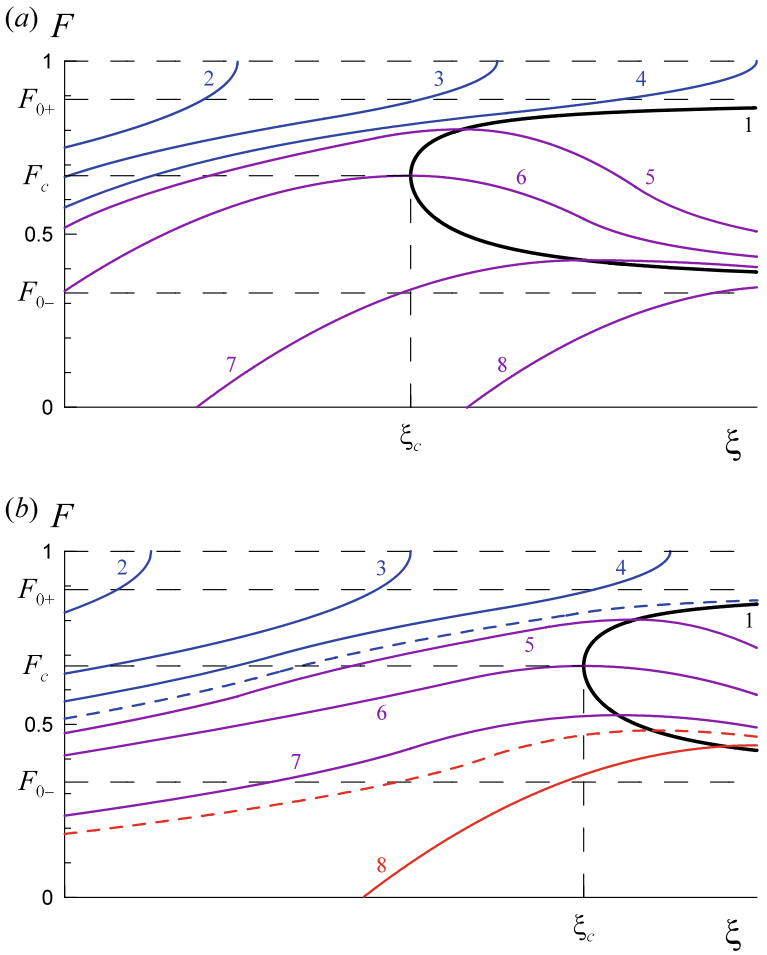


**Fig. 27** (color online) The subcritical part of the phase portrait of Eq. (128) for $M_0 = 3$. **a** NI (curve 1) and surrounding trajectories, bounded (curves 2–4) and unbounded (curves 5–8) on the right; trajectories 7 and 8 are bounded from the left by the singularity $F = 0$. **b** Bounded (curves 2–4 and 8) and global (curves 5–7) trajectories in the presence of a NI (curve 1) and with inequality (135) fulfilled; blue and red dashed lines show the boundaries of the bundle of global trajectories

Thus, in the subcritical region, NI appears only at a sufficiently large depth gradient as a result of the merger of two complex conjugate roots of Eq. (128). NI has two branches that cannot extend far to the left. Indeed, if $c(\xi_1) = c_1 > 0$ and $M(\xi) \geq M_c$ for $\xi < \xi_1$ then, with decreasing $\xi$, we will inevitably arrive at the singularity $c = 0$ ($H = 0$) for a finite $\xi$.

Let us assume that $M(\xi) = M_c$ at $\xi = \xi_c$ and grows monotonically for $\xi > \xi_c$. Then NI branches, $F = F_{0\pm}(\xi)$, start in the point $\xi = \xi_c$ and each monotonically tends to its own limit (see Fig. 27). The slope of the trajectories is negative between

the branches and positive outside. Therefore, trajectories passing above $F_{0+}(\xi)$ end up reaching $F = 1$ at finite $\xi$. But any trajectory that crosses any branch remains between them up to $\xi = +\infty$, i.e. is not bounded on the right, as well as all trajectories lying below it (see Fig. 27a).

Monotonic growth of $M(\xi)$ does not require so fast an increase in depth. In the borderline case, when $M(\xi)$ tends to the finite limit $M_0 > M_c$ when $\xi \to +\infty$,

$$H(\xi) \sim M_0\xi, \quad F(\xi) \to F_{0-} > 0, \quad U(\xi) \approx F_{0-}^2 c(\xi) \sim \xi^{1/2}, \quad W(\xi) \sim \xi^{-3/2}, \tag{130}$$

that is, the flow and wave velocities grow in the same way, and the channel is narrowed.

If $M(\xi)$ grows with no limit then $F_{0-}(\xi) \approx M^{-1}(\xi) \to 0$. Consider the trajectory passing through the point $(\xi_3,\ F_3)$ into the $\xi > \xi_3$ region and denote $c_3 = c(\xi_3)$ and $a_3 = c_3 F_3$. From Eq. (123) we find

$$a(\xi) = a_3 + \int_{\xi_3}^{\xi} \frac{\mathrm{d}y}{c(y)[1 - F^4(y)]} = a_3 + \frac{1}{1 - F^4(\xi_d)} \int_{\xi_3}^{\xi} \frac{\mathrm{d}y}{c(y)}, \tag{131}$$

where $\xi_d$ is between $\xi_3$ and $\xi$, and see that the integral $I_{F+}(\xi)$ (see Eq. (112)) again plays a crucial role. If it converges, $a(\xi)$ tends to $a_{3+} > 0$ as $\xi \to +\infty$, and relations (108) are fulfilled. If $c(\xi)$ grows more slowly than $\xi$, e.g., $\xi^p$ with $\frac{1}{2} \le p < 1$, the integral diverges and

$$a(\xi) \sim \xi^{1-p}, \quad F(\xi) \sim \xi^{1-2p}, \quad U(\xi) \sim \xi^{2-3p}, \quad W(\xi) \sim \xi^{p-2}, \quad H(\xi) \sim \xi^{2p}. \tag{132}$$

At $p = 1/2$ these relations turn to Eq. (130), and when $p < 1/2$, NI disappears and all trajectories become bounded on the right.

Consider now the continuation of the trajectory passing through the point $(\xi_3,\ F_3)$ to the left, into the region $\xi < \xi_3$. For $a(\xi)$ not to vanish (together with $F(\xi)$) at some finite $\xi$, the integral $I_{F-}(\xi_3)$ must converge and provide a positive limiting value $a_{3-}$ for $a(\xi)$ when $\xi \to -\infty$. Since $M(\xi) < 0$ and $F(\xi)$ grows monotonically, the following inequalities hold:

$$a_3 - \frac{I_{F-}(\xi_3)}{1 - F_3^4} < a_{3-} < a_3 - I_{F-}(\xi_3).$$

For an unlimited continuation of the trajectory to the left, it is necessary that

$$a_3 \equiv c_3 F_3 > I_{F-}(\xi_3). \tag{133}$$

Because $\max\left[F(1 - F^4)\right] = M_c^{-1}$ at $F = F_c = 5^{-1/4}$, we obtain the condition

$$c_3 \ge M_c\, I_{F-}(\xi_3), \tag{134}$$

sufficient for the trajectory passing through the point $(\xi_3,\ F_c)$ to continue with no limit to the left as well. Together with this trajectory, all the above-lying (with $F_3 > F_c$) and some part of the below-lying (with $F_3 < F_c$) trajectories also continue with no limit to the left. The condition (133) cuts off low-lying trajectories which inevitably reach $F = 0$ at some finite $\xi$ (curves 7 and 8 in Fig. 27a and curve 8 in Fig. 27b).

Thus, we see that, for the existence of global subcritical flows of C class, the flow depth $H(\xi)$ must increase indefinitely both to the left (faster than $\xi^2$), for the inequality

$$c(\xi_c) \geq M_c\, I_{F-}(\xi_c), \tag{135}$$

to be hold, and to the right (faster than $M_c\xi$) to ensure the monotonic growth of $M\xi$) for $\xi > \xi_c$, which is necessary to maintain NI. When these conditions are met, the set of global trajectories forms a bundle of trajectories strung on the trajectory passing through the point $(\xi_c,\ F_c)$ (in Fig. 27b the bundle boundaries are shown by dashed lines).

Note that for $M(\xi) > 0$ all trajectories in the supercritical part of the phase portrait ($F > 1$) are bounded on the right by the singularity $F = f = 1$, as in Fig. 20. Global supercritical trajectories can arise if, to the right of some point $\xi_m \geq -\infty$, function $c(\xi)$ decreases monotonically (i.e., $M(\xi) < 0$) that leads to the appearance of NI $f = f_0(\xi)$ described, according to Eq. (123), by the equation

$$f_0^5(\xi) = -M(\xi)\Big[1 - f_0^4(\xi)\Big]. \tag{136}$$

As seen in Fig. 26b, for any $M < 0$ there is one positive root $f_0 < 1$ such that

$$f_0(\xi) = \Big[-M(\xi)\Big]^{1/5} + \tfrac{1}{5}\,M(\xi) + O(|M|^{9/5}), \quad (-M) \ll 1, \tag{137}$$

$$f_0(\xi) = 1 + \tfrac{1}{4}\,M^{-1}(\xi) + O(M^{-2}), \quad (-M) \gg 1. \tag{138}$$

The existence of global solutions and the asymptotic behavior of $f(\xi)$ depend on the convergence of integrals (114). For the trajectory passing through the point $(\xi_4,\ f_4)$, we write Eq. (124) in the form

$$c(\xi)\,\frac{\mathrm{d}a}{\mathrm{d}\xi} = -\frac{f^4(\xi)}{1 - f^4(\xi)} = -\frac{c^4(\xi)}{a^4(\xi)[1 - f^4(\xi)]}$$

and integrate it

$$a^5(\xi) \equiv \left[\frac{c(\xi)}{f(\xi)}\right]^5 = a^5(\xi_4) - 5\int_{\xi_4}^{\xi} \frac{c^3(y)\mathrm{d}y}{1 - f^4(y)} = \left[\frac{c(\xi_4)}{f_4}\right]^5 - \frac{5}{1 - f^4(\xi_f)}\int_{\xi_4}^{\xi} c^3(y)\mathrm{d}y, \tag{139}$$

where $\xi_f$ is between $\xi_4$ and $\xi$. The trajectory will be global if the integral $I_{f+}(x_4)$ converges and $f_4$ is small enough for positiveness of the limit $a_{4+}^5$ of the right-hand side of Eq. (139) when $\xi \to +\infty$. Then $a(\xi) \to a_{4+}$, and relations (108) are valid.

For $\xi \to -\infty$, all trajectories are unlimited, but the behavior of function $f(\xi))$ depends on the convergence of the integral $I_{f-}(x_4)$. If it converges, $a(\xi) \to a_{4-} > 0$, and relations (108) hold. If it diverges and, for example, $c(\xi) \sim (-\xi)^q$ with $-1/3 < q < 1/2$, then

$$\begin{array}{ll} a(\xi) \sim (-\xi)^{(1+3q)/5}, & f(\xi) \sim (-\xi)^{(2q-1)/5}, \\ U(\xi) \sim (-\xi)^{(2+q)/5}, & W(\xi) \sim (-\xi)^{-(2+11q)/5}. \end{array} \tag{140}$$

For $q > 0$, we have $M(\xi) \sim -q(-\xi)^{2q-1} < 0$, and NI $f = f_0(\xi) \approx M^{1/5}(\xi)$ appears, to which $f(\xi)$ tends asymptotically. And when $q \geq 1/2$, they both tend to a finite non-zero limit, so that, in this case, we have for $\xi \to -\infty$

$$a(\xi) \sim U(\xi) \sim c(\xi), \quad W(\xi) \sim c^{-3}(\xi), \quad H(\xi) \sim c^2(\xi). \tag{141}$$

Let us describe in more detail the phase portrait of flows with the depth decreasing in such a manner that $M(\xi) < 0$ monotonically increases. Let $M(\xi)$ has a negative (finite or infinite) limit $M_-$ when $\xi \to -\infty$, whereas $M(\xi)$ goes to zero when $\xi \to +\infty$ faster than $\xi^{-5/3}$ to secure the existence of global trajectories. Then NI $f_0(\xi)$ decreases monotonically from $f_0(M_-)$ (see Fig. 26b) to zero. Each trajectory lying above NI or intersecting it is bounded on the right, but there are also global trajectories that lie entirely below NI and approach it from below as $\xi \to -\infty$ (see Fig. 28a).

Since $M(\xi) < 0$, in the subcritical part of the phase portrait ($f > 1$, $F < 1$) all trajectories are bounded on the right by the singularity $F = f = 1$. Suppose, however, that for some $\xi_3$ condition (134) is satisfied, so that there are trajectories that are unbounded from the left. From underlying trajectories, bounded on both sides, they are separated by a separatrix. For greater clarity, this part of the phase portrait is shown in Fig. 28b in coordinates $(\xi,\ F)$.

## 10 Discussion and Conclusion

Thus, in this chapter, we have studied some specific features of long surface waves propagating in the inhomogeneous environment, in canals with a variable cross-section and spatially varying current. In a particular case, the canal can be unbounded in width.

We have analyzed two classes of related problems. Firstly, we considered the mutual transformation of co- and counter-current propagating waves and calculated the transformation coefficients, that is, the reflection and transmission coefficients. It has been shown that in super-critical flows with $U > c$, the transmission coefficient can be greater than unity which means that the transmitted wave can be amplified by

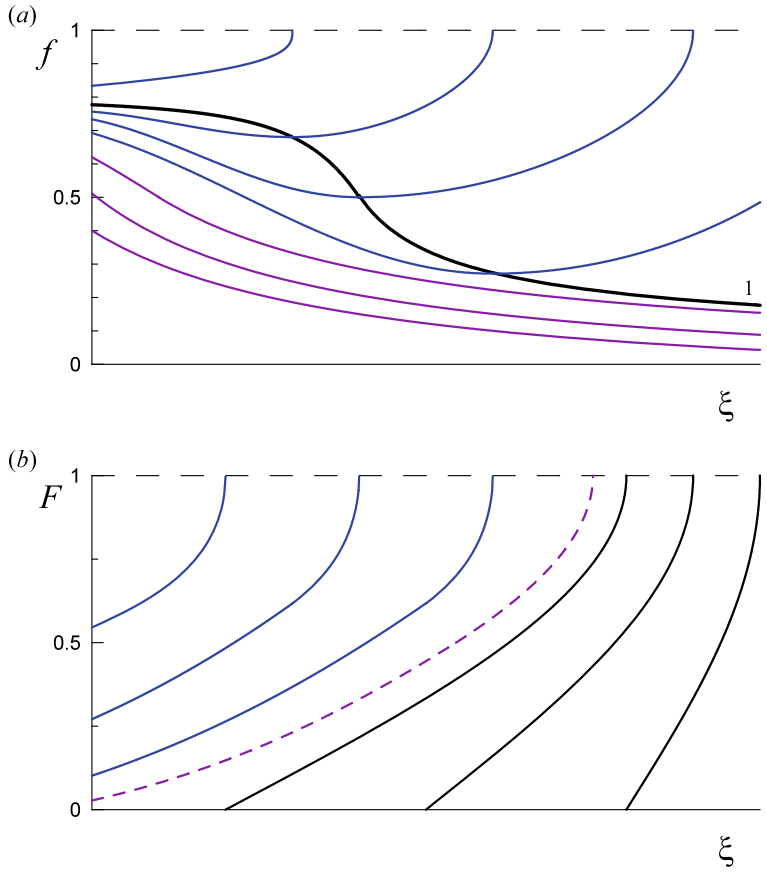


**Fig. 28** (color online) Qualitative view of the phase portrait for $M(\xi) < 0$: **a** the supercritical part ($f < 1$, $f_0(M_-) = 0.8$), line 1 is the NI; **b** the subcritical part ($F < 1$), the dashed line shows the separatrix

a current. This phenomenon is related to the existence of negative energy waves. The coefficient of amplification has been calculated. The most interesting phenomena in such a case are the wave transformation in currents that transit from sub- to supercritical regime and vice versa.

Secondly, we have shown that in spatially inhomogeneous flows of specific configurations, the linear waves can propagate in opposite (co-current and counter-current) directions independently, without reflection. We have found that there are three classes of RL flows, both sub- and supercritical, and have studied their properties in detail. It is interesting to note that for the A-class flows the critical point $U = c$ is not a singular one, whereas the B- and C-class flows can be either sub-critical or supercritical. However, under certain conditions, each class contains global flows.

The phenomenon of reflectionless propagation in inhomogeneous media is well-known in general (see, for example, [5, 6, 12, 15, 16, 24, 25] and references therein); here we have generalized it to moving fluids. The practical importance of such a regime is related to the possibility of the most efficient energy transport which can have, however, both positive and negative effects depending on the particular situation.

**Acknowledgements** SC acknowledges the financial support from the Ministry of Science and Higher Education of the Russian Federation (subsidy No. 075-GZ/C3569/278). YS acknowledges the funding of this study from the State Task Programme in the sphere of scientific activity of the Ministry of Science and Higher Education of the Russian Federation (project No. FSWE-2023-0004).
Data Availability: Any data related to this paper are available upon request from one of the authors (SC).

## References

1. V. M. Babich and V. S. Buldyrev, Asymptotic Methods in the Short-Wave Diffraction Problems (Springer, 2011).
2. V. V. Babikov, The Phase-Function Method in Quantum Mechanics (Nauka, Moscow, 1976, in Russian).
3. C. M. Bender and S. A. Orszag, Advanced Mathematical Methods for Scientists and Engineers (McGraw-Hill, New York, 1978).
4. D. I. Blokhintsev, Acoustics of Moving Inhomogeneous Media (Taylor & Francis, 1998).
5. L. M. Brekhovskikh and O. A. Godin, Acoustics of Layered Media, v. 1 (Springer-Verlag, 1990).
6. L. M. Brekhovskikh and O. A. Godin, Acoustics of Layered Media, v. 2 (Springer-Verlag, 1992).
7. F. Calogero, Variable Phase Approach to Potential Scattering (Academic Press, New York, 1967).
8. S. Churilov, A. Ermakov, and Y. Stepanyants, Wave scattering in spatially inhomogeneous currents, Phys. Rev. D 96, 064016 (2017).
9. S. Churilov and Y. Stepanyants, Hydrodynamic models of astrophysical wormholes. The general concept, Phys. Fluids 33, 077121 (2021).
10. S. M. Churilov and Y. A. Stepanyants, Reflectionless wave propagation on shallow water with variable bathymetry and current, J. Fluid Mech. 931, A15 (2022).
11. S. M. Churilov and Y. A. Stepanyants, Reflectionless wave propagation on shallow water with variable bathymetry and current. Part 2, J. Fluid Mech. 939, A15 (2022).
12. I. Didenkulova, E. Pelinovsky, and T. Soomere, Long surface wave dynamics along a convex bottom, J Geophys. Res. – Oceans 114, C07006 (2009). https://doi.org/10.1029/2008JC005027.
13. A. Ermakov and Y. Stepanyants, Transformation of long surface and tsunami-like waves in the ocean with a variable bathymetry. Pure Appl. Geophys. 177, 1675–1693 (2020).
14. A. L. Fabrikant and Yu. A. Stepanyants, Propagation of Waves in Shear Flows (World Scientific, Singapore, 1998).
15. V. L. Ginzburg, The Propagation of Electromagnetic Waves in Plasmas (Pergamon Press, 1970).
16. R. Grimshaw, E. Pelinovsky, and T. Talipova, Non-reflecting internal wave beam propagation in the deep ocean, J. Phys. Oceanogr. 40 (4), 802–813 (2010).

17. Yu. A. Kravtsov and Yu. I. Orlov, Geometrical Optics of Inhomogeneous Media (Springer-Verlag, 1990).
18. L. D. Landau and E. M. Lifshitz, Fluid Mechanics (Butterworth-Heinemann, Burlington, MA, 1987).
19. L. D. Landau and E. M. Lifshitz, Quantum Mechanics (Pergamon Press, 1965).
20. V. P. Maslov, The Complex WKB Method in Nonlinear Equations I: Linear Theory, (Birkhäuser, 1994).
21. M. E. McIntyre, On the "wave momentum myth", J. Fluid Mech. 106, 331–347 (1981).
22. F. W. J. Olver, Asymptotics and Special Functions (Academic Press, New York and London, 1974).
23. L. A. Ostrovsky, S. A. Rybak, and L. Sh. Tsimring, Negative energy waves in hydrodynamics, Sov. Phys. Uspekhi 29 (11) 1040–1052 (1986).
24. E. Pelinovsky, I. Didenkulova, E. Shurgalina, and N. Aseeva, Nonlinear wave dynamics in self-consistent water channels, J. Phys. A: Math. Theor. 50, 505501 (2017).
25. E. Pelinovsky, O. Kaptsov, Travelling waves in shallow seas of variable depth, Symmetry 14 (7), 1448 (2022).
26. C. Peloquin, L.-P. Euvé, T. Philbin, and G. Rousseaux, Analog wormhole and black hole laser effects in hydrodynamics, Phys. Rev. D 93 084032 (2016).
27. J. J. Synge, Geometrical Optics. An Introduction into Hamilton's Method (Cambridge University Press, 1937).

# Factorization Conditions for Nonlinear Second-Order Differential Equations


**G. González, H. C. Rosu, O. Cornejo-Pérez, and S. C. Mancas**

**Abstract** For the case of nonlinear second-order differential equations with a constant coefficient of the first derivative term and polynomial nonlinearities, the factorization conditions of Rosu & Cornejo-Pérez are approached in two ways: (i) by commuting the subindices of the factorization functions in the two factorization conditions and (ii) by leaving invariant only the first factorization condition achieved by using monomials or polynomial sequences. For the first case the factorization brackets commute and the generated equations are only equations of Ermakov-Pinney type. The second modification is non commuting, leading to nonlinear equations with different nonlinear force terms, but the same first-order part as the initially factored equation. It is illustrated for monomials with the examples of the generalized Fisher and FitzHugh-Nagumo initial equations. A polynomial sequence example is also included.

G. González
Cátedra CONAHCYT–Universidad Autónoma de San Luis Potosí, San Luis Potosí 78000, Mexico
e-mail: gabriel.gonzalez@uaslp.mx

Coordinación para la Innovación y la Aplicación de la Ciencia y la Tecnología, Universidad Autónoma de San Luis Potosí, San Luis Potosí 78000, Mexico

H. C. Rosu
IPICyT, Instituto Potosino de Investigación Científica y Tecnológica, Camino a la presa San José 2055, Col. Lomas 4a Sección, 78216 San Luis Potosí, S.L.P., Mexico
e-mail: hcr@ipicyt.edu.mx

O. Cornejo-Pérez
Facultad de Ingeniería, Universidad Autónoma de Querétaro, Centro Universitario Cerro de las Campanas, 76010 Santiago de Querétaro, Mexico
e-mail: octavio.cornejo@uaq.mx

S. C. Mancas (✉)
Department of Mathematics, Embry-Riddle Aeronautical University,
Daytona Beach 32114-3900, USA
e-mail: mancass@erau.edu



S. Manukure and W.-X. Ma (eds.), *Nonlinear and Modern Mathematical Physics*,
Springer Proceedings in Mathematics & Statistics 459,
https://doi.org/10.1007/978-3-031-59539-4_3

**Keywords** Nonlinear second-order differential equation · Factorization condition · Generalized Fisher equation · FitzHugh-Nagumo equation · Implicit solution

## 1 Introduction

Many dynamical systems in mechanics and in physics in general are described by non linear second order differential equations or evolve under the action of internal forces with small non-linear components, especially during external forcing or along the relaxing stage after the forcing has been canceled. In their homogeneous form,

$$\frac{d^2x}{dt^2} + \gamma(x)\frac{dx}{dt} + f(x) = 0\,, \tag{1}$$

these equations are traditionally known in the literature as Liénard equations [1–3], although in the case of the constant parameter $\gamma(x) = \gamma$, they may be considered as of Duffing type, because the Duffing oscillator corresponding to $\gamma > 0$ and $f(x) = r_1 x + r_2 x^3$, with $r_1$ and $r_2$ two real constants, is a representative example. The simplest physical description of (1) in the latter case is that of a particle attached to a spring which provides a restoring force which is close to linear, i.e., $r_1 > 0$ and $|r_2| \ll 1$. Two types of springs can be introduced, known as soft and hard [4], for $r_2 < 0$ and $r_2 > 0$, respectively. In the case of soft springs, in the extension phase the restoring force becomes progressively weaker than for the linear spring. The hard springs which become stiffer than the linear one while increasing the extension are less frequent.

Moreover, if one goes beyond mechanical oscillators and nonlinear electronic circuits, one comes across a second important and widespread category of equations of constant $\gamma$ coefficient which are obtained by the travelling wave reduction of reaction-diffusion equations and nonlinear evolution equations. In such cases, the coefficient $\gamma$ that we denote by $\nu$ is the constant velocity of the travelling fronts [5]. The nonlinear force $f$ covers the phenomenology due to (bio)chemical reactions or any process capable of producing new components.

A simple way to obtain particular solutions of these non linear second order differential equations consists in using the factorization method, where the second-order differential operator

$$D^2 + \gamma(x)D + \frac{f(x)}{x}\,, \qquad D = \frac{d}{dt}\,, \tag{2}$$

is factored in terms of two different first-order differential operators in the operatorial form of Eq. (1)

$$\left(D - \phi_2(x)\right)\left(D - \phi_1(x)\right)x = 0\,. \tag{3}$$

This may provide particular solutions of (1) by a single quadrature of $(D - \phi_1(x))\, x = 0$. To match the factored operator in (3) to the operator (2), the factoring functions $\phi_i$ should satisfy the conditions

$$\phi_1 + \phi_2 + x\frac{d\phi_1}{dx} = -\gamma \tag{4}$$

$$\phi_1\phi_2 = \frac{f(x)}{x} \tag{5}$$

that have been introduced in 2005 by two of the authors [6, 7]. They applied this kind of factorization to many well-known equations with polynomial nonlinearities by taking additional advantage from the polynomial factorization of the nonlinear part. The second condition shows that $\sqrt{f(x)/x}$ is the geometric mean of the functions $\phi_i$ that can be chosen from combinations of the factors of $f(x)/x$ if $f(x)$ is a polynomial which does not have the zero degree power. This also assures that from (3) one can obtain a particular solution of (1) by the quadrature of $(D - \phi_1(x))\, x = 0$,

$$\int \frac{dx}{x\phi_1(x)} = t - t_0 \tag{6}$$

since $\phi_1$ can be chosen as one of the factors of $f(x)/x$.

Moreover, as in supersymmetric quantum mechanics [8, 9], the reverting of the factorization brackets has been used in [6, 7] to obtain particular solutions of equations with identical operator part, but different polynomial part $\tilde{f}$, of the form

$$\frac{d^2x}{dt^2} + \gamma(x)\frac{dx}{dt} + \tilde{f}(x) = 0\,, \quad \tilde{f}(x) = f(x) + \phi_2(\phi_{1,x} - \phi_{2,x})x^2\,, \tag{7}$$

where the subscript $x$ denotes the derivative with respect to $x$. As well known, the reverting of the factorization brackets in quantum mechanics is equivalent to going to the Darboux-transformed partner equation of a given linear Schrödinger equation and it is also based on the logarithmic derivative connection between the solutions of the Riccati and Schrödinger equations. Such logarithmic connections between the solutions of different nonlinear evolution equations are also well known being a very useful tool for obtaining new analytic solutions [10, 11].

On the other hand, with a different grouping of terms, one can also obtain particular solutions of 'supersymmetric' nonlinear equations of the form

$$\frac{d^2x}{dt^2} + \tilde{\gamma}\frac{dx}{dt} + f(x) = 0\,, \quad \tilde{\gamma} = \gamma + (\phi_{1,x} - \phi_{2,x})x\,, \tag{8}$$

i.e., with the same polynomial nonlinearities, but a different operator part which turns nonlinear in damping. Resorting again to the mechanical and electronic circuit description, Eq. (7) describes springs with additional stiffness, whereas Eq. (8) describes more complicated oscillators that can display positive and negative damp-

ing and chaotic dynamics, such as the cases of Rayleigh's equation of violin strings and van der Pol equation of self-excited valve circuit [4] which are amongst the simplest particular cases of (8).

All these calculus properties have yielded many interesting particular solutions of the kink and soliton type for well-known nonlinear equations obtained by the traveling wave change of variables from evolution equations [6, 7, 12–22] and have been also widely implemented in Matlab and Maple algorithms [23].

In this chapter, we discuss similar nonlinear equations and their particular solutions obtained through some additional conditions and/or modifications of the factorization functions in the factorization conditions (4) and (5) for Eq. (1) of the Duffing type (constant parameter $\gamma(x) = \gamma$) and traveling wave reductions of reaction-diffusion equations with $\gamma = \nu$. Regarding the variable $\gamma$ class, some cases have been presented previously in [7] and their study with the same focus as here is left for future work.

In particular, we will consider here the effect of two types of modifications of the factorization brackets in Eqs. (4) and (5):

- The first modification is performed in a way that keeps invariant the two factorization conditions, which leads to a commutative factorization setting in which the reverting of the factorization brackets does not generate a new equation.
- The second type of modification is by adding a polynomial into the multiplication brackets in such a way that only the first factorization condition is kept invariant which generates a non-commutative factorization.

The chapter is organized as follows. In the second section, the conditions for having a commutative factorization scheme are presented together with some physical examples of this approach. In the third section, a non-commutative factorization which generalizes the Rosu and Cornejo-Pérez factorization is introduced and some examples are presented for illustrative purposes. The conclusions are summarized in the last section.

## 2 Commutative Factorization Setting

We now study the consequences of interchanging the subindexes in the RCP pair of factorization conditions. This is equivalent to adding another pair of conditions obtained by commuting the subindexes in both equations. However, one can instantly find that this is a minimal change since the second factorization condition keeps its form under such an interchange. Therefore, proceeding in this way, we obtain the following triplet of different factorization conditions

$$\phi_1 + \phi_2 + x\frac{d\phi_1}{dx} = -\gamma \tag{9}$$

$$\phi_2 + \phi_1 + x\frac{d\phi_2}{dx} = -\gamma \tag{10}$$

$$\phi_2\phi_1\ (= \phi_1\phi_2) = \frac{f(x)}{x}\ . \tag{11}$$

In this case, by comparing the first two equations, one can see that $d\phi_1/dx = d\phi_2/dx$ implying

$$\phi_2 = \phi_1 + c_0\ , \tag{12}$$

where $c_0$ is an arbitrary real constant. In other words, these extended (commuting) factorization conditions introduce the additional restriction on the factoring functions of being different only by a constant. Furthermore, from (8) one has $\tilde{\gamma} = \gamma$, so that the interchange of the factorization brackets does not produce a new equation in this case. Thus, in factored form, one deals with equations of the type

$$(D - \phi_1 - c_0)(D - \phi_1)x = 0\ , \tag{13}$$

where $\phi_1$ satisfies

$$x\frac{d\phi_1}{dx} + 2\phi_1 = -\gamma - c_0\ , \tag{14}$$

which is obtained by substituting (12) into (9). For constant $\gamma$, (14) implies

$$\phi_1(x) = -\frac{\gamma + c_0}{2} + \frac{\kappa_1}{x^2}\ , \qquad \phi_2(x) = -\frac{\gamma - c_0}{2} + \frac{\kappa_1}{x^2}\ , \tag{15}$$

where $\kappa_1$ is an arbitrary integration constant. Besides, $f(x)$ is obtained from (11) as

$$f(x) = \frac{\gamma^2 - c_0^2}{4}x - \frac{\kappa_1\gamma}{x} + \frac{\kappa_1^2}{x^3}\ . \tag{16}$$

A direct connection, not depending on $\gamma$, between the factoring functions and the nonlinear term $f(x)$ is obtained by substituting (12) in (11)

$$\phi_{1,2} = \frac{\mp c_0 - \sqrt{c_0^2 + 4f(x)/x}}{2}\ . \tag{17}$$

(i) *Case* $\gamma = 0$. For this case, let us take $c_0 = -2a$ and $\kappa_1 = b$ in (15), writing the factorization functions as

$$\phi_1(x) = a + \frac{b}{x^2}\ , \qquad \phi_2(x) = -a + \frac{b}{x^2}\ . \tag{18}$$

These factorization functions provide the standard Ermakov-Pinney differential equation

$$\frac{d^2x}{dt^2} - a^2x + \frac{b^2}{x^3} = 0\,, \tag{19}$$

which admits the following commuting factorizations

$$\left(D \pm a - \frac{b}{x^2}\right)\left(D \mp a - \frac{b}{x^2}\right)x = 0\,, \tag{20}$$

providing two particular solutions from each of the first-order equations

$$\frac{dx}{dt} = \pm ax + \frac{b}{x}\,. \tag{21}$$

For each of the signs of the linear term, these particular solutions are given by

$$x(t) = \pm\sqrt{-\frac{b}{a} + \frac{e^{2a(t+c)}}{a}}\,, \quad x(t) = \pm\sqrt{\frac{b}{a} + \frac{e^{-2a(t-c)}}{a}}\,, \tag{22}$$

respectively, where $c$ is an integration constant. These particular Ermakov solutions correspond to a different nonlinear superposition compared to that of Pinney [24]. If one writes the general Ermakov solution for $d^2x/dt^2 - a^2x + b^2x^{-3} = 0$ in the known form $x_g = \sqrt{\alpha_1 x_1^2 + \alpha_2 x_2^2 + 2\alpha_3 x_1 x_2}$ with the superposition constants $\alpha_i$ of $x_{1,2} = e^{2ac}e^{\pm at}$ related by $\alpha_1\alpha_2 - \alpha_3^2 = -b^2/W^2$, where $W$ is the Wronskian determinant of $x_{1,2}$, then one can see that they correspond to $\alpha_1 = 1/a$, $\alpha_2 = 0$, and $\alpha_3 = b/W$.

Moreover, if $\gamma = 0$, one can obtain the general solution as follows. Substituting $\phi_2 = \frac{f(x)}{\phi_1 x}$ in the first factorization condition, the Abel equation of the second kind [13]

$$x\phi_1\frac{d\phi_1}{dx} + \phi_1^2 + \frac{f(x)}{x} = 0 \tag{23}$$

is obtained, which for $f(x) = -a^2x + b^2/x^3$ has the solution

$$\phi_1(x) = \pm\sqrt{a^2 + \frac{\tilde{\kappa}}{x^2} + \frac{b^2}{x^4}}\,, \tag{24}$$

where $\tilde{\kappa}$ is an integration constant. For $\tilde{\kappa} = \pm 2ab$, one obtains the previous particular cases in Eq. (18). Next, from

$$\frac{dx}{dt} = \phi_1(x)x = \pm\sqrt{a^2x^2 + \tilde{\kappa} + \frac{b^2}{x^2}} \tag{25}$$

for the positive sign, one obtains the solutions

$$x(t) = \pm\frac{1}{2a}\sqrt{e^{2a(t-t_0)} - 2\tilde{\kappa} + (\tilde{\kappa}^2 - 4a^2b^2)e^{-2a(t-t_0)}} \tag{26}$$

whereas for the negative sign, the solutions are

$$x(t) = \pm\frac{1}{2a}\sqrt{e^{-2a(t-t_0)} - 2\tilde{\kappa} + (\tilde{\kappa}^2 - 4a^2b^2)e^{2a(t-t_0)}}\,, \tag{27}$$

all of which are general Ermakov-Pinney solutions. The solutions (22) are obtained for $\tilde{\kappa} = 2ab$ and $t_0 = -\left(c + \frac{\ln(4a)}{2a}\right)$.

(ii) *Case* $\gamma = constant \neq 0$. For this case, the simplest factorization is obtained by setting $\phi_1 = \phi_2 = \phi$ ($c_0 = 0$), making identical the two factorization brackets. In this special case, we have

$$\phi(x) = -\frac{\gamma}{2} + \frac{b}{x^2}\,, \tag{28}$$

which one can easily verify that satisfies the triplet factorization conditions. The obtained second order non linear differential equation is of the following Ermakov-Pinney type

$$\frac{d^2x}{dt^2} + \gamma\frac{dx}{dt} + \frac{\gamma^2}{4}x - \frac{\gamma b}{x} + \frac{b^2}{x^3} = 0\,, \tag{29}$$

or in operatorial form

$$\left(D + \frac{\gamma}{2} - \frac{b}{x^2}\right)^2 x = 0 \tag{30}$$

which yields the particular solutions given by

$$x(t) = \pm\sqrt{\frac{2b}{\gamma} + \frac{e^{-\gamma(t-2c)}}{\gamma}}\,, \tag{31}$$

where $c$ is an integration constant.

Another possible pair of factorization functions for this case is

$$\phi_1(x) = a_1 + \frac{b}{x^2}\,, \qquad \phi_2(x) = -a_2 + \frac{b}{x^2}\,, \tag{32}$$

which generate the following equation

$$\frac{d^2x}{dt^2} + (a_2 - a_1)\frac{dx}{dt} - a_1a_2x - \frac{(a_2 - a_1)b}{x} + \frac{b^2}{x^3} = 0\,. \tag{33}$$

Thus, for $\gamma = a_2 - a_1$, Eq. (33) admits the following commuting factorizations

$$\left(D + a_2 - \frac{b}{x^2}\right)\left(D - a_1 - \frac{b}{x^2}\right) x = 0 \,, \tag{34}$$

$$\left(D - a_1 - \frac{b}{x^2}\right)\left(D + a_2 - \frac{b}{x^2}\right) x = 0 \,, \tag{35}$$

which lead to two particular solutions obtained from

$$\frac{dx}{dt} = a_1 x + \frac{b}{x} \,, \qquad \frac{dx}{dt} = -a_2 x + \frac{b}{x} \,. \tag{36}$$

These solutions are

$$x(t) = \pm\sqrt{\frac{-b}{a_1} + \frac{e^{2a_1(t+c_1)}}{a_1}} \,, \qquad x(t) = \pm\sqrt{\frac{b}{a_2} + \frac{e^{-2a_2(t-c_2)}}{a_2}} \,, \tag{37}$$

respectively; $c_1$ and $c_2$ are integration constants.

In closing this section, we notice that multiplying each of the factorization brackets by an exponential factor in the independent variable,

$$e^{\pm c_0 t}\,(D - \phi_1)\, e^{\pm c_0 t}\,(D - \phi_1)\, x = 0 \,, \tag{38}$$

is another way of producing the triplet of commuting factorization conditions. However, in this case, only the constants $\pm c_0$ are introduced in the factorization brackets.

## 3 Non-commutative Factorization Setting

We move now to the study of additive extensions of the factorization functions,

$$\tilde{\phi}_1(x) = \phi_1 + \epsilon_1(x) \,, \qquad \tilde{\phi}_2(x) = \phi_2 + \epsilon_2(x) \,, \tag{39}$$

where the $\epsilon$ functions are arbitrary functions so far. Of course, both factorization conditions can change under the additive extension, but to keep a link with the initial equation defined through the $\phi$ factorization functions, we are interested in those $\tilde{\phi}$ functions for which the first factorization condition is satisfied for the same $\gamma$ parameter while the product one is changed to a different nonlinear force $\tilde{f}$,

$$\tilde{\phi}_1 + \tilde{\phi}_2 + x\frac{d\tilde{\phi}_1}{dx} = -\gamma \tag{40}$$

$$\tilde{\phi}_1 \tilde{\phi}_2 = \frac{\tilde{f}(x)}{x} \,. \tag{41}$$

Therefore the factored equation $\left(D-\tilde{\phi}_2\right)\left(D-\tilde{\phi}_1\right)x=0$ is

$$\frac{d^2x}{dt^2}+\gamma\frac{dx}{dt}+\tilde{f}(x)=0\,. \tag{42}$$

The additions $\epsilon_1(x)$ and $\epsilon_2(x)$ are not independent, but related through the following relation

$$\epsilon_1(x)=-\frac{\int\epsilon_2(x)dx}{x}\,, \tag{43}$$

obtained by substituting (39) into (40) and (41), (for zero integration constant). This condition can be fulfilled by power functions or a finite sum of power functions. For the monomial case, $\epsilon_1(x)=-\mathrm{a}x^m$ and $\epsilon_2(x)=\mathrm{a}(m+1)x^m$, $m\in\mathbf{N}$, the nonlinear force $\tilde{f}(x)$ has the expression

$$\tilde{f}_m(x)=\mathrm{a}\big[(m+1)\phi_1-\phi_2\big]x^{m+1}-\mathrm{a}^2(m+1)x^{2m+1}\,. \tag{44}$$

From the physical point of view, it is useful to think of (42) as an equation that replaces (1) under small perturbations of the nonlinear force. In this perturbative context, the most interesting cases are the lowest powers, $m=0$ and $m=1$, which provide the following $\tilde{f}_m(x)$

$$\tilde{f}_0(x)=f(x)+\mathrm{a}(\phi_1-\phi_2-\mathrm{a})x\,, \tag{45}$$

$$\tilde{f}_1(x)=f(x)+\mathrm{a}(2\phi_1-\phi_2)x^2-2\mathrm{a}^2x^3\,. \tag{46}$$

## 3.1 Examples

We illustrate the monomial extension with two cases that are traveling wave frame forms of reaction-diffusion equations and also provide a finite polynomial sequence case. In the traveling wave context, the $\gamma$ parameter is the velocity $\nu$ of the traveling wave.

(1). *The generalized Fisher equation*

The generalized Fisher equation has the form [6]

$$x''+\nu x'+x(1-x^n)=0\,,\quad \nu\neq 0\,,\quad n\geq 1\,, \tag{47}$$

where the primes stand for derivatives with respect to $\zeta=s-\nu t$. In the reaction-diffusion form, the case $n=2$ has been proposed by Fisher as an equation governing the population dynamics in the genetics context of the alleles. It has become over the years the fundamental law of population genetics. The general solution, obtained using *Mathematica*, can be written in terms of Kummer's confluent hypergeometric

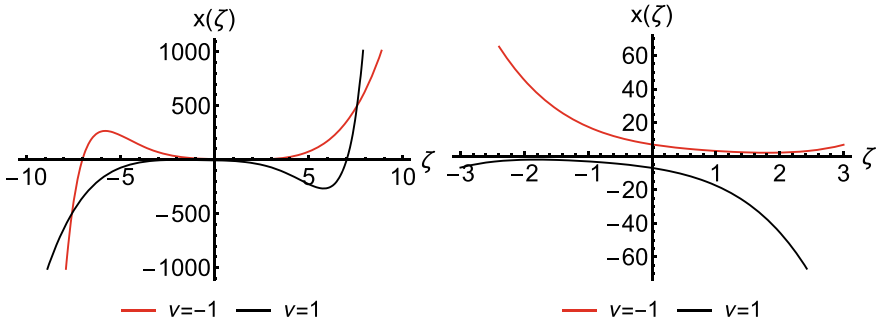


(a) $n = 2; c_1 = 1, c_2 = 0.$ (b) $n = 2; c_1 = -1, c_2 = 0.$

**Fig. 1** Particular solutions obtained from (48) for the values of $n$ and constants of integration as displayed

function of the second kind (the Tricomi function), $U$, as

$$x(\zeta) = \frac{1}{\nu}\left[\frac{\zeta}{\nu} + \frac{\zeta^2}{2} - \frac{\zeta^{n+2}}{n+2} - U(1, n+3; \nu\zeta) + c_1 e^{\nu\zeta}\right] + c_2 \,. \tag{48}$$

where $c_1$ and $c_2$ are integration constants. Plots of particular solutions derived from this general Fisher solution are provided in Fig. 1.

On the other hand, Eq. (47) can be factored with [6]

$$\phi_1 = h_n^{-1}\left(1 - x^{n/2}\right) \,, \qquad \phi_2 = h_n\left(1 + x^{n/2}\right) \,, \qquad h_n^2 = 1 + n/2 \,. \tag{49}$$

for $\nu_n = -\left(h_n + h_n^{-1}\right)$.

The monomially-only-extended factoring functions read

$$\tilde{\phi}_1(x) = h_n^{-1}\left(1 - x^{n/2}\right) - \mathrm{a}x^m \,, \qquad \tilde{\phi}_2(x) = h_n\left(1 + x^{n/2}\right) + \mathrm{a}(m+1)x^m \,, \tag{50}$$

which lead to

$$\tilde{f}(x) = f(x) + \mathrm{a}\left[\frac{m+1}{h_n} - h_n - \mathrm{a}(m+1)x^m - \left(\frac{m+1}{h_n} + h_n\right)x^{n/2}\right]x^{m+1} \tag{51}$$

Using (50), a particular solution of

$$x'' + \nu_n x' + x(1 - x^n) + \mathrm{a}\left[\frac{m+1}{h_n} - h_n - \mathrm{a}(m+1)x^m - \left(\frac{m+1}{h_n} + h_n\right)x^{n/2}\right]x^{m+1} = 0 \,, \tag{52}$$

is obtained from

$$\frac{dx}{d\zeta} - h_n^{-1}\left(1 - x^{n/2}\right)x + \mathrm{a}x^{m+1} = 0 \,, \tag{53}$$

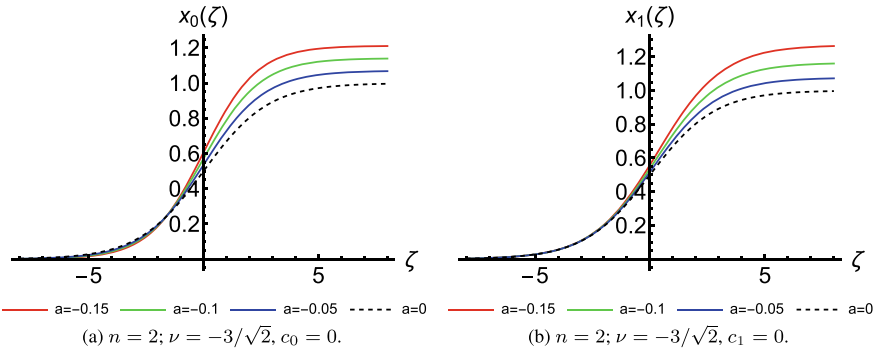


(a) $n = 2; \nu = -3/\sqrt{2}, c_0 = 0.$ (b) $n = 2; \nu = -3/\sqrt{2}, c_1 = 0.$

**Fig. 2** Particular solutions from (55) for negative values of a and the values of $n$, $\nu$, and constants of integration as displayed

as

$$\int \frac{dx}{x(h_n \mathrm{a} x^m - x^{n/2} + 1)} = \frac{1}{h_n} \int d\zeta \,. \tag{54}$$

For $n = 2$ and the cases $m = 0$ and $m = 1$, the quadrature in the latter equation provides the following particular solutions

$$x_0(\zeta) = \frac{1 - \sqrt{2}\mathrm{a}}{2} e^{\frac{1-\sqrt{2}\mathrm{a}}{2}\left(\frac{\zeta}{\sqrt{2}} - c_0\right)} \operatorname{sech} \frac{1 - \sqrt{2}\mathrm{a}}{2} \left(\frac{\zeta}{\sqrt{2}} - c_0\right), \quad x_1(\zeta) = \frac{e^{\frac{\zeta}{\sqrt{2}} - c_1}}{1 + \left(1 + \sqrt{2}\mathrm{a}\right) e^{\frac{\zeta}{\sqrt{2}} - c_1}}, \tag{55}$$

respectively, where $c_0$ and $c_1$ are integration constants. This kind of particular solutions are presented in Fig. 2 and have typical traveling wave front profiles.

The differences between the nonlinear forces for these cases are given by the expressions

$$\Delta f_0(\zeta) = \tilde{f}_0 - f = -\frac{\mathrm{a}}{\sqrt{2}} \left(\sqrt{2}\mathrm{a} + 1 + 3x_0(\zeta)\right) x_0(\zeta) \,, \tag{56}$$

$$\Delta f_1(\zeta) = \tilde{f}_1 - f = -2\mathrm{a}(\mathrm{a} + \sqrt{2}) x_1^3(\zeta) \tag{57}$$

and are plotted in Fig. 3. For small values of the parameter a, they still have the switching profile of the solutions.

(2). *The FitzHugh-Nagumo Equation*

The FitzHugh-Nagumo equation,

$$x'' + \nu x' + f(x) = 0 \,, \qquad f(x) = x(x-1)(\beta - x) \,, \tag{58}$$

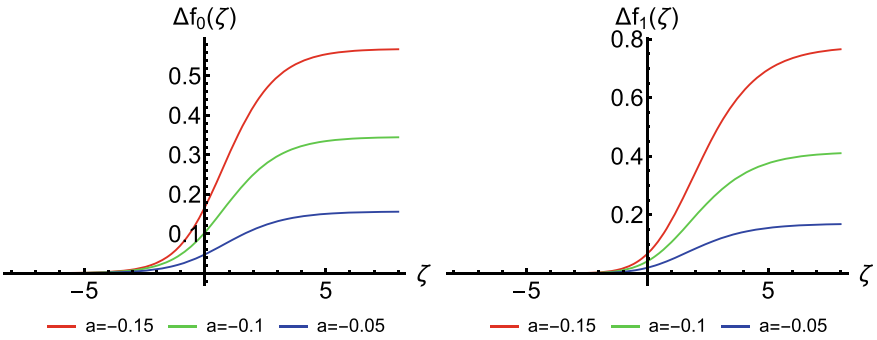


**Fig. 3** Differences between the nonlinear forces as given by (56) and (57), respectively

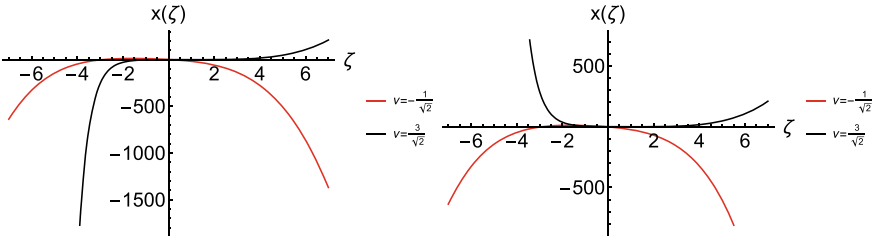


(a) $\beta = \pm 1$; $c_1 = 1$, $c_2 = 0$. (b) $\beta = \pm 1$; $c_1 = -1$, $c_2 = 0$.

**Fig. 4** Particular solutions obtained from (59) for the values of $\beta$ and constants of integration as displayed. The values of $\nu$, $-1/\sqrt{2}$ and $3/\sqrt{2}$, correspond to positive and negative $\beta$, respectively

emerged in a simplified system of two equations modelling the transmission of electrical impulses through a nerve axon with the variable $x$ representing the axon membrane potential. In the homogeneous Eq. (58) the effect of a slow negative feedback on the membrane potential is not taken into account which eliminates the evolution equation of the feedback. The general solution is

$$x(\zeta) = -\frac{1}{\nu}\left[\frac{2p_1(\nu)+\beta\nu^2}{\nu^3}\zeta - \frac{2p_1(\nu)+\beta\nu^2}{\nu^2}\frac{\zeta^2}{2} + \frac{p_1(\nu)}{\nu}\frac{\zeta^3}{3} - \frac{\zeta^4}{4} + \tilde{c}_1 e^{-\nu\zeta}\right] + \tilde{c}_2\,, \quad (59)$$

where $p_1(\nu) = 3 + (\beta+1)\nu$ and $\tilde{c}_{1,2}$ are arbitrary integration constants. Some particular solutions derived from this general Fitz-Hugh-Nagumo solution are plotted in Fig. 4. Their profiles are not very different from the particular Fisher solutions obtained from the general Fisher solution.

For the particular value $\nu_\beta = (1-2\beta)/\sqrt{2}$, Eq. (58) is a particular case of the generalized Burgers-Huxley equation and can be factorized [7] with $\phi_1(x) = (x-1)/\sqrt{2}$ and $\phi_2(x) = \sqrt{2}(\beta - x)$, which we use in the monomially-only-extended factorization functions

$$\tilde{\phi}_1 = \frac{x-1}{\sqrt{2}} - \mathrm{a}x^m \,, \qquad \tilde{\phi}_2 = \sqrt{2}(\beta - x) + \mathrm{a}(m+1)x^m \tag{60}$$

to factorize the equation

$$x'' + \nu_\beta x' + \tilde{f}(x) = 0 \,, \tag{61}$$

where

$$\tilde{f}(x) = f(x) - \mathrm{a}\left(\sqrt{2}\beta + \frac{m+1}{\sqrt{2}}\right)x^{m+1} + \mathrm{a}\left(\sqrt{2} + \frac{m+1}{\sqrt{2}}\right)x^{m+2} - \mathrm{a}^2(m+1)x^{2m+1} \,. \tag{62}$$

A particular solution of (61) is obtained from

$$\frac{dx}{d\zeta} - \frac{1}{\sqrt{2}}(x-1)x + \mathrm{a}x^{m+1} = 0 \tag{63}$$

through the following quadrature

$$\int \frac{dx}{x(x-1-\sqrt{2}\mathrm{a}x^m)} = \frac{1}{\sqrt{2}}\int d\zeta \,. \tag{64}$$

For the $m = 0$ and $m = 1$ cases, the particular solutions are given by

$$x_0(\zeta) = \frac{\sqrt{2}(1+\sqrt{2}\mathrm{a})}{\sqrt{2} - e^{(1+\sqrt{2}\mathrm{a})\frac{\zeta+2c_0}{\sqrt{2}}}} \,, \qquad x_1(\zeta) = \frac{\sqrt{2}}{\sqrt{2}(1-\sqrt{2}\mathrm{a}) - e^{\frac{\zeta+2c_1}{\sqrt{2}}}} \tag{65}$$

respectively, where $c_0$ and $c_1$ are integration constants. These solutions plotted in Fig. 5 are manifestly singular; they blow up at finite traveling variables given by $\zeta_0^*(a) = \ln 2/(\sqrt{2}+2a) - 2c_0$ and $\zeta_1^*(a) = \sqrt{2}\ln[\sqrt{2}(1-\sqrt{2}a)] - 2c_1$, respectively.

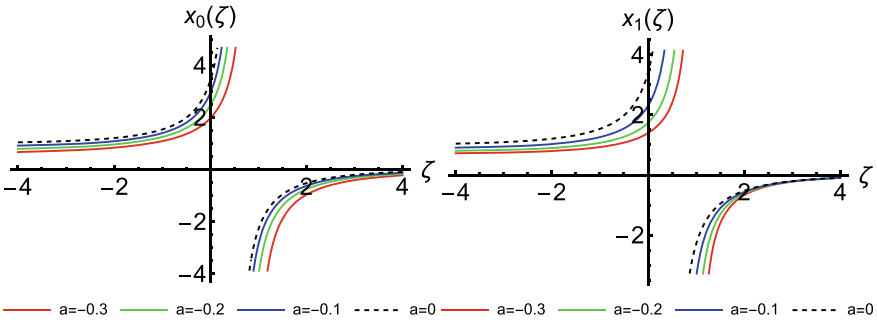


**Fig. 5** Particular solutions as obtained from (65) for zero integration constants and the displayed values of the parameter a

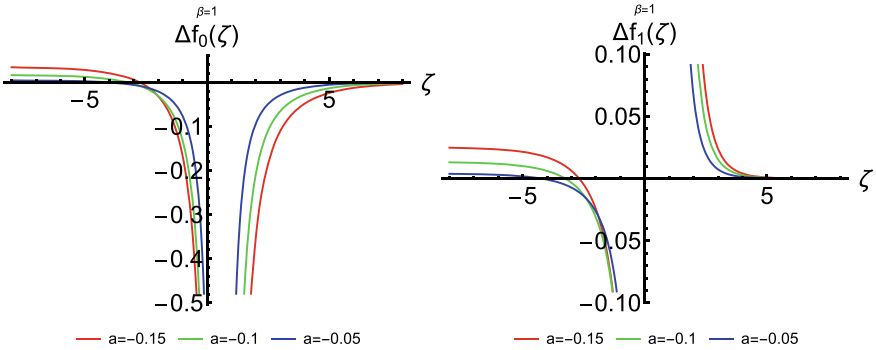


**Fig. 6** Differences between the nonlinear forces as given by (66) and (67), respectively, for the displayed values of the parameters

From (62), one can also obtain the differences between the nonlinear functions of the two equations

$$\Delta f_0(\zeta) = \tilde{f}_0 - f = \frac{\mathrm{a}}{\sqrt{2}}\left[3x_0(\zeta) - 2\beta - \sqrt{2}\mathrm{a} - 1\right]x_0(\zeta)\,, \tag{66}$$

$$\Delta f_1(\zeta) = \tilde{f}_1 - f = \sqrt{2}\mathrm{a}\left[(2 - \sqrt{2}\mathrm{a})x_1(\zeta) - \beta - 1\right]x_1^2(\zeta)\,, \tag{67}$$

for $m = 0$ and $m = 1$, respectively. These differences are plotted in Fig. 6 for several values of the parameter a and $\beta = 1$.

The interesting feature to be noticed is that the particular solutions obtained for the monomially-only-extended FitzHugh-Nagumo equation depend only on the parameter a, while the forces depend also on the parameter $\beta$. This is due to the fact that the factoring functions $\phi_1(x)$ and $\tilde{\phi}_1(x)$ do not depend on $\beta$.

(3). *Polynomial sequence example*

Finally, we discuss a polynomial sequence extension of the factorization functions involving $N$ terms of a $\gamma = 0$ initial case for which the factorization functions $\phi_{1,2}$ are both zero, i.e., a degenerate $D^2x = 0$ case. Then, we have

$$\tilde{\phi}_1(x) = -\sum_{m=0}^{N} \mathrm{a}_m x^m\,, \qquad \tilde{\phi}_2(x) = \sum_{m=0}^{N} (m+1)\mathrm{a}_m x^m\,, \tag{68}$$

which one can easily verify that satisfies the conditions given in Eqs. (40) and (41).

Using the first pair of factorization functions, the corresponding second order non linear differential equation has the form

$$\frac{d^2x}{dt^2} - \left(\sum_{m=0}^{N} \mathrm{a}_m x^m\right)\left(\sum_{m=0}^{N} (m+1)\mathrm{a}_m x^m\right) x \equiv \frac{d^2x}{dt^2} - \left[\sum_{m=0}^{N}\left(\sum_{l=0}^{m}(m-l+1)\mathrm{a}_l \mathrm{a}_{m-l}\right) x^m\right] x = 0\,, \tag{69}$$

which admits the following non-commuting factorization

$$\left(D - \sum_{m=0}^{N}(m+1)\mathrm{a}_m x^m\right)\left(D + \sum_{m=0}^{N} \mathrm{a}_m x^m\right) x = 0\,. \tag{70}$$

One particular solution for Eq. (69) can be obtained from the first order equation

$$\frac{dx}{dt} = -\sum_{m=0}^{N} \mathrm{a}_m x^{m+1}\,. \tag{71}$$

While for $N < 2$ one can easily obtain simple explicit solutions of (71), for $N \geq 2$, the solutions will be in general implicit solutions depending on the roots of the cubic, quartic, a.s.o., algebraic equations.

Let us consider the $N = 2$ case for which $\sum_{m=0}^{2} \mathrm{a}_m x^{m+1} = x(\mathrm{a}_0 + \mathrm{a}_1 x + \mathrm{a}_2 x^2) = \mathrm{a}_2 x(x-\alpha_1)(x-\alpha_2)$, where $\alpha_{1,2}$ are the roots of the quadratic algebraic equation. Then, we have the quadrature

$$\int \frac{dx}{x(x-\alpha_1)(x-\alpha_2)} = -\mathrm{a}_2 \int dt\,. \tag{72}$$

The classification of the solutions in terms of the roots is the following [25]:

(i). If $\alpha_{1,2} = \frac{1}{2\mathrm{a}_2}\left(-\mathrm{a}_1 \pm \sqrt{\Delta}\right)$ , $\Delta = \mathrm{a}_1^2 - 4\mathrm{a}_0\mathrm{a}_2 > 0$, then by the method of partial fraction decompositions, one obtains

$$\frac{1}{\alpha_1\alpha_2(\alpha_1-\alpha_2)}\left[\ln x^{(\alpha_1-\alpha_2)} + \ln(x-\alpha_1)^{\alpha_2} - \ln(x-\alpha_2)^{\alpha_1}\right] = -\mathrm{a}_2(t-t_0)\,, \tag{73}$$

which leads to the implicit solution

$$\frac{(x-\alpha_1)^{\alpha_2}}{(x-\alpha_2)^{\alpha_1}} x^{(\alpha_1-\alpha_2)} = e^{-\mathrm{a}_2\alpha_1\alpha_2(\alpha_1-\alpha_2)(t-t_0)} \equiv e^{-\frac{\mathrm{a}_0}{\mathrm{a}_2}\sqrt{\Delta}(t-t_0)}\,. \tag{74}$$

(ii). When $\alpha_1 = \alpha_2 = \alpha$ $(= -\frac{\mathrm{a}_1}{2\mathrm{a}_2})$, $\Delta = 0$, the implicit solution is

$$-\frac{1}{x-\alpha} + \frac{1}{\alpha}\ln\left|\frac{x}{x-\alpha}\right| = -\alpha\,(\mathrm{a}_2 t + \mathrm{c}) \equiv \frac{\mathrm{a}_1}{2}(t-t_0)\,. \tag{75}$$

(iii). If $\alpha_1 = \bar{\alpha}_2 = r + is$, $\Delta < 0$, the implicit solution is

$$-\ln\left|\sqrt{(x-r)^2+s^2}\right| + \frac{\ln|x|}{s} + \frac{r}{s}\arctan\frac{x-r}{s} = \mathrm{a}_2(r^2+s^2)(t-t_0)\ . \tag{76}$$

(iv). In the degenerate case $\alpha_1 = \alpha_2 = 0$, i.e., $\mathrm{a}_0 = \mathrm{a}_1 = 0$, one obtains the simple explicit solution

$$\frac{1}{2x^2} = \mathrm{a}_2(t-t_0)\ . \tag{77}$$

In all cases, $t_0$ is an arbitrary integration constant.

In a very limited amount of these kinds of zero $\gamma$ cases, one can also obtain implicit solutions with two integration constants (general solutions). As in the Ermakov-Pinney case, this is obtained through the Abel equation of the second kind for the factorization function $\tilde{\phi}_1$, which reads

$$\tilde{\phi}_1\frac{d\tilde{\phi}_1}{dx} + \frac{1}{x}\tilde{\phi}_1^2 = \sum_{m=0}^{N}\left(\sum_{l=0}^{m}(m-l+1)\mathrm{a}_l\mathrm{a}_{m-l}\right)x^{m-1}\ . \tag{78}$$

In terms of the function $\psi = \tilde{\phi}_1^2$, this equation is a linear first order equation, which in the $N = 2$ leads to the solution

$$\tilde{\phi}_1(x) = \pm\sqrt{(\mathrm{a}_0 + \mathrm{a}_1x + \mathrm{a}_2x^2)^2 + \frac{k_1}{x^2}}\ , \tag{79}$$

where $k_1$ is an integration constant. Then, from

$$\frac{dx}{dt} = \tilde{\phi}_1(x)x = \pm\sqrt{(\mathrm{a}_0x + \mathrm{a}_1x^2 + \mathrm{a}_2x^3)^2 + k_1}\ , \tag{80}$$

one can obtain for $\mathrm{a}_0 = \mathrm{a}_1 = 0, \mathrm{a}_2 \neq 0$ (case (iv) above) the general implicit solution

$$\sqrt{(a_2x^3)^2 + k_1}\,{}_2F_1\left(\frac{2}{3}, 1, \frac{7}{6}; -\frac{(a_2x^3)^2}{k_1}\right) = k_1(t-t_0)\ , \tag{81}$$

where ${}_2F_1$ is Gauss' hypergeometric function. For $k_1 = 0$, one obtains the explicit singular solution given in (77).

## 4 Conclusions

We have discussed some minimal extensions of the factorization conditions of Rosu and Cornejo-Pérez in the case of the constant $\gamma$ coefficient of the first derivative with emphasis on the generated nonlinear equations and their particular solutions. The necessary conditions to have commutative factorizations have been introduced which lead to equations of the Ermakov-Pinney type at most as has been shown in this paper. For the non-commutative factorization case, one can obtain equations with the same $\gamma$ parameter through designed additive monomial extensions of the factorization functions. The new equations have nonlinear forces that differ from the initial nonlinear elastic forces by supplementary terms. In the mechanical context of spring models, one may seek applications in cases of weak nonlinear nanoelasticity [26, 27]. On the other hand, in this paper, the illustrative examples have been chosen from the vast area of reaction-diffusion equations in which a huge variety of travelling fronts are present and $\gamma$ is just the constant velocity of their motion. We have presented such kinds of modified counterparts of the generalized Fisher equation and the FitzHugh-Nagumo equation, and their particular solutions have been obtained by the factorization method. A polynomial sequence extension in the case $\gamma = 0$ has been also provided, for which various types of implicit solutions have been given for the $N = 2$ size of the sequence. We hope to extend these ideas in future work to the more general case of dissipation depending on the spatial coordinate and time and also to inhomogeneous equations of this kind [28] with the goal of enlarging the class of nonlinear equations with analytic solutions and identifying their possible applications.

### *CRediT Authorship Contribution Statement*

**G. González**: Conceptualization, Methodology, Writing—review & editing.
**H. C. Rosu**: Writing—original draft, Supervision, Formal analysis.
**O. Cornejo-Pérez**: Investigation, Conceptualization, Writing—review.
**S. C. Mancas**: Calculations, Investigation, Writing—review & editing.

### *Declaration of Competing Interests*

The authors declare they have no known competing financial interests or personal relationships that could have appeared to influence the work reported in this paper.

## References


1. T. Harko, S.D. Liang, Exact solutions of the Liénard and generalized Liénard type ordinary nonlinear differential equations obtained by deforming the phase space coordinates of the linear harmonic oscillator, J. Eng. Math. 98 (2016) 93–111.
2. V. K. Chandrasekar, M. Senthilvelan, and M. Lakshmanan, Unusual Liénard-type nonlinear oscillator, Phys. Rev. E 72 (2005) 066203.
3. R. Iacono and F. Russo, Class of solvable nonlinear oscillators with isochronous orbits, Phys. Rev. E 83 (2011) 027601.
4. D.W. Jordan, P. Smith, Nonlinear Ordinary Differential Equations, Second Ed., Clarendon Press, Oxford, 1987.
5. P.C. Fife, Mathematical Aspects of Reacting and Diffusing Systems, Springer, Berlin Heidelberg, 1979.
6. H.C. Rosu, O. Cornejo-Pérez, Supersymmetric pairing of kinks for polynomial nonlinearities, Phys. Rev. E 71 (2005) 046607.
7. O. Cornejo-Pérez, H.C. Rosu, Nonlinear second order ODE's: Factorizations and particular solutions, Prog. Theor. Phys. 114 (2005) 533–538.
8. F. Cooper, A. Khare, U. Sukhatme, Supersymmetry in Quantum Mechanics, World Scientific, Singapore, 2001.
9. S.-H. Dong, Factorization Method in Quantum Mechanics, Springer, Dordrecht, 2007.
10. J.D. Cole, On a quasi-linear parabolic equation occurring in aerodynamics, Quart. Appl. Math. IX (1951) 225–236.
11. X. Lü, W.-X. Ma, Study of lump dynamics based on a dimensionally reduced Hirota billinear equation, Nonlinear Dyn. 85 (2016) 1217–1222.
12. O. Cornejo-Pérez, J. Negro, L.M. Nieto, H.C. Rosu, Traveling-wave solutions for Korteweg-de Vries-Burgers equations through factorizations. Found. Phys. 36 (2006) 1587–1599.
13. P.G. Estévez, Ş Kuru, J. Negro, L.M. Nieto, Factorization of a class of almost linear second-order differential equations. J. Phys. A: Math. Theor. 40 (2007) 9819–9824.
14. E.S. Fahmy, Travelling wave solutions for some time-delayed equations through factorizations, Chaos, Solitons & Fractals 38 (2008) 1209–1216.
15. O. Cornejo-Pérez, Traveling wave solutions for some factorized nonlinear PDEs, J. Phys. A: Math. Theor. 42 (2009) 035204.
16. Ö. Yeşiltaş, Factorization and Lie point symmetries of general Liénard-type equation in the complex plane, Phys. Scr. 80 (2009) 055003.
17. M. Justin, G. Betchewe, S.Y. Doka, K.T. Crepin, Exact solutions of a semiconductor nonlinear reaction-diffusion equation through factorization method, Appl. Math. Comput. 219 (2012) 2917–2922.
18. S.C. Mancas, H.C. Rosu, Integrable dissipative nonlinear second order differential equations via factorizations and Abel equation, Phys. Lett. A 377 (2013) 1434–1438.
19. A.K. Tiwari, S.N. Pandey, V.K. Chandrasekar, M. Lakshmanan, Factorization technique and isochronous condition for coupled quadratic and mixed Liénard-type nonlinear systems, Appl. Math. Comp. 252 (2015) 457–472.
20. E.S. Selima, X. Yao, A.-M. Wazwaz, Multiple and exact soliton solutions of the perturbed KdV equation of long surface waves in a convective fluid via Painlevé analysis, factorization, and simplest equation method, Phys. Rev. E 95 (2017) 062211.
21. H.C. Rosu, O. Cornejo-Pérez, M. Pérez-Maldonado, J.A. Belinchón, Extension of a factorization method of nonlinear second order ODE's with variable coefficients, Rev. Mex. Fís. 63 (2017) 218–222.
22. D.C. Bitang A. Ziem, A. Mvogo, T.C. Kofané, Effects of transport memory in wave fronts in a bistable reaction-diffusion system, Physica A 517 (2019) 36–46.
23. G.W. Griffiths and W.E. Schiesser, *Traveling Wave Analysis of Partial Differential Equations, Numerical and Analytical Methods with MATLAB and MAPLE*, Academic Press, 2012.
24. E. Pinney, The nonlinear differential equation $y'' + p(x)y + cy^{-3} = 0$, Proc. Am. Math. Soc. 1 (1951) 681.

25. S.C. Mancas, H.C. Rosu, Integrable Abel equations and Vein's Abel equation, Math. Meth. Appl. Sci. 39 (2016) 1376–1387.
26. I. Goldhirsch, C. Goldenberg, Granular and nano-elasticity, arXiv:cond-mat/0201081.
27. J.H. Song, X. Wang, E. Riedo, Z. Wang, Elastic property of vertically aligned nanowires, Nano Letters 5 (2005) 1954–1958.
28. O. Cornejo-Pérez, S.C. Mancas, H.C. Rosu, C. A. Rico-Olvera, Factorization method for some inhomogeneous Liénard equations, Rev. Mex. Fís. 67 (2021) 443–446.

# Symbolic Computation of Solitary Wave Solutions and Solitons Through Homogenization of Degree


**Willy Hereman and Ünal Göktaş**

**Abstract** A simplified Hirota method for the computation of solitary waves and solitons of nonlinear partial differential equations (PDEs) is presented. A change of dependent variable transforms the PDE into an equation that is homogeneous of degree. Solitons are then computed using a perturbation-like scheme involving linear and nonlinear operators in a finite number of steps. The method is applied to fifth-order Korteweg-de Vries (KdV) equations due to Lax, Sawada-Kotera, and Kaup-Kupershmidt. The method works for non-quadratic homogeneous equations for which the bilinear form might be unknown. Furthermore, homogenization of degree allows one to compute solitary wave solutions of nonlinear PDEs that do not have solitons. Examples include the Fisher and FitzHugh-Nagumo equations, and a combined KdV-Burgers equation. When applied to a wave equation with a cubic source term, one gets a "bi-soliton" solution describing the coalescence of two wavefronts. The method is largely algorithmic and implemented in *Mathematica*.

**Keywords** Hirota method · Solitary waves · Solitons · Symbolic computation

W. Hereman (✉)
Department of Applied Mathematics and Statistics, Colorado School of Mines, Golden, CO 80401-1887, USA
e-mail: whereman@mines.edu
URL: https://people.mines.edu/whereman

Ü. Göktaş
Department of Computer Science and Engineering, Texas A&M University, College Station, TX 77843-3112, USA
e-mail: ugoktas@tamu.edu



S. Manukure and W.-X. Ma (eds.), *Nonlinear and Modern Mathematical Physics*,
Springer Proceedings in Mathematics & Statistics 459,
https://doi.org/10.1007/978-3-031-59539-4_4

In memory of Prof. R. Hirota (1932–2015)
Photograph courtesy of J. Hietarinta.

## 1 Introduction

In the 1970s, Hirota [42, 43] started working on an algebraic method to compute solitons of completely integrable nonlinear partial differential equations (PDEs). His method has three major steps. Given a nonlinear PDE, (i) change the dependent variable (a.k.a. apply Hirota's transformation) so that the transformed PDE is homogeneous of degree in a new dependent variable (or variables), (ii) express that homogeneous equation into one or more bilinear equations using the Hirota operators, (iii) solve the bilinear equation(s) using a perturbation-like scheme that terminates after a finite number of steps.

Finding the Hirota transformation is quite challenging and often requires insight and ingenuity. Based on experience, Hietarinta [37] provides some useful tips for finding a suitable candidate thereby reducing the guesswork.

Next, finding the appropriate bilinear form for the homogeneous equation can also be a difficult task. In particular in cases where the homogeneous equation is cubic or quartic in the new dependent variable and would have to be decoupled into a pair of bilinear equations, either involving an extra independent variable or an additional function [40]. To circumvent this difficulty, we will not use the bilinear form of the homogeneous equation but include it for completeness.

To compute solitons, the type of solutions one seeks for the homogeneous equation is quite specific. They are a *finite* sums of polynomials in exponential functions with different traveling wave arguments. The terms in that sum are computed order-by-order, using a "tracking" or "bookkeeping" parameter ($\epsilon$) which is set equal to one[1] after the exact solutions are computed.

Hirota's method [45–49] can be found in many books on solitons and complete integrability [2, 3, 16, 77, 82], books on differential equations (e.g., [108]), encyclopedia (e.g., [112]), and survey papers [9, 70, 71, 78, 92] most noteworthy those by Hietarinta [38–40].

Hietarinta's papers have a wealth of information about Hirota's method: how to use it to construct regular and oscillatory solitons (breathers), Bäcklund transformations and Lax pairs, and as a tool in a computer-aided search for possibly new completely integrable systems. His surveys have a plethora of examples including nonlinear Schrödinger (NLS) equations, the sine- and sinh-Gordon equations, shallow water wave equations, the Sasa-Satsuma equation, and systems of coupled equations such as the Hirota-Satsuma and Davey-Stewartson systems.

Hirota wrote a book [49] about his method. As far as we know, the only other book about the bilinear method is by Matsuno [74]. Several theses, for example, [89, 115, 126] have been written about Hirota's method and it is the subject of thousands of research papers.

Of course, there are several mathematically more rigorous methods to compute solitons, such as the Inverse Scattering Transform (IST), the Wronskian determinant methods, the Riemann-Hilbert approach, the dressing method, the Darboux and

[1] Unlike the *small* parameter $\epsilon$ used in perturbation methods where one seeks *approximate* solutions up to some order in $\epsilon$.

Bäcklund transformation methods, etc. In contrast to the more advanced analytic methods that use complex analysis, such as IST and the Riemann-Hilbert method, Hirota's method can not solve the initial value problem for nonlinear PDEs. Regardless, Hirota's method is a direct, powerful, and effective method to quickly find the explicit form of solitons. Apart from soliton solutions, Hirota's method can be used to find rational (lump) solutions of PDEs and the method applies to various types of discrete equations as well. A discussion of those is beyond the scope of this paper.

A mathematical foundation for the Hirota method by Sato and other researchers at the Kyoto School of Mathematics can be found in, for example, [13, 14, 54, 66, 86, 116]. There are deep connections of Hirota's method with infinite dimensional Lie algebras, transformation groups, Grassmanian manifolds, Wronskians, Gramians, Pfaffians, Bell polynomials, Plücker relations, etc. We refer the interested reader to the literature.

This survey paper is based on one (WH) of the authors' thirty years of experience with Hirota's method mainly from the perspective of applications and computer implementation. He argues that if one seeks solutions involving exponentials, replacing a nonlinear PDE (which usually consists of both linear and nonlinear terms) with an equation that is homogeneous in degree in a new dependent variable (or variables) is quite important, perhaps more so than working with Hirota's bilinear form(s) of the transformed equation. Therefore, "homogenization of degree" is at the core of what is now called[2] the *simplified* Hirota method in which Hirota's bilinear operators are no longer used. Instead, we use a perturbation-like scheme involving linear and nonlinear operators to solve the homogeneous equation without first recasting it into bilinear form.

Although the bilinear representation of the PDE is not used in our approach, dismissing it would be a mistake because it is a valuable tool in the search for completely integrable equations [36, 37] and theoretical considerations (see, e.g., [116] and the references therein).

The concept of homogenization of degree is illustrated for the Burgers equation and the ubiquitous Korteweg-de Vries (KdV) equation. For the Burgers equation, a truncated Laurent series of its solution yields the Cole-Hopf transformation, which allows one to transform the Burgers equation into the heat equation. The latter is homogeneous of degree one (linear) and can be solved by separation of variables and other methods. Using Hirota's method, traveling wave solutions of the heat equation involving one or more exponentials readily lead to multiple kink solutions of the Burgers equation. Contrary to solitons, these do not collide elastically but coalesce into a single wavefront.

In the case of the KdV equation, a truncated Laurent series reveals the transformation that Hirota used to replace the KdV by a quadratic (bilinear) equation. The connection between Hirota's transformation and the truncated Laurent expansion, a.k.a. truncated Painlevé expansion or singular manifold expansion, has been long known [17, 81, 84]. As the examples will show, it is a crucial step in the application of any flavor of Hirota's method.

[2] Some authors [65, 97, 114, 123] call it the Hereman or Hereman-Nuseir method.

The idea of homogenization is further illustrated on a class of completely integrable fifth-order KdV equations, including those of Lax [67], Sawada-Kotera (SK) and Caudrey-Dodd-Gibbon (CDG) [28, 95], and Kaup-Kupershmidt (KK) [19, 50, 57]. Their solitons are computed with a straightforward algorithm involving linear and nonlinear operators which are not necessarily quadratic. Also, the cubic operators we introduce are not the same as the trilinear operators discussed in [25, 40] because we split off the linear operator the same way as for quadratic equations.

The computations for the KK case are complicated, lengthy, and nearly impossible without using a symbolic manipulation program such as *Maple* or *Mathematica*. One reason is that the homogeneous equation is of fourth degree. Another reason is that the structure of the soliton solutions is quite different from those of the KdV, Lax, and SK equations. Although the soliton solutions of the KK equation were already presented in [30], and these for the Lax and SK equations have been computed long before that, from time to time their computation resurfaces in the literature, most recently in [56, 63, 64, 104, 107, 113, 114].

Homogenization of degree also allows one to find solitary wave solutions of nonlinear PDEs that are either not completely integrable or for which the bilinear form is unknown. A couple of such examples, mainly from mathematical biology, will be shown. We pay particular attention to a FitzHugh-Nagumo (FHN) equation with convection term for it has a so-called *bi-soliton* solution that describes the coalescence of wavefronts. The same happens for Burgers and wave equations with cubic source terms which are also discussed in detail.

The simplified Hirota method has been successfully used by many authors to find solitary wave and soliton solutions. Most notably, Wazwaz has extensively applied the method to find bi-soliton solutions [109, 110] and soliton solutions of a large number of PDEs involving one or more space variables (see, e.g., [111–113] and many of his other papers). Additional applications to PDEs with multiple space variables can be found in, e.g., [65, 97, 114, 123].

Before applying the (simplified) Hirota method, it is a good idea to test if the PDE has the Painlevé property [2, 11] by running, e.g., the `PainleveTest.m` code [6]. The Laurent series used in the Painlevé test often provides insight in which homogenizing transformation to use.

We developed a *Mathematica* package, called `PDESolitonSolutions.m` [22]. It uses the homogenization method to solve several polynomial PDEs that are completely integrable as well as some that do not have soliton solutions. In this paper we focus on $(1 + 1)$-dimensional PDEs although our code already works for some PDEs involving up to three space variables $(x, y, z)$ in addition to time $(t)$. We cover only two examples of PDEs with multiple space variables. One of the examples is the well-studied Kadomtsev-Petviashvili (KP) equation.

The paper is organized as follows. In Sect. 2 we discuss the homogenization of the Burgers and KdV equations using logarithmic derivative transformations.

After a brief review of the original Hirota method, we describe the simplified version in Sect. 3 still using the KdV equation as the prime example.

In Sect. 4, we apply the simplified Hirota method to the Lax, SK, and KK equations. For each we compute the one-, two- and three-soliton solutions explicitly.

In Sect. 5 we show how the method needs to be adjusted to find solitons for the modified KdV (mKdV) equation.

To show how the simplified method can be applied to PDEs that are not "solitonic" in Sect. 6 we compute solitary wave solutions of the Fisher and FHN equations with and without convection terms. Additional examples include a combined KdV-Burgers equation, a Burgers and wave equation with cubic source terms, and an equation due to Calogero. For each of these equations we compute exact travelling wave solutions. None has soliton solutions although some have bi-soliton solutions.

Section 7 covers an equation in $(1 + 1)$ dimensions which has two-soliton but not three-soliton solutions.

In Sect. 8 we compute multi-soliton solutions for the KP equation and an equation in $(3 + 1)$ dimensions studied by Geng and Ma [21].

Section 9 covers software to automate Hirota's method. In particular, we discuss the implementation and limitations of `PDESolitonSolutions.m` and review related software packages.

Finally, some conclusions are drawn in Sect. 10 followed by a brief discussion of future work.

## 2 Homogenization of Nonlinear PDEs

### 2.1 The Burgers Equation

Our initial example is the Burgers (a.k.a. Burgers-Bateman) equation,

$$u_t + 2uu_x - u_{xx} = 0, \tag{1}$$

named after Harry Bateman (1882–1946) and Johannes Burgers (1895–1981). The subscripts denote partial derivatives, e.g., $u_{xx} = \frac{\partial^2 u}{\partial x^2}$ and later on $u_{3x} = \frac{\partial^3 u}{\partial x^3}$, etc. Note that the coefficient of the diffusion term ($u_{xx}$) has been normalized. Equation (1) can be linearized with a logarithmic derivative transformation due to Cole and Hopf. First integrate[3] the Burgers equation with respect to $x$, yielding

$$\partial_t \left( \int^x u \, dx \right) + u^2 - u_x = 0. \tag{2}$$

Then substitute

$$u = c \, (\ln f)_x = c \left( \frac{f_x}{f} \right), \tag{3}$$

[3] Alternatively, set $u = v_x$ and integrate with respect to $x$ to get $v_t + v_x^2 - v_{xx} = 0$. Substitution of $v = c \, \ln f$ yields (4). The same can be done for other equations in this paper.

where $c$ is a constant, to get

$$f(f_t - f_{xx}) + (c+1)f_x^2 = 0. \tag{4}$$

Setting $c = -1$ yields the heat equation

$$f_t - f_{xx} = 0. \tag{5}$$

Then,

$$u(x,t) = -(\ln f)_x = -\frac{f_x}{f} \tag{6}$$

is the well-known Cole-Hopf transformation.[4] We now show where this mysterious transformation comes from. As in the Painlevé test [6], substitute a Laurent series

$$u(x,t) = f^{\alpha}(x,t)\sum_{k=0}^{\infty} u_k(x,t)f^k(x,t) \tag{7}$$

into (1). Note that $f(x,t)$ is the manifold of the poles since $\alpha$ is a negative integer. The most singular terms $f^{2\alpha-1}$ and $f^{\alpha-2}$ will balance when $\alpha = -1$ and vanish for $u_0(x,t) = -f_x$. Truncating (7) at the constant level term in $f$ yields an auto-Bäcklund transformation,

$$u(x,t) = -\frac{f_x}{f} + u_1(x,t) = -(\ln f)_x + u_1(x,t), \tag{8}$$

provided $u_1(x,t)$ is also a solution of the Burgers equation. For the zero solution ($u_1 = 0$) (8) becomes the Cole-Hopf transformation (6). The transformation allows us to replace the Burgers equation which has a mismatch of linear and quadratic terms in $u$ by an equation that is homogeneous in degree in the new field variable $f$. The fact that the resulting equation happens to be of *first* degree (linear) is advantageous for it can be solved by separation of variables eventually resulting in a large class of solutions of (1).

Setting the stage for what follows, we consider a couple of simple solutions of (5). Substituting $f(x,t) = 1 + \mathrm{e}^{\theta} = 1 + \mathrm{e}^{kx-\omega t+\delta}$, where $k$ is the wave number, $\omega$ the angular frequency, and $\delta$ a phase constant, into (5) yields the dispersion law $\omega = -k^2$. Hence,

[4] This transformation is consistent with the scaling symmetry [29] of the Burgers equation which is invariant under $x \to \lambda^{-1}x$, $t \to \lambda^{-2}t$, $u \to \lambda u$ with an arbitrary constant $\lambda$. Hence, one would expect a *first* derivative of $\ln f$.

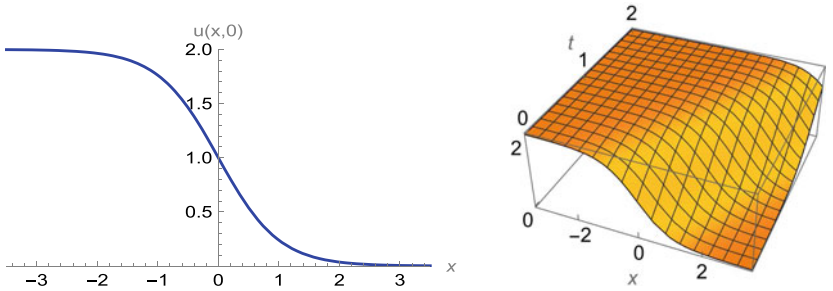


**Fig. 1** 2D and 3D graphs of the one-kink solution (10) for $K = 1$ and $\Delta = 0$

$$
\begin{aligned}
u(x,t) &= -(\ln f)_x = -\frac{f_x}{f} = -k\left(\frac{\mathrm{e}^{\theta}}{1+\mathrm{e}^{\theta}}\right) = -k\left(\frac{\mathrm{e}^{\theta}\mathrm{e}^{-\frac{\theta}{2}}}{(1+\mathrm{e}^{\theta})\mathrm{e}^{-\frac{\theta}{2}}}\right) \\
&= -k\left(\frac{\mathrm{e}^{\frac{\theta}{2}}}{\mathrm{e}^{\frac{\theta}{2}}+\mathrm{e}^{-\frac{\theta}{2}}}\right) = -\tfrac{1}{2}k\left(\frac{2\mathrm{e}^{\frac{\theta}{2}}}{\mathrm{e}^{\frac{\theta}{2}}+\mathrm{e}^{-\frac{\theta}{2}}}\right) \\
&= -\tfrac{1}{2}k\left(\frac{\mathrm{e}^{\frac{\theta}{2}}+\mathrm{e}^{-\frac{\theta}{2}}+\mathrm{e}^{\frac{\theta}{2}}-\mathrm{e}^{-\frac{\theta}{2}}}{\mathrm{e}^{\frac{\theta}{2}}+\mathrm{e}^{-\frac{\theta}{2}}}\right) = -\tfrac{1}{2}k\left(1+\tanh\tfrac{\theta}{2}\right)
\end{aligned}
\tag{9}
$$

with $\theta = kx + k^2t + \delta$, or, simply

$$
u(x,t) = K\,(1 - \tanh\Theta)\,, \tag{10}
$$

with $\Theta = Kx - 2K^2t + \Delta$, $K = -\frac{k}{2}$, and $\Delta = -\frac{\delta}{2}$. This kink-shaped solution (shock wave) of the Burgers equation is pictured in Fig. 1.

Due to its linearity, $f(x,t) = 1 + \sum_{i=1}^{N} \mathrm{e}^{\theta_i}$ where $\mathrm{e}^{\theta_i} = \mathrm{e}^{k_i\,x + k_i^2\,t + \delta_i}$ with $k_i$ and $\delta_i$ arbitrary constants, also solves (5) yielding a $N$-kink solution

$$
u(x,t) = -\frac{k_i \sum_{i=1}^{N} \mathrm{e}^{\theta_i}}{1 + \sum_{i=1}^{N} \mathrm{e}^{\theta_i}} \tag{11}
$$

for any integer $N \geq 1$. Figure 2 shows solution (11) for the case where two wavefronts ($N = 2$) coalesce into a single kink-shaped wavefront as time progresses. For a more detailed analysis of solutions of type (11) we refer to [106].

## 2.2 The Korteweg-de Vries Equation

Next we explore the homogenization of the ubiquitous KdV equation,

$$
u_t + 6uu_x + u_{3x} = 0, \tag{12}
$$

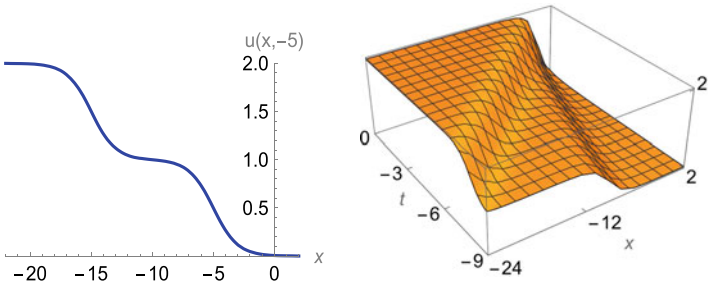


**Fig. 2** 2D and 3D graphs of the two-kink solution (11) for $k_1 = -1, k_2 = -2$, and $\delta_1 = \delta_2 = 0$

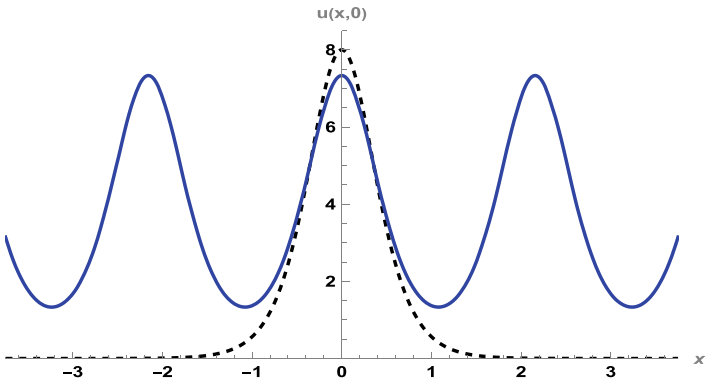


**Fig. 3** Graphs of the solitary wave (dashed line) and cnoidal wave (solid line) solutions for $k = 2$, $m = \frac{9}{10}$, and $\delta = 0$

named after Diederik Korteweg (1848–1941) and Gustav de Vries (1866–1934).

In [61] they derived the equation and its solitary wave and cnoidal wave solutions:

$$u(x,t) = 2k^2 \operatorname{sech}^2(kx - 4k^3t + \delta), \tag{13}$$

$$u(x,t) = \tfrac{4}{3}k^2(1-m) + 2k^2 m \operatorname{cn}^2(kx - 4k^3t + \delta; m), \tag{14}$$

where $m \in (0, 1)$ is the modulus of the Jacobi elliptic cosine (cn) function. Both solutions are shown in Fig. 3. As $m$ approaches 1, the peaks of the periodic solution get a little taller, the valleys become lower and flatter before they eventually spread out horizontally to become the pulse-type hyperbolic secant solution.

The interaction of the more complicated soliton solutions (to be discussed later in this paper) were first observed in numerical simulations by Zabusky and Kruskal [122] in 1965.

To compute soliton solutions with Hirota's method the original KdV equation needs to be replaced by an equation (in a new field variable) that is homogeneous of degree. To get a candidate transformation, again substitute a Laurent series (7) into (12). The most singular terms $f^{2\alpha-1}$ and $f^{\alpha-3}$ will balance when $\alpha = -2$. The

terms $f^{-5}$ and $f^{-4}$ vanish when $u_0(x,t) = -f_x$ and $u_1(x,t) = 2f_{xx}$. Hence, we obtain an auto-Bäcklund transformation for the KdV equation

$$u(x,t) = -\frac{2{f_x}^2}{f^2} + \frac{2f_{xx}}{f} + u_2(x,t) = 2(\ln f)_{xx} + u_2(x,t), \tag{15}$$

where $u_2(x,t)$ is also a solution of the KdV equation. Taking $u_2 = 0$ yields the Hirota transformation[5] that "bilinearizes" the KdV equation. To see the effect of a logarithmic derivative transformation substitute

$$u = c\,(\ln f)_{xx} = c\left(\frac{ff_{xx} - {f_x}^2}{f^2}\right), \tag{16}$$

where $c$ is an undetermined constant, into the integrated version of (12):

$$\partial_t\left(\int^x u\,dx\right) + 3u^2 + u_{xx} = 0. \tag{17}$$

This yields

$$f^3(f_{xt} + f_{4x}) - f^2(f_x f_t - 3(c-1)f_{xx}^2 + 4f_x f_{3x}) + 3(c-2)f_x^2(f_x^2 - 2ff_{xx}) = 0. \tag{18}$$

Setting $c = 2$ (confirming what we learned from the truncated Laurent series), (18) simplifies into[6]

$$f(f_{xt} + f_{4x}) - f_x f_t + 3f_{xx}^2 - 4f_x f_{3x} = 0, \tag{19}$$

which is homogeneous of *second* degree in $f$. Hirota [49] introduced the transformation $u = 2\,(\ln f)_{xx}$ in the early 1970s and realized that (19) can be written in bilinear form

$$\left(D_x D_t + D_x^4\right)(f\cdot f) = 0, \tag{20}$$

with operators $D_x$ and $D_t$ defined (see, e.g., [46, 49]) as

$$D_x^m(f\cdot g) = (\partial_x - \partial_{x'})^m f(x,t)g(x',t)\Big|_{x'=x}, \tag{21}$$

$$D_t^n(f\cdot g) = (\partial_t - \partial_{t'})^n f(x,t)g(x,t')\Big|_{t'=t}, \tag{22}$$

with $m$ and $n$ positive integers.

[5] Note that the KdV equation is invariant [29] when $x \to \lambda^{-1}x$, $t \to \lambda^{-3}t$, $u \to \lambda^2 u$. Therefore, a *second* derivative of $\ln f$ makes sense.

[6] Many authors, in particular those working on the mathematical foundation of Hirota's method, use $\tau$ instead of $f$ and investigate the rich mathematical properties of the "tau" function.

Working with these Hirota operators is easy because it amounts to applying Leibniz rule for derivatives of products of functions with every other sign flipped. Thus,

$$D_x^m(f\cdot g) = \sum_{j=0}^{m} \frac{(-1)^{m-j} m!}{j!(m-j)!} \left(\frac{\partial^j f}{\partial x^j}\right)\left(\frac{\partial^{m-j} g}{\partial x^{m-j}}\right), \tag{23}$$

and, more general,

$$D_x^m D_t^n(f\cdot g) = (\partial_x - \partial_{x'})^m (\partial_t - \partial_{t'})^n f(x,t) g(x',t')\Big|_{x'=x,t'=t} \tag{24}$$

$$= \sum_{j=0}^{m}\sum_{i=0}^{n} \frac{(-1)^{n+m-i-j} m!n!}{j!(m-j)!i!(n-i)!} \left(\frac{\partial^{i+j} f}{\partial t^i \partial x^j}\right)\left(\frac{\partial^{n+m-i-j} g}{\partial t^{n-i}\partial x^{m-j}}\right). \tag{25}$$

For example,

$$D_x^4(f\cdot g) = f_{4x}g - 4f_{3x}g_x + 6f_{xx}g_{xx} - 4f_x g_{3x} + f g_{4x}, \tag{26}$$

and

$$D_x D_t(f\cdot g) = f_{xt}g - f_t g_x - f_x g_t + f g_{xt}. \tag{27}$$

With the above one can readily verify that $\left(D_x D_t + D_x^4\right)(f\cdot f) = 0$ yields (19).

## 3 Solving the Homogeneous PDE

### 3.1 Hirota's Method

We now show how Hirota computed soliton solutions of (20). He sought a solution of the form

$$f(x,t) = 1 + \sum_{n=1}^{\infty} \epsilon^n f^{(n)}(x,t) = 1 + \epsilon f^{(1)} + \epsilon^2 f^{(2)} + \ldots, \tag{28}$$

where $\epsilon$ is a formal parameter. The building blocks of solitons are exponentials with different plane-wave arguments. Actually, $f^{(1)}$ will be the sum of a chosen but fixed number ($N$) of exponentials $\mathrm{e}^{\theta_i} = \mathrm{e}^{k_i x - \omega_i t + \delta_i}$ $(i = 1, \ldots, N)$. Then, $f^{(2)}$ will have products of just two of these exponentials such as $\mathrm{e}^{2\theta_i}$ and $\mathrm{e}^{\theta_i+\theta_j}$ $(i, j = 1, \ldots, N)$. In turn, $f^{(3)}$ will have products of three exponentials, for example, $\mathrm{e}^{3\theta_i}$, $\mathrm{e}^{2\theta_i+\theta_j}$, $\mathrm{e}^{\theta_i+2\theta_k}$, and $\mathrm{e}^{\theta_i+\theta_j+\theta_k}$ $(i, j, k = 1, \ldots, N)$. The role of $\epsilon$ is to keep track of how many exponentials are in the mix because terms involving products of two exponentials can never be equated to terms with products of three exponentials, etc. In other words, $\epsilon$ serves as a *bookkeeping* parameter which can be set to one once the computations

are done. As we will see in all the examples that follow, when solitons exist (28) will truncate and therefore be a *finite* sum of exponentials.

Substituting (28) into (20) and splitting order-by-order in $\epsilon$ gives

$$\begin{aligned}
&O(\epsilon^0): \ B(1\cdot 1) = 0,\\
&O(\epsilon^1): \ B(1\cdot f^{(1)} + f^{(1)}\cdot 1) = 0,\\
&O(\epsilon^2): \ B(1\cdot f^{(2)} + f^{(1)}\cdot f^{(1)} + f^{(2)}\cdot 1) = 0,\\
&O(\epsilon^3): \ B(1\cdot f^{(3)} + f^{(1)}\cdot f^{(2)} + f^{(2)}\cdot f^{(1)} + f^{(3)}\cdot 1) = 0,\\
&O(\epsilon^4): \ B(1\cdot f^{(4)} + f^{(1)}\cdot f^{(3)} + f^{(2)}\cdot f^{(2)} + f^{(3)}\cdot f^{(1)} + f^{(4)}\cdot 1) = 0,\\
&\quad\ \vdots \qquad\qquad \vdots\\
&O(\epsilon^n): \ B\left(\sum_{j=0}^{n} f^{(j)}\cdot f^{(n-j)}\right) = 0, \quad n \geq 0, \quad \text{with } f^{(0)} = 1,
\end{aligned} \tag{29}$$

where for the present example $B = D_x D_t + D_x^4$.

To illustrate, we compute the one- and two-soliton solutions of (12). Note that the first equation in (29) is trivially satisfied. Using (26) and (27), the second equation reduces[7] to $f_{xt}^{(1)} + f_{4x}^{(1)} = 0$.

**One-soliton Solution of the KdV Equation**

If we take $f^{(1)} = \mathrm{e}^{\theta} \equiv \mathrm{e}^{k\,x-\omega\,t+\delta}$, that second equation yields the dispersion law $\omega = k^3$. Next, one can readily verify that $B(f^{(1)}\cdot f^{(1)})$ is zero. Consequently, $f^{(2)}$ is zero and so are $f^{(3)}$, $f^{(4)}$, etc. Therefore, there are only two terms in (28). Explicitly,

$$f = 1 + \mathrm{e}^{\theta} = 1 + \mathrm{e}^{k\,x-k^3\,t+\delta} \tag{30}$$

after setting $\epsilon = 1$. Hence,

$$\begin{aligned}
u(x,t) &= 2\left(\frac{f f_{xx} - {f_x}^2}{f^2}\right) = \frac{2k^2\,\mathrm{e}^{\theta}}{\left(1+\mathrm{e}^{\theta}\right)^2} = \frac{2k^2\,\mathrm{e}^{\theta}\mathrm{e}^{-\theta}}{\left[\mathrm{e}^{-\frac{\theta}{2}}\left(1+\mathrm{e}^{\theta}\right)\right]^2}\\
&= \tfrac{1}{2}k^2\mathrm{sech}^2\left[\tfrac{1}{2}(kx - k^3t + \delta)\right] = 2\,K^2\mathrm{sech}^2\left(Kx - 4\,K^3t + \Delta\right),
\end{aligned} \tag{31}$$

where $K = \frac{k}{2}$ and $\Delta = \frac{\delta}{2}$. Figure 4 shows a 3D graph of this so-called *solitary wave solution* or *one-soliton solution* for $K = 2$ and $\Delta = 0$.

**Two-soliton Solution of the KdV Equation**

Starting with $f^{(1)} = \mathrm{e}^{\theta_1} + \mathrm{e}^{\theta_2}$, where $\mathrm{e}^{\theta_i} = \mathrm{e}^{k_i\,x-\omega_i\,t+\delta_i}$, the first nontrivial equation in (29) yields $\omega_i = k_i^3$. Then, $B(f^{(1)}\cdot f^{(1)}) = -6k_1k_2(k_1-k_2)^2\mathrm{e}^{\theta_1+\theta_2}$ which determines the form of $f^{(2)}$, namely, $f^{(2)} = a_{12}\mathrm{e}^{\theta_1+\theta_2}$, with some constant coefficient $a_{12}$ to be computed. Then, $B(1\cdot f^{(2)}) = B(f^{(2)}\cdot 1) = f_{xt}^{(2)} + f_{4x}^{(2)} = 3a_{12}k_1k_2(k_1+k_2)^2\mathrm{e}^{\theta_1+\theta_2}$.

[7] With $B = D_x D_t + D_x^4$, one has $B(1.f) = B(f.1) = f_{xt} + f_{4x}$ for any function $f$.

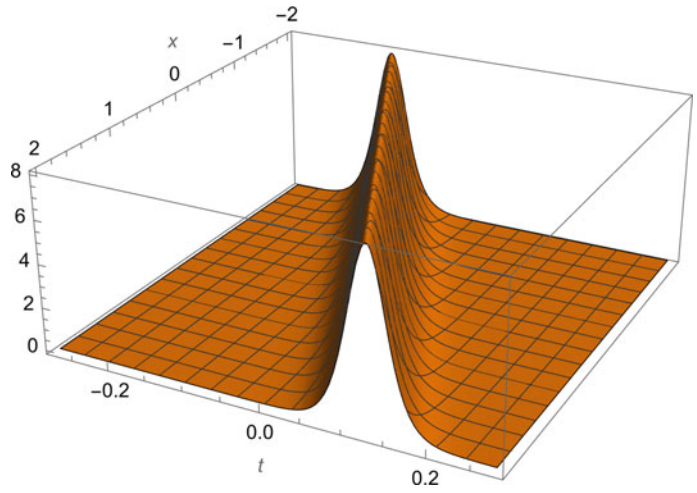


**Fig. 4** 3D graph of the hump-shaped solution (31) for $K = 2$ and $\Delta = 0$

Substitution of the pieces into the third equation of (29) then gives

$$a_{12} = \left(\frac{k_1 - k_2}{k_1 + k_2}\right)^2. \tag{32}$$

One can show that from $O(\epsilon^3)$ onward one can set $f^{(3)}$, $f^{(4)}$, etc., equal to zero. Thus, $f$ contains only four terms. With $\epsilon = 1$, using

$$f = 1 + \mathrm{e}^{\theta_1} + \mathrm{e}^{\theta_2} + a_{12}\mathrm{e}^{\theta_1+\theta_2}, \tag{33}$$

and $u = 2(\ln f)_{xx}$, this yields

$$u(x,t) = \frac{2\left[k_1^2\mathrm{e}^{\theta_1} + k_2^2\mathrm{e}^{\theta_2} + 2(k_1 - k_2)^2\mathrm{e}^{\theta_1+\theta_2} + a_{12}(k_2^2\mathrm{e}^{\theta_1} + k_1^2\mathrm{e}^{\theta_2})\mathrm{e}^{\theta_1+\theta_2}\right]}{\left(1 + \mathrm{e}^{\theta_1} + \mathrm{e}^{\theta_2} + a_{12}\,\mathrm{e}^{\theta_1+\theta_2}\right)^2}. \tag{34}$$

Setting $k_i = 2K_i$, $\delta_i = 2\Delta_i + \ln\left(\frac{K_2+K_1}{K_2-K_1}\right)$, the above can be written as

$$\begin{aligned} u(x,t) &= \frac{4\left(K_2^2 - K_1^2\right)\left[(K_2^2 - K_1^2) + K_1^2\cosh(2\Theta_2) + K_2^2\cosh(2\Theta_1)\right]}{\left[(K_2 - K_1)\cosh(\Theta_2 + \Theta_1) + (K_2 + K_1)\cosh(\Theta_2 - \Theta_1)\right]^2} \\ &= 2\left(K_2^2 - K_1^2\right)\left(\frac{K_1^2\mathrm{sech}^2(\Theta_1) + K_2^2\mathrm{csch}^2(\Theta_2)}{\left[K_1\tanh(\Theta_1) - K_2\coth(\Theta_2)\right]^2}\right), \end{aligned} \tag{35}$$

where $\Theta_i = K_i x - 4K_i^3 t + \Delta_i$ $(i = 1, 2)$. The elastic scattering of two solitons for the KdV equation is shown in Figs. 5 and 6 for $k_1 = 2$, $k_2 = \frac{3}{2}$, and $\delta_1 = \delta_2 = 0$.

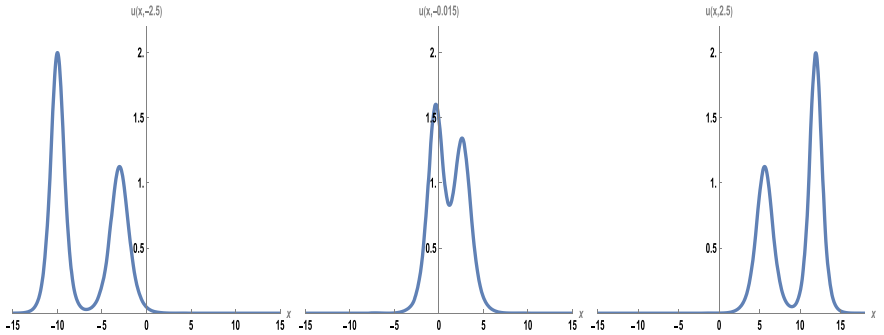


**Fig. 5** Graph of the two-soliton solution (35) of the KdV equation at three different moments in time

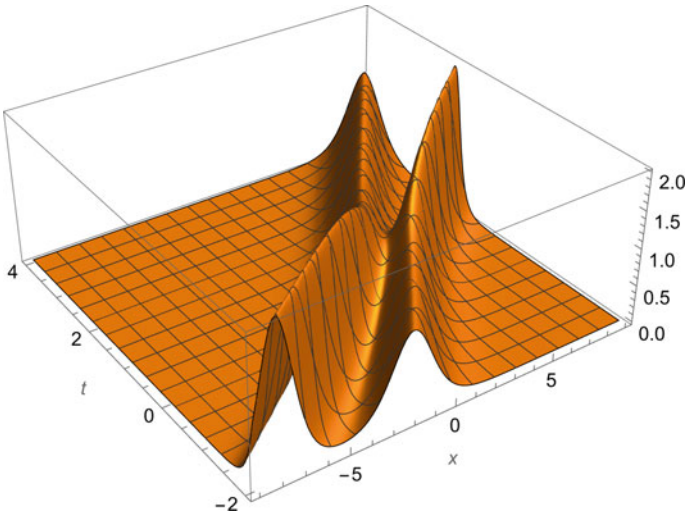


**Fig. 6** Bird's eye view of a two-soliton collision for the KdV equation. Notice the phase shift after collision: the taller (faster) soliton is shifted forward and the shorter (slower) soliton backward relative to where they would have been if they had not collided

## *3.2 Simplified Hirota Method*

In this Section we use a simplified version of Hirota's method which does not use the bilinear representation (20). Instead, we write (19) in the form

$$f\,\mathcal{L}f + \mathcal{N}(f, f) = 0, \tag{36}$$

where

$$\mathcal{L}f = f_{xt} + f_{4x} \tag{37}$$

and

$$\mathcal{N}(f,g) = -f_x g_t + 3f_{xx}g_{xx} - 4f_x g_{3x} \tag{38}$$

define a linear differential operator $\mathcal{L}$ and a quadratic differential operator $\mathcal{N}$. Note that the latter is linear in each of the auxiliary functions $f(x,t)$ and $g(x,t)$. So, we could also call it "bilinear" but, of course, $\mathcal{N}$ differs from Hirota's bilinear operator $B$. Substituting (28) into (36), and setting the coefficients of powers of $\epsilon$ to zero yields[8]

$$\begin{aligned}
&O(\epsilon^1): \ \mathcal{L}f^{(1)} = 0,\\
&O(\epsilon^2): \ \mathcal{L}f^{(2)} = -\mathcal{N}(f^{(1)}, f^{(1)}),\\
&O(\epsilon^3): \ \mathcal{L}f^{(3)} = -\left(f^{(1)}\mathcal{L}f^{(2)} + \mathcal{N}(f^{(1)}, f^{(2)}) + \mathcal{N}(f^{(2)}, f^{(1)})\right),\\
&\qquad\vdots \qquad\qquad \vdots\\
&O(\epsilon^n): \ \mathcal{L}f^{(n)} = -\sum_{j=1}^{n-1}\left(f^{(j)}\mathcal{L}f^{(n-j)} + \mathcal{N}(f^{(j)}, f^{(n-j)})\right), \quad n \geq 2.
\end{aligned} \tag{39}$$

The $N$-soliton solution of the KdV is then generated from

$$f^{(1)} = \sum_{i=1}^{N} \mathrm{e}^{\theta_i} \equiv \sum_{i=1}^{N} \mathrm{e}^{k_i x - \omega_i t + \delta_i}, \tag{40}$$

where $N$ is a natural number, by solving the equations (39) successively to determine $f^{(2)}$, $f^{(3)}$, etc. The first equation, $\mathcal{L}f^{(1)} = 0$, yields the dispersion relation $\omega_i = k_i^3$. With (40) one readily computes

$$-\mathcal{N}(f^{(1)}, f^{(1)}) = -\sum_{i,j=1}^{N} 3k_i k_j^2 (k_i - k_j)\mathrm{e}^{\theta_i+\theta_j} = \sum_{1\leq i<j\leq N} 3k_i k_j (k_i - k_j)^2 \mathrm{e}^{\theta_i+\theta_j}. \tag{41}$$

Note that there are no terms $\mathrm{e}^{2\theta_i}$. Hence, $f^{(2)}$ must be of the from

$$f^{(2)} = \sum_{1\leq i<j\leq N} a_{ij}\mathrm{e}^{\theta_i+\theta_j}, \tag{42}$$

with constants[9] $a_{ij}$ to be determined. Next, compute

$$\mathcal{L}f^{(2)} = \sum_{1\leq i<j\leq N} 3k_i k_j (k_i + k_j)^2 a_{ij}\, \mathrm{e}^{\theta_i+\theta_j}, \tag{43}$$

[8] Details of the derivation are given in the Appendix.

[9] The $a_{ij}$ are often called phase factors because they can be absorbed in the exponents via $a_{ij} = \mathrm{e}^{A_{ij}}$.

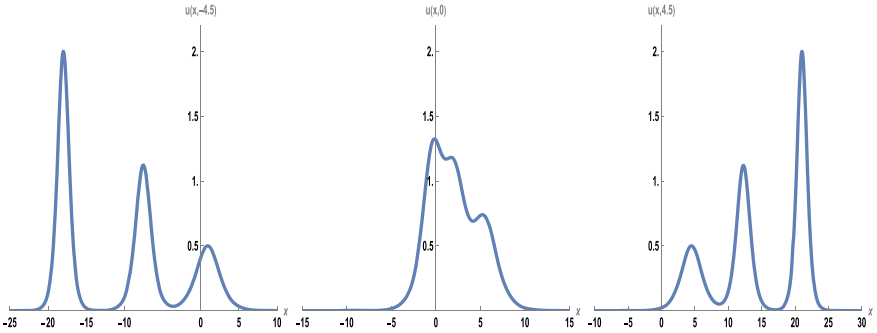


**Fig. 7** Graph of the three-soliton solution of the KdV equation at three different moments in time

and equate (41) with (43) to get

$$a_{ij} = \left(\frac{k_i - k_j}{k_i + k_j}\right)^2, \qquad 1 \le i < j \le N. \tag{44}$$

To keep matters transparent we show some details of the computation of the three-soliton solution and the result for the four-soliton solution.

**Three-soliton Solution of the KdV Equation**

Proceeding in a similar way with the third equation in (39) leads to the explicit form of $f^{(3)}$. For $N = 3$, we find

$$f^{(3)} = b_{123} \mathrm{e}^{\theta_1+\theta_2+\theta_3} \tag{45}$$

with

$$b_{123} = a_{12}\, a_{13}\, a_{23} = \left[\frac{(k_1 - k_2)\,(k_1 - k_3)\,(k_2 - k_3)}{(k_1 + k_2)\,(k_1 + k_3)\,(k_2 + k_3)}\right]^2. \tag{46}$$

For $N = 3$, one can verify that $f^{(n)} = 0$ for $n > 3$. Thus,

$$\begin{aligned} f = 1 &+ \mathrm{e}^{\theta_1} + \mathrm{e}^{\theta_2} + \mathrm{e}^{\theta_3} + a_{12}\,\mathrm{e}^{\theta_1+\theta_2} + a_{13}\,\mathrm{e}^{\theta_1+\theta_3} + a_{23}\,\mathrm{e}^{\theta_2+\theta_3} \\ &+ a_{12}\, a_{13}\, a_{23}\,\mathrm{e}^{\theta_1+\theta_2+\theta_3} \end{aligned} \tag{47}$$

after setting $\epsilon = 1$. Notice that (47) has no terms in $\mathrm{e}^{2\theta_1}$, $\mathrm{e}^{2\theta_2}$, $\mathrm{e}^{2\theta_1+\theta_2}$, $\mathrm{e}^{\theta_1+2\theta_2}$, etc. The explicit expression of $u(x, t)$ (not shown due to length) then follows from $u(x, t) = 2(\ln f)_{xx}$.

The elastic collision of three solitons for the KdV equation is shown in Figs. 7 and 8 for $k_1 = 2$, $k_2 = \frac{3}{2}$, $k_3 = 1$, and $\delta_1 = \delta_2 = \delta_3 = 0$.

**Four-soliton Solution of the KdV Equation**

The computation of the four-soliton solution proceeds along the same lines. After setting $\epsilon = 1$,

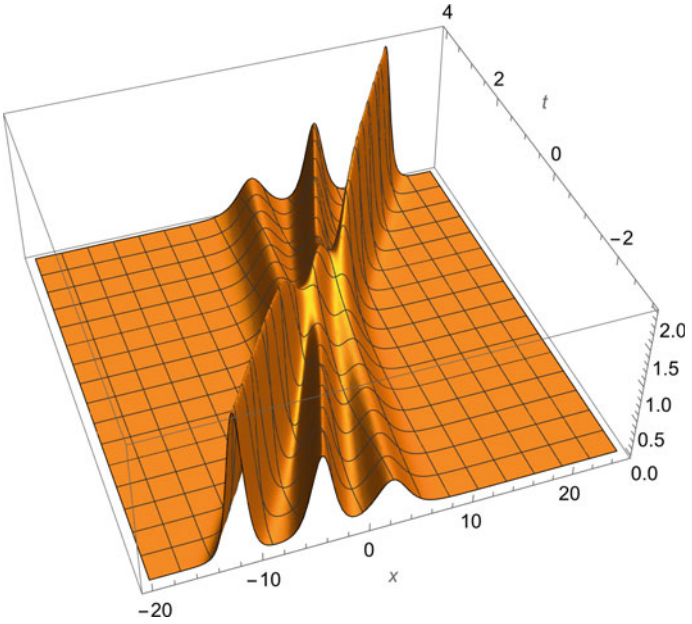


**Fig. 8** Bird's eye view of three solitons colliding for the KdV equation. Notice the phase shift after collision: the faster soliton has advanced and the slower ones are behind. The shortest of the three solitons is shifted the most

$$f = 1 + \mathrm{e}^{\theta_1} + \mathrm{e}^{\theta_2} + \mathrm{e}^{\theta_3} + \mathrm{e}^{\theta_4} + a_{12}\,\mathrm{e}^{\theta_1+\theta_2} + a_{13}\,\mathrm{e}^{\theta_1+\theta_3} + a_{14}\,\mathrm{e}^{\theta_1+\theta_4} + a_{23}\,\mathrm{e}^{\theta_2+\theta_3} + a_{24}\,\mathrm{e}^{\theta_2+\theta_4} + a_{34}\,\mathrm{e}^{\theta_3+\theta_4} + a_{12}a_{13}a_{23}\,\mathrm{e}^{\theta_1+\theta_2+\theta_3} + a_{12}a_{14}a_{24}\,\mathrm{e}^{\theta_1+\theta_2+\theta_4} + a_{13}a_{14}a_{34}\mathrm{e}^{\theta_1+\theta_3+\theta_4} + a_{23}a_{24}a_{34}\mathrm{e}^{\theta_2+\theta_3+\theta_4} + a_{12}a_{13}a_{14}a_{23}a_{24}a_{34}\mathrm{e}^{\theta_1+\theta_2+\theta_3+\theta_4}, \quad (48)$$

with $a_{ij}$ as defined in (44).

The four-soliton solution $u(x,t)$ of the KdV equation follows from $u(x,t) = 2(\ln f)_{xx}$. Its analytic expression is not shown for it would fill pages.

***N*-soliton Solution of the KdV Equation**

Hirota introduced [46, Eq. (5.38)] a concise formula for the function $f$ leading to the $N$-soliton solution of the KdV equation,

$$f = \sum_{\mu=0,1} \mathrm{e}^{\left[\sum_{i<j}^{(N)} \mu_i \mu_j A_{ij} + \sum_{i=1}^{N} \mu_i \theta_i\right]}, \quad (49)$$

where $\sum_{\mu=0,1}$ denotes the sum over the $2^N$ combinations of $\mu_1 = 0, 1$, $\mu_2 = 0, 1$, $\ldots$, $\mu_N = 0, 1$. Furthermore, $\sum_{i<j}^{(N)}$ indicates summation over all possible pairs $(i, j)$ with $i$ and $j$ chosen from the $N$ elements $\{1, 2, ..., N\}$ but $i < j$, and $a_{ij} = \mathrm{e}^{A_{ij}}$.

Inspired by the result obtained by the IST, the $N$-soliton solution can be written in a compact form [20, 42, 101, 103] as

$$u(x,t) = 2\,(\ln\det(I+M))_{xx} \tag{50}$$

where $I$ is the $N \times N$ identity matrix and

$$M_{\ell m} = \frac{\mathrm{e}^{\Theta_\ell+\Theta_m}}{K_\ell + K_m} \quad \text{with } \Theta_\ell = K_\ell x - 4K_\ell^3 t + \Delta_\ell. \tag{51}$$

Note that $\det(I+M)$ will match $f$ in (30), (33), (47), and (48) when $k_i = 2K_i$ and $\delta_i = 2\Delta_i - \ln(2K_i)$ with $K_i > 0$.

## 4 Application to a Class of Fifth-Order Evolution Equations

In this section we investigate the soliton solutions of a three-parameter family of fifth-order KdV equations,

$$u_t + \alpha u^2 u_x + \beta u_x u_{xx} + \gamma u u_{3x} + u_{5x} = 0, \tag{52}$$

where $\alpha$, $\beta$, and $\gamma$ are nonzero real parameters. With $u = \frac{1}{\gamma}\tilde{u}$ one gets

$$\tilde{u}_t + \tfrac{\alpha}{\gamma^2}\tilde{u}^2\tilde{u}_x + \tfrac{\beta}{\gamma}\tilde{u}_x\tilde{u}_{xx} + \tilde{u}\tilde{u}_{3x} + \tilde{u}_{5x} = 0, \tag{53}$$

showing that the individual values of the parameters are less important than the ratios $\frac{\alpha}{\gamma^2}$ and $\frac{\beta}{\gamma}$. Table 1 shows the values of these ratios for which (52) is known to be completely integrable together with values of $(\alpha, \beta, \gamma)$ used in the literature. The names of the equations are also listed together with a couple of references. Using scales on $u$, $x$, and $t$, the named equations cannot be transformed into one another; they are fundamentally different.[10]

Integrate (52),

$$\partial_t\left(\int^x u\,dx\right) + \tfrac{1}{3}\alpha u^3 + \tfrac{1}{2}(\beta-\gamma)u_x^2 + \gamma u u_{xx} + u_{4x} = 0, \tag{54}$$

and substitute (16) where $c$ is a constant, to get

$$\begin{aligned} &6f^5(f_{xt}+f_{6x}) - 3f^4(2f_xf_t + \ldots + 12f_xf_{5x}) + 2f^3\left((\ldots)f_{xx}^3 + \ldots + (\ldots)f_x^2f_{4x}\right) \\ &+3f^2f_x^2\left((\ldots)f_{xx}^2 + (\ldots)f_xf_{3x}\right) + 2f_x^4(360 - 6\beta c + \alpha c^2 - 12\gamma c)(3ff_{xx} - f_x^2) = 0, \end{aligned} \tag{55}$$

[10] After a trivial scaling the CDG equation becomes the SK equation. They are the *same* equations which often goes unnoticed in the literature (see, e.g., [64, 91]).

**Table 1** Completely integrable fifth-order evolutions equations of type (52)

| $\frac{\alpha}{\gamma^2}$ | $\frac{\beta}{\gamma}$ | $(\alpha, \beta, \gamma)$ | Name | References |
|---|---|---|---|---|
| $\frac{3}{10}$ | 2 | (30, 20, 10) | Lax | [67] |
| | | (120, 40, 20) | | [94] |
| $\frac{1}{5}$ | 1 | (45, 15, 15) | Sawada-Kotera | [95] |
| | | (180, 30, 30) | Caudrey-Dodd-Gibbon | [10, 15] |
| $\frac{1}{5}$ | $\frac{5}{2}$ | (20, 25, 10) | Kaup-Kupershmidt | [19, 50, 57] |

which is of sixth degree. In the next subsections we investigate the integrable cases listed in Table 1. For each case the constant $c$ can be obtained from substituting a Laurent series into (52).

## 4.1 The Lax Equation

Using $\alpha = \frac{3}{10}\gamma^2$, $\beta = 2\gamma$, and $c = \frac{20}{\gamma}$, (55) reduces to a homogeneous *trilinear* equation

$$f^2(f_{xt} + f_{6x}) - f(f_x f_t - 5f_{xx} f_{4x} + 6f_x f_{5x}) + 10(f_{xx}^3 - 2f_x f_{xx} f_{3x} + f_x^2 f_{4x}) = 0, \tag{56}$$

which can be written in bilinear form consisting of two coupled equations (see [49, p. 56] and [46, 94]):

$$\begin{aligned} &\left(D_x D_s + D_x^4\right)(f \cdot f) = 0, \\ &\left(D_x D_t + D_x^6\right)(f \cdot f) - \tfrac{5}{3}\left(D_s^2 + D_s D_x^3\right)(f \cdot f) = 0, \end{aligned} \tag{57}$$

for only one function $f$ but with an extra independent variable $s$ which corresponds to the time variable in the KdV equation. This comes as no surprise because the Lax equation belongs to the family of KdV flows [82, p. 114] each with its own time variable. Upon elimination of $s$ via suitable cross differentiations one obtains (56).

Note that (56) can also be recast in terms of Hirota trilinear operators [40, Eq. (8.113)]. Completely integrable trilinear equations have been studied [25, 40, 41, 69] but are less common than their bilinear counterparts. Specific examples can be found in, for example, [72, 93, 96].

We will not use (57) in the subsequent computation of solitons. Instead, we write the cubic equation (56) as

$$f^2 \mathcal{L} f + f\mathcal{N}_1(f, f) + \mathcal{N}_2(f, f, f) = 0, \tag{58}$$

with operators

$$\begin{aligned} \mathcal{L}f &= f_{xt} + f_{6x}, \\ \mathcal{N}_1(f,g) &= -(f_t g_x - 5 f_{xx} g_{4x} + 6 f_x g_{5x}), \\ \mathcal{N}_2(f,g,h) &= 10(f_{xx} g_{xx} h_{xx} - 2 f_x g_{xx} h_{3x} + f_x g_x h_{4x}), \end{aligned} \tag{59}$$

where $f$, $g$, and $h$ are auxiliary functions.

Upon substitution of (28) into (58) the first four equations of the perturbation scheme become[11]

$$\begin{aligned} O(\epsilon^1) &: \mathcal{L}f^{(1)} = 0, \\ O(\epsilon^2) &: \mathcal{L}f^{(2)} = -\mathcal{N}_1(f^{(1)}, f^{(1)}), \\ O(\epsilon^3) &: \mathcal{L}f^{(3)} = -\left(2f^{(1)}\mathcal{L}f^{(2)} + \mathcal{N}_1(f^{(1)}, f^{(2)}) + \mathcal{N}_1(f^{(2)}, f^{(1)})\right. \\ &\qquad \left. + f^{(1)}\mathcal{N}_1(f^{(1)}, f^{(1)}) + \mathcal{N}_2(f^{(1)}, f^{(1)}, f^{(1)})\right), \\ O(\epsilon^4) &: \mathcal{L}f^{(4)} = -\left(2f^{(1)}\mathcal{L}f^{(3)} + \left(2f^{(2)} + {f^{(1)}}^2\right)\mathcal{L}f^{(2)} + \mathcal{N}_1(f^{(1)}, f^{(3)})\right. \\ &\qquad + \mathcal{N}_1(f^{(3)}, f^{(1)}) + \mathcal{N}_1(f^{(2)}, f^{(2)}) + f^{(1)}\left(\mathcal{N}_1(f^{(1)}, f^{(2)})\right. \\ &\qquad \left. + \mathcal{N}_1(f^{(2)}, f^{(1)})\right) + f^{(2)}\mathcal{N}_1(f^{(1)}, f^{(1)}) + \mathcal{N}_2(f^{(1)}, f^{(1)}, f^{(2)}) \\ &\qquad \left. + \mathcal{N}_2(f^{(1)}, f^{(2)}, f^{(1)}) + \mathcal{N}_2(f^{(2)}, f^{(1)}, f^{(1)})\right), \end{aligned} \tag{60}$$

where we used the first equation to simplify the other ones. Starting from (40), one can proceed as in KdV case to construct soliton solutions of any order $N$. The only difference is that for the Lax equation $\omega_i = k_i^5$ instead of $\omega_i = k_i^3$. For example, the one-soliton solution

$$u(x,t) = \tfrac{5}{\gamma}k^2 \operatorname{sech}^2\left[\tfrac{1}{2}(kx - k^5 t + \delta)\right] = \tfrac{20}{\gamma}K^2 \operatorname{sech}^2\left(Kx - 16\,K^5 t + \Delta\right), \tag{61}$$

where $K = \frac{k}{2}$ and $\Delta = \frac{\delta}{2}$, solves

$$u_t + \tfrac{3}{10}\gamma^2 u^2 u_x + 2\gamma u_x u_{xx} + \gamma u u_{3x} + u_{5x} = 0. \tag{62}$$

## 4.2 The Sawada-Kotera Equation

Using $\alpha = \frac{1}{5}\gamma^2$, $\beta = \gamma$, and $c = \frac{30}{\gamma}$ one gets a quadratic equation,

$$f(f_{xt} + f_{6x}) - f_x f_t - 10 f_{3x}^2 + 15 f_{xx} f_{4x} - 6 f_x f_{5x} = 0, \tag{63}$$

[11] The derivation is given in the Appendix.

which can be written in bilinear form [46] as

$$\left(D_x D_t + D_x^6\right)(f \cdot f) = 0. \tag{64}$$

Ignoring the bilinear representation, we write (63) in the form (36) with

$$\mathcal{L} f = f_{xt} + f_{6x}, \tag{65}$$
$$\mathcal{N}(f, g) = -f_x g_t - 10 f_{3x} g_{3x} + 15 f_{xx} g_{4x} - 6 f_x g_{5x}, \tag{66}$$

and proceed as in the KdV case, leading to the following soliton solutions.

**One-soliton Solution of the SK Equation**
The solitary wave solution

$$\begin{aligned} u(x,t) &= \tfrac{15}{2\gamma} k^2 \operatorname{sech}^2\left[\tfrac{1}{2}(kx - k^5 t + \delta)\right] \\ &= \tfrac{30}{\gamma} K^2 \operatorname{sech}^2\left(Kx - 16\,K^5 t + \Delta\right), \end{aligned} \tag{67}$$

where $K = \frac{k}{2}$ and $\Delta = \frac{\delta}{2}$, solves

$$u_t + \tfrac{1}{5}\gamma^2 u^2 u_x + \gamma u_x u_{xx} + \gamma u u_{3x} + u_{5x} = 0. \tag{68}$$

**Higher-order Soliton Solutions of the SK Equation**
The computation of higher-order soliton solutions is analogous to the KdV equation; see (33), (47), and (48). Except that the dispersion relation is now quintic, $\omega_i = k_i^5$, and the $a_{ij}$ must be replaced by

$$a_{ij} = \frac{(k_i - k_j)^2 (k_i^2 - k_i k_j + k_j^2)}{(k_i + k_j)^2 (k_i^2 + k_i k_j + k_j^2)} = \frac{(k_i - k_j)^3 (k_i^3 + k_j^3)}{(k_i + k_j)^3 (k_i^3 - k_j^3)}. \tag{69}$$

The actual two- and three-soliton solutions $u(x, t)$ of the SK equation are very long expressions (not shown).

## *4.3 The Kaup-Kupershmidt Equation*

Using $\alpha = \frac{1}{5}\gamma^2$, $\beta = \frac{5}{2}\gamma$, and $c = \frac{15}{\gamma}$, (55) becomes a *quartic* equation,

$$\begin{aligned} &4f^3(f_{xt} + f_{6x}) - f^2(4 f_t f_x - 5 {f_{3x}}^2 + 24 f_x f_{5x}) \\ &-30 f f_x (f_{xx} f_{3x} - 2 f_x f_{4x}) + 15 {f_x}^2 (3 {f_{xx}}^2 - 4 f_x f_{3x}) = 0, \end{aligned} \tag{70}$$

which can be written as a coupled system of bilinear equations (see [49, p. 36] and [88, 104]),

$$\left(D_x D_t + \tfrac{1}{16} D_x^6\right)(f\cdot f) + \tfrac{15}{4} D_x^2 (f\cdot g) = 0, \tag{71}$$

$$D_x^4 (f\cdot f) - 4fg = 0, \tag{72}$$

for two unknown functions $f$ and $g$. One can verify that upon elimination of $g$ in (71) and (72) indeed yields (70).

In what follow, we will ignore the bilinear system and write (70) in operator form as

$$f^3 \mathcal{L} f + f^2 \mathcal{N}_1(f, f) + f\mathcal{N}_2(f, f, f) + \mathcal{N}_3(f, f, f, f) = 0. \tag{73}$$

This homogeneous equation involves one linear operator and three nonlinear operators defined as

$$\mathcal{L} f = 4(f_{xt} + f_{6x}), \tag{74}$$

$$\mathcal{N}_1(f, g) = -(4 f_t g_x - 5 f_{3x} g_{3x} + 24 f_x g_{5x}), \tag{75}$$

$$\mathcal{N}_2(f, g, h) = -30 f_x (g_{xx} h_{3x} - 2 g_x h_{4x}), \tag{76}$$

$$\mathcal{N}_3(f, g, h, j) = 15 f_x g_x (3 h_{xx} j_{xx} - 4 h_x j_{3x}), \tag{77}$$

for auxiliary functions $f(x,t)$, $g(x,t)$, $h(x,t)$, and $j(x,t)$. The nonlinear operators are bilinear, trilinear, and quadrilinear, respectively.

Substituting (28) into (73) and equating the coefficients of powers of $\epsilon$ to zero yields[12] the perturbation scheme of which the first four equations read

$$\begin{aligned}
O(\epsilon^1) &: \mathcal{L} f^{(1)} = 0,\\
O(\epsilon^2) &: \mathcal{L} f^{(2)} = -\mathcal{N}_1(f^{(1)}, f^{(1)}),\\
O(\epsilon^3) &: \mathcal{L} f^{(3)} = -\Big(3 f^{(1)} \mathcal{L} f^{(2)} + 2 f^{(1)} \mathcal{N}_1(f^{(1)}, f^{(1)}) + \mathcal{N}_1(f^{(2)}, f^{(1)})\\
&\quad + \mathcal{N}_1(f^{(1)}, f^{(2)}) + \mathcal{N}_2(f^{(1)}, f^{(1)}, f^{(1)})\Big),\\
O(\epsilon^4) &: \mathcal{L} f^{(4)} = -\Big(3 f^{(1)} \mathcal{L} f^{(3)} + 3\left(f^{(2)} + {f^{(1)}}^2\right) \mathcal{L} f^{(2)} + \mathcal{N}_1(f^{(1)}, f^{(3)})\\
&\quad + \mathcal{N}_1(f^{(3)}, f^{(1)}) + \mathcal{N}_1(f^{(2)}, f^{(2)}) + 2 f^{(1)} \left(\mathcal{N}_1(f^{(1)}, f^{(2)})\right.\\
&\quad \left. + \mathcal{N}_1(f^{(2)}, f^{(1)})\right) + \left(2 f^{(2)} + {f^{(1)}}^2\right) \mathcal{N}_1(f^{(1)}, f^{(1)})\\
&\quad + \mathcal{N}_2(f^{(1)}, f^{(1)}, f^{(2)}) + \mathcal{N}_2(f^{(1)}, f^{(2)}, f^{(1)}) + \mathcal{N}_2(f^{(2)}, f^{(1)}, f^{(1)})\\
&\quad + f^{(1)} \mathcal{N}_2(f^{(1)}, f^{(1)}, f^{(1)}) + \mathcal{N}_3(f^{(1)}, f^{(1)}, f^{(1)}, f^{(1)})\Big),
\end{aligned} \tag{78}$$

where we used the first equation to simplify the subsequent ones. Clearly, the number of terms grows at each order in $\epsilon$ and the computational complexity increases accordingly. Full details of the step-by-step solution of the perturbation scheme for the KK equation with coefficients $\alpha = 20$, $\beta = 25$, and $\gamma = 10$, can be found [30, 85] where we used *Macsyma* to perform the lengthy computations. Here we sum-

[12] Details of the derivation are given in the Appendix.

marize the results for general $\alpha, \beta$, and $\gamma$ subject to the conditions $\alpha = \frac{1}{5}\gamma^2$, and $\beta = \frac{5}{2}\gamma$.

**One-soliton Solution of the KK Equation**

Taking $f^{(1)} = \mathrm{e}^{\theta} = \mathrm{e}^{kx-\omega t+\delta}$, $\mathcal{L}f^{(1)} = 0$ yields $\omega = k^5$. In contrast to the KdV case, the right hand side of the second equation,

$$-\mathcal{N}(f^{(1)}, f^{(1)}) = 15k^6\,\mathrm{e}^{2\theta}, \tag{79}$$

does not vanish but has a term in $\mathrm{e}^{2\theta}$. Thus, $f^{(2)}$ must be of the form

$$f^{(2)} = a\,\mathrm{e}^{2\theta}, \tag{80}$$

with undetermined constant coefficient $a$. Then,

$$\mathcal{L}f^{(2)} = 240ak^6\,\mathrm{e}^{2\theta} \tag{81}$$

and equating the right hand sides of (79) and (81) yields $a = \frac{1}{16}$. Next, we check that we can set $f^{(n)} = 0$ for $n \geq 3$ by verifying that the right hand sides of the subsequent equations in (78) are all zero. This is indeed the case and the perturbation scheme terminates after two steps. Setting $\epsilon = 1$,

$$f = 1 + \mathrm{e}^{\theta} + \tfrac{1}{16}\,\mathrm{e}^{2\theta}, \tag{82}$$

and $u = \frac{15}{\gamma}(\ln f)_{xx}$ yields

$$u = \tfrac{240}{\gamma}k^2\left[\frac{\mathrm{e}^{\theta}(16 + 4\mathrm{e}^{\theta} + \mathrm{e}^{2\theta})}{(16 + 16\mathrm{e}^{\theta} + \mathrm{e}^{2\theta})^2}\right] \tag{83}$$

which solves

$$u_t + \tfrac{1}{5}\gamma^2u^2u_x + \tfrac{5}{2}\gamma u_xu_{xx} + \gamma uu_{3x} + u_{5x} = 0. \tag{84}$$

The one-soliton solution can also be written as

$$u = \tfrac{240}{\gamma}k^2\left(\frac{\left[1 - \tanh^2(\frac{\theta}{2})\right]\left[21 - 30\tanh\frac{\theta}{2} + 13\tanh^2(\frac{\theta}{2})\right]}{\left[33 - 30\tanh\frac{\theta}{2} + \tanh^2(\frac{\theta}{2})\right]^2}\right) \tag{85}$$

$$= \tfrac{240}{\gamma}k^2\left(\frac{4 + 17\cosh\theta - 15\sinh\theta}{[16 + 17\cosh\theta - 15\sinh\theta]^2}\right), \tag{86}$$

where $\theta = kx - k^5t + \delta$. Figure 9 shows the 2D and 3D graphs of the one-soliton solution for $\gamma = 10$, $k = 2$, and $\delta = 0$. In comparison with the solitary wave solution of the KdV equation shown in Figs. 3 and 4, the solution of the KK equation is wider and flatter at the top.

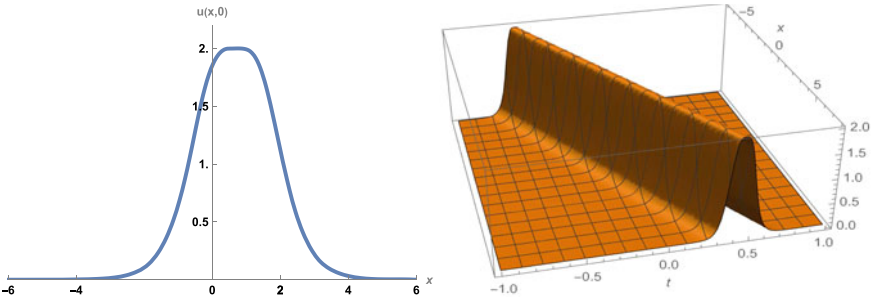


**Fig. 9** 2D and 3D graphs of solution (85) with $\gamma = 10$, $k = 2$, and $\delta = 0$

**Two-soliton Solution of the KK Equation**

Starting from

$$f^{(1)} = \mathrm{e}^{\theta_1} + \mathrm{e}^{\theta_2}, \tag{87}$$

where $\theta_i = k_i x - k_i^5 t + \delta_i$ $(i = 1, 2)$, we compute

$$-\mathcal{N}_1(f^{(1)}, f^{(1)}) = 15k_1^6\,\mathrm{e}^{2\theta_1} + 15k_2^6\,\mathrm{e}^{2\theta_2} + 10k_1k_2(2k_1^4 - k_1^2k_2^2 + 2k_2^4)\,\mathrm{e}^{\theta_1+\theta_2}. \tag{88}$$

Thus $f^{(2)}$ must be of the form

$$f^{(2)} = a_1\,\mathrm{e}^{2\theta_1} + a_2\,\mathrm{e}^{2\theta_2} + a_{12}\,\mathrm{e}^{\theta_1+\theta_2}, \tag{89}$$

with the (constant) coefficients $a_1$, $a_2$, and $a_{12}$ to be determined. Then,

$$\begin{aligned}\mathcal{L}f^{(2)} = {} & 240a_1k_1^6\,\mathrm{e}^{2\theta_1} + 240a_2k_2^6\,\mathrm{e}^{2\theta_2} \\ & + 20a_{12}k_1k_2(k_1+k_2)^2(k_1^2+k_1k_2+k_2^2)\,\mathrm{e}^{\theta_1+\theta_2}.\end{aligned} \tag{90}$$

Equating (88) with (90) determines $a_1 = a_2 = \frac{1}{16}$, as expected, and

$$a_{12} = \frac{2k_1^4 - k_1^2k_2^2 + 2k_2^4}{2(k_1+k_2)^2(k_1^2+k_1k_2+k_2^2)}. \tag{91}$$

Therefore,

$$f^{(2)} = \tfrac{1}{16}\,\mathrm{e}^{2\theta_1} + \tfrac{1}{16}\,\mathrm{e}^{2\theta_2} + \frac{(2k_1^4 - k_1^2k_2^2 + 2k_2^4)}{2(k_1+k_2)^2(k_1^2+k_1k_2+k_2^2)}\,\mathrm{e}^{\theta_1+\theta_2}. \tag{92}$$

The main difference with the the KdV, Lax, and SK equations is that the terms $\mathrm{e}^{2\theta_1}$ and $\mathrm{e}^{2\theta_2}$ in $f^{(2)}$ no longer drop out. At $O(\epsilon^3)$ one gets

$$f^{(3)} = b_{12}\left(\mathrm{e}^{\theta_1+2\theta_2} + \mathrm{e}^{2\theta_1+\theta_2}\right), \tag{93}$$

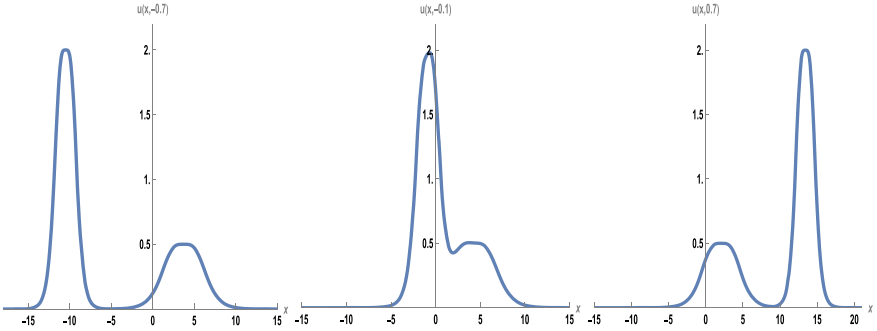


**Fig. 10** Graph of the two-soliton solution of the KK equation at three different moments in time

with

$$b_{12} = \frac{(k_1 - k_2)^2(k_1^2 - k_1k_2 + k_2^2)}{16(k_1 + k_2)^2(k_1^2 + k_1k_2 + k_2^2)}. \tag{94}$$

At the next order

$$f^{(4)} = b_{12}^2\, \mathrm{e}^{2(\theta_1+\theta_2)} = \frac{(k_1 - k_2)^4(k_1^2 - k_1k_2 + k_2^2)^2}{256(k_1 + k_2)^4(k_1^2 + k_1k_2 + k_2^2)^2}\, \mathrm{e}^{2(\theta_1+\theta_2)}. \tag{95}$$

After verification that all $f^{(n)}$ are zero for $n \geq 5$ and setting $\epsilon = 1$,

$$\begin{aligned} f = 1 + \mathrm{e}^{\theta_1} + \mathrm{e}^{\theta_2} + \tfrac{1}{16}\,\mathrm{e}^{2\theta_1} + \tfrac{1}{16}\,\mathrm{e}^{2\theta_2} + a_{12}\,\mathrm{e}^{\theta_1+\theta_2} \\ + b_{12}\left(\mathrm{e}^{2\theta_1+\theta_2} + \mathrm{e}^{\theta_1+2\theta_2}\right) + b_{12}^2\,\mathrm{e}^{2(\theta_1+\theta_2)}. \end{aligned} \tag{96}$$

The explicit expression of $u(x, t)$ (not shown due to length) then follows from $u = \frac{15}{\gamma}(\ln f)_{xx}$. The collision of two solitons for the KK equation is shown in Figs. 10 and 11 for $k_1 = 2$, $k_2 = 1$, and $\delta_1 = \delta_2 = 0$.

**Three-soliton Solution of the KK Equation**

Starting with

$$f^{(1)} = \sum_{i=1}^{3} \mathrm{e}^{\theta_i} = \mathrm{e}^{\theta_1} + \mathrm{e}^{\theta_2} + \mathrm{e}^{\theta_3}, \tag{97}$$

where $\theta_i = k_i x - k_i^5 t + \delta_i$, the equations of the perturbation scheme are solved order-by-order yielding expressions for $f^{(2)}, f^{(3)}, \ldots, f^{(6)}$ because, as it turns out, $f^{(n)} = 0$ for $n \geq 7$. The latter requires verification that the right hand sides at $O(\epsilon^7)$ and beyond all vanish in order for the perturbation scheme to terminate. The computations

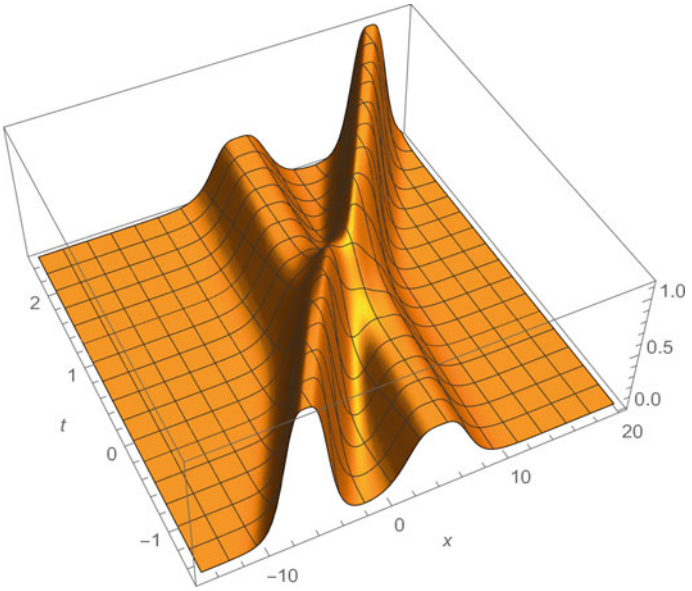


**Fig. 11** Bird's eye view of the collision of two solitons for the KK equation. Notice the phase shift after the collision

are very lengthy, time consuming, and currently at the limit of what *Mathematica* can handle.[13] Summarizing the results:

$$f^{(2)} = \tfrac{1}{16} \sum_{i=1}^{3} \mathrm{e}^{2\theta_i} + \sum_{1 \le i < j \le 3} a_{ij}\, \mathrm{e}^{\theta_i + \theta_j}, \tag{98}$$

with phase factors

$$a_{ij} = \frac{2k_i^4 - k_i^2 k_j^2 + 2k_j^4}{2(k_i + k_j)^2 (k_i^2 + k_i k_j + k_j^2)}, \qquad 1 \le i < j \le 3. \tag{99}$$

Next,

$$f^{(3)} = \sum_{1 \le i < j \le 3} b_{ij} \left( \mathrm{e}^{2\theta_i + \theta_j} + \mathrm{e}^{\theta_i + 2\theta_j} \right) + c_{123}\, \mathrm{e}^{\theta_1 + \theta_2 + \theta_3}, \tag{100}$$

where

$$b_{ij} = \frac{(k_i - k_j)^2 (k_i^2 - k_i k_j + k_j^2)}{16(k_i + k_j)^2 (k_i^2 + k_i k_j + k_j^2)}, \qquad 1 \le i < j \le 3, \tag{101}$$

[13] With the code PDESolitonSolutions.m discussed in Sect. 9, the computation of the three-soliton solution takes about 4 min on a Dell XPS-15 laptop with Intel Core i7 processor at 4.7GHz and 32 GB of memory.

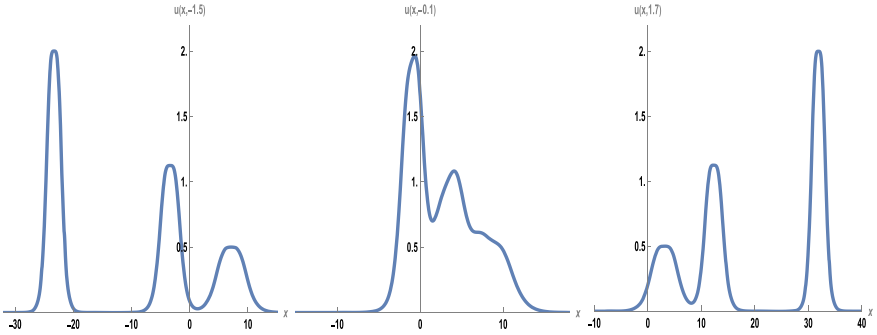


**Fig. 12** Graph of the three-soliton solution of the KK equation at three different moments in time

and

$$c_{123} = \tfrac{1}{D}\left[(2k_1^4 - k_1^2k_2^2 + 2k_2^4)(k_3^8 + k_1^4k_2^4) + (2k_1^4 - k_1^2k_3^2 + 2k_3^4)(k_2^8 + k_1^4k_3^4)\right.$$
$$\left.+(2k_2^4 - k_2^2k_3^2 + 2k_3^4)(k_1^8 + k_2^4k_3^4)\right] - \tfrac{1}{2D}\left[(k_1^2 + k_2^2)(k_1^4 + k_2^4)(k_3^6 + k_1^2k_2^2k_3^2)\right.$$
$$+(k_1^2 + k_3^2)(k_1^4 + k_3^4)(k_2^6 + k_1^2k_2^2k_3^2) + (k_2^2 + k_3^2)(k_2^4 + k_3^4)(k_1^6 + k_1^2k_2^2k_3^2)$$
$$\left.+12k_1^4k_2^4k_3^4\right] \tag{102}$$

with

$$D = 4\prod_{1\le i<j\le 3}(k_i + k_j)^2\,(k_i^2 + k_ik_j + k_j^2). \tag{103}$$

Carrying on,

$$f^{(4)} = \sum_{1\le i<j\le 3} b_{ij}^2\,\mathrm{e}^{2(\theta_i+\theta_j)} + 16\left(a_{23}b_{12}b_{13}\,\mathrm{e}^{2\theta_1+\theta_2+\theta_3}\right.$$
$$\left.+\,a_{13}b_{12}b_{23}\mathrm{e}^{\theta_1+2\theta_2+\theta_3} + a_{12}b_{13}b_{23}\,\mathrm{e}^{\theta_1+\theta_2+2\theta_3}\right), \tag{104}$$
$$f^{(5)} = 256\,b_{12}b_{13}b_{23}\left(b_{12}\,\mathrm{e}^{2\theta_1+2\theta_2+\theta_3} + b_{13}\mathrm{e}^{2\theta_1+\theta_2+2\theta_3}\right.$$
$$\left.+\,b_{23}\,\mathrm{e}^{\theta_1+2\theta_2+2\theta_3}\right), \tag{105}$$
$$f^{(6)} = 16\,(16b_{12}b_{13}b_{23})^2\,\mathrm{e}^{2(\theta_1+\theta_2+\theta_3)}. \tag{106}$$

Finally, after setting $\epsilon = 1$,

$$f = 1 + f^{(1)} + f^{(2)} + f^{(3)} + f^{(4)} + f^{(5)} + f^{(6)}, \tag{107}$$

and $u(x,t) = \frac{15}{\gamma}(\ln f)_{xx}$ (not shown due to length) then solves (84).

The collision of three solitons for the KK equation is shown in Figs. 12 and 13 for $k_1 = 2, k_2 = \frac{3}{2}, k_3 = 1$, and $\delta_1 = \delta_2 = \delta_3 = 0$.

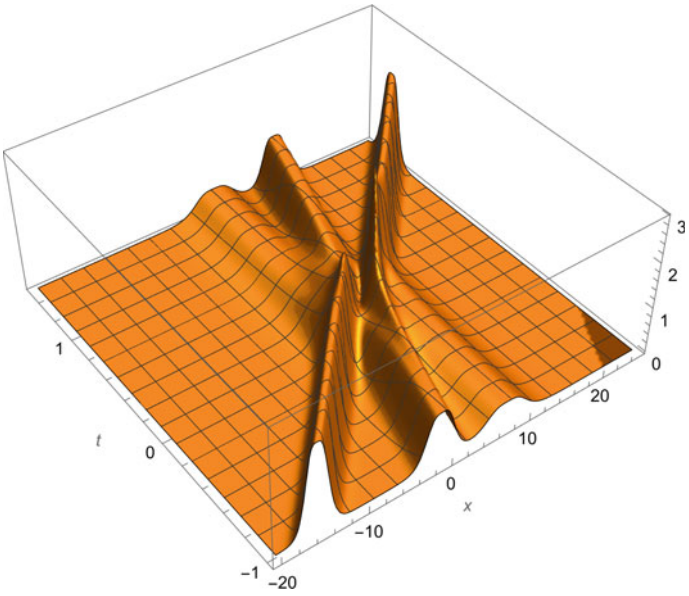


**Fig. 13** Bird's eye view of the collision of three solitons for the KK equation. Notice the phase shift after the collision

## 5 The Modified KdV Equation

Of course, not every polynomial soliton equation in $(1+1)$ dimensions can be solved with a solution of type (28). Consider, for example, the mKdV equation,

$$u_t + 24u^2u_x + u_{3x} = 0, \tag{108}$$

which after integration becomes

$$\partial_t \left( \int^x u\, dx \right) + 8u^3 + u_{xx} = 0. \tag{109}$$

The Laurent series for (108) suggests the transformation

$$u = \pm\tfrac{1}{2}i\, (\ln \tilde{f})_x = \pm\tfrac{1}{2}i \left( \frac{\tilde{f}_x}{\tilde{f}} \right). \tag{110}$$

Substitution of either of these branches into (109) yields

$$\tilde{f}(\tilde{f}_t + \tilde{f}_{3x}) - 3\tilde{f}_x \tilde{f}_{xx} = 0. \tag{111}$$

Although homogeneous of second degree and deceptively simple, it has no solution of the form $\tilde{f} = 1 + \mathrm{e}^{\theta}$ where $\theta = k\,x - \omega\,t + \delta$. Indeed, the term in $\mathrm{e}^{\theta}$ vanishes for $\omega = k^3$ but the term $-3k^3\mathrm{e}^{2\theta}$ is only zero when $k = 0$. It is clear from (110) that to obtain a real-valued solution, i.e., $u^\star = u$, $\tilde{f}$ must be a complex function. One can readily verify that $u = \pm\frac{1}{2}i\,(\ln(f + i\,g))_x$, for real functions $f$ and $g$ does not work either. So, $\tilde{f}$ must be a ratio of complex functions. Hence,

$$u = \pm\tfrac{1}{2}i\,\left(\ln\left(\frac{f + i\,g}{h + i\,j}\right)\right)_x, \tag{112}$$

where $f, g, h,$ and $j$ are real functions. From $u^\star = u$ it follows that $h = f$ and $j = -g$. Observe that (108) remains invariant when $u$ is replaced by its negative. Therefore, without loss of generality, we continue with the plus sign,

$$u = \tfrac{1}{2}i\,\left(\ln\left(\frac{f + i\,g}{f - i\,g}\right)\right)_x = \left(\arctan\left(\tfrac{f}{g}\right)\right)_x = \frac{f_x g - f g_x}{f^2 + g^2}, \tag{113}$$

which is Hirota's transformation for the mKdV equation [43]. Note that the roles of $f$ and $g$ can thus be interchanged in the computations below.

Goldstein [23] gave a different argument[14] to arrive at (113). Accounting for the $\pm$ signs in (110), he argued that the solution may have two families of singularities and therefore assumed[15]

$$u = \tfrac{1}{2}i\,\left(\frac{F_x}{F} - \frac{G_x}{G}\right) = \tfrac{1}{2}i\,\left(\ln\left(\frac{F}{G}\right)\right)_x. \tag{114}$$

Note that the two terms (in the first equality above) indeed account for the two branches in (110). Setting $F = f + i\,g$ and $G = f - i\,g$ then gives (113).

Applying Hirota's transformation (113) to (109) yields

$$\begin{aligned} &f^3(g_t + g_{3x}) - g^3(f_t + f_{3x}) - f^2(f_t g + 3f_x g_{xx} + 3f_{xx}g_x + f_{3x}g) \\ &+g^2(f g_t + f g_{3x} + 3f_x g_{xx} + 3f_{xx}g_x) + 6f g_x(f_x^2 + g_x^2) \\ &-6f_x g(f_x^2 + g_x^2) + 6f g(f_x f_{xx} - g_x g_{xx}) = 0, \end{aligned} \tag{115}$$

which is clearly not of the usual form the simplified Hirota method applies to. The terms in (115) can be regrouped as

$$\begin{aligned} &(f^2 + g^2)(f_t g - f g_t - f g_{3x} + 3f_x g_{xx} - 3f_{xx}g_x + f_{3x}g) \\ &-6(f_x g - f g_x)(f f_{xx} - f_x^2 + g g_{xx} - g_x^2) = 0. \end{aligned} \tag{116}$$

[14] The argument is based on modified singular manifold expansion methods [17, 24, 81].

[15] With $u = \pm\frac{1}{2}\,i\,(\ln(F/G))_x$, (108) can be replaced by $(D_t + D_x^3)(F\cdot G) = 0$ and $D_x^2(F\cdot G) = 0$ where $G = F^\star$. See, e.g., [28] for explicit expressions of $F$ and $G$ for the two- and three-soliton cases.

Taking advantage of the fact that there are two free functions in play, Hirota [43, 45] then set the factors multiplying $f^2 + g^2$ and $f_x g - f g_x$ separately equal to zero, to get the coupled system

$$f(g_t + g_{3x}) - g(f_t + f_{3x}) - 3(f_x g_{xx} - f_{xx} g_x) = 0, \tag{117}$$
$$f f_{xx} - f_x^2 + g g_{xx} - g_x^2 = 0, \tag{118}$$

which can be written in bilinear form as

$$(D_t + D_x^3)(f \cdot g) = 0, \tag{119}$$
$$D_x^2(f \cdot f + g \cdot g) = 0. \tag{120}$$

Ignoring the bilinear form, one could write (117) and (118) as

$$f\,\mathcal{L}g - g\,\mathcal{L}f + \mathcal{N}_1(f, g) = 0, \tag{121}$$
$$\mathcal{N}_2(f, f) + \mathcal{N}_2(g, g) = 0, \tag{122}$$

with

$$\mathcal{L}f = f_t + f_{3x} \tag{123}$$

and

$$\mathcal{N}_1(f, g) = -3(f_x g_{xx} - f_{xx} g_x), \tag{124}$$
$$\mathcal{N}_2(f, g) = f g_{xx} - f_x g_x. \tag{125}$$

With a suitable adaptation of the method in Sect. 3.2, one could then seek a solution of (121) and (122) using

$$f = f^{(0)} + \epsilon f^{(1)} + \epsilon^2 f^{(2)} + \ldots, \tag{126}$$
$$g = g^{(0)} + \epsilon g^{(1)} + \epsilon^2 g^{(2)} + \ldots. \tag{127}$$

Based on the interchangeability of $f$ and $g$, one can either take $f^{(0)} = g^{(1)} = 0$ and $g^{(0)} = 1$, or equivalently, $g^{(0)} = f^{(1)} = 0$ and $f^{(0)} = 1$. In either case, $\mathcal{L}\mathrm{e}^{\theta_i} = \mathcal{L}\mathrm{e}^{k_i x - \omega_i t + \delta_i} = 0$ determines the dispersion relation $\omega_i = k_i^3$. Proceeding with the former case but skipping the details of the computations we summarize the results.

**One-soliton Solution of the mKdV Equation**

With

$$f = \mathrm{e}^{\theta} = \mathrm{e}^{kx - k^3 t + \delta} \quad \text{and} \quad g = 1, \tag{128}$$

one gets

$$u = \frac{f_x}{1+f^2} = k\frac{\mathrm{e}^{\theta}}{1+\mathrm{e}^{2\theta}} = \tfrac{1}{2}k\,\mathrm{sech}\,\theta$$
$$= \tfrac{1}{2}k\,\mathrm{sech}\,(kx - k^3t + \delta) = K\,\mathrm{sech}\left(2\,Kx - 8\,K^3t + \delta\right) \tag{129}$$

with $K = \frac{k}{2}$.

**Two-soliton Solution of the mKdV Equation**

Now

$$f = \mathrm{e}^{\theta_1} + \mathrm{e}^{\theta_2},$$
$$g = 1 - a_{12}\mathrm{e}^{\theta_1+\theta_2}, \tag{130}$$

with $\theta_i = k_i x - k_i^3 t + \delta_i$ and $a_{12} = \left(\frac{k_1-k_2}{k_1+k_2}\right)^2$. Then,

$$u = \frac{k_1\mathrm{e}^{\theta_1} + k_2\mathrm{e}^{\theta_2} + a_{12}\,(k_1\mathrm{e}^{\theta_2} + k_2\mathrm{e}^{\theta_1})\mathrm{e}^{\theta_1+\theta_2}}{1 + \mathrm{e}^{2\theta_1} + \mathrm{e}^{2\theta_2} + \dfrac{8k_1k_2}{(k_1+k_2)^2}\,\mathrm{e}^{\theta_1+\theta_2} + a_{12}^2\,\mathrm{e}^{2\theta_1+2\theta_2}}. \tag{131}$$

**Three-soliton Solution of the mKdV Equation**

After some computations one finds that

$$f = \mathrm{e}^{\theta_1} + \mathrm{e}^{\theta_2} + \mathrm{e}^{\theta_3} - b_{123}\mathrm{e}^{\theta_1+\theta_2+\theta_3},$$
$$g = 1 - a_{12}\,\mathrm{e}^{\theta_1+\theta_2} - a_{13}\,\mathrm{e}^{\theta_1+\theta_3} - a_{23}\,\mathrm{e}^{\theta_2+\theta_3}, \tag{132}$$

with $\theta_i = k_i x - k_i^3 t + \delta_i$, $a_{ij} = \left(\frac{k_i-k_j}{k_i+k_j}\right)^2$, and $b_{123} = a_{12}a_{13}a_{23}$.

***N*-soliton Solution of the mKdV Equation**

A concise formula [35, 52, 73] for the function $\tilde{F} = g + i\,f$ leading to the $N$-soliton solution $u = \frac{1}{2}i\,\left(\ln\left(\frac{\tilde{F}}{\tilde{F}^\star}\right)\right)_x$ of the mKdV equation is given[16] by

$$\tilde{F} = \sum_{\mu=0,1} \mathrm{e}^{\left[\sum_{i<j}^{(N)} \mu_i\mu_j A_{ij} + \sum_{j=1}^{N} \mu_j(\theta_j + i\frac{\pi}{2})\right]}, \tag{133}$$

where the summations have the same meaning as in (49) and again $a_{ij} = \mathrm{e}^{A_{ij}}$. The extra $i\frac{\pi}{2}$ takes care of the complex coefficients and sign reversals.

The $N$-soliton solution can be written [43, 100, 102] as

$$u(x,t) = \frac{1}{2i}\left(\ln\frac{\det(I + iM)}{\det(I - iM)}\right)_x, \tag{134}$$

[16] Recall that the roles of $f$ and $g$ can be interchanged because $-u$ solves (108) whenever $u$ does. $\tilde{F}$ is $F$ with the roles of $f$ and $g$ reversed.

where $I$ is the $N \times N$ identity matrix and

$$M_{\ell m} = \frac{\mathrm{e}^{\Theta_\ell + \Theta_m}}{K_\ell + K_m} \quad \text{with } \Theta_\ell = K_\ell x - 4K_\ell^3 t + \Delta_\ell. \tag{135}$$

Note that $\frac{\det(I+iM)}{\det(I-iM)}$ matches $\frac{\tilde{F}}{F^*} = \frac{g+i\,f}{g-i\,f}$ with $f$ and $g$ in (128), (130), and (132) when $k_i = 2K_i$ and $\delta_i = 2\Delta_i - \ln(2K_i)$ with $K_i > 0$.

## 6 Application to Non-solitonic PDEs

### 6.1 The Fisher Equation with Convection

One of the examples discussed in [26] is the Fisher equation with convection term [76, 79],

$$u_t + \alpha u u_x - u_{xx} - u(1-u) = 0, \quad \alpha \neq 0, \tag{136}$$

where $\alpha$ is the convection coefficient. This equation can also be viewed as a Burgers equation with quadratic source term. Motivated by a truncated Laurent series, use

$$u = -\tfrac{2}{\alpha}(\ln f)_x = -\tfrac{2}{\alpha}\left(\frac{f_x}{f}\right) \tag{137}$$

to replace (136) with a homogeneous equation of second degree

$$f(f_{3x} + f_x - f_{xt}) + f_x(f_t - f_{xx} + \tfrac{2}{\alpha} f_x) \equiv f\,\mathcal{L}f + \mathcal{N}(f, f) = 0, \tag{138}$$

where

$$\mathcal{L}f = f_{3x} + f_x - f_{xt}, \tag{139}$$

$$\mathcal{N}(f, g) = f_x(g_t - g_{xx} + \tfrac{2}{\alpha} g_x). \tag{140}$$

Seeking a solution of type (28), $\mathcal{L}f^{(1)} = \mathcal{L}(\sum_{i=1}^{N} \mathrm{e}^{\theta_i})$ yields $\omega_i = -(1 + k_i^2)$. The second equation in (39) then becomes

$$\mathcal{L}f^{(2)} = -\sum_{i=1}^{N} k_i \left(1 + \tfrac{2}{\alpha} k_i\right) \mathrm{e}^{2\theta_i} - \sum_{1 \leq i < j \leq N} \left(k_i + k_j + \tfrac{4}{\alpha} k_i k_j\right) \mathrm{e}^{\theta_i + \theta_j}. \tag{141}$$

If we were to include the terms $\mathrm{e}^{2\theta_i}$ in $f^{(2)}$ the perturbation scheme would not terminate. Hence, we are forced to set all wave numbers equal to $k_i = -\frac{\alpha}{2}$ ($i = 1, 2, \ldots, N$). Thus, $N = 1$ and only a solitary solution can be obtained. Note that both sums in (141) vanish when $k_i = -\frac{\alpha}{2}$. Hence, $f^{(2)} = 0$ and

$$f(x,t) = 1 + \mathrm{e}^{\theta} = 1 + \mathrm{e}^{-\frac{\alpha}{2}x + \frac{1}{4}(4+\alpha^2)t + \delta}. \tag{142}$$

Finally, from (137)

$$u(x,t) = \frac{\mathrm{e}^{\theta}}{1+\mathrm{e}^{\theta}} = \tfrac{1}{2}\left(1 - \tanh\left[\tfrac{1}{2}\left(\tfrac{\alpha}{2}x - \tfrac{1}{4}(4+\alpha^2)t - \delta\right)\right]\right), \tag{143}$$

since $k = -\frac{\alpha}{2}$. The graphs of the kink solution (143) in 2D and 3D are similar to those in Fig. 1.

## 6.2 The Fisher Equation

A transformation to homogenize the Fisher equation [18, 80] without convection,

$$u_t - u_{xx} - u(1-u) = 0, \tag{144}$$

is remarkably different from (137). Indeed, a truncated Laurent series suggests

$$u = -6(\ln f)_{xx} + \tfrac{6}{5}(\ln f)_t, \tag{145}$$

which yields

$$\begin{aligned} &f(f_{4x} + f_{xx} - \tfrac{6}{5}f_{xxt} + \tfrac{1}{5}f_{tt} - \tfrac{1}{5}f_t) - 4f_x f_{3x} + 3f_{xx}^2 - f_x^2 \\ &-\tfrac{6}{5}f_t f_{xx} + \tfrac{12}{5}f_x f_{xt} + \tfrac{1}{25}f_t^2 \equiv f\,\mathcal{L}f + \mathcal{N}(f,f) = 0. \end{aligned} \tag{146}$$

Here,

$$\mathcal{L}f = f_{4x} + f_{xx} - \tfrac{6}{5}f_{xxt} + \tfrac{1}{5}f_{tt} - \tfrac{1}{5}f_t, \tag{147}$$

$$\mathcal{N}(f,g) = -4f_x g_{3x} + 3f_{xx}g_{xx} - f_x g_x - \tfrac{6}{5}f_t g_{xx} + \tfrac{12}{5}f_{xt}g_x + \tfrac{1}{25}f_t g_t. \tag{148}$$

Solving (39) with $f^{(1)} = \sum_{i=1}^{N} \mathrm{e}^{\theta_i} = \sum_{i=1}^{N} \mathrm{e}^{k_i x - \omega_i t + \delta_i}$ as a starting point, one gets $\omega_i = -5k_i^2$ or $\omega_i = -(1+k_i^2)$.

**Case 1**: For $\omega_i = -5k_i^2$ the second equation in (39) reads

$$\mathcal{L}f^{(2)} = \sum_{i=1}^{N} k_i^2(1-6k_i^2)\,\mathrm{e}^{2\theta_i} + 2\sum_{1\le i<j\le N} c_{ij}\,\mathrm{e}^{\theta_i+\theta_j}, \tag{149}$$

where $c_{ij} = k_i k_j\left[1 + 2k_i k_j - 4(k_i^2 + k_j^2)\right]$. If we put terms $\mathrm{e}^{2\theta_i}$ in $f^{(2)}$ the perturbation scheme does not terminate. Hence, $k_i = \pm\frac{1}{\sqrt{6}}$ $(i = 1, 2, \ldots, N)$ which also

makes $c_{ij} = 0$. This leads us to conclude that a multi-soliton solution does not exist and $N = 1$. With $k = \pm\frac{1}{\sqrt{6}}$ we have $\omega = -\frac{5}{6}$. Using (145) with $f = 1 + \mathrm{e}^{\theta}$ gives

$$u(x,t) = \frac{\mathrm{e}^{2\theta}}{(1+\mathrm{e}^{\theta})^2} = \frac{1}{(1+e^{-\theta})^2} = \tfrac{1}{4}\left(1 + \tanh\tfrac{\theta}{2}\right)^2, \tag{150}$$

where each of these forms of the solution appears in the literature (see, e.g., [4]). Explicitly, for $k = -\frac{1}{\sqrt{6}}$,

$$u(x,t) = \tfrac{1}{4}\left(1 - \tanh\left[\tfrac{1}{2}\left(\tfrac{1}{\sqrt{6}}x - \tfrac{5}{6}t - \delta\right)\right]\right)^2, \tag{151}$$

which is a wave traveling to the right. The graph of this kink solution is the same as in Fig. 1 but with a steeper slope due to the square in (151). For $k = \frac{1}{\sqrt{6}}$,

$$u(x,t) = \tfrac{1}{4}\left(1 + \tanh\left[\tfrac{1}{2}\left(\tfrac{1}{\sqrt{6}}x + \tfrac{5}{6}t + \delta\right)\right]\right)^2, \tag{152}$$

which is a left-traveling wave, a bit steeper than the one shown in Fig. 1 after a vertical flip. Note that (152) does not follow from (143) in the limit for $\alpha \to 0$.

**Case 2**: For $\omega_i = -(1 + k_i^2)$ the second equation in (39) becomes

$$\mathcal{L}f^{(2)} = -\tfrac{1}{25}\left(\sum_{i=1}^{N}(1+k_i^2)(1+6k_i^2)\,\mathrm{e}^{2\theta_i} + 2\sum_{1\le i<j\le N} c_{ij}\,\mathrm{e}^{\theta_i+\theta_j}\right), \tag{153}$$

where $c_{ij} = \left[1 + 35k_ik_j + 46k_i^2k_j^2 - 2(k_i^2 + k_j^2)(7 + 10k_ik_j)\right]$. So, for real wave numbers $k_i$ the terms $\mathrm{e}^{2\theta_i}$ do not vanish. No solitary wave solutions or solitons can be obtained in this case.

### 6.3 The FitzHugh-Nagumo Equation with Convection

The FHN equation with convection term [58],

$$u_t + \alpha u u_x - u_{xx} + u(1-u)(a-u) = 0, \tag{154}$$

where $\alpha$ denotes the convection coefficient and $a$ is an arbitrary constant, is also called the Burgers-Huxley equation [87].

A truncated Laurent series suggests two possible transformations, namely,

$$u = \sqrt{m}\,(\ln f)_x = \sqrt{m}\left(\frac{f_x}{f}\right), \quad m > 0. \tag{155}$$

and

$$u = -\frac{2}{\sqrt{m}}(\ln f)_x = -\frac{2}{\sqrt{m}}\left(\frac{f_x}{f}\right), \quad m > 0, \tag{156}$$

where we have replaced $\alpha$ by $\frac{m-2}{\sqrt{m}}$ in (154) to simplify their forms and the computations below. Using (155), (154) transforms into

$$\begin{aligned} &f(f_{3x} - af_x - f_{xt}) + f_x\left(f_t - (m+1)f_{xx} + \sqrt{m}(1+a)f_x\right) \\ &\equiv f\,\mathcal{L}f + \mathcal{N}(f,f) = 0, \end{aligned} \tag{157}$$

where

$$\mathcal{L}f = f_{3x} - af_x - f_{xt}, \tag{158}$$

$$\mathcal{N}(f,g) = f_x\left(g_t - (m+1)g_{xx} + \sqrt{m}(1+a)g_x\right). \tag{159}$$

To compute a single solitary wave solution we take $f = 1 + \mathrm{e}^{\theta}$. Then, $\mathcal{L}\mathrm{e}^{\theta} = 0$ yields $\omega = a - k^2$. Next, $\mathcal{N}(\mathrm{e}^{\theta}, \mathrm{e}^{\theta}) = 0$ determines $k = \frac{1}{\sqrt{m}}$ or $k = \frac{a}{\sqrt{m}}$. Thus, $\omega = \frac{am-1}{m}$ or $\omega = \frac{a(m-a)}{m}$, respectively. Returning to $u$, we obtain the solitary wave solutions

$$u(x,t) = \tfrac{1}{2}\left(1 + \tanh\left[\tfrac{1}{2}\left(\frac{1}{\sqrt{m}}x - \frac{(am-1)}{m}t + \delta\right)\right]\right) \tag{160}$$

and

$$u(x,t) = \tfrac{1}{2}a\left(1 + \tanh\left[\tfrac{1}{2}\left(\frac{a}{\sqrt{m}}x - \frac{a(m-a)}{m}t + \delta\right)\right]\right). \tag{161}$$

Although it is impossible to find a two-soliton solution, a so-called *bi-soliton* solution can be computed which describes coalescent wave fronts. Indeed, taking $f = 1 + \mathrm{e}^{\theta_1} + \mathrm{e}^{\theta_2}$, with $\omega_i = a - k_i^2$ $(i = 1, 2)$, after some computations one gets

$$u(x,t) = \frac{\mathrm{e}^{\theta_1} + a\,\mathrm{e}^{\theta_2}}{1 + \mathrm{e}^{\theta_1} + \mathrm{e}^{\theta_2}}, \tag{162}$$

where

$$\theta_1 = \tfrac{1}{\sqrt{m}}x - \left(\tfrac{am-1}{m}\right)t + \delta_1, \quad \theta_2 = \tfrac{a}{\sqrt{m}}x - \left(\tfrac{a(m-a)}{m}\right)t + \delta_2. \tag{163}$$

Since $\alpha = \frac{m-2}{\sqrt{m}}$, possible[17] values for $m$ are

$$m = \tfrac{1}{2}\left(4 + \alpha^2 \pm \alpha\sqrt{8 + \alpha^2}\right), \quad m > 0. \tag{164}$$

This solution can be found in [30, 58] where it was obtained with a different method.

[17] For any positive value of $m$, the pair $(\alpha, m)$ must still satisfy $\alpha = \frac{m-2}{\sqrt{m}}$.

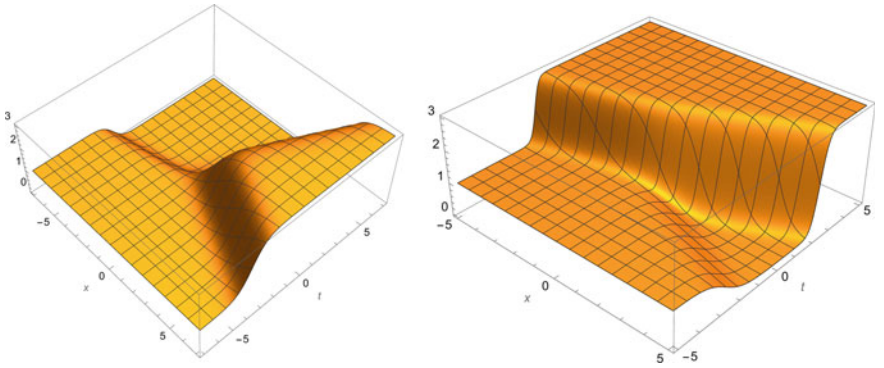


**Fig. 14** 3D graphs of solution (162) with (163) (left) and (167) (right) both for $a = 3$, $\alpha = 1$ (i.e., $m = 4$), and $\delta_1 = \delta_2 = 0$

Skipping the details, with (156) one obtains the following solutions

$$u(x,t) = \tfrac{1}{2}\left(1 - \tanh\left[\tfrac{1}{2}\left(\frac{\sqrt{m}}{2}x + \frac{(4a-m)}{4}t - \delta\right)\right]\right) \tag{165}$$

and

$$u(x,t) = \tfrac{1}{2}a\left(1 - \tanh\left[\tfrac{1}{2}\left(\frac{a\sqrt{m}}{2}x + \frac{a(4-am)}{4}t - \delta\right)\right]\right), \tag{166}$$

with $m$ given in (164). The bi-soliton solution corresponding to (156) is (162) with

$$\theta_1 = -\tfrac{\sqrt{m}}{2}x - \left(\tfrac{4a-m}{4}\right)t + \delta_1, \quad \theta_2 = -\tfrac{a\sqrt{m}}{2}x - \left(\tfrac{a(4-am)}{4}\right)t + \delta_2. \tag{167}$$

Solution (162) with either (163) or (167) describes the coalescence of two wave fronts pictured in Fig. 14.

Finally, for $m = 2$ (i.e., $\alpha = 0$), one gets a solitary wave solution of the FHN equation without convection [5].

## *6.4 A Burgers Equation with a Cubic Source Term*

Consider the Burgers equation with a polynomial source term of third degree,

$$u_t + \alpha u u_x - u_{xx} = 3u(2-u)(u+1), \tag{168}$$

which is of the kind treated in [99, Eq. (26)]. Equation (168) can also be viewed as an equation of FitzHugh-Naguma-type with convection term.[18] Such equations are known to have coalescent wave fronts [27, 58]. Based on a truncated Laurent series, there are potentially two homogenizing transformations:

$$u = \sqrt{m}\,(\ln f)_x = \sqrt{m}\left(\frac{f_x}{f}\right), \quad m > 0. \tag{169}$$

and

$$u = -\frac{2}{3\sqrt{m}}\,(\ln f)_x = -\frac{2}{3\sqrt{m}}\left(\frac{f_x}{f}\right), \quad m > 0, \tag{170}$$

where we used $\alpha = \frac{3m-2}{\sqrt{m}}$ in (168) to simplify their forms. Starting with (169), substitution into (168) yields

$$f\,(6f_x - f_{xt} + f_{3x}) + f_x\left(f_t + 3\sqrt{m}\,f_x - (1+3\,m)\,f_{xx}\right) \tag{171}$$

$$\equiv f\,\mathcal{L}f + \mathcal{N}(f,f) = 0. \tag{172}$$

Here, $\mathcal{L}$ and $\mathcal{N}$ are defined by

$$\mathcal{L}f = 6f_x - f_{xt} + f_{3x}, \tag{173}$$

$$\mathcal{N}(f,g) = f_x\left(g_t + 3\sqrt{m}g_x - (1+3\,m)\,g_{xx}\right). \tag{174}$$

For the single solitary wave solution, $\mathcal{L}\mathrm{e}^{\theta} = 0$ yields $\omega = -(k^2+6)$. Next, $\mathcal{N}(\mathrm{e}^{\theta}, \mathrm{e}^{\theta}) = 0$ determines $k = -\frac{1}{\sqrt{m}}$ or $k = \frac{2}{\sqrt{m}}$. Thus, $\omega = -\frac{6m+1}{m}$ or $\omega = -\frac{2(3m+2)}{m}$, respectively. So, with $f = 1 + \mathrm{e}^{\theta}$ we obtain the solitary wave solutions

$$u(x,t) = -\tfrac{1}{2}\left(1 - \tanh\left[\tfrac{1}{2\sqrt{m}}x - \frac{(6\,m+1)}{2\,m}t - \frac{\delta}{2}\right]\right) \tag{175}$$

and

$$u(x,t) = 1 + \tanh\left[\frac{1}{\sqrt{m}}x + \frac{(3\,m+2)}{m}t + \frac{\delta}{2}\right], \tag{176}$$

where, with regard to $\alpha = \frac{3m-2}{\sqrt{m}}$, possible values[19] for $m$ are

$$m = \tfrac{1}{18}\left(12 + \alpha^2 \pm \alpha\sqrt{24+\alpha^2}\right), \quad m > 0. \tag{177}$$

As with the FHN equation with convection term, no two-soliton solution exists but a bi-soliton solution can be found which describes coalescent wave fronts. Indeed, taking $f = 1 + \mathrm{e}^{\theta_1} + \mathrm{e}^{\theta_2}$ where $\omega_i = -(k_i^2 + 6)$ $(i = 1, 2)$ one gets

[18] Except that $u - 1$ is now replaced by $u + 1$.

[19] For any positive value of $m$, the pair $(\alpha, m)$ must still satisfy $\alpha = \frac{3m-2}{\sqrt{m}}$.

$$u(x,t) = \frac{\sqrt{m}(k_1 e^{\theta_1} + k_2 e^{\theta_2})}{1 + e^{\theta_1} + e^{\theta_2}}$$
$$= \frac{2\, e^{\frac{2}{\sqrt{m}}x + \frac{2(3m+2)}{m}t + \delta_1} - e^{-\frac{1}{\sqrt{m}}x + \frac{(6m+1)}{m}t + \delta_2}}{1 + e^{\frac{2}{\sqrt{m}}x + \frac{2(3m+2)}{m}t + \delta_1} + e^{-\frac{1}{\sqrt{m}}x + \frac{(6m+1)}{m}t + \delta_2}}, \tag{178}$$

because $k_1 = \frac{2}{\sqrt{m}}$ and $k_2 = -\frac{1}{\sqrt{m}}$ with $m$ in (177). For $m = 1$, a solution of (168) with $\alpha = 1$ then reads

$$u(x,t) = \frac{2e^{2x+10t+\delta_1} - e^{-x+7t+\delta_2}}{1 + e^{2x+10t+\delta_1} + e^{-x+7t+\delta_2}}. \tag{179}$$

The solution procedure using (170) is similar and leads to

$$u(x,t) = -\tfrac{1}{2}\left(1 + \tanh\left[\tfrac{3\sqrt{m}}{4}x + \frac{3(3\,m+8)}{8}t + \frac{\delta}{2}\right]\right) \tag{180}$$

and

$$u(x,t) = 1 - \tanh\left[\frac{3\sqrt{m}}{2}x - \frac{3(3\,m+2)}{2}t - \frac{\delta}{2}\right], \tag{181}$$

with $m$ given in (177). The bi-soliton solution corresponding to (170) reads

$$u(x,t) = -\frac{2}{3\sqrt{m}}\frac{(k_1 e^{\theta_1} + k_2 e^{\theta_2})}{(1 + e^{\theta_1} + e^{\theta_2})}$$
$$= -\frac{e^{\frac{3\sqrt{m}}{2}x + \frac{3(3m+8)}{4}t + \delta_1} - 2\, e^{-3\sqrt{m}x + 3(3m+2)t + \delta_2}}{1 + e^{\frac{3\sqrt{m}}{2}x + \frac{3(3m+8)}{4}t + \delta_1} + e^{-3\sqrt{m}x + 3(3m+2)t + \delta_2}}, \tag{182}$$

because $k_1 = \frac{3\sqrt{m}}{2}$ and $k_2 = -3\sqrt{m}$ with $m$ in (177). For $m = 1$, a bi-soliton solution of (168) with $\alpha = 1$ then becomes

$$u(x,t) = -\frac{e^{\frac{3}{2}x + \frac{33}{4}t + \delta_1} - 2e^{-3x+15t+\delta_2}}{1 + e^{\frac{3}{2}x + \frac{33}{4}t + \delta_1} + e^{-3x+15t+\delta_2}}. \tag{183}$$

Solutions (179) and (183), describing two coalescent wave fronts, are shown in Fig. 15.

Returning to $\alpha$ via (177) also allows one to consider the case $\alpha = 0$ (i.e., $m = \frac{2}{3}$), leading to solutions of (168) with a cubic source but without convection.

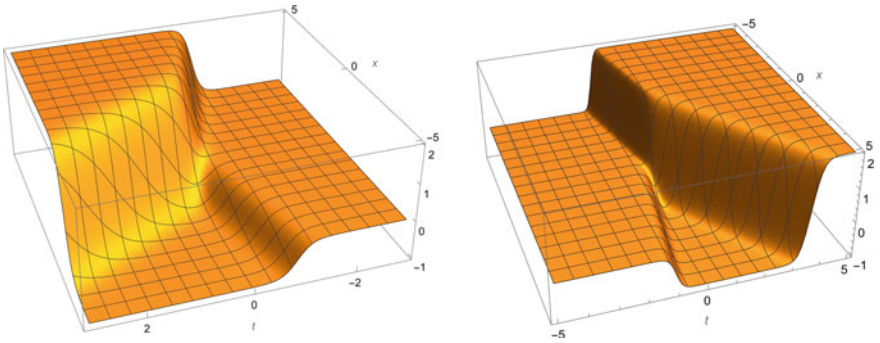

**Fig. 15** 3D graphs of (179) (left) and (183) (right) for $\delta_1 = -\delta_2 = 1$

## 6.5 A Wave Equation with Cubic Source Term

Consider the wave equation,

$$\tfrac{1}{8}u_{tt} + u_t + uu_x - \tfrac{1}{8}u_{xx} = u(u-1)(u+2), \tag{184}$$

which is a special case of an equation investigated in [99, Eq. (2)]. The Laurent series solution suggests the transformation

$$u = \tfrac{1}{2}\kappa\left[(\ln f)_t - \kappa(\ln f)_x\right] = \tfrac{1}{2}\kappa\left(\frac{f_t - \kappa f_x}{f}\right), \tag{185}$$

with $\kappa = \pm 1$. We first consider the case where $\kappa = 1$. Using

$$u = \tfrac{1}{2}\left(\frac{f_t - f_x}{f}\right), \tag{186}$$

allows one to replace (184) by

$$\begin{aligned} &f\,(16f_t + 8f_{tt} + f_{3t} - 16f_x - 8f_{xt} - f_{xtt} - f_{xxt} + f_{3x}) \\ &-(3f_t - f_x)\,(4f_t + f_{tt} - 4f_x - 2f_{xt} + f_{xx}) \\ &\equiv f\,\mathcal{L}f + \mathcal{N}(f,f) = 0, \end{aligned} \tag{187}$$

with

$$\mathcal{L}f = 16f_t + 8f_{tt} + f_{3t} - 16f_x - 8f_{xt} - f_{xtt} - f_{xxt} + f_{3x}, \tag{188}$$

$$\mathcal{N}(f,g) = -(3f_t - f_x)\,(4g_t + g_{tt} - 4g_x - 2g_{xt} + g_{xx})\,. \tag{189}$$

Then, $\mathcal{L}\mathrm{e}^{\theta} = 0$ yields $\omega = -k$, $\omega = 4 - k$, or $\omega = 4 + k$. With $f = 1 + \mathrm{e}^{\theta}$, one readily obtains

$$u(x,t) = -\tfrac{1}{2}(\omega + k)\left(\frac{\mathrm{e}^{\theta}}{1+\mathrm{e}^{\theta}}\right) = -\tfrac{1}{4}(\omega + k)\left(1 + \tanh\tfrac{\theta}{2}\right). \tag{190}$$

Obviously, the choice $\omega = -k$ must be rejected. For $\omega = 4 - k$, one finds that $\mathcal{N}(\mathrm{e}^{\theta}, \mathrm{e}^{\theta}) \equiv 0$ and

$$u(x,t) = -\left(1 + \tanh\left[\tfrac{1}{2}\,(kx - (4-k)t + \delta)\right]\right) \tag{191}$$

with arbitrary $k$ and $\delta$. For $\omega = 4 + k$, $\mathcal{N}(\mathrm{e}^{\theta}, \mathrm{e}^{\theta}) = 0$ determines $k = -2$ or $k = -3$ resulting in $\omega = 2$ or $\omega = 1$, respectively. The case $k = -2$ (i.e., $\omega = 2$) is rejected for it leads to $u(x,t) \equiv 0$. For $k = -3$ (i.e., $\omega = 1$) one gets

$$u(x,t) = \tfrac{1}{2}\Big(1 - \tanh\left[\tfrac{1}{2}\,(3x + t - \delta)\right]\Big), \tag{192}$$

which is different from (191) when $k = -3$.

Attempting to find a solution of type (28), $\mathcal{L}f^{(1)} = \mathcal{L}(\sum_{i=1}^{N} \mathrm{e}^{\theta_i})$ determines $\omega_i = -k_i, 4 - k_i$, or $4 + k_i$. As with the solitary wave solution, to avoid trivial solutions we continue with $\omega_i = 4 - k_i$ and $\omega_i = 4 + k_i$.

Here again, it is impossible to find a two-soliton solution but a bi-soliton solution can be computed. Indeed, taking $f = 1 + \mathrm{e}^{\theta_1} + \mathrm{e}^{\theta_2} + a_{12}\mathrm{e}^{\theta_1+\theta_2}$, leads to $a_{12} = 0$. Then, for $\omega_i = 4 - k_i$ $(i = 1, 2)$, after some computation one gets

$$u(x,t) = -2\left(\frac{\mathrm{e}^{\theta_1} + \mathrm{e}^{\theta_2}}{1 + \mathrm{e}^{\theta_1} + \mathrm{e}^{\theta_2}}\right), \tag{193}$$

where $\theta_1 = k_1 x - (4 - k_1)t + \delta_1$ and $\theta_2 = k_2 x - (4 - k_2)t + \delta_2$. Solution (193) agrees with the result in [99, Eq. (37)]. As shown in Fig. 16, (193) describes two coalescent wave fronts. For $\omega_i = 4 + k_i$, after some computations one gets $k_1 = -2$, $k_2 = -3$, and $a_{12} = 1$, resulting in (192) with $\delta$ replaced by $\delta_2$.

The computations for $\kappa = -1$ in (185) are similar but only lead to

$$u(x,t) = \tfrac{1}{2}\Big(1 + \tanh\left[\tfrac{1}{2}\,(x - 3t + \delta)\right]\Big) \tag{194}$$

which does not follow from (191) when $k = 1$.

## 6.6 A Combined KdV-Burgers Equation

A combined KdV-Burgers equation [98],

$$u_t + 6uu_x + u_{3x} - 5\beta u_{xx} = 0, \tag{195}$$

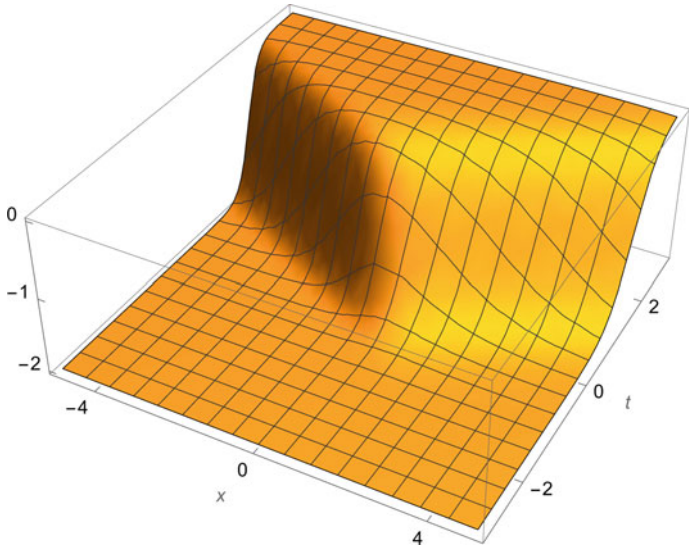


**Fig. 16** 3D graph of (193) with $k_1 = 1$, $k_2 = -2$, and $\delta_1 = \delta_2 = 0$

where $\beta > 0$, is used in models where both dispersive and dissipative effects are relevant. A Laurent series of the solution of (195) suggests the transformation

$$u = 2(\ln f)_{xx} - 2\beta(\ln f)_x, \tag{196}$$

which we substitute into the integrated KdV-Burgers equation,

$$\partial_t \left( \int^x u \, dx \right) + 3u^2 + u_{xx} - 5\beta u_x = 0 \tag{197}$$

to get

$$\begin{aligned} &f(f_{xt} - \beta f_t + 5\beta^2 f_{xx} - 6\beta f_{3x} + f_{4x}) \\ &- f_x f_t + \beta^2 f_x^2 + 6\beta f_x f_{xx} + 3f_{xx}^2 - 4 f_x f_{3x} = 0. \end{aligned} \tag{198}$$

This homogeneous equation is of the form $f\,\mathcal{L}f + \mathcal{N}(f, f) = 0$. Therefore, we can proceed as in the KdV case and solve (39) step-by-step with

$$\mathcal{L}f = f_{xt} - \beta f_t + 5\beta^2 f_{xx} - 6\beta f_{3x} + f_{4x}, \tag{199}$$

$$\mathcal{N}(f, g) = -f_x g_t + \beta^2 f_x g_x + 6\beta f_x g_{xx} + 3 f_{xx} g_{xx} - 4 f_x g_{3x}. \tag{200}$$

We summarize the results. First, $\mathcal{L}e^{\theta} = \mathcal{L}e^{kx-\omega t+\delta} = 0$ yields $(\beta - k)(\omega - k^3 + 5\beta k^2) = 0$. Thus, two cases have to be considered.

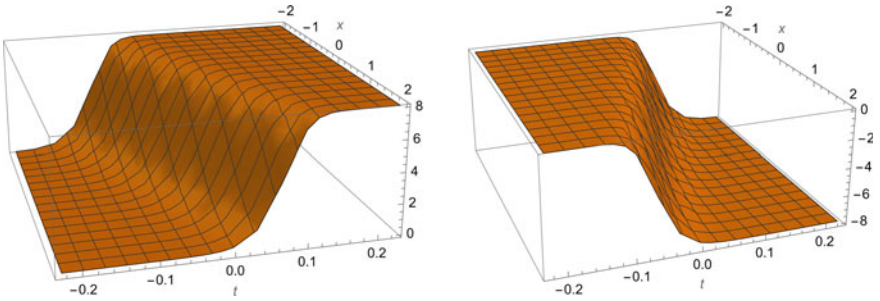


**Fig. 17** 3D graphs of (201) (left) and (202) (right) for $\beta = 2$ and $\delta = 0$

**Case 1**: When $\omega = k^2(k - 5\beta)$ and $k \neq \beta$, $\mathcal{N}(\mathrm{e}^{\theta}, \mathrm{e}^{\theta}) = 0$ determines $k = -\beta$. So, $\omega = -6\beta^3$. Inserting $f = 1 + \mathrm{e}^{\theta}$ into (196) yields

$$u(x,t) = 2\beta^2 \left( \frac{\mathrm{e}^{\theta}(2 + \mathrm{e}^{\theta})}{(1 + \mathrm{e}^{\theta})^2} \right) = \tfrac{1}{2}\beta^2 \left(3 - \tanh \tfrac{\theta}{2}\right) \left(1 + \tanh \tfrac{\theta}{2}\right), \tag{201}$$

with $\theta = -\beta x + 6\beta^3 t + \delta$.

**Case 2**: When $k = \beta$, $\mathcal{N}(\mathrm{e}^{\theta}, \mathrm{e}^{\theta}) = 0$ determines $\omega = -6\beta^3$, yielding

$$u(x,t) = -2\beta^2 \left( \frac{\mathrm{e}^{2\theta}}{(1 + \mathrm{e}^{\theta})^2} \right) = -\tfrac{1}{2}\beta^2 \left(1 + \tanh \tfrac{\theta}{2}\right)^2, \tag{202}$$

with $\theta = \beta x + 6\beta^3 t + \delta$. Solutions (201) and (202) are shown in Fig. 17 for $\beta = 2$ and $\delta = 0$.

An attempt to find a multi-soliton or bi-soliton solutions based on (28) failed. Assuming $k_i \neq \beta$ (discussed in Case 2) and working with (28), $\mathcal{L} f^{(1)} = \mathcal{L}(\sum_{i=1}^{N} \mathrm{e}^{\theta_i})$ determines $\omega_i = k_i^2(k_i - 5\beta)$. The second equation in (39) then becomes

$$\mathcal{L} f^{(2)} = -\beta \sum_{i=1}^{N} k_i^2 (k_i + \beta)\, \mathrm{e}^{2\theta_i} - \sum_{1 \leq i < j \leq N} c_{ij}\, \mathrm{e}^{\theta_i + \theta_j}, \tag{203}$$

where $c_{ij} = k_i k_j \left[ 2\beta^2 + \beta(k_i + k_j) + 6k_i k_j - 3(k_i^2 + k_j^2) \right]$. Putting terms $\mathrm{e}^{2\theta_i}$ in $f^{(2)}$ prevents the perturbation scheme from terminating. Hence, $k_i = -\beta$ $(i = 1, 2, \ldots, N)$ which also makes $c_{ij} = 0$. But if the wave numbers have to be equal then $N = 1$ and that brings us back to Case 1 and (201).

## 6.7 An Equation due to Calogero

For the equation

$$u_t - 3(3uu_x^2 + u^4u_x + u^2u_{xx}) - u_{3x} = 0 \tag{204}$$

due to Calogero [8], the Laurent series (7) has $\alpha = -\frac{1}{2}$. Therefore, to apply the simplified Hirota method we first change the dependent variable. Setting $u = \sqrt{v}$ with $v > 0$ gives

$$4v^2v_t - 3v_x^3 - 12v^2v_x^2 - 12v^4v_x + 6vv_xv_{xx} - 12v^3v_{xx} - 4v^2v_{3x} = 0, \tag{205}$$

which looks more complicated than (204) but has a truncated Laurent series with $\alpha = -1$. Then, with the transformation

$$v = \tfrac{1}{2}(\ln f)_x = \tfrac{1}{2}\left(\frac{f_x}{f}\right) \tag{206}$$

(205) can be replaced by an equation of fourth degree,

$$\begin{aligned} &f(4f_x^2f_{xt} - 3f_{xx}^3 + 6f_xf_{xx}f_{3x} - 4f_x^2f_{4x}) - f_x^2(4f_xf_t + 3f_{xx}^2 - 4f_xf_{3x}) \\ &\equiv f\mathcal{N}_1(f,f,f) + \mathcal{N}_2(f,f,f,f) = 0, \end{aligned} \tag{207}$$

with

$$\mathcal{N}_1(f,g,h) = 4f_xg_xh_{xt} - 3f_{xx}g_{xx}h_{xx} + 6f_xg_{xx}h_{3x} - 4f_xg_xh_{4x}, \tag{208}$$

$$\mathcal{N}_2(f,g,h,j) = -f_xg_x(4h_xj_t + 3h_{xx}j_{xx} - 4h_xj_{3x}). \tag{209}$$

If one seeks a solution to (207) of type (28), then $\mathcal{N}_1(\mathrm{e}^\theta, \mathrm{e}^\theta, \mathrm{e}^\theta)$ with $\theta = kx - \omega t + \delta$ yields $\omega = -\frac{1}{4}k^3$. Fortuitously, if the dispersion law holds then $\mathcal{N}_2(\mathrm{e}^\theta, \mathrm{e}^\theta, \mathrm{e}^\theta, \mathrm{e}^\theta) = 0$ and, therefore, $f = 1 + \mathrm{e}^\theta$ solves (207). Using (206) and $u = \sqrt{v}$, after some algebra one gets

$$u = \tfrac{1}{2}\sqrt{k}\sqrt{1 + \tanh\left[\tfrac{1}{8}\left(4kx + k^3t + 4\delta\right)\right]}, \tag{210}$$

where $k > 0$. This solution was computed in [30] with a different method. It is graphed in Fig. 18 for $k = 4$ and $\delta = 0$.

If one tries to find a multi-soliton solution with $f^{(1)} = \sum_{i=1}^{N} \mathrm{e}^{\theta_i}$ with $\theta_i = k_ix + \frac{1}{4}k_i^3t + \delta_i$, then $\mathcal{N}_1(f^{(1)}, f^{(1)}, f^{(1)})$ only vanishes if the wave numbers are equal.

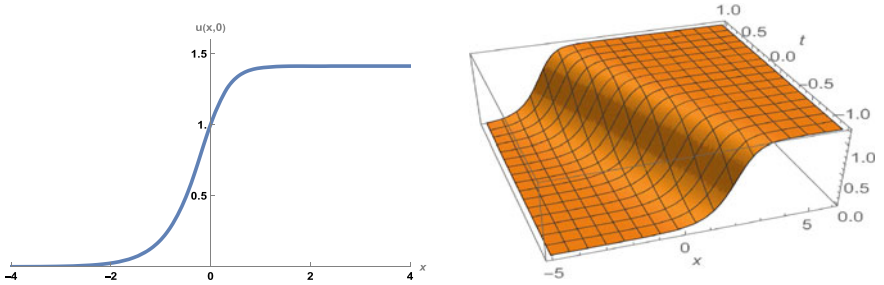


**Fig. 18** 2D and 3D graphs of (210) for $k = 4$ and $\delta = 0$

## 7 An Equation with Two but Not Three Solitons

Equations that have two-soliton but not three-soliton solutions have been discovered. The best known example is the sine-Gordon equation in two space variables which already appears in early work by Hirota [44] and was later studied in greater generality in [59]. Another example is a $(3+1)$-dimensional eight-order equation due to Kac-Wakimoto [90, 105].

With respect to equations in $(1+1)$ dimensions, Hietarinta (see [36, 37] and references therein) did an extensive search of bilinear forms for which the necessary condition to have a three-soliton solution is violated. Although the appropriate bilinear forms are given explicitly, the equations in the original field variable $u$ are not always available in his papers. Reversing the process, i.e., finding the nonlinear PDE (or a system thereof) that leads to a (known) bilinear form is not straightforward. Consult, e.g., [36, 37, 40, 70] for strategies and explicit examples.

Taking a different example, we study the soliton solutions of a polynomial equation in $(1+1)$ dimensions,

$$u_t + \tfrac{15}{784}u^3u_x + \tfrac{15}{28}uu_xu_{xx} + \tfrac{15}{56}u^2u_{3x} + \tfrac{5}{2}u_{xx}u_{3x} + u_xu_{4x} + uu_{5x} + u_{7x} = 0, \tag{211}$$

which appears in [51, Eq. (19) for $K = 56$]. The authors claim that this equation has at most a two-soliton solution. However, they do not give the constraint on the wave numbers $k_i$ that prevents the existence of, e.g., a three-soliton solution. We therefore investigate (211) in more detail.

Based on a truncated Laurent series, we substitute

$$u = 56\,(\ln f)_{xx} = 56\left(\frac{ff_{xx} - {f_x}^2}{f^2}\right) \tag{212}$$

into the integrated form of (211),

$$\partial_t\left(\int^x u\,dx\right) + \tfrac{15}{3136}u^4 + \tfrac{15}{56}u^2u_{xx} + \tfrac{5}{4}u_{xx}^2 + uu_{4x} + u_{6x} = 0, \tag{213}$$

yielding

$$f\,(f_{xt}+f_{8x})-f_x f_t+35{f_{4x}}^2-56f_{3x}f_{5x}+28f_{xx}f_{6x}-8f_x f_{7x}=0, \tag{214}$$

which is of the form $f\mathcal{L}f+\mathcal{N}(f,f)=0$ with

$$\mathcal{L}f=f_{xt}+f_{8x}, \tag{215}$$
$$\mathcal{N}(f,g)=-f_x g_t+35f_{4x}g_{4x}-56f_{3x}g_{5x}+28f_{xx}g_{6x}-8f_x g_{7x}. \tag{216}$$

As usual, $\mathcal{L}\mathrm{e}^{\theta}=0$ yields the dispersion relation $\omega=k^7$. So, with $f=1+\mathrm{e}^{\theta}$ we obtain the solitary wave solution

$$u(x,t)=14k^2\mathrm{sech}^2\left[\tfrac{1}{2}\left(kx-k^7t+\delta\right)\right]. \tag{217}$$

Seeking a solution of the form (28), as before $\mathcal{L}f^{(1)}=\mathcal{L}(\sum_{i=1}^{N}\mathrm{e}^{\theta_i})=0$ with $\theta_i=k_ix-\omega_it+\delta_i$ yields $\omega_i={k_i}^7$.

For the two-soliton solution, taking $f=1+\mathrm{e}^{\theta_1}+\mathrm{e}^{\theta_2}+a_{12}\mathrm{e}^{\theta_1+\theta_2}$, after some computations one gets

$$a_{12}=\left(\frac{(k_1-k_2)\left({k_1}^2-k_1k_2+{k_2}^2\right)}{(k_1+k_2)\left({k_1}^2+k_1k_2+{k_2}^2\right)}\right)^2 \tag{218}$$

and, then from (212),

$$u(x,t)=56\left(\frac{{k_1}^2\mathrm{e}^{\theta_1}+{k_2}^2\mathrm{e}^{\theta_2}+a_{12}\mathrm{e}^{\theta_1+\theta_2}(k_1+k_2)^2}{1+\mathrm{e}^{\theta_1}+\mathrm{e}^{\theta_2}+a_{12}\mathrm{e}^{\theta_1+\theta_2}}-\frac{\left(k_1\mathrm{e}^{\theta_1}+k_2\mathrm{e}^{\theta_2}+a_{12}\mathrm{e}^{\theta_1+\theta_2}(k_1+k_2)\right)^2}{(1+\mathrm{e}^{\theta_1}+\mathrm{e}^{\theta_2}+a_{12}\mathrm{e}^{\theta_1+\theta_2})^2}\right) \tag{219}$$

with $\theta_i=k_ix-{k_i}^7t+\delta_i$.

The collision of two solitons for Eq. (211) is shown in Figs. 19 and 20 for $k_1=1$, $k_2=2$, and $\delta_1=\delta_2=0$.

The existence of a two-soliton solution comes as no surprise because (214) can be written in bilinear form as

$$\left(D_xD_t+D_x^8\right)(f\cdot f)=0, \tag{220}$$

which satisfies the conditions[20] for the existence of a two-soliton solution (see, for example, [34, Eq. (22)] and [46, Eq. (5.47)]).

In an attempt to find a three-soliton solution, one would take

[20] For a derivation of such conditions see, e.g., [74].

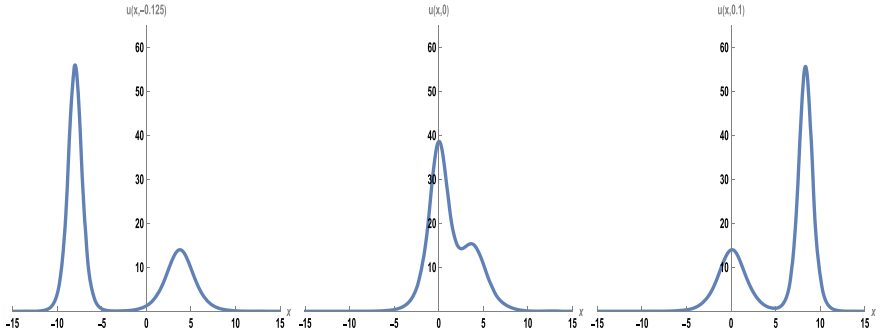


**Fig. 19** Graph of the two-soliton solution (219) of (211) at three different moments in time

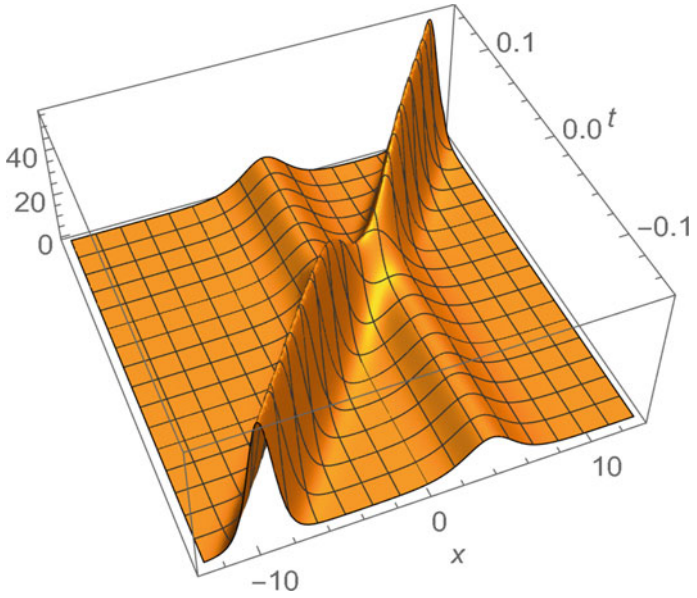


**Fig. 20** Bird's eye view of the collision of two solitons for Eq. (211). Notice the phase shift after the collision

$$f = 1 + \mathrm{e}^{\theta_1} + \mathrm{e}^{\theta_2} + \mathrm{e}^{\theta_3} + a_{12}\mathrm{e}^{\theta_1+\theta_2} + a_{13}\mathrm{e}^{\theta_1+\theta_3} + a_{23}\mathrm{e}^{\theta_2+\theta_3} + b_{123}\mathrm{e}^{\theta_1+\theta_2+\theta_3} \tag{221}$$

with

$$a_{ij} = \left( \frac{(k_i - k_j)\left({k_i}^2 - k_i k_j + {k_j}^2\right)}{(k_i + k_j)\left({k_i}^2 + k_i k_j + {k_j}^2\right)} \right)^2 \tag{222}$$

and $b_{123} = a_{12}a_{13}a_{23}$ and substitute it into (214). A lengthy computation shows that the equation is only satisfied if the wave numbers are equal or zero. Actually, this

agrees with Hietarinta's earlier studies of equations that have a bilinear form. Indeed, for an $N$-soliton solution to exist, the condition [46, 74]

$$S[P,n]=\sum_{\sigma=\pm 1} P\left(\sum_{i=1}^{n}\sigma_i k_i, -\sum_{i=1}^{n}\sigma_i\omega_i\right)\prod_{i<j}^{(n)} P(\sigma_i k_i-\sigma_j k_j, -\sigma_i\omega_i+\sigma_j\omega_j)\sigma_i\sigma_j = 0 \quad (223)$$

must hold for $n = 2, 3, \ldots, N$. In (223), $P$ is the polynomial corresponding to the bilinear operator $B$, $\sum_{\sigma=\pm 1}$ indicates the summation over all possible combinations of $\sigma_1 = \pm 1,\ \sigma_2 = \pm 1,\ \ldots,\ \sigma_n = \pm 1$ and $\prod_{i<j}^{(n)}$ means the product of all possible combinations of the $n$ elements with $i < j$, and all $k_i, \omega_i$ subject to the dispersion law $\omega_i(k_i)$. Note that (223) is a condition for $P$ and not for the $k_i$. Also, all $\omega_i$ are replaced in terms of the $k_i$ because (223) is evaluated on the dispersion law.

For (220), $P(D_x, D_t) = B = D_x D_t + D_x^8$ and the three-soliton condition $S[P, 3] = 0$ (see, [34, Eq. (28)]) gives[21]

$$\begin{aligned}&(k_1k_2k_3)^4\left[(k_1^2-k_2^2)(k_1^2-k_3^2)(k_2^2-k_3^2)\right]^2\\&(k_1^2k_2^2+k_1^2k_3^2+k_2^2k_3^2)(k_1^4+k_2^4+k_3^4+k_1^2k_2^2+k_1^2k_3^2+k_2^2k_3^2)=0.\end{aligned} \quad (224)$$

Thus, the wave numbers must be either equal, each other's opposites, or zero. In conclusion, the non-existence of a three-soliton solution agrees with the claim in [51].

## 8 Soliton Solutions in Multiple Space Dimensions

### *8.1 The Kadomtsev-Petviashvili Equation*

Arguably, the KP equation [2, 16, 55],

$$(u_t + 6uu_x + u_{3x})_x + 3\sigma u_{yy} = 0 \quad (225)$$

for $u(x, y, t)$ and $\sigma = \pm 1$, is one of the most studied soliton equations involving more than one space variable. We only consider the so-called KPII equation [7, 60] where $\sigma = 1$. A Laurent series of its solution suggests the transformation $u = 2(\ln f)_{xx}$. We therefore integrate (225) twice,

$$\partial_t\left(\int^x u\,dx\right) + 3u^2 + u_{xx} + 3\partial_y^2\left(\int^x\left(\int^x u\,dx\right)dx\right) = 0, \quad (226)$$

[21] Based on symmetry considerations, simplified expressions of (223) are given in [71, Eq. (2.9)] and [83, Eqs. (4.3) and (4.4)]. A computer implementation can be found in [126, pp. 27–29 and p. 82].

before replacing $u$ in terms of $f$. The resulting equation,

$$f(f_{xt} + f_{4x} + 3f_{yy}) - f_x f_t + 3f_{xx}^2 - 4f_x f_{3x} - 3f_y^2 = 0, \tag{227}$$

can be written in bilinear form

$$\left(D_x D_t + D_x^4 + 3D_y^2\right)(f \cdot f) = 0, \tag{228}$$

where $D_y$ is the Hirota operator defined in a similar way as $D_x$ and $D_t$ in (21) and (22), respectively.

Continuing with (227), the computation of soliton solutions is similar to the KdV case in Sect. 2.2. Indeed, the forms of $f(x, y, t)$ for multi-soliton solutions remain the same except that $\theta_i = k_i x + l_i y - \omega_i t + \delta_i$ with $\omega_i = \frac{k_i^4 + 3l_i^2}{k_i}$. Setting $l_i = k_i P_i$ simplifies matters. Then $\theta_i = k_i \left(x + P_i y - (k_i^2 + 3P_i^2)t\right) + \delta_i$ and the phase factors are

$$a_{ij} = \frac{(k_i - k_j)^2 - (P_i - P_j)^2}{(k_i + k_j)^2 - (P_i - P_j)^2} \tag{229}$$

and $b_{123} = a_{12}\, a_{13}\, a_{23}$.

Setting $k = 2K$ and $\delta = 2\Delta$, we obtain the solitary wave solution

$$u(x, y, t) = 2\, K^2 \mathrm{sech}^2\left[K\left(x + Py - (4\,K^2 + 3P^2)t\right) + \Delta\right] \tag{230}$$

which is essentially one-dimensional.

The lengthy expressions for the two- and three-soliton solutions are not shown for brevity. A graph of the two-soliton solution of (225) at $t = 0.35$ for $K_1 = \frac{1}{2}$, $K_2 = 1$, $P_1 = -\frac{1}{8}$, $P_2 = \frac{3}{16}$ and $\Delta_1 = \Delta_2 = 0$ is shown in Fig. 21. Various types of soliton interactions have been reported in the literature and observed at flat beaches [1].

## 8.2 A (3 + 1)-dimensional Evolution Equation

Consider the (3 + 1)-dimensional evolution equation [21],

$$3W_{xz} - 2\,(2W_t + W_{3x} - 2\,W W_x)_y + 2\left(W_x \partial_x^{-1} W_y\right)_x = 0, \tag{231}$$

which can be written as

$$3u_{xxz} - (2u_{xt} + u_{4x} - 2u_x u_{xx})_y + 2(u_{xx} u_y)_x = 0 \tag{232}$$

after substituting $W = u_x$. Integrating (232) twice with respect to $x$, yields

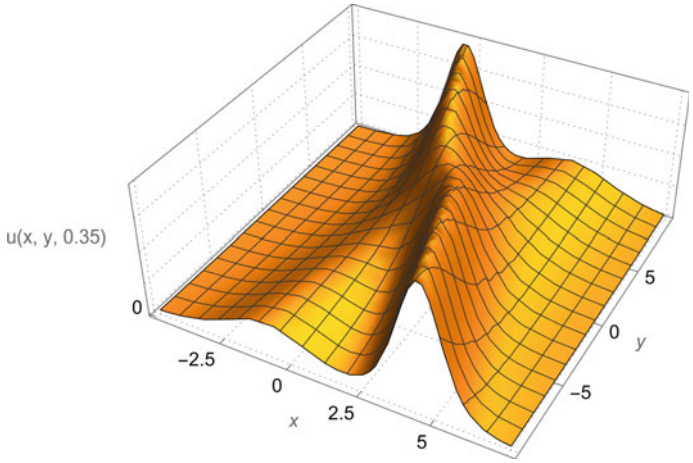


**Fig. 21** Snapshot of a two-soliton solution for the KP equation

$$3u_z - 2\partial_t\left(\int^x u_y\,dx\right) - u_{xxy} + 2u_x u_y = 0. \tag{233}$$

A Laurent series solution of (232) suggests the transformation $u = -3\,(\ln f)_x$ which indeed allows one to replace (233) by a homogeneous equation,

$$f(-2f_{yt} + 3f_{xz} - f_{xxxy}) + 2f_y f_t - 3(f_x f_z + f_{xx} f_{xy} - f_x f_{xxy}) + f_{3x} f_y = 0, \tag{234}$$

of the form $f\mathcal{L}f + \mathcal{N}(f, f) = 0$ with

$$\mathcal{L}f = -2f_{yt} + 3f_{xz} - f_{xxxy}, \tag{235}$$

$$\mathcal{N}(f, g) = 2f_y g_t - 3(f_x g_z + f_{xx} g_{xy} - f_x g_{xxy}) + f_{3x} g_y. \tag{236}$$

To compute a single solitary wave solution we set $f = 1 + \mathrm{e}^{\theta}$, where $\theta = kx + ly + mz - \omega t + \delta$. Then, $\mathcal{L}\mathrm{e}^{\theta} = 0$ yields $\omega = \frac{k(k^2 l - 3m)}{2l}$. Since $\mathcal{N}(\mathrm{e}^{\theta}, \mathrm{e}^{\theta}) = 0$ we readily obtain a solitary wave solution

$$u(x, t) = -\frac{3}{2}k\left(1 + \tanh\left[\frac{1}{2}\left(kx + ly + mz - \frac{k(k^2 l - 3\,m)t}{2l} + \delta\right)\right]\right). \tag{237}$$

For a two-soliton solution we take $f = 1 + \mathrm{e}^{\theta_1} + \mathrm{e}^{\theta_2} + a_{12}\mathrm{e}^{\theta_1+\theta_2}$, with $\theta_i = k_i x + l_i y + m_i z - \omega_i t + \delta_i$ and $\omega_i = \frac{k_i(k_i^2 l_i - 3m_i)}{2l_i}$. After some computations

$$a_{12} = \frac{k_1 k_2 l_1 l_2 (k_1 - k_2)(l_1 - l_2) - (k_1 l_2 - k_2 l_1)(l_1 m_2 - l_2 m_1)}{k_1 k_2 l_1 l_2 (k_1 + k_2)(l_1 + l_2) - (k_1 l_2 - k_2 l_1)(l_1 m_2 - l_2 m_1)}. \tag{238}$$

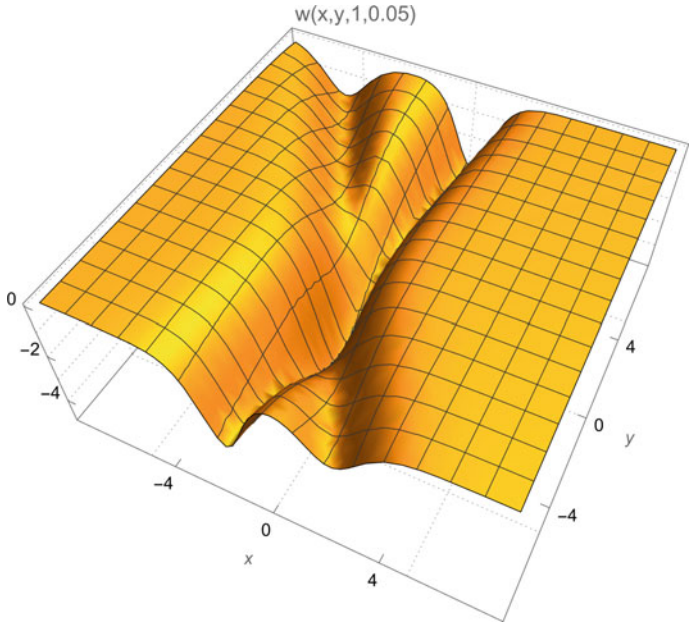


**Fig. 22** Plot of a two-soliton solution for (231) at $t = 0.05$ and $z = 1$ with $k_1 = 2, k_2 = \frac{3}{2}$, $l_1 = -\frac{1}{4}, l_2 = \frac{3}{4}, m_1 = 4, m_2 = \frac{9}{4}$, and $\delta_1 = \delta_2 = 0$

Thus, a two-soliton solution exists without having to impose any restrictions on the components $(k_i, l_i, m_i)$ of the wave vector. In [21], the authors took $l_i = k_i$ and $m_i = k_i^3$ from the outset and therefore only computed a special two-soliton solution for which $\omega_i = -k_i^3$. Assuming a traveling frame $\theta_i = k_i(x + y) + k_i^3(t + z)$ from the start is too restrictive. Indeed, by a change of variables $(x, y, z, t) \to (\xi, \eta)$ with $\xi = x + y$ and $\eta = t + z$, one can readily show that after two integrations with respect to $\xi$ Eq. (231) becomes the integrated KdV equation, that is, (17) with $t$ replaced by $\eta$, $x$ by $\xi$, and $u(x, t)$ by $u(\xi, \eta)$.

Moving on with our computations, a three-soliton solution does not exist for arbitrary wave numbers. Indeed,

$$f = 1 + \mathrm{e}^{\theta_1} + \mathrm{e}^{\theta_2} + \mathrm{e}^{\theta_3} + a_{12}\mathrm{e}^{\theta_1+\theta_2} + a_{13}\mathrm{e}^{\theta_1+\theta_3} + a_{23}\mathrm{e}^{\theta_2+\theta_3} + b_{123}\mathrm{e}^{\theta_1+\theta_2+\theta_3} \tag{239}$$

only yields a three-soliton solution if $l_i = k_i$ with $m_i$ still arbitrary (and a lengthy computation shows that the same holds for a four-soliton solution). The dispersion law and coefficients then simplify into $\omega_i = \frac{1}{2}(k_i^3 - 3m_i)$, $a_{ij} = ((k_i - k_j)/(k_i + k_j))^2$, and $b_{123} = a_{12}a_{13}a_{23}$, which are the same as for the KdV equation.

A graph of a two-soliton solution of (231) at $t = 0.05$ and $z = 1$ with $k_1 = 2, k_2 = \frac{3}{2}, l_1 = -\frac{1}{4}, l_2 = \frac{3}{4}, m_1 = 4, m_2 = \frac{9}{4}$, and $\delta_1 = \delta_2 = 0$ is shown in Fig. 22.

## 9 Symbolic Software

Symbolic software for Hirota's method comes in two flavors: (i) code that aims at finding the bilinear form of a nonlinear PDE and (ii) code to compute soliton solutions with and without the use of the bilinear form.

### *9.1 Early Developments of Soliton Software*

As part of the design of symbolic software for soliton theory, in the early 1990s Hereman and Zhuang [28, 31–33] implemented the Hirota method in *Macsyma*, a commercial computer algebra system now superseded by *Maxima*,[22] a descendant of the original *DOE Macsyma* system. The code `HIROTA_SINGLE.MAX` is able to automatically compute up to three-soliton solutions of well-known nonlinear PDEs that can be transformed into a single bilinear equation of KdV-type [31, 34], including the KdV, Boussinesq, KP, SK, and shallow water wave equations. To compute soliton solutions of these mostly $(1+1)$-dimensional PDEs, the bilinear form must be given explicitly. The code can also verify condition (223) for the existence of three- or four-soliton solutions ($n = 3$ or 4). To cover bilinear equations of mKdV-type [35], Hereman and Zhuang made `HIROTA_SYSTEM.MAX` [28, 126] which was applied to various extensions of the mKdV equation taken from [52]. Codes for the sine-Gordon equation, NLS equations, and various other types of soliton equations which have quite complicated bilinear forms [37] were not developed. The code `HIROTA_SINGLE.MAX` was converted into *Mathematica* syntax and released under the name `hirota.m`. Further details about these open source codes[23] can be found in [32, 126].

Although the simplified Hirota method (which does not use the bilinear form) was already published in [30, 85], its implementation did not start until 2012 and is still ongoing. Cook et al. [12] made the code `Homogenize-And-Solve.m` to automate the computation of the soliton solutions discussed in Sect. 4 and other soliton equations in $(1+1)$-dimensions. That code is now superseded by `PDESolitonSolutions.m` [22].

### *9.2 Implementation and Limitations of PDESolitonSolutions.m*

The current version of `PDESolitonSolutions.m` [22] computes up to three-soliton solutions for a given single PDE in one dependent variable (called $u$ below)

[22] *Maxima* is freely available from SourceForge at https://maxima.sourceforge.io/.

[23] The codes are still available at https://people.mines.edu/whereman..

which is function of up to three space variables $(x, y, z)$ and time $(t)$. The PDE must have polynomial terms with constant coefficients. Presently, the code can not handle systems of PDEs. The algorithm largely follows the steps of Sect. 3.2:

(i) The PDE is integrated with respect to $x$ as many times as possible.
(ii) The code first attempts to find a transformation to homogenize the given PDE based on the (truncated) Laurent series expansion of its solution. If unsuccessful, the code tries a transformation of type $u = c\,(\ln f)_{nx}$, with integer $1 \leq n \leq n_{\max}$ (with default value $n_{\max} = 4$) and constant $c$. Starting with $n = 1$, the code seeks the lowest value of $n$ and matching $c$ so that the PDE is transformed into an equation that is homogeneous in $f$.
(iii) A solution of type $f(x, y, z, t) = 1 + \sum_{n=1}^{p} \epsilon^n f^{(n)}(x, y, z, t)$ is sought where $1 \leq p \leq p_{\max}$ (with default value $p_{\max} = 8$). The bookkeeping parameter $\epsilon$ helps with splitting expressions into single exponentials, products of two exponentials, etc. Substituting the above sum for $f$ into a homogeneous equation for $f$ (of degree $d$) yields an expression of degree $\ell_{\max} = d\ p_{\max}$ in $\epsilon$.
(iv) Starting with $f^{(1)} = \sum_{i=1}^{N} \phi_i(x, y, z, t)$, where the natural number $N$ refers to the $N$-soliton solution one aims to compute and $\phi_i(x, y, z, t) \equiv \mathrm{e}^{\theta_i} = \mathrm{e}^{k_i x + l_i y + m_i z - \omega_i t + \delta_i}$, at order $\epsilon$ the code balances the linear terms in $\phi_i$ to determine the dispersion relation $\omega_i(k_i, l_i, m_i)$.
(v) Next, based on the monomials in the functions $\phi_i$ that occur at order $\epsilon^2$, the code builds $f^{(2)} = \sum_{i,j} a_{ij} \phi_i \phi_j$ and computes the coefficients $a_{ij}$ (and possible constraints for $k_i, l_i$, and $m_i$) by balancing like products of two exponentials. Note that $i = j$ is allowed to account for terms in $\phi_i^2$.
(vi) At the next orders in $\epsilon$, expressions for $f^{(3)}$, $f^{(4)}$, etc., are computed the same way. If at some order $n < p_{\max}$ in $\epsilon$ the function $f^{(n)}$ becomes identically zero, the code verifies that $f^{(n+1)}, \ldots, f^{(p_{\max})}$ can be set to zero. It also verifies whether or not the coefficients of $\epsilon^{n+1}, \ldots, \epsilon^{\ell_{\max}}$ in the expression mentioned in (iii) all vanish. For non-solitonic equations this may lead to (additional) constraints on the wave numbers. If both verifications are successful, the code returns the solutions after explicitly verifying that the final $f$ indeed satisfies the homogenized PDE. If none of the $f^{(n)}$ become zero, the code reports that a $N$-soliton solution could not be computed. The code will return a solitary wave solution for $N = 1$ and a bi-soliton solution for $N = 2$, provided such solutions exist.

Some remarks are warranted:

(i) The current code only considers integration with respect to $x$ ignoring the possibility to integrate the given PDE with respect to $y$ or $z$.
(ii) In addition to transformations based on a truncated Laurent series, currently only single-term logarithmic derivative transformations with respect to $x$ up to fourth-order are used. At present only transformations involving one new dependent variable $(f)$ are considered. Therefore, the current code can not find solutions of, for example, the mKdV equation.
(iii) With regard to the growing complexity of $f^{(n)}$ as $n$ increases, $p_{\max} = 8$ has been set as default value.

(iv) The current code is limited to three space variables and time. To prevent long expressions and avoid *Mathematica*'s conversion of products of exponentials into a single exponential, the explicit form of $\phi_i(x, y, z, t)$ is never used. Instead, the code uses rules for derivatives of $\phi_i(x, y, z, t)$, such as $\phi_i(x, y, z, t)_{nx} = k_i^n \phi_i(x, y, z, t)$ and $\phi_i(x, y, z, t)_{mt} = (-\omega_i)^m \phi_i(x, y, z, t)$.

(v) For example for the two-soliton case, $f^{(2)} = a_{11}\phi_1^2 + a_{12}\phi_1\phi_2 + a_{22}\phi_2^2$ where some of these terms might not be included. Indeed, after substitution of $f = 1 + f^{(1)} = 1 + \phi_1 + \phi_2$ into the homogeneous equation, the code generates the list of monomials of type $\phi_i\phi_j$ (including $\phi_i^2$) that occur at order $\epsilon^2$ and makes a linear combination of those monomials with undetermined coefficients $a_{ij}$ to create $f^{(2)}$ with the minimal number of terms. The coefficients $a_{ij}$ are then computed by requiring that like terms in $\phi_i\phi_j$ vanish.
The same procedure is used to compute $N$-soliton solutions. Starting from $f = 1 + f^{(1)} = 1 + \phi_1 + \phi_2 + \ldots + \phi_N$, the code constructs the minimal expressions for all subsequent $f^{(n)}$ in which each term is a product of $n$ (not necessarily distinct) functions taken from $\{\phi_1, \phi_2, \ldots, \phi_N\}$. The code determines which of these products are actually needed and combines them with undetermined coefficients.

(vi) For homogeneous equations of high degree, some symbolic verifications can be quite slow. To speed things up, the code does no longer *symbolically* verify that coefficients of higher orders in $\epsilon$ in the perturbation scheme vanish as soon as two consecutive coefficients of lower orders terms already vanished identically. Once two consecutive expressions are determined to be zero, the code *numerically* tests if the expressions at higher order are also zero. This applies to both the computation of the $f^{(n)}$ as well as the coefficients of $\epsilon$ in the perturbation scheme.
Furthermore, verifying that the (lengthy) expressions of $f$ indeed solve the homogeneous equation can be time consuming, especially for cubic and quartic equations. Indeed, checking that (107) satisfies (70) is computationally very expensive. Therefore, after the solution is substituted into the homogeneous equation, all independent variables, wave numbers $(k_i, l_i, m_i)$, phase constants $\delta_i$, and parameters in the PDE (if present) are repeatedly replaced by random real numbers in $[-2, 2]$. In each case it is checked if the resulting expression is zero within machine precision. Likewise, the solitary wave and one-soliton solutions for $u(x, y, z, t)$ are tested symbolically but the numerical approach is used to verify that the often long expressions of two- and three-soliton solutions $u(x, y, z, t)$ indeed solve the original PDE.

## 9.3 Other Software Packages for Hirota's Method

As early as 1988, Ito [53] designed code in REDUCE to interactively investigate nonlinear PDEs with Hirota's bilinear and Wronskian operators.

In [124], Zhou et al. introduced the *Maple* package `Bilinearization` to convert (mainly) nonlinear evolution equations of KdV-type into their bilinear form using logarithmic-derivative transformations. To cover the mKdV and nonlinear Schrödinger equations, they later extended the algorithm to work for arctan and rational transformations. They also added the code `Multisoliton` to compute up to three-soliton solutions for single bilinear equations and simple systems of bilinear equations. Ye et al. [120, 121] presented a more efficient method to do the same but only with logarithmic-derivative transformations. Their method is also implemented in *Maple*. When successful, these *Maple* codes return the bilinear form explicitly.

Yang and Ruan [117–119] have produced the *Maple* packages `HBFTrans`, `HBFTrans2`, and `HBFGen` to transform nonlinear PDEs into their bilinear forms, again based on logarithmic derivative transformations. In their newest algorithms, they take advantage of the properties of the Hirota operators and the scaling invariance[24] of the original equation. Doing so, makes their codes more efficient and faster.

Based on the Bell polynomial approach [68, 69], Miao et al. [75] developed the *Maple* package `PDEBellII` to compute bilinear forms, bilinear Bäcklund transformations, Lax pairs, and conservation laws of KdV-type equations. In contrast to `PDEBell`, developed earlier by Yang and Chen, `PDEBellII` does no longer use scaling invariance to make it applicable to a broader class of nonlinear PDEs.

For completeness, we mention the new computational method of Kumar et al. [62] for the construction of bilinear forms which, as far as we know, has not been implemented yet.

## 10 Conclusions and Future Work

Hirota's bilinear method is an effective method to construct soliton solutions of completely integrable nonlinear PDEs. In this paper we discussed a simplified version of Hirota's method (which does not use Hirota's bilinear operators) and used it to construct solitary and soliton solutions of various soliton equations as well as some nonlinear polynomial equations that do not have solitons.

We showed that the Hirota transformation is crucial to obtain a PDE that is homogeneous of degree (in the new dependent variable). We focused on logarithmic derivative transformations but, as we saw with the mKdV equation, rational and arctan transformations might be required, or combinations thereof. To homogenize, e.g., the Davey-Stewartson system, one needs a mixture of rational and logarithmic derivative transformations. There is no systematic way for finding these transformations but the first few terms of a Laurent series solution and scaling invariance of the PDE can help determine a suitable candidate thereby reducing the guess work.

The actual recasting of the transformed PDE into bilinear form in terms of Hirota's operators, which assumes a quadratic equation or a tricky decoupling into quadratic

[24] Dilation or scaling symmetry is a special Lie-point symmetry shared by many integrable PDEs [29].

equations, is not required to compute solitary wave solutions or solitons. Indeed, without bilinear forms, exact solutions of the transformed equation can still be constructed straightforwardly by solving a perturbation-like scheme on the computer using a symbolic manipulation package.

The simplified version of Hirota's method is largely algorithmic and now available as the *Mathematica* program `PDESolitonSolutions.m`. In future releases a broader class of transformations (likely involving two functions $f$ and $g$) will be considered to make the code applicable to a large set of PDEs including mKdV-type equations. A future version of the code might follow the algorithm presented in this paper even closer. It will use the perturbation schemes involving the linear and nonlinear operators which will automatically be generated by splitting the homogeneous equations into linear and nonlinear pieces. This "divide-and-conquer" strategy is expected to make the computations faster. An extension of the algorithm and code to systems of PDEs is being investigated.

**Acknowledgements** One of the authors (WH) thanks Solomon Manukure and Wen-Xiu Ma for the invitation to give a plenary talk on this subject at the 6th International Workshop on Nonlinear and Modern Mathematical Physics (NMMP2022). Both authors are grateful for the opportunity to write this chapter for the Proceedings of NMMP2022. We thank Jarmo Hietarinta for providing a photograph of Prof. Hirota. We gratefully acknowledge Wuning Zhuang (Master student) who helped with early implementations of the Hirota method in *Macsyma* and Ameina Nuseir (Ph.D. student) who first computed the soliton solutions of the Kaup-Kuperschmidt equation. We also thank Andrew Cook (REU student) who helped write *Mathematica* code for the simplified Hirota method.

## Appendix

In the derivations below we use that $\mathcal{L}(f)$ is linear in $f$, $\mathcal{N}_1(f, g)$ is bilinear (i.e., linear in both $f$ and $g$), $\mathcal{N}_2$ is trilinear, and $\mathcal{N}_3$ is quadrilinear.

**Bilinear Scheme**

For the derivation of the perturbation scheme for an equation of type (36) we need Cauchy's product formula (to regroup terms in powers of $\epsilon$),

$$\left(\sum_{p=1}^{\infty} \epsilon^p\, a_p\right)\left(\sum_{q=1}^{\infty} \epsilon^q\, b_q\right) = \sum_{n=2}^{\infty} \epsilon^n \sum_{j=1}^{n-1} a_j\, b_{n-j}. \tag{240}$$

Then,

$$
\begin{aligned}
f\,\mathcal{L}f &= \left(1+\sum_{r=p}^{\infty}\epsilon^p\,f^{(p)}\right)\,\mathcal{L}\left(\sum_{q=1}^{\infty}\epsilon^q\,f^{(q)}\right)\\
&= \left(1+\sum_{p=1}^{\infty}\epsilon^p\,f^{(p)}\right)\,\sum_{q=1}^{\infty}\epsilon^q\,\mathcal{L}f^{(q)}\\
&= \sum_{q=1}^{\infty}\epsilon^q\,\mathcal{L}f^{(q)}+\left(\sum_{p=1}^{\infty}\epsilon^p\,f^{(p)}\right)\left(\sum_{q=1}^{\infty}\epsilon^q\,\mathcal{L}f^{(q)}\right)\\
&= \sum_{n=1}^{\infty}\epsilon^n\,\mathcal{L}f^{(n)}+\sum_{n=2}^{\infty}\epsilon^n\sum_{j=1}^{n-1}f^{(j)}\mathcal{L}f^{(n-j)},
\end{aligned}
\tag{241}
$$

where we have applied (240) with $a_p = f^{(p)}$ and $b_q = \mathcal{L}f^{(q)}$. Similarly, we compute

$$
\begin{aligned}
\mathcal{N}(f,f) &= \mathcal{N}\left(1+\sum_{p=1}^{\infty}\epsilon^p\,f^{(p)},\;1+\sum_{q=1}^{\infty}\epsilon^q\,f^{(q)}\right)\\
&= \mathcal{N}\left(\sum_{p=1}^{\infty}\epsilon^p\,f^{(p)},\;\sum_{q=1}^{\infty}\epsilon^q\,f^{(q)}\right)\\
&= \sum_{n=2}^{\infty}\epsilon^n\sum_{j=1}^{n-1}\mathcal{N}(f^{(j)},f^{(n-j)}),
\end{aligned}
\tag{242}
$$

where again we applied (240) and used the bilinearity of $\mathcal{N}(f,g)$. Adding (241) and (242), the coefficient of $\epsilon^n$ is

$$
\mathcal{L}f^{(n)}+\sum_{j=1}^{n-1}\left(f^{(j)}\mathcal{L}f^{(n-j)}+\mathcal{N}(f^{(j)},f^{(n-j)})\right)=0,\quad n\geq 2. \tag{243}
$$

**Trilinear Scheme**

For the derivation of the perturbation scheme for equations of type (58) we need Cauchy's product formula for three sums:

$$
\left(\sum_{p=1}^{\infty}\epsilon^p\,a_p\right)\left(\sum_{q=1}^{\infty}\epsilon^q\,b_q\right)\left(\sum_{r=1}^{\infty}\epsilon^r\,c_r\right)=\sum_{n=3}^{\infty}\epsilon^n\sum_{j=2}^{n-1}\sum_{\ell=1}^{j-1}a_\ell\,b_{n-j}\,c_{j-\ell}. \tag{244}
$$

Substituting (28) into (58) and applying (240) and (244) yields the following term in $\epsilon^n$:

$$\mathcal{L}f^{(n)} + \sum_{j=1}^{n-1} \left(2f^{(j)}\mathcal{L}f^{(n-j)} + \mathcal{N}_1(f^{(j)}, f^{(n-j)})\right) + \sum_{j=2}^{n-1}\sum_{\ell=1}^{j-1} \left(f^{(\ell)}f^{(n-j)}\mathcal{L}f^{(j-\ell)}\right.$$
$$\left. + f^{(\ell)}\mathcal{N}_1(f^{(n-j)}, f^{(j-\ell)}) + \mathcal{N}_2(f^{(\ell)}, f^{(n-j)}, f^{(j-\ell)})\right) = 0, \quad n \geq 3. \tag{245}$$

**Quadrilinear Scheme**

Setting up the perturbation scheme for equations of type (73) requires the formula

$$\left(\sum_{p=1}^{\infty} \epsilon^p a_p\right)\left(\sum_{q=1}^{\infty} \epsilon^q b_q\right)\left(\sum_{r=1}^{\infty} \epsilon^r c_r\right)\left(\sum_{s=1}^{\infty} \epsilon^s d_s\right)$$
$$= \sum_{n=4}^{\infty} \epsilon^n \sum_{j=3}^{n-1}\sum_{\ell=2}^{j-1}\sum_{m=1}^{\ell-1} a_m\, b_{n-j}\, c_{j-\ell}\, d_{\ell-m}. \tag{246}$$

Substituting (28) into (73) and applying (240), (244), and (246) yields the following at $O(\epsilon^n)$:

$$\mathcal{L}f^{(n)} + \sum_{j=1}^{n-1} \left(3f^{(j)}\mathcal{L}f^{(n-j)} + \mathcal{N}_1(f^{(j)}, f^{(n-j)})\right)$$
$$+ \sum_{j=2}^{n-1}\sum_{\ell=1}^{j-1} \left(3f^{(\ell)}f^{(n-j)}\mathcal{L}f^{(j-\ell)} + 2f^{(\ell)}\mathcal{N}_1(f^{(n-j)}, f^{(j-\ell)}) + \mathcal{N}_2(f^{(\ell)}, f^{(n-j)}, f^{(j-\ell)})\right)$$
$$+ \sum_{j=3}^{n-1}\sum_{\ell=2}^{j-1}\sum_{m=1}^{\ell-1} \left(f^{(m)}f^{(n-j)}f^{(j-\ell)}\mathcal{L}f^{(\ell-m)} + f^{(m)}f^{(n-j)}\mathcal{N}_1(f^{(j-\ell)}, f^{(\ell-m)})\right.$$
$$\left. + f^{(m)}\mathcal{N}_2(f^{(n-j)}, f^{(j-\ell)}, f^{(\ell-m)}) + \mathcal{N}_3(f^{(m)}, f^{(n-j)}, f^{(j-\ell)}, f^{(\ell-m)})\right) = 0,$$
$$n \geq 4. \tag{247}$$

## References


1. Ablowitz, M.J., Baldwin, D.E.: Nonlinear shallow ocean-wave soliton interactions on flat beaches. Phys. Rev. E 81, Art. No. 036305, 5pp (2012). https://doi.org/10.1103/PhysRevE.86.036305
2. Ablowitz, M.J., Clarkson, P.A.: Solitons, Nonlinear Evolution Equations and Inverse Scattering. Lond. Math. Soc. Lect. Note Ser., vol. 149. Cambridge Univ. Press, Cambridge (1991)
3. Ablowitz, M.J., Segur, H.: Solitons and the Inverse Scattering Transform. SIAM, Philadelphia (1981)

4. Ablowitz, M.A., Zeppetella, A.: Explicit solutions of Fisher's equation for a special wave speed. Bull. Math. Biology 41, 835–840 (1979). https://doi.org/10.1007/BF02462380
5. Aronson, G.G., Weinberger, H.F.: Nonlinear diffusion in population genetics, combustion, and nervepulse propagation. In: Goldstein, J.A. (ed) Partial Differential Equations and Related Topics, Lecture Notes Math., vol. 446, pp. 5–49, Springer, Berlin, (1975). https://doi.org/10.1007/BFb0070595
6. Baldwin, D., Hereman W.: Symbolic software for the Painlevé test of nonlinear ordinary and partial differential equations. J. Nonl. Math. Phys. 13(1), 90–110 (2006). https://doi.org/10.2991/jnmp.2006.13.1.8
7. Biondini, G., Pelinovsky, D.E.: Kadomtsev-Petviashvili equation. Scholarpedia 3(10), Art. No. 6539, 9pp (2008). https://doi.org/10.4249/scholarpedia.6539
8. Calogero, F.: The evolution partial differential equation $u_t = u_{3x} + 3(u_{xx}u^2 + 3u_x^2u) + 3u_xu^4$. J. Math. Phys. 28, 538–555 (1987). https://doi.org/10.1063/1.527639
9. Caudrey, P.J.: Memories of Hirota's method: application to the reduced Maxwell-Bloch system in the early 1970s. Philos. Trans. Roy. Soc. A 369(1939), 1215–1227 (2011). https://doi.org/10.1098/rsta.2010.0337
10. Caudrey, P.J., Dodd, R.K., Gibbon, J.D.: A new hierarchy of Korteweg-de Vries equations. Proc. R. Soc. Lond. A 351, 407–422 (1976). https://doi.org/10.1098/rspa.1976.0149
11. Conte, R. (ed), The Painlevé Property–One Century Later. CRM Ser. Math. Phys., Springer, New York (1999)
12. Cook, A., Hereman, W., Göktaş, Ü.: `Homogenize-And-Solve.m`: A *Mathematica* program for the symbolic computation of solitary wave and soliton solutions of some scalar nonlinear evolution equations with polynomial terms. Dept. Appl. Math. Stat., Colorado School of Mines, Golden, Colorado (2012). https://people.mines.edu/whereman.
13. Date, E.: Transformation groups for soliton equations. In: Stone, M. (ed) Bosonization, pp. 427–507, World Scientific, Singapore (1994). https://doi.org/10.1142/9789812812650_0032
14. Date, E., Jimbo, M., Kashiwara, M., Miwa, T.: Transformation groups for soliton equations. In: Jimbo, M., Miwa, T. (eds) Proc. RIMS Symp. Nonlinear Integrable Systems–Classical and Quantum Theory, pp. 39–119, World Scientific, Singapore (1983)
15. Dodd, R.K., Gibbon, J.D.: The prolongation structure of a higher order Korteweg-de Vries equation. Proc. R. Soc. Lond. A 358(1694), 287–296 (1977). https://doi.org/10.1098/rspa.1978.0011
16. Drazin, P.G., Johnson, R.S.: Solitons: An Introduction. Cambridge Texts Appl. Math., Cambridge Univ. Press, Cambridge (1989)
17. Estévez, P.G., Gordoa, P.R., Martinez Alonso, L., Medina Reus, E.: Modified singular manifold expansion: application to the Boussinesq and Mikhailov-Shabat systems. J. Phys. A: Math. Gen. 26, 1915–1925 (1993). https://doi.org/10.1088/0305-4470/26/8/018
18. Fisher, R.A.: The wave of advance of an advantageous gene. Ann. Eugenics 7, 355–369 (1937). https://doi.org/10.1111/j.1469-1809.1937.tb02153.x
19. Fordy A., Gibbons, J.: Some remarkable nonlinear transformations. Phys. Lett. A 75(5), 325 (1980). https://doi.org/10.1016/0375-9601(80)90829-4
20. Gardner, C.S., Greene, J.M., Kruskal, M.D., Miura, R.M.: Korteweg-de Vries equation and generalizations. VI. Methods for exact solution. Commun. Pure Appl. Math. 27(1), 97–133 (1974). https://doi.org/10.1002/cpa.3160270108
21. Geng, X., Ma, Y.: N-soliton solution and its Wronskian form of a $(3 + 1)$-dimensional nonlinear evolution equation. Phys. Lett. A 369(4), 285–289 (2007). https://doi.org/10.1016/j.physleta.2007.04.099
22. Göktaş, Ü., Hereman, W.: `PDESolitonSolutions.m`: A *Mathematica* package for the symbolic computation of solitary wave and soliton solutions of polynomial nonlinear PDEs using a simplified version of Hirota's method. Dept. Appl. Math. Stat., Colorado School of Mines, Golden, Colorado (2023). https://people.mines.edu/whereman.
23. Goldstein, P.P.: Hints on the Hirota bilinear method. Acta Phys. Polonica A 112(6), 1171–1184 (2007). https://doi.org/10.12693/APhysPolA.112.1171

24. Gordoa, P.R., Estévez, P.G.: Double singular manifold method for the mKdV equation. Theor. Math. Phys. 99, 653–657 (1994). https://doi.org/10.1007/BF01017047
25. Grammaticos, B., Ramani, A., Hietarinta, J.: Multilinear operators: the natural extension of Hirota's bilinear formalism. Phys. Lett. A 190(1), 65–70 (1994). https://doi.org/10.1016/0375-9601(94)90367-0
26. Hayek, M.: Exact and traveling-wave solutions for convection-diffusion-reaction equation with power-law nonlinearity. Appl. Math. Comp. 218(6), 2407–2420 (2011). https://doi.org/10.1016/j.amc.2011.07.034
27. Hereman, W.: Application of a Macsyma program for the Painlevé test to the FitzHugh-Nagumo equation. In: Conte, R., Boccara, N. (eds) Partially Integrable Evolution Equations in Physics. Math. Phys. Sci., vol. 310, pp. 585–586, Kluwer, Dortrecht (1990). https://doi.org/10.1007/978-94-009-0591-7_29
28. Hereman, W.: Symbolic software for the study of nonlinear partial differential equations, In: Vichnevexsky, R., Knight, D., Richter, G. (eds) Advances in Computer Methods for Partial Differential Equations VII, pp. 326–332, IMACS, New Brunswick (1992)
29. Hereman, W., Adams, P.J., Eklund, H.L., Hickman, M.S., Herbst, B.M.: Direct methods and symbolic software for conservation laws of nonlinear equations. In: Yan, Z. (ed) Advances of Nonlinear Waves and Symbolic Computation, ch. 2, pp. 19–79. Nova Science Publishers, New York (2009)
30. Hereman, W., Nuseir, A.: Symbolic methods to construct exact solutions of nonlinear partial differential equations. Math. Comp. Simulat. 43(1), 13–27 (1997). https://doi.org/10.1016/S0378-4754(96)00053-5
31. Hereman, W., Zhuang, W.: Symbolic computation of solitons with Macsyma. In: Ames W.F., van der Houwen, P.J. (eds) Computational and Applied Mathematics II: Differential Equations, pp. 287–296, North-Holland, Amsterdam (1992)
32. Hereman, W., Zhuang, W.: Symbolic computation of solitons via Hirota's bilinear method. Technical Report, Dept. Math. Comp. Sci., Colorado School of Mines, Golden, Colorado, 33pp (1994). https://people.mines.edu/whereman.
33. Hereman, W., Zhuang, W. Symbolic software for soliton theory. Acta Appl. Math. 39(1–3), 361–378 (1995). https://doi.org/10.1007/BF00994643
34. Hietarinta, J.: A search for bilinear equations passing Hirota's three-soliton condition. I. KdV-type bilinear equations. J. Math. Phys. 28(8), 1732–1742 (1987). https://doi.org/10.1063/1.527815
35. Hietarinta, J.: A search for bilinear equations passing Hirota's three-soliton condition. II. mKdV-type bilinear equations. J. Math. Phys. 28(9), 2094–2101 (1987). https://doi.org/10.1063/1.527421
36. Hietarinta, J.: Recent results from the search for bilinear equations having three-soliton solutions. In: Degasperis, A., Fordy, A.P. (eds) Nonlinear Evolution Equations: Integrability and Spectral Methods, pp. 307–317, Manchester Univ. Press, Manchester (1989)
37. Hietarinta, J.: Hirota's bilinear method and partial integrability. In: Conte, R., Boccara, N. (eds) Partially Integrable Evolution Equations in Physics. Math. Phys. Sci., vol. 310, pp. 459–478, Kluwer, Dortrecht (1990). https://doi.org/10.1007/978-94-009-0591-7_17
38. Hietarinta, J.: Introduction to the bilinear method. In: Kosmann-Schwarzbach, Y., Grammaticos, B., Tamizhmani, K.M. (eds) Integrability of Nonlinear Systems, Lect. Notes Phys., vol. 495, pp. 95–103, Springer, Berlin (1997). https://doi.org/10.1007/BFb0113694
39. Hietarinta, J.: Hirota's bilinear method and its generalization. Int. J. Mod. Phys. 12(1), 43–51 (1997). https://doi.org/10.1142/S0217751X97000062
40. Hietarinta, J.: Hirota's bilinear method and its connection with integrability. In: Mikhailov, A.V. (ed) Integrability. Lect. Notes Phys., vol. 767, ch. 8, pp. 279–314, Springer, Berlin (2009). https://doi.org/10.1007/978-3-540-88111-7_9
41. Hietarinta, J., Grammaticos, B., Ramani, A.: Integrable trilinear PDE's. In: Makhankov, V.G., Bishop, A.R., Holm, D.D. (eds) Proc. 10th Int. Workshop Nonl. Evolution Eqs. Dyn. Systems (NEEDS '94), pp. 54–63, World Scientific, Singapore (1995). https://doi.org/10.48550/arXiv.solv-int/9411003

42. Hirota, R.: Exact solution of the Korteweg-de Vries equation for multiple collisions of solitons. Phys. Rev. Lett. 27(18), 1192–1194 (1971). https://doi.org/10.1103/PhysRevLett.27.1192
43. Hirota, R.: Exact solution of the modified Korteweg-de Vries equation for multiple collisions of solitons. J. Phys. Soc. Jpn. 33(5), 1456–1458 (1972). https://doi.org/10.1143/JPSJ.33.1456
44. Hirota, R.: Exact three-soliton solution of the two-dimensional sine-Gordon equation. J. Phys. Soc. Jpn. 35(5), 1566 (1973). https://doi.org/10.1143/JPSJ.35.1566
45. Hirota, R.: Direct method of finding exact solutions of nonlinear evolution equations. In: Miura, R. (ed) Bäcklund Transformations, the Inverse Scattering Method, Solitons, and Their Applications, Lect. Notes Math., vol. 515, pp. 40–68, Springer, Berlin (1976). https://doi.org/10.1007/BFb0081162
46. Hirota, R.: Direct methods in soliton theory. In: Bullough, R.K., Caudrey, P.J. (eds) Solitons, Topics Current Phys., vol. 17, ch. 5, pp. 157–176, Springer, Berlin (1980). https://doi.org/10.1007/978-3-642-81448-8_5
47. Hirota, R.: Bilinear forms of soliton theory. In: Jimbo, M., Miwa, T. (eds) Proc. RIMS Symp. Non-linear Integrable Systems–Classical Theory and Quantum Theory, pp. 15-37, World Scientific, Singapore (1983)
48. Hirota, R.: Fundamental properties of the binary operators in soliton theory and their generalization. In: Takeno, S. (ed) Dynamical Problems in Soliton Theory, Springer Ser. Synergetics, vol. 30, pp. 42–49, Springer, Berlin (1985). https://doi.org/10.1007/978-3-662-02449-2_7
49. Hirota, R.: The Direct Method in Soliton Theory, Cambridge Tracts Math., vol. 155, Cambridge Univ. Press, Cambridge (2004). https://doi.org/10.1017/CBO9780511543043
50. Hirota, R., Ramani, A.: The Miura transformation of Kaup's equation and of Mikhailov's equation. Phys. Lett. A 76(2), 95–96 (1980). https://doi.org/10.1016/0375-9601(80)90578-2
51. Il'in, I.A., Noshchenko, D.S., Perezhogin, A.S.: On classification of higher-order integrable nonlinear partial differential equations. Chaos Solitons Fractals 76, 278–281 (2015). https://doi.org/10.1016/j.chaos.2015.04.004
52. Ito, M.: An extension of nonlinear evolution equations of the K-dV (mK-dV) type to higher orders. J. Phys. Soc. Jpn. 49(2), 771–778 (1980). https://doi.org/10.1143/JPSJ.49.771
53. Ito M.: A REDUCE program for Hirota's bilinear operator and Wronskian operations. Comp. Phys. Comm. 50(3), 321–330 (1988). https://doi.org/10.1016/0010-4655(88)90188-9
54. Jimbo, M., Miwa, T.: Solitons and infinite dimensional Lie algebras. Publ. RIMS, Kyoto Univ. 19, 943–1001 (1983). https://doi.org/10.2977/prims/1195182017
55. Kadomtsev, B.B., Petviashvili, V.I.: On the stability of solitary waves in weakly dispersive media. Sov. Phys. Dokl. 15, 539–541 (1970)
56. Karakoc, S.B.G., Ali, K.K, Sucu, D.Y.: A new perspective for analytical and numerical soliton solutions of the Kaup-Kupershmidt and Ito equations. J. Comput. Appl. Math. 421, Art. No. 114850, 13pp (2023). https://doi.org/10.1016/j.cam.2022.114850
57. Kaup, D.: On the inverse scattering problem for the cubic eigenvalue problems of the class $\psi_{3x} + 6Q\psi_x + 6R\psi = \lambda\psi$. Stud. Appl. Math. 62(3), 189–216 (1980). https://doi.org/10.1002/sapm1980623189
58. Kawahara, T., Tanaka, M.: Interactions of traveling fronts: an exact solution of a nonlinear diffusion equation. Phys. Lett. A 97(8), 311–314 (1983). https://doi.org/10.1016/0375-9601(83)90648-5
59. Kobayashi, K.K., Izutsu, M.: Exact solution of the $n$-dimensional sine-Gordon equation. J. Phys. Soc. Jpn. 41(3), 1091–1092 (1976). https://doi.org/10.1143/JPSJ.41.1091
60. Kodama, Y.: Solitons in Two-Dimensional Shallow Water. CBMS-NSF Reg. Conf. Ser. Appl. Math., vol. 92. SIAM, Philadelphia (2018)
61. Korteweg, D.J., de Vries, G.: XLI. On the change of form of long waves advancing in a rectangular canal, and on a new type of long stationary waves. Philos. Mag. (Ser. 5) 39(240), 422–443 (1895). https://doi.org/10.1080/14786449508620739
62. Kumar, S., Mohan, B.: A novel and efficient method for obtaining Hirota's bilinear form for the nonlinear evolution equation in $(n + 1)$ dimensions. Partial Diff. Eqs. Appl. Math. 5, Art. No. 100274, 5pp (2022). https://doi.org/10.1016/j.padiff.2022.100274

63. Kumar, S., Mohan, B.: A generalized nonlinear fifth-order KdV-type equation with multiple soliton solutions: Painlevé analysis and Hirota bilinear technique. Phys. Scr. 97(12), Art. No. 125214, 9pp (2022). https://doi.org/10.1088/1402-4896/aca2fa
64. Kumar, S., Mohan, B., Kumar, A.: Generalized fifth-order nonlinear evolution equation for the Sawada-Kotera, Lax, and Caudrey-Dodd-Gibbon equations in plasma physics: Painlevé analysis and multi-soliton solutions. Phys. Scr. 97(3), Art. No. 035201, 9pp (2022). https://doi.org/10.1088/1402-4896/ac4f9d
65. Lakestani, M., Manafian, J., Partohaghighi, M.: Some new soliton solutions for the nonlinear the fifth-order integrable equations. Comp. Meth. Diff. Eqs. 10(2), 445–460 (2022). https://doi.org/10.22034/cmde.2020.30833.1462
66. Lambert, F., Springael, J., Colin, S., Willox, R.: An elementary approach to hierarchies of soliton equations. J. Phys. Soc. Jpn. 76(5), Art. No. 054005, 10pp (2007). https://doi.org/10.1143/JPSJ.76.054005
67. Lax, P.: Integrals of nonlinear equations of evolution and solitary waves. Comm. Pure Appl. Math. 21(5), 467–490 (1968). https://doi.org/10.1002/cpa.3160210503
68. Ma, W.-X.: Bilinear equations and resonant solutions characterized by Bell polynomials. Rep. Math. Phys 72(1), 41–56 (2013). https://doi.org/10.1016/S0034-4877(14)60003-3
69. Ma, W.-X.: Trilinear equations, Bell polynomials, and resonant solution. Front. Math. China 8(5), 1139–1156 (2013). https://doi.org/10.1007/s11464-013-0319-5
70. Ma, W.-X.: Soliton solutions by means of Hirota bilinear forms. Partial Diff. Eqs. Appl. Math. 5, Art. No. 100220, 5pp (2022). https://doi.org/10.1016/j.padiff.2021.100220
71. Ma, W.-X.: $N$-soliton solutions and the Hirota conditions in $(1 + 1)$-dimensions. Int. J. Nonl. Sci. Numer. Simul. 23(1), 123–133 (2022). https://doi.org/10.1515/ijnsns-2020-0214
72. Matsukidaira, J., Satsuma, J., Strampp, W.: Soliton equations expressed by trilinear forms and their solutions. Phys. Lett. A. 147(8–9), 467–471 (1990). https://doi.org/10.1016/0375-9601(90)90608-Q
73. Matsuno, Y.: Bilinearization of nonlinear evolution equations. II. Higher-order modified Korteweg-de Vries equations. J. Phys. Soc. Jpn. 49(2), 787–794 (1980). https://doi.org/10.1143/JPSJ.49.787
74. Matsuno, Y.: Bilinear Transformation Method. Academic Press, Orlando (1984)
75. Miao, Q., Wang, Y., Chen, Y., Yang, Y.: PDEBellII: A Maple package for finding bilinear forms, bilinear Bäcklund transformations, Lax pairs and conservation laws of the KdV-type equations. Comp. Phys. Commun. 185(1), 357–367 (2014). https://doi.org/10.1016/j.cpc.2013.09.005
76. Mimura, M., Ohara, K.: Standing wave solutions for a Fisher type equation with a non-local convection. Hiroshima Math. J. 16(3), 33–50 (1985). https://doi.org/10.32917/HMJ/1206130536
77. Miwa, T., Jimbo, M., Date, E.: Solitons: Differential Equations, Symmetries and Infinite Dimensional Algebras. Cambridge Tracts Math., vol. 135, Cambridge Univ. Press, Cambridge (2000)
78. Mohan, B., Meenay, D., Das, S., Rohilla, D.K., Parihar, N., Ajay, Malik, D.: Application of Hirota's direct method to nonlinear partial differential equations: Bilinear form and soliton solutions. Hans Shodh Sudha 3(2), 31–38 (2022). https://www.hansshodhsudha.com/volume3-issue2/manuscript%203.pdf
79. Murray, J.D.: Lectures on Nonlinear Differential-Equation Models in Biology. Clarendon Press, Oxford (1977)
80. Murray, J.D.: Mathematical Biology. Biomathematics Texts, vol. 19, Springer, Berlin (1989)
81. Musette, M., Conte, R.: The two-singular-manifold method: I. Modified Korteweg-de Vries and sine-Gordon equations. J. Phys. A: Math. Gen. 27(11), 3895–3913 (1994). https://doi.org/10.1088/0305-4470/27/11/036
82. Newell, A.C.: Solitons in Mathematics and Physics. CBMS-NSF Regional Conf. Ser. Appl. Math., vol. 48, SIAM, Philadelphia (1985)
83. Newell, A.C., Yunbo, Z.: The Hirota conditions. J. Math. Phys. 27(8), 2016–2021 (1986). https://doi.org/10.1063/1.527020

84. Nozaki, K.: Hirota's method and the singular manifold expansion. J. Phys. Soc. Jpn. 56(9), 3052–3054 (1987). https://doi.org/10.1143/JPSJ.56.3052
85. Nuseir, A.: Symbolic Computation of Exact Solutions of Nonlinear Partial Differential Equations Using Direct Methods. Ph.D. Thesis, Dept. Math. Comp. Sci., Colorado School of Mines, Golden, Colorado (1995). https://people.mines.edu/whereman.
86. Ohta, Y., Satsuma, J., Takahashi, D., Tokihiro, T.: An elementary introduction to Sato theory. Prog. Theor. Phys. Suppl. 94, 210–241 (1988). https://doi.org/10.1143/PTPS.94.210
87. Öziş, T., Aslan, İ.: Symbolic computation and construction of new exact traveling wave solutions to Fitzhugh-Nagumo and Klein-Gordon equations. Z. Naturforsch. 64a, 15–20 (2009). https://doi.org/10.1515/zna-2009-1-203
88. Parker, A.: On soliton solutions of the Kaup-Kupershmidt equation. I. Direct bilinearisation and solitary wave. Physica D 137(1–2), 25–33 (2000). https://doi.org/10.1016/S0167-2789(99)00166-9
89. Pekcan, A.: The Hirota Direct Method. MS Thesis, Dept. Math., Bilkent Univ., Ankara, Turkey (2005). http://www.thesis.bilkent.edu.tr/0002895.pdf
90. Pekcan, A.: The Kac-Wakimoto equation is not integrable. Preprint, arXiv:1611.10254v1, 30 Nov. 2016, 7pp (2016). https://doi.org/10.48550/arXiv.1611.10254
91. Saleem, S., Hussain, M.Z.: Numerical solution of nonlinear fifth-order KdV-type partial differential equations via Haar wavelet. Int. J. Appl. Comput. Math 6, Art. No. 164, 16pp (2020). https://doi.org/10.1007/s40819-020-00907-1
92. Satsuma, J.: Bilinear formalism in soliton theory. In: Kosmann-Schwarzbach, Y., Grammaticos, B., Tamizhmani, K.M. (eds) Integrability of Nonlinear Systems, Lect. Notes Phys., vol. 495, pp. 297–313, Springer, Berlin (1997). https://doi.org/10.1007/BFb0113699
93. Satsuma, J., Kajiwara, K., Matsukidaira, J., Hietarinta, J.: Solutions of the Broer-Kaup system through its trilinear form. J. Phys. Soc. Jpn. 61(9), 3096–3102 (1992). https://doi.org/10.1143/JPSJ.61.3096
94. Satsuma, J., Kaup, D.J.: A Bäcklund transformation for a higher order Korteweg-de Vries equation. J. Phys. Soc. Jpn. 43(2), 692–697 (1977). https://doi.org/10.1143/JPSJ.43.692
95. Sawada, K., Kotera, T.: A method of finding $N$-soliton solutions of the KdV and KdV-like equation. Prog. Theor. Phys. 51(5), 1355–1367 (1974). https://doi.org/10.1143/PTP.51.1355
96. Schiff, J.: Integrability of Chern-Simons-Higgs vortex equations and a reduction of the self-dual yang-mills equations to three dimensions. In: Levi, D., Winternitz, P. (eds) Painlevé Transcendents. NATO ASI Ser., vol. 278, pp. 393–405, Springer, Boston (1992). https://doi.org/10.1007/978-1-4899-1158-2_26
97. Singh, S., Saha Ray, S.: Painlevé integrability and new soliton solutions for $(2+1)-$dimensional Bogoyavlensky-Konopelchenko equation and generalized Bogoyavlensky-Konopelchenko equation with variable coefficients in fluid mechanics. Int. J. Mod. Phys. B 37(14), Art. No. 2350131, 29pp (2023). https://doi.org/10.1142/S021797922350131X
98. Su, C.H., Gardner, C.S.: Korteweg-de Vries equation and generalizations. III. Derivation of the Korteweg-de Vries equation and Burgers equation. J. Math. Phys. 10(3), 536–539 (1969). https://doi.org/10.1063/1.1664873
99. Vladimirov, V.A., Mączka, C.: Exact solutions of generalized Burgers equation, describing travelling fronts and their interaction. Rep. Math. Phys. 60(2), 317–328 (2007). https://doi.org/10.1016/S0034-4877(07)80142-X
100. Wadati, M.: The modified Korteweg-de Vries equation. J. Phys. Soc. Jpn. 34(5), 1289–1296 (1973). https://doi.org/10.1143/JPSJ.34.1289
101. Wadati, M., Sawada, K.: New representations of the soliton solution for the Korteweg-de Vries equation. J. Phys. Soc. Jpn. 48(1), 312–318 (1980). https://doi.org/10.1143/JPSJ.48.312
102. Wadati, M., Sawada, K.: Application of the trace method to the modified Korteweg-de Vries equation. J. Phys. Soc. Jpn. 48(1), 319–325 (1980). https://doi.org/10.1143/JPSJ.48.319
103. Wadati, M., Toda M.: The exact $N$-soliton solution of the Korteweg-de Vries equation. J. Phys. Soc. Jpn. 32(5), 1403–1411 (1972). https://doi.org/10.1143/JPSJ.32.1403

104. Wang, P.: Bilinear form and soliton solutions for the fifth-order Kaup-Kupershmidt equation. Mod. Phys. Lett. B 31(6), Art. No. 1750057, 8pp (2017). https://doi.org/10.1142/S0217984917500579
105. Wang, D.-S., Piao, L., Zhang, N.: Some new types of exact solutions for the Kac-Wakimoto equation associated with $\mathfrak{e}_6^{(1)}$. Phys. Scr. 95(3), Art. No. 035202, 8pp (2020). https://doi.org/10.1088/1402-4896/ab51e5
106. Wang, S., Tang, X.-y., Lou S.-Y., Soliton fission and fusion: Burgers equation and Sharma-Tasso-Olver equation, Chaos Solitons Fractals 21(1), 231–239 (2004). https://doi.org/10.1016/j.chaos.2003.10.014
107. Wang, P., Xiao, S.-H.: Soliton solutions for the fifth-order Kaup-Kupershmidt equation. Phys. Scr. 93(10), Art. No. 105201, 10pp (2018). https://doi.org/10.1088/1402-4896/aad6ad
108. Wazwaz, A.-M.: The KdV equation. In: Dafermos, C.M., Pokorný, M. (eds) Handbook of Differential Equations: Evolutionary Equations, vol. 4, ch. 9, pp. 485–568, Elsevier, Amsterdam (2008)
109. Wazwaz, A.-M.: Combined equations of the Burgers hierarchy: multiple kink solutions and multiple singular kink solutions. Phys. Scr. 82(2), Art. No. 025001, 6pp (2010). https://doi.org/10.1088/0031-8949/82/02/025001
110. Wazwaz, A.-M.: Burgers hierarchy: Multiple kink solutions and multiple singular kink solutions. J. Franklin Inst. 347(3), 618–626 (2010). https://doi.org/10.1016/j.jfranklin.2010.01.003
111. Wazwaz, A.-M.: New $(3+1)$-dimensional nonlinear equations with KdV equation constituting its main part: multiple soliton solutions. Math. Meth. Appl. Sci. 39(4), 886–891 (2015). https://doi.org/10.1002/mma.3528
112. Wazwaz, A.-M.: $(3+1)$-dimensional nonlinear evolution equations and couplings of fifth-order equations in the solitary waves theory: Multiple soliton solutions. In: Meyers, R.A. (ed) Encyclopedia of Complexity and Systems Science, pp. 1–46, Springer, Berlin (2015). https://doi.org/10.1007/978-3-642-27737-5_5-7
113. Wazwaz, A.-M.: The simplified Hirota's method for studying three extended higher-order KdV-type equations. J. Ocean Engr. Sci. 1(3), 181–185 (2016). https://doi.org/10.1016/j.joes.2016.06.003
114. Wei, L.: Exact soliton solutions for the general fifth Korteweg-de Vries equation. Zh. Vychisl. Mat. Mat. Fiz, 49(8), 1497–1502 (2009) and Comp. Math. Math. Phys., 49(8), 1429–1434 (2009). https://doi.org/10.1134/s0965542509080120
115. Willox, R.: On a Direct Bilinear Operator Method in Soliton Theory. Ph.D. Thesis, Free Univ. Brussels (V.U.B.), Brussels, Belgium (1993)
116. Willox, R., Satsuma, J.: Sato theory and transformation groups. A unified approach to integrable systems. In: Grammaticos, B., Kosmann-Schwarzbach, Y., Tamizhmani, K.M. (eds) Discrete Integrable Systems, Lect. Notes Phys., vol. 644, pp. 17–55, Springer, Berlin (2004). https://doi.org/10.1007/978-3-540-40357-9_2
117. Yang, X.D., Ruan, H.Y.: A Maple package on symbolic computation of Hirota bilinear form for nonlinear equations. Commun. Theor. Phys. 52(5), 801–807 (2009). https://doi.org/10.1088/0253-6102/52/5/07
118. Yang, X.D., Ruan, H.Y.: HBFTrans2: A Maple package to construct Hirota bilinear form for nonlinear equations. Commun. Theor. Phys. 55(5), 747–752 (2011). https://doi.org/10.1088/0253-6102/55/5/03
119. Yang, X.D., Ruan, H.Y.: HBFGen: A maple package to construct the Hirota bilinear form for nonlinear equations. Appl. Math. Comp. 219(15), 8018–8025 (2013). https://doi.org/10.1016/j.amc.2013.02.037
120. Ye, Y.C., Wang, L.H., Chang, Z.W., He, J.S.: An efficient algorithm of logarithmic transformation to Hirota bilinear form of KdV-type bilinear equation. Appl. Math. Comput. 218(5), 2200–2209 (2011). https://doi.org/10.1016/j.amc.2011.07.036
121. Ye, Y.-C., Zhou, Z.-X.: A universal way to determine Hirota's bilinear equation of KdV type. J. Math. Phys. 54(8), Art. No. 081506, 17pp (2013). https://doi.org/10.1063/1.4818836

122. Zabusky, N.J., Kruskal, M.D.: Interaction of “solitons" in a collisionless plasma and the recurrence of initial states. Phys. Rev. Lett. 15(6), 240–243 (1965). https://doi.org/10.1103/PhysRevLett.15.240
123. Zhang, L.-L., Yu J.-P., Ma, W.-X., Khalique C.M., Sun, Y.-L.: Kink solutions of two generalized fifth-order nonlinear evolution equations. Mod. Phys. Lett. B 36(3), Art. No. 2150555, 15pp (2022). https://doi.org/10.1142/S0217984921505552
124. Zhou, Z.J., Fu, J.Z., Li, Z.B.:, An implementation for the algorithm of Hirota bilinear form of PDE in the Maple system. Appl. Math. Comput. 183(2), 872–877 (2006). https://doi.org/10.1016/j.amc.2006.06.034
125. Zhou, Z.J., Fu, J.Z., Li, Z.B.:, Maple packages for computing Hirota’s bilinear equation and multisoliton solutions of nonlinear evolution equations. Appl. Math. Comput. 217(1), 92–104 (2010). https://doi.org/10.1016/j.amc.2010.05.012
126. Zhuang, W.: Symbolic Computation of Exact Solutions of Nonlinear Evolution and Wave Equations. MS Thesis T-4162, Dept. Math. Comp. Sci., Colorado School of Mines, Golden, Colorado (1991). https://people.mines.edu/whereman.

# Propagation of Bright Solitons for KdV-Type Equations Involving Triplet Dispersion


**Kamyar Hosseini, Evren Hincal, Olivia A. Obi, and Ranjan Das**

**Abstract** In the present paper, a series of KdV-type equations with triplet dispersion, as mathematical models of waves on shallow water surfaces, are explored. Bright solitons of the governing equations involving triple-spatial dispersion, spatio-temporal dispersion, and dualtemporal-spatial dispersion are formally constructed using the Kudryashov method. The impact of triplet dispersion as well as the nonlinear parameter on the propagation of bright solitons is investigated in detail. Results reveal how the propagation of bright solitons can systematically be controlled.

**Keywords** KdV-type equations · Triplet dispersion · Kudryashov method · Bright solitons · Propagation

## 1 Introduction

The KdV equation

$$u_t + 6uu_x + u_{xxx} = 0,$$

is known as a mathematical model of waves on shallow water surfaces. The history of the KdV equation [1] goes back to Scott's experiments in 1834 and theoretical studies accomplished by Rayleigh and Boussinesq around 1871, and finally, Korteweg and de Vries in 1895. Today, researchers deal with many nonlinear partial differential equa-

K. Hosseini (✉) · E. Hincal · O. A. Obi
Department of Mathematics, Near East University TRNC, Mersin 10, Turkey
e-mail: kamyar_hosseini@yahoo.com

K. Hosseini · E. Hincal
Department of Computer Science and Mathematics, Lebanese American University, Beirut, Lebanon

Faculty of Art and Science, University of Kyrenia, Kyrenia, TRNC, Mersin 10, Turkey

R. Das
Department of Mathematics, Arya Vidyapeeth College, Guwahati 781016, Assam, India



S. Manukure and W.-X. Ma (eds.), *Nonlinear and Modern Mathematical Physics*,
Springer Proceedings in Mathematics & Statistics 459,
https://doi.org/10.1007/978-3-031-59539-4_5

tions (NLPDEs) along with their exact solutions, which are referred to as KdV-type equations. For example, Wazwaz [2] employed Hirota's bilinear method to derive multiple solitons of the perturbed KdV equation. The scholar of [3] extracted solitons of the modified KdV (mKdV) equation using the tanh-coth method. Zhang and Ma [4] applied an ansatz method to construct rational solutions of a KdV-like equation. Newly, the following KdV-type equations, as mathematical models of waves on shallow water surfaces, were introduced

$$u_t + \alpha u u_x + \beta_1 u_{xxx} + \beta_2 u_{xxt} + \beta_3 u_{xtt} = 0, \tag{1}$$

$$u_t + \alpha u^2 u_x + \beta_1 u_{xxx} + \beta_2 u_{xxt} + \beta_3 u_{xtt} = 0, \tag{2}$$

by Biswas et al. [5] which involve triplet dispersion. Biswas et al. [5] derived solitary waves of the above KdV-type equations using an ansatz method. It should be pointed out that Eqs. (1) and (2) are reduced to KdV and mKdV equations, i.e.

$$u_t + \alpha u u_x + \beta_1 u_{xxx} = 0,$$
$$u_t + \alpha u^2 u_x + \beta_1 u_{xxx} = 0,$$

by considering $\beta_2 = \beta_3 = 0$. The principal aim of the current paper is to acquire bright solitons of the above KdV-type equations by applying the Kudryashov method [6–8]. Among the efficient methods [9–18] to obtain soliton waves of NLPDEs, Kudryashev's method has received considerable attention from academic scholars. Onder et al. [19] utilized the Kudryashov method to find soliton waves of a coupled nonlinear Schrödinger system. Hosseini et al. [20] found dark solitons of a nonlinear Schrödinger equation with the parabolic law using the Kudryashov method. More applications of the Kudryashov method can be found in [21–26].

This paper is organized as follows: In Sect. 2, the Kudryashov method is explained in short. In Sect. 3, after applying a special hypothesis and deriving the reduced forms of the KdV-type equations, their bright solitons are retrieved using the Kudryashov method. In Sect. 4, the impact of triplet dispersion as well as the nonlinear parameter on the propagation of bright solitons is investigated in detail. By reviewing the results, the present paper ends in the last section.

## 2 Kudryashov Method

In the current section, the Kudryashov method is explained in short. The first step of this method is taking the following series

$$U(\epsilon) = a_0 + a_1 K(\epsilon) + a_2 K^2(\epsilon) + \cdots + a_N K^N(\epsilon), \quad a_N \neq 0, \tag{3}$$

as the solution of

$$P(U(\epsilon), U'(\epsilon), U''(\epsilon), \ldots) = 0. \tag{4}$$

For more information, $a_i, i = 0, 1, \ldots, N$ are unknowns, $N$ is the balance number, and $K(\epsilon)$ is

$$K(\epsilon) = \frac{1}{(A - B)\sinh(\epsilon) + (A + B)\cosh(\epsilon)},$$

satisfying

$$(K'(\epsilon))^2 = K^2(\epsilon)(1 - 4ABK^2(\epsilon)). \tag{5}$$

The second step is applying (3)–(5) and solving the resulting system to derive unknowns. Finally, solitons of Eq. (4) are constructed by inserting unknowns into Eq. (3).

## 3 KdV-Type Equations and Their Bright Solitons

In the present section, after applying a special hypothesis and deriving the reduced forms of the KdV-type equations, their bright solitons are retrieved using the Kudryashov method. To this end, the following hypothesis is employed

$$u(x, t) = U(\epsilon), \quad \epsilon = x - \omega t, \tag{6}$$

where $\omega$ is the soliton velocity. So, the first KdV-type equation becomes

$$-\omega U'(\epsilon) + \alpha U(\epsilon)U'(\epsilon) + \beta_1 U'''(\epsilon) - \omega\beta_2 U'''(\epsilon) + \omega^2\beta_3 U'''(\epsilon) = 0.$$

Integrating the above equation w.r.t. $\epsilon$ leads to

$$-\omega U(\epsilon) + \frac{1}{2}\alpha U^2(\epsilon) + (\beta_1 - \omega\beta_2 + \omega^2\beta_3)U''(\epsilon) = 0. \tag{7}$$

From $U''$ and $U^2$, we find that $N = 2$, and consequently, Eq. (3) takes the form

$$U(\epsilon) = a_0 + a_1 K(\epsilon) + a_2 K^2(\epsilon), \quad a_2 \neq 0, \tag{8}$$

where $a_0$, $a_1$, and $a_2$ are unknowns. Applying (5), (7), and (8) yields the following system

$$
\begin{aligned}
&\alpha a_0 - 2\omega = 0,\\
&-\beta_3\omega^2 + (\beta_2+1)\omega - \alpha a_0 - \beta_1 = 0,\\
&4\beta_3\omega^2 a_2 - \frac{1}{2}(8\beta_2+2)a_2\omega + \frac{1}{2}\alpha a_1^2 + a_2(\alpha a_0 + 4\beta_1) = 0,\\
&-A\beta_3 B\omega^2 + A\beta_2 B\omega - AB\beta_1 + \frac{1}{8}\alpha a_2 = 0,\\
&-A\beta_3 B\omega^2 + A\beta_2 B\omega - AB\beta_1 + \frac{1}{48}\alpha a_2 = 0,
\end{aligned}
$$

with the following solutions:
Case 1:

$$
\begin{aligned}
&a_0 = 0,\\
&a_1 = 0,\\
&a_2 = \frac{3AB\left(4\beta_2+1\pm\sqrt{-64\beta_1\beta_3+16\beta_2^2+8\beta_2+1}\right)}{2\beta_3\alpha},\\
&\omega = \frac{4\beta_2+1\pm\sqrt{-64\beta_1\beta_3+16\beta_2^2+8\beta_2+1}}{8\beta_3}.
\end{aligned}
$$

Thus, solitons of the first KdV-type equation are derived as

$$
u_{1,2}(x,t) = \frac{3AB\left(4\beta_2+1\pm\sqrt{-64\beta_1\beta_3+16\beta_2^2+8\beta_2+1}\right)}{2\beta_3\alpha}\left(\frac{1}{(A-B)\sinh(x-\omega t)+(A+B)\cosh(x-\omega t)}\right)^2,
$$

where

$$
\omega = \frac{4\beta_2+1\pm\sqrt{-64\beta_1\beta_3+16\beta_2^2+8\beta_2+1}}{8\beta_3}.
$$

Case 2:

$$
\begin{aligned}
&a_0 = \frac{4\beta_2-1\pm\sqrt{-64\beta_3\beta_1+16\beta_2^2-8\beta_2+1}}{4\beta_3\alpha},\\
&a_1 = 0\\
&a_2 = \frac{3\left(-4\beta_2+1\mp\sqrt{-64\beta_3\beta_1+16\beta_2^2-8\beta_2+1}\right)AB}{2\beta_3\alpha},\\
&\omega = \frac{4\beta_2-1\pm\sqrt{-64\beta_3\beta_1+16\beta_2^2-8\beta_2+1}}{8\beta_3}.
\end{aligned}
$$

Consequently, solitons of the first KdV-type equation are acquired as

$$u_{3,4}(x,t) = \frac{4\beta_2 - 1 \pm \sqrt{-64\beta_3\beta_1 + 16\beta_2^2 - 8\beta_2 + 1}}{4\beta_3\alpha} + \frac{3\Big(-4\beta_2 + 1 \mp \sqrt{-64\beta_3\beta_1 + 16\beta_2^2 - 8\beta_2 + 1}\Big)AB}{2\beta_3\alpha} \Big(\frac{1}{(A-B)\sinh(x-\omega t) + (A+B)\cosh(x-\omega t)}\Big)^2,$$

where

$$\omega = \frac{4\beta_2 - 1 \pm \sqrt{-64\beta_3\beta_1 + 16\beta_2^2 - 8\beta_2 + 1}}{8\beta_3}.$$

Now, by considering (2) and (6), the second KdV-type equation becomes

$$-\omega U'(\epsilon) + \alpha U^2(\epsilon)U'(\epsilon) + \beta_1 U'''(\epsilon) - \omega\beta_2 U'''(\epsilon) + \omega^2\beta_3 U'''(\epsilon) = 0.$$

Integrating the above equation w.r.t. $\epsilon$ yields

$$-\omega U(\epsilon) + \frac{1}{3}\alpha U^3(\epsilon) + (\beta_1 - \omega\beta_2 + \omega^2\beta_3)U''(\epsilon) = 0. \tag{9}$$

From $U''$ and $U^3$, it is found that $N = 1$, and accordingly, we have

$$U(\epsilon) = a_0 + a_1 K(\epsilon), \quad a_1 \neq 0, \tag{10}$$

where $a_0$ and $a_1$ are unknowns. By employing (5), (9), and (10), the following system is generated

$$\begin{aligned}
&\alpha a_0^2 - 3\omega = 0,\\
&-\omega\beta_3 + (\beta_2 + 1)\omega - \alpha a_0^2 - \beta_1 = 0,\\
&\alpha a_0 a_1^2 = 0,\\
&\frac{1}{3}\alpha a_1^3 - 8AB(\omega^2\beta_3 - \omega\beta_2 + \beta_1)a_1 = 0.
\end{aligned}$$

Applying Maple results in
Case 1:

$$a_0 = 0,$$
$$a_1 = \pm 2\sqrt{-\frac{-3AB\sqrt{-4\beta_3\beta_1 + \beta_2^2 + 2\beta_2 + 1} - 3AB\beta_2 - 3AB}{\alpha\beta_3}},$$

$$\omega = \frac{\beta_2 + 1 + \sqrt{-4\beta_3\beta_1 + \beta_2^2 + 2\beta_2 + 1}}{2\beta_3}.$$

Thus, solitons of the second KdV-type equation are derived as

$$u_{1,2}(x,t) = \pm 2\sqrt{-\frac{-3AB\sqrt{-4\beta_3\beta_1 + \beta_2^2 + 2\beta_2 + 1} - 3AB\beta_2 - 3AB}{\alpha\beta_3}}\,\frac{1}{(A-B)\sinh(x-\omega t) + (A+B)\cosh(x-\omega t)},$$

where

$$\omega = \frac{\beta_2 + 1 + \sqrt{-4\beta_3\beta_1 + \beta_2^2 + 2\beta_2 + 1}}{2\beta_3}.$$

Case 2:

$$a_0 = 0,$$
$$a_1 = \pm 2\sqrt{-\frac{-3AB\sqrt{-4\beta_3\beta_1 + \beta_2^2 + 2\beta_2 + 1} - 3AB\beta_2 - 3AB}{\alpha\beta_3}},$$
$$\omega = \frac{\beta_2 + 1 - \sqrt{-4\beta_3\beta_1 + \beta_2^2 + 2\beta_2 + 1}}{2\beta_3}.$$

Consequently, solitons of the second KdV-type equation are acquired as

$$u_{3,4}(x,t) = \pm 2\sqrt{-\frac{3AB\sqrt{-4\beta_3\beta_1 + \beta_2^2 + 2\beta_2 + 1} - 3AB\beta_2 - 3AB}{\alpha\beta_3}}\,\frac{1}{(A-B)\sinh(x-\omega t) + (A+B)\cosh(x-\omega t)},$$

where

$$\omega = \frac{\beta_2 + 1 - \sqrt{-4\beta_3\beta_1 + \beta_2^2 + 2\beta_2 + 1}}{2\beta_3}.$$

## 4 A Comprehensive Analysis

In the present section, the impact of triplet dispersion as well as the nonlinear parameter on the propagation of bright solitons is investigated in detail. First, we portray the first bright soliton of Eq. (1) for the following parameter regimes

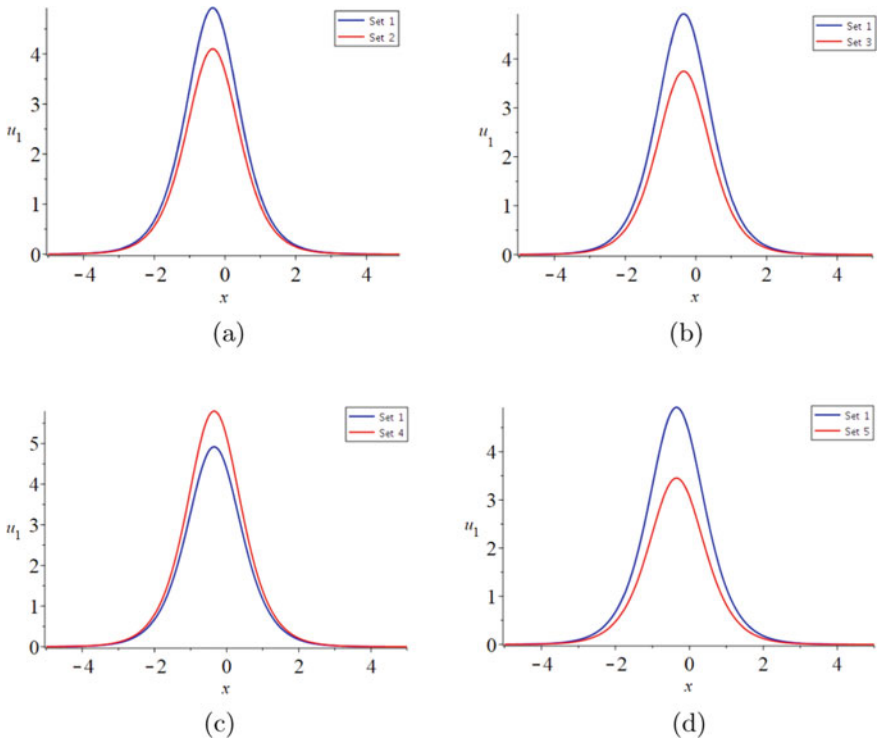


**Fig. 1** The first bright soliton of Eq. (1) for **a** Sets 1 and 2, **b** Sets 1 and 3, **c** Sets 1 and 4, and **d** Sets 1 and 5 when $t = 0$

$$\begin{aligned}
&\text{Set 1} : \{A = 2, B = 1, \alpha = 1, \beta_1 = 1, \beta_2 = 2, \beta_3 = 1\},\\
&\text{Set 2} : \{A = 2, B = 1, \alpha = 1.2, \beta_1 = 1, \beta_2 = 2, \beta_3 = 1\},\\
&\text{Set 3} : \{A = 2, B = 1, \alpha = 1, \beta_1 = 1.25, \beta_2 = 2, \beta_3 = 1\},\\
&\text{Set 4} : \{A = 2, B = 1, \alpha = 1, \beta_1 = 1, \beta_2 = 2.2, \beta_3 = 1\},\\
&\text{Set 5} : \{A = 2, B = 1, \alpha = 1, \beta_1 = 1, \beta_2 = 2, \beta_3 = 1.2\},
\end{aligned}$$

in Fig. 1 when $t = 0$.

From Fig. 1a, b, and d, it is seen that by increasing $\alpha$, $\beta_1$, and $\beta_3$, the amplitude of the wave profile decreases while it increases by increasing $\beta_2$ as shown in Fig. 1c. Such information is useful in controlling the propagation of bright solitons in the first KdV-type equation. As another case study, we depict the first bright soliton of Eq. (2) for the following parameter regimes

$$\begin{aligned}
&\text{Set 1} : \{A = 2, B = 1, \alpha = 1, \beta_1 = 1, \beta_2 = 2, \beta_3 = 1\},\\
&\text{Set 2} : \{A = 2, B = 1, \alpha = 1.3, \beta_1 = 1, \beta_2 = 2, \beta_3 = 1\},
\end{aligned}$$

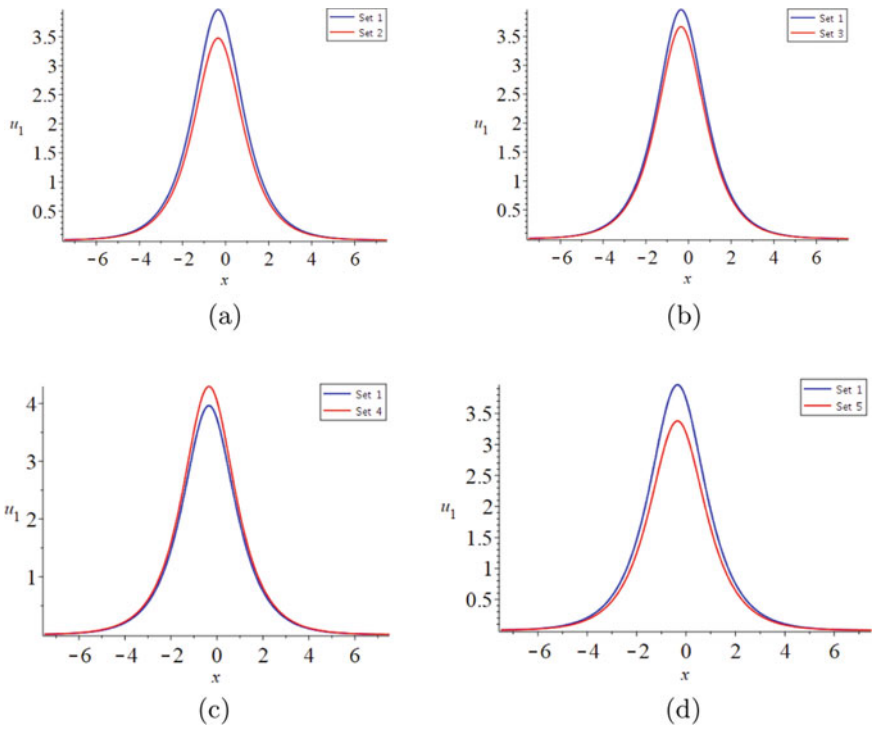


**Fig. 2** The first bright soliton of Eq. (2) for **a** Sets 1 and 2, **b** Sets 1 and 3, **c** Sets 1 and 4, and **d** Sets 1 and 5 when $t = 0$

$$\text{Set } 3 : \{A = 2, B = 1, \alpha = 1, \beta_1 = 1.7, \beta_2 = 2, \beta_3 = 1\},$$
$$\text{Set } 4 : \{A = 2, B = 1, \alpha = 1, \beta_1 = 1, \beta_2 = 2.4, \beta_3 = 1\},$$
$$\text{Set } 5 : \{A = 2, B = 1, \alpha = 1, \beta_1 = 1, \beta_2 = 2, \beta_3 = 1.3\},$$

in Fig. 2 when $t = 0$.

By looking at Fig. 2a, b, and d, it is observed that by increasing $\alpha$, $\beta_1$, and $\beta_3$, the amplitude of the wave profile decreases while it increases by increasing $\beta_2$ as illustrated in Fig. 2c. Using this information, the propagation of bright solitons in the second KdV-type equation can be controlled.

## 5 Conclusion

In the present paper, the authors explored a family of mathematical models of waves on shallow water surfaces called KdV-type equations with triplet dispersion. Using the Kudryashov method, as a pioneering method, bright solitons of the govern-

ing equations involving triple-spatial dispersion, spatio-temporal dispersion, and dualtemporal-spatial dispersion were formally derived. The influence of triplet dispersion as well as the nonlinear parameter on the propagation of bright solitons was examined by representing a series of 2D plots. As a result, the propagation of bright solitons in KdV-type equations can be readily controlled. As the authors could not obtain the dark solitons of the KdV-type equations by the Kudryashov method, so, other methods [27–30] in the future will be used to do this.

## 6 Conflict of Interest

The authors declare no conflict of interest.

## References

1. de Jager, E.M.: On the origin of the Korteweg−De Vries equation. arXiv.math/0602661, (2006).
2. Wazwaz, A.M.: Multiple-soliton solutions of the perturbed KdV equation. Commun. Nonlinear Sci. Numer. Simulat. 15, 3270–3273 (2010).
3. Wazwaz, A.M.: New sets of solitary wave solutions to the KdV, mKdV, and the generalized KdV equations. Commun. Nonlinear Sci. Numer. Simulat. 13, 331–339 (2008).
4. Zhang, Y., Ma, W.X.: Rational solutions to a KdV-like equation. Appl. Math. Comput. 256, 252–256 (2015).
5. Biswas, A., Coleman, N., Kara, A.H., Khan, S., Moraru, L., Moldovanu, S., Iticescu, C., Yıldırım, Y.: Shallow water waves and conservation laws with dispersion triplet. Appl. Sci. 12, 3647 (2022).
6. Kudryashov, N.A.: Method for finding highly dispersive optical solitons of nonlinear differential equation. Optik 206, 163550 (2020).
7. Kudryashov, N.A.: Highly dispersive solitary wave solutions of perturbed nonlinear Schrödinger equations. Appl. Math. Comput. 371, 124972 (2020).
8. Kudryashov, N.A.: Highly dispersive optical solitons of the generalized nonlinear eighth-order Schrödinger equation. Optik 206, 164335 (2020).
9. Ma, W.X., Manukure, S., Wang, H., Batwa, S.: Lump solutions to a (2+1)-dimensional fourth-order nonlinear PDE possessing a Hirota bilinear form. Mod. Phys. Lett. B 35, 2150160 (2021).
10. Manukure, S., Zhou, Y., Ma, W.X.: Lump solutions to a (2+1)-dimensional extended KP equation. Comput. Math. Appl. 75, 2414–2419 (2018).
11. Zhou, Y., Manukure, S., Ma, W.X.: Lump and lump-soliton solutions to the Hirota−Satsuma−Ito equation. Commun. Nonlinear Sci. Numer. Simul. 68, 56–62 (2019).
12. Ma, W.X: Inverse scattering and soliton solutions of nonlocal complex reverse-spacetime mKdV equations. J. Geom. Phys. 157, 103845 (2020).
13. Manukure, S., Zhou, Y.: A study of lump and line rogue wave solutions to a (2+1)-dimensional nonlinear equation. J. Geom. Phys. 167, 104274 (2021).
14. Savaissou, N., Gambo, B., Rezazadeh, H., Bekir, A., Doka, S.Y.: Exact optical solitons to the perturbed nonlinear Schrödinger equation with dual-power law of nonlinearity. Opt. Quant. Electron. 52, 318 (2020).
15. Liu, J.G., Eslami, M., Rezazadeh, H., Mirzazadeh, M.: The dynamical behavior of mixed type lump solutions on the (3+1)-dimensional generalized Kadomtsev−Petviashvili−Boussinesq equation. Int. J. Nonlinear Sci. Numer. Simul. 21, 661–665 (2020).

16. Ismael, H.F., Bulut, H., Baskonus, H.M., Gao, W.: Dynamical behaviors to the coupled Schrödinger−Boussinesq system with the beta derivative. AIMS Math. 6, 7909–7928 (2021).
17. Jhangeer, A., Baskonus, H.M., Yel, G., Gao, W.: New exact solitary wave solutions, bifurcation analysis and first order conserved quantities of resonance nonlinear Schrödinger's equation with Kerr law nonlinearity. J. King Saud Univ. Sci. 33, 101180 (2021).
18. Baskonus, H.M., Sulaiman, T.A., Bulut, H., Aktürk, T.: Investigations of dark, bright, combined dark-bright optical and other soliton solutions in the complex cubic nonlinear Schrödinger equation with $\delta$-potential. Superlattices Microstruct. 115, 19–29 (2018).
19. Onder, I., Secer, I., Bayram, M.: Optical soliton solutions of time-fractional coupled nonlinear Schrödinger system via Kudryashov-based methods. Optik 272, 170362 (2022).
20. Hosseini, K., Hincal, E., Mirzazadeh, M., Salahshour, S., Obi, O.A., Rabiei, F.: A nonlinear Schrödinger equation including the parabolic law and its dark solitons. Optik 273, 170363 (2022).
21. Salahshour, S., Hosseini, K., Mirzazadeh, M., Baleanu, D.: Soliton structures of a nonlinear Schrödinger equation involving the parabolic law. Opt. Quant. Electron. 53, 672 (2021).
22. Hosseini, K., Salahshour, S., Mirzazadeh, M.: Bright and dark solitons of a weakly nonlocal Schrödinger equation involving the parabolic law nonlinearity. Optik 227, 166042 (2021).
23. Hosseini, K., Matinfar, M., Mirzazadeh, M.: Soliton solutions of high-order nonlinear Schrödinger equations with different laws of nonlinearities. Regul. Chaotic Dyn. 26, 105–112 (2021).
24. Hosseini, K., Mirzazadeh, M., Baleanu, D., Raza, N., Park, C., Ahmadian, A., Salahshour, S.: The generalized complex Ginzburg−Landau model and its dark and bright soliton solutions. Eur. Phys. J. Plus 136, 709 (2021).
25. Hosseini, K., Salahshour, S., Sadri, K., Mirzazadeh, M., Park, C., Ahmadian, A.: The (2+1)-dimensional hyperbolic nonlinear Schrödinger equation and its optical solitons. AIMS Math. 6, 9568–9581 (2021).
26. Hosseini, K., Mirzazadeh, M., Salahshour, S., Baleanu, D., Zafar, A.: Specific wave structures of a fifth-order nonlinear water wave equation. J. Ocean Eng. Sci. 7, 462–466 (2022).
27. Akinyemi, L., Morazara, E.: Integrability, multi-solitons, breathers, lumps and wave interactions for generalized extended Kadomtsev−Petviashvili equation. Nonlinear Dyn. 111, 4683–4707 (2023).
28. Altawallbeh, Z., Az-Zo'bi, E., Alleddawi, A.O., Senol, M., Akinyemi, L.: Novel liquid crystals model and its nematicons. Opt. Quant. Electron. 54, 861 (2022).
29. Mathanaranjan, T., Rezazadeh, H., Şenol, M., Akinyemi, L.: Optical singular and dark solitons to the nonlinear Schrödinger equation in magneto-optic waveguides with anti-cubic nonlinearity. Opt. Quant. Electron. 53, 722 (2021).
30. Zhao, Y.H., Mathanaranjan, T., Rezazadeh, H., Akinyemi, L., Inc, M.: New solitary wave solutions and stability analysis for the generalized (3+1)-dimensional nonlinear wave equation in liquid with gas bubbles. Results Phys. 43, 106083 (2022).

# A Natural Full-Discretization of the Korteweg-de-Vries Equation


**Xingbiao Hu and Yingnan Zhang**

**Abstract** In this paper, we propose an integrable full-discretization of the Korteweg-de-Vries (KdV) equation. Our method is based on the compatibility between the integrable equation and its Bäcklund transformation. By using this approach, we derive a discrete equation that is a natural discretization of the KdV equation. Specifically, in the natural limit, the discrete system approaches the continuous KdV equation. We demonstrate that the integrability of the discrete system is confirmed by a Lax pair and a Bäcklund transformation.

**Keywords** Integrable discretization · Korteweg-de-Vries equation · Bäcklund transformation

## 1 Introduction

In this paper, we investigate the full-discretization of the Korteweg-de-Vries (KdV) equation, which is a well-known completely integrable equation used to describe shallow water waves [1]. The KdV equation has attracted significant interest since the seminal numerical experiment performed by Zabusky and Kruskal [2]. Over the years, various approaches have been used to discretize the KdV equation, and several discrete analogues have been developed. Taha and Ablowitz discretized the Lax pair of the KdV equation to obtain both a space discrete analogue and a fully discrete analogue, which they applied to simulate the KdV equation [3]. In [4], Ohta and

X. Hu
LSEC, ICMSEC, Academy of Mathematics and Systems Science, Chinese Academy of Sciences, Beijing 100190, China
e-mail: hxb@lsec.cc.ac.cn

School of Mathematical Sciences, University of Chinese Academy of Sciences, Beijing 100049, China

Y. Zhang (✉)
School of Mathematical Sciences, Nanjing Normal University, Nanjing 210024, Jiangsu, China
e-mail: ynzhang@njnu.edu.cn



S. Manukure and W.-X. Ma (eds.), *Nonlinear and Modern Mathematical Physics*,
Springer Proceedings in Mathematics & Statistics 459,
https://doi.org/10.1007/978-3-031-59539-4_6

Hirota introduced a semi-discrete analogue and left the time variable smooth. The Lotka-Volterra equation can also be viewed as an integrable semi-discretization of the Korteweg-de-Vries equation [5–7]. As for the full-discrete analogues, the lattice KdV developed by Hirota [8] and Nijhoff et al. [9] is a well-known example, and it can be reduced to the continuous KdV equation, though not in a standard limit. Schiff also constructed a full-discretization of the KdV equation using a loop group approach in [10]. Other notable works include those by Suris [11], Tempesta [12], and their respective references.

The idea of obtaining integrable discretizations through a suitable interpretation of Bäcklund transformations is well established. The generation of integrable differential-difference equations from Bäcklund transformations was first explored by Chiu and Ladik in [13], and Levi and Benguria in [14, 15]. In our previous work [16], we demonstrated that by introducing a convergence condition, we can obtain an integrable discretization of a soliton equation through the compatibility between the integrable equation and its Bäcklund transformation. In [16, 17], we applied this method to discretize the space and time variables of the KdV equation separately. In this paper, we extend our approach and show that by using two sets of Bäcklund transformations, we can discretize both the space and time variables simultaneously.

The main procedure we used in obtaining integrable discretizations through Bäcklund transformations involves working with bilinear equations and bilinear Bäcklund transformations. Compared to the traditional bilinear method [8, 18, 19] used to discretize soliton equations, the procedure presented in [16] is from a different viewpoint of the bilinear method and is much more direct. The traditional method, as shown in the left chart of Fig. 1, is to discretize the bilinear form of the soliton equation first and then confirm the integrability. Due to non-uniqueness, there is some freedom in $(eq1)$ when we discretize the smooth bilinear differential equation. Subsequently $(eq2)$ is obtained from $(eq1)$ by considering its integrabilities (soliton solutions or Bäcklund transformation). Different from the traditional approach, the procedure shown on the right of Fig. 1 preserves the integrability first and then discretize the equation. Given an integrable bilinear equation and its Bäcklund transformation, an expanded system $(eq3)$ of bilinear equations compatible with the original bilinear equation can be obtained. In $(eq3)$, there are some free parameters inherited from the associated Bäcklund transformations. Using properties of the $\tau$-function or the ideas in [14], it is natural to introduce some discrete variables in the new integrable system. By considering continuum limit, we impose a convergence condition on the new integrable system. Then the parameters can be determined and an integrable discretization of the original bilinear system can be derived. We will give a brief review of this approach with the KdV equation in next section.

The paper is organized in the following. In Sect. 2, we will review the integrable semi-discretizations of the KdV equation obtained in [16, 17]. In Sect. 3, we will show the full-discretization of the KdV equation and prove its integrability. Section 4 devotes to conclusions and discussions.

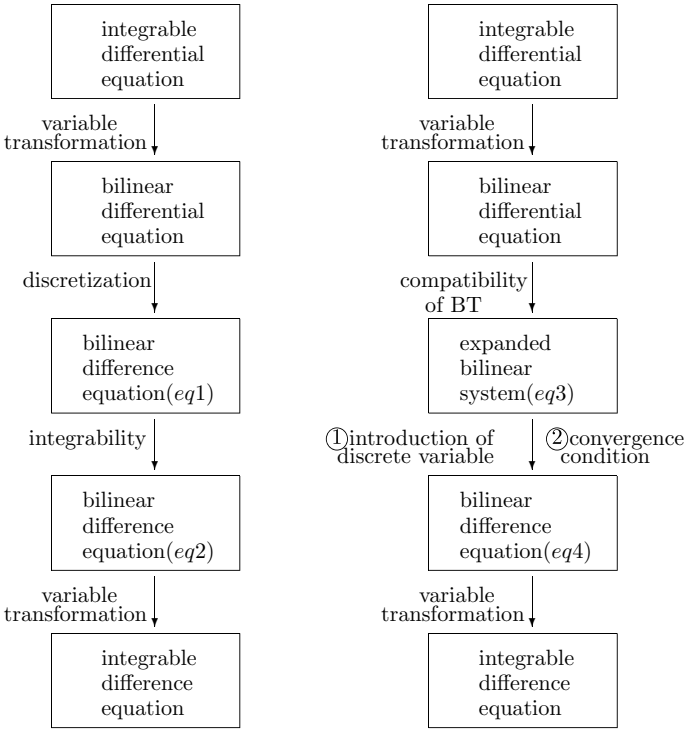


**Fig. 1** Flow charts of bilinear method of integrable discretization—Left chart: traditional approach; Right chart: approach based on BT

## 2 Semi-discretization of the KdV Equation Based on the Bäcklund Transformation

In this section, we will provide a brief review of two semi-discretized versions of the KdV equation presented in [16, 17]. One semi-discretization is applied to the space variable, while the other is applied to the time variable. Our approach is based on the bilinear method and the utilization of Bäcklund transformations.

The Korteweg-de Vries (KdV) equation can be written as

$$u_t + u_{xxx} + 12uu_x = 0. \tag{1}$$

Here, $u$, $x$, and $t$ are quantities that can be rescaled to produce any desired coefficients in (1). The KdV equation is a completely integrable equation and has a Lax pair and infinite conservation quantities. For more details, see [1] and references therein.

The dependent variable transformation $u = (\ln f)_{xx}$ converts (1) to the bilinear form

$$D_x(D_t + D_x^3) f \cdot f = 0. \tag{2}$$

Here the $D$-operator is defined by

$$D_t^m D_x^n a(t,x) \cdot b(t,x) = \frac{\partial^m}{\partial s^m} \frac{\partial^n}{\partial y^n} a(t+s, x+y) b(t-s, x-y) \mid_{s=0, y=0}, \quad m, n = 0, 1, 2, \ldots, \tag{3}$$

or by the exponential identity

$$\begin{aligned} \exp(\delta D_z) a(z) \cdot b(z) &= \exp(\delta \partial_y)(a(z+y) b(z-y)) \mid_{y=0}, \\ &= a(z+\delta) b(z-\delta). \end{aligned} \tag{4}$$

The following bilinear Bäcklund transformation (BT) of (2) has been given in [20]:

$$(D_x^2 - \lambda D_x) f \cdot g = 0, \tag{5}$$

$$(D_t + D_x^3 + \mu) f \cdot g = 0, \tag{6}$$

where $\lambda$ and $\mu$ are arbitrary constants. For details of the $D$-operator and the bilinear Bäcklund transformation, see [20].

## 2.1 Semi-discretization of the Space Variable

To discretize the space variable, we consider (2) and (5) together as a new system

$$D_x(D_t + D_x^3) f \cdot f = 0, \tag{7}$$

$$(D_x^2 - \lambda D_x) f \cdot g = 0. \tag{8}$$

Taking $f \to f_n$, $g \to f_{n-h}$ and $\lambda = \frac{2}{h}$, where $n$ is a discrete variable and $h$ is the step size, we get a differential-difference system

$$D_x(D_t + D_x^3) f_n \cdot f_n = 0, \tag{9}$$

$$(D_x^2 - \frac{2}{h} D_x) f_n \cdot f_{n-h} = 0, \tag{10}$$

From properties of the Bäcklund transformation, the above system is also integrable. One can rewrite (10) as

$$[D_x^2 \cosh(\frac{h}{2}D_n) - \frac{2}{h}D_x \sinh(\frac{h}{2}D_n)]f_n \cdot f_n = 0. \tag{11}$$

Expanding this equation in powers of $h$, we get

$$[D_x^2 - D_x D_n + O(h^2)]f_n \cdot f_n = 0, \tag{12}$$

which means that $D_x = D_n + O(h^2)$. Thus the discrete variable $n$ can be viewed as an approximation to $x$ and $h$ is just the step size in the $x$-direction. We do not discretize $x$ directly but take it as an auxiliary variable. In the bilinear equations, we still write it as $x$ without confusion.

Applying the dependent variable transformation $v_n = (\ln f_n)_x$, $u_n = v_{n,x}$, $p_n = u_{n,x}$, $q_n = p_{n,x}$, $r_n = q_{n,x}$ to (9)–(10), we get

$$u_{n,t} + r_n + 12u_n p_n = 0, \tag{13}$$

$$(u_{n+\frac{h}{2}} + u_{n-\frac{h}{2}}) = \frac{2}{h}(v_{n+\frac{h}{2}} - v_{n-\frac{h}{2}}) - (v_{n+\frac{h}{2}} - v_{n-\frac{h}{2}})^2, \tag{14}$$

$$(p_{n+\frac{h}{2}} + p_{n-\frac{h}{2}}) = \frac{2}{h}(u_{n+\frac{h}{2}} - u_{n-\frac{h}{2}}) - 2(u_{n+\frac{h}{2}} - u_{n-\frac{h}{2}})(v_{n+\frac{h}{2}} - v_{n-\frac{h}{2}}), \tag{15}$$

$$\begin{aligned}(q_{n+\frac{h}{2}} + q_{n-\frac{h}{2}}) = \frac{2}{h}(p_{n+\frac{h}{2}} - p_{n-\frac{h}{2}}) - 2(p_{n+\frac{h}{2}} - p_{n-\frac{h}{2}})(v_{n+\frac{h}{2}} - v_{n-\frac{h}{2}}) \\ -2(u_{n+\frac{h}{2}} - u_{n-\frac{h}{2}})^2,\end{aligned} \tag{16}$$

$$\begin{aligned}(r_{n+\frac{h}{2}} + r_{n-\frac{h}{2}}) = \frac{2}{h}(q_{n+\frac{h}{2}} - q_{n-\frac{h}{2}}) - 6(p_{n+\frac{h}{2}} - p_{n-\frac{h}{2}})(u_{n+\frac{h}{2}} - u_{n-\frac{h}{2}}) \\ -2(q_{n+\frac{h}{2}} - q_{n-\frac{h}{2}})(v_{n+\frac{h}{2}} - v_{n-\frac{h}{2}}).\end{aligned} \tag{17}$$

Under the natural limit $h \to 0$, the above system tends to the KdV Eq. (1). The discussions above can be summarized as the following theorem.

**Theorem 1** *The system (9)–(10) is an integrable discretization of the KdV Eq. (2). Using transformations $v_n = (\ln f_n)_x$, $u_n = v_{n,x}$, $p_n = u_{n,x}$, $q_n = p_{n,x}$, $r_n = q_{n,x}$, this system can be converted to (13)–(17), which converge to the KdV Eq. (1) as $h \to 0$.*

The bilinear Eqs. (9) and (10) have the Bäcklund transformation (BT)

$$(D_x e^{-\frac{h}{2}D_n})f_n \cdot g_n = (-\frac{1}{h}e^{-\frac{h}{2}D_n} + \beta e^{\frac{h}{2}D_n})f_n \cdot g_n, \tag{18}$$

$$D_x^2 f_n \cdot g_n = \gamma f_n g_n, \tag{19}$$

$$(D_t + D_x^3 + 3\gamma D_x)f_n \cdot g_n = 0, \tag{20}$$

where $\beta$ and $\gamma$ are arbitrary constants. Setting $v_n = (\ln g_n)_x$, $u_n = v_{n,x}$, $p_n = u_{n,x}$, $q_n = p_{n,x}$, $f_n = \phi_n g_n$ and $\psi_n = \phi_{n,x}$ in (18)–(20), we can get a Lax pair for the discrete Eqs. (13)–(17):

$$\beta\begin{pmatrix}\phi_{n+1}\\ \psi_{n+1}\end{pmatrix}=\begin{pmatrix}\frac{1}{h}+v_n-v_{n+1} & 1\\ \gamma-u_n-u_{n+1} & \frac{1}{h}+v_n-v_{n+1}\end{pmatrix}\begin{pmatrix}\phi_n\\ \psi_n\end{pmatrix},$$

$$\begin{pmatrix}\phi_{n,t}\\ \psi_{n,t}\end{pmatrix}=\begin{pmatrix}2p_n & -4(\gamma+u_n)\\ 2q_n-4(\gamma-2u_n)(\gamma+u_n) & -2p_n\end{pmatrix}\begin{pmatrix}\phi_n\\ \psi_n\end{pmatrix}.$$

See the details in [16].

## 2.2 Semi-discretization of the Time Variable

To discretize the time variable, we need derive a higher order Bäcklund transformation. In fact, we have the following proposition [17].

**Proposition 1** *If $f$ and $g$ are two solutions of (2) and satisfy the BT (5)–(6), they also satisfy*

$$(D_xD_t-\frac{1}{2}D_x^4+\frac{3}{2}\lambda D_x^3+\mu D_x)f\cdot g=0. \tag{21}$$

Proposition 1 means that (21) is also compatible with the original Eq. (2). Similarly as the case of space variable, setting $f\to f_{m+k}$, $g\to f_m$, $\mu=-\frac{3}{k}$ and $\gamma=0$, from (2) and (21), we get an integrable differential-difference system

$$D_x(D_t+D_x^3)f_m\cdot f_m=0, \tag{22}$$

$$(D_xD_t-\frac{1}{2}D_x^4-\frac{3}{k}D_x)f_{m+k}\cdot f_m=0. \tag{23}$$

The integrability is inherited from the compatibility between (2) and (21). Here we view $t$ as an auxiliary variable and $k$ as the step size.

With $\eta_m=(\ln f_m)_t$, $u_m=(\ln f_m)_{xx}$, the system (22)–(23) can be transformed to

$$v_{m,x}=u_m, \tag{24}$$

$$\eta_{m,x}+6u_m^2+u_{m,xx}=0, \tag{25}$$

$$\begin{aligned}&\frac{3}{k}(u_{m+1}-u_m)+17(u_{m+1}u_{m+1,x}+u_mu_{m,x})+(u_{m+1}u_{m,x}+u_{m+1,x}u_m)\\&+\frac{3}{2}(u_{m+1,xxx}+u_{m,xxx})+3(v_{m+1}-v_m)(u_{m+1,xx}-u_{m,xx})\\&+3(v_{m+1}-v_m)^2(u_{m+1,x}+u_{m,x})+12(v_{m+1}-v_m)(u_{m+1}^2-u_m^2)\\&-(u_{m+1}-u_m)(\eta_{m+1}-\eta_m)+2(v_{m+1}-v_m)^3(u_{m+1}-u_m)=0.\end{aligned} \tag{26}$$

Here we have omitted the detailed derivation process and written subscript $m+k$ as $m+1$. Replacing $u_m$ by $u(x,t)$, $u_{m+1}$ by $u(x,t+k)$, and similarly for $v$ and $\eta$, and

then taking the limit $k \to 0$, Eqs. (24)–(26) tends to the KdV Eq. (1). A Lax pair for the integrable differential-difference system (24)–(26) is

$$L_m \Psi_m = \lambda \Psi_m, \tag{27}$$
$$\Psi_{m+1} = A_m \Psi_m, \tag{28}$$

where

$$L_m = \partial_x^2 + 2u_m, \tag{29}$$
$$A_m = k a_m \partial_x^3 + k b_m \partial_x^2 + k c_m \partial_x + (k d_m + 1). \tag{30}$$

$$a_m = -4, \tag{31}$$
$$b_m = 4(v_{m+1} - v_m), \tag{32}$$
$$c_m = -2(v_{m+1} - v_m)^2 - 2(5u_m + u_{m+1}), \tag{33}$$
$$d_m = -\frac{1}{3}(\eta_{m+1} - \eta_m) + \frac{2}{3}u_{m+1,x} - \frac{20}{3}u_{m,x} + \frac{2}{3}(v_{m+1} - v_m)^3 + 2(v_{m+1} - v_m)(3u_m + u_{m+1}) \tag{34}$$

and $\partial_x^i$ is the quasi differential operator. The compatibility of the above system is

$$L_{m+1} A_m = A_m L_m, \tag{35}$$

which gives the Eq. (24)–(26).

## 3 Full Discretization of the KdV Equation

In this section, we present a fully discrete approximation of the KdV Eq. (1). In contrast to the semi-discrete case, where only one discrete variable is introduced, the fully discrete case requires the introduction of two discrete variables, necessitating the use of two sets of Bäcklund transformations. Specifically, the integrable fully discrete approximation of the KdV Eq. (2) is given by:

$$D_x(D_t + D_x^3) f_{n,m} \cdot f_{n,m} = 0, \tag{36}$$
$$(D_x^2 \exp(\frac{h}{2}D_n) - \frac{2}{h}D_x \exp(\frac{h}{2}D_n)) f_{n+1,m} \cdot f_{n,m} = 0, \tag{37}$$
$$(D_x D_t \exp(\frac{k}{2}D_m) - \frac{1}{2}D_x^4 \exp(\frac{k}{2}D_m) - \frac{3}{k}D_x \exp(\frac{k}{2}D_m)) f_{n,m+1} \cdot f_{n,m} = 0. \tag{38}$$

Equation (36) corresponds to the original bilinear KdV Eq. (2), whereas Eqs. (37) and (38) are obtained from the Bäcklund transformations (5) and (21), respectively. The discrete variables $n$ and $m$ correspond to the continuous variables $x$ and $t$. Let $\eta_{n,m} = (\ln f_{n,m})_t$, $\beta_{n,m} = (\ln f_{n,m})_{xt}$, $v_{n,m} = (\ln f_{n,m})_x$, $u_{n,m} = (\ln f_{n,m})_{xx}$, $p_{n,m} = (\ln f_{n,m})_{xxx}$, $q_{n,m} = (\ln f_{n,m})_{xxxx}$, $r_{n,m} = (\ln f_{n,m})_{xxxxx}$. Then Eqs. (36)–(38) can be transformed into a nonlinear system

$$(u_{n+1,m} + u_{n,m}) = \frac{2}{h}(v_{n+1,m} - v_{n,m}) - (v_{n+1,m} - v_{n,m})^2, \tag{39}$$

$$\begin{aligned}(p_{n+1,m} + p_{n,m}) = {} & \frac{2}{h}(u_{n+1,m} - u_{n,m}) \\ & -2(u_{n+1,m} - u_{n,m})(v_{n+1,m} - v_{n,m}),\end{aligned} \tag{40}$$

$$\begin{aligned}(q_{n+1,m} + q_{n,m}) = {} & \frac{2}{h}(p_{n+1,m} - p_{n,m}) - 2(p_{n+1,m} - p_{n,m})(v_{n+1,m} - v_{n,m}) \\ & -2(u_{n+1,m} - u_{n,m})^2,\end{aligned} \tag{41}$$

$$\begin{aligned}(r_{n+1,m} + r_{n,m}) = {} & \frac{2}{h}(q_{n+1,m} - q_{n,m}) - 2(q_{n+1,m} - q_{n,m})(v_{n+1,m} - v_{n,m}) \\ & -6(p_{n+1,m} - p_{n,m})(u_{n+1,m} - u_{n,m}),\end{aligned} \tag{42}$$

$$\beta_{n,m} + 6u_{n,m}^2 + q_{n,m} = 0, \tag{43}$$

$$\begin{aligned}\frac{3}{k}(v_{n,m+1} - v_{n,m}) = {} & (\beta_{n,m+1} + \beta_{n,m}) + (\eta_{n,m+1} - \eta_{n,m})(v_{n,m+1} - v_{n,m}) \\ & -\frac{1}{2}[(q_{n,m+1} + q_{n,m}) + 4(v_{n,m+1} - v_{n,m})(p_{n,m+1} - p_{n,m}) \\ & +3(u_{n,m+1} + u_{n,m})^2 + 6(v_{n,m+1} - v_{n,m})^2(u_{n,m+1} + u_{n,m}) \\ & +(v_{n,m+1} - v_{n,m})^4].\end{aligned} \tag{44}$$

From Eq. (43), we have

$$\begin{aligned}(\beta_{n+1,m} - \beta_{n,m}) + 6(u_{n+1,m} + u_{n,m})(u_{n+1,m} - u_{n,m}) \\ +(q_{n+1,m} - q_{n,m}) = 0.\end{aligned} \tag{45}$$

Inserting Eq. (39) into the above formulae, we obtain

$$\begin{aligned}(\beta_{n+1,m} - \beta_{n,m}) + (q_{n+1,m} - q_{n,m}) + \frac{12}{h}(v_{n+1,m} - v_{n,m})(u_{n+1,m} - u_{n,m}) \\ -6(v_{n+1,m} - v_{n,m})^2(u_{n+1,m} - u_{n,m}) = 0.\end{aligned} \tag{46}$$

Note that $u = v_x$, $p = u_x$, $q = p_x$, $\beta = \eta_x$. Thus integrating Eq. (46) about $x$, we have

$$\begin{aligned}(\eta_{n+1,m} - \eta_{n,m}) + (p_{n+1,m} - p_{n,m}) \\ +\frac{6}{h}(v_{n+1,m} - v_{n,m})^2 - 2(v_{n+1,m} - v_{n,m})^3 = 0.\end{aligned} \tag{47}$$

Here we have taken all the integral constants as zero. Eliminating $\beta$ in Eq. (44) and then differentiating it with respect to $x$, we obtain

$$\begin{aligned}
&\frac{3}{k}(u_{n,m+1}-u_{n,m})+\frac{3}{2}(r_{n,m+1}+r_{n,m})+(u_{n,m+1}p_{n,m}+u_{n,m}p_{n,m+1})\\
&+17(u_{n,m+1}p_{n,m+1}+u_{n,m}p_{n,m})+3(v_{n,m+1}-v_{n,m})(q_{n,m+1}-q_{n,m})\\
&+12(v_{n,m+1}-v_{n,m})(u^2_{n,m+1}-u^2_{n,m})+3(v_{n,m+1}-v_{n,m})^2(p_{n,m+1}+p_{n,m})\\
&+2(v_{n,m+1}-v_{n,m})^3(u_{n,m+1}-u_{n,m})-(\eta_{n,m+1}-\eta_{n,m})(u_{n,m+1}-u_{n,m})\\
&=0. \qquad (48)
\end{aligned}$$

It can be observed that the system of Eqs. (39)–(42), (47)–(48) converges to the semi-discrete Eqs. (13)–(17) as $h \to 0$, and to the semi-discrete Eqs. (24)–(26) as $k \to 0$.

In the next, we will show the integrability of the full discrete Eqs. (36)–(38).

**Proposition 2** *The Bäcklund transformation of the bilinear Eqs.* (36)–(38) *is*

$$D_x e^{-\frac{h}{2}D_n} f_{n,m}\cdot g_{n,m} = (\gamma e^{\frac{h}{2}D_n} - \frac{1}{h}e^{-\frac{h}{2}D_n}) f_{n,m}\cdot g_{n,m}, \qquad (49)$$

$$D_x^2 f_{n,m}\cdot g_{n,m} = \lambda f_{n,m} g_{n,m}, \qquad (50)$$

$$(D_t + D_x^3 + 3\lambda D_x + \mu) f_{n,m}\cdot g_{n,m} = 0, \qquad (51)$$

$$\begin{aligned}
&(D_t e^{\frac{k}{2}D_m} - 2D_x^3 e^{\frac{k}{2}D_m} - 6\lambda D_x e^{\frac{k}{2}D_m} + (\mu - \frac{3}{k})e^{\frac{k}{2}D_m}\\
&\qquad -\theta e^{-\frac{k}{2}D_m}) f_{n,m}\cdot g_{n,m} = 0, \qquad (52)
\end{aligned}$$

*where $\lambda$, $\mu$, $\gamma$ and $\theta$ are Bäcklund parameters.*

***Proof*** Assume $f_{n,m}$ is solutions of Eqs. (36)–(38). All we need to do is to prove that the $g_{n,m}$ given by (49)–(52) is also a solution of the Eqs. (36)–(38), i.e.

$$\begin{aligned}
P_1 &\equiv D_x(D_t + D_x^3) g_{n,m}\cdot g_{n,m} = 0,\\
P_2 &\equiv [D_x^2 \cosh(\frac{h}{2}D_n) - \frac{2}{h}D_x \sinh(\frac{h}{2}D_n)] g_{n,m}\cdot g_{n,m} = 0,\\
P_3 &\equiv [D_x D_t \cosh(\frac{k}{2}D_m) - \frac{1}{2}D_x^4 \cosh(\frac{k}{2}D_m)\\
&\qquad -\frac{3}{k}D_x \sinh(\frac{k}{2}D_m)] g_{n,m}\cdot g_{n,m} = 0
\end{aligned}$$

In fact, $P_1 = 0, P_2 = 0$ can be proved in a same way in [16]. In the following, we will prove $P_3 = 0$. Firstly, in a similar way in [17], we can prove that $f_{n,m}$, $g_{n,m}$ satisfy

$$(D_x D_t - \frac{1}{2}D_x^4 + \mu D_x + \frac{9}{2}\lambda^2) f_{n,m}\cdot g_{n,m} = 0. \qquad (53)$$

Secondly, we have the following identities,

$$\begin{aligned}
&(D_x D_t e^{\frac{1}{2}D_m} a \cdot a)(e^{\frac{1}{2}D_m} b \cdot b) - (e^{\frac{1}{2}D_m} a \cdot a)(D_x D_t e^{\frac{1}{2}D_m} b \cdot b) \\
&= D_x \cosh(\frac{1}{2}D_m)(D_t a \cdot b) \cdot (ab) + D_x(D_t e^{\frac{1}{2}D_m} a \cdot b) \cdot (e^{-\frac{1}{2}D_m} a \cdot b) \\
&\quad - \sinh(\frac{1}{2}D_m)[(D_x D_t a \cdot b) \cdot (ab) + (D_x a \cdot b) \cdot (D_t a \cdot b)], \qquad (54)
\end{aligned}$$

$$\begin{aligned}
&(D_x^4 e^{\frac{1}{2}D_m} a \cdot a)(e^{\frac{1}{2}D_m} b \cdot b) - (e^{\frac{1}{2}D_m} a \cdot a)(D_x^4 e^{\frac{1}{2}D_m} b \cdot b) \\
&= 4D_x(D_x^3 e^{\frac{1}{2}D_m} a \cdot b) \cdot (e^{-\frac{1}{2}D_m} a \cdot b) - 3D_x^2 \sinh(\frac{1}{2}D_m)(D_x^2 a \cdot b) \cdot (ab) \\
&\quad -2D_x \cosh(\frac{1}{2}D_m)[(D_x^3 a \cdot b) \cdot (ab) + 3(D_x^2 a \cdot b) \cdot (D_x a \cdot b)] \\
&\quad - \sinh(\frac{1}{2}D_m)[(D_x^4 a \cdot b) \cdot (ab) + 2(D_x^3 a \cdot b) \cdot (D_x a \cdot b)]. \qquad (55)
\end{aligned}$$

$$\begin{aligned}
&D_x \cosh(\frac{1}{2}D_m)(D_x a \cdot b) \cdot (ab) \\
&= D_x(D_x e^{\frac{1}{2}D_m} a \cdot b) \cdot (e^{-\frac{1}{2}D_m} a \cdot b) - \sinh(\frac{1}{2}D_m)(D_x^2 a \cdot b) \cdot (ab). \qquad (56)
\end{aligned}$$

By using (54)–(56) and the relations (49)–(53), we have

$$\begin{aligned}
&-(e^{\frac{k}{2}D_m} f_{n,m} \cdot f_{n,m}) P_3 \\
&\equiv [(D_x D_t e^{\frac{k}{2}D_m} - \frac{1}{2}D_x^4 e^{\frac{k}{2}D_m} - \frac{3}{k}D_x e^{\frac{k}{2}D_m}) f_{n,m} \cdot f_{n,m}](e^{\frac{k}{2}D_m} g_{n,m} \cdot g_{n,m}) \\
&\quad -(e^{\frac{k}{2}D_m} f_{n,m} \cdot f_{n,m})[(D_x D_t e^{\frac{k}{2}D_m} - \frac{1}{2}D_x^4 e^{\frac{k}{2}D_m} - \frac{3}{k}D_x e^{\frac{k}{2}D_m}) g_{n,m} \cdot g_{n,m}] \\
&= D_x \cosh(\frac{k}{2}D_m)(D_t f_{n,m} \cdot g_{n,m}) \cdot (f_{n,m} g_{n,m}) \\
&\quad +D_x(D_t e^{\frac{k}{2}D_m} f_{n,m} \cdot g_{n,m}) \cdot (e^{-\frac{k}{2}D_m} f_{n,m} \cdot g_{n,m}) \\
&\quad - \sinh(\frac{k}{2}D_m)[(D_x D_t f_{n,m} \cdot g_{n,m}) \cdot (f_{n,m} g_{n,m}) + (D_x f_{n,m} \cdot g_{n,m}) \cdot (D_t f_{n,m} \cdot g_{n,m})] \\
&\quad -2D_x(D_x^3 e^{\frac{k}{2}D_m} f_{n,m} \cdot g_{n,m}) \cdot (e^{-\frac{k}{2}D_m} f_{n,m} \cdot g_{n,m}) \\
&\quad +\frac{3}{2}D_x^2 \sinh(\frac{k}{2}D_m)(D_x^2 f_{n,m} \cdot g_{n,m}) \cdot (f_{n,m} g_{n,m}) \\
&\quad +D_x \cosh(\frac{k}{2}D_m)[(D_x^3 f_{n,m} \cdot g_{n,m}) \cdot (f_{n,m} g_{n,m}) + 3(D_x^2 f_{n,m} \cdot g_{n,m}) \cdot (D_x f_{n,m} \cdot g_{n,m})] \\
&\quad +\frac{1}{2} \sinh(\frac{k}{2}D_m)[(D_x^4 f_{n,m} \cdot g_{n,m}) \cdot (f_{n,m} g_{n,m}) + 2(D_x^3 f_{n,m} \cdot g_{n,m}) \cdot (D_x f_{n,m} \cdot g_{n,m})] \\
&\quad -\frac{6}{k} \sinh(\frac{k}{2}D_m)(D_x f_{n,m} \cdot g_{n,m}) \cdot (f_{n,m} g_{n,m})
\end{aligned}$$

$$
\begin{aligned}
&= D_x(D_t e^{\frac{k}{2}D_m} f_{n,m}\cdot g_{n,m})\cdot(e^{-\frac{k}{2}D_m} f_{n,m}\cdot g_{n,m})\\
&\quad -2D_x(D_x^3 e^{\frac{k}{2}D_m} f_{n,m}\cdot g_{n,m})\cdot(e^{-\frac{k}{2}D_m} f_{n,m}\cdot g_{n,m})\\
&\quad +(2\mu-\frac{6}{k})\sinh(\frac{k}{2}D_m)(D_x f_{n,m}\cdot g_{n,m})\cdot(f_{n,m}g_{n,m})\\
&\quad -6\lambda D_x\cosh(\frac{k}{2}D_m)(D_x f_{n,m}\cdot g_{n,m})\cdot(f_{n,m}g_{n,m})\\
&= D_x(D_t e^{\frac{k}{2}D_m} f_{n,m}\cdot g_{n,m})\cdot(e^{-\frac{k}{2}D_m} f_{n,m}\cdot g_{n,m})\\
&\quad -2D_x(D_x^3 e^{\frac{k}{2}D_m} f_{n,m}\cdot g_{n,m})\cdot(e^{-\frac{k}{2}D_m} f_{n,m}\cdot g_{n,m})\\
&\quad +(\mu-\frac{3}{k})D_x(e^{\frac{k}{2}D_m} f_{n,m}\cdot g_{n,m})\cdot(e^{-\frac{k}{2}D_m} f_{n,m}\cdot g_{n,m})\\
&\quad -6\lambda D_x(D_x e^{\frac{k}{2}D_m} f_{n,m}\cdot g_{n,m})\cdot(e^{-\frac{1}{2}D_m} f_{n,m}\cdot g_{n,m})\\
&= 0
\end{aligned}
\tag{57}
$$

Thus we complete the proof.

Setting $v_{n,m}=(\ln g_{n,m})_x$, $u_{n,m}=v_{n,m,x}$, $p_{n,m}=u_{n,m,x}$, $q_{n,m}=p_{n,m,x}$, $f_{n,m}=\phi_{n,m}g_{n,m}$, $\psi_{n,m}=\phi_{n,m,x}$, and $\Phi_{n,m}=(\phi_{n,m},\psi_{n,m})^T$, the bilinear Eqs. (49)–(52) can be transformed to Lax pair of the discrete system (39)–(42), (47)–(48).

$$\gamma\Phi_{n+1,m}=A_{n,m}\Phi_{n,m}, \tag{58}$$

$$B_{n,m}\Phi_{n,m+1}=\theta\Phi_{n,m}, \tag{59}$$

where $\gamma$, $\theta$ are constants,

$$A_{n,m}=\begin{pmatrix}\frac{1}{h}+v_{n,m}-v_{n+1,m} & 1\\ \lambda-u_{n,m}-u_{n+1,m} & \frac{1}{h}+v_{n,m}-v_{n+1,m}\end{pmatrix},$$

$$B_{n,m}=\begin{pmatrix}\alpha_1 & \alpha_2\\ \alpha_3 & \alpha_4\end{pmatrix},$$

$$
\begin{aligned}
\alpha_1 &= -\frac{3}{k}+2p_{n,m}+4p_{n,m+1}+12\lambda v_{n,m}+6u_{n,m}v_{n,m}-6u_{n,m+1}v_{n,m}\\
&\quad +2v_{n,m}^3-12\lambda v_{n,m+1}-6u_{n,m}v_{n,m+1}+6u_{n,m+1}v_{n,m+1}-6v_{n,m}^2v_{n,m+1}\\
&\quad +6v_{n,m}v_{n,m+1}^2-2v_{n,m+1}^3-\eta_{n,m}+\eta_{n,m+1},
\end{aligned}
\tag{60}
$$

$$\alpha_2=-12\lambda-6u_{n,m}-6u_{n,m+1}-6v_{n,m}^2+12v_{n,m}v_{n,m+1}-6v_{n,m+1}^2, \tag{61}$$

$$
\begin{aligned}
\alpha_3 &= -12\lambda^2+3q_{n,m}+3q_{n,m+1}+6\lambda u_{n,m}+12u_{n,m}^2+6\lambda u_{n,m+1}+12u_{n,m+1}^2\\
&\quad +6p_{n,m}v_{n,m}-6p_{n,m+1}v_{n,m}-6\lambda v_{n,m}^2+6u_{n,m}v_{n,m}^2+6u_{n,m+1}v_{n,m}^2\\
&\quad -6p_{n,m}v_{n,m+1}+6p_{n,m+1}v_{n,m+1}+12\lambda v_{n,m}v_{n,m+1}-12u_{n,m}v_{n,m}v_{n,m+1}\\
&\quad -12u_{n,m+1}v_{n,m}v_{n,m+1}-6\lambda v_{n,m+1}^2+6u_{n,m}v_{n,m+1}^2+6u_{n,m+1}v_{n,m+1}^2,
\end{aligned}
\tag{62}
$$

$$\begin{aligned}\alpha_4 = &-\frac{3}{k} - 4p_{n,m} - 2p_{n,m+1} + 12\lambda v_{n,m} - 6u_{n,m}v_{n,m} + 6u_{n,m+1}v_{n,m} + 2v_{n,m}^3 \\ &- 12\lambda v_{n,m+1} + 6u_{n,m}v_{n,m+1} - 6u_{n,m+1}v_{n,m+1} - 6v_{n,m}^2 v_{n,m+1} \\ &+ 6v_{n,m}v_{n,m+1}^2 - 2v_{n,m+1}^3 - \eta_{n,m} + \eta_{n,m+1}. \end{aligned} \tag{63}$$

We can check that the compatibility conditions

$$B_{n+1,m}A_{n,m+1} - A_{n,m}B_{n,m} = 0, \tag{64}$$

gives the discrete system (39)–(42), (47)–(48).

**Theorem 2** *The bilinear system* (36)–(38) *is an integrable discretization of the bilinear KdV Eq.* (2)*. Through the variable transformation* $\eta_{n,m} = (\ln f_{n,m})_t$, $v_{n,m} = (\ln f_{n,m})_x$, $u_{n,m} = (\ln f_{n,m})_{xx}$, $p_{n,m} = (\ln f_{n,m})_{xxx}$, $q_{n,m} = (\ln f_{n,m})_{xxxx}$, $r_{n,m} = (\ln f_{n,m})_{xxxxx}$, *it turns to the full discrete system* (39)–(42), (47)–(48) *which tends to the KdV Eq.* (1) *under the natural limits* $h \to 0$, $k \to 0$.

## 4 Conclusion and Discussion

In this paper, we have presented a full discretization of the KdV equation using the bilinear method and the compatibility between the integrable differential equation and its Bäcklund transformation. Unlike the semi-discretizations in [16, 17], the full discretization requires two sets of Bäcklund transformations to discretize both the space and time variables.

Our approach has significant potential and warrants further investigation. In the future, we plan to discretize the initial boundary value problems of the KdV equation to conduct numerical studies. Additionally, we will explore the extension of our method to other types of equations, such as the NLS equation.

**Acknowledgements** This work was supported by the National Natural Science Foundation of China (Grant no. 12071447, 11931017) and the Natural Science Foundation of Jiangsu Province (Grant no. BK20211266).

## References

1. Miura, R. M. The Korteweg-deVries equation: a survey of results. SIAM Review, 1976, 18.3 : 412–459.
2. Zabusky, N. J. and Kruskal,M. D. Interaction of solitons in a collisionless plasma and the recurrence of initial states. Physic Review Letter, 1965, 15:240–243.
3. Taha, T. R., and Ablowitz, M. J. Analytical and numerical aspects of certain nonlinear evolution equations. I. Analytical. Journal of Computational Physics, 1984, 55(2): 192–202.

4. Ohta,Y. and Hirota, R. A discrete KdV equation and its Casorati determinant solution. Journal of the Physical Society of Japan, 1991, 60(6): 2095–2095.
5. Moser,J. Three integrable Hamiltonian systems connected with isospectral deformations. Surveys in applied mathematics. Academic Press, 1976: 235–258.
6. Kac, M. and Pierre van Moerbeke. On an explicitly soluble system of nonlinear differential equations related to certain Toda lattices. Advances in Mathematics, 1975, 16(2): 160–169.
7. Bogoyavlensky, O. I. Integrable discretizations of the KdV equation. Physics Letters A, 1988, 134(1): 34–38.
8. Hirota R. Nonlinear partial difference equations I. A difference analogue of the Korteweg-de Vries equation. Journal of the Physical Society of Japan, 1977, 43(4): 1424–1433.
9. Nijhoff, F. and Capel,H. The discrete Korteweg-de Vries equation. Acta Applicandae Mathematica, 1995, 39(1-3): 133–158.
10. Schiff,J. Loop groups and discrete KdV equations. Nonlinearity, 2003, 16:257–275.
11. Suris, Y. B. The problem of integrable discretization: Hamiltonian approach. Birkhäuser, 2012.
12. Tempesta, P. Discretization of nonlinear evolution equations over associative function algebras. Nonlinear Analysis: Theory, Methods and Applications, 2010, 72(7–8): 3237–3246.
13. Chiu, S. C. and Ladik, J. F. Generating exactly soluble nonlinear discrete evolution equations by a generalized Wronskian technique. Journal of Mathematical Physics, 1977, 18(4): 690–700.
14. Levi, D. Benguria R. Bäcklund transformations and nonlinear differential difference equations. Proceedings of the National Academy of Sciences, 1980, 77(9): 5025–5027.
15. Levi, D. Nonlinear differential difference equations as Bäcklund transformations. Journal of Physics A: Mathematical and General, 1981, 14(5): 1083–1098.
16. Zhang, Y., Chang, X., Hu, J., Hu, X. and Tam, H.W. Integrable discretization of soliton equations via bilinear method and Bäcklund transformation. Science China Mathematics, 2015, 58: 279–296.
17. Zhang, Y., Tam, H. W. and Hu, X. B. Integrable discretization of time and its application on the Fourier pseudospectral method to the Kortewegde Vries equation. Journal of Physics A: Mathematical and Theoretical, 2014, 47(4): 045202.
18. Hu, X. B., Zhu, Z. N. and Wang, D. L. A differential- difference Caudrey-Dodd-Gibbon-Kotera-Sawada equation. Journal of the Physical Society of Japan, 2000, 69(4): 1042–1049.
19. Hu, X. B., Clarkson, P. A. Bäcklund transformations and nonlinear superposition formulae of a differential-difference KdV equation. Journal of Physics A: Mathematical and General, 1998, 31(5): 1405.
20. Hirota, R. Direct Method in Soliton Theory(translated by Nagai A, Nimmo J and Gilson C). Cambridge University Press, 2004.

# Damped Nonlinear Schrödinger Equation with Stark Effect


**Yi Hu, Yongki Lee, and Shijun Zheng**

**Abstract** The problem of singularity formation for damped NLS (dNLS) has been an interesting and meanwhile challenging one in both mathematical and physical literature. We study the $L^2$-critical damped NLS with a Stark potential. We prove that the threshold for global existence and finite time blow-up of this equation is given by $\|Q\|_2$, where $Q$ is the unique positive radial solution of $\Delta Q + |Q|^{4/d} Q = Q$ in $H^1(\mathbb{R}^d)$. Moreover, in any small neighborhood of $Q$, there exists an initial data $u_0$ above the ground state such that the solution flow admits the log-log blow-up speed. This verifies the structural stability for the "log-log law" associated to the NLS mechanism under the perturbation by a damping term and a Stark potential. The proof of our main theorem is based on the Avron-Herbst formula and the analogous result for the unperturbed dNLS. The method of our analysis allows to further prove a general blow-up criterion. Moreover, we give a concentration compactness description for the limiting behavior of blow-up solutions, which might have independent analytical interest.

**Keywords** Damped nonlinear Schrödinger equation · Stark potential · Avron-Herbst formula

**2020 Mathematics Subject Classification** 35B40 · 35Q55

Y. Hu · Y. Lee · S. Zheng (✉)
Department of Mathematical Sciences, Georgia Southern University, Statesboro, GA 30458, USA
e-mail: szheng@georgiasouthern.edu

Y. Hu
e-mail: yihu@georgiasouthern.edu

Y. Lee
e-mail: yongkilee@georgiasouthern.edu



S. Manukure and W.-X. Ma (eds.), *Nonlinear and Modern Mathematical Physics*,
Springer Proceedings in Mathematics & Statistics 459,
https://doi.org/10.1007/978-3-031-59539-4_7

## 1 Introduction

Consider the damped nonlinear Schrödinger equation (dNLS) with Stark effect:

$$iu_t = -\Delta u + (E \cdot x)u - |u|^{p-1}u - iau, \qquad u(0) = u_0 \in \mathcal{H}^1. \tag{1.1}$$

Here $p \in (1, 1 + \frac{4}{n-2})$ if $n \geq 3$ and $p \in (1, \infty)$ if $n = 1, 2$. The solution $u = u(t, x) : \mathbb{R}^{1+n} \to \mathbb{C}$ is the wave function, $V(x) = V_E(x) := E \cdot x$ is a Stark potential with $E \in \mathbb{R}^n \setminus \{0\}$, and $-iau$ is a linear damping to the system with $a > 0$ being the coefficient of friction. The initial data $u_0$ is in the energy space $\mathcal{H}^1 := \left\{\phi \in H^1 : x\phi \in L^2\right\}$, whose norm is given by $\|\phi\|_{\mathcal{H}^1} := \left(\|\phi\|_{H^1}^2 + \|x\phi\|_{L^2}^2\right)^{1/2}$, where $H^1$ denotes the usual Sobolev space.

The problem of studying singular solutions for the dNLS has been known technically difficult [10, 14, 16, 39]. In laser optics, it is desirable to understand the effect of small damping on singularity formation (rate of wave collapse, asymptotics of the blow-up profile) for the NLS mechanism. The dNLS (1.1) provides a model for optical self-focusing phenomenon, where an electromagnetic wave is absorbed by the propagation medium.

The damping term $-iau, a > 0$ contributes to the decrease of the mass and thus there does not exists minimal mass blowup solutions, see (2.1) and Remark 3.2. In fact, any initial data $u_0$ with possible large mass can quickly change to small mass because of $\|u(t)\|_2^2 = e^{-2at}\|u_0\|_2^2$. Hence, there are analytical difficulties in determining the blow-up behavior and the blow-up time. In the absence of a potential, i.e., $V = 0$, Darwich [12] showed the existence of blow-up solutions in the log-log regime for $L^2$-critical dNLS based on some modifications of Merle-Raphaël spectral-hypothesis approach [28]. When $V$ is an unbounded potential, such approach does not seem applicable since one would not be able to treat the dNLS (1.1) as a small perturbation of the free dNLS. In addition, there is some difficulty verifying the appropriate spectral hypothesis. Motivated by the $\mathcal{R}$-transform method in [4] for the rotational NLS, we apply the Avron-Herbst transform (3.1) to convert Eq. (1.1) to the unperturbed dNLS, which allows to obtain the blow-up solutions above the ground state solution $Q_0$ of (1.7) with exact log-log blow-up rate in Theorem 1.1. This result on the dNLS (1.1) is two-fold:

(i) It shows that $\|Q_0\|_2$ is the threshold for global existence and blow-up.
(ii) It informs that in any small neighborhood of $Q_0$, there exist blow-up solutions in the log-log regime. Per the authors' best knowledge, such construction of singular solutions of (1.1) is new for Stark potential.

In the remaining of the introduction section, we elaborate on our results in Theorems 1.1 and 1.2. The associated energy of the dNLS (1.1) is given by

$$\mathcal{E}_V(u) := \int_{\mathbb{R}^n} \left( |\nabla u|^2 + V_E|u|^2 - \frac{2}{p+1}|u|^{p+1} \right) dx. \tag{1.2}$$

In physics, $E$ may represent an electric field or quantum gravity [11, 38], and damped NLS equations appear in nonlinear optics, plasma physics, and water waves [16, 19, 23, 33].

The hamiltonian $H = H_E := -\Delta + E \cdot x$ arises in the study of hydrogen model in connection with the resonance phenomenon associated with quasi-stationary states [20, 21]. The operator $H_E$ is essentially selfadjoint in $C_0^\infty(\mathbb{R}^3)$, which has absolutely continuous spectrum $\mathbb{R} = (-\infty, \infty)$. The presence of a Stark potential has an resonance effect such that it shifts the discrete energies of the hydrogen atom into resonances (pseudo-eigenvalues) via the hamiltonian $H_{Z,E} = -\Delta - \frac{Z}{|x|} + E \cdot x$, where $Z \geq 0$ is the atomic number. This distinguishes from the harmonic oscillator $-\Delta + |x|^2$ in that $H_{Z,E}$ has weaker decaying "bound state", and so $V_E = E \cdot x$ is also called the spatially damped oscillator.

On the other hand, when $a > 0$, the linear term $-iau$ is present as a temporal damping effect for the NLS equation. So it might be of analytical interest to study the Schrödinger type system as (1.1). There has been a large body of literature in the field of wave dispersion-dissipation in physics and numerics [1, 6, 19, 24, 25].

If $E = 0$ and $a = 0$, then Eq. (1.1) becomes the classic NLS

$$iu_t = -\Delta u - |u|^{p-1}u\,, \qquad u(0) = u_0 \in H^1 \tag{1.3}$$

and its well-posedness and blowup have been studied extensively in the $H^1$-subcritical and $H^1$-critical cases $p \leq 1 + \frac{4}{n-2}$, see [9, 37]. The following quantities are conserved in time for (1.3):

$$\text{(Mass)} \qquad \mathcal{M}(u) := \|u(t)\|_{L^2}^2 \tag{1.4}$$

$$\text{(Energy)} \qquad \mathcal{E}_0(u) := \|\nabla u(t)\|_{L^2}^2 - \frac{2}{p+1}\|u(t)\|_{L^{p+1}}^{p+1} \tag{1.5}$$

$$\text{(Momentum)} \qquad \mathcal{P}(u) := \mathrm{Im}\left(\int_{\mathbb{R}^n} \overline{u}\nabla u\, dx\right). \tag{1.6}$$

In the $L^2$-critical regime $p = 1 + \frac{4}{n}$, if we let $Q = Q_0$ be the unique positive and radial solution in $H^1$ to the elliptic equation

$$\Delta Q + |Q|^{\frac{4}{n}}Q = Q\,, \tag{1.7}$$

then Weinstein [40] showed that $\|Q\|_{L^2}$ is the threshold for global existence and finite time blowup of the Cauchy problem (1.3) in $H^1$. Namely, if $\|u_0\|_{L^2} < \|Q\|_{L^2}$, then the solution $u(t)$ of (1.3) is global in $H^1$, while for any $c \geq \|Q\|_{L^2}$, there exists $u_0 \in H^1$ with $\|u_0\|_{L^2} = c$ such that the solution $u(t)$ blows up in finite time $T^* > 0$. Further, Merle [26] showed that the set of all minimal mass blowup solutions at the ground state level $\|Q\|_2$ consists of pseudo-conformal transforms of the solitary wave $e^{it}Q(x)$:

$$S(t,x)=\frac{e^{i\theta}}{|T-t|^{d/2}}Q(\frac{x-x_0}{T-t})e^{-i\frac{|x-x_0|^2}{4(T-t)}}e^{\frac{i}{T-t}} \tag{1.8}$$

where $(\theta, T, x_0) \in \mathbb{R}\times\mathbb{R}\times\mathbb{R}^n$ are parameters.

When the initial data is above the ground state level, under the assumption of certain spectral property (see Remark 2.6), Merle and Raphaël ([28, 29]) proved the sharp blow-up speed for the solutions, i.e., there exists a small universal constant $\alpha^*>0$ such that for all $u_0\in\mathcal{B}_{\alpha^*}$ with negative energy $\mathcal{E}_0(u_0)<0$, the solution $u(t)$ blows up as $t\to T^*$ with the speed (called "log-log law")

$$\|\nabla u(t)\|_{L^2}\approx\left(\frac{\log|\log(T^*-t)|}{T^*-t}\right)^{\frac{1}{2}}, \tag{1.9}$$

where

$$\mathcal{B}_\alpha:=\left\{\phi\in H^1:\|Q\|_{L^2}<\|\phi\|_{L^2}<\|Q\|_{L^2}+\alpha\right\}.$$

This log-log regime is also known to be stable in $H^1$ [36].

If $E=0$ in Eq. (1.1), then one has the damped NLS

$$i\varphi_t=-\Delta\varphi-|\varphi|^{p-1}\varphi-ia\varphi,\qquad \varphi(0)=\varphi_0=u_0\in H^1. \tag{1.10}$$

The local well-posedness in $H^1$ for the dNLS is well-known (see e.g. [9, 39]). Precisely speaking, for every $u_0\in H^1$, there exists $T>0$ and a unique solution $\varphi\in C\left([0,T),H^1\right)$ of the Cauchy problem (1.10), where $[0,T)=[0,T_{max})$ is the maximal time interval of existence. Moreover, if $T_{max}$ is finite, then $\|\nabla\varphi(t)\|_2\to\infty$ as $t\to T_{max}$. Because of the damping term $-ia\varphi$, the dynamics of the solution may behave differently from that of the classic NLS. For instance, the mass, energy, and momentum (1.4)–(1.6) are not conserved. Darwich [12] studied the Cauchy problem (1.10) in the $L^2$-critical regime $p=1+\frac{4}{n}$ when $n\le 4$, and he proved that $\|Q\|_2$ is the sharp threshold for the blow-up phenomenon in $H^1$. Furthermore, there exists $\alpha_0>0$ such that for all $a>0$ and arbitrary $\alpha\in(0,\alpha_0)$, there exists a blow-up solution in the log-log regime corresponding to some $u_0\in\mathcal{B}_\alpha$, see Theorem 2.4.

Motivated by the abovementioned work, in this paper we concentrate on the $L^2$-critical case $p=1+4/n$ for the focusing dNLS (1.1) with a Stark potential. We shall establish the sharp threshold for global existence and the log-log law for the Cauchy problem (1.1) in the weighted Sobolev space $\mathcal{H}^1$. Our main result is stated as follows.

**Theorem 1.1** *Let $p=1+\frac{4}{n}$ and $a>0$. Suppose $u_0\in\mathcal{H}^1(\mathbb{R}^n)$ for $1\le n\le 4$.*

*(a) If $\|u_0\|_{L^2}\le\|Q\|_{L^2}$, then the solution of (1.1) is global in time such that $u(t)\in C([0,\infty),\mathcal{H}^1)$.*

*(b) There exists a small $\alpha_0>0$ such that for arbitrary $\alpha\in(0,\alpha_0)$, there exists $u_0\in\mathcal{B}_\alpha\cap\mathcal{H}^1$ such that the corresponding solution $u(t)$ of (1.1) blows up at $T^*<\infty$ with the log-log speed (1.9).*

The proof of Theorem 1.1 (see Sect. 3) relies on the Avron-Herbst transform (Proposition 3.1) and Theorem 2.4. An alternative, independent proof of part (a) in all dimensions is given as a corollary (Corollary 4.4) of a limiting profile result in Theorem 4.3.

We wish to mention that for the $L^2$-critical NLS (1.3), there exist minimal mass blow-up solutions (1.8) with $\|u_0\|_2 = \|Q\|_2$ and pseudo-conformal blow-up speed $(T^* - t)^{-1}$. However, in the presence of damping, $\|u_0\|_2 = \|Q\|_2$ will lead to a global solution to the Eq. (1.1), so Theorem 1.1 also proves the *none existence of minimal mass blow-up solutions* for (1.1).

Theorem 1.1 shows the structural stability for the NLS mechanism: The log-log law continues to hold when the free NLS $iu_t = -\Delta u - |u|^{4/n}u$ is perturbed with a damping term and a linearly growth potential. Similar results have been obtained for other Schrödinger type equations rencently [4, 15, 34, 35]. However, from the proofs in either [12] or [13], it is not evident whether such log-log regime is topologically stable for the dissipative NLS (1.1) in an electric field.

Our second main result is concerned with finding a sufficient condition on singular (blow-up) solutions for (1.1). By the $A$-$H$ transform in Proposition 3.1, we are able to show that, given any $u_0$ with $\mathcal{E}_0(u_0) < 0$, there exists $a_* = a_*(u_0) > 0$ such that the solution $u(t)$ blows up for all $0 < a < a_0$ by an application of [14, Theorem 1.2], see Theorem 2.8.

**Theorem 1.2** *Let $p$=1+4/$n$, $n \geq 1$. Suppose $u_0 \in \mathcal{H}^1$ and $\mathcal{E}_V(u_0) < \int E \cdot x|u_0|^2$. Then, there exists $a_* = a_*(\|u_0\|_{H^1}) > 0$ such that for all $a \in (0, a_*)$, the corresponding solution $u(t)$ of (1.1) in $C([0, T^*), \mathcal{H}^1)$ blows up finite time on $[0, T^*)$ in the sense that $\|\nabla u(t)\|_2 \to \infty$ as $t \to T^*$.*

Note that this theorem, along with part (a) in Theorem 1.1, implies the blow-up for any initial data in the open region $\{u \in \mathcal{B}_{\alpha_,} \cap \mathcal{H}^\infty : \mathcal{E}_\prime(\sqcap) < \prime\}$ for any prescribed positive $\alpha_0$.

On the other hand, the numerical result in [16] and also [10, 14] suggest that increasing the value of $a > a_*$ can give rise to the effect that *damping arrests self-focusing* so that the solution will survive over infinity time. However, such $a_*$ is dependent on the initial data. Meanwhile, in the case $V_E = 0$, a simple scaling argument informs that given any solution $u$ of $NLS_a$ in (2.5), then $u_\lambda(t, x) := \frac{1}{\lambda^{n/2}} u(\frac{t}{\lambda^2}, \frac{x}{\lambda})$ solves $NLS_{a/\lambda^2}$, cf. [12, Remark 3.2]. Thus, the problem of stability/instability of blow-up for the dNLS can be notably subtle and sensitive.

We would like to comment that the results in this article inform that the Stark potential $V_E = E \cdot x$ does not seem to essentially change the blow-up by its interactions with the damping term and the $L^2$-critical nonlinearity. However, this potential may affect the scattering behavior owing to its interaction with a linear potential potential like $|x|^{-\gamma}$, as was observed in Ozawa's work [32], cf. also [8, Remark, p. 727]. It would be of interest to further study the effect of $V_E$ on the long time asymptotic behavior for Eq. (1.1) when $p < 1 + 4/n$.

## 2 Preliminaries

For the dNLS (1.1) with a Stark potential $V_E$, the local well-posedness in $\mathcal{H}^1$ holds. In fact, following a standard fixed point argument as in [9] or [8, 42], we can easily show the following l.w.p. for (1.1).

**Proposition 2.1** *Let $p \in (1, 1+4/(n-2))$. Suppose $u_0 \in \mathcal{H}^1$. Then there exists $T := T^* \in (0, \infty]$ and a unique solution $u(t)$ in $C\left([0,T), \mathcal{H}^1\right)$ of the Cauchy problem (1.10), where $[0,T)$ is the lifespan for forward time. The blow-up alternative holds: If $T$ is finite, then $\|\nabla u(t)\|_2 \to \infty$ as $t \to T$.*

We omit the detailed proof of the proposition, but instead provide below a description of the "modified conservation laws" on the interval of existence $[0,T)$ for the mass, energy, and momentum of the system.

**Proposition 2.2** *Let $u$ be a solution of the Cauchy problem (1.1) on $[0,T)$. Let $\mathcal{M}(u)$, $\mathcal{E}_0(u)$, and $\mathcal{P}(u)$ be defined as in (1.4)–(1.6), respectively, and let $\mathcal{E}_V(u)$ be the associated energy (1.2). Then*

$$\mathcal{M}(u) = e^{-2at}\mathcal{M}(u_0) \tag{2.1}$$

$$\frac{d}{dt}\mathcal{E}_0(u) = -2i\int_{\mathbb{R}^n} E\cdot u\nabla\overline{u}dx - 2a\|\nabla u(t)\|_{L^2}^2 + 2a\|u(t)\|_{L^{p+1}}^{p+1} \tag{2.2}$$

$$\frac{d}{dt}\mathcal{E}_V(u) = -2a\int_{\mathbb{R}^n} E\cdot x|u|^2dx - 2a\|\nabla u(t)\|_{L^2}^2 + 2a\|u(t)\|_{L^{p+1}}^{p+1} \tag{2.3}$$

$$\mathcal{P}(u) = e^{-2at}\left(-tE\mathcal{M}(u_0) + \mathcal{P}(u_0)\right). \tag{2.4}$$

***Proof*** Equations (2.1) to (2.4) can be verified by straightforward calculations. For instance, to verify the identity (2.1), we multiply both sides of Eq. (1.1) by $\overline{u}$ and integrate them with respect to $x$ to obtain

$$\begin{aligned}\int_{\mathbb{R}^n} iu_t\overline{u}dx &= \int_{\mathbb{R}^n}\left(-\Delta u + E\cdot xu - |u|^{p-1}u - iau\right)\overline{u}dx\\ &= \int_{\mathbb{R}^n}\left(|\nabla u|^2 + E\cdot x|u|^2 - |u|^{p+1} - ia|u|^2\right)dx.\end{aligned}$$

Since

$$\frac{d}{dt}\int_{\mathbb{R}^n}|u|^2dx = 2\,\mathrm{Re}\int u_t\overline{u}dx = 2\,\mathrm{Im}\int iu_t\overline{u}dx = -2a\int_{\mathbb{R}^n}|u|^2dx,$$

we obtain the o.d.e.

$$\frac{d}{dt}\|u(t)\|_{L^2}^2 = -2a\|u(t)\|_{L^2}^2, \qquad \|u(0)\|_{L^2} = \|u_0\|_{L^2},$$

whose solution yields (2.1).

Similarly, Eqs. (2.2) and (2.3) follow from a direct calculation, and Eq. (2.4) follows via solving the Cauchy problem

$$\frac{d}{dt}\mathcal{P}(u) = -E\mathcal{M}(u_0) - 2a\mathcal{P}(u), \qquad \mathcal{P}(u(0)) = \mathcal{P}(u_0).$$

□

**Remark 2.3** If the system is damping-free, i.e. $a = 0$, then the quantities $\mathcal{M}(u)$ and $\mathcal{E}_V(u)$ are conserved. Also, from (2.1)–(2.4), it seems that the Stark potential affects the dynamics of all but $\mathcal{M}(u)$. Indeed, Eq. (2.1) also holds when $E = 0$ (which will be used in the proof of Theorem 1.1 later). Moreover, Eq. (2.1) indicates the nonexistence of solitary waves of the form $u(t, x) = e^{it}\phi(x)$, for otherwise $\|u(t)\|_{L^2} = \|\phi\|_{L^2}$ does not decay in time.

The following theorem is the main result in [12], and it will be applied in the proof of Theorem 1.1.

**Theorem 2.4** (Darwich [12]) *Let $p = 1 + \frac{4}{n}$ and $u_0 \in H^1(\mathbb{R}^n)$, $n = 1, 2, 3, 4$.*

*(a) If $\|u_0\|_{L^2} \le \|Q\|_{L^2}$, then the solution to Eq. (1.10) is global in $H^1$.*
*(b) There exists a $\delta_0 > 0$ such that, for all $a > 0$ and $\delta \in (0, \delta_0)$, there exists a $u_0 \in H^1$ with $\|u_0\|_{L^2} = \|Q\|_{L^2} + \delta$, such that the solution to Eq. (1.10) blows up in finite time in the log-log regime (1.9).*

The proof of Theorem 2.4 is a modification of the approach in [27] to [30]. The initial ansatz for the profile near $t \to T^*$ is given as

$$\varphi(t, x) = \frac{e^{i\theta(t)}}{\lambda(t)^{d/2}} \left(Q_{b(t)} + \eta\right)\left(t, \frac{x - y(t)}{\lambda(t)}\right)$$

for some geometrical parameters $(b, \lambda, y, \theta) = (b(t), \lambda(t), y(t), \theta(t)) \in \mathbb{R}_+ \times \mathbb{R}_+ \times \mathbb{R}^n \times \mathbb{R}$ with $\lambda(t) \sim 1/\|\nabla u(t)\|_2$. These profiles $Q_b$ are regularization of the self-similar solutions of (1.3) that obeys the elliptic equation

$$\Delta Q_b + ib\left(\frac{n}{2} + x \cdot \nabla\right) Q_b + |Q_b|^{\frac{4}{n}} Q_b = Q_b\,.$$

Thus $Q_b$ are resultantly suitable deformation of $Q$ up to some degeneracy of the problem (1.7). The geometrical parameters here are uniquely defined per some orthogonality conditions in the *Spectral Property* [28, p. 164], or [4, 41].

**Remark 2.5** The limit on the dimension $n \le 4$ is required in an interpolation inequality in the proof of [12, Lemma 6.2], see also similar proof for [13, Lemma 4.2].

**Remark 2.6** The *Spectral Property* has not been analytically verified for all dimensions. In one dimension it was proved by Merle and Raphaël [28] using the explicit

expression of $Q$ to (1.7). The recent progress in higher dimensions is attributed to [18], and [41], where is given an improved numerically-assisted proof for $n \leq 10$ and also for $n = 11, 12$ in the radial case. See also the discussions on the rotational NLS in [4, 5], where the spectral property is required.

**Remark 2.7** It is known in the literature that that nonlinear damping arrests blow-up, while linear damping can arrest blow-up only when the parameter $a$ is larger than a threshold value $a_{threshold}$ [3, 16]. At first glimpse one might think that the result in Theorem 2.4 should be valid for a finite range of $a$ dependent on $u_0$. However, a close read of, e.g., Remark 4.5 suggests that even for large damping value of $a$, the solution $u(t)$ can blow up in very short time before the mass going below $\|Q\|_2^2$. On the other hand, when $a = 0$ and $\|u_0\|_2 = \|Q\|_2$, it is easy to construct for the undamped NLS with Stark effect a pseudo-conformal type blow-up solution with blow-up rate $(T - t)^{-1}$ for any prescribed $T > 0$. Also, we can construct a global solution that has blow-up at infinite time. Nevertheless, when $a > 0$, the dNLS (1.1) no longer admits similar blow-up solutions, even though the converted nonlinearity $-e^{-at(p-1)}|\varphi|^{p-1}\varphi \approx -|\varphi|^{p-1}\varphi$ for shorter time under the transform $u = e^{-at}\varphi$. We see here again that even in very short time the role of damping $-iau$ in arresting blow-up is crucial and can be exceptionally subtle.

For the proof of Theorem 1.2 we need the analogous result in [14], where some blow-up conditions for (1.10) were obtained. Let $J(t) := \int |x|^2|\varphi|^2$ be the variance. In the $L^2$-critical regime $p = 1 + \frac{4}{n}$, the virial identity for the free NLS (1.3) reads $\frac{d^2}{dt^2}J(t) = 8\mathcal{E}_0(u_0)$, which can be used to show that $u_0 \mapsto u(t)$ is a blow-up solution of (1.3) if $\mathcal{E}_0(u_0) < 0$. This result was extended for the dNLS (2.5) in the absence of $V_E$ in [14, Theorem 1.2]

$$i\varphi_t = -\Delta\varphi - |\varphi|^{4/n}\varphi - ia\varphi, \qquad \varphi(0) = \varphi_0\,. \tag{2.5}$$

The proof is based on a localized virial identity for the dNLS. Denote $\Sigma := H^1 \cap \{u \in L^2 : \int |x|^2|u|^2 < \infty\}$.

**Theorem 2.8** (Dinh [14]) *Let $p = 1 + 4/n$, $n \geq 1$. Suppose $u_0 \in \Sigma$ and $\mathcal{E}_0(\varphi_0) < 0$. Then, there exists a positive $a_* = a_*(\|u_0\|_{H^1})$ such that for all $a \in (0, a_*)$, the corresponding solution $u(t)$ of (2.5) in $C([0, T^*), \Sigma)$ blows up finite time on $[0, T^*)$.*

The proof of Theorem 1.2 is based on a simple application of the Avron-Herbst formula (3.2) and Theorem 2.8. The $A$-$H$ transform allows us to convert solutions $u(t)$ of (1.1) into solutions $\varphi$ of (2.5). We leave the proof as an easy exercise for the reader.

## 3 Avron-Herbst Formula and Proof of Theorem 1.1

First we introduce the Avron-Herbst formula, as is well-known [2, 8, 11].

**Proposition 3.1** *Let $T \in (0, \infty]$. If $\varphi$ is the solution to the Cauchy problem (1.10) on $[0, T)$, then for $E \in \mathbb{R}^n \setminus \{0\}$, the function*

$$u(t, x) := \varphi\left(t, x + t^2 E\right) e^{-i\left(tE\cdot x + \frac{|E|^2 t^3}{3}\right)} \tag{3.1}$$

*is the solution to the Cauchy problem (1.1) on $[0, T)$.*

*Conversely, if $u$ is the solution to the Cauchy problem (1.1) on $[0, T)$, then the function*

$$\varphi(t, x) := u\left(t, x - t^2 E\right) e^{i\left(tE\cdot x - \frac{2|E|^2 t^3}{3}\right)} \tag{3.2}$$

*is the solution to the Cauchy problem (1.10) on $[0, T)$.*

***Proof*** Both can be verified by direct computation. For example, to verify that $u$ in (3.1) solves the problem (1.1), obviously we have $u(0) = \varphi(0) = u_0$, and

$$\begin{aligned} u_t(t, x) &= \left[\varphi_t\left(t, x + t^2 E\right) + 2tE \cdot \nabla\varphi\left(t, x + t^2 E\right)\right] e^{-i\left(tE\cdot x + \frac{|E|^2 t^3}{3}\right)} \\ &\quad + \varphi\left(t, x + t^2 E\right) e^{-i\left(tE\cdot x + \frac{|E|^2 t^3}{3}\right)} \left[-i\left(E \cdot x + |E|^2 t^2\right)\right] \\ &= \left[\varphi_t\left(t, x + t^2 E\right) + 2tE \cdot \nabla\varphi\left(t, x + t^2 E\right) - iE \cdot x\varphi\left(t, x + t^2 E\right)\right. \\ &\quad \left. -i|E|^2 t^2 \varphi\left(t, x + t^2 E\right)\right] e^{-i\left(tE\cdot x + \frac{|E|^2 t^3}{3}\right)} \end{aligned}$$

and

$$\begin{aligned} \Delta u(t, x) &= \Delta\left[\varphi\left(t, x + t^2 E\right)\right] e^{-i\left(tE\cdot x + \frac{|E|^2 t^3}{3}\right)} + 2\nabla\left[\varphi\left(t, x + t^2 E\right)\right] \cdot \nabla\left[e^{-i\left(tE\cdot x + \frac{|E|^2 t^3}{3}\right)}\right] \\ &\quad + \varphi\left(t, x + t^2 E\right) \Delta\left[e^{-i\left(tE\cdot x + \frac{|E|^2 t^3}{3}\right)}\right] \\ &= \left[\Delta\varphi\left(t, x + t^2 E\right) - 2itE \cdot \nabla\varphi\left(t, x + t^2 E\right) - t^2|E|^2 \varphi\left(t, x + t^2 E\right)\right] e^{-i\left(tE\cdot x + \frac{|E|^2 t^3}{3}\right)}. \end{aligned}$$

Then Eq. (1.1) holds if we bring $u$, $u_t$, and $\Delta u$ into both sides and use Eq. (1.10) for $\varphi$. □

Now we prove Theorem 1.1 using the Avron-Herbst transform (3.1)–(3.2).

***Proof of Theorem*** 1.1 To prove (a), note that if $\|u_0\|_{L^2} \leq \|Q\|_{L^2}$, then according to Theorem 2.4, there exists a global solution $\varphi$ to the Cauchy problem (1.10) with

$\varphi(0) = u_0$. Applying formula (3.1) to $\varphi$, we obtain a global solution $u$ to the problem (1.1).

To prove (b), let $\alpha_0 := \delta_0$ in Theorem 2.4. Then for each $\alpha \in (0, \alpha_0)$, there exists an initial value $\|u_0\|_{L^2} = \|Q\|_{L^2} + \alpha$ with which the solution $\varphi$ to the Cauchy problem (1.10) blows up in finite time $T^*$ at the log-log speed (1.9). Then we obtain $u$ in terms of $\varphi$ on $[0, T^*)$ through formula (3.1), and $[0, T^*)$ is the maximal time interval for $u$ because otherwise we can use formula (3.2) to extend $\varphi$ beyond $T^*$. To show that $u$ blows up in the log-log regime, we have

$$\begin{aligned}\nabla u(t,x) &= \nabla\varphi\left(t, x + t^2E\right) e^{-i\left(tE\cdot x + \frac{|E|^2t^3}{3}\right)} + \varphi\left(t, x + t^2E\right) e^{-i\left(tE\cdot x + \frac{|E|^2t^3}{3}\right)}(-itE) \\ &=: \mathrm{I} + \mathrm{II}.\end{aligned}$$

It is easy to see that

$$\|\mathrm{I}\|_{L^2} = \|\nabla\varphi(t)\|_{L^2} \approx \left(\frac{\log|\log(T^*-t)|}{T^*-t}\right)^{\frac{1}{2}} \quad \text{as } t \to T^*.$$

Also, by the identiy (2.1) (and Remark 2.3), we have

$$\|\mathrm{II}\|_{L^2} = t|E|\,\|\varphi(t)\|_{L^2} = te^{-at}|E|\,\|u_0\|_{L^2},$$

which is a bounded function on $[0, \infty)$ with maximum occurring at $t = \frac{1}{a}$. Combining both estimates, we have

$$\|\nabla u(t)\|_{L^2} \approx \|\mathrm{I}\|_{L^2} + \|\mathrm{II}\|_{L^2} \approx \left(\frac{\log|\log(T^*-t)|}{T^*-t}\right)^{\frac{1}{2}} \quad \text{as } t \to T^*.$$

□

**Remark 3.2** We have noted in the introduction section that, in the presence of damping, Theorem 1.1 (a) indicates that there always exists a global solution of (1.1) when $\|u_0\|_2 = \|Q\|_2$. Indeed, we will give another proof of this property in the next section as a corollary of a limiting profile result (Theorem 4.3), which basically says that the mass of a blowup solution will concentrate and will be no less than $\|Q\|_2$. This, together with the mass decay (2.1), will explain why there are no blow-up solutions at the level $\|Q\|_2$, see Corollary 4.4.

## 4 A Limiting Profile Result for Eq. (1.1)

In this section, we will first prove a limiting profile result about the mass concentration of blow-up solutions of Eq. (1.1) in Theorem 4.3, and then give an alternative proof of Theorem 1.1 (a) for all dimensions. Throughout this section, we assume $p = 1 + \frac{4}{n}$.

In [22], Hmidi and Keraani proved a refined version of compactness lemma adapted to the analysis of the blow-up phenomenon for the Cauchy problem (1.3) in the $L^2$-critical case. Their result is as follows.

**Theorem 4.1** ([22]) *Let $\{v_k\}$ be a bounded sequence in $H^1(\mathbb{R}^n)$ such that*

$$\limsup_{k\to\infty} \|\nabla v_k\|_{L^2} \le M \tag{4.1}$$

*and*

$$\limsup_{k\to\infty} \|v_k\|_{L^{2+\frac{4}{n}}} \ge m. \tag{4.2}$$

*Then there exists a sequence $\{x_k\} \subseteq \mathbb{R}^n$ such that (up to a subsequence)*

$$v_k(\cdot + x_k) \rightharpoonup V \quad \text{and} \quad \|V\|_{L^2} \ge \left(\frac{n}{n+2}\right)^{\frac{n}{4}} \frac{m^{\frac{n}{2}+1}+1}{M^{\frac{n}{2}}} \|Q\|_{L^2}.$$

We will also use the following lemma from [31].

**Lemma 4.2** *([31]) Let $T \in (0,\infty)$, and assume that $f : [0,T) \to \mathbb{R}^+$ is a continuous function. If $\lim_{t\to T} f(t) = \infty$, then there exists a sequence $\{t_k\}$ in $\subseteq [0,T)$ such that*

$$t_k \to T \quad \text{and} \quad \frac{\int_0^{t_k} f(\tau)\, d\tau}{f(t_k)} \to 0 \quad \text{as} \quad k \to \infty.$$

Now we present the main result in this section.

**Theorem 4.3** (Concentration of mass) *Consider the Cauchy problem (1.1) with $p = 1 + \frac{4}{n}$. Suppose that the solution $u$ of (1.1) blows up at finite time $T^* < \infty$, i.e. $\|\nabla u(t)\|_{L^2} \to \infty$ as $t \to T^*$. Then for any function $w(t)$ satisfying $w(t)\|\nabla u(t)\|_{L^2} \to \infty$ as $t \to T^*$, there exists a function $x(t) \in \mathbb{R}^n$ such that (up to a subsequence)*

$$\liminf_{t\to T^*} \|u(t)\|_{L^2(|x-x(t)|<w(t))} \ge \|Q\|_{L^2}. \tag{4.3}$$

***Proof*** Let $G(u)$ be the r.h.s. of the Eq. (2.2), i.e.

$$G(u) := -2i \int_{\mathbb{R}^n} E \cdot u \nabla \overline{u} dx - 2a\|\nabla u(t)\|_{L^2}^2 + 2a\|u(t)\|_{L^{2+\frac{4}{n}}}^{2+\frac{4}{n}}.$$

Integrating (2.2) on $[0,t)$, we have

$$\mathcal{E}_0(u(t)) = \mathcal{E}_0(u_0) + \int_0^t G(u(\tau)) d\tau. \tag{4.4}$$

Now we give an estimate of $G(u)$. By Hölder's inequality and the mass decay (2.1), we have

$$\left|\int_{\mathbb{R}^n} E\cdot u\nabla\overline{u}dx\right| \le \|E\cdot u(t)\|_{L^2}\|\nabla u(t)\|_{L^2}$$
$$= |E|\,\|u(t)\|_{L^2}\|\nabla u(t)\|_{L^2} \le |E|\,\|u_0\|_{L^2}\|\nabla u(t)\|_{L^2},$$

and by Gagliardo-Nirenberg inequality and (2.1), we have

$$\|u(t)\|^{2+\frac{4}{n}}_{L^{2+\frac{4}{n}}} \le C\,\|u(t)\|^{\frac{4}{n}}_{L^2}\,\|\nabla u(t)\|^2_{L^2} \le C\,\|u_0\|^{\frac{4}{n}}_{L^2}\,\|\nabla u(t)\|^2_{L^2},$$

so

$$|G(u(t))| \le 2|E|\,\|u_0\|_{L^2}\|\nabla u(t)\|_{L^2} + 2a\,\|\nabla u(t)\|^2_{L^2} + 2aC\,\|u_0\|^{\frac{4}{n}}_{L^2}\,\|\nabla u(t)\|^2_{L^2}$$
$$\lesssim \|\nabla u(t)\|_{L^2} + \|\nabla u(t)\|^2_{L^2}. \tag{4.5}$$

Since $\|\nabla u(t)\|_{L^2}\to\infty$ as $t\to T^*$, by Lemma 4.2, there exists a sequence $t_k\to T^*$ such that

$$\frac{\int_0^{t_k}\left(\|\nabla u(\tau)\|_{L^2}+\|\nabla u(\tau)\|^2_{L^2}\right)d\tau}{\|\nabla u(t_k)\|_{L^2}+\|\nabla u(t_k)\|^2_{L^2}}\to 0,$$

so by (4.5) we have

$$\frac{\int_0^{t_k} G(u(\tau))\,d\tau}{\|\nabla u(t_k)\|^2_{L^2}}\to 0. \tag{4.6}$$

Let

$$\rho(t) := \frac{\|\nabla Q\|_{L^2}}{\|\nabla u(t)\|_{L^2}}, \qquad v(t,x) := \rho^{\frac{n}{2}}u(t,\rho x), \qquad \rho_k := \rho(t_k), \qquad v_k(x) := v(t_k,x).$$

Now we check that $\{v_k\}$ defined above satisfies the assumptions in Theorem 4.1. Firstly, by the mass decay (2.1), we have

$$\|v_k\|_{L^2} = \|u(t_k)\|_{L^2} \le \|u_0\|_{L^2},$$

showing the boundedness of $\{v_k\}$. Secondly, since

$$\|\nabla v_k\|_{L^2} = \rho_k\|\nabla u(t_k)\|_{L^2} = \|\nabla Q\|_{L^2},$$

we know that inequality (4.1) is satisfied with $M = \|\nabla Q\|_{L^2}$. Finally, by (1.5), (4.4), and (4.6), we have

$$\begin{aligned}
\mathcal{E}_0(v_k) &= \|\nabla v_k\|_{L^2}^2 - \frac{n}{n+2}\|v_k\|_{L^{2+\frac{4}{n}}}^{2+\frac{4}{n}} \\
&= \rho_k^2\|\nabla u(t_k)\|_{L^2}^2 - \frac{n}{n+2}\left(\rho_k^2\|u(t_k)\|_{L^{2+\frac{4}{n}}}^{2+\frac{4}{n}}\right) \\
&= \rho_k^2\,\mathcal{E}_0(u(t_k)) \\
&= \rho_k^2\,\mathcal{E}_0(u_0) + \rho_k^2\int_0^{t_k} G(u(\tau))d\tau \\
&= \frac{\|\nabla Q\|_{L^2}^2\mathcal{E}_0(u_0)}{\|\nabla u(t_k)\|_{L^2}^2} + \|\nabla Q\|_{L^2}^2\frac{\displaystyle\int_0^{t_k} G(u(\tau))d\tau}{\|\nabla u(t_k)\|_{L^2}^2} \to 0 \qquad \text{as } k\to\infty,
\end{aligned}$$

or equivalently,

$$\|v_k\|_{L^{2+\frac{4}{n}}}^{2+\frac{4}{n}} \to \frac{n+2}{n}\|\nabla v_k\|_{L^2}^2 = \frac{n+2}{n}\|\nabla Q\|_{L^2}^2,$$

so inequality (4.2) is also satisfied with $m = \left(\frac{n+2}{n}\|\nabla Q\|_{L^2}^2\right)^{\frac{n}{2n+4}}$. Hence by Theorem 4.1, there exists a sequence $\{x_k\} \subseteq \mathbb{R}^n$ such that

$$\rho_k^{\frac{n}{2}}u(t_k, \rho_k\cdot + x_k) \rightharpoonup V \tag{4.7}$$

weakly in $H^1$, and

$$\begin{aligned}
\|V\|_{L^2} &\geq \left(\frac{n}{n+2}\right)^{\frac{n}{4}}\frac{m^{\frac{n}{2}+1}+1}{M^{\frac{n}{2}}}\|Q\|_{L^2} \\
&= \left(\frac{n}{n+2}\right)^{\frac{n}{4}}\frac{\left(\frac{n+2}{n}\|\nabla Q\|_{L^2}^2\right)^{\frac{n}{4}}+1}{\|\nabla Q\|_{L^2}^{\frac{n}{2}}}\|Q\|_{L^2} \geq \|Q\|_{L^2}.
\end{aligned}$$

By (4.7), for every $R > 0$, there is

$$\liminf_{k\to\infty}\int_{|x|\leq R}\rho_k^n\,|u(t_k, \rho_k x + x_k)|^2\,dx \geq \int_{|x|\leq R}|V|^2\,dx,$$

or equivalently,

$$\liminf_{k\to\infty}\int_{|x-x_k|\leq \rho_k R}|u(t_k, x)|^2\,dx \geq \int_{|x|\leq R}|V|^2\,dx.$$

Now let $w(t)$ be a function satisfying $w(t)\|\nabla u(t)\|_{L^2} \to \infty$ as $t \to T^*$. Then $\frac{w(t_k)}{\rho_k} \to \infty$ as $k \to \infty$, so $\frac{w(t_k)}{\rho_k} \geq R$ for $k$ large enough. Hence,

$$\begin{aligned}\liminf_{k\to\infty} \sup_{y\in\mathbb{R}^n} \int_{|x-y|\leq w(t_k)} |u(t_k,x)|^2\,dx &\geq \liminf_{k\to\infty} \sup_{y\in\mathbb{R}^n} \int_{|x-y|\leq \rho_k R} |u(t_k,x)|^2\,dx \\ &\geq \liminf_{k\to\infty} \int_{|x-x_k|\leq \rho_k R} |u(t_k,x)|^2\,dx \\ &\geq \int_{|x|\leq R} |V|^2\,dx,\end{aligned}$$

and letting $R \to \infty$, we have

$$\liminf_{k\to\infty} \sup_{y\in\mathbb{R}^n} \int_{|x-y|\leq w(t_k)} |u(t_k,x)|^2\,dx \geq \int_{\mathbb{R}^n} |V|^2\,dx \geq \|Q\|_{L^2}^2.$$

For every $t \in [0, T^*)$, the function

$$y \mapsto \int_{|x-y|\leq w(t)} |u(t,x)|^2\,dx$$

is continuous and vanishes as $|y| \to \infty$, so the supremum is attained at some point $x(t) \in \mathbb{R}^n$. Therefore,

$$\liminf_{k\to\infty} \int_{|x-x(t_k)|\leq w(t_k)} |u(t_k,x)|^2\,dx = \liminf_{k\to\infty} \sup_{y\in\mathbb{R}^n} \int_{|x-y|\leq w(t_k)} |u(t_k,x)|^2\,dx \geq \|Q\|_{L^2}^2,$$

and the proof of Theorem 4.3 is complete. □

Now we give an alternative proof of Theorem 1.1 (a) by virtue of the mass concentration property (4.3) in Theorem 4.3.

**Corollary 4.4** *Theorem 1.1 (a) holds for all dimensions.*

***Proof*** Since $u_0 \in \mathcal{H}^1$, according to Proposition 2.1, there exist $0 < T^* \leq \infty$ and a unique solution $u(t)$ in $C([0, T^*), \mathcal{H}^1)$. Assume $u$ blows up at $T^* < \infty$. Then by (4.3) (taking $w(t) \equiv 1$), we have (up to a subsequence)

$$\liminf_{t\to T^*} \|u(t)\|_{L^2(|x-x(t)|<1)} \geq \|Q\|_{L^2}$$

for some function $x(t) \in \mathbb{R}^n$. However by (2.1), $\|u(t)\|_{L^2}$ decays in $t$, so its limit inferior will be strictly less than $\|Q\|_{L^2}$, contradictory to the prior inequality. □

**Remark 4.5** By Theorem 4.3, if $\|u_0\|_{L^2} > \|Q\|_{L^2}$ and $u$ blows up at finite time $T^*$, then $T^* \leq \frac{1}{a} \log\left(\frac{\|u_0\|_{L^2}}{\|Q\|_{L^2}}\right)$.

## 5 Concluding Remarks

It is commonly known that, unlike the standard NLS, the damped NLS is non-hamiltonian, which does not enjoy conservation laws in mass, energy or momentum. This can bring in difficulties to the study of singularity formation of dNLS. In this article, we consider the linearly damped NLS (1.1) under a (weak) waveguide potential $V$, where $V(x) = E \cdot x$ represents the Stark effect. In the absence of a potential, the existence of blow-up solutions for dNLS has been obtained in e.g. [6, 12–14, 16]. Our main result, Theorem 1.1, shows the existence of blow-up solutions in the log-log regime above the ground state level $\|Q\|_2$. Furthermore, Theorem 1.2 gives a general blow-up criterion for (1.1). These two theorems together suggest that given any $u_0$ in $\left\{\phi \in \mathcal{H}^1 : \|Q\|_{L^2} < \|\phi\|_{L^2} < \|Q\|_{L^2} + \alpha\right\}$ for some $\alpha > 0$, there exists $a_* = a_*(\|u_0\|_{H^1}) > 0$ such that for all $a \in (0, a_*)$, the solution $u(t)$ blows up in finite time with log-log speed. This can be viewed as a remarkable structural stability for NLS type systems. Observe that, in view of (2.1), Theorem 1.1 (a), and Corollary 4.4, the "damping arrests self-focusing" phenomenon occurs in the presence of Stark effect too, if one increases the value of $a > 0$.

The advantage of our analysis and transform method is that the work is not overwhelmed by complex technical details. The line of approach can be applied to treat other unbounded perturbations, e.g., a confining harmonic potential. In application, the abovementioned results might provide a priori information for observation in the lab as well as numerical simulations [3, 7, 17, 19]. Following this direction of investigation, our work might leave open the question concerning the construction of blow-up solutions for a general potential $V$.

**Acknowledgements** The authors thank the referees' careful reading and very helpful comments regarding the improvement on the presentation of the initial manuscript. S.Z. is partially supported by NNSFC grant No. 12071323 as Co-PI.

## References

1. G. Akrivis, V. Dougalis, O. Karakashian, V. McKinney, Numerical approximation of singular solutions of the damped nonlinear Schrödinger equation, ENUMATH 97 (Heidelberg), World Scientific, 1998, 117–124.
2. J. E. Avron, I. W. Herbst, Spectral and scattering theory of Schrödinger operators related to the Stark effect, Comm. Math. Phys. 52, (1977), no. 3, 239–254.
3. W. Bao, D. Jaksch, An explicit unconditionally stable numerical method for solving damped nonlinear Schrödinger equations with a focusing nonlinearity, SIAM J. Numer. Anal. 41 (4), (2003), 1406–1426.
4. N. Basharat, Y. Hu, S. Zheng, Blowup rate for mass critical rotational nonlinear Schrödinger equations, Contemporary Mathematics 725, (2019), 1–12.
5. N. Basharat, H. Hajaiej, Y. Hu, S. Zheng, Threshold for blowup and stability for nonlinear Schrödinger equation with rotation, Annales Henri Poincaré 24, (2023), 1377–1416.
6. P. Bégout, J.I. Díaz, Finite time extinction for a critically damped Schrödinger equation with a sublinear nonlinearity, Advances in Differential Equations 28, (2023), 311–340.

7. J. Cai, H. Zhang, Efficient schemes for the damped nonlinear Schrödinger equation in high dimensions, Applied Mathematics Letters 102, (2020), 106158.
8. R. Carles, Y. Nakamura, Nonlinear Schrödingere equations with Stark potential, Hokkaido Math. J. 33, (2004), 719–729.
9. T. Cazenave, Semilinear Schrödinger Equations, Courant Lecture Notes in Mathematics 10, American Mathematical Society, Courant Institute of Mathematical Sciences, 2003.
10. J. Cui, J. Hong, L. Sun, On global existence and blow-up for damped stochastic nonlinear Schrödinger equation, Discrete and Continuous Dynamical Systems-Series B 24, (2017), 6837.
11. H. L. Cycon, R. G. Froese, W. Kirsch, B. Simon, Schrödinger operators with application to quantum mechanics and global geometry, Springer Study Edition, Texts and Monographs in Physics, Springer-Verlag, Berlin, 1987.
12. M. Darwich, Blowup for the damped $L^2$-critical nonlinear Schrödinger equation, Adv. Differential Equations 17, (2012), 337–367.
13. M. Darwich, L. Molinet, Some remarks on the nonlinear Schrödinger equation with fractional dissipation, J. Math. Phys. 57 (2016), 101502.
14. V. D. Dinh, Blow-up criteria for linearly damped nonlinear Schrödinger equations, Evol. Equ. Control Theory 10, (2021), no. 3, 599–617.
15. C. Fan, Y. Su, D. Zhang, A note on log-log blow up solutions for stochastic nonlinear Schrödinger equations, Stoch PDE: Anal Comp 10, (2022), 1500–1514.
16. G. Fibich, Self-focusing in the damped nonlinear Schrödinger equation, SIAM J. Appl. Math. 61(5), (2001), 1680–1705.
17. G. Fibich, M. Klein, Nonlinear-damping continuation of the nonlinear Schrödinger equation - A numerical study, Physica D: Nonlinear Phenomena 241, (2012), 519–527.
18. G. Fibich, F Merle, P Raphaël, Proof of a spectral property related to the singularity formation for the $L^2$ critical nonlinear Schrödinger equation, Physica D: Nonlinear Phenomena 220 (1), (2006), 1–13.
19. G. Fotopoulos, N.I. Karachalios, V. Koukouloyannis, K. Vetas, The linearly damped nonlinear Schrödinger equation with localized driving: spatiotemporal decay estimates and the emergence of extreme wave events, Z. Angew. Math. Phys. 71, (2020), 1–23.
20. S. Graffi and V. Grecchi, Resonances in Stark effect and perturbation theory, Commun. Math. Phys. 62 (1978), 83–96.
21. E. Harrell II, Perturbation theory and atomic resonances since Schrödinger's time, Spectral theory and mathematical physics, 227–248, Proc. Sympos. Pure Math., 76, Part 1, Amer. Math. Soc., Providence, RI, 2007.
22. T. Hmidi and S. Keraani, Blowup theory for the critical nonlinear Schrödinger equations revisited, Int. Math. Res. Not. 46, (2005), 2815–2828.
23. C. Kharif, R. Kraenkel, M. Manna, R. Thomas, The modulational instability in deep water under the action of wind and dissipation, Journal of Fluid Mechanics 664, (2010), 138–149.
24. P. Laurençot, Long-time behaviour for weakly damped driven nonlinear Schrödinger equations in $\mathbb{R}^N$, $N \geq 3$, Nonlinear Differential Equations Appl. 2, (1995), 357–369.
25. B. Malomed, Multidimensional dissipative solitons and solitary vortices, Chaos, Solitons and Fractals 163, (2022), 112526.
26. F. Merle, Determination of blow-up solutions with minimal mass for nonlinear Schrödinger equations with critical power, Duke Math. J. 69, (1993), no. 2, 427–454.
27. F. Merle and P. Raphaël, On universality of blow-up profile for $L^2$ critical nonlinear Schrödinger equation, Invent. Math. 156, (2004), 565–672.
28. F. Merle, P. Raphaël, Blow up dynamic and upper bound on the blow up rate for critical nonlinear Schrödinger equation, Ann. of Math. 161, (2005), no. 1, 157–222.
29. F. Merle, P. Raphaël, Profiles and quantization of the blow up mass for critical nonlinear Schrödinger equation, Comm. Math. Phys. 253, (2005), no. 3, 675–704.
30. F. Merle, P. Raphaël. On a sharp lower bound on the blow-up rate for the $L^2$ critical nonlinear Schrödinger equation, J. Amer. Math. Soc., 19, (2006), 37–90.
31. M. Ohta, G. Todorova, Remarks on global existence and blowup for damped nonlinear Schrödinger equations, Discrete Contin. Dyn. Syst. 23, (2009), no. 4, 1313–1325.

32. T. Ozawa, Non-existence of wave operators for Stark effect Hamiltonians, *Mathematische Zeitschrift* 207, (1991), 335–339.
33. V. Perez-Garcia, M. Porras, L. Vazquez, The nonlinear Schrödinger equation with dissipation and the moment method, Phys. Lett. A 202, (1995), 176–182.
34. F. Planchon, P. Raphaël, Existence and stability of the log-log blow-up dynamics for the $L^2$-critical nonlinear Schrödinger equation in a domain, Ann. Henri Poincaré 8, (2007), 1177–1219.
35. C.-M. Sun, J.-Q. Zheng, Low regularity blowup solutions for the mass-critical NLS in higher dimensions, Journal de Mathématiques Pures et Appliquées 134, (2020), 255–298.
36. P. Raphaël, Stability of the log-log bound for blow-up solutions to the critical nonlinear Schrödinger equation, Math.Ann., 331, (2005), 577–609.
37. T. Tao, *Nonlinear dispersive equations: Local and global analysis*, CBMS Regional Conference Series in Mathematics 106, American Mathematical Society, Providence, RI, 2006.
38. T. Tsurumi, M. Wadati, Free fall of atomic laser beam with weak inter-atomic interaction, J. Phys. Soc. Jpn. 70, (2001), 60–68.
39. M. Tsutsumi, Nonexistence of global solutions to the Cauchy problem for the damped nonlinear Schrödinger equations, SIAM J. Math. Anal. 15, (1984), 357–366.
40. M. Weinstein, Nonlinear Schrödinger equations and sharp interpolation estimates, Comm. Math. Phys. 87, (1983), no. 4, 567–576.
41. K. Yang, S. Roudenko, Y.-X. Zhao, Blow-up dynamics and spectral property in the $L^2$-critical nonlinear Schrödinger equation in high dimensions, Nonlinearity 31, (2018), no.9, 4354–4392.
42. S. Zheng, Fractional regularity for nonlinear Schrödinger equations with magnetic fields, Contemporary Mathematics 581, (2012), 271–285.

# Effect of Electron's Drift Velocity in Nonlinear Ion-Acoustic Solitons in a Negative Ion Beam Plasma


**J. Kalita, R. Das, K. Hosseini, E. Hincal, and S. Salahshour**

**Abstract** In the present paper, the authors have explored the existence of KdV and mKdV solitons in a collisionless and unmagnetized plasma model involving positive ion and negative ion beams together with thermal electrons. For various selections of $Q'(= m_b/m_i$, negative ion beam to positive ion mass ratio) larger and less than one, low amplitude rarefactive and compressive KdV solitons are created in the plasma under the effect of the electron's drift velocity $v'_e$. In two intervals of drift velocity $v'_e$ for $0 \leq v'_e \leq 26$ and $26.5 \leq v'_e \leq 28.5$ when $Q'$ is less than one, the existence of the mKdV solitons is demonstrated.

**Keywords** KdV and mKdV solitons · Positive ion · Negative ion beam · Electron's drift velocity

J. Kalita
Department of Mathematics, Gauhati University, Guwahati 781014, Assam, India

R. Das
Department of Mathematics, Arya Vidyapeeth College, Guwahati 781016, Assam, India

K. Hosseini (✉) · E. Hincal
Department of Mathematics, Near East University TRNC, Mersin 10, Turkey
e-mail: kamyar_hosseini@yahoo.com

Faculty of Art and Science, University of Kyrenia, Kyrenia, TRNC, Mersin 10, Turkey

S. Salahshour
Faculty of Engineering and Natural Sciences, Istanbul Okan University, Istanbul, Turkey

Faculty of Engineering and Natural Sciences, Bahcesehir University, Istanbul, Turkey



S. Manukure and W.-X. Ma (eds.), *Nonlinear and Modern Mathematical Physics*,
Springer Proceedings in Mathematics & Statistics 459,
https://doi.org/10.1007/978-3-031-59539-4_8

## 1 Introduction

Nonlinear phenomena in different mediums and diverse physical situations have long been the subject of inquiry. Over the past three decades, a wide range of acceptable approaches has been exerted to extensively explore the nonlinear ion-acoustic solitary waves (NLIASWs) in plasma, both theoretically and empirically. Starting with the theoretical studies of [1] in a straightforward model of cold plasma, the KdV equation has been applied to examine the presence of IASWs in plasma in multicomponent plasmas that incorporate varied physical circumstances. According to Watanabe's [2] theoretical work and Ludwig et al. [3] experimental observations, ion-acoustic solitons (IASs) are formed in a significant part by negative ions. Modified KdV solitons in plasma including negative ions have been seen by Nakamura and Tsukayabashi [4]. Negative ion beams have a long history that spans several decades, and there are numerous scientific and technological uses for them today, ranging from nuclear fusion and industrial applications to sources for accelerators and spallation neutron sources [5]. Burgess [6] has looked at how optical scattering methods might be used to determine the $H^-$ concentrations in plasma sources that are relevant to the negative ion beam. The observation of the change in the collective ion characteristic in Thomson scattering in a plasma containing negative ions in that experiment offers a more promising possibility. The impact of negative ions in the plasma and the excitation of solitary waves and double-layer in the plasma was subsequently discussed by various scholars (Watanabe [2], Hase et al. [7], Tagare and Reddy [8], Verheest [9], and Baboolal et al. [10]). Solitons that are compressive and rarefactive are seen in a negative-ion plasma. By investigating the effects of the electron's drift motion along the magnetic field's direction, Kalita et al. [11] looked into the effect of IASs. The drift velocity's limiting value is discussed, as well as the upper and lower bounds on the existence of solitons with different velocities. The existence of modified KdV solitons has only been proven by Kalita and Kalita [12] for negative to positive ion mass ratios $Q' > 1$. In light of the plasma's electron inertia, Khuel and Zhang [13] investigated how ion drift affects small amplitude IAS. The existence of IASs has been shown to depend on the ion-drift velocity being less than the electron thermal velocity. The movement of IASWs in a heated plasma of negatively charged ions and its interaction with the drifting motion of electrons were explored in [14]. For various values of $Q' > 1$ or $Q' < 1$, it is demonstrated that rarefactive and compressive solitons exist depending on the drift velocity $v'_e$. It is discovered that the compressive soliton for $Q' > 1$ and the rarefactive soliton for $Q' < 1$ but small, are at their highest near $v'_e = 0$ when $r < 0.5$ demonstrating the characteristic change in solitons for the inclusion of $v'_e$. The presence of IASs in a magnetized ion beam plasma has been explored by Kalita et al. [15]. In a heated magnetoplasma with the electrons initially drifting in the magnetic field's direction, the study on IASWs by Kalita and Bhatta [16] has been completed. They proved that the parametric domains contain both compressive and rarefactive solitons. For various selections of $v'_e$ and $Q'$, the authors of [17] have examined the presence of mKdV solitons. In a negative-ion plasma, Chattopadhyaya et al. [18] discovered that

the ions' drift motion significantly contributes to the stimulation of IASWs and double layers. Islam et al. [19] have studied IASWs in a magnetized plasma composed of non-thermal and isothermal electrons. Sharma et al. [20] demonstrated that IAW instability can be caused by the passage of an ion beam through a magnetized plasma containing negative ions via the Cerenkov type beam-plasma interaction. Rehman [21] studied the quantum soliton waves, which include cold positive ions, negative ions, and Fermi electron gas. He also examined how low-frequency ion-acoustic waves spread when negative ions are present in quantum plasma. Using the linear kinetic theory, the authors in [22] have investigated the impact of negative ions on drift ion wave instability in a weakly collisional magnetized plasma. The researchers of [23] examined the dust IASs with the electron's drift velocity in an unmagnetized plasma using the mkdV equation. They have shown the existence of the mKdV solitons in two new drift velocities for $94 \leq v_e' \leq 104$ and $303.75 \leq v_e' \leq 306$. In a non-magnetized plasma made up of two-temperature electrons that follow a kappa-type distribution, a positive ion beam, and a positive warm ion fluid, Kaur et al. [24] looked at the nonlinear propagation of IASWs. The KdV equation was used in a plasma system of the ion beam to investigate the influence of magnetically quantized degenerate trapped electron and positron on small amplitude IASWs by Deka and Dev [25]. They have proven that solitary waves of both compressive and rarefactive types exist in this kind of plasma environment. Recently, by adopting the method of reductive perturbation, in polarised quantum plasma containing relativistic degenerate electrons and positrons, Mohsenpoura et al. [26] examined the oblique propagation of the ion-acoustic quantum soliton. This equation demonstrated that two ion-acoustic modes (slow and fast) exist when a negative ion is present. More results are found in [27–36]. The existence of KdV and mKdV solitons is inferred using the reductive perturbation method (RPM) in a collisionless and unmagnetized plasma model that includes thermal electrons and positive and negative ion beams. The RPM is typically used with nonlinear waves of small amplitude [37, 38]. In order to introduce space and time variables, which are suitable for describing long-wave length phenomena, this method rescales both space and time in the governing equations of the system.

This study is arranged as follows: The basic equations are provided in the second section. The third section represents the construction of KdV and mKdV models. The solitary waves are retrieved in the fourth section, and finally, the outcomes are analyzed in the fifth section.

## 2 Basic Equations of Motion

In the current analysis, the motion of IAWs in a plasma involving positive ions, negative ion beams, and electrons is considered. The one-dimensional collision-free plasma equations are:

For the ions

$$\frac{\partial n_i}{\partial t} + \frac{\partial}{\partial x}(n_i v_i) = 0 \tag{1}$$

$$\frac{\partial v_i}{\partial t} + v_i \frac{\partial v_i}{\partial x} + \frac{\partial \phi}{\partial x} = 0 \tag{2}$$

For the negative ion beams

$$\frac{\partial n_b}{\partial t} + \frac{\partial}{\partial x}(n_b v_b) = 0 \tag{3}$$

$$\frac{\partial v_b}{\partial t} + v_b \frac{\partial v_b}{\partial x} = \frac{1}{Q'} \frac{\partial \phi}{\partial x} \tag{4}$$

For the electrons

$$\frac{\partial n_e}{\partial t} + \frac{\partial}{\partial x}(n_e v_e) = 0 \tag{5}$$

$$\frac{\partial v_e}{\partial t} + v_e \frac{\partial v_e}{\partial x} = \frac{1}{Q}\left(\frac{\partial \phi}{\partial x} - \frac{1}{n_e}\frac{\partial n_e}{\partial x}\right) \tag{6}$$

Poisson equation

$$\frac{\partial^2 \phi}{\partial x^2} = n_e + \frac{\alpha}{1-\alpha} n_b - \frac{1}{1-\alpha} n_i \tag{7}$$

where $i$, $b$, and $e$ denote for ions, negative ion beams, and electrons, respectively. $Q' = m_b/m_i$, $Q = m_e/m_i$ and $\alpha = n_{b0}/n_{i0}$ represent respectively the ratio of negative ion beam mass to ion mass, electron mass to ion mass, and ion beam to ion density ratio. By normalizing densities to equilibrium plasma density $n_0$, time $t$ to the ion plasma period $w_{pi}^{-1} = \left(m_i/4\pi n_0 e^2\right)^{\frac{1}{2}}$, distances to the Debye length $\lambda_D = \left(T_e/4\pi n_0 e^2\right)^{\frac{1}{2}}$, velocities to $c_s = \left(T_e/m_i\right)^{\frac{1}{2}}$, and potential $\phi$ to $T_e/e$, the set of Eqs. (1)–(7) is represented in a non-dimensional form.

## 3 Derivation of KdV and mKdV Equations

The stretched variables

$$\xi = \varepsilon^{\frac{1}{2}}(x - Ut), \quad \tau = \varepsilon^{\frac{3}{2}} t \tag{8}$$

are utilized to obtain the KdV equation from (1) to (7). In (8), $\varepsilon$ and $U$ are respectively the small dimensionless expansion parameter and phase velocity of IAW. The derivatives of space and time are thus substituted by

$$\frac{\partial}{\partial x} = \varepsilon^{\frac{1}{2}} \frac{\partial}{\partial \xi}$$
$$\frac{\partial}{\partial t} = \varepsilon^{\frac{1}{2}} \left( \varepsilon \frac{\partial}{\partial \tau} - U \frac{\partial}{\partial \xi} \right)$$

respectively. We asymptotically expand the flow variables as

$$\begin{aligned} n_i &= 1 + \varepsilon n_{i1} + \varepsilon^2 n_{i2} + \cdots \\ n_b &= 1 + \varepsilon n_{b1} + \varepsilon^2 n_{b2} + \cdots \\ n_e &= 1 + \varepsilon n_{e1} + \varepsilon^2 n_{e2} + \cdots \\ v_i &= \varepsilon v_{i1} + \varepsilon^2 v_{i2} + \cdots \\ v_b &= \varepsilon v_{b1} + \varepsilon^2 v_{b2} + \cdots \\ v_e &= v_e' + \varepsilon v_{e1} + \varepsilon^2 v_{e2} + \cdots \\ \phi &= \varepsilon \phi_1 + \varepsilon^2 \phi_2 + \cdots \end{aligned} \tag{9}$$

Using (8) and (9) in (1)–(7) under the conditions $n_{i1} = n_{e1} = n_{b1} = 0$, $v_{i1} = 0$, $v_{b1} = 0$, $v_{e1} = v_e'$, and $\phi_1 = 0$ at $|\xi| \to \infty$, we get

$$\begin{aligned} &n_{i1} = \frac{\phi_1}{U^2}, n_{e1} = \frac{\phi_1}{1 - Q(U - v_e')^2}, n_{b1} = \frac{\phi_1}{Q'U^2}, v_{i1} = \frac{\phi_1}{U}, v_{e1} = \frac{(U - v_e')\phi_1}{1 - Q(U - v_e')^2}, \\ &v_{b1} = -\frac{1}{Q'U}\phi_1, n_{e1} + \frac{\alpha}{1-\alpha} n_{b1} - \frac{1}{1-\alpha} n_{i1} = 0 \end{aligned} \tag{10}$$

Owing to the values of $n_{i1}, n_{e1}$, and $n_{b1}$ as well as the last equation of (10), we arrive at the phase velocity equation as

$$\frac{1}{1 - Q(U - v_e')^2} - \frac{\alpha}{(1-\alpha)Q'U^2} - \frac{1}{(1-\alpha)U^2} = 0 \tag{11}$$

From the set of $\varepsilon^2$-order equations, the KdV equation can be obtained with the help of (10) and (1)-(7) as

$$\frac{\partial \phi_1}{\partial \tau} + p\phi_1 \frac{\partial \phi_1}{\partial \xi} + q \frac{\partial^3 \phi_1}{\partial \xi^3} = 0 \tag{12}$$

where $p = \dfrac{A}{2B}$ and $q = \dfrac{1}{2B}$ with

$$A = \frac{3Q(U - v')^2 - 1}{\{1 - Q(U - v_e')^2\}^3} - \frac{3\alpha}{(1-\alpha)Q'U^4} + \frac{3}{(1-\alpha)U^4}$$
$$B = \frac{Q(U - v_e')^2}{\{1 - Q(U - v_e')^2\}^2} + \frac{\alpha}{(1-\alpha)Q'U^3} + \frac{1}{(1-\alpha)U^3}$$

We are more concerned with researching the existence of mKdV solitons in plasma that is impacted by electron drift velocity; than, we are with proving the existence of KdV solitons, which has been extensively researched in the past. As a result, we must set $p = 0$ in place certain assumptions in order to derive the mKdV equations that incorporate higher order nonlinearity in the system (12). This gives

$$\alpha_c = \frac{X + Z}{X + Y}$$

where $X = \dfrac{3Q(U - v')^2 - 1}{\{1 - Q(U - v_e')^2\}^3}$, $Y = \dfrac{3}{Q'U^4}$ and $Z = \dfrac{3}{U^4}$.

The critical density ratio is represented here by the corresponding $\alpha_c = n_{b0}/n_{i0}$ determined by $p = 0$. We focus on finding the mKdV solitons for various values of $\alpha_c$. To acquire the mKdV equation from (1)–(7), we take the new variables

$$\xi = \varepsilon(x - Ut), \quad \tau = \varepsilon^3 t \tag{13}$$

instead of (8).

Using (13) and (9) in (1)–(7), the mKdV equation can be derived as

$$\frac{\partial \phi_1'}{\partial \tau} + p'(\phi_1')^2 \frac{\partial \phi_1'}{\partial \xi} + q' \frac{\partial^3 \phi_1'}{\partial \xi^3} = 0, \quad \phi_1' = \phi_1, \tag{14}$$

where $p' = \dfrac{C}{4D}$ and $q' = \dfrac{1}{2D}$ with

$$C = \frac{4Q(U - v_e')^2 - 15Q^2(U - v_e')^4 - 1}{\{1 - Q(U - v_e')^2\}^5} + \frac{15\alpha_c}{Q^3U^6(1 - \alpha_c)} + \frac{15}{U^6(1 - \alpha_c)}$$

$$D = \frac{Q(U - v_e')}{\{1 - Q(U - v_e')^2\}^2} + \frac{\alpha_c}{Q'U^3(1 - \alpha_c)} + \frac{1}{U^3(1 - \alpha_c)}$$

## 4 Solitary Waves

With the use of $\eta = \xi - V\tau$, the soliton of Eq. (12) can be found as

$$\phi_1 = \frac{3V}{p} sech^2\left(\frac{1}{2}\sqrt{\frac{V}{q}}\eta\right) \tag{15}$$

where $V$ signifies the velocity. The amplitude and the width of the wave are

$$\phi_0 = \frac{3V}{p}, \quad \Delta = 2\sqrt{\frac{q}{V}}.$$

The soliton of Eq. (14) can be retrieved subject to $\phi_1' = 0$ and $\partial^2\phi_1'/\partial\eta^2 = 0$ as $\eta \to \pm\infty$ as

$$\phi_1' = \sqrt{\frac{6V}{p'}} sech\left(\sqrt{\frac{V}{q'}}\eta\right) \tag{16}$$

where $\phi_0' = \sqrt{\frac{6V}{p'}}$ and $\Delta' = \sqrt{\frac{q'}{V}}$.

## 5 Results and Discussion

It is seen that the drifting influence of the electrons plays a crucial role in the creation of KdV or mKdV solitons in the current model containing negative ions in a plasma and a negative ion beam. To investigate the characteristics of IASWs for a negative ion beam plasma with the impact of electron drift, we create the profile of the solitary waves depicted in figures [1–8]. By using the method of reductive perturbation, we have presented a study on the existence of KdV soliton and mKdV soliton of small amplitude in our plasma model under the impact of electron's drift velocity $v_e'$ for various selections of $Q'$ greater or less than one. It is perceived that the KdV soliton's amplitude Fig. 1a increases rapidly at small values of $Q' < 1$, and after a certain value of $Q'$ stays nearly constant, reaching its maximum value in each case. With bigger $\alpha$ and higher values of $Q'$ the saturation value of the amplitude is observed to be less. At smaller $Q'$ and smaller temperature ratio $\alpha$, the width Fig. 1b of the KdV soliton rapidly drops. The width, however gradually diminishes as the temperature

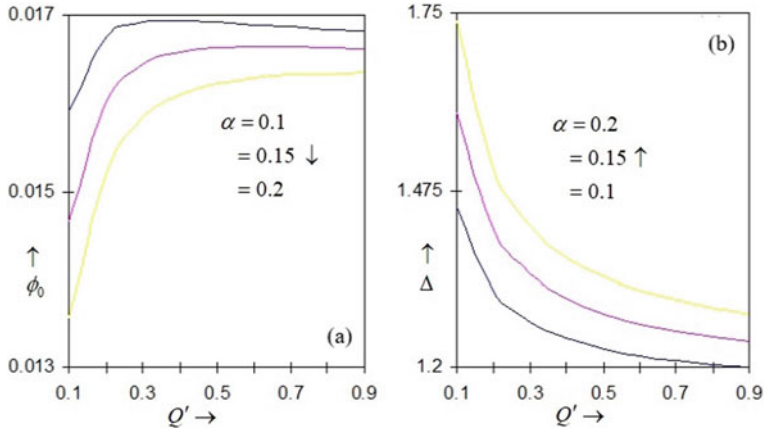


**Fig. 1** Compressive KdV soliton's amplitude $\phi_0(a)$ and width $\Delta(b)$ for $v_s' = 40$, $V = 0.1$, and $\alpha = 0.1, 0.15, 0.2$ versus $Q' < 1$

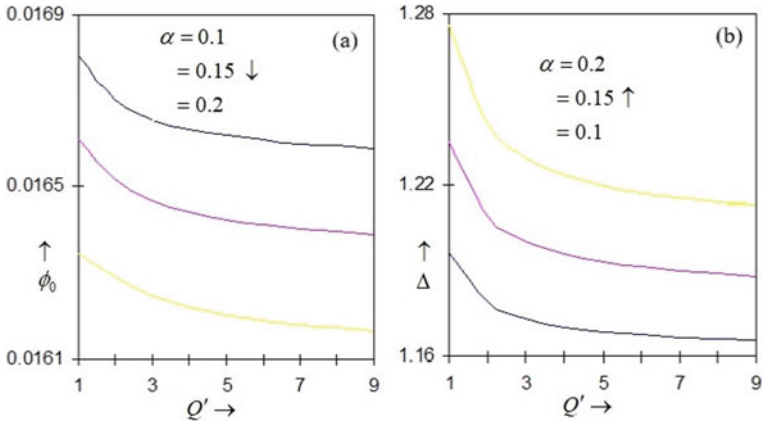


**Fig. 2** Compressive KdV soliton's amplitude $\phi_0(a)$ and width $\Delta(b)$ for $v_s' = 40$, $V = 0.1$, and $\alpha = 0.1, 0.15, 0.2$ versus $Q' > 1$

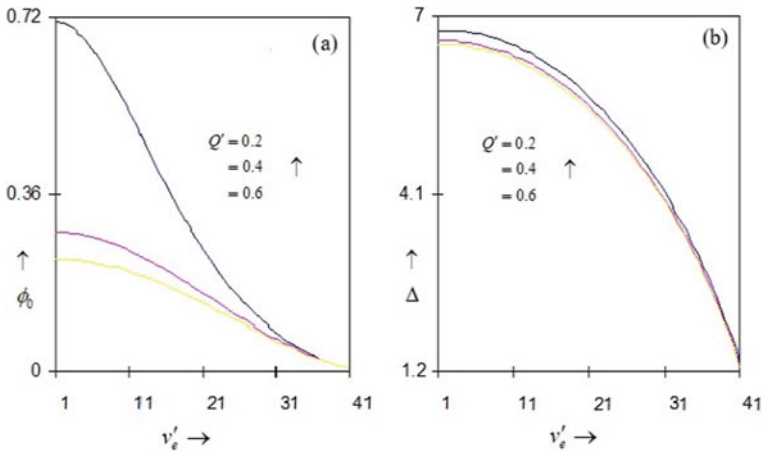


**Fig. 3** Compressive KdV soliton's amplitude $\phi_0(a)$ and width $\Delta(b)$ for $\alpha = 0.05$ and $V = 0.05$ and different values of $Q' < 1$ versus the drift velocity $v_e'$

ratio increases, reaching a minimum value for higher values of $Q'$ for a certain value of $v_e'$. Figure 2a shows that for $v_e' = 40$, $V = 0.1$, and $\alpha = 0.1, 0.15, 0.2$, the amplitude of the KdV soliton decreases with increasing values of $Q' > 1$. For the same set of values, the KdV soliton's width Fig. 2b likewise drops. Furthermore, it is vital to point out that the compressive KdV solitons have much higher amplitudes at smaller $v_e'$ Fig. 3a for $\alpha = 0.05$ and $V = 0.05$ as well as for various mass ratios $Q' = 0.2, 0.4, 0.6$. They are seen to be extremely small and tend to zero in $v_e'$'s upper existence region. Ironically, the widths of KdV solitons demonstrate an ignorable difference Fig. 3b for $Q' = 0.2, 0.4$, though they are prominent for $Q' = 0.4, 0.6$ It is noteworthy to notice that the growth scenario of the amplitude Fig. 4a and

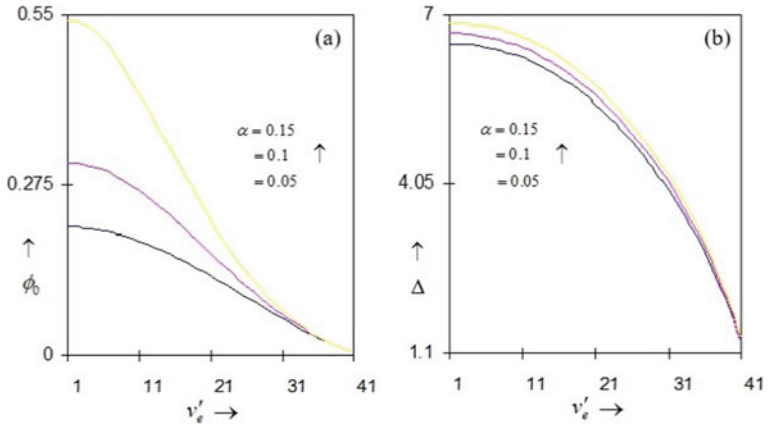


**Fig. 4** Compressive KdV soliton's amplitude $\phi_0(a)$ and width $\Delta(b)$ for the fixed $Q' < 1, V = 0.05$, and different values of $\alpha$ versus the drift velocity $v'_e$

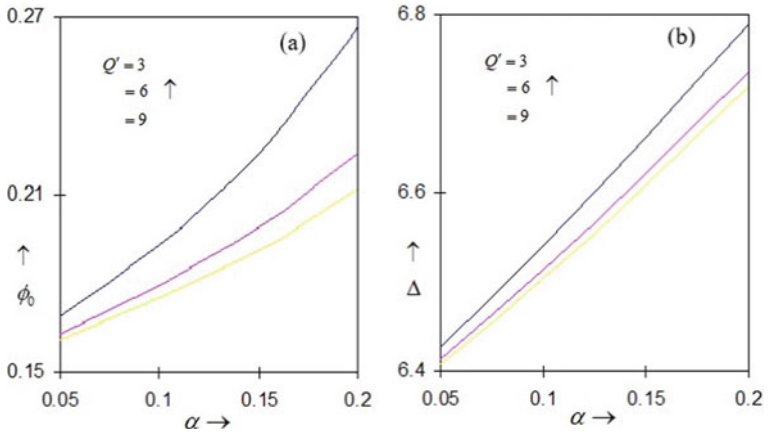


**Fig. 5** Compressive KdV soliton's amplitude $\phi_0(a)$ and width $\Delta(b)$ for $v'_e = 3, V = 0.05$, and and different values of $Q' > 1$ versus the density ratio $\alpha$

width Fig. 4b of KdV solitons are comparable to Fig. 3 for various selections of. The amplitude Fig. 5a of the KdV soliton is observed to rise evenly with $\alpha$ for $V = 0.05$, and $Q' = 3, 6, 9$. Additionally, the KdV soliton's width Fig. 5b grows linearly. The mKdV soliton's amplitude Fig. 6a grows as $\alpha$ rises for a fixed value of $Q' < 1$, $V = 0.2$, and for various selections of $v'_e$. The growth pattern of the width Fig. 6b of mKdV soliton is similar to that of the amplitude. The amplitude of mKdV solitons decreases very slowly in the lower regime of $v'_e$, and then decreases more rapidly in the upper regime of $v'_e$ for $\alpha = 0.01$ and $V = 0.15$, and $Q' = 0.7, 0.8, 0.9$ Fig. 7a. However, the widths Fig. 7b of the mKdV soliton are almost constant in the lower regime of $v'_e$ and decrease more rapidly in the upper regime of $v'_e$ for $\alpha = 0.01$ and $V = 0.1$. For

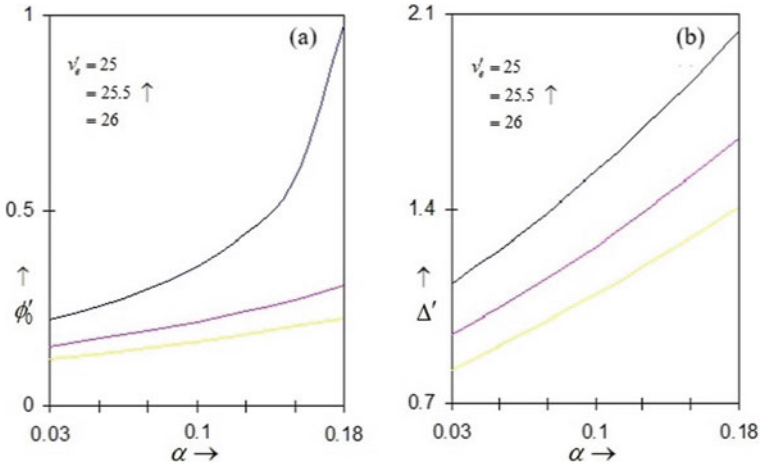


**Fig. 6** Amplitude $\phi_0'(a)$ and width $\Delta'(b)$ of mKdV solitons for $Q' = 0.25$, $V = 0.20$, and different values of $v_s'$ versus the density ratio $\alpha$

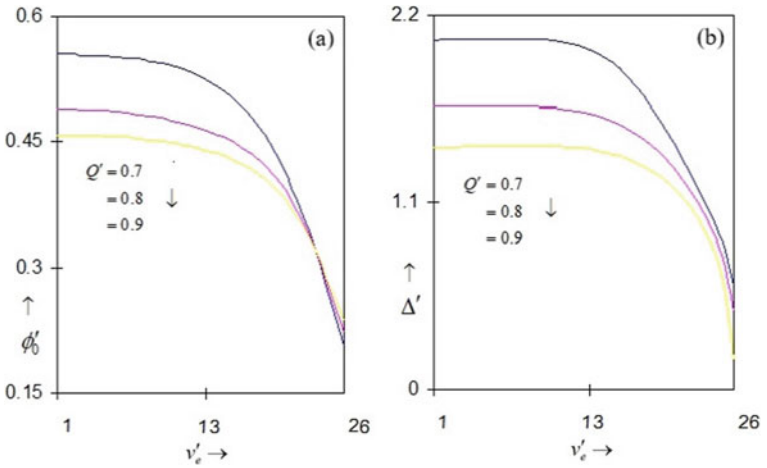


**Fig. 7** Amplitude $\phi_0'(a)$ and width $\Delta'(b)$ of mKdV solitons versus $v_e'$ for $\alpha = 0.01$, $V = 0.15$, and different values of $Q' < 1$

$\alpha = 0.02$ and $V = 0.2$, the amplitude Fig. 8a of mKdV solitons against $v_e'$ decreases rapidly, but linearly for various selections of $Q' = 0.013, 0.014, 0.015$. Further, for a very tiny range of $v_e'$, it is perceived that the corresponding width of the mKdV solitons decreases uniformly and then slightly increases parabolically, thereafter decreases in a diverging manner higher yet constrained regime of $v_e'$. Figure 9 shows the soliton solution $\phi_1$ with $\eta$ for $\alpha = 0.05$(red), 0.10(pink), 0.15(yellow). The investigation of nonlinear wave behaviors, mathematical modeling, and the consequences in plasma

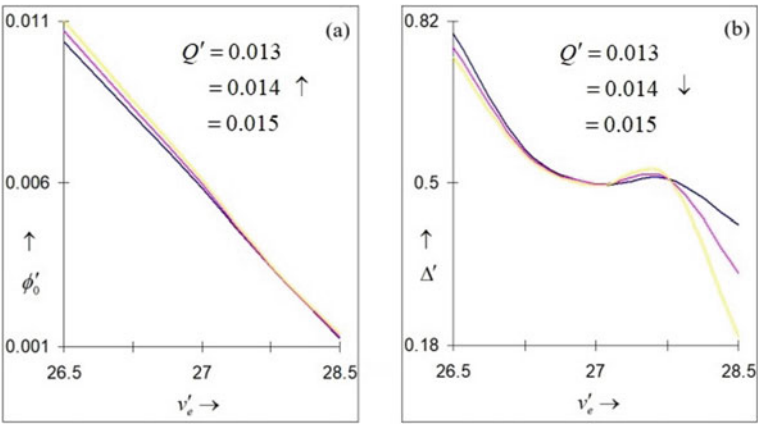


**Fig. 8** Amplitude $\phi_0'(a)$ and width $\Delta'(b)$ of mKdV solitons versus $v_e'$ for $\alpha = 0.02$, $V = 0.20$, and different values of $Q' < 1$

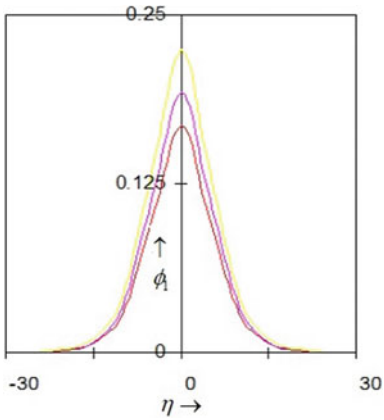


**Fig. 9** Variation of the amplitude for compressive KdV solitons with $\eta$ for $\alpha = 0.05$(red), 0.10(pink), 0.15(yellow)

physics is related to the effect of electron drift velocity in nonlinear ion-acoustic solitons in a negative ion beam plasma [39–44].

## 6 Conclusion

The effect of the electron's drift velocity in a multi-ion plasma system consisting positive ions, negative ion beams, and electrons has been discussed in this investigation. Using the usual reductive perturbation method, the KdV and mKdV equations have been obtained. Small amplitude compressive KdV solitons were produced in the plasma for various selections of $Q'$, bigger and less than one, under the influence

of the electron's drift velocity $v_e'$. It was shown that the mKdV solitons occur in two drift velocity $v_e'$ intervals when $Q'$ is smaller than one.

**Conflict of Interests** The authors declare no conflict of interest.
Data Availability Statement Inquiries about data availability should be directed to the authors.

## References


1. Washimi, H., Taniuti, T.: Propagation of ion-acoustic solitary waves of small amplitude. Phys. Rev. Lett. 17, 996–997 (1966).
2. Watanabe, S.: Ion acoustic soliton in plasma with negative ion. J. Phys. Soc. Jpn. 53, 950–956 (1984).
3. Ludwig, C.G., Ferreira, L.C., Nakamura, Y.: Observation of ion-acoustic rarefaction solitons in a multicomponent plasma with negative ions. Phys. Rev. Lett. 52, 275–278 (1984).
4. Nakamura, Y., Tsukayabashi, I.: Observation of modified Korteweg−de Vries solitons in a multicomponent plasma with negative ions. Phys. Rev. Lett. 52, 2356–2359 (1984).
5. Bacal, M., Wada, M.: Negative hydrogen ion production mechanisms. Appl. Phys. Rev. 2, 021305 (2015).
6. Burgess, D.D.: Possibilities for direct optical observation of negative hydrogen ions in ion beam plasma sources via Rayleigh or Thomson scattering. Plasma Phys. Contr. Fusion 27, 349–354 (1985).
7. Hase, Y., Watanabe, S., Tanaca, H.: Cylindrical ion acoustic soliton in plasma with negative ion. J. Phys. Soc. Jpn. 54, 4115–4125 (1985).
8. Tagare, G.S., Reddy, V.R.: Effect of higher-order nonlinearity on propagation of nonlinear ion-acoustic waves in a collisionless plasma consisting of negative ions. J. Plasma Phys. 35, 219–237 (1986).
9. Verheest, F.: Ion-acoustic double layers in multi-species plasmas maintained by negative ions. J. Plasma Phys. 42, 395–406 (1989).
10. Baboolal, S., Bharuthram, R., AHellberg, M.: On the existence of ion-acoustic double layers in negative-ion plasmas. J. Plasma Phys. 46, 247–254 (1991).
11. Kalita, C.B., Kalita, K.M., Chutia, J.: Drifting effect of electrons on fully non-linear ion acoustic waves in a magnetoplasma. J. Phys. A: Math. Gen. 19, 3559–3563 (1986).
12. Kalita, C.B., Kalita, K.M.: Modified Korteweg−de Vries solitons in a warm plasma with negative ions. Phys. Fluids B 2, 674–676 (1990).
13. Khuel, H.H., Zhang, Y.C.: Effects of ion drift on small-amplitude ion-acoustic solitons. Phys. Fluids B 3, 26–28 (1991).
14. Kalita, C.B., Devi, N.: Solitary waves in a warm plasma with negative ions and drifting effect of electron. Phys. Fluids B 5, 440 (1993).
15. Kalita, C.B., Kalita, K.M., Bhatta, P.R.: Solitons in a magnetized ion-beam plasma system. J. Plasma Phys. 50, 349–357 (1993).
16. Kalita, C.B., Bhatta, P.R.: Highly nonlinear ion-acoustic solitons in a warm magnetoplasma with drifting effect of electrons. Phys. Plasmas 1, 2172 (1994).
17. Kalita, C.B., Das, R.: A comparative study of modified Korteweg−de Vries (MKdV) and Korteweg−de Vries (KdV) solitons in plasmas with negative ions under the influence of electrons' drift motion. Phys. Plasmas 5, 3588 (1998).
18. Chattopadhayaya, S., Bhattacharya, K.S., Paul, N.S.: On the effects of drift motion and negative ions on ion-acoustic solitary waves and double-layers in plasmas. Indian J. Phys. B 76, 59–65 (2002).

19. Islam, S., Bandyopadhyay, A., Das, P.K.: Ion-acoustic solitary waves in a multispecies magnetized plasma consisting of non-thermal and isothermal electrons. J. Plasma Phys. 74, 765–806 (2008).
20. Sharma, C.S., Gahlot, A.: Ion beam driven ion-acoustic waves in a plasma cylinder with negative ions. Phys. Plasmas 15, 073705 (2008).
21. Rehman, S.U.: Linear and nonlinear quantum ion acoustic waves in a plasma with positive, negative ions and Fermi electron gas. Phys. Plasmas 17, 062303 (2010).
22. Rosenberg, M., Merlino, R.: Drift instability in a positive ion-negative ion plasma. J. Plasma Phys. 79, 949–952 (2013).
23. Das, R., Karmakar, K.: Modified Korteweg−de Varies solitons in a dusty plasma with electron inertia and drifting effect of electrons. Can. J. Phys. 91, 839–843 (2013).
24. Kaur, N., Singh, K., Saini, N.S.: Effect of ion beam on the characteristics of ion-acoustic Gardner solitons and double layers in a multicomponent superthermal plasma. Phys. Plasmas 24, 092108 (2017).
25. Deka, K.M., Dev, A.N.: Wave propagation with degenerate electron-positron in magnetically quantised ion beam plasma. Pramana J. Phys. 95, 65 (2021).
26. Mohsenpour, T., Ehsani, H., Behzadipour, M.: Ion-acoustic solitons in negative ion plasma with relativistic degenerate electrons and positrons. Waves Random Complex Media (2021), https://doi.org/10.1080/17455030.2021.1919338.
27. Baboolal, S., Bharuthram, R., Hellberg, A.M.: Cut-off conditions and existence domains for large-amplitude ion-acoustic solitons and double layers in fluid plasmas. J. Plasma Phys. 44, 1–23 (1990).
28. Kalita, C.B., Barman, N.S.: Effect of ion and ion-beam mass ratio on the formation of ion acoustic solitons in magnetized plasma in the presence of electron inertia. Phys. Plasmas 16, 052101 (2009).
29. Kalita, C.B., Das, R.: Modified Korteweg de Vries (MKdV) and Korteweg de Vries (KdV) solitons in a warm plasma with negative ions and electrons' drift motion. J. Phys. Soc. Jpn. 71, 2918–2924 (2002).
30. Chattopadhyay, S., Paul, S.N., Ray, D.: Influence of negative ions on ion-acoustic solitary waves in a two-electron-temperature plasma. Fizika A 18, 89 (2009).
31. Bailung, H., Sharma, K.S., Nakamura, Y.: Effect of ion beam on the propagation of rarefactive solitons in multicomponent plasma with negative ion. Phys. Plasmas 17, 062103 (2010).
32. Knist, S., Greiner, F., Biss, F., Piel, A.: Influence of negative ions on drift waves in a low-density Ar/O2-plasma. Plasma Phys. 51, 769–784 (2011).
33. Das, R.: Effect of ion temperature on small-amplitude ion acoustic solitons in a magnetized plasma ion-beam plasma in presence of electron inertia, Astrophys. Space Sci. 341, 543–549 (2012).
34. Kumar, A., Mathew, V.: Streaming instabilityin negative ion plasma. Phys. Plasmas 24, 092107 (2017).
35. Paul, I., Chatterjee, A., Paul, S.N.: Nonlinear propagation of ion acoustic waves in quantum plasma in the presence of an ion beam. Laser Part. Beams 37, 370–380 (2019).
36. Kaur, R., Singh, K., Saini, N.S.: Ion acoustic cnoidal waves in ion-beam dense plasma in the presence of quantizing magnetic field. IEEE Trans. Plasma Sci. 49, 1686 (2021).
37. Taniuti T., Wei C.C.: Reductive perturbation mathod in nonlinear wave propagation. I. J. Phys. Soc. Jpn. 24, 941–946 (1968).
38. Asano, N., Taniuti T., Yajima. N.: Perturbation mathod for a nonlinear wave modulation. II. J. Math. Phys. 10, 2020–2024 (1969).
39. Miura, R.M.: Korteweg−de Vries equation and generalizations. I. A remarkable explicit nonlinear transformation. J. Math. Phys. 9, 1202–1204 (1968).
40. Gardner, C.S., Greene, J.M., Kruskal, M.D., Miura, R.M.: Method for solving the Korteweg−de Vries equation. Phys. Rev. Lett. 19, 1095 (1967).
41. Miura, R.M., Gardner, C.S., Kruskal, M.D.: Korteweg−de Vries equation and generalizations. II. Existence of conservation laws and constants of motion. J. Math. Phys. 9, 1204–1209 (1968).

42. Miura, R.M.: The Korteweg−de Vries equation: a survey of results. SIAM Rev. 18, 412–459 (1976).
43. Kruskal, M.D., Miura, R.M., Gardner, C.S., Zabusky, N.J.: Korteweg−de Vries equation and generalizations. V. Uniqueness and nonexistence of polynomial conservation laws. J. Math. Phys. 11, 952–960 (1970).
44. Zabusky, N.J., Kruskal, M.D.: Interaction of "solitons" in a collisionless plasma and the recurrence of initial states. Phys. Rev. Lett. 15, 240 (1965).

# Darboux Transformation and Exact Solution for Novikov Equation


**Hongcai Ma, Xiaoyu Chen, and Aiping Deng**

**Abstract** In this paper, the lax pair of Novikov equation is given in $3 \times 3$ matrices form. Based on the spectral problem and the lax pair of Novikov equation, we construct the Darboux transformation and give the theoretical proof. By selecting the appropriate seed solution and using the obtained Darboux transformation, we can acquire the new exact solution of this equation. Finally, three-dimensional distribution and density plots of the new solution are shown. Exact solutions are depend on the different chosen seed solutions.

**Keywords** Novikov equation · Darboux transformation · Lax pair · Exact solution

## 1 Introduction

With the continuous development of science and technology as well as scientific research tools, the importance of nonlinear phenomena in nature is gradually increasing [1]. Compared with linear phenomena, the nature and structure of nonlinear phenomena are more complex. The solution is the most important step in the study of partial differential equations [2]. The effective solution methods for linear systems are generally not applicable to nonlinear partial differential systems. Some methods, include inverse scattering transform, Hirota bilinear method, Riemann-Hilbert method and the Painlev*é* test method are extremely useful method to acquire various soliton solutions [3–5]. The Darboux transformation is one of the most important approaches to acquire soliton solution for differential equations [6–9]. In this paper, we use the Darboux transformation method to study the Novikov equation.

H. Ma (✉) · A. Deng
School of Mathemaics and Staisics, Donghua University, Shanghai 201620, China
e-mail: hongcaima@hotmail.com

X. Chen
Experimental School, Donghua University, Shanghai 201620, China
e-mail: cxytianxia1@163.com



S. Manukure and W.-X. Ma (eds.), *Nonlinear and Modern Mathematical Physics*,
Springer Proceedings in Mathematics & Statistics 459,
https://doi.org/10.1007/978-3-031-59539-4_9

The Novikov equation has the following form

$$u_t - u_{xxt} + 4u^2u_x - u^2u_{xxx} - 3uu_xu_{xx} = 0, \tag{1}$$

that is equivalent to

$$m_t + u^2m_x + 3uu_xm = 0, \quad m = u - u_{xx}. \tag{2}$$

This equation has been discovered by Novikov as a new integrable equation with cubic nonlinearities which can be thought as a generalization of the Camassa-Holm equation [10–12].

For Eq. (2), Adler have searched its B$\ddot{a}$cklund transformation [13], Wu et al have acquired Global weak solutions [14], Holliman et al have studied its cauchy problem in Sobolev spaces [15, 16], Li have obtained a parametric representation for N-soliton solutions [17], Shi et al have investigated mixed lump-soliton solution [18].

The structure of the paper is as follows. In Sect. 2, based on the Lax pair, we formulate the Darboux transformation matrix of the Novikov equation and give a theoretical proof. In Sect. 3, we select the different seed solutions $m = u = 0$ and $m = u = 1$, acquire the new exact solutions by the constructed Darboux transformation in Sect. 2 and demonstrate three-dimensional distribution plot and their dynamic properties.

## 2 Lax Pair and Darboux Transformation

### *2.1 Lax Pair*

The Eq. (2) has the following 3×3 matrix form Lax representation [19]

$$\Phi_x = M\Phi, \quad \Phi_t = N\Phi, \quad \Phi = \begin{pmatrix} \phi_1 \\ \phi_2 \\ \phi_3 \end{pmatrix}, \tag{3}$$

with

$$M = \begin{pmatrix} 0 & \lambda m & 0 \\ 0 & 0 & \lambda m \\ 1 & 0 & 0 \end{pmatrix}, \quad N = \begin{pmatrix} n_1 - uu_x & n_2 - \lambda mu^2 & u_x^2 \\ n_3 & -2n_1 & -n_2 - \lambda mu^2 \\ -u^2 & n_3 & n_1 + uu_x \end{pmatrix}, \tag{4}$$

where

$$n_1 = \frac{1}{3\lambda^2}, \quad n_2 = \frac{u_x}{\lambda}, \quad n_3 = \frac{u}{\lambda}.$$

Here $\lambda$ is an arbitrary complex number called the spectral parameter, and $\phi$ is called the eigenfunction associated with $\lambda$, and $u, m$ is a potential function of position with respect to $x, t$ which are two independent variables. Equation (2) is equivalent to the compatibility condition $\Phi_{xt} = \Phi_{tx}$, i.e. the zero curvature equation [20]

$$M_t - N_x + [M, N] = 0, \tag{5}$$

where $[M, N] = MN - NM$.

## 2.2 Darboux Transformation

Firstly, we introduce a gauge transformation

$$\overline{\Phi} = T\Phi. \tag{6}$$

It is easy to see that the Lax pair (3) is transformed to

$$\overline{\Phi}_x = \overline{M\Phi}, \quad \overline{M} = (T_x + TM)T^{-1}, \tag{7}$$

$$\overline{\Phi}_t = \overline{N\Phi}, \quad \overline{N} = (T_t + TN)T^{-1}. \tag{8}$$

where $T$ is a Darboux matrix. Our aim now is to find the specific form of $T$ such that $\overline{M}$ and $\overline{N}$ obtained under transformation (6) have the same forms as $M$ and $N$ respectively. After confirming the specific form of the matrix $T$, the original seed solution $(u, m)$ in $M, N$ is mapped into a new solution $(\overline{u}, \overline{m})$ in $\overline{M}, \overline{N}$.

Without loss of generality, we assume that the Darboux matrix $T$ in Eq. (6) is of form

$$T = \begin{pmatrix} t_{11} & t_{12} & t_{13} \\ t_{21} & t_{22} & t_{23} \\ t_{31} & t_{32} & t_{33} \end{pmatrix} = \begin{pmatrix} \lambda^N + \sum\limits_{i=0}^{N-1} b_{11}^{(i)}\lambda^i & \sum\limits_{i=0}^{N-1} b_{12}^{(i)}\lambda^i & \sum\limits_{i=0}^{N-1} b_{13}^{(i)}\lambda^i \\ \sum\limits_{i=0}^{N-1} b_{21}^{(i)}\lambda^i & \lambda^N + \sum\limits_{i=0}^{N-1} b_{22}^{(i)}\lambda^i & \sum\limits_{i=0}^{N-1} b_{23}^{(i)}\lambda^i \\ \sum\limits_{i=0}^{N-1} b_{31}^{(i)}\lambda^i & \sum\limits_{i=0}^{N-1} b_{32}^{(i)}\lambda^i & \lambda^N + \sum\limits_{i=0}^{N-1} b_{11}^{(i)}\lambda^i \end{pmatrix},$$

where $b_{ij}^{(k)}(i, j = 1, 2, 3, k = 1, 2, \ldots, N-1)$ are functions of $x, t$ to be determined, and $b_{21}^{(N-1)} = b_{31}^{(N-1)} = b_{32}^{(N-1)} = 0, b_{12}^{(N-1)} = b_{23}^{(N-1)}, b_{11}^{(N-1)} + b_{33}^{(N-1)} = 2b_{22}^{(N-1)} (N \geq 2)$.

Let $\varphi(\lambda_j)$, $\phi(\lambda_j)$ and $\chi(\lambda_j)$ be the three basic solutions of the equation (2) associated with $\lambda_j$. For the sake of convenience, we introduce

$$\begin{aligned}\varphi(\lambda_j) &= (\varphi_1(\lambda_j), \varphi_2(\lambda_j), \varphi_3(\lambda_j))^T,\\ \phi(\lambda_j) &= (\phi_1(\lambda_j), \phi_2(\lambda_j), \phi_3(\lambda_j))^T,\\ \chi(\lambda_j) &= (\chi_1(\lambda_j), \chi_2(\lambda_j), \chi_3(\lambda_j))^T.\end{aligned} \tag{9}$$

According to the $tr(M) = tr(N) = 0$ and Eq. (6), we get

$$\begin{aligned}[det(\overline{\varphi}, \overline{\phi}, \overline{\chi})]_x &= [detT \cdot det(\varphi, \phi, \chi)]_x = 0,\\ [det(\overline{\varphi}, \overline{\phi}, \overline{\chi})]_t &= [detT \cdot det(\varphi, \phi, \chi)]_t = 0.\end{aligned} \tag{10}$$

Let $\lambda_j (\lambda_i \neq \lambda_j, i \neq j; \lambda_j \neq 0, j = 1, 2, \ldots, 3N)$ be roots of the $3N$-th order polynomial $detT$, these conclusions described above are obtained by direct calculation.

Thus for $\lambda = \lambda_j$, $j = 1, 2, \ldots, 3N$, there are constants $\gamma_j^{(1)}, \gamma_j^{(2)}$ such that the following equation

$$\begin{cases} t_{11}\varphi_1 + t_{12}\varphi_2 + t_{13}\varphi_3 + \gamma_j^{(1)}(t_{11}\phi_1 + t_{12}\phi_2 + t_{13}\phi_3) + \gamma_j^{(2)}(t_{11}\chi_1 + t_{12}\chi_2 + t_{13}\chi_3) = 0,\\ t_{21}\varphi_1 + t_{22}\varphi_2 + t_{23}\varphi_3 + \gamma_j^{(1)}(t_{21}\phi_1 + t_{22}\phi_2 + t_{23}\phi_3) + \gamma_j^{(2)}(t_{21}\chi_1 + t_{22}\chi_2 + t_{23}\chi_3) = 0,\\ t_{31}\varphi_1 + t_{32}\varphi_2 + t_{33}\varphi_3 + \gamma_j^{(1)}(t_{31}\phi_1 + t_{32}\phi_2 + t_{33}\phi_3) + \gamma_j^{(2)}(t_{31}\chi_1 + t_{32}\chi_2 + t_{33}\chi_3) = 0. \end{cases}$$

Also, it can be rewritten in the form of a linear system of equation

$$\begin{cases} t_{11} + \sigma_j^{(1)} t_{12} + \sigma_j^{(2)} t_{13} = 0,\\ t_{21} + \sigma_j^{(1)} t_{22} + \sigma_j^{(2)} t_{23} = 0,\\ t_{31} + \sigma_j^{(1)} t_{32} + \sigma_j^{(2)} t_{33} = 0, \end{cases} \tag{11}$$

where

$$\begin{aligned}\sigma_j^{(1)} &= \frac{\varphi_2(\lambda_j) + \gamma_j^{(1)}\phi_2(\lambda_j) + \gamma_j^{(2)}\chi_2(\lambda_j)}{\varphi_1(\lambda_j) + \gamma_j^{(1)}\phi_1(\lambda_j) + \gamma_j^{(2)}\chi_1(\lambda_j)},\\ \sigma_j^{(2)} &= \frac{\varphi_3(\lambda_j) + \gamma_j^{(1)}\phi_3(\lambda_j) + \gamma_j^{(2)}\chi_3(\lambda_j)}{\varphi_1(\lambda_j) + \gamma_j^{(1)}\phi_1(\lambda_j) + \gamma_j^{(2)}\chi_1(\lambda_j)}.\end{aligned} \tag{12}$$

Then, we can obtain the following Riccati equations according to Eqs. (3) and (11),

$$\begin{aligned}\sigma_{jx}^{(1)} &= \lambda m[\sigma_j^{(2)} - (\sigma_j^{(1)})^2],\\ \sigma_{jx}^{(2)} &= 1 - \sigma_j^{(1)}\sigma_j^{(2)},\\ t_{11x} &= -\sigma_{jx}^{(1)} t_{12} - \sigma_j^{(1)} t_{12x} - \sigma_{jx}^{(2)} t_{13} - \sigma_j^{(2)} t_{13x},\\ t_{21x} &= -\sigma_{jx}^{(1)} t_{22} - \sigma_j^{(1)} t_{22x} - \sigma_{jx}^{(2)} t_{23} - \sigma_j^{(2)} t_{23x},\\ t_{31x} &= -\sigma_{jx}^{(1)} t_{32} - \sigma_j^{(1)} t_{32x} - \sigma_{jx}^{(2)} t_{33} - \sigma_j^{(2)} t_{33x}.\end{aligned} \tag{13}$$

As a consequent, we have

**Theorem 1.** Matrices $\overline{M}$ and $\overline{N}$ given by Eqs. (7), (8) are respectively have the same forms as $M$ and $N$, and relations between the original eigenfunctions $u, m$ and the new gain ones $\overline{u}, \overline{m}$ are

$$\begin{cases} \overline{m} = m + b_{11}^{(N-2)} - 2b_{22}^{(N-2)}, \\ \overline{u} = u + (\overline{m} - m)[b_{33}^{(N-1)} - b_{22}^{(N-1)}]. \end{cases} \tag{14}$$

Equation (6) make up the Darboux transformation of the Eq. (2). Now, we give a detailed proof of Theorem 1 with respect to matrix $\overline{M}$.

**Proof.** Let

$$(T_x + TM)T^* = \begin{pmatrix} f_{11}(\lambda) & f_{12}(\lambda) & f_{13}(\lambda) \\ f_{21}(\lambda) & f_{22}(\lambda) & f_{23}(\lambda) \\ f_{31}(\lambda) & f_{32}(\lambda) & f_{33}(\lambda) \end{pmatrix}, \tag{15}$$

where $T^*$ is the adjoint matrix of $T$. We can find that $f_{sl}(\lambda)(s, l = 1, 2, 3)$ are both $3N$ or $3N + 1$ degree polynomials of $\lambda$. Here, $f_{12}(\lambda)$ , $f_{23}(\lambda)$ are $3N + 1$ degree and the rest are $3N$ degree with respect to $\lambda$. Then $f_{sl}(\lambda)(s, l = 1, 2, 3) = 0$ when $\lambda = \lambda_j$, this result is directly calculated by using Eq. (13).

Since $T^{-1} = T^*/\det T$, Eq. (13) can be written as

$$T_x + TM = P(\lambda)T = \begin{pmatrix} p_{11}^{(0)} & p_{12}^{(1)}\lambda + p_{12}^{(0)} & p_{13}^{(0)} \\ p_{21}^{(0)} & p_{22}^{(0)} & p_{23}^{(1)}\lambda + p_{23}^{(0)} \\ p_{31}^{(0)} & p_{32}^{(0)} & p_{33}^{(0)} \end{pmatrix} T, \tag{16}$$

where $p_{sl}^{(k)}(s, l = 1, 2, 3; k = 0, 1)$ are independent of $\lambda$. Comparing the coefficients of $\lambda^k, k = N - 1, N, N + 1$ at both ends of the Eq. (16), it implies

$$\lambda^{N+1} : p_{12}^{(1)} = p_{23}^{(1)} = m, \tag{17}$$

with

$$\begin{aligned} &\lambda^N : p_{11}^{(0)} = p_{13}^{(0)} = p_{21}^{(0)} = p_{22}^{(0)} = p_{32}^{(0)} = p_{33}^{(0)} = 0, p_{31}^{(0)} = 1, \\ &p_{12}^{(0)} = p_{23}^{(0)} = \frac{b_{12x}^{(N-1)} + m(b_{11}^{(N-2)} - b_{22}^{(N-2)})}{b_{22}^{(N-1)}}, \end{aligned} \tag{18}$$

and

$$
\begin{aligned}
\lambda^{N-1}:& b_{11x}^{(N-1)}+b_{13}^{(N-1)}=p_{12}^{(0)}b_{21}^{(N-1)}+mb_{21}^{(N-2)},\\
& b_{21x}^{(N-1)}+b_{23}^{(N-1)}=mb_{31}^{(N-2)}+p_{23}^{(0)}b_{31}^{(N-1)},\\
& b_{31x}^{(N-1)}+b_{33}^{(N-1)}=b_{11}^{(N-1)},\quad b_{12x}^{(N-1)}+mb_{11}^{(N-2)}=mb_{22}^{(N-2)}+p_{12}^{(0)}b_{22}^{(N-1)},\\
& b_{22x}^{(N-1)}+mb_{21}^{(N-2)}=mb_{32}^{(N-2)}+p_{23}^{(0)}b_{32}^{(N-1)},\quad b_{32x}^{(N-1)}+mb_{31}^{(N-2)}=b_{12}^{(N-1)},\\
& b_{13x}^{(N-1)}+mb_{12}^{(N-2)}=mb_{23}^{(N-2)}+p_{12}^{(0)}b_{23}^{(N-1)},\\
& b_{23x}^{(N-1)}+mb_{22}^{(N-2)}=mb_{33}^{(N-2)}+p_{23}^{(0)}b_{33}^{(N-2)},\quad b_{33x}^{(N-1)}+mb_{32}^{(N-2)}=b_{12}^{(N-1)}.
\end{aligned}
$$

Combining Eqs. (2.2) , (14), it is not difficult to acquire $P(\lambda)=\overline{M}$.

Here, coefficients $b_{ij}^{(k)}(i,j=1,2,3,k=1,2,\ldots,N-1)$ can solved by Cramer rule in linear system (11). We can also prove $\overline{N}$ has the same form as $N$ by similar steps.

## 3 New Exact Solution and Dynamical Properties

As we all known before, different seed solutions of the same equation will yield different exact solutions after Darboux transformation.

### *3.1 Seed Solution $m=u=0$*

Choose seed solution $m=u=0$ and solve the Eq. (4) for $\lambda=\lambda_j$, $j=1,2,\ldots,3N$, we deduce that

$$
\Phi(\lambda_j)=\begin{pmatrix}\phi_1(\lambda_j)\\ \phi_2(\lambda_j)\\ \phi_3(\lambda_j)\end{pmatrix}=\begin{pmatrix}c_1+k_1e^{\rho_1(\lambda_j)t}\\ c_2+k_2e^{\rho_2(\lambda_j)t}\\ c_1x+k_3e^{\rho_3(\lambda_j)t}\end{pmatrix},\tag{19}
$$

where $c_j$ and $k_j$, $j=1,2,3$ are arbitrary constants but $c_1\neq 0$ and

$$
\rho_1=\rho_3=\frac{1}{3\lambda^2},\quad \rho_2=-\frac{2}{3\lambda^2}.\tag{20}
$$

According to Eqs. (11) and (14), we find

$$
\overline{m}=b_{11}^{(N-2)}-b_{22}^{(N-2)},\quad \overline{u}=[b_{11}^{(N-2)}-b_{22}^{(N-2)}][b_{33}^{(N-1)}-b_{22}^{(N-1)}],\tag{21}
$$

and

$$
b_{11}^{(N-2)}=\frac{\Delta_1}{\Delta},\quad b_{22}^{(N-2)}=\frac{\Delta_2}{\Delta},\quad b_{33}^{(N-1)}=\frac{\Delta_{33}}{\Delta},\quad b_{22}^{(N-1)}=\frac{\Delta_{22}}{\Delta},\tag{22}
$$

where $\Delta, \Delta_k$ are the determinant of the $3N \times 3N$ coefficient matrix of the linear system (11), i.e.

$$\Delta = \begin{vmatrix} 1 & \lambda_1 & \cdots & \lambda_1^{N-1} & \sigma_1^{(1)} & \sigma_1^{(1)}\lambda_1 & \cdots & \sigma_1^{(1)}\lambda_1^{N-1} & \sigma_1^{(2)} & \sigma_1^{(2)}\lambda_1 & \cdots & \sigma_1^{(2)}\lambda_1^{N-1} \\ 1 & \lambda_2 & \cdots & \lambda_2^{N-1} & \sigma_2^{(1)} & \sigma_2^{(1)}\lambda_2 & \cdots & \sigma_2^{(1)}\lambda_2^{N-1} & \sigma_2^{(2)} & \sigma_2^{(2)}\lambda_2 & \cdots & \sigma_2^{(2)}\lambda_2^{N-1} \\ \cdots & \cdots & \cdots & \cdots & \cdots & \cdots & \cdots & \cdots & \cdots & \cdots & \cdots & \cdots \\ 1 & \lambda_j & \cdots & \lambda_j^{N-1} & \sigma_j^{(1)} & \sigma_j^{(1)}\lambda_j & \cdots & \sigma_j^{(1)}\lambda_j^{N-1} & \sigma_j^{(2)} & \sigma_j^{(2)}\lambda_j & \cdots & \sigma_j^{(2)}\lambda_j^{N-1} \\ \cdots & \cdots & \cdots & \cdots & \cdots & \cdots & \cdots & \cdots & \cdots & \cdots & \cdots & \cdots \\ 1 & \lambda_{3N} & \cdots & \lambda_{3N}^{N-1} & \sigma_{3N}^{(1)} & \sigma_{3N}^{(1)}\lambda_{3N} & \cdots & \sigma_{3N}^{(1)}\lambda_{3N}^{N-1} & \sigma_{3N}^{(2)} & \sigma_{3N}^{(2)}\lambda_1 & \cdots & \sigma_{3N}^{(2)}\lambda_{3N}^{N-1} \end{vmatrix},$$

$$\Delta_1 = \begin{vmatrix} 1 & \cdots & -\lambda_1^N & \lambda_1^{N-1} & \sigma_1^{(1)} & \sigma_1^{(1)}\lambda_1 & \cdots & \sigma_1^{(1)}\lambda_1^{N-1} & \sigma_1^{(2)} & \sigma_1^{(2)}\lambda_1 & \cdots & \sigma_1^{(2)}\lambda_1^{N-1} \\ 1 & \cdots & -\lambda_2^N & \lambda_2^{N-1} & \sigma_2^{(1)} & \sigma_2^{(1)}\lambda_2 & \cdots & \sigma_2^{(1)}\lambda_2^{N-1} & \sigma_2^{(2)} & \sigma_2^{(2)}\lambda_2 & \cdots & \sigma_2^{(2)}\lambda_2^{N-1} \\ \cdots & \cdots & \cdots & \cdots & \cdots & \cdots & \cdots & \cdots & \cdots & \cdots & \cdots & \cdots \\ 1 & \cdots & -\lambda_j^N & \lambda_j^{N-1} & \sigma_j^{(1)} & \sigma_j^{(1)}\lambda_j & \cdots & \sigma_j^{(1)}\lambda_j^{N-1} & \sigma_j^{(2)} & \sigma_j^{(2)}\lambda_j & \cdots & \sigma_j^{(2)}\lambda_j^{N-1} \\ \cdots & \cdots & \cdots & \cdots & \cdots & \cdots & \cdots & \cdots & \cdots & \cdots & \cdots & \cdots \\ 1 & \cdots & -\lambda_{3N}^N & \lambda_{3N}^{N-1} & \sigma_{3N}^{(1)} & \sigma_{3N}^{(1)}\lambda_{3N} & \cdots & \sigma_{3N}^{(1)}\lambda_{3N}^{N-1} & \sigma_{3N}^{(2)} & \sigma_{3N}^{(2)}\lambda_1 & \cdots & \sigma_{3N}^{(2)}\lambda_{3N}^{N-1} \end{vmatrix},$$

$$\Delta_2 = \begin{vmatrix} 1 & \cdots & \lambda_1^{N-1} & \sigma_1^{(1)} & \sigma_1^{(1)}\lambda_1 & \cdots & -\sigma_1^{(1)}\lambda_1^N & \sigma_1^{(1)}\lambda_1^{N-1} & \sigma_1^{(2)} & \sigma_1^{(2)}\lambda_1 & \cdots & \sigma_1^{(2)}\lambda_1^{N-1} \\ 1 & \cdots & \lambda_2^{N-1} & \sigma_2^{(1)} & \sigma_2^{(1)}\lambda_2 & \cdots & -\sigma_2^{(1)}\lambda_2^N & \sigma_2^{(1)}\lambda_2^{N-1} & \sigma_2^{(2)} & \sigma_2^{(2)}\lambda_2 & \cdots & \sigma_2^{(2)}\lambda_2^{N-1} \\ \cdots & \cdots & \cdots & \cdots & \cdots & \cdots & \cdots & \cdots & \cdots & \cdots & \cdots & \cdots \\ 1 & \cdots & \lambda_j^{N-1} & \sigma_j^{(1)} & \sigma_j^{(1)}\lambda_j & \cdots & -\sigma_j^{(1)}\lambda_j^N & \sigma_j^{(1)}\lambda_j^{N-1} & \sigma_j^{(2)} & \sigma_j^{(2)}\lambda_j & \cdots & \sigma_j^{(2)}\lambda_j^{N-1} \\ \cdots & \cdots & \cdots & \cdots & \cdots & \cdots & \cdots & \cdots & \cdots & \cdots & \cdots & \cdots \\ 1 & \cdots & \lambda_{3N}^{N-1} & \sigma_{3N}^{(1)} & \sigma_{3N}^{(1)}\lambda_{3N} & \cdots & -\sigma_{3N}^{(1)}\lambda_{3N}^N & \sigma_{3N}^{(1)}\lambda_{3N}^{N-1} & \sigma_{3N}^{(2)} & \sigma_{3N}^{(2)}\lambda_1 & \cdots & \sigma_{3N}^{(2)}\lambda_{3N}^{N-1} \end{vmatrix},$$

$$\Delta_{33} = \begin{vmatrix} 1 & \lambda_1 & \cdots & \lambda_1^{N-1} & \sigma_1^{(1)} & \sigma_1^{(1)}\lambda_1 & \cdots & \sigma_1^{(1)}\lambda_1^{N-1} & \sigma_1^{(2)} & \sigma_1^{(2)}\lambda_1 & \cdots & -\sigma_1^{(2)}\lambda_1^N \\ 1 & \lambda_2 & \cdots & \lambda_2^{N-1} & \sigma_2^{(1)} & \sigma_2^{(1)}\lambda_2 & \cdots & \sigma_2^{(1)}\lambda_2^{N-1} & \sigma_2^{(2)} & \sigma_2^{(2)}\lambda_2 & \cdots & -\sigma_2^{(2)}\lambda_2^N \\ \cdots & \cdots & \cdots & \cdots & \cdots & \cdots & \cdots & \cdots & \cdots & \cdots & \cdots & \cdots \\ 1 & \lambda_j & \cdots & \lambda_j^{N-1} & \sigma_j^{(1)} & \sigma_j^{(1)}\lambda_j & \cdots & \sigma_j^{(1)}\lambda_j^{N-1} & \sigma_j^{(2)} & \sigma_j^{(2)}\lambda_j & \cdots & -\sigma_j^{(2)}\lambda_j^N \\ \cdots & \cdots & \cdots & \cdots & \cdots & \cdots & \cdots & \cdots & \cdots & \cdots & \cdots & \cdots \\ 1 & \lambda_{3N} & \cdots & \lambda_{3N}^{N-1} & \sigma_{3N}^{(1)} & \sigma_{3N}^{(1)}\lambda_{3N} & \cdots & \sigma_{3N}^{(1)}\lambda_{3N}^{N-1} & \sigma_{3N}^{(2)} & \sigma_{3N}^{(2)}\lambda_1 & \cdots & -\sigma_{3N}^{(2)}\lambda_{3N}^N \end{vmatrix},$$

$$\Delta_{22} = \begin{vmatrix} 1 & \lambda_1 & \cdots & \lambda_1^{N-1} & \sigma_1^{(1)} & \sigma_1^{(1)}\lambda_1 & \cdots & -\sigma_1^{(1)}\lambda_1^N & \sigma_1^{(2)} & \sigma_1^{(2)}\lambda_1 & \cdots & \sigma_1^{(2)}\lambda_1^{N-1} \\ 1 & \lambda_2 & \cdots & \lambda_2^{N-1} & \sigma_2^{(1)} & \sigma_2^{(1)}\lambda_2 & \cdots & -\sigma_2^{(1)}\lambda_2^N & \sigma_2^{(2)} & \sigma_2^{(2)}\lambda_2 & \cdots & \sigma_2^{(2)}\lambda_2^{N-1} \\ \cdots & \cdots & \cdots & \cdots & \cdots & \cdots & \cdots & \cdots & \cdots & \cdots & \cdots & \cdots \\ 1 & \lambda_j & \cdots & \lambda_j^{N-1} & \sigma_j^{(1)} & \sigma_j^{(1)}\lambda_j & \cdots & -\sigma_j^{(1)}\lambda_j^N & \sigma_j^{(2)} & \sigma_j^{(2)}\lambda_j & \cdots & \sigma_j^{(2)}\lambda_j^{N-1} \\ \cdots & \cdots & \cdots & \cdots & \cdots & \cdots & \cdots & \cdots & \cdots & \cdots & \cdots & \cdots \\ 1 & \lambda_{3N} & \cdots & \lambda_{3N}^{N-1} & \sigma_{3N}^{(1)} & \sigma_{3N}^{(1)}\lambda_{3N} & \cdots & -\sigma_{3N}^{(1)}\lambda_{3N}^N & \sigma_{3N}^{(2)} & \sigma_{3N}^{(2)}\lambda_1 & \cdots & \sigma_{3N}^{(2)}\lambda_{3N}^{N-1} \end{vmatrix}.$$

For $N = 1$, we have similar results

$$\overline{m} = b_{11} - 2b_{22}, \quad \overline{u} = (b_{11} - 2b_{22})(b_{22} - b_{33}), \tag{23}$$

and

$$b_{11} = \frac{\Delta_{11}}{\Delta}, \quad b_{22} = \frac{\Delta_{22}}{\Delta}, \quad b_{33} = \frac{\Delta_{33}}{\Delta}, \tag{24}$$

where

$$\Delta = \begin{vmatrix} 1 & \sigma_1^{(1)} & \sigma_1^{(2)} \\ 1 & \sigma_2^{(1)} & \sigma_2^{(2)} \\ 1 & \sigma_3^{(1)} & \sigma_3^{(2)} \end{vmatrix}, \quad \Delta_{11} = \begin{vmatrix} -\lambda_1 & \sigma_1^{(1)} & \sigma_1^{(2)} \\ -\lambda_2 & \sigma_2^{(1)} & \sigma_2^{(2)} \\ -\lambda_3 & \sigma_3^{(1)} & \sigma_3^{(2)} \end{vmatrix},$$
$$\Delta_{22} = \begin{vmatrix} 1 & -\sigma_1^{(1)}\lambda_1 & \sigma_1^{(2)} \\ 1 & -\sigma_2^{(1)}\lambda_2 & \sigma_2^{(2)} \\ 1 & -\sigma_3^{(1)}\lambda_3 & \sigma_3^{(2)} \end{vmatrix}, \quad \Delta_{33} = \begin{vmatrix} 1 & \sigma_1^{(1)} & -\sigma_1^{(2)}\lambda_1 \\ 1 & \sigma_2^{(1)} & -\sigma_2^{(2)}\lambda_2 \\ 1 & \sigma_3^{(1)} & -\sigma_3^{(2)}\lambda_3 \end{vmatrix}. \tag{25}$$

To better analyze the exact solution, we show the three dimensional plots of the solution (23) and its density plots in the $x - t - u(m)$ coordinate in Fig. 1.

Figure 1 displays the one exact solution $\overline{m}$ and $\overline{u}$ with seed solution $m = u = 0$. (a) and (b) shows the peakon solution $\overline{m}$, (c) and (d) shows the peakon solution $\overline{u}$. A part of the image of the solution is truncated due to the restriction of the range of $\overline{m}$ and $\overline{u}$.

## 3.2 Seed Solution $m = u = 1$

Choose seed solution $m = u = 1$ and solve the Eq. (4) for $\lambda = \lambda_j$, $j = 1, 2, 3$, we deduce that

$$\Phi(\lambda_j) = \begin{pmatrix} \phi_1(\lambda_j) \\ \phi_2(\lambda_j) \\ \phi_3(\lambda_j) \end{pmatrix} = \begin{pmatrix} \tau e^{\rho(\lambda_j)x + k_i(\lambda_j)t} \\ \tau c_1(\lambda_j) e^{\rho(\lambda_j)x + k_i(\lambda_j)t} \\ \tau c_2(\lambda_j) e^{\rho(\lambda_j)x + k_i(\lambda_j)t} \end{pmatrix}, \quad i = 1, 2, 3, \tag{26}$$

where $\tau$ is arbitrary constants and

$$c_1 = \lambda^{-\frac{1}{3}}, \quad c_2 = \lambda^{-\frac{2}{3}}, \quad \rho = \frac{2}{3}\lambda \tag{27}$$

with

$$k_1 = \frac{(-2916\lambda^9 + 108\lambda^3 + 12\sqrt{3}\sqrt{3402\lambda^{10} - 1296\lambda^8 + 135\lambda^6 + 54\lambda^4 - 9\lambda^2 + 4} - 108\lambda)^{\frac{1}{3}}}{18\lambda^3}$$
$$- \frac{2(18\lambda^6 - 3\lambda^2 + 1)}{3\lambda^3(-2916\lambda^9 + 108\lambda^3 + 12\sqrt{3}\sqrt{3402\lambda^{10} - 1296\lambda^8 + 135\lambda^6 + 54\lambda^4 - 9\lambda^2 + 4} - 108\lambda)^{\frac{1}{3}}}$$
$$+ \frac{1}{3\lambda^2},$$

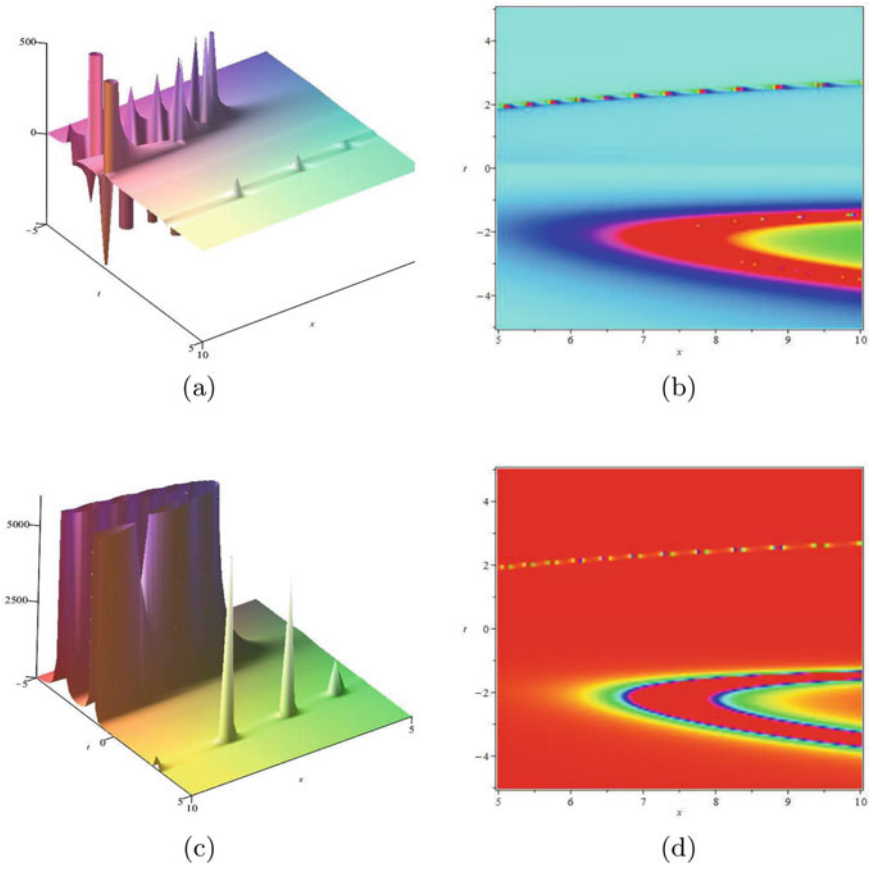


**Fig. 1** Taking the parameters as $\lambda_1 = \frac{1}{3}, \lambda_2 = \frac{1}{\sqrt{3}}, \lambda_3 = 1, \gamma_1^{(1)} = 0, \gamma_1^{(2)} = \sqrt{3}, \gamma_2^{(1)} = -\sqrt{3}, \gamma_2^{(2)} = 0, \gamma_3^{(1)} = 1 + \sqrt{3}, \gamma_3^{(2)} = 1 - \sqrt{3}$

$$
\begin{aligned}
k_2 = {} & \frac{(-2916\lambda^9 + 108\lambda^3 + 12\sqrt{3}\sqrt{3402\lambda^{10} - 1296\lambda^8 + 135\lambda^6 + 54\lambda^4 - 9\lambda^2 + 4} - 108\lambda)^{\frac{1}{3}}}{36\lambda^3} \\
& + \frac{18\lambda^6 - 3\lambda^2 + 1}{3\lambda^3(-2916\lambda^9 + 108\lambda^3 + 12\sqrt{3}\sqrt{3402\lambda^{10} - 1296\lambda^8 + 135\lambda^6 + 54\lambda^4 - 9\lambda^2 + 4} - 108\lambda)^{\frac{1}{3}}} \\
& + i\sqrt{3}\,\frac{(-2916\lambda^9 + 108\lambda^3 + 12\sqrt{3}\sqrt{3402\lambda^{10} - 1296\lambda^8 + 135\lambda^6 + 54\lambda^4 - 9\lambda^2 + 4} - 108\lambda)^{\frac{1}{3}}}{36\lambda^3} \\
& + \frac{i(18\lambda^6 - 3\lambda^2 + 1)}{3\lambda^3(-2916\lambda^9 + 108\lambda^3 + 12\sqrt{3}\sqrt{3402\lambda^{10} - 1296\lambda^8 + 135\lambda^6 + 54\lambda^4 - 9\lambda^2 + 4} - 108\lambda)^{\frac{1}{3}}} \\
& + \frac{1}{3\lambda^2},
\end{aligned}
$$

$$
\begin{aligned}
k_3 = & -\frac{(-2916\lambda^9+108\lambda^3+12\sqrt{3}\sqrt{3402\lambda^{10}-1296\lambda^8+135\lambda^6+54\lambda^4-9\lambda^2+4}-108\lambda)^{\frac{1}{3}}}{36\lambda^3} \\
& + \frac{18\lambda^6-3\lambda^2+1}{3\lambda^3(-2916\lambda^9+108\lambda^3+12\sqrt{3}\sqrt{3402\lambda^{10}-1296\lambda^8+135\lambda^6+54\lambda^4-9\lambda^2+4}-108\lambda)^{\frac{1}{3}}} \\
& - i\sqrt{3}\,\frac{(-2916\lambda^9+108\lambda^3+12\sqrt{3}\sqrt{3402\lambda^{10}-1296\lambda^8+135\lambda^6+54\lambda^4-9\lambda^2+4}-108\lambda)^{\frac{1}{3}}}{36\lambda^3} \\
& - \frac{i(18\lambda^6-3\lambda^2+1)}{3\lambda^3(-2916\lambda^9+108\lambda^3+12\sqrt{3}\sqrt{3402\lambda^{10}-1296\lambda^8+135\lambda^6+54\lambda^4-9\lambda^2+4}-108\lambda)^{\frac{1}{3}}} \\
& + \frac{1}{3\lambda^2}.
\end{aligned}
$$

For the simple case ($N = 1$), we can obtain new exact solutions from $m = u = 1$

$$\overline{m} = 1 + b_{11} - 2b_{22}, \quad \overline{u} = (1 + b_{11} - 2b_{22})(b_{22} - b_{33}), \tag{28}$$

where $b_{ij}, i, j = 1, 2, 3$ is defined by Eqs. (24) and (25).

## 4 Conclusions

In this paper, based on a $3 \times 3$ matrix spectral problem and the Lax pair of Novikov equation, we successfully construct $N$-fold Darboux transformation matrix. The paper aims to obtain precise solutions with different seed solutions. Results indicated that the change of related parameters and seed solutions has a great influence on the waveform of the acquired exact solution. By selecting appropriate parameters, we acquire the three dimensional plots and density plots of exact solution with seed solution $m = u = 0$. This solution we found does not appear in the literature previously associated with this Eq. (2). Lastly, these soliton solutions deserve further study and may have relevance in physics or related disciplines. In the future, we hope we can seek the rogue wave solution, breather solution and other forms of solutions for Eq. (2) base on the results achieved so far.

## References


1. Thomas, L., Saaty.: Modern nonlinear equations. Courier Corporation (2012)
2. Jihuan, H.: Some asymptotic methods for strongly nonlinear equations. J. Mod. Phy. 20(10), 1141–1199 (2006)
3. Calogero., Francesco, D., Antonio.:Spectral transform and solitons. Elsevier (2011)
4. Newell., Alan, C.: The inverse scattering transform. In: Solitons, pp. 177–242. Springer (1980)
5. Ma, W.X., Zhou, Y.: Lump solutions to nonlinear partial differential equations via hirota bilinear forms. J. Diff. Equ. 264(4), 2633–2659 (2018)

6. Yang, D.Y., Tian, B., Qu, Q.X., Zhang, C.R., Chen, S.S., Wei, C.C.: Lax pair, conservation laws, Darboux transformation and localized waves of a variable-coefficient coupled Hirota system in an inhomogeneous optical fiber. Chaos Solitons Fractals. 150, 110487 (2021)
7. Shen, Y., Tian, B., Zhou, T.Y., Gao, X.T.: N-fold Darboux transformation and solitonic interactions for the Kraenkel-Manna-Merle system in a saturated ferromagnetic material. Nonlinear Dyn. 111(3), 2641–2649 (2023)
8. Wang, M., Tian, B., Zhou, T.Y.: Darboux transformation, generalized Darboux transformation and vector breathers for a matrix Lakshmanan-Porsezian-Daniel equation in a Heisenberg ferromagnetic spin chain. Chaos Solitons Fractals. 152, 111411 (2021)
9. Rogers, C., Schief, W.K.: Bäcklund and Darboux transformations: geometry and modernapplications in soliton theory. Cambridge University Press (2002).
10. Novikov., Vladimir.: Generalizations of the Camassa–Holm equation. J. Phys. A: Math. Theor. 42(34), 342002 (2009)
11. Li, J., Wu, X., Yu, Y., Zhu, W.: Non-uniform dependence on initial data for the Camassa–Holm equation in the critical besov space. J. Math. Flu. Mec. 23(2), 1–11 (2021)
12. Madiyeva, A., Pelinovsky, D.E.: Growth of perturbations to the peaked periodic waves in the Camassa–Hol equation. J. Math. Ana. 53(3), 3016–3039 (2021)
13. Adler, V.E.: Backlund transformation for the Krichever-Novikov equation. Int. Math. Res. Not. 1998(1) 1–4 (1998). https://doi.org/10.1155/S1073792898000014
14. Wu, X.L., Yin, Z.Y.: Global weak solutions for the Novikov equation. J. Phys. A: Math. Theor. 44(5), 055202 (2011)
15. Himonas, A.A., Holliman, C.: The Cauchy problem for the Novikov equation. J. Non. 25(2), 449–479 (2012)
16. Yan, W., Li, Y.S., Zhang, Y.M.: The Cauchy problem for the Novikov equation. J. Non. Diff. Equ. Appl. 20(3), 1157–1169 (2013)
17. Wu, L., Li, C., Li, N.: Soliton solutions to the Novikov equation and a negative flow of the Novikov hierarchy. J. Appl. Math. Lett. 87, 134–140 (2019)
18. Shi, K.Z., Shen, S.F., Ren, B.: Dynamics of mixed lump-soliton for extended (2+1)-dimensional asymmetric Nizhnik-Novikov-Veselov equation. J. Comm. Theor. Phys. 74(3), 035001 (2022)
19. Ma, R., Zhang, Y., Xiong, N., Feng, B.F.: Short wave limit of the Novikov equation and its integrable semi-discretizations. J. Phys. A: Math. Theor. 54(49), 495701 (2021)
20. Sakovich, S.Y.: On zero-curvature representations of evolution equations. J. Phys. A: Math. Gene. 28(10), 2861 (1995)

# Construction of Multi-wave Solutions of Nonlinear Equations with Variable Coefficients Arising in Fluid Mechanics


**Hongcai Ma, Yidan Gao, and Aiping Deng**

**Abstract** The nonlinear development equations play an important role in describing natural phenomena, so it is very important to solve the nonlinear development equations. In this paper, the (2+1)-dimensional variable coefficient Date-Jimbo-Kashiwara-Miwa equation, and the variable coefficient shallow water wave equation are studied by using exp-function method, which can be regarded as a special multi-soliton method. The one-wave solution, two-wave solution, three-wave solution and four-wave solution are solved with the mathematical software Maple, and corresponding figures are drawn to better observe the state of the solution.

**Keywords** Exp-function method · The (2+1)-dimensional variable coefficient Date-Jimbo-Kashiwara-Miwa equation · The (2+1)-dimensional variable coefficient shallow water wave equation · Multi-wave solutions

## 1 Introduction

Soliton theory plays an important role in the nonlinear development of science and has been applied to almost all natural sciences. Due to their abilities to describe a lot of natural phenomena quite accurately, the research on nonlinear equations is flourishing. Obtaining exact solutions of nonlinear equations has become one of the important research. Through the continuous efforts of scholars, there have been many methods to attain the exact solutions of nonlinear equations: homogeneous balance method [1], sine-cosine method [2], jacobi elliptic function [3], mapping method [4], extend F-expansion method [5], etc.

H. Ma (✉) · Y. Gao · A. Deng
Department of Applied Mathematics, Donghua University, Shanghai 201620, China
e-mail: hongcaima@hotmail.com

Y. Gao
e-mail: gydana@163.com



S. Manukure and W.-X. Ma (eds.), *Nonlinear and Modern Mathematical Physics*,
Springer Proceedings in Mathematics & Statistics 459,
https://doi.org/10.1007/978-3-031-59539-4_10

In this article, we are going to solve two equations with time-dependent variables by using the exp-function method. This method was first proposed by Ma et al. in 2010, they applied this method to study the three wave solutions of (3+1)-dimensional potential Yu-Toda-Sasa-Fukuyama Equation [6]. Exact solutions of many nonlinear equations have been solved by using this method [7–11]. The multiple exp-function method can be regarded as a generalization of Hirota's perturbation scheme, so the multi-wave solutions are soliton-type.

In this article, we will use the exp-function method to explore the multi-wave solutions of two equations with variable coefficients depending on time. The first equation is the (2+1)-dimensional variable coefficient Date-Jimbo-Kashiwara-Miwa equation (vcDJKM) [12, 13]:

$$u_{xxxxy} + 4u_{xxy}u_x + 2u_{xxx}u_y + 6u_{xy}u_{xx} - \alpha u_{yyy} - 2\beta g(t)u_{xxt} + h(t)u_{xxy} = 0, \tag{1}$$

where $g(t)$ and $h(t)$ are variable coefficients, which depending on time. The variable coefficients $g(t)$ and $h(t)$ may be caused by the geometrical and physical inhomogeneities, such as varying radius, material density, and so on. When $g(t) = 1$ and $h(t) = 0$, the Eq. (1) is reduced to the famous (2+1)-dimensional DJKM equation. Khalid et al. obtained the analytical soliton solutions of (1) [14]. Adem et al. acquired the complexiton solutions of (1) [15]. Yuan et al. gave N-soliton solutions in the Wronskian and Grammian [16]. Kang and Xia constructed abundant solutions of (1) [17].

The second equation is the (2+1)-dimensional variable coefficients shallow water wave equation (vcSWW) [18–20]:

$$u_{xt} + 2\alpha(t)u_xu_{xy} + \alpha(t)u_yu_{xx} + \beta(t)u_{xy} + \frac{1}{2}\rho\alpha(t)u_{xxxy} = 0. \tag{2}$$

When $\alpha(t) = -2$, $\beta(t) = \alpha$, $\rho = -1$, we obtain the (2+1)-dimensional extended shallow water wave equation [21]:

$$u_{xt} - 4u_xu_{xy} - 2u_yu_{xx} + \alpha u_{xy} + u_{xxxy} = 0, \tag{3}$$

where famous Korteweg-de Vries equation is obtained by assuming $x = y$ and $\beta(t) = 0$ in (2) [22, 23]:

$$u_{xt} - 6u_xu_{xx} + u_{xxxx} = 0. \tag{4}$$

The (2) is reduced to the (2+1)-dimensional breaking soliton equation [24], when $\alpha(t) = -2$, $\beta(t) = 0$, $\rho = -1$:

$$u_{xt} - 4u_xu_{xy} - 2u_yu_{xx} + u_{xxxy} = 0. \tag{5}$$

This article is arranged as follows: in Sect. 2, we use the exp-function method to solve the four types wave solutions of the (2+1)-dimensional vcDJKM equation

and draw corresponding figures. Similarly, in Sect. 3, we also use exp-function to solve four types wave solutions of the (2+1)-dimensional vcSWW equation, and draw corresponding figures. In Sect. 4, we make a brief summary of the previous research, and put forward some problems for future considerations.

## 2 Multi-wave Solutions of the (2+1)-Dimensional vcDJKM Equation

In this part, we will use exp-function method introduced in [6] to explore multi-wave solutions of the (2+1)-dimensional vcDJKM equation. For each wave solution, we take two different sets of parameters and plot corresponding 3D figures, density plots, and values of $x$ or $y$ for the given parameters.

### *2.1 One-Wave Solution*

We take the linear conditions,

$$\eta_{1,x} = k_1\eta_1, \eta_{1,y} = l_1\eta_1, \eta_{1,t} = -\omega_1(t)\eta_1, \tag{6}$$

with

$$\eta_1 = c_1 e^{k_1 x + l_1 y - \omega_1(t)}, \tag{7}$$

where $c_1$ is an arbitrary constant.

In order to gain one-wave solution of (1), we assume that the form of $p$ and $q$ are as follows:

$$p = a_0 + a_1\eta_1, q = b_0 + b_1\eta_1, \tag{8}$$

and the solution is a rational function,

$$u = \frac{p}{q}, \tag{9}$$

where $a_0, a_1, b_0$ and $b_1$ are constants. By applying Eq. (9) into Eq. (1), we obtain

$$a_1 = \frac{b_1(2k_1b_0 + a_0)}{b_0}, \omega_1 = -\int \frac{l_1(k_1^4 + k_1^2h(t) - l_1^2\alpha)}{2\beta k_1^2 g(t)}dt. \tag{10}$$

We take the parameter and the wave frequencies determined by (10) into (9), we get the one-wave solution of (1):

$$u = \frac{a_0 + \frac{b_1(2k_1b_0+a_0)}{b_0}c_1e^{k_1x+l_1y+\int \frac{l_1(k_1^4+k_1^2h(t)-l_1^2\alpha)}{2\beta k_1^2 g(t)}dt}}{b_0 + b_1c_1e^{k_1x+l_1y+\int \frac{l_1(k_1^4+k_1^2h(t)-l_1^2\alpha)}{2\beta k_1^2 g(t)}dt}}. \tag{11}$$

## 2.2 Two-Wave Solution

Similarly, we take the linear conditions,

$$\eta_{i,x} = k_i\eta_i, \eta_{i,y} = l_i\eta_i, \eta_{i,t} = -\omega_i(t)\eta_i, (1 \le i \le 2), \tag{12}$$

with

$$\eta_i = c_ie^{k_ix+l_iy-\omega_i(t)}, (1 \le i \le 2), \tag{13}$$

where $c_i$ $(1 \le i \le 2)$ are arbitrary constants.

In order to gain two-wave solution of (1), we assume that the form of $p$ and $q$ are as follows:

$$p = 2(k_1\eta_1 + k_2\eta_2 + a_{12}(k_1 + k_2)\eta_1\eta_2), q = 1 + \eta_1 + \eta_2 + a_{12}\eta_1\eta_2, \tag{14}$$

and

$$u = \frac{p}{q}, \tag{15}$$

where the $a_{12}$ is a constant will be determined later. We take (15) into (1), then we solve the algebraic system with Maple, and obtain the result

$$a_{12} = \frac{k_1^2k_2^2(k_1 - k_2)^2 + \alpha(k_1l_2 - k_2l_1)^2}{k_1^2k_2^2(k_1 + k_2)^2 + \alpha(k_1l_2 - k_2l_1)^2}, \tag{16}$$

and

$$\omega_1 = -\int \frac{l_1(k_1^4 + k_1^2h(t) - l_1^2\alpha)}{2\beta k_1^2 g(t)}dt, \omega_2 = -\int \frac{l_2(k_2^4 + k_2^2h(t) - l_2^2\alpha)}{2\beta k_2^2 g(t)}dt. \tag{17}$$

Then we gain the two-wave solution of (1) as:

$$u = \frac{2(k_1\eta_1 + k_2\eta_2 + a_{12}(k_1 + k_2)\eta_1\eta_2)}{1 + \eta_1 + \eta_2 + a_{12}\eta_1\eta_2}, \tag{18}$$

where $a_{12}$ is determined by (16), and $\omega_1, \omega_2$ are determined by (17).

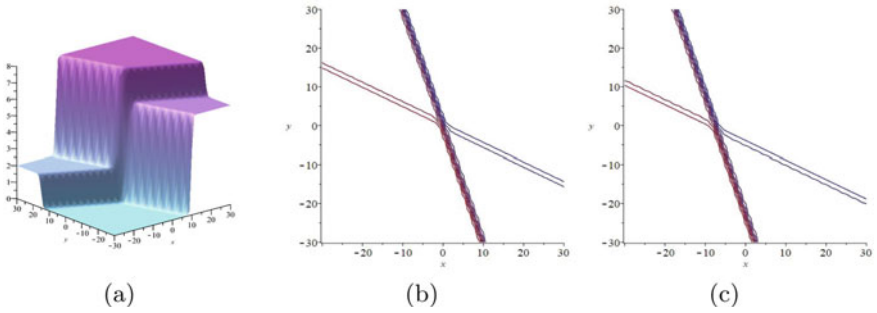


**Fig. 1** The two-wave solution of (1) with the parameters as $\alpha = \beta = c_1 = l_2 = k_1 = g(t) = 1, c_2 = l_1 = 2, k_2 = 3, h(t) = 6$. **a** 3D figure, **b** density plot at $t = 0$ and **c** density plot at $t = 3$

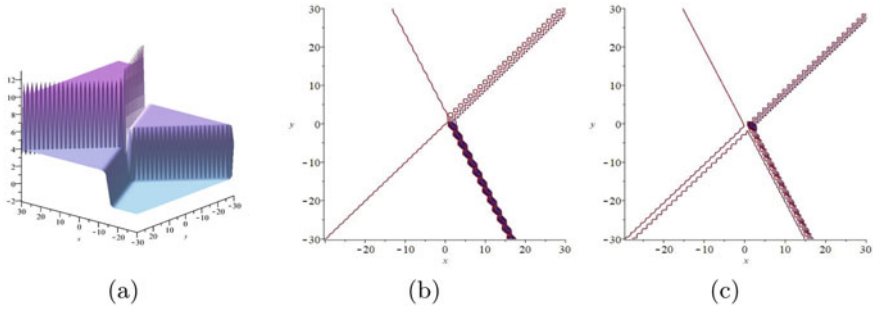


**Fig. 2** The two-wave solution of (1) with the parameters as $-\alpha = c_1 = l_1 = 1, \beta = c_2 = k_1 = 2, l_2 = -k_2 = -3, h(t) = tanh(t), g(t) = 6$. **a** 3D figure, **b** density plot at $t = 0$ and **c** density plot at $t = 3$

When taking the parameters as $\alpha = \beta = c_1 = l_2 = k_1 = g(t) = 1, c_2 = l_1 = 2, k_2 = 3, h(t) = 6$, the 3D figure and density plots of (18) are shown in Fig. 1. And Fig. 2 shows the 3D figure and density plots of (18) with the parameters as $-\alpha = c_1 = l_1 = 1, \beta = c_2 = k_1 = 2, l_2 = -k_2 = -3, h(t) = tanh(t), g(t) = 6$.

## 2.3 Three-Wave Solution

Similarly, we choose the linear conditions,

$$\eta_{i,x} = k_i \eta_i, \eta_{i,y} = l_i \eta_i, \eta_{i,t} = -\omega_i(t)\eta_i, (1 \le i \le 3), \tag{19}$$

with

$$\eta_i = c_i e^{k_i x + l_i y - \omega_i(t)}, (1 \le i \le 3), \tag{20}$$

where $c_i$ $(1 \le i \le 3)$ are arbitrary constants.

In order to describe the three-wave solution of (1), we assume that

$$\begin{aligned} p = 2(k_1\eta_1 + k_2\eta_2 + k_3\eta_3 + a_{12}(k_1 + k_2)\eta_1\eta_2 + a_{13}(k_1 + k_3)\eta_1\eta_3 \\ + a_{23}(k_2 + k_3)\eta_2\eta_3 + a_{12}a_{13}a_{23}(k_1 + k_2 + k_3)\eta_1\eta_2\eta_3), \end{aligned} \tag{21}$$

and

$$q = 1 + \eta_1 + \eta_2 + \eta_3 + a_{12}\eta_1\eta_2 + a_{13}\eta_1\eta_3 + a_{23}\eta_2\eta_3 + a_{12}a_{13}a_{23}\eta_1\eta_2\eta_3, \tag{22}$$

in addition to this, we have three-wave solution,

$$u = \frac{p}{q}. \tag{23}$$

Just like before, we take (23) into (1), then we solve the algebraic system with Maple, and we obtain

$$a_{ij} = \frac{k_i^2 k_j^2 (k_i - k_j)^2 + \alpha(k_i l_j - k_j l_i)^2}{k_i^2 k_j^2 (k_i + k_j)^2 + \alpha(k_i l_j - k_j l_i)^2}, (1 \le i < j \le 3), \tag{24}$$

with the wave frequencies

$$\omega_i = -\int \frac{l_i(k_i^4 + k_i^2 h(t) - l_i^2\alpha)}{2\beta k_i^2 g(t)} dt, (1 \le i \le 3). \tag{25}$$

In the form of (24) and (25), it is easy to get three-wave solution to (1). We provide two examples where $h(t)$ and $g(t)$ go to special functions. We also obtain 3D figures and corresponding density maps of the two states of (1) with different parameters. At the same time, we also draw the value graph of $x$ with different values of $y$ to study the trend of $x$. Figure 3 shows the pictures of (23) with the parameters as $\alpha = \beta =$

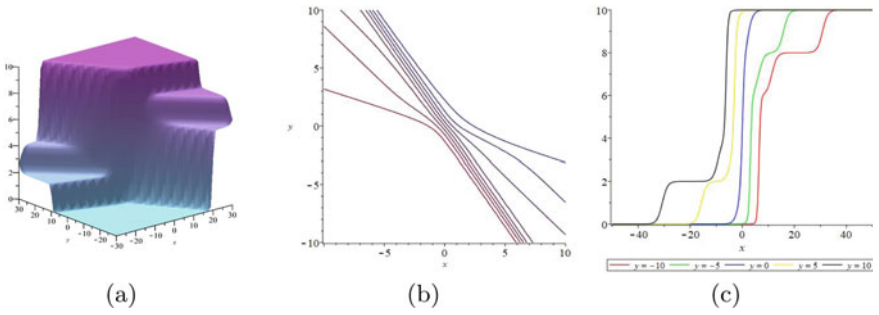


**Fig. 3** The pictures of (23) with the parameters as $\alpha = \beta = c_1 = l_1 = k_1 = k_3 = g(t) = 1, c_2 = l_2 = c_3 = 2, l_3 = k_2 = 3, h(t) = 6$. **a** 3D figure, **b** density plot at $t = 0$, **c** the value graph of $x$ with different values of $y$

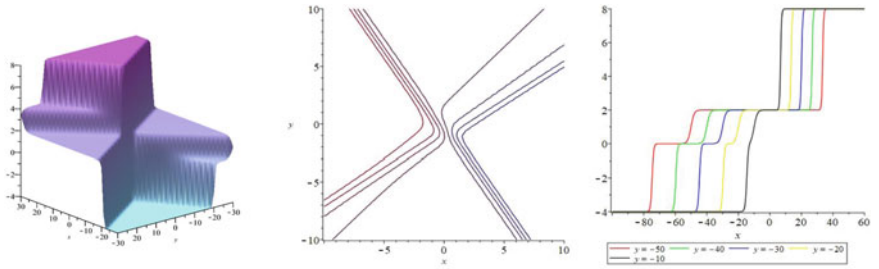


**Fig. 4** The pictures of (23) with the parameters as $\alpha = \beta = -l_1 = k_1 = c_1 = 1, c_2 = l_2 = c_3 = -k_3 = 2, l_3 = k_2 = g(t) = 3, h(t) = cos(t)$. **a** 3D figure, **b** density plot at $t = 0$, **c** the value graph of $x$ with different values of $y$

$c_1 = l_1 = k_1 = k_3 = g(t) = 1, c_2 = l_2 = c_3 = 2, l_3 = k_2 = 3, h(t) = 6$. And Fig. 4 shows the pictures of (23) with the parameters as $\alpha = \beta = -l_1 = k_1 = c_1 = 1, c_2 = l_2 = c_3 = -k_3 = 2, l_3 = k_2 = g(t) = 3, h(t) = cos(t)$.

## 2.4 Four-Wave Solution

Again, we choose the linear conditions,

$$\eta_{i,x} = k_i \eta_i, \eta_{i,y} = l_i \eta_i, \eta_{i,t} = -\omega_i(t)\eta_i, (1 \le i \le 4), \tag{26}$$

with

$$\eta_i = c_i e^{k_i x + l_i y - \omega_i(t)}, (1 \le i \le 4), \tag{27}$$

where $c_i$ $(1 \le i \le 4)$ are arbitrary constants.

Let us try the polynomial form of the four-wave solution,

$$\begin{aligned} p = {} & 2(k_1\eta_1 + k_2\eta_2 + k_3\eta_3 + k_4\eta_4 + a_{12}(k_1 + k_2)\eta_1\eta_2 + a_{13}(k_1 + k_3)\eta_1\eta_3 \\ & + a_{14}(k_1 + k_4)\eta_1\eta_4 + a_{23}(k_2 + k_3)\eta_2\eta_3 + a_{24}(k_2 + k_4)\eta_2\eta_4 + a_{34}(k_3 + k_4)\eta_3\eta_4 \\ & + a_{12}a_{13}a_{23}(k_1 + k_2 + k_3)\eta_1\eta_2\eta_3 + a_{13}a_{14}a_{34}(k_1 + k_3 + k_4)\eta_1\eta_3\eta_4 \\ & + a_{12}a_{14}a_{24}(k_1 + k_2 + k_4)\eta_1\eta_2\eta_4 + a_{23}a_{24}a_{34}(k_2 + k_3 + k_4)\eta_2\eta_3\eta_4), \end{aligned} \tag{28}$$

and

$$\begin{aligned} q = {} & 1 + \eta_1 + \eta_2 + \eta_3 + \eta_4 + a_{12}\eta_1\eta_2 + a_{13}\eta_1\eta_3 + a_{14}\eta_1\eta_4 + a_{23}\eta_2\eta_3 \\ & + a_{24}\eta_2\eta_4 + a_{34}\eta_3\eta_4 + a_{12}a_{13}a_{23}\eta_1\eta_2\eta_3 + a_{13}a_{14}a_{34}\eta_1\eta_3\eta_4 \\ & + a_{12}a_{14}a_{24}\eta_1\eta_2\eta_4 + a_{23}a_{24}a_{34}\eta_2\eta_3\eta_4, \end{aligned} \tag{29}$$

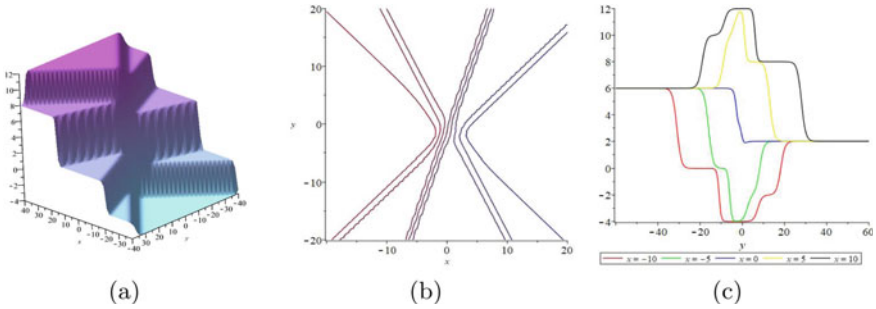


**Fig. 5** The pictures of (30) with the parameters as $\alpha = \beta = -l_1 = l_2 = l_4 = k_4 = c_1 = c_3 = 1, c_2 = c_4 = k_2 = -k_3 = l_3 = 2, k_1 = 3, g(t) = \frac{1}{t^2}, h(t) = sin(t)$. **a** 3D figure, **b** density plot at $t = 0$, **c** the value graph of $x$ with different values of $y$

in addition to this, we have four-wave solution,

$$u = \frac{p}{q}. \tag{30}$$

By the multiple exp-function method and using the linear conditions, we acquire the solution with Maple,

$$a_{ij} = \frac{k_i^2 k_j^2 (k_i - k_j)^2 + \alpha(k_i l_j - k_j l_i)^2}{k_i^2 k_j^2 (k_i + k_j)^2 + \alpha(k_i l_j - k_j l_i)^2}, (1 \le i < j \le 4), \tag{31}$$

and the wave frequencies,

$$\omega_i = -\int \frac{l_i(k_i^4 + k_i^2 h(t) - l_i^2 \alpha)}{2\beta k_i^2 g(t)} dt, (1 \le i \le 4). \tag{32}$$

Two specific solutions of the four-wave solution are plotted in Figs. 5 and 6. In each figure, the first plot is three-dimensional diagram, and the other plots demonstrate the $y$-curves with different $x$-values at $t = 0$. The results show that when time is constant, the peak value of $y$ increases with the increase of $x$.

## 3 Multi-wave Solutions of the (2+1)-Dimensional vcSWW Equation

In this part, we will also use exp-function method introduced in [6] to study the (2+1)-dimensional vcSWW equation. When $\rho = 1$, (2) becomes

$$u_{xt} + 2\alpha(t)u_x u_{xy} + \alpha(t)u_y u_{xx} + \beta(t)u_{xy} + \frac{1}{2}\alpha(t)u_{xxxy} = 0, \tag{33}$$

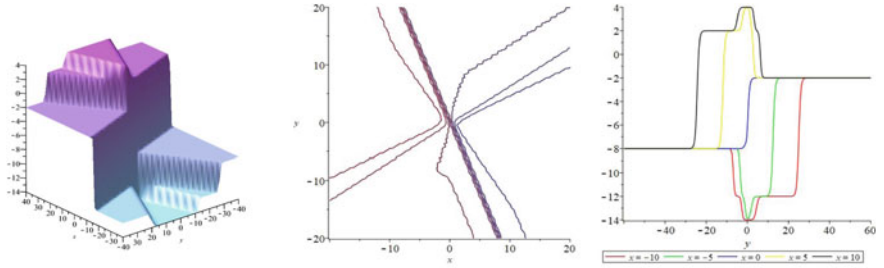


**Fig. 6** The pictures of (30) with the parameters as $\alpha = k_1 = k_3 = c_1 = c_3 = 1, -\beta = c_2 = c_4 = -k_2 = l_3 = l_4 = g(t) = 2, l_1 = -l_2 = -3, h(t) = t$. **a** 3D figure, **b** density plot at $t = 0$, **c** the value graph of $x$ with different values of $y$

we call (33) as the new (2+1)-dimensional variable coefficient shallow water wave equation (vcsww).

Next, in this section, we will use the exp-function to explore the multi-wave solutions of (33). For each wave solution we also take two different sets of parameters and plot corresponding figures.

## *3.1 One-Wave Solution*

We obtain the linear conditions,

$$\eta_{1,x} = k_1\eta_1, \eta_{1,y} = l_1\eta_1, \eta_{1,t} = -\omega_1(t)\eta_1, \tag{34}$$

with

$$\eta_1 = c_1 e^{k_1 x + l_1 y - \omega_1(t)}, \tag{35}$$

where $c_1$ is arbitrary constant.

In order to obtain one-wave solution of (33), we assume that the form of $p$ and $q$ are as follow:

$$p = a_0 + a_1\eta_1, q = b_0 + b_1\eta_1, \tag{36}$$

and the solution is the rational function,

$$u = \frac{p}{q}, \tag{37}$$

where $a_0, a_1, b_0$, and $b_1$ are constants. By applying Eq. (37) into Eq. (2), we obtain

$$a_1 = \frac{b_1(2k_1b_0 + a_0)}{b_0}, \omega_1 = \int \frac{l_1\alpha(t)k_1^2}{2} + l_1\beta(t)dt. \tag{38}$$

We take the parameter and the wave frequencies determined by (38) into (37), the one-wave solution of (33) is

$$u = \frac{a_0 + \frac{b_1(2k_1b_0+a_0)}{b_0}c_1e^{k_1x+l_1y-\frac{b_1(2k_1b_0+a_0)}{b_0}}}{b_0 + b_1c_1e^{k_1x+l_1y-\frac{b_1(2k_1b_0+a_0)}{b_0}}}. \tag{39}$$

### 3.2 Two-Wave Solution

Similarly, we take the linear conditions,

$$\eta_{i,x} = k_i\eta_i, \eta_{i,y} = l_i\eta_i, \eta_{i,t} = -\omega_i(t)\eta_i, (1 \le i \le 2), \tag{40}$$

with

$$\eta_i = c_ie^{k_ix+l_iy-\omega_i(t)}, (1 \le i \le 2), \tag{41}$$

where $c_i$ $(1 \le i \le 2)$ are arbitrary constants.

In order to gain two-wave solution of (33), we assume that the form of $p$ and $q$ are as follow:

$$p = 2(k_1\eta_1 + k_2\eta_2 + a_{12}(k_1 + k_2)\eta_1\eta_2), q = 1 + \eta_1 + \eta_2 + a_{12}\eta_1\eta_2, \tag{42}$$

and

$$u = \frac{p}{q}, \tag{43}$$

where the $a_{12}$ is constant will be determined later. We take (43) into (33), then we solve the algebraic system with Maple, and obtain the result,

$$a_{12} = \frac{(k_1 - k_2)^2}{(k_1 + k_2)^2}, \tag{44}$$

and

$$\omega_1 = \int \frac{l_1\alpha(t)k_1^2}{2} + l_1\beta(t)dt, \omega_2 = \int \frac{l_2\alpha(t)k_2^2}{2} + l_2\beta(t)dt. \tag{45}$$

Then we gain the two-wave solution of (1) as:

$$u = \frac{2(k_1\eta_1 + k_2\eta_2 + a_{12}(k_1 + k_2)\eta_1\eta_2)}{1 + \eta_1 + \eta_2 + a_{12}\eta_1\eta_2}, \tag{46}$$

where $a_{12}$ is determined by (44), and $\omega_1$, $\omega_2$ is determined by (45).

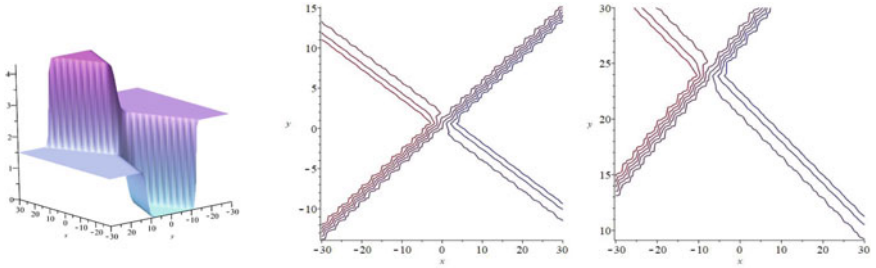


**Fig. 7** The two-wave solution of (33) with the parameters as $l_1 = 2, k_1 = \frac{3}{4}, l_2 = -3, k_2 = \frac{7}{5}, \alpha(t) = sinh(t), \beta(t) = 6, c_1 = 1, c_2 = 1.5$. **a** 3D figure, **b** density plot at $t = 0$ and **c** density plot at $t = 3$

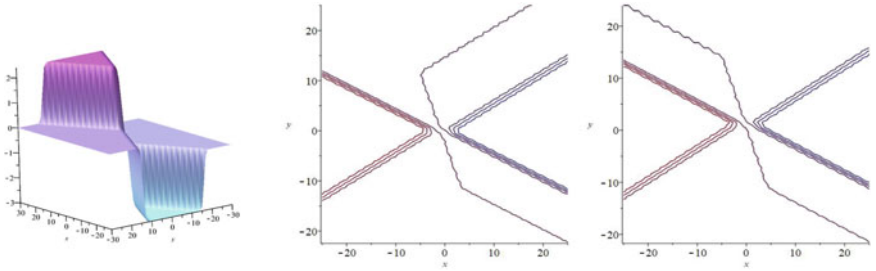


**Fig. 8** The two-wave solution of (33) with the parameters as $l_1 = -3, k_1 = -1.5, l_2 = -2, k_2 = 1.2, \alpha(t) = sin(t), \beta(t) = cos(t), c_1 = 1, c_2 = 1.5$. **a** 3D figure, **b** density plot at $t = 0$ and **c** density plot at $t = 3$

When taking the parameters as $l_1 = 2, k_1 = \frac{3}{4}, l_2 = -3, k_2 = \frac{7}{5}, \alpha(t) = sinh(t), \beta(t) = 6, c_1 = 1, c_2 = 1.5$, the 3D figure and density plots of (46) are shown in Fig. 7. And Fig. 8 shows the 3D figure and density plots of (46) with the parameters as $l_1 = -3, k_1 = -1.5, l_2 = -2, k_2 = 1.2, \alpha(t) = sin(t), \beta(t) = cos(t), c_1 = 1, c_2 = 1.5$.

### *3.3 Three-Wave Solution*

Similarly, we choose the linear conditions,

$$\eta_{i,x} = k_i \eta_i, \eta_{i,y} = l_i \eta_i, \eta_{i,t} = -\omega_i(t)\eta_i, (1 \leq i \leq 3), \tag{47}$$

with

$$\eta_i = c_i e^{k_i x + l_i y - \omega_i(t)}, (1 \leq i \leq 3), \tag{48}$$

where $c_i$ $(1 \leq i \leq 3)$ are arbitrary constants.

In order to describe the three-wave solution of (33), we assume that

$$\begin{aligned} p = {} & 2(k_1\eta_1 + k_2\eta_2 + k_3\eta_3 + a_{12}(k_1 + k_2)\eta_1\eta_2 + a_{13}(k_1 + k_3)\eta_1\eta_3 \\ & + a_{23}(k_2 + k_3)\eta_2\eta_3 + a_{12}a_{13}a_{23}(k_1 + k_2 + k_3)\eta_1\eta_2\eta_3), \end{aligned} \tag{49}$$

and

$$q = 1 + \eta_1 + \eta_2 + \eta_3 + a_{12}\eta_1\eta_2 + a_{13}\eta_1\eta_3 + a_{23}\eta_2\eta_3 + a_{12}a_{13}a_{23}\eta_1\eta_2\eta_3, \tag{50}$$

in addition to this, we have three-wave solution,

$$u = \frac{p}{q}. \tag{51}$$

Just like before, we take (51) into (33), then we solve the algebraic system with Maple, and we obtain,

$$a_{ij} = \frac{(k_i - k_j)^2}{(k_i + k_j)^2}, (1 \leq i < j \leq 3), \tag{52}$$

with the wave frequencies,

$$\omega_i = \int \frac{l_i \alpha(t) k_i^2}{2} + l_i \beta(t) dt, (1 \leq i \leq 3). \tag{53}$$

In the form of (52) and (53), it is easy to get three-wave solution of (33). We provide two examples where $\alpha(t)$ and $\beta(t)$ go to special functions. We also obtain 3D figures and corresponding density maps of the two states of (33) with different parameters. At the same time, we also draw the value graph of $x$ with different values of $y$ to study the trend of $x$. Figure 9 shows the pictures of (51) with the parameters as $l_1 = -\frac{3\sqrt{2}}{8}, k_1 = \frac{3}{4}, l_2 = -\frac{3\sqrt{2}}{4}, k_2 = 5, l_3 = -\frac{5}{6}, k_3 = \frac{5}{12}, \alpha(t) = 1, \beta(t) = 4\sqrt{2}, c_1 = 0.5, c_2 = 0.8, c_3 = 1.2$. And Fig. 10 shows the pictures of (51) with the parameters as $l_1 = -\frac{5}{8}, k_1 = \frac{7}{4}, l_2 = -\frac{3}{4}, k_2 = -\frac{3}{5}, l_3 = -\frac{11}{6}, k_3 = \frac{7}{12}, \alpha(t) = t, \beta(t) = sin(t), c_1 = 0.5, c_2 = 0.8, c_3 = 1.2$.

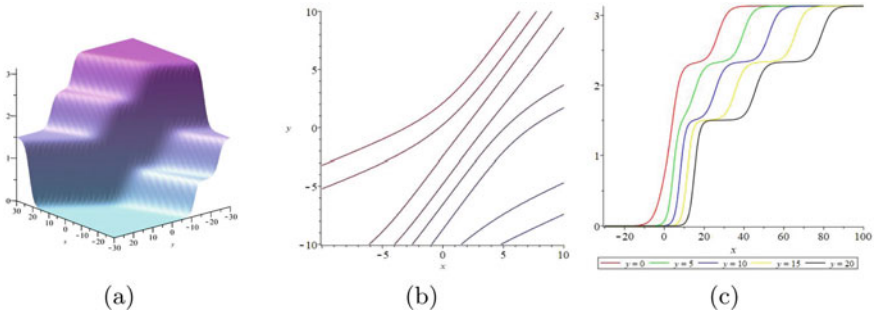


**Fig. 9** The pictures of (51) with the parameters as $l_1 = -\frac{3\sqrt{2}}{8}, k_1 = \frac{3}{4}, l_2 = -\frac{3\sqrt{2}}{4}, k_2 = 5, l_3 = -\frac{5}{6}, k_3 = \frac{5}{12}, \alpha(t) = 1, \beta(t) = 4\sqrt{2}, c_1 = 0.5, c_2 = 0.8, c_3 = 1.2$. **a** 3D figure, **b** density plot at $t = 0$, **c** the value graph of $x$ with different values of $y$

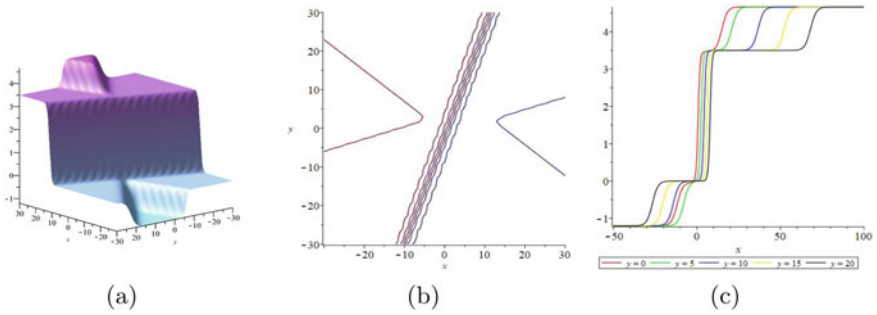


**Fig. 10** The pictures of (51) with the parameters as $l_1 = -\frac{5}{8}, k_1 = \frac{7}{4}, l_2 = -\frac{3}{4}, k_2 = -\frac{3}{5}, l_3 = -\frac{11}{6}, k_3 = \frac{7}{12}, \alpha(t) = t, \beta(t) = sin(t), c_1 = 0.5, c_2 = 0.8, c_3 = 1.2$. **a** 3D figure, **b** density plot at $t = 0$, **c** the value graph of $x$ with different values of $y$

## *3.4 Four-Wave Solution*

Again, we choose the linear conditions,

$$\eta_{i,x} = k_i \eta_i, \eta_{i,y} = l_i \eta_i, \eta_{i,t} = -\omega_i(t)\eta_i, (1 \le i \le 4), \tag{54}$$

with

$$\eta_i = c_i e^{k_i x + l_i y - \omega_i(t)}, (1 \le i \le 4), \tag{55}$$

where $c_i$ $(1 \le i \le 4)$ are arbitrary constants.

Let us try the polynomial form of the four-wave solution,

$$
\begin{aligned}
p = {} & 2(k_1\eta_1 + k_2\eta_2 + k_3\eta_3 + k_4\eta_4 + a_{12}(k_1 + k_2)\eta_1\eta_2 + a_{13}(k_1 + k_3)\eta_1\eta_3 \\
& + a_{14}(k_1 + k_4)\eta_1\eta_4 + a_{23}(k_2 + k_3)\eta_2\eta_3 + a_{24}(k_2 + k_4)\eta_2\eta_4 + a_{34}(k_3 + k_4)\eta_3\eta_4 \\
& + a_{12}a_{13}a_{23}(k_1 + k_2 + k_3)\eta_1\eta_2\eta_3 + a_{13}a_{14}a_{34}(k_1 + k_3 + k_4)\eta_1\eta_3\eta_4 \\
& + a_{12}a_{14}a_{24}(k_1 + k_2 + k_4)\eta_1\eta_2\eta_4 + a_{23}a_{24}a_{34}(k_2 + k_3 + k_4)\eta_2\eta_3\eta_4),
\end{aligned} \tag{56}
$$

and

$$
\begin{aligned}
q = {} & 1 + \eta_1 + \eta_2 + \eta_3 + \eta_4 + a_{12}\eta_1\eta_2 + a_{13}\eta_1\eta_3 + a_{14}\eta_1\eta_4 + a_{23}\eta_2\eta_3 \\
& + a_{24}\eta_2\eta_4 + a_{34}\eta_3\eta_4 + a_{12}a_{13}a_{23}\eta_1\eta_2\eta_3 + a_{13}a_{14}a_{34}\eta_1\eta_3\eta_4 \\
& + a_{12}a_{14}a_{24}\eta_1\eta_2\eta_4 + a_{23}a_{24}a_{34}\eta_2\eta_3\eta_4,
\end{aligned} \tag{57}
$$

in addition to this, we have four-wave solution,

$$u = \frac{p}{q}. \tag{58}$$

By the exp-function method and using the linear conditions, we acquire the solution with Maple,

$$a_{ij} = \frac{(k_i - k_j)^2}{(k_i + k_j)^2}, (1 \le i < j \le 4), \tag{59}$$

with the wave frequencies

$$\omega_i = \int \frac{l_i\alpha(t)k_i^2}{2} + l_i\beta(t)dt, (1 \le i \le 4). \tag{60}$$

Two specific solutions of those four-wave solution are plotted in Figs. 11 and 12. In each figure, the first plot is three-dimensional diagram, the second plot is density plot, and the third plot exhibits the $x$-curves at $t = 0$. Figure 11 shows the pictures

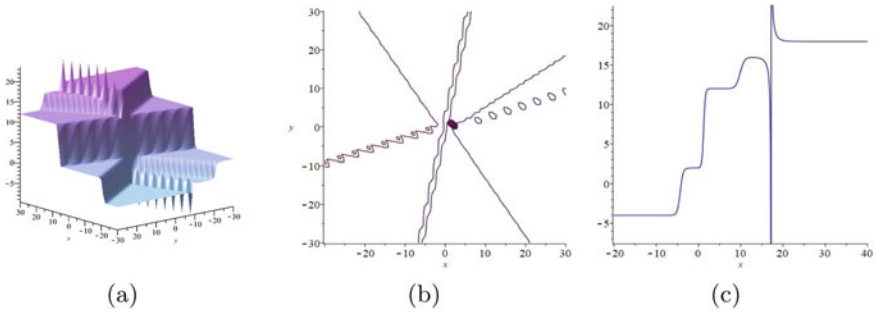


**Fig. 11** The pictures of (58) with the parameters as $-l_2 = k_4 = c_2 = c_4 = 1, l_1 = -k_3 = \beta(t) = 2, k_1 = l_3 = -l_4 = 3, \alpha(t) = 4, k_2 = 5, c_1 = c_3 = 0.8$. **a** 3D figure, **b** density plot at $t = 0$, **c** the value graph of $x$ with $y = 5$ at $t = 0$

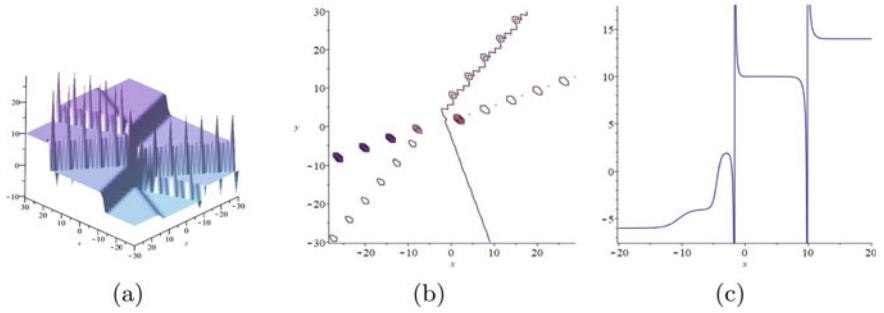


**Fig. 12** The pictures of (58) with the parameters as $l_2 = -k_4 = 1, -k_1 = -l_4 = \beta(t) = c_2 = c_4 = 2, k_2 = -l_3 = 3, k_3 = 4, l_1 = 5, c_1 = c_3 = -0.5, \alpha(t) = sinh(t)$. **a** 3D figure, **b** density plot at $t = 0$, **c** the value graph of $x$ with $y = 5$ at $t = 0$

of (58) with the parameters as $-l_2 = k_4 = c_2 = c_4 = 1, l_1 = -k_3 = \beta(t) = 2, k_1 = l_3 = -l_4 = 3, \alpha(t) = 4, k_2 = 5, c_1 = c_3 = 0.8$. And Fig. 12 shows the pictures of (58) with the parameters as $l_2 = -k_4 = 1, -k_1 = -l_4 = \beta(t) = c_2 = c_4 = 2, k_2 = -l_3 = 3, k_3 = 4, l_1 = 5, c_1 = c_3 = -0.5, \alpha(t) = sinh(t)$.

## 4 Conclusions

In this paper, we study the (2+1)-dimensional vcDJKM equation and the (2+1)-dimensional vcsww equation. According to the exp-function method, we obtain the one-wave solution, two-wave solution, three-wave solution and four-wave solution of the two equations respectively, and we take two sets of different values for the variable coefficients to enrich their various states. The results show that both equations have multi-wave solution determined by $p$ and $q$.

The nonlinear equations with variable coefficients can describe the physical linearity more accurately than the general equations, so they have more research value. As far as we know, the content of using this method to study variable coefficient equation is not very much. Since we have given the forms of $p$ and $q$, the obtained solutions are solitonic, so the forms of the solutions are very limited. Therefore, it is worth studying the different forms of $p$ and $q$. The solutions obtained here are soliton-type, and we can introduce a very powerful formula for soliton solutions in [25–34]:

$$f = \sum_{\mu=0,1} exp(\sum_{j=1}^{N} \mu_j \eta_j + \sum_{1 \le i < j \le N}^{N} \mu_i \mu_j \theta_{ij}). \tag{61}$$

In addition, we only have four types of wave solutions for the two equations, and perhaps there are other types of wave solutions for these equations, which we have yet to solve. We hope that our conclusions can enrich the literature which study the behavior of nonlinear evolution equations.

## References


1. Wang, M.L., Zhou, Y.B., Li, Z.B.: Application of a homogeneous balance method to exact solutions of nonlinear equations in mathematical physics. Phys. Lett. A. **216**, 67–75 (1996)
2. Wazwaz, A.M.: A sine-cosine method for handlingnonlinear wave equations. Mathl. Comput. Modelling. **40**, 499–508 (2004)
3. Liu, S.K., Fu, Z.T., Liu, S.D., Zhao, Q.: Jacobi elliptic function expansion method and periodic wave solutions of nonlinear wave equations. Phys. Lett. A. **289**, 69–74 (2001)
4. Zeng, X., Yong, X.L.: A new mapping method and its applications to nonlinear partial differential equations. Phys. Lett. A. **372**, 6602–6607 (2008)
5. Wang, M.L., Li, X.Z.: Extended F-expansion method and periodic wave solutions for the generalized Zakharov equations. Phys. Lett. A. **343**, 48–54 (2005)
6. Ma, W.X., Huang, T.W., Zhang, Y.: A multiple exp-function method for nonlinear differential equations and its application. Phys. Scr. **82**, (2010)
7. Darvishi, M.T., Najafi, M., Najafi, M.: Application of multiple exp-function method to obtain multi-soliton solutions of (2+1)-and (3+1)-dimensional breaking soliton equations. Am. J. Comput. Appl. Math. **1**(2), 41–47 (2011)
8. Ma, W.X., Zhu, Z.N.: Solving the (3+1)-dimensional generalized KP and BKP equations by the multiple exp-function algorithm. Appl. Math. Comput. **218**, 11871–11879 (2012)
9. Adem, A.R.: The generalized (1+1)-dimensional and (2+1)-dimensional Ito equations: Multiple exp-function algorithm and multiple wave solutions. Comput. Math. Appl. **71**, 1248–1258 (2016)
10. Wan, P.B., Manafian, J., Ismael, H.F., Mohammed, S.A.: Investigating one-, two-, and triple-wave solutions via multiple exp-function method arising in engineering sciences. Adv. Math. Phys. **2020**, 8018064 (2020)
11. Nisar, K.S., Ilhan, O.A., Abdulazeez, S.T., Manafian, J., Mohammed, S.A., Osman, M.S.: Novel multiple soliton solutions for some nonlinear pdes via multiple exp-function method. Result. Phys. **21**, 103769 (2021)
12. Date, E., Jimbo, M., Kashiwara, M., Miwa, T.: Transformation groups for soliton equations: Iv. A new hierarchy of soliton equations of KP-type. Phys. D. **4**, 343–365 (1982)
13. Wazwaz, A.M.: A (2+1)-dimensional time-dependent Date–Jimbo–Kashiwara–Miwa equation: Painlevé integrability and multiple soliton solutions. Comput. Math. Appl. **79**, 1145–1149 (2020)
14. Ali, K.K., Mehanna, M.S., Wazwaz, A.M.: Analytical and numerical treatment to the (2+1)-dimensional Date-Jimbo-Kashiwara-Miwa equation. N.a. Eng. **10**(1), 187–200 (2021)
15. Adem, A.R., Yildirim, Y., Yaşar, E.: Complexiton solutions and soliton solutions: (2+1)-dimensional Date-Jimbo-Kashiwara-Miwa equation. Pramana. **92**, (2019)
16. Yuan, Y.Q., Tian, B., Sun, W.R., Chai, J., Liu, L.: Wronskian and grammian solutions for a (2+1)-dimensional Date-Jimbo-Kashiwara-Miwa equation. Comput. Math. Appl. **74**, 873–879 (2017)
17. Kang, Z.Z., Xia, T.C.: Construction of abundant solutions of the (2+1)-dimensional time-dependent Date-Jimbo-Kashiwara-Miwa equation. Appl. Math. Lett. **103**, 106163 (2020)
18. Xin, X.P., Zhang, L.L., Xia, Y.R., Liu, H.Z.: Nonlocal symmetries and exact solutions of the (2+1)-dimensional generalized variable coefficient shallow water wave equation. Appl. Math. Lett. **94**, 112–119 (2019)

19. Lan, Z.Z., Gao, Y.T., Yang, J.W., Su, C.Q., Zuo, D.W.: Solitons, bäcklund transformation, lax pair, and infinitely many conservation law for a (2+1)-dimensional generalised variable-coefficient shallow water wave equation. Z. Naturforsch. **71**(1), 69–79 (2016)
20. Tian, B., Shan, W.R., Zhang, C.Y., Wei, G.M., Gao, Y.T.: Transformations for a generalized variable-coefficient nonlinear schrödinger model from plasma physics, arterial mechanics and optical fibers with symbolic computation. Eur. Phys. J. B. **47**, 329–332 (2005)
21. Wang, Y.H., Wang, H., Zhang, H.S.,and Temuer C.L.: Exact interaction solutions of an extended (2+1)-dimensional shallow water wave equation. Commun. Theor. Phys. **68**(2), (2017)
22. Nijhoff, F., Capel, H.: The discrete Korteweg-de Vries equation. N.a. Appl. Math. **39**, 133–158 (1995)
23. Boiti, M., Pempinelli, F.: Similarity solutions of the Korteweg-de Vries equation. Il Nuovo Cimento B (1971-1996). **51**, 70–78 (1979)
24. Chen, Y., Li, B., Zhang, H.Q.: Symbolic computation and construction of soliton-like solutions to the (2+1)-dimensional breaking soliton equation. Commun. Theor. Phys. **40**(2), (2003)
25. Liu, Y.Q., Wen, X.Y., Wang, D.S.: The N-soliton solution and localized wave interaction solutions of the (2+1)-dimensional generalized Hirota-Satsuma-Ito equation. Comput. Math. Appl. **77**, 947–966 (2019)
26. Dong, J.J., Li, B., Yuen, M.W.: Soliton molecules and mixed solutions of the (2+1)-dimensional bidirectional Sawada–Kotera equation. Commun. Theor. Phys. **72**(2), 025002 (2020)
27. Zhang, Z., Yang, S.X., Li, B.: Soliton molecules, asymmetric solitons and hybrid solutions for (2+1)-dimensional fifth-order KdV equation. Chin. Phys. Lett. **36**(12), 120501 (2019)
28. Ma, H.C., Cheng, Q.X., Deng, A.P.: Soliton molecules and some novel hybrid solutions for the (2+1)-dimensional generalized Konopelchenko–Dubrovsky–Kaup–Kupershmidt equation. Commun. Theor. Phys. **72**(9), 095001 (2020)
29. Ma, H.C., Cheng, Q.X., Deng, A.P.: Solitons, breathers, and lump solutions to the (2+1)-dimensional generalized Calogero–Bogoyavlenskii–Schiff equation. Complex. **2021**, 7264345 (2021)
30. Ma, H.C., Cheng, Q.X., Deng, A.P.: Soliton molecules, asymmetric soliton and some novel hybrid solutions for the isospectral BKP equation. Mod. Phys. Lett. B. **35**(10), 2150174 (2021)
31. Ma, H.C., Wang, Y.X., Deng, A.P.: Soliton molecules and some novel mixed solutions for the extended Caudrey-Dodd-Gibbon equation. J. Geom. Phys. **168**, 104309 (2021)
32. Ma, H.C., Huang, H.Y., Deng, A.P.: Soliton molecules and some interaction solutions for the (3+1)-dimensional Jimbo-Miwa equation. J. Geom. Phys. **170**, 104362 (2021)
33. Ma, H.C., Huang, H.Y., Deng, A.P.: Soliton molecules and some novel hybrid solutions for (3+1)-dimensional B-type Kadomtsev–Petviashvili equation. Mod. Phys. Lett. B. **35**(23), 2150388 (2021)
34. Ma, H.C., Huang, H.Y., Deng, A.P.: Solitons and soliton molecules in two nonlocal alice-bob fifth-order KdV systems. Int. J. Appl. Comput. Math. **60**, 3051–3062 (2021)

# Nonlocal Integrable Equations in Soliton Theory


**Wen-Xiu Ma**

**Abstract** This article is to provide a brief overview of the study of nonlocal integrable equations in soliton theory. The concept of nonlocality is explained, a little history of nonlocal dynamics is given, and basic problems of nonlocal differential equations are discussed. With the AKNS matrix spectral problems being taken as examples, a classification of the corresponding nonlocal integrable NLS equations and mKdV equations is presented. The identification of those nonlocal integrable equations is made within the zero curvature formulation, where local and nonlocal group reductions of matrix spectral problems are carefully conducted in pairs. Illustrative integrable models include six couples of scalar nonlocal integrable NLS equations and five couples of scalar nonlocal integrable mKdV equations.

**Keywords** Matrix spectral problem · Zero curvature equation · Nonlocal integrable equation · NLS equations · mKdV equations

**2010 Mathematics Subject Classification** 37K15 · 35Q55 · 37K40

## 1 What About?

In mathematics, local and nonlocal concepts are balanced, particularly in calculus. For a local operator $A$ acting on functions, it is possible, in principle, to compute the value $(Au)(x)$ using only knowledge of the values of $u$ in an arbitrarily small

W.-X. Ma (✉)
Department of Mathematics, Zhejiang Normal University, Jinhua 321004, Zhejiang, China
e-mail: mawx@cas.usf.edu

Department of Mathematics, King Abdulaziz University, Jeddah 21589, Saudi Arabia

Department of Mathematics and Statistics, University of South Florida, Tampa, FL 33620-5700, USA

Material Science Innovation and Modelling, North-West University, Mafikeng Campus, Private Bag X2046, Mmabatho 2735, South Africa



S. Manukure and W.-X. Ma (eds.), *Nonlinear and Modern Mathematical Physics*,
Springer Proceedings in Mathematics & Statistics 459,
https://doi.org/10.1007/978-3-031-59539-4_11

neighborhood of a point $x$. For a nonlocal operator, this is not possible. In calculus, two basic operations are differentiation and integration. The first is local and the second is nonlocal.

In the theory of differential equations, a nonlocal differential equation is a kind of mathematical equation that describes the evolution of a system with a nonlocal interaction. Unlike local equations, which describe the evolution of a system at a specific point in space and time, nonlocal equations take into account the interaction of the system with its big environment. The ordinary differential equation (ODE) $y' = y$ is local, but the ODE $y' = y(-t)$ is nonlocal, since its motion at time $t$ depends on two times, $t$ and $-t$. It remains open how to solve such general linear nonlocal ODEs, even with constant coefficients. The partial differential equation (PDE) $u_t = u_{xx}$ is local, and similarly, the PDE $u_t = u_{xx}(-x, -t)$ is nonlocal. The first is the heat equation, a prototypical equation in mathematical physics. The second one provides solutions to the linearized Boussinesq equation $u_{tt} + u_{xxxx} = 0$, which describes a vibrating elastic beam; but yet, its well-posedness theory has not been established.

In a nonlinear world, by integrable equations, we mean a kind of nonlinear ODEs and PDEs. An integrable ODE is a Hamiltonian equation defined on a $2n$-dimensional symplectic manifold, which possesses $n$ independent constants of motion commuting under the corresponding Poisson bracket [1]. A PDE is called to be integrable, if its eigenfunctions of associated linear problems, known as Lax pairs [2], provide a complete set of functions in a normed infinite-dimensional vector space of functions, so that any solution can be represented by its corresponding generalized Fourier series with respect to that set of eigenfunctions. Lax pairs, generating infinitely many conservation laws and symmetries, play an essential role in establishing such complete integrability. Moreover, by virtue of Lax pairs, the inverse scattering transform is often used to solve Cauchy problems of integrable PDEs [3]. This method involves decomposing the initial wave profile into a set of elementary waves that satisfy a Lax pair of linear spectral problems, and then using these waves to construct the solution of a Cauchy problem of an integrable PDE.

In this article, by integrable equations, we mean integerable PDEs. It is known that group reductions of Lax pairs lead to constrained integrable equations, not only local but also nonlocal. This motivates us to study nonlocal integrable equations, based on matrix spectral problems. Primary characteristics of nonlocalities are time reverse, space reverse and spacetime reverse utilities [4]. By checking invariance of Lax pairs under similarity transformations, a certain classification of nonlocal integrable equations associated with a given spectral problem can be achieved [5]. However, nonlocal equations are almost impossible to solve using conventional techniques. We just started studying nonlocal PDEs, particularly integrable ones, and many of their mathematical theories need to be developed from scratch.

In what follows, we will provide a little history of nonlocal dynamics and highlight the study of nonlocal integrable equations. By conducting group reductions of the (1+1)-dimensional AKNS matrix spectral problems in pairs, the corresponding nonlocal integrable NLS equations and mKdV equations are constructed and classified into six classes and five classes, respectively, three NLS classes of which

possess a mixed type nonlocality involving all three reflection coordinates. Concluding remarks are given in the final section.

## 2 Little History and Driving Force

One popular example of nonlocal dynamics is pantograph modeling [6], which has a long history in pantograph mechanics and pantograph transport [7]. Particularly, in 1821, the eidograph was invented to improve upon the practical utility of the pantograph [8]. In theoretical physics, two-place physics [9] is an inspiring example of nonlocal theories, which aims to explain the correlated natural phenomena happened at two different spaces and/or times [10].

Furthermore, cryptographic theories, for example, the RSA cryptographic system, involve public keys and private keys, applying data mining algorithms, which are essentially nonlocal problems [11]. The notion of non-locality in quantum mechanics, a property of the universe that is independent of our description of nature, was introduced in the context of the EPR controversy on the phenomenon of entanglement between quantum systems [12]. Unsupervised machine learning in artificial intelligence actually deal with a nonlocal superposition concept as well [13].

Recently, it has been found that PT symmetric potentials in quantum mechanics can guarantee that the energy spectrum is real and that time evolution is unitary [14]. The importance of nonlocal integrable equations stems from an observation that a nonlocal integrable nonlinear Schrödinger equation can be viewed as a linear Schrödinger equation, in quantum mechanics, with a PT symmetric nonlocal potential [15]. The classical nonlinear Schrödinger equation describes waves in nonlinear dispersive media under the first-order perturbation with respect to wave number, one principal application of which is to the propagation of light in nonlinear optical fibers. The modified Korteweg-de Vries equation corresponds to the second-order perturbation theory of water waves, waveguides, etc., and it is also generalized to nonlocal situations [4], being PT symmetric. The study of nonlocal integrable equations [16] is primarily driven by these two kinds of integrable equations.

## 3 What to Do?

One fundamental problem in mathematical theories of nonlocal differential equations is: how can we determine solutions to nonlocal ODEs, for example, to an $n$th-order nonlocal homogeneous linear ODE:

$$y^{(n)}(t) + c_1 y^{(n-1)}(\alpha_1 t) + \cdots + c_{n-1} y'(\alpha_{n-1} t) + y(-t) = 0,\ \alpha_i = \pm 1,\ 1 \le i \le n-1, \tag{1}$$

with constant coefficients $c_i$, $1 \le i \le n-1$? It is clear, however, that the first-order nonlocal equation

$$y' = cy(-t),\ c = \text{const.} \neq 0, \tag{2}$$

has an elementary function solution:

$$y(t) = \cos(ct - \frac{\pi}{4}) \text{ or } \sin(-ct - \frac{\pi}{4}),$$

and the second-order nonlocal equation

$$y'' = cy(-t),\ c = \text{const.} \neq 0, \tag{3}$$

has two linearly independent elementary function solutions:

$$y(t) = \sin \omega t,\ \cosh \omega t,\ \text{when } c = \omega^2,$$

and

$$y(t) = \cos \omega t,\ \sinh \omega t,\ \text{when } c = -\omega^2.$$

A more general example is

$$y'' + y'(-t) + y(2t) = 0, \tag{4}$$

for which any good idea to solve should be of great importance. Nonlocal ODEs may define novel special functions that could have important applications in many areas of mathematics and physics.

A second interesting problem is: what can we say about the well-posedness of initial-value and/or boundary-value problems for nonlocal PDEs? For example, how about the Cauchy problem for the spacetime reverse heat equation

$$u_t = u_{xx}(-x, -t)? \tag{5}$$

Does its Cauchy problem have a unique solution? The maximum principle does not hold for this nonlocal equation, which is used to show the uniqueness of a solution to the Cauchy problem of the local heat equation. Interestingly, this nonlocal problem can be solved by separation of variables and Fourier series. The solution to a Cauchy problem of this nonlocal equation (5) for $-\pi \leq x \leq \pi$ is given by

$$u(x,t) = \frac{a_0}{2} + \sqrt{2}\sum_{n=1}^{\infty}[-a_n \sin(n^2 t - \frac{\pi}{4}) \cos nx + b_n \cos(n^2 t - \frac{\pi}{4}) \sin nx], \tag{6}$$

where $a_n$ and $b_n$ are the Fourier coefficients of an initial displacement:

$$a_n = \frac{1}{\pi}\int_{-\pi}^{\pi} f(x) \cos nx\, dx,\ n \geq 0,\ b_n = \frac{1}{\pi}\int_{-\pi}^{\pi} f(x) \sin nx\, dx,\ n \geq 1.$$

There exists the same well-posedness problem for nonlocal integrable equations. It is known that the inverse scattering transform has been used to formulate the solution to the Cauchy problem for the space reverse integrable nonlinear Schrödinger equation [17], and Dabrboux transformation, the Hirota bilinear method and Riemann-Hilbert problems are also successfully applied to construction of soliton solutions to a few other nonlocal integrable equations (see, e.g., [16, 18–21]). Nevertheless, the existence and the uniqueness of solutions to initial value problems and/or boundary value problems still remain open. The questions are even harder to answer for mixed type nonlocal integrable nonlinear Schrödinger equations, some paradigmatic examples of which are

$$iu_t = u_{xx} + [uu(x,-t) + u(-x,t)u(-x,-t)]u, \tag{7}$$

$$iu_t = u_{xx} \pm [uu^*(-x,t) + u(-x,-t)u^*(x,-t)]u, \tag{8}$$

and

$$iu_t = u_{xx} \pm [uu^*(-x,t) + u(x,-t)u^*(-x,-t)]u, \tag{9}$$

where $u^*$ is the complex conjugate of $u$ (see the next section for details).

Mathematical theories of nonlocal differential equations provide a powerful tool for modeling and analyzing complex physical phenomena and have the potential to lead to new discoveries and insights in mathematical physics. Related research is ongoing. We are committed to continual innovation to better understand and finally know how to solve nonlocal differential equations, including nonlocal integrable ones.

## 4 Classification Under Pairs of Group Reductions

We would like to present a classification of nonlolcal integrable NLS equations and mKdV equations, associated with the (1+1)-dimensional AKNS matrix spectral problems, by taking group reductions in pairs.

A common general scheme for constructing integrable equations is the zero curvature formulation (see, e.g, [22, 23]). Let $u$ and $\lambda$ denote the potential and the spectral parameter, respectively. Consider a Lax pair of matrix spectral problems:

$$-i\phi_x = U\phi, \ -i\phi_t = V\phi, \tag{10}$$

where $U = U(u,\lambda)$ and $V = V(u,\lambda)$ are given spatial and temporal spectral matrices, respectively, and $\phi$ is a matrix eigenfunction. An integrable equation is determined by the associated zero curvature equation

$$U_t - V_x + i[U,V] = 0, \tag{11}$$

which is the compatibility condition of (10). Let $m, n$ be two arbitrary natural numbers, and assume that

$$u = u(p, q), \ p = (p_{jk})_{1\le j\le m,\ 1\le k\le n}, \ q = (q_{kj})_{1\le k\le n,\ 1\le j\le m}. \tag{12}$$

For each $r \in \mathbb{N}$ and two pairs of arbitrary constants, $\alpha_1, \alpha_2$ and $\beta_1, \beta_2$, where $\alpha_1 \neq \alpha_2$ and $\beta_1 \neq \beta_2$, we formulate a pair of spectral matrices as follows:

$$U = \lambda\Lambda + P(u), \ \Lambda = \mathrm{diag}(\alpha_1 I_m, \alpha_2 I_n), \ P = \begin{bmatrix} 0 & p \\ q & 0 \end{bmatrix}, \tag{13}$$

and

$$V^{[r]} = \lambda^r \Omega + Q^{[r]}(u, \lambda), \ \Omega = \mathrm{diag}(\beta_1 I_m, \beta_2 I_n), \tag{14}$$

where $I_k$ is the identity matrix of order $k$, and $Q^{[r]}$ is traceless and $\deg_\lambda Q^{[r]} \le r - 1$.

Let $\alpha = \alpha_1 - \alpha_2, \beta = \beta_1 - \beta_2$ and $I_{m,n} = \mathrm{diag}(I_m, -I_n)$. Particularly, upon taking

$$Q^{[2]} = \frac{\beta}{\alpha}\lambda P - \frac{\beta}{\alpha^2} I_{m,n}(P^2 + iP_x), \tag{15}$$

the corresponding zero curvature equation gives the matrix integrable NLS equations:

$$p_t = -\frac{\beta}{\alpha^2} i(p_{xx} + 2pqp), \ q_t = \frac{\beta}{\alpha^2} i(q_{xx} + 2qpq), \tag{16}$$

and upon taking

$$Q^{[3]} = \frac{\beta}{\alpha}\lambda^2 P - \frac{\beta}{\alpha^2}\lambda I_{m,n}(P^2 + iP_x) - \frac{\beta}{\alpha^3}(i[P, P_x] + P_{xx} + 2P^3), \tag{17}$$

the corresponding zero curvature equation presents the matrix integrable mKdV equations:

$$p_t = -\frac{\beta}{\alpha^3}(p_{xxx} + 3pqp_x + 3p_x qp), \ q_t = -\frac{\beta}{\alpha^3} i(q_{xxx} + 3q_x pq + 3qpq_x). \tag{18}$$

For the spatial spectral matrix $U$, determined by (13), we can conduct possible group reductions generated from using a constant invertible matrix $C$ of the form:

$$C = \begin{bmatrix} C_1 & 0 \\ 0 & C_2 \end{bmatrix}, \tag{19}$$

where $C_1$ and $C_2$ are invertible square matrices of order $m$ and $n$, respectively, and Hermitian when the conjugate transpose is involved or symmetric when only the transpose is involved. The key is to keep the corresponding zero curvature equation to hold after a group reduction.

For the matrix integrable NLS equations (16), local reductions come with the case of replacing $\lambda$: $\lambda \to \lambda^*$. The complex local group reduction is

$$U^\dagger(x,t,\lambda^*) = CU(x,t,\lambda)C^{-1}, \tag{20}$$

and the corresponding local potential reduction reads

$$q(x,t) = C_2^{-1} p^\dagger(x,t) C_1. \tag{21}$$

Nonlocal reductions come with the cases of replacing $\lambda$: $\lambda \to -\lambda^*, -\lambda, \lambda$. The reverse-space, reverse-time and reverse-spacetime group reductions are

$$U^\dagger(-x,t,-\lambda^*) = -CU(x,t,\lambda)C^{-1}, \tag{22}$$

$$U^T(x,-t,-\lambda) = -CU(x,t,\lambda)C^{-1}, \tag{23}$$

$$U^T(-x,-t,\lambda) = CU(x,t,\lambda)C^{-1}, \tag{24}$$

respectively, and the corresponding nonlocal potential reductions read

$$q(x,t) = -C_2^{-1} p^\dagger(-x,t) C_1, \tag{25}$$

$$q(x,t) = -C_2^{-1} p^T(x,-t) C_1, \tag{26}$$

$$q(x,t) = C_2^{-1} p^T(-x,-t) C_1. \tag{27}$$

For the matrix integrable mKdV equations (18), local reductions are associated with the cases of replacing $\lambda$: $\lambda \to \lambda^*, -\lambda$ (see, e.g., [24, 25]). The complex and real local group reductions are

$$U^\dagger(x,t,\lambda^*) = CU(x,t,\lambda)C^{-1}, \tag{28}$$

$$U^T(x,t,-\lambda) = -CU(x,t,\lambda)C^{-1}, \tag{29}$$

and the corresponding local potential reductions read

$$q(x,t) = C_2^{-1} p^\dagger(x,t) C_1, \tag{30}$$

$$q(x,t) = C_2^{-1} p^T(x,t) C_1. \tag{31}$$

Nonlocal group reductions are associated with the cases of replacing $\lambda$: $\lambda \to -\lambda^*, \lambda$. The complex and real reverse-spacetime group reductions are

$$U^\dagger(-x,-t,-\lambda^*) = -C_2 U(x,t,\lambda)C^{-1}, \tag{32}$$

$$U^T(-x,-t,\lambda) = C_2 U(x,t,\lambda) C^{-1}, \tag{33}$$

and the corresponding nonlocal potential reductions read

$$q(x,t) = -C_2^{-1} p^\dagger(-x,-t) C_1, \tag{34}$$

$$q(x,t) = C_2^{-1} p^T(-x,-t) C_1. \tag{35}$$

We will discuss about how to reduce the matrix integrable NLS and mKdV equations and classify the reduced nonlocal integrable counterparts, by conducting pairs of group reductions of the associated matrix spectral problems.

## 4.1 Pairs of Group Reductions Yielding Nonlocal Integrabe Equations

Let us conduct a pair of group reductions as follows:

$$U^\dagger(\tilde{x},\tilde{t},\pm\lambda^*) \text{ or } U^T(\tilde{x},\tilde{t},\pm\lambda) = \pm\Sigma U(x,t,\lambda)\Sigma^{-1}, \tag{36}$$

and

$$U^\dagger(\tilde{x},\tilde{t},\pm\lambda^*) \text{ or } U^T(\tilde{x},\tilde{t},\pm\lambda) = \pm\Delta U(x,t,\lambda)\Delta^{-1}, \tag{37}$$

where $(\tilde{x},\tilde{t})$ could be any of the three reflection coordinates, $(-x,t)$, $(x,-t)$ and $(-x,-t)$, and

$$\Sigma = \begin{bmatrix} \Sigma_1 & 0 \\ 0 & \Sigma_2 \end{bmatrix}, \ \Delta = \begin{bmatrix} \Delta_1 & 0 \\ 0 & \Delta_2 \end{bmatrix}, \tag{38}$$

with $\Sigma_1$, $\Delta_1$ and $\Sigma_2$, $\Delta_2$ being invertible square matrices of orders $m$ and $n$, respectively, and Hermitian when the conjugate transpose is involved or symmetric when only the transpose is involved (see, e.g., [26–33]).

For the matrix integrable NLS equations (16), we can have six pairs of group reductions, which yield nonlocal integrable NLS equations. Those six pairs of local and nonlocal reductions correspond to types $(\lambda^*,-\lambda^*)$, $(\lambda^*,-\lambda)$, $(\lambda^*,\lambda)$, $(-\lambda^*,-\lambda)$, $(-\lambda^*,\lambda)$ and $(-\lambda,\lambda)$. All six pairs of group reductions lead to the nonlocal potential reductions:

$$\begin{cases} q(x,t) = \Sigma_2^{-1} p^\dagger(x,t)\Sigma_1, \ q(x,t) = -\Delta_2^{-1} p^\dagger(-x,t)\Delta_1, \\ q(x,t) = \Sigma_2^{-1} p^\dagger(x,t)\Sigma_1, \ q(x,t) = -\Delta_2^{-1} p^T(x,-t)\Delta_1, \\ q(x,t) = \Sigma_2^{-1} p^\dagger(x,t)\Sigma_1, \ q(x,t) = \Delta_2^{-1} p^T(-x,-t)\Delta_1, \\ q(x,t) = -\Sigma_2^{-1} p^\dagger(-x,t)\Sigma_1, \ q(x,t) = -\Delta_2^{-1} p^T(x,-t)\Delta_1, \\ q(x,t) = -\Sigma_2^{-1} p^\dagger(-x,t)\Sigma_1, \ q(x,t) = \Delta_2^{-1} p^T(-x,-t)\Delta_1, \\ q(x,t) = -\Sigma_2^{-1} p^T(x,-t)\Sigma_1, \ q(x,t) = \Delta_2^{-1} p^T(-x,-t)\Delta_1, \end{cases} \tag{39}$$

respectively, and the associated temporal spectral matrices satisfy

$$\begin{cases} (V^{[2]})^{\dagger}(x,t,\lambda^*) = \Sigma V^{[2]}(x,t,\lambda)\Sigma^{-1}, (V^{[2]})^{\dagger}(-x,t,-\lambda^*) = \Delta V^{[2]}(x,t,\lambda)\Delta^{-1}, \\ (V^{[2]})^{\dagger}(x,t,\lambda^*) = \Sigma V^{[2]}(x,t,\lambda)\Sigma^{-1}, (V^{[2]})^{T}(x,-t,-\lambda) = \Delta V^{[2]}(x,t,\lambda)\Delta^{-1}, \\ (V^{[2]})^{\dagger}(x,t,\lambda^*) = \Sigma V^{[2]}(x,t,\lambda)\Sigma^{-1}, (V^{[2]})^{T}(-x,-t,\lambda) = \Delta V^{[2]}(x,t,\lambda)\Delta^{-1}, \\ (V^{[2]})^{\dagger}(-x,t,-\lambda^*) = \Sigma V^{[2]}(x,t,\lambda)\Sigma^{-1}, (V^{[2]})^{T}(x,-t,-\lambda) = \Delta V^{[2]}(x,t,\lambda)\Delta^{-1}, \\ (V^{[2]})^{\dagger}(-x,t,-\lambda^*) = \Sigma V^{[2]}(x,t,\lambda)\Sigma^{-1}, (V^{[2]})^{T}(-x,-t,\lambda) = \Delta V^{[2]}(x,t,\lambda)\Delta^{-1}, \\ (V^{[2]})^{T}(x,-t,-\lambda) = \Sigma V^{[2]}(x,t,\lambda)\Sigma^{-1}, (V^{[2]})^{T}(-x,-t,\lambda) = \Delta V^{[2]}(x,t,\lambda)\Delta^{-1}, \end{cases} \tag{40}$$

respectively, so that the corresponding zero curvature equation holds true under each of the six pairs of group reductions.

For the matrix integrable mKdV equations (18), we have one pair of local group reductions, corresponding to type $(\lambda^*, -\lambda)$, which leads to Sasa-Satsuma type equations [34], and five pairs of local and nonlocal group reductions, corresponding to types $(\lambda^*, -\lambda^*)$, $(\lambda^*, \lambda)$, $(-\lambda, -\lambda^*)$, $(-\lambda, \lambda)$ and $(-\lambda^*, \lambda)$. All five pairs of local and nonlocal group reductions yield the nonlocal potential reductions:

$$\begin{cases} q(x,t) = \Sigma_2^{-1} p^{\dagger}(x,t)\Sigma_1, \ q(x,t) = -\Delta_2^{-1} p^{\dagger}(-x,-t)\Delta_1, \\ q(x,t) = \Sigma_2^{-1} p^{\dagger}(x,t)\Sigma_1, \ q(x,t) = \Delta_2^{-1} p^{T}(-x,-t)\Delta_1, \\ q(x,t) = -\Sigma_2^{-1} p^{T}(x,t)\Sigma_1, \ q(x,t) = -\Delta_2^{-1} p^{\dagger}(-x,-t)\Delta_1, \\ q(x,t) = -\Sigma_2^{-1} p^{T}(x,t)\Sigma_1, \ q(x,t) = \Delta_2^{-1} p^{T}(-x,-t)\Delta_1, \\ q(x,t) = -\Sigma_2^{-1} p^{\dagger}(-x,-t)\Sigma_1, \ q(x,t) = \Delta_2^{-1} p^{T}(-x,-t)\Delta_1, \end{cases} \tag{41}$$

respectively, and the associated temporal spectral matrices satisfy

$$\begin{cases} (V^{[3]})^{\dagger}(x,t,\lambda^*) = \Sigma V^{[3]}(x,t,\lambda)\Sigma^{-1}, (V^{[3]})^{\dagger}(-x,-t,-\lambda^*) = -\Delta V^{[3]}(x,t,\lambda)\Delta^{-1}, \\ (V^{[3]})^{\dagger}(x,t,\lambda^*) = \Sigma V^{[3]}(x,t,\lambda)\Sigma^{-1}, (V^{[3]})^{T}(-x,-t,\lambda) = \Delta V^{[3]}(x,t,\lambda)\Delta^{-1}, \\ (V^{[3]})^{T}(x,t,-\lambda) = -\Sigma V^{[3]}(x,t,\lambda)\Sigma^{-1}, (V^{[3]})^{\dagger}(-x,-t,-\lambda^*) = -\Delta V^{[3]}(x,t,\lambda)\Delta^{-1}, \\ (V^{[3]})^{T}(x,t,-\lambda) = \Sigma V^{[3]}(x,t,\lambda)\Sigma^{-1}, (V^{[3]})^{T}(-x,-t,\lambda) = \Delta V^{[3]}(x,t,\lambda)\Delta^{-1}, \\ (V^{[3]})^{\dagger}(-x,-t,-\lambda^*) = -\Sigma V^{[3]}(x,t,\lambda)\Sigma^{-1}, (V^{[3]})^{T}(-x,-t,\lambda) = \Delta V^{[3]}(x,t,\lambda)\Delta^{-1}, \end{cases} \tag{42}$$

respectively, so that the corresponding zero curvature equation holds true under each of the five pairs of group reductions.

## 4.2 Examples in the Case of $m = 1$ and $n = 2$

Let us set $m = 1$ and $n = 2$ and consider two choices of pairs of group reductions with

$$\Sigma_1 = 1, \ \Sigma_2^{-1} = \begin{bmatrix} \sigma & 0 \\ 0 & \sigma \end{bmatrix}, \ \Delta_1 = 1, \ \Delta_2^{-1} = \begin{bmatrix} 0 & \delta \\ \delta & 0 \end{bmatrix}; \tag{43}$$

and

$$\Sigma_1 = 1, \ \Sigma_2^{-1} = \begin{bmatrix} 0 & \sigma \\ \sigma & 0 \end{bmatrix}, \ \Delta_1 = 1, \ \Delta_2^{-1} = \begin{bmatrix} \delta & 0 \\ 0 & \delta \end{bmatrix}, \tag{44}$$

where $\sigma$ and $\delta$ are real constants satisfying $\sigma^2 = \delta^2 = 1$, i.e., $(\sigma, \delta) = (1, 1), (1, -1), (-1, 1)$ or $(-1, -1)$.

### 4.2.1 Reduced Spatial Spectral Matrices

We point out that if the first choice leads to a reduced spatial spectral matrix

$$U = \begin{bmatrix} \alpha_1\lambda & p_1 & f(p_1) \\ g(p_1) & \alpha_2\lambda & 0 \\ h(p_1) & 0 & \alpha_2\lambda \end{bmatrix}, \tag{45}$$

then the second choice gives another reduced spatial spectral matrix

$$U = \begin{bmatrix} \alpha_1\lambda & p_1 & f(p_1) \\ h(p_1) & \alpha_2\lambda & 0 \\ g(p_1) & 0 & \alpha_2\lambda \end{bmatrix}, \tag{46}$$

where the (2,1)th and (3,1)th entries are exchanged with the (3,1)th and (2,1)th entries of the previous spatial spectral matrix, respectively. Therefore, we will only list the reduced spatial spectral matrices under the first choice (43).

Considering the matrix integrable NLS equations (16), we have the following six reduced spatial spectral matrices.

(a) Type ($\lambda^*$,$-\lambda^*$):

$$U = \begin{bmatrix} \alpha_1\lambda & p_1 & -\sigma\delta p_1(-x, t) \\ \sigma p_1^* & \alpha_2\lambda & 0 \\ -\delta p_1^*(-x, t) & 0 & \alpha_2\lambda \end{bmatrix}. \tag{47}$$

(b) Type ($\lambda^*$,$-\lambda$):

$$U = \begin{bmatrix} \alpha_1\lambda & p_1 & -\sigma\delta p_1^*(x, -t) \\ \sigma p_1^* & \alpha_2\lambda & 0 \\ -\delta p_1(x, -t) & 0 & \alpha_2\lambda \end{bmatrix}. \tag{48}$$

(c) Type ($\lambda^*$,$\lambda$):

$$U = \begin{bmatrix} \alpha_1\lambda & p_1 & \sigma\delta p_1^*(-x, -t) \\ \sigma p_1^* & \alpha_2\lambda & 0 \\ \delta p_1(-x, -t) & 0 & \alpha_2\lambda \end{bmatrix}. \tag{49}$$

(d) Type ($-\lambda^*$,$-\lambda$):

$$U = \begin{bmatrix} \alpha_1\lambda & p_1 & \sigma\delta p_1^*(-x,-t) \\ -\sigma p_1^*(-x,t) & \alpha_2\lambda & 0 \\ -\delta p_1(x,-t) & 0 & \alpha_2\lambda \end{bmatrix}. \tag{50}$$

(e) Type $(-\lambda^*,\lambda)$:

$$U = \begin{bmatrix} \alpha_1\lambda & p_1 & -\sigma\delta p_1^*(x,-t) \\ -\sigma p_1^*(-x,t) & \alpha_2\lambda & 0 \\ \delta p_1(-x,-t) & 0 & \alpha_2\lambda \end{bmatrix}. \tag{51}$$

(f) Type $(-\lambda,\lambda)$:

$$U = \begin{bmatrix} \alpha_1\lambda & p_1 & -\sigma\delta p_1(-x,-t) \\ -\sigma p_1(x,-t) & \alpha_2\lambda & 0 \\ \delta p_1(-x,t) & 0 & \alpha_2\lambda \end{bmatrix}. \tag{52}$$

Considering the matrix integrable mKdV equations (18), we have the following five reduced spatial spectral matrices.
(a) Type $(\lambda^*,-\lambda^*)$:

$$U = \begin{bmatrix} \alpha_1\lambda & p_1 & -\sigma\delta p_1(-x,-t) \\ \sigma p_1^* & \alpha_2\lambda & 0 \\ -\delta p_1^*(-x,-t) & 0 & \alpha_2\lambda \end{bmatrix}. \tag{53}$$

(b) Type $(\lambda^*,\lambda)$:

$$U = \begin{bmatrix} \alpha_1\lambda & p_1 & \sigma\delta p_1^*(-x,-t) \\ \sigma p_1^* & \alpha_2\lambda & 0 \\ \delta p_1(-x,-t) & 0 & \alpha_2\lambda \end{bmatrix}. \tag{54}$$

(c) Type $(-\lambda,-\lambda^*)$:

$$U = \begin{bmatrix} \alpha_1\lambda & p_1 & \sigma\delta p_1^*(-x,-t) \\ -\sigma p_1 & \alpha_2\lambda & 0 \\ -\delta p_1^*(-x,-t) & 0 & \alpha_2\lambda \end{bmatrix}. \tag{55}$$

(d) Type $(-\lambda,\lambda)$:

$$U = \begin{bmatrix} \alpha_1\lambda & p_1 & -\sigma\delta p_1(-x,-t) \\ -\sigma p_1 & \alpha_2\lambda & 0 \\ \delta p_1(-x,-t) & 0 & \alpha_2\lambda \end{bmatrix}. \tag{56}$$

(e) Type $(-\lambda^*,\lambda)$:

$$U = \begin{bmatrix} \alpha_1\lambda & p_1 & -\sigma\delta p_1^* \\ -\sigma p_1^*(-x,-t) & \alpha_2\lambda & 0 \\ \delta p_1(-x,-t) & 0 & \alpha_2\lambda \end{bmatrix}. \tag{57}$$

Note that the reduced spatial spectral matrices of type $(\lambda^*, \lambda)$ in both cases of the matrix NLS and mKdV equations are the same. Therefore, the resulting type $(\lambda^*, \lambda)$ nonlocal integrable NLS equations and mKdV equations come from one integrable hierarchy, associated with that reduced spatial spectral matrix.

### 4.2.2 Scalar Nonlocal Integrable NLS and mKdV Equations

The six classes of pairs of local and nonlocal group reductions in two choices generate the following six couples of scalar nonlocal integrable NLS equations.
(a) Type $(\lambda^*, -\lambda^*)$ scalar nonlocal integrable NLS equations are

$$p_{1,t} = -\frac{\beta}{\alpha^2} i[p_{1,xx} + 2\sigma(p_1 p_1^* + p_1(-x,t)p_1^*(-x,t))p_1], \tag{58}$$

$$p_{1,t} = -\frac{\beta}{\alpha^2} i[p_{1,xx} - 2\delta(p_1 p_1^*(-x,t) + p_1^* p_1(-x,t))p_1]. \tag{59}$$

(b) Type $(\lambda^*, -\lambda)$ scalar nonlocal integrable NLS equations are

$$p_{1,t} = -\frac{\beta}{\alpha^2} i[p_{1,xx} + 2\sigma(p_1 p_1^* + p_1(x,-t)p_1^*(x,-t))p_1], \tag{60}$$

$$p_{1,t} = -\frac{\beta}{\alpha^2} i[p_{1,xx} - 2\delta(p_1 p_1(x,-t) + p_1^* p_1^*(x,-t))p_1]. \tag{61}$$

(c) Type $(\lambda^*, \lambda)$ scalar nonlocal integrable NLS equations are

$$p_{1,t} = -\frac{\beta}{\alpha^2} i[p_{1,xx} + 2\sigma(p_1 p_1^* + p_1(-x,-t)p_1^*(-x,-t))p_1], \tag{62}$$

$$p_{1,t} = -\frac{\beta}{\alpha^2} i[p_{1,xx} + 2\delta(p_1 p_1(-x,-t) + p_1^* p_1^*(-x,-t))p_1]. \tag{63}$$

(d) Type $(-\lambda^*, -\lambda)$ scalar nonlocal integrable NLS equations are

$$p_{1,t} = -\frac{\beta}{\alpha^2} i[p_{1,xx} - 2\sigma(p_1 p_1^*(-x,t) + p_1(x,-t)p_1^*(-x,-t))p_1], \tag{64}$$

$$p_{1,t} = -\frac{\beta}{\alpha^2} i[p_{1,xx} - 2\delta(p_1 p_1(x,-t) + p_1^*(-x,t)p_1^*(-x,-t))p_1]. \tag{65}$$

(e) Type $(-\lambda^*, \lambda)$ scalar nonlocal integrable NLS equations are

$$p_{1,t} = -\frac{\beta}{\alpha^2} i[p_{1,xx} - 2\sigma(p_1 p_1^*(-x,t) + p_1(-x,-t)p_1^*(x,-t))p_1], \tag{66}$$

$$p_{1,t} = -\frac{\beta}{\alpha^2} i[p_{1,xx} + 2\delta(p_1 p_1(-x,-t) + p_1^*(-x,t)p_1^*(x,-t))p_1]. \tag{67}$$

(f) Type $(-\lambda, \lambda)$ scalar nonlocal integrable NLS equations are

$$p_{1,t} = -\frac{\beta}{\alpha^2} i[p_{1,xx} - 2\sigma(p_1 p_1(x,-t) + p_1(-x,t)p_1(-x,-t))p_1], \tag{68}$$

$$p_{1,t} = -\frac{\beta}{\alpha^2} i[p_{1,xx} + 2\delta(p_1 p_1(-x,t) + p_1(x,-t)p_1(-x,-t))p_1]. \tag{69}$$

The last three couples of nonlocal integrable NLS equations have the mixed type nonlocality involving all reflection coordinates, $(-x,t)$, $(x,-t)$ and $(-x,-t)$, in (1+1)-dimensions, which is a completely new phenomenon.

The five classes of pairs of local and nonlocal group reductions in two choices generate the following five couples of scalar nonlocal integrable mKdV equations.
(a) Type $(\lambda^*, -\lambda^*)$ scalar nonlocal integrable mKdV equations are

$$p_{1,t} = -\frac{\beta}{\alpha^3}[p_{1,xxx} + 6\sigma|p_1|^2 p_{1,x} + 3\sigma p_1^*(-x,-t)(p_1 p_1(-x,-t))_x], \tag{70}$$

$$p_{1,t} = -\frac{\beta}{\alpha^3}[p_{1,xxx} - 6\delta p_1 p_1^*(-x,-t)p_{1,x} - 3\delta p_1^*(p_1 p_1(-x,-t))_x]. \tag{71}$$

(b) Type $(\lambda^*, \lambda)$ scalar nonlocal integrable mKdV equations are

$$p_{1,t} = -\frac{\beta}{\alpha^3}[p_{1,xxx} + 6\sigma|p_1|^2 p_{1,x} + 3\sigma p_1(-x,-t)(p_1 p_1^*(-x,-t))_x], \tag{72}$$

$$p_{1,t} = -\frac{\beta}{\alpha^3}[p_{1,xxx} + 6\delta p_1 p_1(-x,-t)p_{1,x} + 3\delta p_1^*(p_1 p_1^*(-x,-t))_x]. \tag{73}$$

(c) Type $(-\lambda, -\lambda^*)$ scalar nonlocal integrable mKdV equations are

$$p_{1,t} = -\frac{\beta}{\alpha^3}[p_{1,xxx} - 6\sigma p_1^2 p_{1,x} - 3\sigma p_1^*(-x,-t)(p_1 p_1^*(-x,-t))_x], \tag{74}$$

$$p_{1,t} = -\frac{\beta}{\alpha^3}[p_{1,xxx} - 6\delta p_1 p_1^*(-x,-t)p_{1,x} - 3\delta p_1(p_1 p_1^*(-x,-t))_x]. \tag{75}$$

(d) Type $(-\lambda, \lambda)$ scalar nonlocal integrable mKdV equations are

$$p_{1,t} = -\frac{\beta}{\alpha^3}[p_{1,xxx} - 6\sigma p_1^2 p_{1,x} - 3\sigma p_1(-x,-t)(p_1 p_1(-x,-t))_x], \tag{76}$$

$$p_{1,t} = -\frac{\beta}{\alpha^3}[p_{1,xxx} + 6\delta p_1 p_1(-x,-t)p_{1,x} + 3\delta(p_1 p_1(-x,-t))_x p_1]. \quad (77)$$

(e) Type $(-\lambda^*, \lambda)$ scalar nonlocal integrable mKdV equations are

$$p_{1,t} = -\frac{\beta}{\alpha^3}[p_{1,xxx} - 6\sigma p_1 p_1^*(-x,-t)p_{1,x} - 3\sigma p_1(-x,-t)(|p_1|^2)_x], \quad (78)$$

$$p_{1,t} = -\frac{\beta}{\alpha^3}[p_{1,xxx} + 6\delta p_1 p_1(-x,-t)p_{1,x} + 3\delta p_1^*(-x,-t)(|p_1|^2)_x]. \quad (79)$$

All those nonlocal integrable equations of lower orders come from the ten nonlocal integrable hierarchies associated with the ten reduced spatial spectral matrices generated from the ten pairs of group reductions (see, e.g., [26–33]). They provide significant integrable models for analyzing complex physical phenomena that involve nonlocal effects and nonlocal interactions, and have the potential to lead to new discoveries and insights in various areas of science and technology, and are an active area of research in mathematical physics.

## 5 Concluding Remarks

This article provided a little history of nonlinear dynamics and discussed about problems of nonlocal differential equations, particularly nonlocal integrable equations, in soliton theory. A thorough classification of nonlocal integrable NLS equations and mKdV equations, associated with the AKNS matrix spectral problems, was achieved via conducting group reductions in pairs. All resulting nonlocal integrable equations consist of six classes of NLS equations and five classes of mKdV equations. Three classes are mixed-type nonlocal integrable NLS equations, each of which involves all three reverse-space, reverse-time and reverse-spacetime nonlocalities. Illustrative examples of scalar nonlocal integrable models were explicitly computed in a particular case with four potential components.

The theory of solitons to nonlocal integrable equations, generated from taking one group reduction, has been carefully formulated via Riemann-Hilbert problems very recently [5]. A large task in nonlocal theories, however, still needs to be done. It is of particular importance to explore soliton solutions systematically by combining different approaches, including the Darboux transformation, the Hirota direct method and the Wronskian technique (see, e.g., [18–21, 35–40]). Breathers and algebro-geometric solutions, being other interesting and important solutions, are worth further studies, too. Two-place (or multiple-place) nonlocalities bring difficulty for establishing global existence of solutions or more generally, the well-posedness theory.

It should also be an extremely rewarding experience to look for novel nonlocal integrable equations, associated with other interesting or significant matrix Lie algebras [41]. In the non-semisimple case, group reductions of matrix spectral problems

yield nonlocal integrable couplings (see, e.g., [42]), about which very little is known. We just started the job. There is a long way to go. Definitely, we need new ideas, new research and new tools that will enable us to address problems on nonlocal differential equations in mathematics and their applications in physical and engineering sciences.

Overall, nonlocal integrable equations are a fascinating research area in mathematical physics that has led to important mathematical discoveries and continue to be a rich source of inspiration for new mathematical research.

**Acknowledgements** The work was supported in part by NSFC under the grants 12271488, 11975145 and 11972291, the Ministry of Science and Technology of China (G2023016011L and G2021016032L), and the Natural Science Foundation for Colleges and Universities in Jiangsu Province (17 KJB 110020).

## References

1. Arnol'd, V.I.: Mathematical Methods of Classical Mechanics. Springer-Verlag, New York-Heidelberg (1978)
2. Lax, P.D.: Integrals of nonlinear equations of evolution and solitary waves. Comm. Pure Appl. Math. **21**, 467–490 (1968)
3. Ablowitz, M.J., Segur, J.: Solitons and the Inverse Scattering Transform. SIAM, Philadelphia, PA (1981)
4. Ablowitz, M.J., Musslimani, Z.H.: Integrable nonlocal nonlinear equations, Stud. Appl. Math. **139**, 7–59 (2017)
5. Ma, W.X.: Nonlocal PT-symmetric integrable equations and related Riemann-Hilbert problems. Partial Differ. Equ. Appl. Math. **4**, 100190 (2021)
6. Shapira, A., Tyomkyn, M.: Quasirandom graphs and the pantograph equation. Amer. Math. Monthly **128**, 630–639 (2021)
7. A ninety-six ton electric locomotive. Sci. Amer. **73**, 87 (1895)
8. Wallace, W.: Account of the invention of the pantograph, and a description of the eidograph. Trans. R. Soc. Edinb. **13**, 418–439 (1836)
9. Lou, S.Y., Huang, F.: Alice-Bob physics: coherent solutions of nonlocal KdV systems. Sci. Rep. **7**, 869 (2017)
10. Mackey, M. C., Glass, L.: Oscillation and chaos in physiological control systems. Science **197**, 287–289 (1977)
11. Bernstein, D., Lange, T.: Post-quantum cryptography. Nature **549**, 188–194 (2017)
12. Einstein, A., Podolsky, B., Rosen, N.: Can quantum-mechanical description of physical reality be considered complete? Phys. Rev. **47**, 777–780 (1935)
13. LeCun, Y., Bengio, Y., Hinton, G.: Deep learning. Nature **521**, 436–444 (2015)
14. Bender, C.M., Boettcher, S.: Real spectra in non-Hermitian Hamiltonians having $\mathcal{PT}$ symmetry. Phys. Rev. Lett. **80**, 5243 (1998)
15. Ablowitz, M.J., Musslimani, Z.H.: Integrable nonlocal nonlinear Schrödinger equation. Phys. Rev. Lett. **110**, 064105 (2013)
16. Yang, J.: Physically significant nonlocal nonlinear Schrödinger equation and its soliton solutions. Phys. Rev. E **98**, 042202 (2018)
17. Ablowitz, M.J., Musslimani, Z.H.: Inverse scattering transform for the integrable nonlocal nonlinear Schrödinger equation. Nonlinearity **29**, 915–946 (2016)

18. Ji, J.L., Zhu, Z.N.: On a nonlocal modified Korteweg-de Vries equation: Integrability, Darboux transformation and soliton solutions. Commun. Nonlinear Sci. Numer. Simul. **42**, 699–708 (2017)
19. Song, C.Q., Xiao, D.M., Zhu, Z.N.: Solitons and dynamics for a general integrable nonlocal coupled nonlinear Schrödinger equation. Commun. Nonlinear Sci. Numer. Simul. **45**, 13–28 (2017)
20. Gürses, M., Pekcan, A.: Nonlocal nonlinear Schrödinger equations and their soliton solutions. J. Math. Phys. **59**, 051501 (2018)
21. Rao, J.G., Zhang, Y.S., Fokas, A.S., He, J.S.: Rogue waves of the nonlocal Davey-Stewartson I equation. Nonlinearity **31**, 4090–4107 (2018)
22. Tu, G.Z.: On Liouville integrability of zero-curvature equations and the Yang hierarchy. J. Phys. A: Math. Gen. **22**, 2375–2392 (1989)
23. Ma, W.X.: A new hierarchy of Liouville integrable generalized Hamiltonian equations and its reduction. Chin. Ann. Math. Ser. A **13**,115–123 (1992)
24. Ma, W.X.: Riemann-Hilbert problems and soliton solutions of a multicomponent mKdV system and its reduction. Math. Methods Appl. Sci. **42**, 1099–1113 (2019)
25. Ma, W.X.: A novel kind of reduced integrable matrix mKdV equations and their binary Darboux transformations. Mod. Phys. Lett. B **36**, 2250094 (2022)
26. Ma, W.X.: Riemann-Hilbert problems and soliton solutions of type $(\lambda^*, -\lambda^*)$ reduced nonlocal integrable mKdV hierarchies. Mathematics **10**, 870 (2022)
27. Ma, W.X.: Type $(-\lambda, -\lambda^*)$ reduced nonlocal integrable mKdV equations and their soliton solutions. Appl. Math. Lett. **131**, 108074 (2022)
28. Ma, W.X.: Reduced nonlocal integrable mKdV equations of type $(-\lambda, \lambda)$ and their exact soliton solutions. Commun. Theor. Phys. **74**, 065002 (2022)
29. Ma, W.X.: Nonlocal integrable mKdV equations by two nonlocal reductions and their soliton solutions. J. Geom. Phys. **177**, 104522 (2022)
30. Ma, W.X.: Reduced non-local integrable NLS hierarchies by pairs of local and non-local constraints. Int. J. Appl. Comput. Math. **8**, 206 (2022)
31. Ma, W.X.: Soliton hierarchies and soliton solutions of type $(-\lambda^*, -\lambda)$ reduced nonlocal nonlinear Schrödinger equations of arbitrary even order. Partial Differ. Equ. Appl. Math. **7**, 100515 (2023)
32. Ma, W.X.: Integrable non-local nonlinear Schrödinger hierarchies of type $(-\lambda^*, \lambda)$ and soliton solutions. Rep. Math. Phys. **92**, 19–36 (2023)
33. Ma, W.X.: Soliton solutions to reduced nonlocal integrable nonlinear Schrödinger hierarchies of type $(-\lambda,\lambda)$. Int. J. Geom. Methods Mod. Phys. **20**, 2350098 (2023)
34. Ma, W.X.: Sasa-Satsuma type matrix integrable hierarchies and their Riemann-Hilbert problems and soliton solutions. Physica D **446**, 133672 (0223)
35. Ma, W.X.: Soliton solutions by means of Hirota bilinear forms. Partial Differ. Equ. Appl. Math. **5**, 100220 (2022)
36. Manukure, S., Chowdhury, A., Zhou, Y.: Complexiton solutions to the asymmetric Nizhnik-Novikov-Veselov equation. Int. J. Mod. Phys. B **33**, 1950098 (2019)
37. Zhou, Y., Manukure, S., McAnally, M.: Lump and rogue wave solutions to a (2+1)-dimensional Boussinesq type equation. J. Geom. Phys. **167**, 104275 (2021)
38. Ma, W.X., Zhou, Y.: Lump solutions to nonlinear partial differential equations via Hirota bilinear forms. J. Differ. Equ. **264**, 2633–2659 (2018)
39. Li, Y., Tian, S.F.: Inverse scattering transform and soliton solutions of an integrable nonlocal Hirota equation. Commun. Pure Appl. Anal. **21**, 293–313 (2022)
40. Abdeljabbar, A,: New double Wronskian solutions for a generalized (2+1)-dimensional Boussinesq nonlinear system with variable coefficients. Partial Differ. Equ. Appl. Math. **3**, 100022 (2021)
41. Ma, W.X.: Integrable nonlocal nonlinear Schrödinger equations associated with so(3,R). Proc. Amer. Math. Soc. Ser. B **9**, 1–11 (2022)
42. Xin, X.P., Liu, Y.T., Xia, Y.R., Liu, H.Z.: Integrability, Darboux transformation and exact solutions for nonlocal couplings of AKNS equations. Appl. Math. Lett. **119**, 107209 (2021)

# Multiple Lump and Rogue Wave Solutions of a Modified Benjamin-Ono Equation


**Solomon Manukure and Yuan Zhou**

**Abstract** In this chapter, a (2+1)-dimensional modified Benjamin-Ono (MBO) equation is introduced. Multiple lump (M-lump) and rogue wave solutions are obtained for the equation with the aid of the Hirota bilinear method. The equation is first studied in two parts: an integrable and a nonintegrable part. The nonintegrable part is found to possess 1-lump and line rogue wave solutions whereas the integrable part has only 1-lump solutions. Furthermore, the MBO equation is found to posses both multiple lump and rogue wave solutions. By fixing parameter values, the dynamics of the solutions are studied with 3D and density plots.

**Keywords** M-lump solutions · Rogue waves · Hirota bilinear form · Benjamin Ono equation

**MSC codes** 37K05 · 35Q53

**PACS** 02.30.Ik · 04.20.Fy · 05.45.Yv

## 1 Introduction

Nonlinear partial differential equations (NLPDEs) and their solutions play an important role in the study of nonlinear interactions between physical processes. Evidently, the search for exact solutions to NLPDEs has, in recent times, become a very important exercise in nonlinear science, especially in the area of mathematical physics. The importance of NLPDEs transcends theoretical boundaries. In areas such as physics, engineering, economics, chemistry, biology, finance and many oth-

S. Manukure
Department of Mathematics, Florida A & M University, Tallahassee, FL 32307, USA

Y. Zhou (✉)
School of Data Science, Xianda College of Economics & Humanities Shanghai International Studies University, Shanghai 200083, China
e-mail: 1911068@xdsisu.edu.cn



S. Manukure and W.-X. Ma (eds.), *Nonlinear and Modern Mathematical Physics*,
Springer Proceedings in Mathematics & Statistics 459,
https://doi.org/10.1007/978-3-031-59539-4_12

ers, NLPDEs have been used to study many practical problems [1]. For example, the nonlinear Schrödinger equation (NLSE), which possesses solitary wave solutions, are used to describe wave propagation in fluids and nonlinear media, such as optical fibers [2].

It is well known that many NLPDEs possess soliton solutions, which have been a major focus of research in mathematical physics for many years. Their discovery which dates back to the 19th century has led to many new research areas and directions. In addition to solitons, several other solutions such as lump solutions have also attracted a lot of attention in recent times. Lump solutions are rational function solutions that are analytic and localized in all directions in space [3–5]. Like solitons, they also have many important applications such as the description of nonlinear patterns in plasma and nonlinear optic media [6]. They were first derived from multi-soliton solutions of the KPI equation by Mankov et al. [7, 8], but have recently been observed for many other NLPDEs in higher dimensions such as the higher dimensional counterparts and extensions of the BKP equation [9, 10], the Ito equation [11], the Hirota-Satsuma-Ito equation [12], the Sawada-Kotera equation [13], the Davey-Stewartson II equation [14], the Ishimori equations [15, 16], and the Hietarinta equation [17, 18]. There are also multiple lump waves which have been observed for many equations [10, 19, 20].

Another interesting class of solutions that have also attracted enormous research attention in recent times are rogue waves. These are often lump-type waves [21], that are localized not only in space but also in time [22]. Such waves have been used to describe nonlinear wave phenomena in the ocean [23, 24] and in nonlinear optics [25, 26] and have also been observed in optical fibers [27–29] and plasma [30]. A unique feature of rogue waves is that they appear from nowhere and disappear without a trace [31]. Thus, they arise from constant (or uniform) backgrounds, grow significantly in height or amplitude and recede back into the constant background [32]. Many NLPDEs such as the NLS equation, the Davey-Stewartson equations, the Boussinesq equation and many others have been found to possess rogue wave solutions. It is also important to remark that rogue waves that arise from non-uniform backgrounds have also been reported in literature [33, 34]. In this article, we investigate the existence of M-lump and rogue wave solutions to a novel (2+1)-dimensional extension of the Benjamin-Ono equation by means of the Hirota bilinear method [35]. We will first find 1-lump and line rogue wave solutions to two reductions of this equation.

The Benjamin-Ono equation is the (1+1)-dimensional integrable system:

$$u_{tt} + 3(u^2)_{xx} + u_{xxx} = 0 \tag{1}$$

with a bilinear form given by

$$(D_t^2 + D_x^4) f \cdot f = 0. \tag{2}$$

The equation arises in the study of long internal gravity waves in deep stratified fluids [36, 37]. It is a completely integrable equation which passes the Painléve test and possesses multi-soliton solutions and other integrability-related properties such as

the Bäckland transformation, infinitely many conserved quantities and symmetries (see, [38, 39]).

In this project, we study the following extended MBO equation

$$\alpha u_{tt} + 3(u^2)_{xx} + u_{xxx} + \beta u_{xx} + u_{tx} + \gamma u_{ty} - u_{yy} = 0 \tag{3}$$

whose bilinear form under the transformation

$$u = 2(\ln f)_x, \tag{4}$$

is given by

$$(\alpha D_t^2 + D_x^4 + \beta D_x^2 + D_t D_x + \gamma D_t D_y - D_y^2) f \cdot f = 0, \tag{5}$$

where $D_x$, $D_y$, and $D_t$ are Hirota bilinar derivatives. and $\alpha$, $\beta$, $\gamma$, are arbitrary constants.

For any nonnegative integers $n$, $m$ and differentiable functions $f$, $g$, we define the Hirota bilinear operator as

$$D_x(f \cdot g) = \left(\frac{\partial}{\partial x} - \frac{\partial}{\partial x'}\right) f(x) \cdot g(x') \Big|_{x'=x} \tag{6}$$

or more generally,

$$D_x^m D_t^n (f \cdot g) = \left(\frac{\partial}{\partial x} - \frac{\partial}{\partial x'}\right)^m \left(\frac{\partial}{\partial t} - \frac{\partial}{\partial t'}\right)^n f(x,t) \cdot g(x',t') \Big|_{x'=x, t'=t}. \tag{7}$$

When $f = g$, we have the bilinear partial derivative expression,

$$D_x^m D_t^n f \cdot f = \sum_{j=0}^{m} \sum_{k=0}^{n} (-1)^{m+n-j-k} \binom{m}{j} \binom{n}{k} \left(\frac{\partial}{\partial x}\right)^{m-j} \left(\frac{\partial}{\partial t}\right)^{n-k} f \left(\frac{\partial}{\partial x}\right)^{j} \left(\frac{\partial}{\partial t}\right)^{k} f,$$

where $\binom{n}{k} = \dfrac{n!}{k!(n-k)!}$, $0 \le k \le n$, is the binomial coefficient.

We remark that Eq. (3) is generally not integrable (It is integrable for some fixed parameters). To find lump and rogue wave solutions, we will consider two reductions of the MBO equation. First, for the case where $\beta = 0$, we have;

$$\alpha u_{tt} + 3(u^2)_{xx} + u_{xxxx} + u_{tx} + \gamma u_{ty} - u_{yy} = 0 \tag{8}$$

which is also nonintegrable. The starting point in constructing lump solutions is to find positive quadratic function solutions to Hirota bilinear equations. According to [3], any positive quadratic function solution to a Hirota bilinear equation in the variables $t, x, y$ can be expressed in the form

$$\begin{cases} f &= f_1^2 + f_2^2 + a_7, \\ f_1 &= a_1 x + a_2 y + a_3 t, \\ f_2 &= a_4 x + a_5 y + a_6 t. \end{cases} \tag{9}$$

where $a_i, 1 \leq i \leq 7$ are real constants and $a_7 > 0$. When $f_1$ and $f_2$ are linearly dependent, the function $f$ can be simplified to

$$f = c_1 f_1^2 + a_7 \tag{10}$$

for some real constant $c_1 > 0$. Then, we have

$$u = 2(\ln f)_x = \frac{4a_1 c_1 f_1}{f}. \tag{11}$$

The above solutions satisfy the conditions that,

$$\lim_{x^2+y^2 \to \infty} u \neq 0 \tag{12}$$

for any fixed $t$, and

$$\lim_{t \to \infty} u \neq 0. \tag{13}$$

These solutions are degenerate. We will consider the case where $f_1$ and $f_2$ are linearly independent.

## 2 Lump Solutions

We now find lump solutions to Eq. (8). Suppose $f_1$ and $f_2$ are linearly independent and

$$\text{rank} \begin{pmatrix} a_1 & a_2 \\ a_4 & a_5 \end{pmatrix} = 2. \tag{14}$$

This is equivalent to the determinant condition

$$\Delta := a_1 a_5 - a_2 a_4 = \begin{vmatrix} a_1 & a_2 \\ a_4 & a_5 \end{vmatrix} \neq 0. \tag{15}$$

Then, substituting $f$ in (9) into (5), a direct computation determines the solutions

$$\begin{cases} a_1 = -\dfrac{\alpha a_3^3 + \alpha a_3 a_6^2 + \gamma a_2 a_3^2 + \gamma a_2 a_6^2 - a_2^2 a_3 - 2a_2 a_5 a_6 + a_3 a_5^2}{a_3^2 + a_6^2}, \\ a_4 = -\dfrac{\alpha a_3^2 a_6 + \alpha a_6^3 + \gamma a_3^2 a_5 + \gamma a_5 a_6^2 + a_2^2 a_6 - 2a_2 a_3 a_5 - a_5^2 a_6}{a_3^2 + a_6^2}, \\ a_7 = \dfrac{3\zeta^2}{(a_2 a_6 - a_3 a_5)^2 (a_3^2 + a_6^2)}, \end{cases} \tag{16}$$

where

$$\begin{aligned} \zeta = {} & \alpha^2 a_3^4 + 2\alpha^2 a_3^2 a_6^2 + \alpha^2 a_6^4 + 2\alpha\gamma a_2 a_3^3 + 2\alpha\gamma a_2 a_3 a_6^2 + 2\alpha\gamma a_3^2 a_5 a_6 + 2\alpha\gamma a_5 a_6^3 + \gamma^2 a_2^2 a_3^2 + \gamma^2 a_2^2 a_6^2 \\ & + \gamma^2 a_3^2 a_5^2 + \gamma^2 a_5^2 a_6^2 - 2\alpha a_2^2 a_3^2 + 2\alpha a_2^2 a_6^2 - 8\alpha a_2 a_3 a_5 a_6 + 2\alpha a_3^2 a_5^2 - 2\alpha a_5^2 a_6^2 - 2\gamma a_2^3 a_3 - 2\gamma a_2^2 a_5 a_6 \\ & - 2\gamma a_2 a_3 a_5^2 - 2\gamma a_5^3 a_6 + a_2^4 + 2a_2^2 a_5^2 + a_5^4, \end{aligned}$$

and $a_i$ for $i = \{2, 3, 5, 6\}$ are free parameters. For the function in (4) to be analytic, we require

$$a_7 > 0, \quad a_2 a_6 - a_3 a_5 \neq 0. \tag{17}$$

From (16) we know that, $a_7 > 0$ if and only if $\zeta \neq 0$ and $a_2 a_6 - a_3 a_5 \neq 0$. Condition (15) is a necessary condition for the second condition in (17) since

$$a_1 a_5 - a_2 a_4 = \frac{(a_2 a_6 - a_3 a_5)(\alpha a_3^2 + \alpha a_6^2 + a_2^2 + a_5^2)}{a_3^2 + a_6^2}. \tag{18}$$

We need free parameters to satisfy $\zeta \neq 0$, $a_2 a_6 - a_3 a_5 \neq 0$, and $\alpha(a_3^2 + a_6^2) + a_2^2 + a_5^2 \neq 0$. Consequently, through the transformation (4), we obtain the following class of solutions

$$u = \frac{4a_4 f_2 + 4a_1 f_1}{f}, \tag{19}$$

where $f_1$ and $f_2$ are are given by,

$$\begin{cases} f_1 = -x\dfrac{\alpha a_3^3 + \alpha a_3 a_6^2 + \gamma a_2 a_3^2 + \gamma a_2 a_6^2 - a_2^2 a_3 - 2a_2 a_5 a_6 + a_3 a_5^2)}{a_3^2 + a_6^2} + t a_3 + y a_2, \\ f_2 = -x\dfrac{\alpha a_3^2 a_6 + \alpha a_6^3 + \gamma a_3^2 a_5 + \gamma a_5 a_6^2 + a_2^2 a_6 - 2a_2 a_3 a_5 - a_5^2 a_6}{a_3^2 + a_6^2} + t a_6 + y a_5. \end{cases} \tag{20}$$

These solutions satisfy

$$\lim_{x^2 + y^2 \to \infty} u(x, y, t) = 0 \tag{21}$$

for any fixed $t$, and are therefore localized in all directions in space. They form a class of lump solutions to Eq. (8).

### 2.1 Illustrative Example

Choosing the parameters,

$$a_2 = 1, a_3 = 2, a_5 = -2, a_6 = -1, \alpha = -1, \gamma = 1,$$

we obtain

$$f = \left(2t - \frac{17}{5}x + y\right)^2 + \left(-t + \frac{4}{5}x - 2y\right)^2 + \frac{3721}{15}, \tag{22}$$

and

$$u = \frac{12(38t - 61x + 25y)}{75t^2 - 228tx + 120ty + 183x^2 - 150xy + 75y^2 + 3721}. \tag{23}$$

It could be easily verified that $u$ decays in all spacial directions, i.e., for any fixed $t$,

$$\lim_{x^2+y^2\to\infty} u(x, y, t) = 0. \tag{24}$$

For $t = -2,\ 0$ and 2, we have,

$$u = -\frac{12(-76 - 61x + 25y)}{183x^2 - 150xy + 75y^2 + 456x - 240y + 4021}, \tag{25}$$

$$u = -\frac{12(-61x + 25y)}{183x^2 - 150xy + 75y^2 + 3721} \tag{26}$$

and

$$u = -\frac{12(76 - 61x + 25y)}{183x^2 - 150xy + 75y^2 - 456x + 240y + 4021} \tag{27}$$

respectively, which are depicted by 3D and contour plots below (Figs. 1, 2 and 3).

## 3 Rogue Waves

We now find rogue wave solutions to Eq. (8). Suppose again that $f_1$ and $f_2$ are linearly independent and

$$\text{rank}\begin{pmatrix} a_1 & a_2 \\ a_4 & a_5 \end{pmatrix} < 2. \tag{28}$$

Let $\xi = a_1 x + a_2 y$. Then, we have

$$f_1 = \xi + a_3 t, \quad f_2 = c\xi + a_6 t,$$

for some $c \in \mathbb{R}$. Then, we can rewrite $f$ in the form

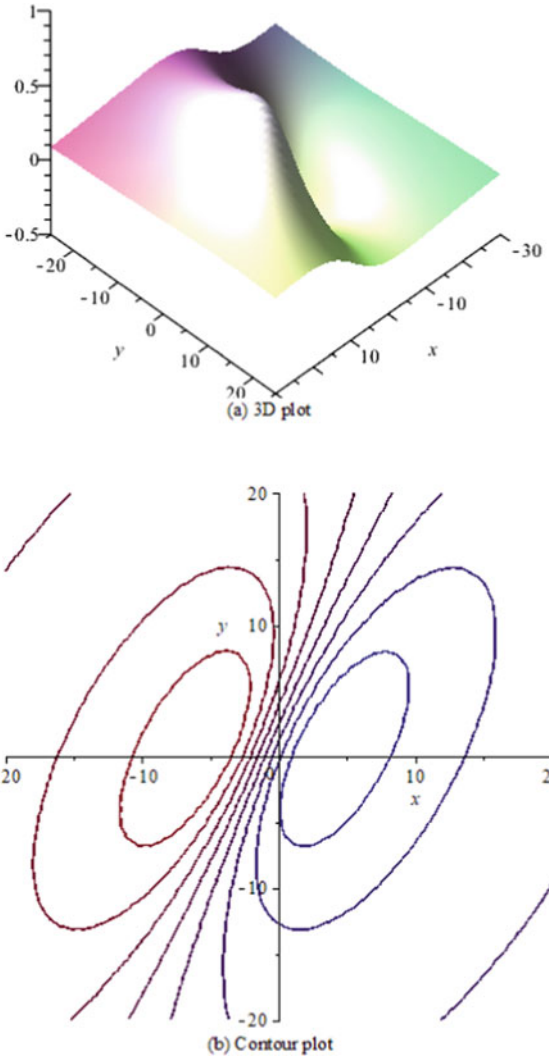


**Fig. 1** Wave profile of solution (25)

$$f = (c_1\xi + c_2 t)^2 + c_3 t^2 + a_7,$$

where $c_1, c_3$ are nonzero constants. The corresponding solutions $u = 2(\ln f)_x$ satisfy

$$\lim_{|t|\to\infty} u(t, x, y) = 0, \tag{29}$$

for $(x, y) \in \mathbb{R}^2$ uniformly and are called line rogue waves.

The above rank condition (28) is equivalent to the condition

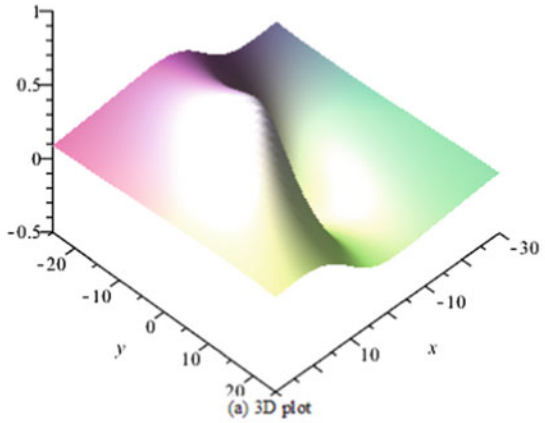

(a) 3D plot

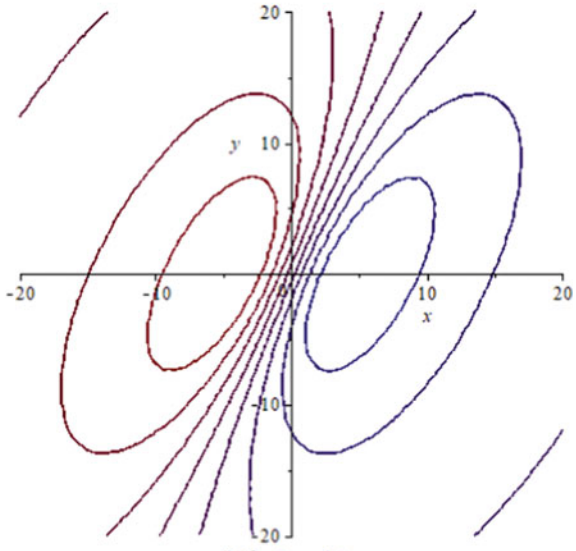

(b) Contour plot

**Fig. 2** Wave profile of solution (26)

$$a_1a_5 - a_2a_4 = \frac{(a_2a_6 - a_3a_5)(\alpha a_3^2 + \alpha a_6^2 + a_2^2 + a_5^2)}{a_3^2 + a_6^2} = 0. \tag{30}$$

This implies that

$$\alpha a_3^2 + \alpha a_6^2 + a_2^2 + a_5^2 = 0, \tag{31}$$

due to condition (17). Consequently,

$$\alpha = -\frac{a_2^2 + a_5^2}{a_3^2 + a_6^2}. \tag{32}$$

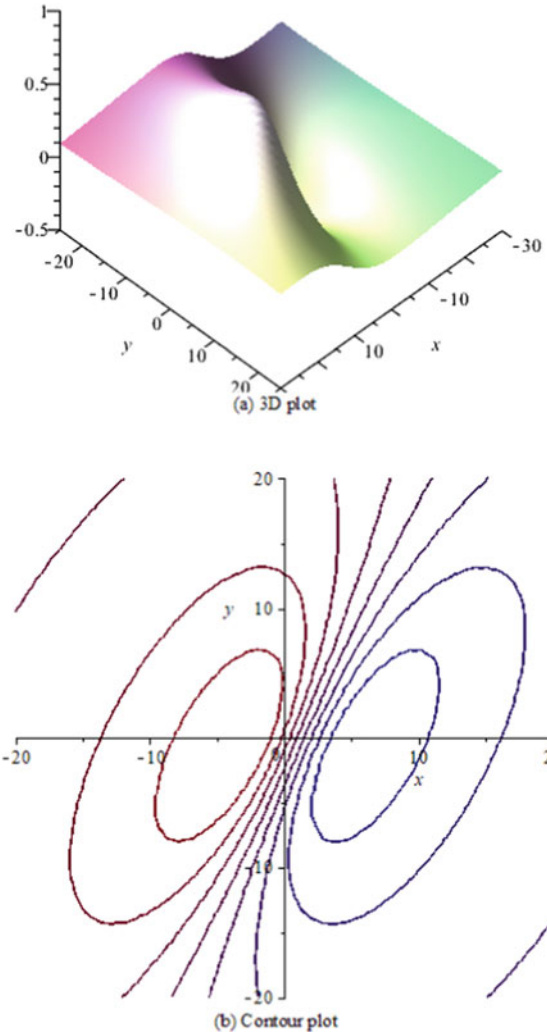


**Fig. 3** Wave profile of solution (27)

Since $a_2^2 + a_5^2 > 0$, $a_3^2 + a_6^2 > 0$, we must have $\alpha < 0$. In other words, when $\alpha \geq 0$ we cannot expect rogue waves. Consequently, we obtain a class of analytic solutions that satisfy condition (29).

### 3.1 Illustrative Example

If we choose parameters

$$a_2 = 1, a_3 = 2, a_5 = -2, a_6 = -1, \gamma = 1,$$

then, $\alpha = -1$, and we obtain we obtain

$$f = \left(2t + \frac{3}{5}x + y\right)^2 + \left(-t - \frac{6}{5}x - 2y\right)^2 + \frac{27}{5}, \tag{33}$$

and

$$u = \frac{12(4t + 3x + 5y)}{25t^2 + 24tx + 40ty + 9x^2 + 30xy + 25y^2 + 27}. \tag{34}$$

The above solution satisfies condition (29) and

$$\lim_{x^2+y^2+t^2\to\infty} u(t, x, y) = 0, \tag{35}$$

unless $3x + 5y = c$ for any fixed $c \in \mathbb{R}$. For $t = -10$, $t = 0$, $t = 10$ and 20, we have,

$$u = \frac{12(-40 + 3x + 5y)}{9x^2 + 30xy + 25y^2 - 240x - 400y + 2527} \tag{36}$$

$$u = \frac{12(3x + 5y)}{9x^2 + 30xy + 25y^2 + 27} \tag{37}$$

$$u = \frac{12(40 + 3x + 5y)}{9x^2 + 30xy + 25y^2 + 240x + 400y + 2527} \tag{38}$$

and

$$u = \frac{12(80 + 3x + 5y)}{9x^2 + 30xy + 25y^2 + 480x + 800y + 10027} \tag{39}$$

respectively, which are depicted by 3D and contour plots below (Figs. 4, 5, 6 and 7).

## 4 Integrable Case

Now, let us consider another reduction of (3). When $\alpha = \gamma = 0$, we obtain the integrable equation;

$$3(u^2)_{xx} + u_{xxx} + \beta u_{xx} + u_{tx} - u_{yy} = 0. \tag{40}$$

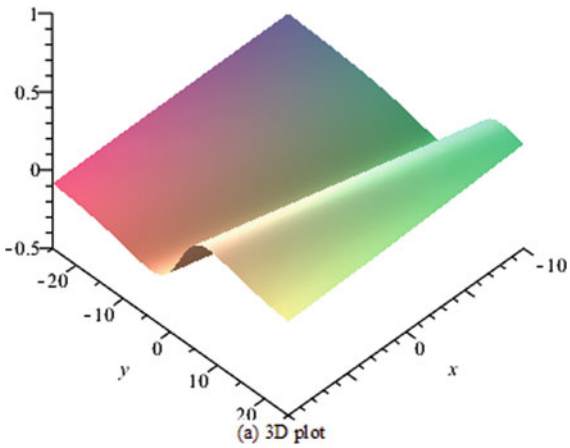


**Fig. 4** Wave profile of solution (36)

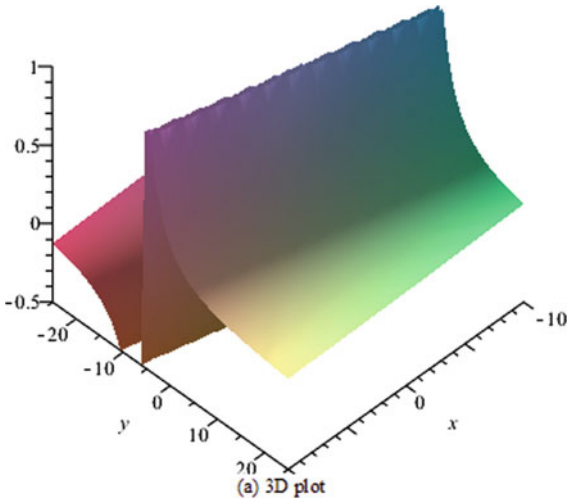


**Fig. 5** Wave profile of solution (37)

This equation has been shown to be Painlevé integrable [40].

Again, substituting (9) into (5), the corresponding solutions under the condition $\alpha = \gamma = 0$, is given by

$$\begin{cases} a_3 = -\dfrac{\beta a_1^3 + \beta a_1 a_4^2 - a_1 a_2^2 + a_1 a_5^2 - 2a_2 a_4 a_5}{a_1^2 + a_4^2}, \\ a_6 = -\dfrac{\beta a_1^2 a_4 + \beta a_4^3 - 2a_1 a_2 a_5 + a_2^2 a_4 - a_4 a_5^2}{a_1^2 + a_4^2}, \\ a_7 = \dfrac{3(a_1^2 + a_4^2)^3}{(a_1 a_5 - a_2 a_4)^2}, \end{cases} \tag{41}$$

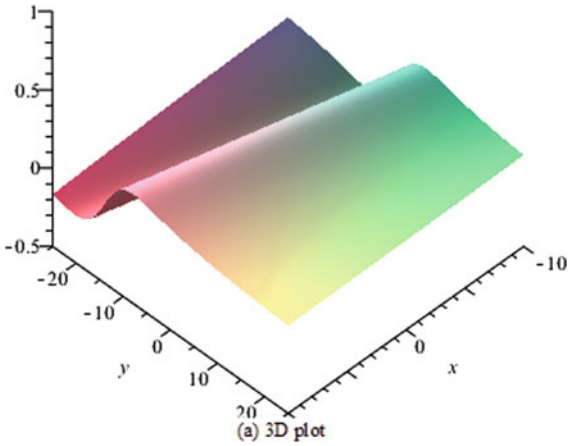


**Fig. 6** Wave profile of solution (38)

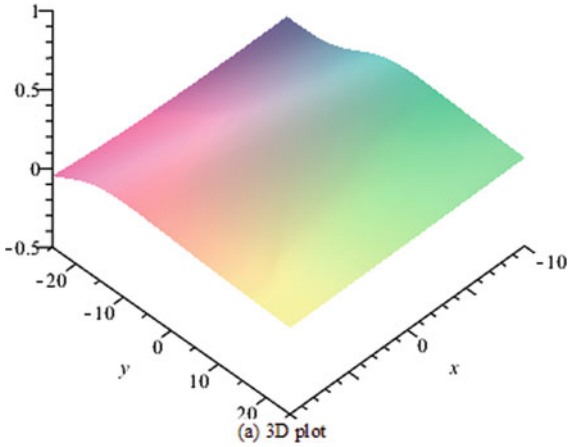


**Fig. 7** Wave profile of solution (39)

where $a_i$ for $i = \{1, 2, 4, 5\}$ are free parameters. To guarantee the analyticity of the function (4), we require

$$a_7 > 0, \quad a_1 a_5 - a_2 a_4 \neq 0 \tag{42}$$

which is a direct consequence of the rank condition. We illustrate some solutions below.

If we choose parameters

$$a_1 = -2, a_2 = -2, a_4 = -1, a_5 = 1, \beta = 2,$$

we obtain

$$f = \left(\frac{18}{5}t - 2x - 2y\right)^2 + \left(\frac{21}{5}t - x + y\right)^2 + \frac{375}{16}, \tag{43}$$

and

$$u = \frac{64(57t - 25x - 15y)}{2448t^2 - 1824tx - 480ty + 400x^2 + 480xy + 400y^2 + 1875}. \tag{44}$$

It could be easily verified that $u$ decays in all spacial directions, i.e., for any fixed $t$,

$$\lim_{x^2+y^2\to\infty} u(x, y, t) = 0. \tag{45}$$

For $t = -2,\ 0$ and 2, we have,

$$u = -\frac{64(-114 - 25x - 15y)}{400x^2 + 480xy + 400y^2 + 3648x + 960y + 11667}, \tag{46}$$

$$u = -\frac{64(-25x - 15y)}{400x^2 + 480xy + 400y^2 + 1875} \tag{47}$$

and

$$u = -\frac{64(114 - 25x - 15y)}{400x^2 + 480xy + 400y^2 - 3648x - 960y + 11667} \tag{48}$$

respectively, which are depicted by 3D and contour plots below (Figs. 8, 9, 10).

We remark that no line rogue waves were found for the integrable version of the MBO equation.

## 5 M-lump Solutions

Now, we consider multiple lump solutions of the MBO Eq. (3). Inspired by [41], we define

$$M = \frac{n(n+1)}{2}, \qquad n = 1, 2, \ldots.$$

We expect multiple lumps for $M = 1, 3, 6, 10, 15, \cdots$. We consider two cases.

### 5.1 In the Case of $X = x + a_1 t$

Let $X = x + a_1 t$, and consider

$$f(x, y, t) = F(X, y) = \sum_{k=0}^{M} \sum_{j=0}^{M-k} a_{k,j} X^{2k} y^{2j}. \tag{49}$$

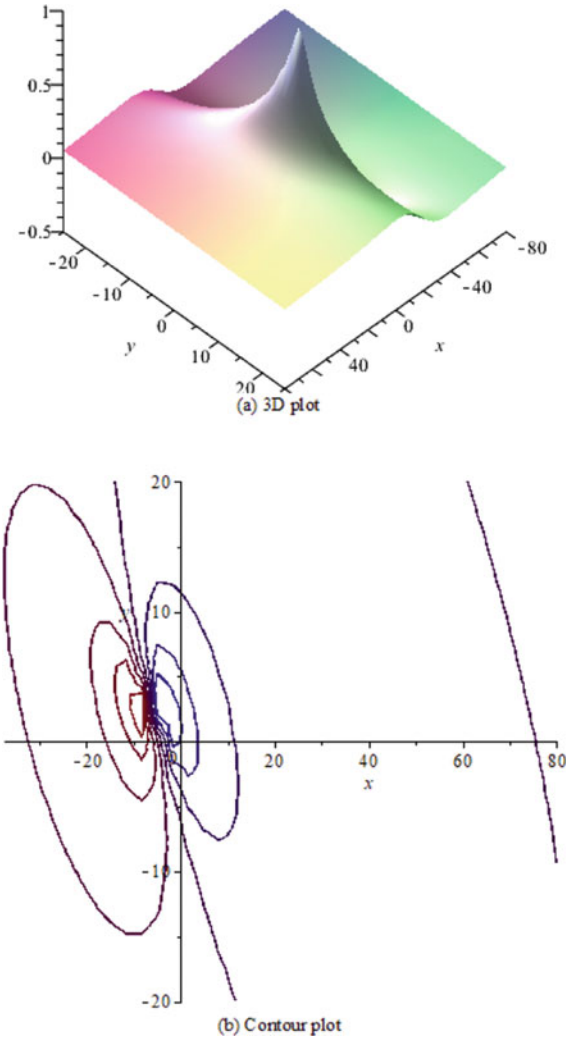


**Fig. 8** Wave profile of solution (46)

When $n = 1$, we have $M = 1$. This is exactly 1-lump solutions.

Let $f_1(x, y, t) = X^2 + a_3 y^2 + a_2$ be a solution of (5). By symbolic computation we get one class of solutions with

$$a_1 = 0, a_2 = -\frac{3}{\beta}, a_3 = -\beta.$$

Therefore

$$f_1(x, y, t) = x^2 - \beta y^2 - \frac{3}{\beta}$$

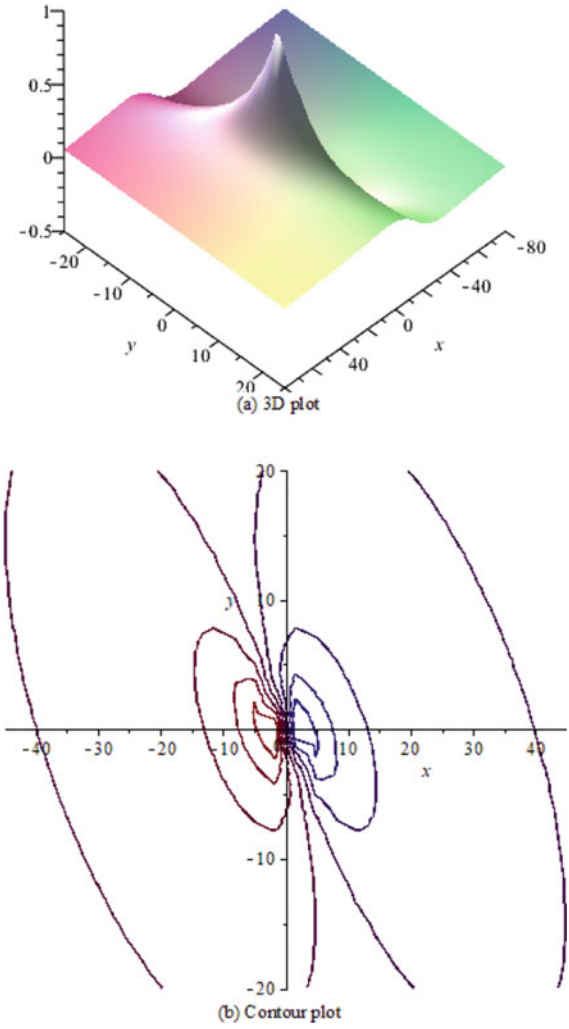


**Fig. 9** Wave profile of solution (47)

When $\beta < 0$, we have $f_1 > 0$ and

$$u(x, y, t) = 2(\ln f_1)_x = \frac{4x}{x^2 - \beta y^2 - \frac{3}{\beta}}. \tag{50}$$

Obviously, the above function $u$ is a static lump solution with the property

$$\lim_{x^2+y^2\to\infty} u(x, y, t) = 0.$$

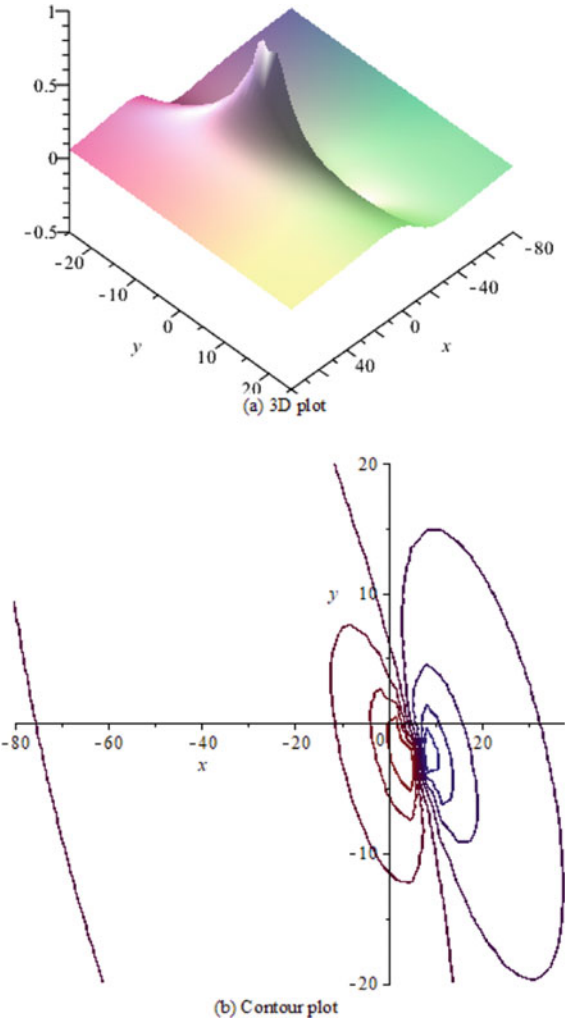


**Fig. 10** Wave profile of solution (48)

Setting $\beta = -1$, we depict the wave profile in Figs. 11, 12 and 13.

When $n = 2$, we have $M = 3$. Let

$$f_2(x, y, t) = X^6 + (a_2 + a_3 y^2)X^4 + (a_4 + a_5 y^2 + a_6 y^4)X^2 + a_7 + a_8 y^2 + a_9 y^4 + a_{10} y^6$$

be a solution of (5). By symbolic computation we get a solution with

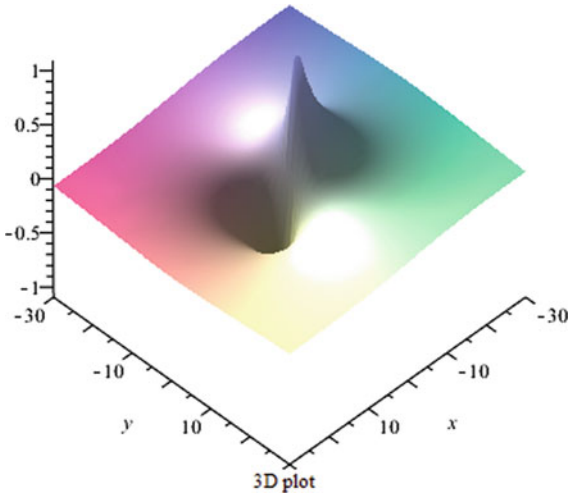


**Fig. 11** Wave profile of solution in Eq. (50) with $\hat{I}^2=-1$

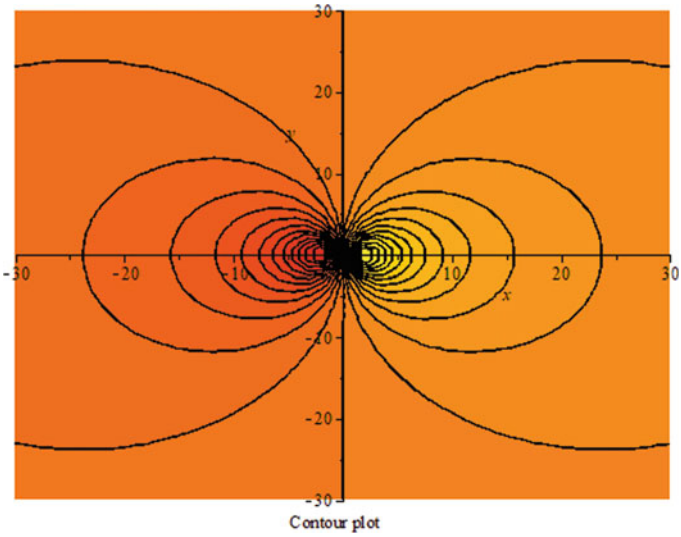


**Fig. 12** Wave profile of solution in Eq. (50) with $\hat{I}^2=-1$

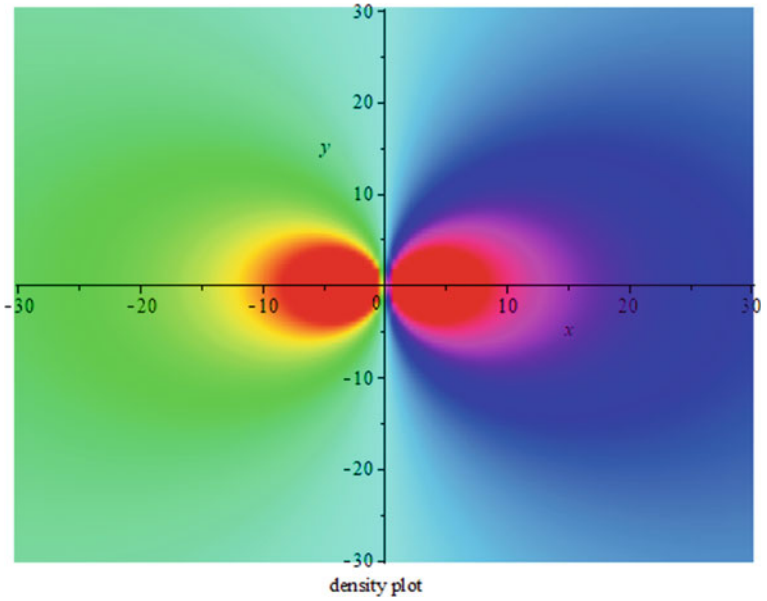


**Fig. 13** Wave profile of solution in Eq. (50) with Î²=-1

$$a_1 = 0, a_2 = -\frac{25}{\beta}, a_3 = -3\beta, a_4 = -\frac{125}{\beta^2}, a_5 = 90,$$
$$a_6 = 3\beta^2, a_7 = -\frac{1875}{\beta^3}, a_8 = -\frac{475}{\beta}, a_9 = -17\beta, a_{10} = -\beta^3. \tag{51}$$

As a result, we have

$$f_2(x, y, t) = x^6 + (-3\beta y^2 - \frac{25}{\beta})x^4 + (3\beta^2 y^4 + 90y^2 - \frac{125}{\beta^2})x^2 - \frac{1875}{\beta^3} - \frac{475}{\beta} y^2 - 17\beta y^4 - \beta^3 y^6.$$

It is easy to see that $f_2 > 0$ when $\beta < 0$, for all $x$, $y$. The corresponding solution

$$u(x, y, t) = 2(\ln f_2(x, y, t))_x = \frac{2[6x^5 + 4x^3(-3\beta y^2 - \frac{25}{\beta}) + 2x(3\beta^2 y^4 + 90y^2 - \frac{125}{\beta^2})]}{f(x, y, t)} \tag{52}$$

is a 3-lump solution. We depict the solution for $\beta = -1$ in Figs. 14, 15 and 16.

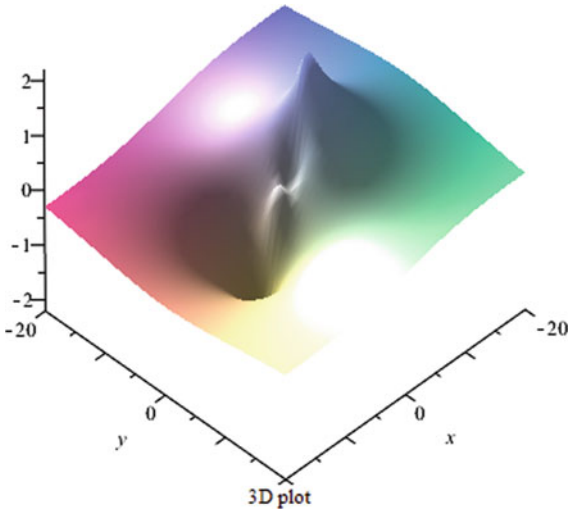


**Fig. 14** Wave profile of solution in Eq. (52) with $\hat{I}^2$=-1

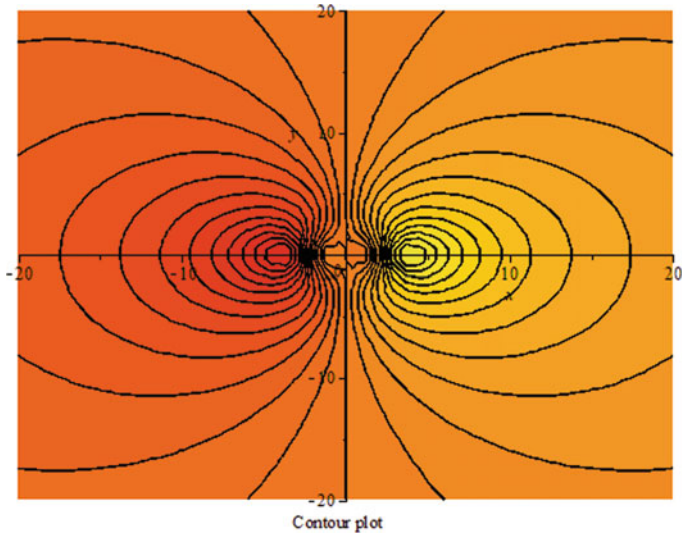


**Fig. 15** Wave profile of solution in Eq. (52) with $\hat{I}^2$=-1

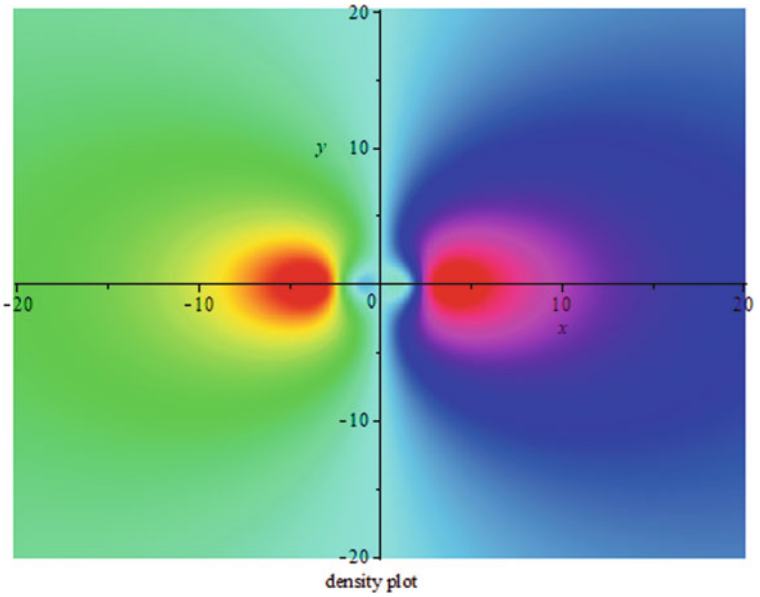


**Fig. 16** Wave profile of solution in Eq. (52) with Î²=-1

When $n = 3$, we have $M = 6$. Let

$$f_3(x, y, t) = X^{12} + (a_2 + a_3 y^2)X^{10} + (a_4 + a_5 y^2 + a_6 y^4)X^8 + (a_7 + a_8 y^2 + a_9 y^4 + a_{10} y^6)X^6 + (a_{11} + a_{12} y^2 + a_{13} y^4 + a_{14} y^6 + a_{15} y^8)X^4 + (a_{16} + a_{17} y^2 + a_{18} y^4 + a_{19} y^6 + a_{20} y^8 + a_{21} y^{10})X^2 + a_{22} + a_{23} y^2 + a_{24} y^4 + a_{25} y^6 + a_{26} y^8 + a_{27} y^{10} + a_{28} y^{12}$$

be a solution of (5). By symbolic computation we get a solution with

$$a_1 = 0, a_2 = -\frac{98}{\beta}, a_3 = -6\beta, a_4 = \frac{735}{\beta^2}, a_5 = 690, a_6 = 15\beta^2, a_7 = -\frac{75460}{3\beta^3},$$
$$a_8 = -\frac{18620}{\beta}, a_9 = -1540\beta, a_{10} = -20\beta^3, a_{11} = -\frac{5187875}{3\beta^4}, a_{12} = \frac{220500}{\beta^2},$$
$$a_{13} = 37450, a_{14} = 1460\beta^2, a_{15} = 15\beta^4, a_{16} = -\frac{159786550}{3\beta^5}, a_{17} = -\frac{565950}{\beta^3},$$
$$a_{18} = \frac{14700}{\beta}, a_{19} = -35420\beta, a_{20} = -570\beta^3, a_{21} = -6\beta^5, a_{22} = \frac{878826025}{9\beta^6},$$
$$a_{23} = \frac{300896750}{3\beta^4}, a_{24} = \frac{16391725}{3\beta^2}, a_{25} = \frac{798980}{3}, a_{26} = 4335\beta^2, a_{27} = 58\beta^4, a_{28} = \beta^6.$$

Consequently, we obtain

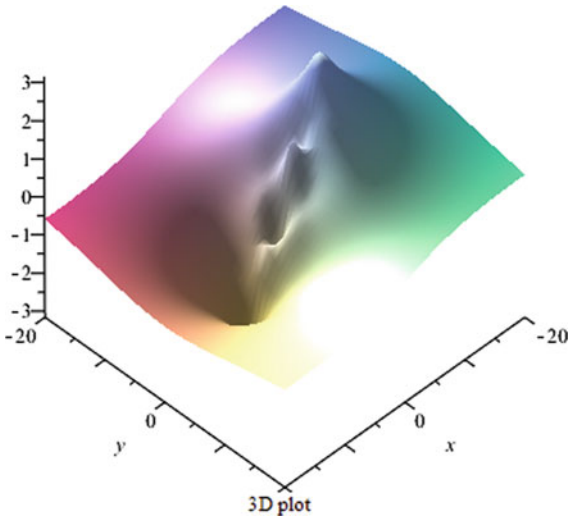


**Fig. 17** Wave profile of solution in Eq. (53) with Î²=-1

$$
\begin{aligned}
f_3(x,y,t) = {} & x^{12} + (-\frac{98}{\beta} - 6\beta y^2)x^{10} + (15\beta^2 y^4 + 690y^2 + \frac{735}{\beta^2})x^8 + (-20\beta^3 y^6 - 1540\beta y^4 \\
& - \frac{18620}{\beta} y^2 - \frac{75460}{3\beta^3})x^6 + (15\beta^4 y^8 + 1460\beta^2 y^6 + 37450y^4 + \frac{220500}{\beta^2} y^2 - \frac{5187875}{3\beta^4})x^4 \\
& + (-6\beta^5 y^{10} - 570\beta^3 y^8 - 35420\beta y^6 + \frac{14700}{\beta} y^4 - \frac{565950}{\beta^3} y^2 - \frac{159786550}{3\beta^5})x^2 \\
& + \beta^6 y^{12} + 58\beta^4 y^{10} + 4335\beta^2 y^8 + \frac{798980}{3} y^6 + \frac{16391725}{3\beta^2 y^4} + \frac{300896750}{3\beta^4} y^2 + \frac{878826025}{9\beta^6}.
\end{aligned}
$$

It is easy to check that $f_3 > 0$ when $\beta < 0$, for all $x$, $y$. The corresponding solution is given by

$$u(x,y,t) = 2(\ln f_3(x,y,t))_x = \frac{2f_{3x}(x,y,t)}{f_3(x,y,t)}, \tag{53}$$

where

$$
\begin{aligned}
f_{3x}(x,y,t) = {} & 12x^{11} + 10x^9(-\frac{98}{\beta} - 6\beta y^2) + 8x^7(15\beta^2 y^4 + 690y^2 + \frac{735}{\beta^2}) + 6x^5(-20\beta^3 y^6 - 1540\beta y^4 \\
& - \frac{18620}{\beta} y^2 - \frac{75460}{3\beta^3}) + 4x^3(15\beta^4 y^8 + 1460\beta^2 y^6 + 37450y^4 + \frac{220500}{\beta^2} y^2 - \frac{5187875}{3\beta^4}) \\
& + 2x(-6\beta^5 y^{10} - 570\beta^3 y^8 - 35420\beta y^6 + \frac{14700}{\beta} y^4 - \frac{565950}{\beta^3} y^2 - \frac{159786550}{3\beta^5}).
\end{aligned}
$$

This is a 6-lump solution. We depict the solution for $\beta = -1$ in Figs. 17 and 18 (Fig. 19).

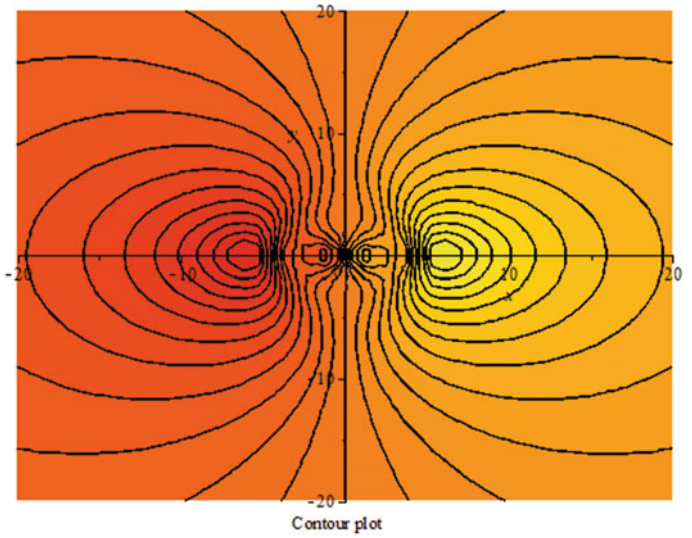


**Fig. 18** Wave profile of solution in Eq. (53) with $\hat{I}^2=-1$

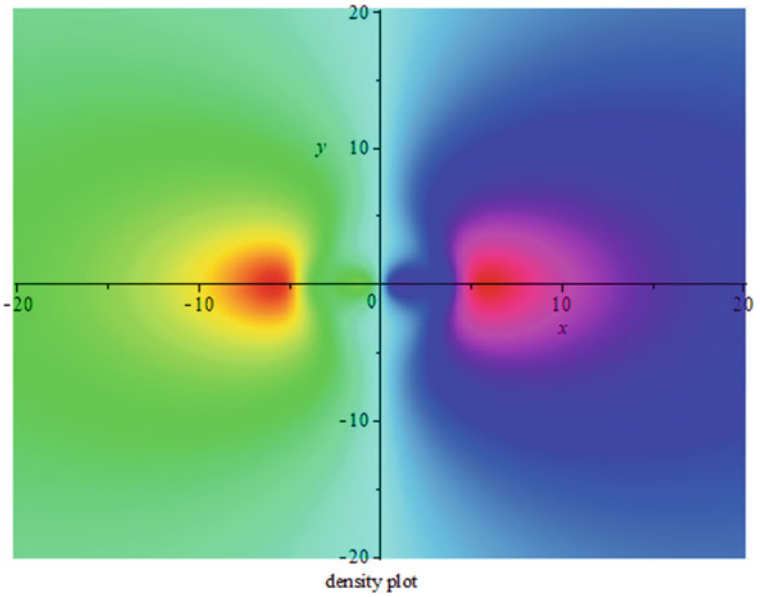


**Fig. 19** Wave profile of solution in Eq. (53) with $\hat{I}^2=-1$

## 5.2 *In the Case of $X = x + a_1 y$*

Now we assume $X = x + a_1 y$ and consider

$$f(x, y, t) = F(X, t) = \sum_{k=0}^{M} \sum_{j=0}^{M-k} a_{k,j} X^{2k} t^{2j}. \tag{54}$$

Let $f_1(x, y, t) = X^2 + a_3 t^2 + a_2$ be a solution of (5). By symbolic computation we get a solution with

$$a_1 = -\frac{1}{\gamma}, a_2 = -\frac{3\gamma^2}{\beta\gamma^2 - 1}, a_3 = \frac{\beta\gamma^2 - 1}{\gamma^2 \alpha}.$$

It follows that

$$f(x, y, t) = (x - \frac{y}{\gamma})^2 - \frac{1 - \beta\gamma^2}{\gamma^2\alpha} t^2 + \frac{3\gamma^2}{1 - \beta\gamma^2}.$$

We need $a_2 > 0, a_3 > 0$ for $f > 0$. So we have

$$\gamma \neq 0, 1 - \beta\gamma^2 > 0, \alpha < 0. \tag{55}$$

A lump solution can, thus, be constructed:

$$u(x, y, t) = 2(\ln f)_x = \frac{4(x - \frac{y}{\gamma})}{(x - \frac{y}{\gamma})^2 - \frac{1-\beta\gamma^2}{\gamma^2\alpha} t^2 + \frac{3\gamma^2}{1-\beta\gamma^2}}. \tag{56}$$

Evidently, the function $u$ possesses the property

$$\lim_{x^2+y^2 \to \infty} u(x, y, t) = 0.$$

We depict the solution in Figs. 20, 21, 22 and 23, for $\alpha = -1, \beta = -1, \gamma = 1$.

When $n = 2$, we have $M = 3$. Let

$$f_2(x, y, t) = X^6 + (a_2 + a_3 t^2)X^4 + (a_4 + a_5 t^2 + a_6 t^4)X^2 + a_7 + a_8 t^2 + a_9 t^4 + a_{10} t^6$$

be a solution of (5). By symbolic computation we get a solution with

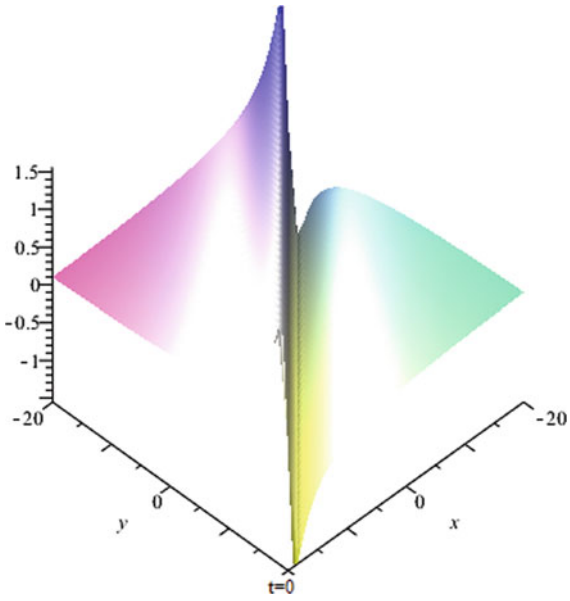


**Fig. 20** Wave profile of solution in Eq. (56) with Î± = âˆ’1, Î² = âˆ’1, Î³ = 1

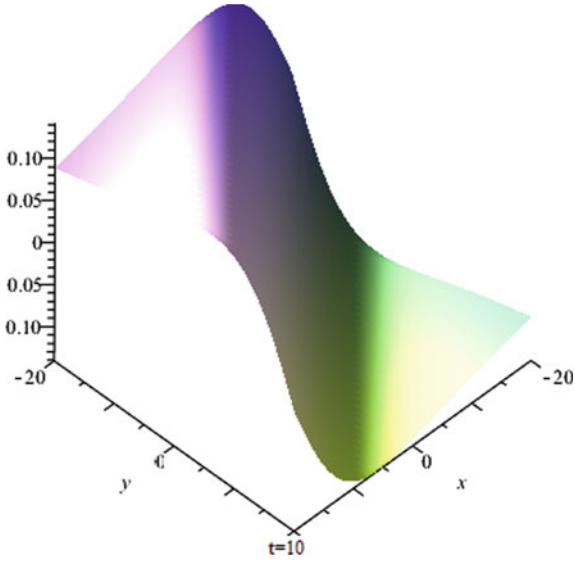


**Fig. 21** Wave profile of solution in Eq. (56) with Î± = âˆ’1, Î² = âˆ’1, Î³ = 1

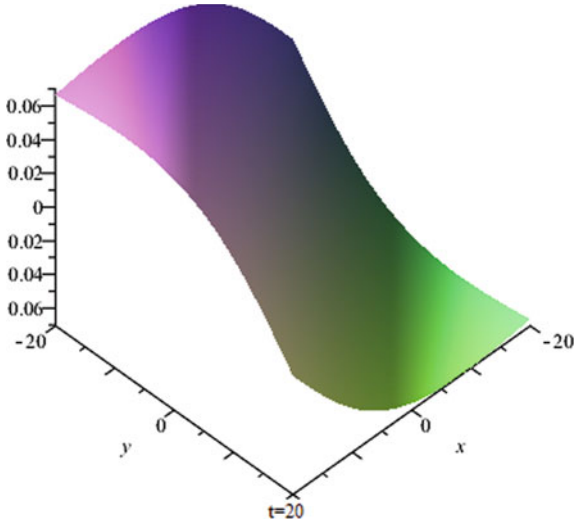


**Fig. 22** Wave profile of solution in Eq. (56) with Î± = âˆ’1, Î² = âˆ’1, Î³ = 1

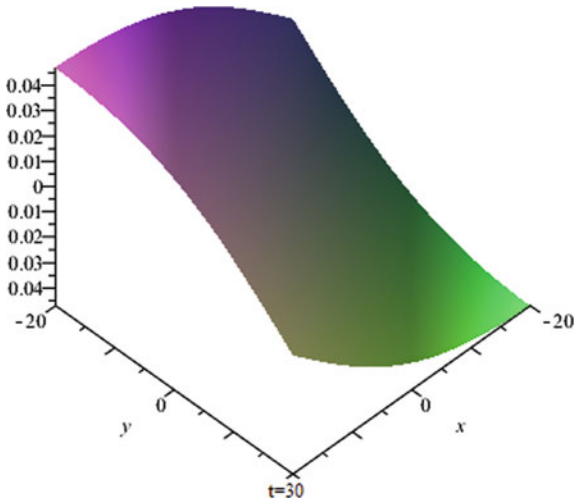


**Fig. 23** Wave profile of solution in Eq. (56) with Î± = âˆ’1, Î² = âˆ’1, Î³ = 1

$$a_1 = -\frac{1}{\gamma}, a_2 = \frac{25\gamma^2}{1-\beta\gamma^2}, a_3 = \frac{3(\beta\gamma^2-1)}{\gamma^2\alpha}, a_4 = -\frac{125\gamma^4}{(\beta\gamma^2-1)^2}, a_5 = -\frac{90}{\alpha},$$
$$a_6 = \frac{3(\beta\gamma^2-1)^2}{\alpha^2\gamma^4}, a_7 = \frac{1875\gamma^6}{(1-\beta\gamma^2)^3}, a_8 = \frac{475\gamma^2}{\alpha(\beta\gamma^2-1)}, a_9 = \frac{17(1-\beta\gamma^2)}{\alpha^2\gamma^2},$$
$$a_{10} = \frac{(\beta\gamma^2-1)^3}{\alpha^3\gamma^6}.$$

Consequently, we obtain

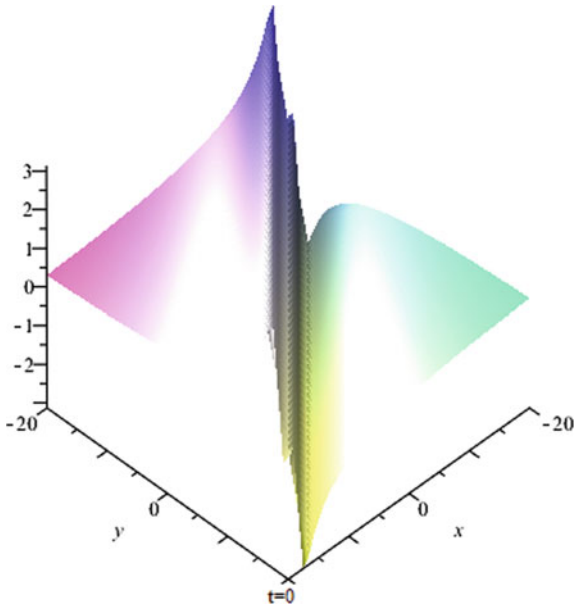


**Fig. 24** Wave profile of solution in Eq. (57) with Î± = âˆ’1, Î² = âˆ’1, Î³ = 1

$$
\begin{aligned}
f_2(x,y,t) =& (x-\frac{y}{\gamma})^6+\left[\frac{3(\beta\gamma^2-1)t^2}{\gamma^2\alpha}+\frac{25\gamma^2}{1-\beta\gamma^2}\right](x-\frac{y}{\gamma})^4\\
&+\left[\frac{3(\beta\gamma^2-1)^2t^4}{\alpha^2\gamma^4}-\frac{90}{\alpha}t^2-\frac{125\gamma^4}{(\beta\gamma^2-1)^2}\right](x-\frac{y}{\gamma})^2\\
&+\frac{(\beta\gamma^2-1)^3t^6}{\alpha^3\gamma^6}+\frac{17(1-\beta\gamma^2)t^4}{\alpha^2\gamma^2}+\frac{475\gamma^2t^2}{\alpha(\beta\gamma^2-1)}+\frac{1875\gamma^6}{(1-\beta\gamma^2)^3}.
\end{aligned}
$$

We denote

$$
\begin{aligned}
f_{2x}(x,y,t) =& 6(x-\frac{x}{y}\gamma)^5+4(x-\frac{y}{\gamma})^3\left[\frac{3(\beta\gamma^2-1)t^2}{\gamma^2\alpha}+\frac{25\gamma^2}{1-\beta\gamma^2}\right] \qquad (57)\\
&+2(x-\frac{y}{\gamma})\left[\frac{3(\beta\gamma^2-1)^2t^4}{\alpha^2\gamma^4}-\frac{90}{\alpha}t^2-\frac{125\gamma^4}{(\beta\gamma^2-1)^2}\right]. \qquad (58)
\end{aligned}
$$

Again, it is easy to see that $f_2 > 0$, when (55) is satisfied. The corresponding solution

$$u(x,y,t) = 2(\ln f_2(x,y,t))_x = \frac{2[f_{2x}(x,y,t)]}{f_2(x,y,t)}$$

is a 3-lump solution. The wave profile is shown in Figs. 24, 25, 26 and 27, for $\alpha = -1, \beta = -1, \gamma = 1$.

When $n = 3$, we have $M = 6$. Let

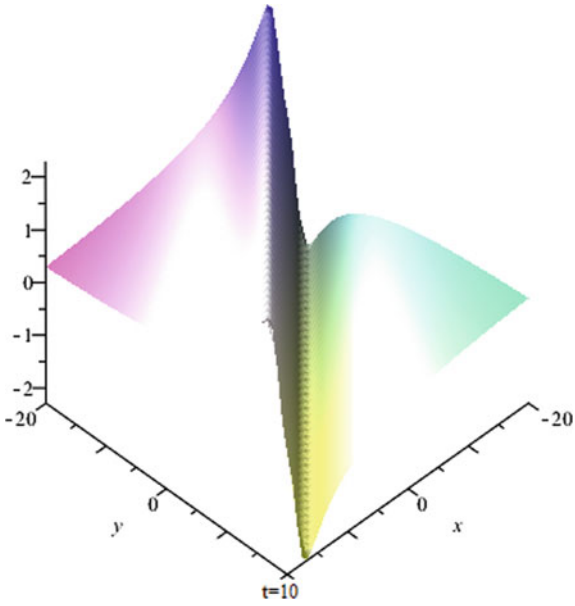


**Fig. 25** Wave profile of solution in Eq. (57) with Î± = âˆ’1, Î² = âˆ’1, Î³ = 1

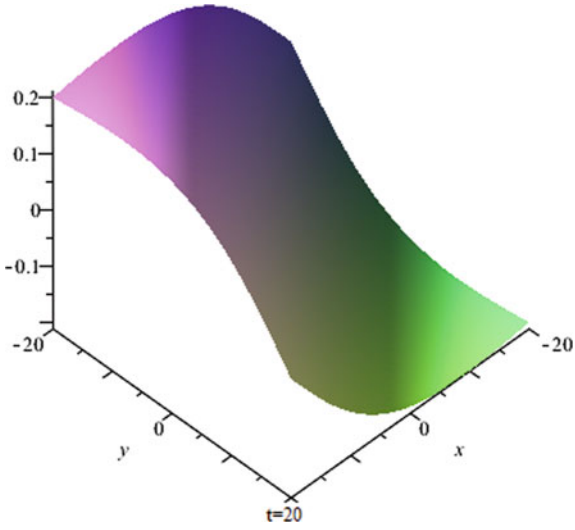


**Fig. 26** Wave profile of solution in Eq. (57) with Î± = âˆ’1, Î² = âˆ’1, Î³ = 1

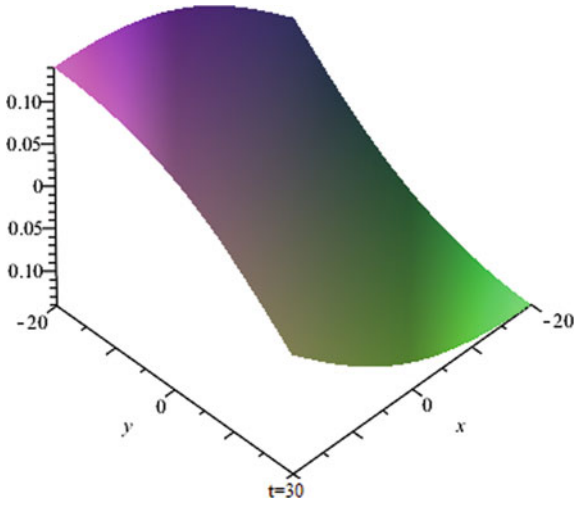


**Fig. 27** Wave profile of solution in Eq. (57) with Î± = âˆ’1, Î² = âˆ’1, Î³ = 1

$$f_3(x,y,t) = X^{12} + (a_2 + a_3t^2)X^{10} + (a_4 + a_5t^2 + a_6t^4)X^8 + (a_7 + a_8t^2 + a_9t^4 + a_{10}t^6)X^6 + (a_{11} + a_{12}t^2 + a_{13}t^4 + a_{14}t^6 + a_{15}t^8)X^4 + (a_{16} + a_{17}t^2 + a_{18}t^4 + a_{19}t^6 + a_{20}t^8 + a_{21}t^{10})X^2 + a_{22} + a_{23}t^2 + a_{24}t^4 + a_{25}t^6 + a_{26}t^8 + a_{27}yt^{10} + a_{28}t^{12}$$

be a solution of (5). By symbolic computation we get a solution with

$$a_1 = -\frac{1}{\gamma}, a_2 = \frac{98\gamma^2}{1-\beta\gamma^2}, a_3 = \frac{6(\beta\gamma^2-1)}{\alpha\gamma^2}, a_4 = -\frac{735\gamma^4}{(\beta\gamma^2-1)^2}, a_5 = -\frac{690}{\alpha},$$
$$a_6 = \frac{15(\beta\gamma^2-1)^2}{\alpha^2\gamma^4}, a_7 = \frac{75460\gamma^6}{3(1-\beta\gamma^2)^3}, a_8 = \frac{18620\gamma^2}{\alpha(\beta\gamma^2-1)}, a_9 = \frac{1540(1-\beta\gamma^2)}{\alpha^2\gamma^2},$$
$$a_{10} = \frac{20(\beta\gamma^2-1)^3}{\alpha^3\gamma^6}, a_{11} = -\frac{5187875\gamma^8}{3(1-\beta\gamma^2)^4}, a_{12} = -\frac{220500\gamma^4}{\alpha(\beta\gamma^2-1)^2}, a_{13} = \frac{37450}{\alpha^2},$$
$$a_{14} = -\frac{1460(1-\beta\gamma^2)^2}{\alpha^3\gamma^4}, a_{15} = \frac{15(1-\beta\gamma^2)^4}{\alpha^4\gamma^8}, a_{16} = \frac{159786550\gamma^{10}}{3(1-\beta\gamma^2)^5}, a_{17} = \frac{565950\gamma^6}{\alpha(\beta\gamma^2-1)^3},$$
$$a_{18} = \frac{14700\gamma^2}{\alpha^2(\beta\gamma^2-1)}, a_{19} = \frac{35420(\beta\gamma^2-1)}{\alpha^3\gamma^2}, a_{20} = \frac{570(1-\beta\gamma^2)^3}{\alpha^4\gamma^6}, a_{21} = \frac{6(\beta\gamma^2-1)^5}{\alpha^5\gamma^{10}},$$
$$a_{22} = \frac{878826025\gamma^{12}}{9(1-\beta\gamma^2)^6}, a_{23} = -\frac{300896750\gamma^8}{3\alpha(\beta\gamma^2-1)^4}, a_{24} = \frac{16391725\gamma^4}{3\alpha^2(\beta\gamma^2-1)^2},$$
$$a_{25} = -\frac{798980}{3\alpha^3}, a_{26} = \frac{4335(\beta\gamma^2-1)^2}{\alpha^4\gamma^4}, a_{27} = -\frac{58(\beta\gamma^2-1)^4}{\alpha^5\gamma^8}, a_{28} = \frac{(\beta\gamma^2-1)^6}{\alpha^6\gamma^{12}}.$$

With $X = x - \frac{y}{\gamma}$, we obtain

$$
\begin{aligned}
f_3(x,y,t) = {} & X^{12} + \left[\frac{6(\beta\gamma^2-1)t^2}{\alpha\gamma^2} + \frac{98\gamma^2}{1-\beta\gamma^2}\right]X^{10} + \left[\frac{15(\beta\gamma^2-1)^2t^4}{\alpha^2\gamma^4} - \frac{690t^2}{\alpha} - \frac{735\gamma^4}{(\beta\gamma^2-1)^2}\right]X^8 \\
& + \left[\frac{20(\beta\gamma^2-1)^3t^6}{\alpha^3\gamma^6} + \frac{1540(1-\beta\gamma^2)t^4}{\alpha^2\gamma^2} + \frac{18620\gamma^2t^2}{\alpha(\beta\gamma^2-1)} + \frac{75460\gamma^6}{3(1-\beta\gamma^2)^3}\right]X^6 \\
& + \left[\frac{15(1-\beta\gamma^2)^4t^8}{\alpha^4\gamma^8} - \frac{1460(1-\beta\gamma^2)^2t^6}{\alpha^3\gamma^4} + \frac{37450t^4}{\alpha^2} - \frac{220500\gamma^4t^2}{\alpha(\beta\gamma^2-1)^2} - \frac{5187875\gamma^8}{3(1-\beta\gamma^2)^4}\right]X^4 \\
& + \left[\frac{6(\beta\gamma^2-1)^5t^{10}}{\alpha^5\gamma^{10}} + \frac{570(1-\beta\gamma^2)^3t^8}{\alpha^4\gamma^6} + \frac{35420(\beta\gamma^2-1)t^6}{\alpha^3\gamma^2} + \frac{14700\gamma^2t^4}{\alpha^2(\beta\gamma^2-1)}\right. \\
& \quad \left. + \frac{565950\gamma^6t^2}{\alpha(\beta\gamma^2-1)^3} + \frac{159786550\gamma^{10}}{3(1-\beta\gamma^2)^5}\right]X^2 \\
& + \frac{(\beta\gamma^2-1)^6t^{12}}{\alpha^6\gamma^{12}} - \frac{58(\beta\gamma^2-1)^4t^{10}}{\alpha^5\gamma^8} + \frac{4335(\beta\gamma^2-1)^2t^8}{\alpha^4\gamma^4} - \frac{798980t^6}{3\alpha^3} + \frac{16391725\gamma^4t^4}{3\alpha^2(\beta\gamma^2-1)^2} \\
& - \frac{300896750\gamma^8t^2}{3\alpha(\beta\gamma^2-1)^4} + \frac{878826025\gamma^{12}}{9(1-\beta\gamma^2)^6}.
\end{aligned}
$$

After some computation, we can verify that $f_3 > 0$ when (55) is satisfied. The resulting solution is given by

$$
u(x,y,t) = 2[\ln f_3(x,y,t)]_x = \frac{2f_{3x}(x,y,t)}{f_3(x,y,t)}, \tag{59}
$$

where

$$
\begin{aligned}
f_{3x}(x,y,t) = {} & 12X^{11} + 10X^9\left[\frac{6(\beta\gamma^2-1)t^2}{\alpha\gamma^2} + \frac{98\gamma^2}{1-\beta\gamma^2}\right] \\
& + 8X^7\left[\frac{15(\beta\gamma^2-1)^2t^4}{\alpha^2\gamma^4} - \frac{690t^2}{\alpha} - \frac{735\gamma^4}{(\beta\gamma^2-1)^2}\right] \\
& + 6X^5\left[\frac{20(\beta\gamma^2-1)^3t^6}{\alpha^3\gamma^6} + \frac{1540(1-\beta\gamma^2)t^4}{\alpha^2\gamma^2} + \frac{18620\gamma^2t^2}{\alpha(\beta\gamma^2-1)} + \frac{15(\beta\gamma^2-1)^2}{\alpha^2\gamma^4}\right] \\
& + 4X^3\left[\frac{15(1-\beta\gamma^2)^4t^8}{\alpha^4\gamma^8} - \frac{1460(1-\beta\gamma^2)^2t^6}{\alpha^3\gamma^4} + \frac{37450t^4}{\alpha^2} - \frac{220500\gamma^4t^2}{\alpha(\beta\gamma^2-1)^2} - \frac{5187875\gamma^8}{3(1-\beta\gamma^2)^4}\right] \\
& + 2X\left[\frac{6(\beta\gamma^2-1)^5t^{10}}{\alpha^5\gamma^{10}} + \frac{570(1-\beta\gamma^2)^3t^8}{\alpha^4\gamma^6} + \frac{35420(\beta\gamma^2-1)t^6}{\alpha^3\gamma^2} + \frac{14700\gamma^2t^4}{\alpha^2(\beta\gamma^2-1)}\right. \\
& \quad \left. + \frac{565950\gamma^6t^2}{\alpha(\beta\gamma^2-1)^3} + \frac{159786550\gamma^{10}}{3(1-\beta\gamma^2)^5}\right].
\end{aligned}
$$

This is a 6-lump solution. We depict the solution in Figs. 28, 29, 30 and 31, for $\alpha = -1, \beta = -1, \gamma = 1$.

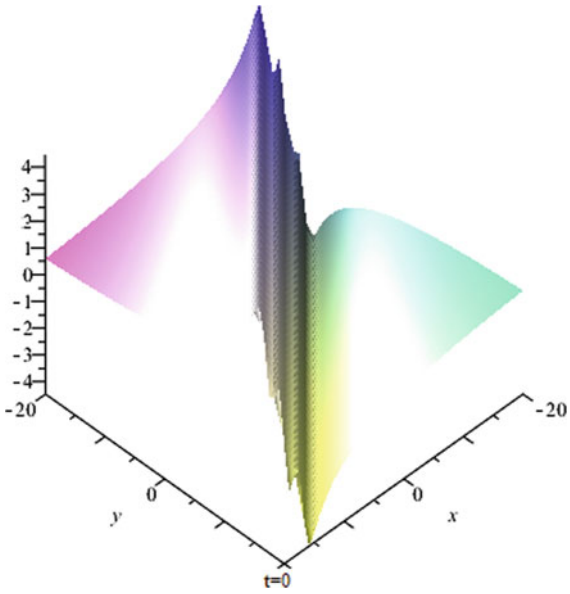


**Fig. 28** Wave profile of solution in Eq. (59) with Î± = âˆ’1, Î² = âˆ’1, Î³ = 1

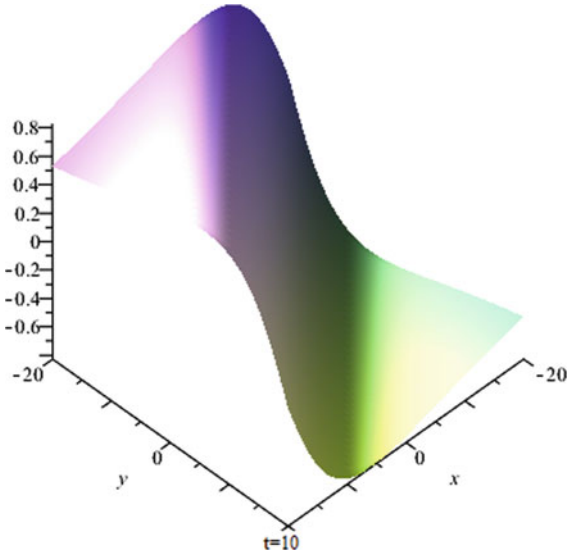


**Fig. 29** Wave profile of solution in Eq. (59) with Î± = âˆ’1, Î² = âˆ’1, Î³ = 1

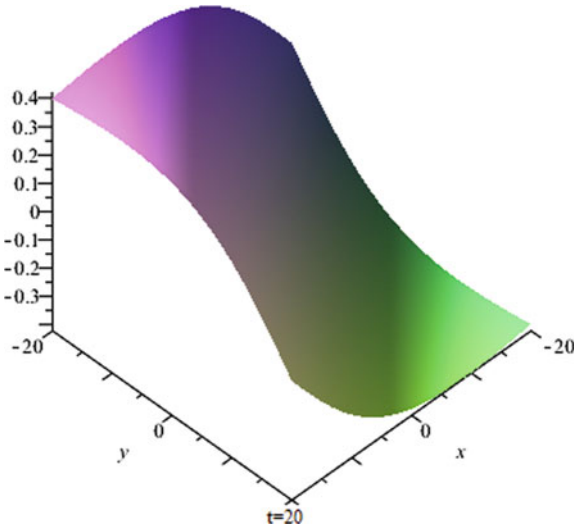


**Fig. 30** Wave profile of solution in Eq. (59) with Î± = âˆ’1, Î² = âˆ’1, Î³ = 1

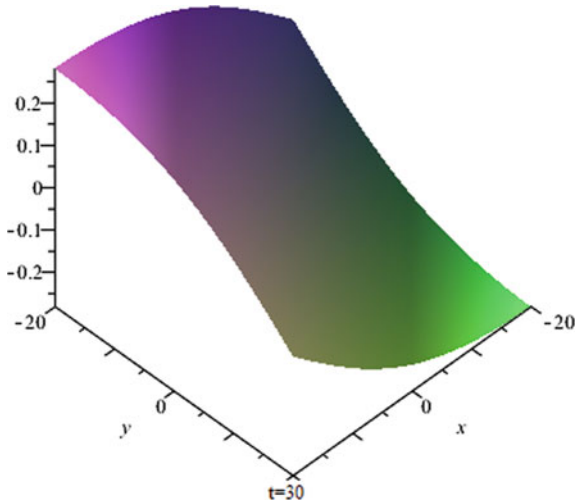


**Fig. 31** Wave profile of solution in Eq. (59) with Î± = âˆ’1, Î² = âˆ’1, Î³ = 1

## 6 Concluding Remarks

In this chapter, we have introduced a new (2+1)-dimensional equation from the well-known Benjamin-Ono equation and studied its multiple lump and rogue wave solutions by means of the Hirota bilinear method. Two reductions were particularly considered: an integrable equation and a nonintegrable one. The nonintegrable equation was found to possess both lump and line rogue wave solutions, whereas the integrable equation was found to posses only lump solutions.

Furthermore, we also found multiple lump solutions to the new equation. For this type of solutions, we considered two cases: $X = x + a_1 t$ and $X = x + a_1 y$. In the first case, we observe multiple lump solutions with multiple peaks and troughs corresponding to the order $M$ of the solution, where $M = \frac{n(n+1)}{2}$, $n = 1, 2, \ldots$. The second case yields multiple lump solutions that are actually rogue waves with multiple line profiles.

## References


1. S. Manukure, T. Booker, A short overview of solitons and applications, Partial Differential Equations in Applied Mathematics 4 (2021) 100140.
2. G. Fibich, The nonlinear Schrödinger equation, Vol. 192, Springer, 2015.
3. W.-X. Ma, Y. Zhou, Lump solutions to nonlinear partial differential equations via Hirota bilinear forms, Journal of Differential Equations 264 (4) (2018) 2633–2659.
4. W.-X. Ma, Lump solutions to the Kadomtsev–Petviashvili equation, Physics Letters A 379 (36) (2015) 1975–1978.
5. S. Manukure, Y. Zhou, W.-X. Ma, Lump solutions to a (2+1)-dimensional extended KP equation, Computers & Mathematics with Applications 75 (7) (2018) 2414–2419.
6. I. S. Aranson, A. Pikovsky, N. F. Rulkov, L. S. Tsimring, Advances in Dynamics, Patterns, Cognition, Springer, 2017.
7. S. Manakov, V. E. Zakharov, L. Bordag, A. Its, V. Matveev, Two-dimensional solitons of the Kadomtsev-Petviashvili equation and their interaction, Physics Letters A 63 (3) (1977) 205–206.
8. P. A. Clarkson, E. Dowie, Rational solutions of the Boussinesq equation and applications to rogue waves, Transactions of Mathematics and its Applications 1 (1) (2017) tnx003.
9. J.-b. Zhang, W.-X. Ma, Mixed lump-kink solutions to the BKP equation, Computers & Mathematics with Applications 74 (3) (2017) 591–596.
10. Y. Zhou, S. Manukure, Rational and interactive solutions to the B-type Kadomtsev-Petviashvili equation, Journal of Applied Analysis & Computation 11 (5) (2021) 2473–2490.
11. J.-Y. Yang, W.-X. Ma, Z. Qin, Lump and lump-soliton solutions to the (2+1)-dimensional Ito equation, Analysis and Mathematical Physics 8 (2018) 427–436.
12. Y. Zhou, S. Manukure, W.-X. Ma, Lump and lump-soliton solutions to the Hirota–Satsuma–Ito equation, Communications in Nonlinear Science and Numerical Simulation 68 (2019) 56–62.
13. H.-Q. Zhang, W.-X. Ma, Lump solutions to the (2+1)-dimensional Sawada–Kotera equation, Nonlinear Dynamics 87 (2017) 2305–2310.
14. J. Satsuma, M. Ablowitz, Two-dimensional lumps in nonlinear dispersive systems, Journal of Mathematical Physics 20 (7) (1979) 1496–1503.
15. K. Imai, K. Nozaki, Lump solutions of the Ishimori-II equation, Progress of theoretical physics 96 (3) (1996) 521–526.
16. K. Imai, Dromion and lump solutions of the Ishimori-I equation, Progress of Theoretical Physics 98 (5) (1997) 1013–1023.
17. S. Manukure, Y. Zhou, A study of lump and line rogue wave solutions to a (2+1)-dimensional nonlinear equation, Journal of Geometry and Physics 167 (2021) 104274.
18. D. Gao, X. Lü, M.-S. Peng, Study on the (2+ 1)-dimensional extension of Hietarinta equation: soliton solutions and bäcklund transformation, Physica Scripta 98 (9) (2023) 095225.
19. B.-Q. Li, Y.-L. Ma, Multiple-lump waves for a (3+1)-dimensional Boiti–Leon–Manna–Pempinelli equation arising from incompressible fluid, Computers & Mathematics with Applications 76 (1) (2018) 204–214.
20. Y. Tian, J.-G. Liu, Study on dynamical behavior of multiple lump solutions and interaction between solitons and lump wave, Nonlinear Dynamics 104 (2021) 1507–1517.

21. W.-X. Ma, Y. Zhou, R. Dougherty, Lump-type solutions to nonlinear differential equations derived from generalized bilinear equations, International Journal of Modern Physics B 30 (28n29) (2016) 1640018.
22. J. M. Dudley, V. Sarano, F. Dias, On Hokusai's Great wave off Kanagawa: Localization, linearity and a rogue wave in sub-antarctic waters, Notes and Records of the Royal Society 67 (2) (2013) 159–164.
23. R. Grimshaw, E. Pelinovsky, T. Taipova, A. Sergeeva, Rogue internal waves in the ocean: Long wave model, The European Physical Journal Special Topics 185 (1) (2010) 195–208.
24. F. Fedele, Rogue waves in oceanic turbulence, Physica D: Nonlinear Phenomena 237 (14-17) (2008) 2127–2131.
25. D. R. Solli, C. Ropers, P. Koonath, B. Jalali, Optical rogue waves, nature 450 (7172) (2007) 1054–1057.
26. D.-I. Yeom, B. J. Eggleton, Rogue waves surface in light, Nature 450 (7172) (2007) 953–954.
27. B. Kibler, J. Fatome, C. Finot, G. Millot, F. Dias, G. Genty, N. Akhmediev, J. M. Dudley, The Peregrine soliton in nonlinear fibre optics, Nature Physics 6 (10) (2010) 790–795.
28. B. Frisquet, B. Kibler, P. Morin, F. Baronio, M. Conforti, G. Millot, S. Wabnitz, Optical dark rogue wave, Scientific Reports 6 (1) (2016) 20785.
29. F. Baronio, B. Frisquet, S. Chen, G. Millot, S. Wabnitz, B. Kibler, Observation of a group of dark rogue waves in a telecommunication optical fiber, Physical Review A 97 (1) (2018) 013852.
30. H. Bailung, S. Sharma, Y. Nakamura, Observation of Peregrine solitons in a multicomponent plasma with negative ions, Physical review letters 107 (25) (2011) 255005.
31. N. Akhmediev, A. Ankiewicz, M. Taki, Waves that appear from nowhere and disappear without a trace, Physics Letters A 373 (6) (2009) 675–678.
32. B. Yang, J. Yang, General rogue waves in the Boussinesq equation, Journal of the Physical Society of Japan 89 (2) (2020) 024003.
33. G. Mu, Z. Qin, R. Grimshaw, Dynamics of rogue waves on a multisoliton background in a vector nonlinear Schrödinger equation, SIAM Journal on Applied Mathematics 75 (1) (2015) 1–20.
34. J. Rao, A. S. Fokas, J. He, Doubly localized two-dimensional rogue waves in the Davey–Stewartson I equation, Journal of Nonlinear Science 31 (4) (2021) 67.
35. R. Hirota, The direct method in soliton theory, no. 155, Cambridge University Press, 2004.
36. T. B. Benjamin, Internal waves of permanent form in fluids of great depth, Journal of Fluid Mechanics 29 (3) (1967) 559–592.
37. H. Ono, Algebraic solitary waves in stratified fluids, Journal of the Physical Society of Japan 39 (4) (1975) 1082–1091.
38. A. S. Fokas, M. J. Ablowitz, The inverse scattering transform for the Benjamin-Ono equation-a pivot to multidimensional problems, Studies in Applied Mathematics 68 (1) (1983) 1–10.
39. R. R. Coifman, M. V. Wickerhauser, The scattering transform for the Benjamin-Ono equation, Inverse Problems 6 (5) (1990) 825.
40. L. Akinyemi, Shallow ocean soliton and localized waves in extended (2+1)-dimensional nonlinear evolution equations, Physics Letters A 463 (2023) 128668.
41. Zhaqilao, A symbolic computation approach to constructing rogue waves with a controllable center in the nonlinear systems, Computers and Mathematics with Applications 75 (9) (2018) 3331–3342.

# On the Inclination of a Parameterized Curve


**John McCuan**

**Abstract** Given a plane curve $\Gamma$ parameterized by arclength $s$ on an open interval $I \subset \mathbb{R}$ by a function $\gamma : I \to \mathbb{R}^2$ with twice continuously differentiable component functions and an initial inclination angle $\theta_0 \in \mathbb{R}$ satisfying $\dot{\gamma}(s_0) = (\cos\theta_0, \sin\theta_0)$ for some $s_0 \in I$, we show there exists a unique function $\psi \in C^1(I)$ with $\dot{\gamma}(s) = (\cos\psi(s), \sin\psi(s))$ for all $s \in I$ and $\psi(s_0) = \theta_0$. Similar results holding for a parameterized curve defined on a compact interval are stated in many differential geometry texts. These results are usually based on a path lifting result for continuous maps into the circle $\mathbb{S}^1$. Our result differs from these treatments both in that the interval $I$ is taken to be open and that the techniques used to obtain the result are via a direct treatment of a system of ordinary differential equations. The system of ordinary differential equations differs from those usually considered in that it contains first order equations of singular type. Such systems seem to have independent interest and the approach presented should have broader application. We give one other related example of a similar singular system of ordinary differential equations, and we strongly suspect the development of a general axiomatic theory of such singular systems should be possible, though we are unaware of such a development. We also discuss the topological approach and offer a version of the path lifting lemma for paths defined on open interval (or any interval). Finally, we discuss applications of our result to the construction, classification, and analysis of plane curves and in relation to structure theorems for plane curves.

**Keywords** Inclination · Universal cover · Plane curve

Let $I$ be an open interval in $\mathbb{R}$ with $s_0 \in I$. Let $\gamma : I \to \mathbb{R}^2$ have coordinate functions $\gamma = (\gamma_1, \gamma_2)$ with $\gamma_j \in C^2(I)$ for $j = 1, 2$ satisfying $\dot{\gamma}_1^2 + \dot{\gamma}_2^2 = 1$ (parameterization by arclength) where

$$\dot{\gamma}_j = \frac{d\gamma_j}{ds} \qquad \text{for } j = 1, 2.$$

J. McCuan (✉)
Georgia Institute of Technology, Mathematics, 686 Cherry Street, Atlanta, GA 30332, USA
e-mail: mccuan@pm.me



S. Manukure and W.-X. Ma (eds.), *Nonlinear and Modern Mathematical Physics*,
Springer Proceedings in Mathematics & Statistics 459,
https://doi.org/10.1007/978-3-031-59539-4_13

We will prove the following:

**Theorem 1** (global solution of singular system of ordinary differential equations) *If* $\theta_0 \in \mathbb{R}$ *satisfies*

$$\begin{cases} \cos\theta_0 = \dot\gamma_1(s_0) \\ \sin\theta_0 = \dot\gamma_2(s_0), \end{cases} \tag{1}$$

*there exists a unique function* $\psi \in C^1(I)$ *satisfying the system of ordinary differential equations*

$$\begin{cases} -\sin\psi\,\dot\psi = \ddot\gamma_1,\ s \in I \\ \cos\psi\,\dot\psi = \ddot\gamma_2,\ s \in I \\ \psi(s_0) = \theta_0. \end{cases} \tag{2}$$

**Theorem 2** (globally defined differentiable inclination) *If* $\theta_0 \in \mathbb{R}$ *satisfies (1) then there exists a unique function* $\psi \in C^1(I)$ *satisfying the system of algebraic equations*

$$\begin{cases} \cos\psi = \dot\gamma_1,\ s \in I \\ \sin\psi = \dot\gamma_2,\ s \in I \\ \psi(s_0) = \theta_0. \end{cases} \tag{3}$$

We obtain Theorem 2 first as a corollary of Theorem 1 and the following assertion of equivalence:

**Theorem 3** (equivalence) *Given* $\gamma : I \to \mathbb{R}^2$ *as above:*

***(a)*** *If* $\psi \in C^1(I)$ *satisfies the transcendental system of algebraic equations (3) then* $\psi$ *is the unique solution of the singular system of ordinary differential equations (2).*

***(b)*** *If* $\psi \in C^1(I)$ *satisfies the singular system of ordinary differential equations (2) then* $\psi$ *is the unique solution of the transcendental system of algebraic equations (3).*

We also obtain Theorem 2 as a corollary of the following topological lifting result:

**Theorem 4** (topological lifting) *If* $I$ *is any interval in* $\mathbb{R}$ *and* $\mathbf{v} : I \to \mathbb{S}^1$ *has coordinate functions* $\mathbf{v} = (v_1, v_2)$ *with* $v_j \in C^0(I)$ *for* $j = 1, 2$ *and* $\mathbf{v}(s_0) = (\cos\theta_0, \sin\theta_0)$ *for some* $\theta_0 \in \mathbb{R}$ *and some* $s_0 \in I$*, then there exists a unique function* $\psi \in C^0(I)$ *for which*

$$\begin{cases} \cos\psi = v_1,\ s \in I \\ \sin\psi = v_2,\ s \in I \\ \psi(s_0) = \theta_0. \end{cases} \tag{4}$$

*The lifting condition (4) is usually formulated as* $p \circ \psi = \mathbf{v}$ *where* $p : \mathbb{R} \to \mathbb{S}^1$ *by* $p(\theta) = (\cos\theta, \sin\theta)$ *is the universal covering map of* $\mathbb{S}^1$.

The organization of the paper is as follows: We begin with a discussion of the construction of plane curves of prescribed curvature. We then prove Theorems 1, 2, and 3 in Sect. 1. Section 2 contains a proof of Theorem 4 and some related discussion

of topological lifting. In Sect. 3 we state two structure theorems for plane curves directly in terms of inclination angle, and in Sect. 4 we give two examples of curves to which the above discussion applies and finally another example of a singular system of ordinary differential equations (ODEs).

## Remarks on the Construction of Plane Curves

The assertion of Theorem 2 is useful in the construction, classification, and analysis of plane curves having prescribed curvature. Say, for example, we wish to classify all $C^2$ curves in the $x$, $y$-plane with signed curvature $k$ satisfying $k = y$ at each point $(x, y)$ on the curve. The usual formulation for $\gamma : I \to \mathbb{R}^2$ defined on an interval $I$ is given by an initial value problem

$$\ddot{\gamma} \cdot \dot{\gamma}^{\perp} = -\dot{\gamma}_2 \ddot{\gamma}_1 + \dot{\gamma}_1 \ddot{\gamma}_2 = \gamma_2, \qquad \gamma(s_0) = (x_0, y_0), \quad \dot{\gamma}(s_0) = \mathbf{v}_0 \tag{5}$$

where $s_0 \in I$ and $\mathbf{v}_0 \in \mathbb{S}^1 = \{\mathbf{v} \in \mathbb{R}^2 : \|\mathbf{v}\| = 1\}$. These curves are called **elastic curves**. They were first (and famously) classified by Euler [5], and the usual procedure for their classification is to trade in the complicated second order equation in (5) for the simple first order system of equations in the initial value problem

$$\begin{cases} \dot{\gamma}_1 = \cos\psi, & \gamma_1(0) = x_0 \\ \dot{\gamma}_2 = \sin\psi, & \gamma_2(0) = y_0 \\ \dot{\psi} = \gamma_2, & \psi(0) = \theta_0 \end{cases} \tag{6}$$

where it is observed that specification of the initial unit tangent $\mathbf{v}_0$ determines some initial angle $\theta_0$ up to an additive multiple of $2\pi$ by

$$\begin{cases} \cos\theta_0 = \dot{\gamma}_1(s_0) \\ \sin\theta_0 = \dot{\gamma}_2(s_0). \end{cases} \tag{7}$$

The introduction of the inclination angle $\psi$ in (6) is based also on the observation that the signed curvature $k$ is given by the formula

$$k = \frac{d\psi}{ds}. \tag{8}$$

Both this observation and the formulation of (6) rely on some result like Theorem 2. Of course, this would be a much more interesting paper if there existed some solutions of (5) which were somehow singular with respect to the inclination angle so that they were missed by a classification of solutions of (6). As it is, Theorem 2 guarantees no such singular elastic curves exist and thus Theorem 2 and all discussion associated with it may be viewed as a technical detail.

On the other hand, it is convenient to have a global result like Theorem 2. A careful look at doCarmo's classical text on differential geometry [3, pp. 23, 36–39] reveals that the formula (8) is only introduced and considered locally and basically with the assumption that $\psi$ is differentiable. Similarly Stoker [14, pp. 21–22] addresses the question by considering the version

$$\begin{cases} \cos\psi = \dot{\gamma}_1(s) \\ \sin\psi = \dot{\gamma}_2(s) \end{cases} \tag{9}$$

of (7) locally. Theorem 2 provides a foundation for the treatments of both doCarmo and Stoker, and this is especially important for Stoker who uses (8) to define curvature.

It is interesting that Stoker returns to the topic [14, p. 27] in the context of a structure theorem for plane curves and offers a kind of global definition with differentiability built in:

$$\psi(s) = \theta_0 + \int_{s_0}^{s} k(\sigma)\, d\sigma. \tag{10}$$

The function $\psi$ defined in (10) is a clearly globally defined continuously differentiable function depending of course on the definition of curvature (which can be done without $\psi$ as given for example in (5)), but most importantly the formula (10) lacks the original connection (3) with the tangent vector to the curve.[1]

In summary, one may find the assumption, but not the justification for the assertion, that the inclination angle is a globally well-defined differentiable function of arclength. It seems to me that one natural global formulation for the existence of $\psi$ is in terms of the singular first order system of ODEs (2). There is a good existence and uniqueness theory for regular first order systems, and there is extensive analysis associated with singular linear ODEs with isolated singular points like Bessel's equation, which can be cast in terms of linear systems. This is the approach taken in Sect. 1 below.

Returning to the construction of curves of prescribed curvature, one may consider

$$\begin{cases} \dot{\gamma}_1 = \cos\psi, & \gamma_1(0) = x_0 \\ \dot{\gamma}_2 = \sin\psi, & \gamma_2(0) = y_0 \\ \dot{\psi} = f, & \psi(0) = \theta_0 \end{cases}$$

in a variety of contexts where the function $f = f(\gamma, \psi, s)$ prescribes the curvature. All such constructions again assume the curve one wishes to parameterize admits/determines a differentiable inclination angle. The Euler elastica mentioned above for which the signed curvature is proportional to the height $y = \gamma_2$ are approached in this way in [11, (2.2) p. 48], [8, p. 387], [9, p. 7], [1, 10]. The approach is used to classify and analyze the meridians of axially symmetric surfaces of

[1] A very similar development is given by Spivak [13, pp. 21–24] obtaining a specifically continuous inclination angle $\psi$ and then freely differentiating $\psi$ without further comment to obtain (10). In [3] doCarmo gives (10) in his treatment of the four vertex theorem.

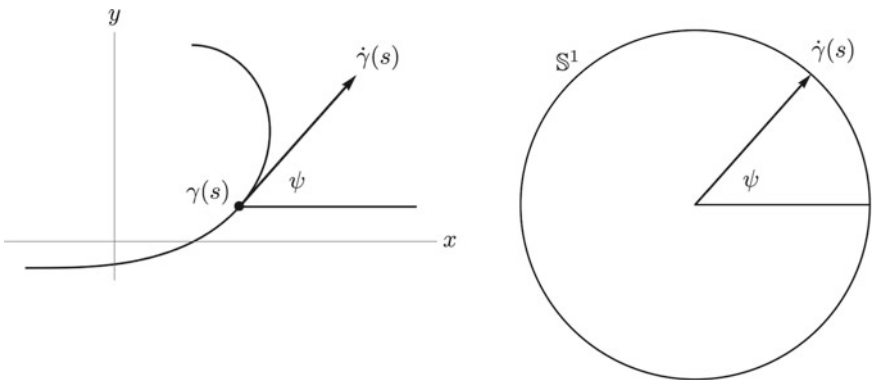


**Fig. 1** The inclination angle of a planar curve

prescribed mean curvature. For constant mean curvature (Delaunay surfaces) see [2] or [4]. For capillary surfaces with mean curvature an affine function of height, see [6, (2.2) p. 17] or [15, (2.2) p. 425]. For more exotic axially symmetric surfaces with prescribed mean curvature see [4, 7, 16]. In view of the structure theorem for planar curves which states that every such curve is essentially determined by the value $k(s) = f$ of the signed curvature as a function of arclength along the curve, it can be said that every regular $C^2$ plane curve is an example. The curve in Fig. 1 was numerically computed with the signed curvature equal to the arclength along the curve with $f(s) = s$.

I have used this approach for constructing and classifying various special curves numerous times without reflecting either on the fact that the existence of a smooth inclination angle was being assumed or the fact that I did not know a reference where that existence was justified.

## Preliminary Remarks Concerning Theorems 2 and 4

Associated with an arclength parameterization $\gamma : I \to \mathbb{R}^2$ as introduced above, the function $\dot{\gamma} : I \to \mathbb{S}^1$ illustrated in Fig. 1 is familiar from differential geometry. In this context, the inclination angle is usually defined informally as the angle between the tangent vector $\dot{\gamma}$ and the positive horizontal direction. The following heuristic discussion is explained in detail in Sect. 2 below.

Having assumed $\gamma$ is an arclength parameterization, we have for each $s \in I$ that $\dot{\gamma}(s) \in \mathbb{S}^1$. Each such point $\dot{\gamma}(s)$ in a circle determines a family of angles by the algebraic relations

$$\begin{cases} \cos\theta = \dot{\gamma}_1(s) \\ \sin\theta = \dot{\gamma}_2(s). \end{cases} \tag{11}$$

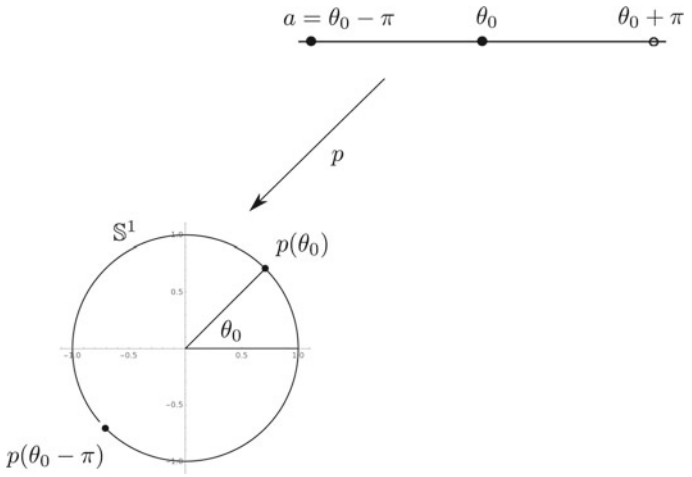


**Fig. 2** Covering map of the circle $\mathbb{S}^1$.

If $\theta$ is one solution of (11), then all the other solutions are given by $\theta + 2\pi j$ for $j \in \{0, \pm 1, \pm 2, \pm 3, \ldots\}$ so that each differs from the others by an integer multiple of $2\pi$. Exactly one of these angles lies in any given interval of length $2\pi$. For example, if $a \in \mathbb{R}$ then there is a unique angle $\theta$ in the interval $[a, a + 2\pi)$ for which (11) holds. Given a curve as in the theorems stated above, the relations (11) restrict the possible choices of the initial angle $\theta_0$ appearing in (1).

On the other hand, if $p$ is the universal covering map of the circle mentioned in Theorem 4, the restriction $p_a : [a, a + 2\pi) \to \mathbb{S}^1$ of that map is one-to-one and onto, and the inverse $p_a^{-1} : \mathbb{S}^1 \to [a, a + 2\pi)$ is well-defined, continuous, and intrinsically differentiable except at $p_a(a) = (\cos(a), \sin(a)) \in \mathbb{S}^1$. See Fig. 2. Thus, given any $\theta_0$ satisfying (1) we can take $a = \theta_0 - \pi$ to obtain some $s_A, s_B \in \mathbb{R}$ with $s_A < s_0 < s_B$ and a function $\psi \in C^0(s_A, s_B)$ given by

$$\psi(s) = p_a^{-1}(\dot{\gamma}(s)) \tag{12}$$

satisfying $p \circ \psi(s) = (\cos\psi, \sin\psi) = \dot{\gamma}(s)$ and $\psi(s_0) = \theta_0$. The relation $p \circ \psi(s) = \dot{\gamma}(s)$ may be assumed to hold and determine $\psi$ uniquely for $s_A < s_0 < s_B$ as long as $\dot{\gamma}(s) \in \{(\cos\theta, \sin\theta) \in \mathbb{S}^1 : |\theta - \theta_0| < \pi\}$ for each arclength $s$ in the same interval $(s_A, s_B)$. Under this assumption, the interval $(s_A, s_B)$ may be written as a union of subsets

$$N_1 = \{s \in (s_A, s_B) : \dot{\gamma}(s) \neq (\pm 1, 0)\}$$
$$N_2 = \{s \in (s_A, s_B) : \dot{\gamma}(s) \neq (0, \pm 1)\}$$

with disjoint complements. At least one of these open sets will contain $s_0$, and on some subinterval one can obtain a unique analytic expression for $\psi$ in terms of some

branch of an inverse trigonometric function applied to one of the functions $\dot{\gamma}_1$ or $\dot{\gamma}_2$. We will obtain such expressions below.

In principle the formulas we will obtain (and the existence/applicability of one of them) do not depend on the twice differentiability of $\gamma$, but if the appropriate function of $\gamma_j$ for $j = 1$ or $j = 2$ is differentiable and $\gamma_j \in C^2(I)$, then the applicable formula can be differentiated to obtain an analytic formula for $\dot{\psi}$ and one can conclude $\psi$ is locally continuously differentiable. We will return to the consideration of situations in which $\dot{\gamma}$ is only assumed to be continuous and the structure of $C^1$ curves in Sects. 2 and 3 respectively.

## 1 Direct Proof of Theorem 2

We begin with a local version of Theorem 1 with arbitrary initial condition at a point $s^* \in I$. This result and its proof are important because they represent an extension of the standard local existence and uniqueness techniques from ODEs to the singular system (2).

**Lemma 1** *If $\theta^* \in \mathbb{R}$ satisfies*

$$\begin{cases} \cos\theta^* = \dot{\gamma}_1(s^*) \\ \sin\theta^* = \dot{\gamma}_2(s^*), \end{cases} \tag{13}$$

*there exists some $\epsilon^* > 0$ and a unique function $\psi \in C^1(I^*)$ where $I^* = (s^* - \epsilon^*, s^* + \epsilon^*)$ such that*

$$\begin{cases} -\sin\psi\,\dot{\psi} = \ddot{\gamma}_1,\ s \in I^* \\ \cos\psi\,\dot{\psi} = \ddot{\gamma}_2,\ s \in I^* \\ \psi(s^*) = \theta^*. \end{cases} \tag{14}$$

*Moreover, we may also assume the solution $\psi$ satisfies*

$$\begin{cases} \cos\psi = \dot{\gamma}_1,\ s \in I^* \\ \sin\psi = \dot{\gamma}_2,\ s \in I^*. \end{cases} \tag{15}$$

***Proof*** We know $\sin^2\theta^* + \cos^2\theta^* = 1$, so either

**(i)** $\sin\theta^* \neq 0$ or
**(ii)** $\cos\theta^* \neq 0$.

Overall then, we consider these two cases, but we will consider the first case in detail. If $\sin\theta^* \neq 0$, there is some $\epsilon > 0$ for which

$$\sin\theta \neq 0 \qquad \text{for} \qquad \theta^* - \epsilon \leq \theta \leq \theta^* + \epsilon. \tag{16}$$

In this case we focus on the first ODE in (14). Specifically the initial value problem

$$\begin{cases} -\sin\psi\,\dot{\psi} = \ddot{\gamma}_1 \\ \psi(s^*) = \theta^* \end{cases} \tag{17}$$

is nonsingular at $(s^*, \theta^*) \in (s^* - \epsilon, s^* + \epsilon) \times (\theta^* - \epsilon, \theta^* + \epsilon)$. By the existence and uniqueness theorem for ODEs, there is some $\epsilon^* > 0$ for which (17) has a unique solution $\psi \in C^1(I^*)$ defined for $s \in I^* = (s^* - \epsilon^*, s^* + \epsilon^*) \subset I$. Without loss of generality, we may assume

$$\theta^* - \epsilon < \psi(s) < \theta^* + \epsilon \quad \text{for } s \in I^* \tag{18}$$

so that according to (16)

$$\sin\psi(s) \neq 0 \qquad \text{for} \qquad s \in I^*. \tag{19}$$

The function $\psi$ also happens to satisfy the first relation in (15) because

$$\begin{aligned} \cos\psi(s) &= \cos\psi(s^*) + \int_{s^*}^{s} [-\sin\psi(\sigma)\,\dot{\psi}(\sigma)]\,d\sigma \\ &= \cos\theta^* + \int_{s^*}^{s} \ddot{\gamma}_1(\sigma)\,d\sigma \\ &= \cos\theta^* + \dot{\gamma}_1(s) - \dot{\gamma}_1(s^*) \\ &= \dot{\gamma}_1(s). \end{aligned} \tag{20}$$

It remains to show the consistency of the second ODE in (14), i.e., that the function $\psi$ satisfies $\cos\psi\,\dot{\psi} = \ddot{\gamma}_2$ for $s \in I^*$.

This will follow immediately if the second relation in (15) holds. We can show this in different ways, but the following way uses techniques from ODEs. The function $y = \dot{\gamma}_2 - \sin\psi$ satisfies $y \in C^1(I^*)$ and the initial condition $y(s^*) = 0$. We proceed to find a first order ODE satisfied by $y$. Differentiating we find

$$\frac{dy}{ds} = \dot{y} = \ddot{\gamma}_2 - \cos\psi\,\dot{\psi}. \tag{21}$$

Since $\gamma$ is parameterized by arclength, we can differentiate the relation $\dot{\gamma}_1^2 + \dot{\gamma}_2^2 \equiv 1$ to obtain

$$\dot{\gamma}_1\,\ddot{\gamma}_1 + \dot{\gamma}_2\,\ddot{\gamma}_2 \equiv 0. \tag{22}$$

This relation may be used to replace $\ddot{\gamma}_2$ in (21) as long as we know $\dot{\gamma}_2 \neq 0$. Since

$$\dot{\gamma}_2(s^*) = \sin\theta^* \neq 0, \tag{23}$$

we know there is some $\eta > 0$ for which $\dot{\gamma}_2(s) \neq 0$ for $s \in J = (s^* - \eta, s^* + \eta)$. Let

$$\eta^* = \sup\{\eta \in (0, \epsilon^*] : \dot{\gamma}_2(s) \neq 0,\ s^* - \eta < s < s^* + \eta\} \tag{24}$$

and $J^* = (s^* - \eta^*, s^* + \eta^*)$.

Returning to (21) this means

$$\dot{y} = -\frac{\dot{\gamma}_1}{\dot{\gamma}_2}\,\ddot{\gamma}_1 - \cos\psi\,\dot{\psi} = \frac{\cos\psi}{\dot{\gamma}_2}\,\sin\psi\,\dot{\psi} - \cos\psi\,\dot{\psi} = -\frac{\cos\psi}{\dot{\gamma}_2}\,(\dot{\gamma}_2 - \sin\psi)\,\dot{\psi}$$

for $s \in J^*$. Thus, the function $y = \dot{\gamma}_2 - \sin\psi \in C^1(I^*)$ satisfies

$$\begin{cases} \dot{y} = -\dfrac{\cos\psi}{\dot{\gamma}_2}\,y\,\dot{\psi} & \text{for } s \in J^* \\ \\ y(s^*) = 0. \end{cases}$$

The unique solution of this problem is $y = \dot{\gamma}_2 - \sin\psi \equiv 0$. In particular, $\dot{\gamma}_2 \equiv \sin\psi$ for $s \in J^*$. We claim finally that $\eta^* = \epsilon^*$, so that $J^* = I^*$ and our discussion of the first case is complete. In fact, if we assume $\eta^* < \epsilon^*$, then by continuity

$$\dot{\gamma}_2(s^* \pm \eta^*) = \sin\psi(s^* \pm \eta^*) \neq 0.$$

This gives an immediate contradiction of the definition (24) of $\eta^*$. Thus we have (15) and consequently (14).

The second case is very similar and leads to the same conclusion(s). □

We next turn our attention to the proof of the equivalence result Theorem 3.

***Proof of Theorem 3 part (a)*** Here we assume $\psi \in C^1(I)$ satisfies (3). Given that $\gamma$ is twice differentiable, it clearly follows that $\psi$ is a solution of (2). Thus, it only remains to show uniqueness.

Let $\tilde{\psi} \in C^1(I)$ be any other solution of (2). Setting $y = \tilde{\psi} - \psi \in C^1(I)$ we see

$$A = \{s \in I : \tilde{\psi}(s) = \psi(s)\} \tag{25}$$

is a nonempty closed set. Given any $s^* \in A$, we may apply Lemma 1 with $\theta^* = \tilde{\psi}(s^*) = \psi(s^*)$ to obtain some $\epsilon^* > 0$ for which (14) has a unique solution on $I^* = (s^* - \epsilon^*, s^* + \epsilon^*)$. It follows that $\tilde{\psi}(s) = \psi(s)$ for $s \in I^*$ and that $A$ is open. Since the only nonempty subset of the open interval $I$ which is both closed and open is the interval $I$ itself, we conclude $A = I$ and $\psi$ is unique. □

***Proof of Theorem 3 part (b)*** Here we assume $\psi \in C^1(I)$ satisfies (2). Applying Lemma 1 at $s^* = s_0$ with $\theta^* = \theta_0$, we obtain some $\epsilon_0 > 0$ for which

$$\psi_0 = \psi\big|_{I_0}$$

is the unique solution of

$$\begin{cases} -\sin\psi\,\dot{\psi} = \ddot{\gamma}_1,\ s \in I_0 \\ \cos\psi\,\dot{\psi} = \ddot{\gamma}_2,\ s \in I_0 \\ \psi(s_0) = \theta_0 \end{cases} \tag{26}$$

where $I_0 = (s_0 - \epsilon_0, s_0 + \epsilon_0)$, and we know

$$\begin{cases} \cos\psi_0 = \dot{\gamma}_1,\ s \in I_0 \\ \sin\psi_0 = \dot{\gamma}_2,\ s \in I_0. \end{cases} \tag{27}$$

Setting

$$B = \{s \in I : \cos\psi(s) = \dot{\gamma}_1(s) \text{ and } \sin\psi(s) = \dot{\gamma}_2(s)\},$$

we have by continuity that $B$ is a closed subset of $I$ containing $I_0$. For any $s^* \in B$, we can apply Lemma 1 with $\theta^* = \psi(s^*)$ to obtain some $\epsilon^* > 0$ for which (15) holds on $I^* = (s^* - \epsilon^*, s^* + \epsilon^*)$. In particular, $I^* \subset B$, and $B$ is open. Again since any nonempty subset of $I$ that is both closed and open is the interval $I$ itself, we know $B = I$, and we have shown existence of a solution of the algebraic system (3).

If $\tilde{\psi} \in C^1(I)$ is any other solution of (3), then noting that any solution of (3) is a solution of (2), the uniqueness shown using the set $A$ from (25) in the proof of part **(a)** above applies here directly. □

The following corollary is an immediate consequence of Theorem 3.

**Corollary 2** (existence implies uniqueness) *If $J$ is any open interval with $s_0 \in J \subset I$, and $\psi \in C^1(J)$ satisfies*

$$\begin{cases} \cos\psi = \dot{\gamma}_1,\ s \in J \\ \sin\psi = \dot{\gamma}_2,\ s \in J \\ \psi(s_0) = \theta_0, \end{cases} \tag{28}$$

*then $\psi$ is the unique function in $C^1(J)$ satisfying (28). Similarly, if $\psi \in C^1(J)$ satisfies*

$$\begin{cases} -\sin\psi\,\dot{\psi} = \ddot{\gamma}_1,\ s \in J \\ \cos\psi\,\dot{\psi} = \ddot{\gamma}_2,\ s \in J \\ \psi(s_0) = \theta_0, \end{cases} \tag{29}$$

*then $\psi$ is the unique function in $C^1(J)$ satisfying (29).*

***Proof*** If $\psi$ solves (28), then differentiation gives that $\psi$ solves (29). But then part **(b)** of Theorem 3 implies $\psi$ is the unique solution of (28). Similarly, if $\psi$ solves (29), then part **(b)** of Theorem 3 implies $\psi$ is the unique solution of (28) and is a solution of (28) in particular. But then part **(a)** of Theorem 3 implies $\psi$ is the unique solution of (29). □

***Proof of Theorem*** 1 We can apply Lemma 1 with $s^* = s_0$ and $\theta^* = \theta_0$ to obtain some interval $I_0 = (s_0 - \epsilon_0, s_0 + \epsilon_0)$ and some $\psi_0 \in C^1(I_0)$ for which $\psi_0$ is the

unique solution in $C^1(I_0)$ for the problem (26) above and for which we also know (27) holds.

Consider the family $\mathcal{F}$ of intervals $J = (\inf J, \sup J)$ for which

$$\inf I \leq \inf J \leq s_0 - \epsilon_0 < s_0 + \epsilon_0 \leq \sup J \leq \sup I \tag{30}$$

and there exists a unique $\psi \in C^1(J)$ for which (28) above holds. Notice (30) is equivalent to the condition $I_0 \subset J \subset I$. We consider

$$U = \bigcup_{J \in \mathcal{F}} J.$$

Since $U$ is a union of intervals each containing the interval $I_0$, we know $U = (\inf U, \sup U)$ is a nonempty open interval. We make two claims:

**Claim 1:** There exists a unique function $\psi = \psi \in C^1(U)$ for which

$$\begin{cases} \cos\psi = \dot{\gamma}_1, \ s \in U \\ \sin\psi = \dot{\gamma}_2, \ s \in U \\ \psi(s_0) = \theta_0, \end{cases} \tag{31}$$

and consequently $U \in \mathcal{F}$.

**Claim 2:** There holds $\inf U = \inf I$ and $\sup U = \sup I$ so that

$$U = I \in \mathcal{F},$$

and since $C^1$ solutions of (3) are solutions of (2) the assertion of Theorem 1 follows.

***Proof of Claim 1*** We attempt to define a function $\Psi \in C^1(U)$ by the formula

$$\Psi(s) = \psi(s) \qquad \text{whenever } s \in J \in \mathcal{F} \tag{32}$$

and $\psi$ is the unique solution of (28) associated with $J$.

For each $\sigma \in U$, there is at least one $J \in \mathcal{F}$ for which $\sigma \in J$, so we can assign some value to $\Psi(\sigma)$. On the other hand, if $J_1, J_2 \in \mathcal{F}$ with $\sigma \in J_1 \cap J_2$, then $J = J_1 \cap J_2$ is an open interval with $I_0 \subset J \subset I$, and by Corollary 2 we see

$$\psi_1\big|_J \equiv \psi_2\big|_J$$

is the unique solution of (28) where $\psi_j$ is the solution associated with $J_j \in \mathcal{F}$ for $j = 1, 2$. In particular, $\psi_1(\sigma) = \psi_2(\sigma)$. This shows $\Psi$ is well-defined by (32), and it follows immediately that $\Psi \in C^1(U)$ and we have shown existence for a solution of (31). Again, we know by Corollary 2 that existence implies uniqueness, so this completes the proof of Claim 1.

***Proof of Claim 2*** Set $s_A = \inf U$ and $s_B = \sup U$. Let $\Psi \in C^1(U)$ continue to denote the unique solution of (31) from Claim 1.

Let us assume by way of contradiction that $s_A > \inf I$. It follows that $s_A \in I$ with $\inf I < s_A \leq s_0 - \epsilon_0$.

Since $\gamma$ is defined on all of $I$ and (31) holds, we know the limits

$$\lim_{s \searrow s_A} \cos \Psi(s) = \dot{\gamma}_1(s_A) \qquad \text{and} \qquad \lim_{s \searrow s_A} \sin \Psi(s) = \dot{\gamma}_2(s_A) \tag{33}$$

exist as well-defined real numbers in $[-1, 1]$. It cannot be the case, furthermore, that both of these numbers are zero or that both of these numbers have absolute value 1.

We now apply another result familiar from the theory of ODEs (or calculus):

**Lemma 3** *Given*

***(i)*** $a, b \in \mathbb{R}$ *with* $a < b$,
***(ii)*** $y \in C^1(J)$ *where* $J = (a, b)$, *and*
***(iii)*** $f \in C^0(y(J) \times J)$,

*if* $y$ *is a solution of*

$$\begin{cases} \dot{y} = f(y, t) & \text{for } t \in J \\ y(t_0) = y_0 \end{cases}$$

*for some* $t_0 \in J$ *then the following hold:*

***(a)*** *If*

$$\lim_{t \searrow a} f(y(t), t) = L \qquad \text{exists as a well-defined real number } L \in \mathbb{R},$$

*then*

$$\lim_{t \searrow a} y(t) = y_a \qquad \text{exists as a well-defined real number } y_a \in \mathbb{R}.$$

***(b)*** *If*

$$\lim_{t \nearrow b} f(y(t), t) = M \qquad \text{exists as a well-defined real number } M \in \mathbb{R},$$

*then*

$$\lim_{t \nearrow b} y(t) = y_b \qquad \text{exists as a well-defined real number } y_b \in \mathbb{R}.$$

If $\dot{\gamma}_1(s_A) \neq 0$, then we can take some $\epsilon > 0$ for which $\cos \Psi(s) \neq 0$ for $s_A < s < s_A + \epsilon$ and consider the ODE in Lemma 3 to be

$$\dot{y} = \frac{\ddot{\gamma}_2}{\cos y}$$

with solution $y = \Psi$ on the interval $(a, b) = (s_A, s_A + \epsilon)$. We conclude from part **(a)** of Lemma 3 in this case that

$$\theta_A = \lim_{s \searrow s_A} \Psi(s) \qquad \text{exists as a well-defined real number.} \tag{34}$$

The ODE is different, but the conclusion (34) is the same if $\dot{\gamma}_1(s_A) = 0$.

Consequently, we may apply Lemma 1 at $s^* = s_A$ with $\theta^* = \theta_A$ to obtain some $\epsilon^*$ and a unique solution $\psi_A \in C^1(I^*)$ of the problem (15), that is

$$\begin{cases} \cos\psi = \dot{\gamma}_1, \ s \in I^* \\ \sin\psi = \dot{\gamma}_2, \ s \in I^* \\ \psi(s_A) = \theta_A \end{cases} \tag{35}$$

where $I^* = (s_A - \epsilon^*, s_A + \epsilon^*) \subset (\inf I, s_0 + \epsilon_0) \subset I$.

We wish next to show $\Psi(s) = \psi_A(s)$ for $s$ in the intersection interval $(s_A, s_A + \epsilon^*)$. We start by defining $\Psi_A : I^* = (s_A - \epsilon^*, s_A + \epsilon^*) \to \mathbb{R}$ by

$$\Psi_A(s) = \begin{cases} \psi_A(s), \ s \le s_A \\ \Psi(s), \ \ s > s_A. \end{cases}$$

Observe that $\Psi_A(s_A) = \theta_A$ and in view of (34) we know $\Psi_A \in C^0(I^*)$. Furthermore $\Psi_A$ is differentiable on $I^* \backslash \{s_A\}$ and (35) holds for $\psi = \Psi_A$ at every $s \in I^*$.

If $\dot{\gamma}(s_A) \neq (\pm 1, 0)$, then there is some $\delta > 0$ for which

$$\sin\Psi(s) \neq 0 \qquad \text{for } s_A < s < s^* + \delta.$$

In particular, $\sin\theta_A = \sin\Psi_A(s_A) \neq 0$, and for $s_A < s < s^* + \delta$ we can write

$$\frac{\Psi_A(s) - \Psi_A(s_A)}{s - s_A} = \frac{\Psi(s) - \theta_A}{s - s_A} = \dot{\Psi}_A(\sigma) = -\frac{\ddot{\gamma}_1(\sigma)}{\sin\Psi_A(\sigma)}$$

for some $\sigma$ with $s_A < \sigma < s$. Since

$$\lim_{\sigma \searrow s_A} \frac{\ddot{\gamma}_1(\sigma)}{\sin\Psi(\sigma)} = \frac{\ddot{\gamma}_1(s_A)}{\sin\theta_A},$$

we see $\Psi_A$ has a right derivative at $s_A$ with value

$$\dot{\Psi}_A(s_A^+) = -\frac{\ddot{\gamma}_1(s_A)}{\sin\theta_A}. \tag{36}$$

Taking the derivative from the left in this case, we find

$$\dot{\Psi}_A(s_A^-) = \lim_{\sigma \nearrow s_A} \dot{\psi}_A(\sigma) = -\frac{\ddot{\gamma}_1(s_A)}{\sin\theta_A}. \tag{37}$$

In view of (36) and (37) we conclude that when $\dot{\gamma}(s_A) \neq (\pm 1, 0)$, $\Psi_A \in C^1(I^*)$ with derivative at $s_A$ the common value

$$\dot{\Psi}_A(s_A) = -\frac{\ddot{\gamma}_1(s_A)}{\sin\theta_A}.$$

Similarly, If $\dot{\gamma}(s_A) \neq (0, \pm 1)$, then $\cos(\theta_A) \neq 0$, and

$$\dot{\Psi}_A(s_A) = \frac{\ddot{\gamma}(s_A)}{\cos(\theta_A)}.$$

We have shown that in all cases $\dot{\Psi}_A(s_A)$ exists and $\Psi_A \in C^1(I^*)$. By uniqueness we conclude $\Psi_A \equiv \psi_A$ as desired. Thus, setting

$$\psi(s) = \begin{cases} \Psi_A(s), & s \in I^* \\ \Psi(s), & s_A < s < s_B, \end{cases}$$

we obtain a function $\Psi_A \in C^1(J)$ for $J = (s_A - \epsilon_*, s_B)$ satisfying (28). By Corollary 2 we know $\Psi_A$ is the unique function satisfying (28) and hence $J \in \mathcal{F}$ contradicting the definition of $s_A$. Therefore, $s_A = \inf I$.

We find similarly that $s_B = \sup I$, so that $U = (s_A, s_B) = I$ and the proof of Theorem 1 is complete. □

Theorem 2 is now immediate.

***Proof of Theorem*** 2 The hypotheses of Theorem 2 are the same as those of Theorem 1, so by Theorem 1 there exists a solution $\psi \in C^1(I)$ of the singular system (2). By part **(b)** of Theorem 3, the function $\psi$ is the unique solution of (3), and this is the conclusion of Theorem 2. □

## 2 Topological Lifting

The existence of the topological lifting asserted in Theorem 4 above may be viewed as fairly standard. Technically, however, it is normally assumed that the domain of **v** is a compact interval, and compactness is used in the proof. A standard reference for such a version of the result is given in Lemma 4.1 (p. 337, Chap. 8) of [12]. Proposition 5 on page 22 of [13] also assumes the domain of **v** is a compact interval though the proof does not use compactness explicitly, and it may be possible to adapt Spivak's argument to prove Theorem 4. I am going to present a different approach which I think expresses more clearly the underlying structure of Theorem 4 and the special structure of the universal covering map $p : \mathbb{R} \to \mathbb{S}^1$ in particular. It should be emphasized that in many of the constructions of curves of prescribed curvature mentioned above, the domain of definition is, or turns out to be, the entire real line $I = \mathbb{R}$ which is decidedly noncompact.

## *Circle Covering and Branches of the Inverse*

Our proof of the topological lifting result Theorem 4 depends on a unified or standardized view of the branches of $p^{-1}$ where $p : \mathbb{R} \to \mathbb{S}^1$ by $p(\theta) = (\cos\theta, \sin\theta)$ is the universal covering map of the circle $\mathbb{S}^1$. We identify **four standard nonsingular branches** of $p^{-1}$ denoted $p_0^{-1}, q_0^{-1}, p_1^{-1}, q_1^{-1}$ from which a family

$$\{p_{2k}^{-1}\}_{k\in\mathbb{Z}} \cup \{q_{2k}^{-1}\}_{k\in\mathbb{Z}} \cup \{p_{2k+1}^{-1}\}_{k\in\mathbb{Z}} \cup \{q_{2k+1}^{-1}\}_{k\in\mathbb{Z}}$$

of nonsingular branches is derived. These depend in turn on four standard nonsingular branches of arccosine and arcsine. Thus, we begin with the familiar real principal branches of arccosine and arcsine as illustrated in Fig. 3. The principal branch of arccosine here is the inverse of

$$\cos|_{[0,\pi]} : [0, \pi] \to [-1, 1]$$

which we will denote $\arccos : [-1, 1] \to [0, \pi]$ and satisfies $\arccos \in C^1(-1, 1) \cap C^0[-1, 1]$. Similarly, the restriction

$$\sin|_{[-\pi/2,\pi/2]} : [-\pi/2, \pi/2] \to [-1, 1]$$

has an inverse $\arcsin \in C^1(-1, 1) \cap C^0[-1, 1]$ as indicated in Fig. 3.

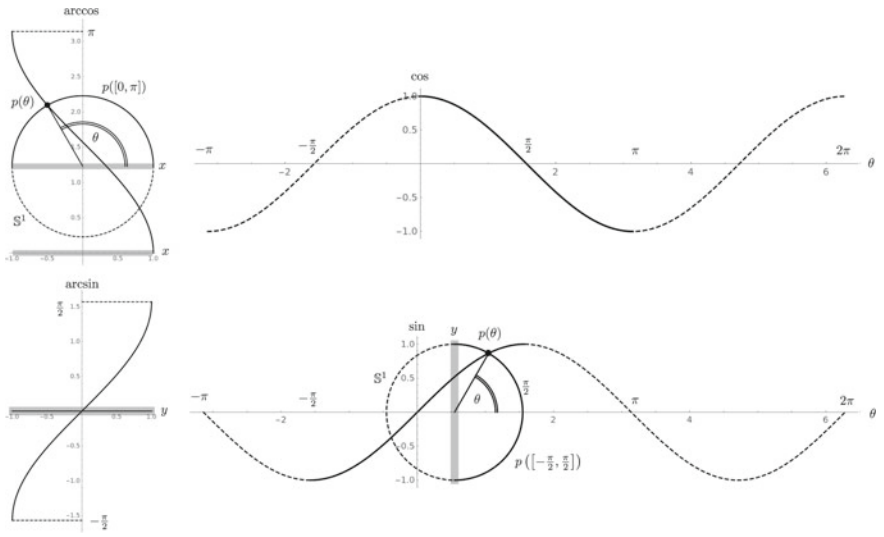


**Fig. 3** Real principal branches of arccosine and arcsine

## 2.1 Decompositions

It will be useful to have appropriate decompositions of the domain $\mathbb{R}$ and codomain $\mathbb{S}^1$ of the covering map $p : \mathbb{R} \to \mathbb{S}^1$. For the real line we start with open intervals

$$V_j = \left(j\frac{\pi}{2} - \frac{\pi}{2}, j\frac{\pi}{2} + \frac{\pi}{2}\right) = \left((j-1)\frac{\pi}{2}, (j+1)\frac{\pi}{2}\right) \quad \text{for } j \in \mathbb{Z}$$

as indicated in Fig. 4. It is readily seen that

$$\bigcup_{j\in\mathbb{Z}} V_j = \mathbb{R}, \qquad V_{2k} = \left(k\pi - \frac{\pi}{2}, k\pi + \frac{\pi}{2}\right), \qquad k \in \mathbb{Z}$$

and

$$\bigcup_{k\in\mathbb{Z}} V_{2k} = \mathbb{R}\backslash \left\{(2k+1)\frac{\pi}{2}\right\}_{k\in\mathbb{Z}} \qquad \text{with} \qquad V_{2m} \cap V_{2n} = \phi, \quad m \neq n.$$

For reasons that should become clear below, we give the intervals $V_j$ for $j \in \mathbb{Z}$ alternate names setting $U_j = V_{j+1}$ as indicated in Fig. 5. The intervals $\{U_j\}_{j\in\mathbb{Z}}$ are of course still an open cover of $\mathbb{R}$. In this instance we observe

$$U_{2k} = V_{2k+1} = (k\pi, (k+1)\pi)\,,$$

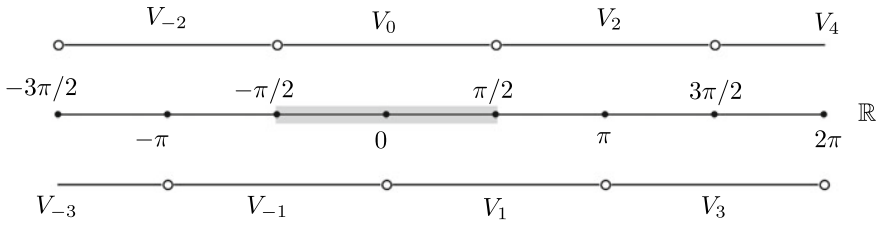


**Fig. 4** Overlapping decomposition of the real line into intervals of length $\pi$.

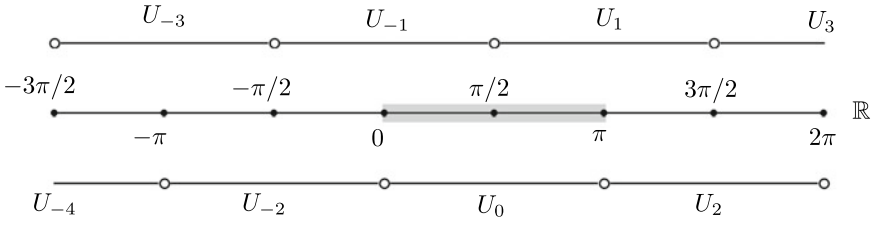


**Fig. 5** Renamed overlapping decomposition of the real line by open intervals

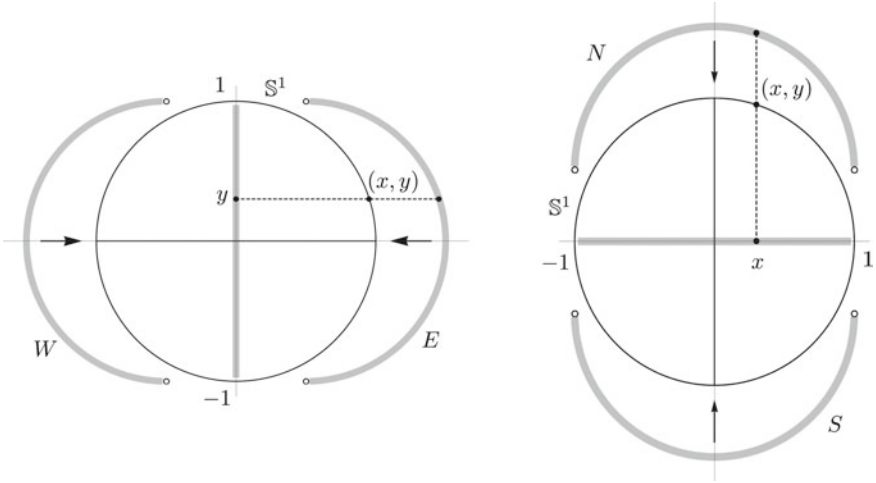


**Fig. 6** Overlapping decomposition of the circle $\mathbb{S}^1$ into compass semicircles

and

$$\bigcup_{k\in\mathbb{Z}} U_{2k} = \mathbb{R}\setminus\{k\pi\}_{k\in\mathbb{Z}} \qquad \text{with} \qquad U_{2m}\cap U_{2n} = \phi, \quad m \neq n.$$

We next consider an overlapping decomposition of $\mathbb{S}^1$ by open **compass semicircles**

$$\begin{aligned} E &= \{(x, y) \in \mathbb{S}^1 : x > 0\} \\ N &= \{(x, y) \in \mathbb{S}^1 : y > 0\} \\ W &= \{(x, y) \in \mathbb{S}^1 : x < 0\} \\ S &= \{(x, y) \in \mathbb{S}^1 : y < 0\} \end{aligned}$$

as indicated in Fig. 6. Finally, we decompose the complement of the compass points $\{(1, 0), (0, 1), (-1, 0), (0, -1)\}$ in the circle $\mathbb{S}^1$ into open quarter circles in the quadrants in the usual manner setting

$$\begin{aligned} \text{I} &= \{(x, y) \in \mathbb{S}^1 : x, y > 0\} = E \cap N \\ \text{II} &= \{(x, y) \in \mathbb{S}^1 : x < 0 < y\} = N \cap W \\ \text{III} &= \{(x, y) \in \mathbb{S}^1 : x, y < 0\} = W \cap S \\ \text{IV} &= \{(x, y) \in \mathbb{S}^1 : y < 0 < x\} = S \cap E. \end{aligned}$$

## 2.2 Restrictions and Inverses

For $\ell \in \mathbb{Z}$, consider the following restrictions of sine and cosine to the intervals in the decomposition sets defined in the previous section:

$$\sin_{2\ell} = \sin\big|_{V_{4\ell}} : V_{4\ell} \to (-1,1), \tag{38}$$

$$\cos_{2\ell} = \cos\big|_{U_{4\ell}} : U_{4\ell} \to (-1,1), \tag{39}$$

$$\sin_{2\ell+1} = \sin\big|_{V_{4\ell+2}} : V_{4\ell+2} \to (-1,1), \tag{40}$$

$$\cos_{2\ell+1} = \cos\big|_{V_{4\ell+2}} : U_{4\ell+2} \to (-1,1). \tag{41}$$

It will be noted that $\sin_{2\ell}$ and $\cos_{2\ell+1}$ are increasing while $\cos_{2\ell}$ and $\sin_{2\ell+1}$ are decreasing. In particular, the inverse of $\sin_0$ is the restriction of the principal branch of arcsine mentioned above to the open interval $(-1,1)$. When we have written $\arcsin \in C^1(-1,1)$ above, it is technically the nonsingular restriction $\sin_0^{-1} \in C^1(-1,1)$ to which we refer. We denote the particular nonsingular principal branch $\sin_0^{-1} : (-1,1) \to (-\pi/2, \pi/2) = V_0$ by

$$\sin_0^{-1} = \sin^{-1}.$$

More generally if the index $j$ of the open interval $V_j$ in Fig. 4 satisfies $j = 4\ell$ for some $\ell \in \mathbb{Z}$, then

$$\sin_{2\ell}^{-1} : (-1,1) \to V_{4\ell} = \Big(2\ell\pi - \frac{\pi}{2}, 2\ell\pi + \frac{\pi}{2}\Big) \quad \text{by} \quad \sin_{2\ell}^{-1} y = 2\ell\pi + \sin^{-1} y \tag{42}$$

as indicated in Fig. 7. We emphasize $\sin_0^{-1} = \sin^{-1}$ with graph near the middle of the illustration is the principal **nonsingular** branch of arcsine, and all of the functions $\sin_j^{-1}$ satisfy

$$\sin_j^{-1} \in C^1(-1,1).$$

Before briefly discussing some details of the other nonsingular branches of arcsine and arccosine, we pause to record the formulas in one place for easy reference as we recorded the restrictions in (38)–(41). Including (42) we have for $\ell \in \mathbb{Z}$

$$\sin_{2\ell}^{-1} : (-1,1) \to V_{4\ell} \quad \text{by} \quad \sin_{2\ell}^{-1} y = 2\ell\pi + \sin^{-1} y \tag{43}$$

$$\cos_{2\ell}^{-1} : (-1,1) \to U_{4\ell} \quad \text{by} \quad \cos_{2\ell}^{-1} x = 2\ell\pi + \cos^{-1} x \tag{44}$$

$$\sin_{2\ell+1}^{-1} : (-1,1) \to V_{4\ell+2} \quad \text{by} \quad \sin_{2\ell+1}^{-1} y = (2\ell+1)\pi - \sin^{-1} y \tag{45}$$

$$\cos_{2\ell+1}^{-1} : (-1,1) \to U_{4\ell+2} \quad \text{by} \quad \cos_{2\ell+1}^{-1} x = 2(\ell+1)\pi - \cos^{-1} x \tag{46}$$

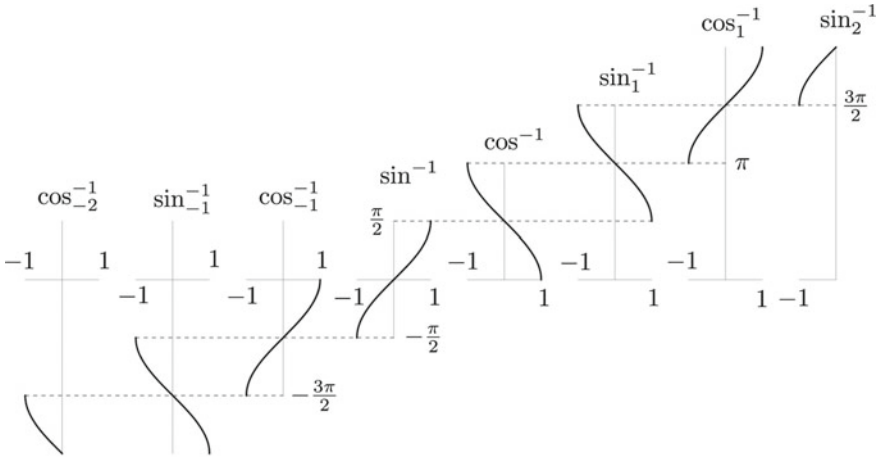


**Fig. 7** Real branches of inverse sine and cosine

with

$$V_{4\ell} = \left(2\ell\pi - \frac{\pi}{2}, 2\ell\pi + \frac{\pi}{2}\right) \tag{47}$$

$$U_{4\ell} = (2\ell\pi, (2\ell+1)\pi) \tag{48}$$

$$V_{4\ell+2} = \left(2\ell\pi + \frac{\pi}{2}, 2\ell\pi + \frac{3\pi}{2}\right) \tag{49}$$

$$U_{4\ell+2} = ((2\ell+1)\pi, (2\ell+2)\pi)\,. \tag{50}$$

We denote by $\cos_0^{-1}$, or simply $\cos^{-1}$, the inverse of the restriction

$$\cos_0 = \cos\big|_{(0,\pi)}\,.$$

We have then $\cos_0^{-1} = \cos^{-1} \in C^1(-1,1)$ and we call this the principal **nonsingular** branch of arccosine. Similarly we obtain decreasing nonsingular branches of arccosine $\cos_{2\ell}^{-1} \in C^1(-1,1)$ for $\ell \in \mathbb{Z}$ given by (44).

Taking the principal nonsingular branches $\sin^{-1}$ and $\cos^{-1}$ as the first two standard nonsingular branches of arcsine and arccosine respectively, we consider two more standard nonsingular branches

$$\sin_1^{-1} : (-1,1) \to V_2 = \left(\frac{\pi}{2}, \frac{3\pi}{2}\right) \qquad \text{and} \qquad \cos_1^{-1} : (-1,1) \to U_2 = (\pi, 2\pi)$$

which are the inverses of the restrictions $\sin_1$ and $\cos_1$ defined in (40) and (41) and are given by

$$\sin_1^{-1} y = \pi - \sin^{-1} y \qquad \text{and} \qquad \cos_1^{-1} x = 2\pi - \cos^{-1} x$$

respectively. These also fall into a family of nonsingular branches given in general by the formulas in (45) and (46) above.

It is also natural to consider at this point certain restrictions of the covering map $p : \mathbb{R} \to \mathbb{S}^1$ with their inverses. For example consider

$$p_0 = p\big|_{V_0} : V_0 = \Big(-\frac{\pi}{2}, \frac{\pi}{2}\Big) \to E$$

where $V_0$ is illustrated in Fig. 4 and $E$ is the eastern compass semicircle in $\mathbb{S}^1$ illustrated in Fig. 6. The function $p_0$ is a bijection with inverse $p_0^{-1} : E \to V_0$ given by

$$p_0^{-1}(x, y) = p^{-1}\big|_{V_0}(x, y) = \sin^{-1} x.$$

We record the general restrictions and inverses in one place for easy reference:

$$p_{2\ell} = p\big|_{V_{4\ell}} : V_{4\ell} \to E \tag{51}$$

$$p_{2\ell+1} = p\big|_{V_{4\ell+2}} : V_{4\ell+2} \to W \tag{52}$$

$$q_{2\ell} = p\big|_{U_{4\ell}} : U_{4\ell} \to N \tag{53}$$

$$q_{2\ell+1} = p\big|_{U_{4\ell+2}} : U_{4\ell+2} \to S \tag{54}$$

with

$$p^{-1}\big|_{V_{4\ell}} : E \to V_{4\ell} \quad \text{by} \quad p_{2\ell}^{-1}(x, y) = \sin_{2\ell}^{-1} y = 2\ell\pi + \sin^{-1} y \tag{55}$$

$$p^{-1}\big|_{V_{4\ell+2}} : W \to V_{4\ell+2} \quad \text{by} \quad p_{2\ell+1}^{-1}(x, y) = \sin_{2\ell+1}^{-1} y = (2\ell+1)\pi - \sin^{-1} y \tag{56}$$

$$p^{-1}\big|_{U_{4\ell}} : N \to U_{4\ell} \quad \text{by} \quad q_{2\ell}^{-1}(x, y) = \cos_{2\ell}^{-1} x = 2\ell\pi + \cos^{-1} x \tag{57}$$

$$p^{-1}\big|_{U_{4\ell+2}} : S \to U_{4\ell+2} \quad \text{by} \quad q_{2\ell+1}^{-1}(x, y) = \cos_{2\ell+1}^{-1} x = (2\ell+1)\pi - \cos^{-1} x \tag{58}$$

We are also now in a position to prove the following result giving a family of compass inverses of the covering map $p$ whose useful formulas depend on the nonsingular $C^1$ inverse trigonometric formulas given above:

**Proposition 1** (compass inverse branches of $p^{-1}$) *For each $\ell \in \mathbb{Z}$, the restrictions*

$$P_{2\ell} = p\big|_{((2\ell-1)\pi,(2\ell+1)\pi)} : ((2\ell-1)\pi, (2\ell+1)\pi) \to \mathbb{S}^1\backslash\{(-1,0)\},$$

$$Q_{2\ell} = p\big|_{\left((2\ell-1)\pi+\frac{\pi}{2},(2\ell+1)\pi+\frac{\pi}{2}\right)} : \left(2\ell\pi - \frac{\pi}{2}, 2\ell\pi + \frac{3\pi}{2}\right) \to \mathbb{S}^1\backslash\{(0,-1)\},$$

$$P_{2\ell+1} = p\big|_{(2\ell\pi,(2\ell+2)\pi)} : (2\ell\pi, (2\ell+2)\pi) \to \mathbb{S}^1\backslash\{(1,0)\}, \text{ and}$$

$$Q_{2\ell+1} = p\big|_{\left(2\ell\pi+\frac{\pi}{2},(2\ell+2)\pi+\frac{\pi}{2}\right)} : \left(2\ell\pi + \frac{\pi}{2}, (2\ell+2)\pi + \frac{\pi}{2}\right) \to \mathbb{S}^1\backslash\{(0,1)\}$$

*are bijections with unique well-defined continuous inverses given as follows:*

***(E)*** $P_{2\ell}^{-1} : \mathbb{S}^1\backslash\{(-1,0)\} \to ((2\ell-1)\pi, (2\ell+1)\pi)$ *by*

$$P_{2\ell}^{-1}(x,y) = \begin{cases} \sin_{2\ell}^{-1} y = 2\ell\pi + \sin^{-1} y, & (x,y) \in E \\ \cos_{2\ell}^{-1} x = 2\ell\pi + \cos^{-1} x, & (x,y) \in N \\ \cos_{2\ell-1}^{-1} x = 2\ell\pi - \cos^{-1} x, & (x,y) \in S. \end{cases}$$

***(N)***

$$Q_{2\ell}^{-1} : \mathbb{S}^1\backslash\{(0,-1)\} \to \left(2\ell\pi - \frac{\pi}{2}, 2\ell\pi + \frac{3\pi}{2}\right)$$

*by*

$$Q_{2\ell}^{-1}(x,y) = \begin{cases} \sin_{2\ell}^{-1} y = 2\ell\pi + \sin^{-1} y, & (x,y) \in E \\ \cos_{2\ell}^{-1} x = 2\ell\pi + \cos^{-1} x, & (x,y) \in N \\ \sin_{2\ell+1}^{-1} y = (2\ell+1)\pi - \sin^{-1} y, & (x,y) \in W. \end{cases}$$

***(W)*** $P_{2\ell+1}^{-1} : \mathbb{S}^1\backslash\{(1,0)\} \to (2\ell\pi, (2\ell+2)\pi)$ *by*

$$P_{2\ell+1}^{-1}(x,y) = \begin{cases} \cos_{2\ell}^{-1} x = 2\ell\pi + \cos^{-1} x, & (x,y) \in N \\ \sin_{2\ell+1}^{-1} y = (2\ell+1)\pi - \sin^{-1} y, & (x,y) \in W \\ \cos_{2\ell+1}^{-1} x = 2(\ell+1)\pi - \cos^{-1} x, & (x,y) \in S. \end{cases}$$

***(S)***

$$Q_{2\ell+1}^{-1} : \mathbb{S}^1\backslash\{(0,1)\} \to \left(2\ell\pi + \frac{\pi}{2}, (2\ell+2)\pi + \frac{\pi}{2}\right)$$

*by*

$$Q_{2\ell+1}^{-1}(x,y) = \begin{cases} \sin_{2\ell+1}^{-1} y = (2\ell+1)\pi - \sin^{-1} y, & (x,y) \in E \\ \sin_{2\ell+2}^{-1} y = (2\ell+2)\pi + \sin^{-1} y, & (x,y) \in W \\ \cos_{2\ell+1}^{-1} x = 2(\ell+1)\pi - \cos^{-1} x, & (x,y) \in S. \end{cases}$$

*In particular, the functions $P_{2\ell}$, $Q_{2\ell}$, $P_{2\ell+1}$, and $Q_{2\ell+1}$ for $\ell \in \mathbb{Z}$ are homeomorphisms of their respective domains onto compass semicircles in $\mathbb{S}^1$.*

Remark(s) on the proof: Since each of the expressions above is continuous and in fact $C^1$ with respect to the independent variable appearing in the formula for a particular compass semicircle, the most important part of the proof is showing the given formulas agree on overlapping semicircles so that the inverse functions are well-defined.

Consider for example the formula for $Q_{2\ell}^{-1}(x, y)$ and a point $(x, y) \in E \cap N = \mathrm{I}$. The fact that $(x, y) \in \mathrm{I}$ tells us $x, y > 0$ and

$$x = \sqrt{1 - y^2}.$$

We also know,

$$\sin_{2\ell}^{-1} y \in \left(2\ell\pi, 2\ell\pi + \frac{\pi}{2}\right) \subset (2\ell\pi, (2\ell + 1)\pi) = U_{4\ell},$$

the last set being the domain of the restriction

$$\cos_{2\ell} = \cos\Big|_{U_{4\ell}}.$$

Therefore,

$$\begin{aligned} \cos(\sin_{2\ell}^{-1} y) &= \cos(\sin^{-1} y) \\ &= \sqrt{1 - \sin^2(\sin^{-1} y)} \\ &= \sqrt{1 - y^2} \\ &= x. \end{aligned}$$

This means $\cos_{2\ell}^{-1} x = \sin_{2\ell}^{-1} y$ as required in the first two formulas defining $Q_{2\ell}^{-1}$ when applied on the intersection $E \cap N = \mathrm{I}$.

If $(x, y) \in N \cap W = \mathrm{II}$, then $x < 0 < y$ and

$$x = -\sqrt{1 - y^2}.$$

In this case we have

$$\sin_{2\ell+1}^{-1} y \in \left(2\ell\pi + \frac{\pi}{2}, (2\ell + 1)\pi\right) \subset (2\ell\pi, (2\ell + 1)\pi) = U_{4\ell}.$$

Then

$$\begin{aligned} \cos(\sin_{2\ell+1}^{-1} y) &= \cos(\pi - \sin^{-1} y) \\ &= -\cos(\sin^{-1} y) \end{aligned}$$

$$
\begin{aligned}
&= -\sqrt{1 - \sin^2(\sin^{-1} y)} \\
&= -\sqrt{1 - y^2} \\
&= x.
\end{aligned}
$$

Again this means $\cos_{2\ell}^{-1} x = \sin_{2\ell+1}^{-1} y$ as required in the second and third formulas defining $Q_{2\ell}^{-1}$ when applied on the intersection $N \cap W = \mathrm{II}$.

The many verifications of the formulas in the proposition follow from similar calculations using the definitions of the overlapping partition intervals and the standard nonsingular inverse trigonometric functions defined above. □

**Proposition 2** (general maximal inverse branches of $p^{-1}$) *Given $\theta^* \in \mathbb{R}$, the restriction*

$$
p^* = p\big|_{(\theta^*-\pi,\theta^*+\pi)} : (\theta^* - \pi, \theta^* + \pi) \to \mathbb{S}^1 \backslash \{(\cos\theta^*, \sin\theta^*)\}
$$

*is a bijection admitting a well-defined continuous inverse*

$$
(p^*)^{-1} : \mathbb{S}^1 \backslash \{(\cos\theta^*, \sin\theta^*)\} \to (\theta^* - \pi, \theta^* + \pi).
$$

*In particular, $p^*$ is a homeomorphism.*

I omit the proof of this result, though it may be useful in some applications to write down explicit formulas for $(p^*)^{-1}$ in terms of the standard trigonometric inverses depending on the location of $p(\theta^*) \in \mathbb{S}^1$ or alternatively the location of $\theta^*$ among the overlapping partition intervals $U_j$ and $V_j$ in $\mathbb{R}$.

## 2.3 Proof of Theorem 4

As in the proof of Theorem 1, we begin again with a local version of Theorem 4 with arbitrary initial condition at a point $s^* \in I$. This result also generalizes the introductory discussion above and an attempt is made to capture in this result and its proof the essential structure of the universal covering map of the circle as mentioned in the introduction.

**Lemma 4** *If $\mathbf{v} : I \to \mathbb{S}^1$ and $s^* \in I$ satisfy $\mathbf{v}(s^*) = p(\theta^*)$, that is,*

$$
\begin{cases} \cos\theta^* = v_1(s^*) \\ \sin\theta^* = v_2(s^*) \end{cases} \tag{59}
$$

*for some $\theta^* \in \mathbb{R}$, then there exists some $\epsilon^* > 0$ such that setting $I^* = (s^* - \epsilon^*, s^* + \epsilon^*)$ there exists a unique function $\psi \in C^0(I^*)$ for which*

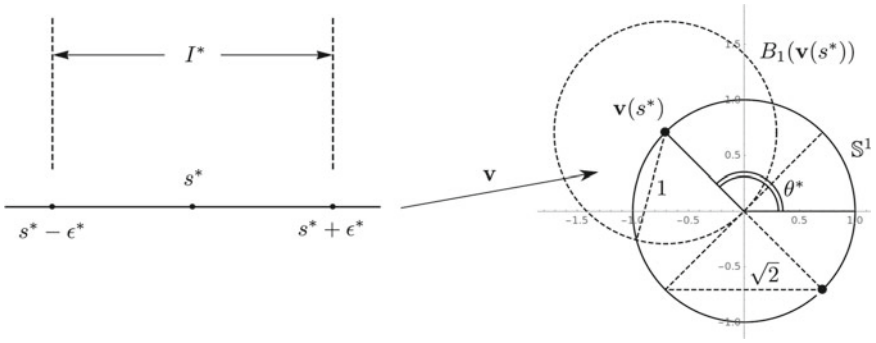


**Fig. 8** Continuous mapping into a semicircle

$$\begin{cases} \cos\psi = v_1, \ s \in I^* \\ \sin\psi = v_2, \ s \in I^* \\ \psi(s^*) = \theta^*. \end{cases} \tag{60}$$

***Proof*** By continuity, there exists some $\epsilon^* > 0$ for which

$$\mathbf{v}(I^*) \subset B_1(\mathbf{v}(s^*)) = \{\mathbf{x} \in \mathbb{S}^1 : \|\mathbf{x} - \mathbf{v}(s^*)\| < 1\} \subset \mathbb{S}^1 \backslash \{(-\cos\theta^*, -\sin\theta^*)\} \tag{61}$$

where $I^* = (s^* - \epsilon^*, s^* + \epsilon^*)$ as in the statement of the lemma. See Fig. 8.

We recall the universal covering map $p : \mathbb{R} \to \mathbb{S}^1$ with

$$p(\theta) = (\cos\theta, \sin\theta)$$

for which the restriction

$$p^* = p\big|_{(\theta^* - \pi, \theta^* + \pi)} : (\theta^* - \pi, \theta^* + \pi) \to \mathbb{S}^1 \backslash \{(-\cos\theta^*, -\sin\theta^*)\}$$

is a homeomorphism, i.e., continuous bijection with continuous inverse.

Thus, setting $\psi : I^* \to \mathbb{R}$ by

$$\psi \equiv (p^*)^{-1} \circ \mathbf{v}$$

we have $\psi \in C^0(I^*)$ and $p \circ \psi = \mathbf{v}$. Also, $\psi(s^*) = \theta^*$ so that (60) holds.

To see uniqueness, consider $\tilde{\psi} \in C^0(I^*)$ for which (60) holds. The set

$$A = \{s \in I^* : \tilde{\psi}(s) = \psi(s)\}$$

is nonempty and closed by the continuity of $\tilde{\psi}$ and $\psi$. If $\sigma \in A$, then

$$\tilde{\psi}(\sigma) = \psi(\sigma) = (p^*)^{-1} \circ \mathbf{v}(\sigma) \in (\theta^* - \pi, \theta^* + \pi).$$

By the continuity of $\tilde{\psi}$, there is some $\delta > 0$ for which $\tilde{\psi}(s) \in (\theta^* - \pi, \theta^* + \pi)$ for $\sigma - \delta < s < \sigma + \delta$. Therefore, we have

$$\tilde{\psi}(s) = (p^*)^{-1} \circ p \circ \tilde{\psi}(s) = (p^*)^{-1} \circ \mathbf{v}(s) = \psi(s)$$

for $\sigma - \delta < s < \sigma + \delta$. This shows $(\sigma - \delta, \sigma + \delta) \subset A$, and $A$ is open. Since the only nonempty subsets of $I^*$ which are both open and closed are the open interval $I^*$ itself, we have shown $A = I^*$, and $\tilde{\psi} \equiv \psi$. □

**Note:** An alternative proof of Lemma 4 may be given avoiding the direct use of Proposition 2 along the following lines: We start with the observation that

$$\mathbb{R} = \bigcup_{j \in \mathbb{Z}} V_j,$$

so there is some $j \in \mathbb{Z}$ for which $\theta^* \in V_j$. At this point, one considers various cases. If $j$ is even, then either $j = 4\ell$ or $j = 4\ell + 2$ for some $\ell \in \mathbb{Z}$, and the value $\ell$ is unique because $V_{2m} \cap V_{2n} = \phi$ for $m \neq n$. If $j = 4\ell$, then

$$\mathbf{v}(s^*) = p\big|_{V_{4\ell}}(s_*) \in E.$$

Since the compass semicircle $E$ is open in $\mathbb{S}^1$, there exists some $\epsilon^* > 0$ for which $\mathbf{v}(s) \in E$ and

$$p \circ p^{-1}\big|_{V_{4\ell}} \circ \mathbf{v}(s) = p \circ P_{2\ell}^{-1} \circ \mathbf{v}(s) = \mathbf{v}(s) \qquad \text{for } s^* - \epsilon^* < s < s^* + \epsilon^*.$$

In particular, setting

$$\psi(s) = P_{2\ell}^{-1} \circ \mathbf{v}(s) \qquad \text{for } s^* - \epsilon^* < s < s^* + \epsilon^*,$$

we have $\psi \in C^0(I^*)$ and $p \circ \psi(s) = \mathbf{v}(s)$ for $s \in I^*$. There also holds $\psi(s^*) = \theta^*$, so the existence claim of the proposition is established. As for uniqueness, if $\tilde{\psi} \in C^0(I^*)$ and

$$p \circ \tilde{\psi}(s) = \mathbf{v}(s) \qquad \text{for } s \in I^*,$$

then since $\mathbf{v}(s) \in E$, we have

$$\tilde{\psi}(s) = P_{2\ell}^{-1} \circ p \circ \tilde{\psi}(s) = P_{2\ell}^{-1} \circ \mathbf{v}(s) = \psi(s) \qquad \text{for } s \in I^*.$$

Thus, the case $\theta^* \in V_{4\ell}$ leads to the conclusion of the lemma. The cases $\theta^* \in V_{4\ell+2}$ and $\theta^* \in V_{2k+1} = U_{2k}$ for some $k \in \mathbb{Z}$ are handled similarly.

***Proof of Theorem 4*** Applying Lemma 4 at $s^* = s_0$ with $\theta^* = \theta_0$ we obtain $\epsilon_0 > 0$ and a unique function $\psi_0 \in C^0(I_0)$ for which $\psi_0(s_0) = \theta_0$ and

$$\mathbf{v}(s) = p \circ \psi_0(s) \qquad \text{for } s \in I_0$$

where $I_0 = (s_0 - \epsilon_0, s_0 + \epsilon_0)$.

Let $\mathcal{F}$ be the family of open intervals $J = (\inf J, \sup J)$ for which

$$\inf I \leq \inf J \leq s_0 - \epsilon_0 < s_0 + \epsilon_0 \leq \sup J \leq \sup I$$

and for which there exists a unique $\psi = \psi_J \in C^0(J)$ with

$$\mathbf{v}(s) = p \circ \psi(s), \qquad s \in J,$$

that is, there exists a well-defined, unique continuous lifting of the restriction

$$\mathbf{v}\big|_J.$$

Setting

$$s_A = \inf_{J \in \mathcal{F}} (\inf J) \qquad \text{and} \qquad s_B = \sup_{J \in \mathcal{F}} (\sup J),$$

as usual, we make two claims:

**Claim 1:** There exists a unique function $\psi = \Psi \in C^0(s_A, s_B)$ with $\psi(s_0) = \theta_0$ and

$$\mathbf{v}(s) = p \circ \psi(s), \qquad s \in (s_A, s_B),$$

that is, $\Psi$ is a unique continuous lifting, and $(s_A, s_B) \in \mathcal{F}$.

**Claim 2:** There holds $s_A = \inf I$ and $s_B = \sup I$ so that

$$(s_A, s_B) = I \in \mathcal{F}.$$

The second claim gives the assertion of the theorem.

***Proof of Claim 1*** We define $\Psi : (s_A, s_B) \to \mathbb{R}$ by

$$\Psi(s) = \psi(s) \qquad \text{whenever } s \in J \in \mathcal{F} \text{ and } \psi = \psi_J.$$

We need to show $\Psi$ is a well-defined, unique continuous lifting of $\mathbf{v}$. Since continuity is local and $(s_A, s_B)$ is open, continuity follows if $\Psi$ is well-defined.

Since it is clear by definition that

$$\bigcup_{J \in \mathcal{F}} J = (s_A, s_B),$$

we have for each $\sigma \in (s_A, s_B)$ at least one $J \in \mathcal{F}$ with $\sigma \in J$ and at least one value $\psi_J(\sigma)$ which may be assigned to $\Psi(\sigma)$. Assume $\sigma \in J_1 \cap J_2$ for some $J_j \in \mathcal{F}$, and

let $\psi_j$ denote the continuous lifting on $J_j$, for $j = 1, 2$. Note that $J_1 \cap J_2$ is an open interval and

$$I_0 \subset C = \{s \in J_1 \cap J_2 : \psi_1(s) = \psi_2(s)\}.$$

Since $\psi_1$ and $\psi_2$ are continuous, $C$ is a closed set. If $s^* \in C$, then we can apply Lemma 4 at $s^*$ with $\theta^* = \psi_1(s^*) = \psi_2(s^*)$ to obtain some $\epsilon^* > 0$ for which $I^* = (s^* - \epsilon^*, s^* + \epsilon^*) \subset J_1 \cap J_2$, and there is a unique continuous lifting $\psi : I^* \to \mathbb{R}$ of

$$\mathbf{v}\big|_{I^*} \tag{62}$$

with $\psi(s^*) = \theta^*$. Since

$$(\psi_1)\big|_{I^*} \qquad \text{and} \qquad (\psi_2)\big|_{I^*}$$

are both continuous liftings of the restriction (62) satisfying $\psi_j(s^*) = \theta^*$ for $j = 1, 2$, we conclude

$$(\psi_1)\big|_{I^*} \equiv (\psi_2)\big|_{I^*},$$

and $s^* \in I^* \subset C$. This means $C$ is open as well. Since the only nonempty subset of the open interval $J_1 \cap J_2$ which is both closed and open is the interval $J_1 \cap J_2$ itself, we conclude $C = J_1 \cap J_2$ and $\psi_1(\sigma) = \psi_2(\sigma)$ in particular. This establishes existence of the continuous lifting $\Psi : (s_A, s_B) \to \mathbb{R}$ with $\Psi(s_0) = \psi_0(s_0) = \theta_0$. It remains to show uniqueness.

If $\tilde{\psi} \in C^0(s_A, s_B)$ is a lifting of

$$\mathbf{v}\big|_{(s_A, s_B)} \tag{63}$$

with $\tilde{\psi}(s_0) = \theta_0$, then for each $\sigma \in (s_A, s_B)$, there is some $J \in \mathcal{F}$ with $\sigma \in J$. If $\psi_J$ is the lifting associated with the interval $J \in \mathcal{F}$, then since

$$\tilde{\psi}\big|_J$$

is a continuous lifting with $\tilde{\psi}(s_0) = \theta_0$, we know by the uniqueness of $\psi_J$ that

$$\tilde{\psi}(\sigma) = \psi_J(\sigma) = \Psi(\sigma).$$

Thus, $\Psi$ is unique and Claim 1 is established.

***Proof of Claim 2*** Let $\Psi \in C^0(U)$ denote the unique continuous lifting on $U = (s_A, s_B)$ obtained in the proof of Claim 1 above. If we assume $s_B < \sup I$, then $s_B \in I$ and $\mathbf{v}(s_B)$ is a well-defined point in $\mathbb{S}^1$. In fact, $\mathbf{v}(s_B)$ is an element of (at least) one of the open compass semicircles, $E$, $N$, $W$, or $S$. Consider the case

$$\mathbf{v}(s_B) \in E = \left\{(\cos\theta, \sin\theta) : -\frac{\pi}{2} < \theta < \frac{\pi}{2}\right\} \subset \mathbb{S}^1.$$

Because $\mathbf{v}$ is continuous and $\Psi$ is a lifting,

$$\lim_{s\nearrow s_B} p\circ\Psi(s)=\lim_{s\nearrow s_B}\mathbf{v}(s)=\mathbf{v}(s_B).$$

In particular, for some $\epsilon>0$, there holds

$$p\circ\Psi(s)\in E\qquad\text{for}\qquad s_B-\epsilon<s<s_B. \tag{64}$$

From this we know

$$\Psi(s)\in p^{-1}E=\bigcup_{\ell\in\mathbb{Z}}V_{4\ell}.$$

Let $\sigma\in(s_B-\epsilon,s_B)$ be fixed. Since $V_{4m}\cap V_{4n}=\phi$ for $m\neq n$, there exists a unique $\ell\in\mathbb{Z}$ for which $\Psi(\sigma)\in V_{4\ell}$. For any other $s\in(s_B-\epsilon,s_B)$ we know similarly that $\Psi(s)\in V_{4m}$ for some $m\in\mathbb{Z}$. If $m<\ell$, then

$$4m<4m+2\leq 4\ell-2<4\ell,$$

and it follows from the continuity of $\Psi$ that there is some $s^*\in(s_B-\epsilon,s_B)$ between $s$ and $\sigma$ for which

$$\Psi(s^*)\in V_{4\ell-2}.$$

Consequently, $\mathbf{v}(s^*)=p\circ\Psi(s^*)\in W$ which contradicts (64). If $\ell<m$ we obtain a similar contradiction. From this we conclude

$$\Psi(s)\in V_{4\ell}=\left(2\ell\pi-\frac{\pi}{2},2\ell\pi+\frac{\pi}{2}\right)\subset\subset((2\ell-1)\pi,(2\ell+1)\pi)\qquad\text{for}\qquad s\in(s_B-\epsilon,s_B).$$

Therefore,

$$\Psi(s)=P_{2\ell}^{-1}\circ p\circ\Psi(s)=P_{2\ell}^{-1}\circ\mathbf{v}(s)\qquad\text{for}\qquad s\in(s_B-\epsilon,s_B),$$

and there exists a well-defined value

$$\theta_B=\lim_{s\nearrow s_B}\Psi(s)=P_{2\ell}^{-1}\circ\mathbf{v}(s_B)\in\left[2\ell\pi-\frac{\pi}{2},2\ell\pi+\frac{\pi}{2}\right].$$

Note that $\Psi_B:(s_A,s_B]\to\mathbb{R}$ by

$$\Psi_B(s)=\begin{cases}\Psi(s), & s\in(s_A,s_B)\\ \theta_B, & s=s_B\end{cases}$$

satisfies $\Psi_B\in C^0(s_A,s_B]$. Furthermore, we can now apply Lemma 4 at $s^*=s_B$ with $\theta^*=\theta_B$ to obtain some $\epsilon^*>0$ and a unique continuous lifting $\psi\in C^0(I^*)$ on $I^*=(s_B-\epsilon^*,s_B+\epsilon^*)\subset(s_B-\epsilon,s_B+\epsilon)\subset I$. Thus, we consider $\Psi^*:(s_A,s_B+\epsilon^*)\to\mathbb{R}$ by

$$\Psi^*(s) = \begin{cases} \Psi(s), & s \in (s_A, s_B) \\ \psi(s), & s \in [s_B, s_B + \epsilon^*). \end{cases}$$

Since $\psi(s^*) = \theta_B = \Psi_B(s^*)$, we know $\Psi^* \in C^0(s_A, s_B + \epsilon^*)$. Also, $\Psi^*$ satisfies $p \circ \Psi^*(s) = \mathbf{v}(s)$ for $s \in (s_A, s_B + \epsilon^*)$, so $\Psi^*$ is a lifting of $\mathbf{v}$. It remains to show $\Psi^*$ is the unique such lifting.

If $\tilde{\psi} \in C^0(s_A, s_B + \epsilon^*)$ with $\tilde{\psi}(s_0) = \theta_0$ and $p \circ \tilde{\psi}(s) = \mathbf{v}(s)$ for $s \in (s_A, s_B + \epsilon^*)$, then first of all,

$$\tilde{\psi}\big|_{(s_A, s_B)} \equiv \Psi$$

due to the uniqueness of $\Psi$. This implies

$$\tilde{\psi}(s_B) = \lim_{s \nearrow s_B} \Psi(s) = \Psi_B(s_B) = \theta_B.$$

And this implies

$$\tilde{\psi}\big|_{(s_B - \epsilon^*, s_B + \epsilon^*)} \equiv \psi$$

due to the uniqueness of the local lifting $\psi$ at $s^* = s_B$. This shows $\tilde{\psi} \equiv \Psi^*$, and $\Psi^*$ is unique. This contradicts the definition of $s_B$, and we conclude $s_B = \sup I$ as claimed.

There are various other cases to consider. First of all, we are still working under the assumption that $\mathbf{v}(s_B) \in E$. The cases $\mathbf{v}(s_B) \in N$, $\mathbf{v}(s_B) \in W$, and $\mathbf{v}(s_B) \in S$ all lead to similar contradictions and the conclusion $s_B = \sup I$. Then the assumption $s_A > \inf I$ leads to similar cases and similar contradictions. We conclude $U = (s_A, s_B) = I$ and the theorem holds. □

**Remark:** It is also straightforward to allow certain more general possibilities in the argument(s) above. For example, if $I$ is assumed to be a half-closed interval of the form $[\min I, \sup I)$ where $\min I \in \mathbb{R}$ with $s_0 \in I_* = (\min I, \sup I)$ and $\theta_0$ given as in Theorem 4, then it can be shown that

$$\lim_{s \searrow s_A} \psi(s) = \theta_A$$

exists where $s_A = \min I$ and $\psi$ is the continuous lifting of

$$\mathbf{v}\big|_{I_*}.$$

It follows that $\psi$ can be extended to a unique continuous lifting of $\mathbf{v} : I \to \mathbb{S}^1$. The situation when $\mathbf{v}(s_0) = p(\theta_0)$ is specified at an endpoint $s_0 = \min I$ can also be considered separately in this case using a variant of the argument above. As a consequence, we can state the following general version of Theorem 4.

**Lemma 5** *Let $I \subset \mathbb{R}$ be* **any interval**, *open, closed, or half-open/closed. If $\mathbf{v} = (v_1, v_2) : I \to \mathbb{S}^1$ is continuous and there are values $s_0 \in I$ and $\theta_0 \in \mathbb{R}$ with*

$$\begin{cases} \cos\theta_0 = v_1(s_0) \\ \sin\theta_0 = v_2(s_0), \end{cases} \tag{65}$$

*then there exists a unique function $\psi \in C^0(I)$ such that*

$$p \circ \psi = \mathbf{v} \qquad \text{and} \qquad \psi(s_0) = \theta_0. \tag{66}$$

### 2.4 Second Proof of Theorem 1

We can apply Theorem 4 with $\mathbf{v} = \dot\gamma$ to obtain a continuous lifting $\psi_c \in C^0(I)$ with

$$\dot\gamma = p \circ \psi_c \qquad \text{and} \qquad \psi_c(s_0) = \theta_0.$$

Since the condition $\psi = \psi_c \in C^1(I)$ can be verified locally. We observe that all the local expressions for $\psi_c$ are given in terms of standard nonsingular ($C^1$) inverse trigonometric functions of the coordinate functions $v_1$ and/or $v_2$. Furthermore, if we know $\gamma_1, \gamma_2 \in C^2(I)$, then we know the coordinate functions $v_1 = \dot\gamma_1$ and $v_2 = \dot\gamma_2$ are in $C^1(I)$. Thus, the local compositions are in $C^1(I)$ and Theorem 1 follows. □

## 3 Structure of Plane Curves

Theorem 1 may be applied to the construction of plane curves of prescribed curvature to obtain the following structure theorem for plane curves:

**Theorem 5** (structure theorem for $C^2$ curves) *If $I$ is an open interval with*

***(i)*** $s_0 \in I$,
***(ii)*** $\mathbf{x}_0 \in \mathbb{R}^2$,
***(iii)*** $\mathbf{v}_0 \in \mathbb{S}^1$, *and*

*$k \in C^0(I)$, then there exists a unique curve $\gamma : I \to \mathbb{R}^2$ parameterized by arclength and satisfying $\gamma(s_0) = \mathbf{x}_0$, $\dot\gamma(s_0) = \mathbf{v}_0$ and*

$$\ddot\gamma \cdot (-\dot\gamma_2, \dot\gamma_1) = \frac{d\psi}{ds} = k$$

*is the signed curvature associated with $\gamma$ and where $\psi \in C^1(I)$ is the inclination angle determined by $\gamma$ and any value $\theta_0 \in \mathbb{R}$ with $(\cos\theta_0, \sin\theta_0) = \mathbf{v}_0$.*

Theorem 4 may be applied to obtain the following structure theorem for $C^1$ plane curves:

**Theorem 6** (structure theorem for $C^1$ curves) *If $I$ is an open interval with*

***(i)*** $s_0 \in I$,
***(ii)*** $\mathbf{x}_0 \in \mathbb{R}^2$, *and*

$\mathbf{v} = (v_1, v_2) : I \to \mathbb{S}^1$ *with* $v_j \in C^0(I)$ *for* $j = 1, 2$, *then there exists a unique curve* $\gamma : I \to \mathbb{R}^2$ *parameterized by arclength and satisfying* $\gamma(s_0) = \mathbf{x}_0$, *and*

$$\dot{\gamma} = (\cos\psi, \sin\psi) = \mathbf{v}$$

*where* $\psi \in C^0(I)$ *is the inclination angle determined by* $\gamma$ *and any value* $\theta_0 \in \mathbb{R}$ *with* $(\cos\theta_0, \sin\theta_0) = \mathbf{v}(s_0)$.

## 4 Examples

Here we give examples of two plane curves to which the main result Theorem 1 applies and another example of a singular system of ODEs to which the techniques of the first proof of Theorem 1 apply.

### *4.1 Example Curves*

The examples of curves are both counterclockwise spirals. Consider $\alpha : (0, \infty) \to \mathbb{R}^2$ by

$$\alpha(t) = \frac{1}{t}(\cos t, \sin t).$$

When parameterized by arclength, a natural arclength interval is $\mathbb{R}$ with $\gamma(0) = \alpha(1)$ and signed curvature given by

$$k = -\frac{2}{|\gamma|^2(|\gamma|^2 + 1)^{3/2}}.$$

The curve has infinite length as it spirals for $t > 1$ and also for $0 < t < 1$ where it is asymptotic to the line $y = 1$ as indicated on the left in Fig. 9.

As a second example, consider $\alpha : \mathbb{R} \to \mathbb{R}^2$ by

$$\alpha(t) = \frac{1}{e^t}(\cos t, \sin t).$$

Here

$$k = -\frac{1}{|\gamma|\sqrt{2}}.$$

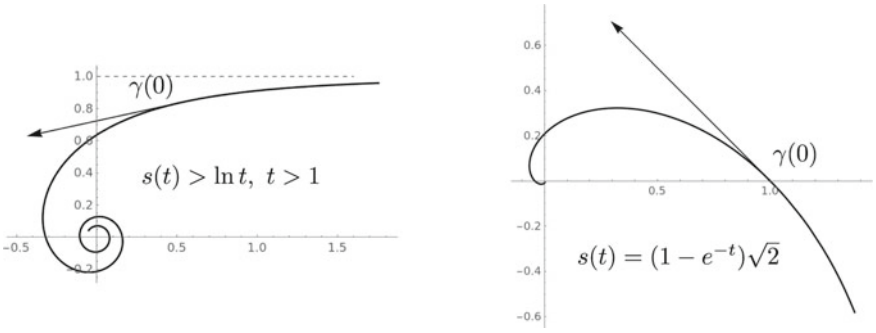


**Fig. 9** Curves with prescribed curvature and natural arclength domains given by open intervals: $\gamma : \mathbb{R} \to \mathbb{R}^2$ (left) and $\gamma : (-\infty, \sqrt{2}) \to \mathbb{R}^2$ (right)

This curve also spirals around the origin infinitely many times but has length in the spirals starting from $(1, 0)$ given by $\sqrt{2} < \infty$. Thus, the natural arclength domain is $(-\infty, \sqrt{2})$ as indicated in Fig. 9.

## *4.2 Another Singular System*

Given $\gamma \in C^2(I \to \mathbb{R}^2)$ as above, a technically different singular system of ordinary differential equations sharing the same singular/nonsingular character displayed by (2) and indeed an alternative for analytically defining the inclination $\psi \in C^1(I)$ determined by $\gamma$ is

$$\begin{cases} -\dot{\gamma}_2\, \dot{\psi} = \ddot{\gamma}_1,\ s \in I \\ \dot{\gamma}_1\, \dot{\psi} = \ddot{\gamma}_2,\ s \in I \\ \psi(s_0) = \theta_0. \end{cases} \tag{67}$$

We make two simple observations about the system (67).

First, in view of the condition

$$\dot{\gamma}_1^2 + \dot{\gamma}_2^2 = 1 \tag{68}$$

at least one of the ordinary differential equations in (67) is nonsingular at each $s \in I$. It will be recalled that this is a feature shared with the singular system (2). Proceeding as with the system (2) we may consider the case $\dot{\gamma}_2(s_0) \neq 0$ so that on some interval the first equation in (67) determines a unique function $\psi$ locally.

Letting $\psi_0$ denote the solution of (2) given by Theorem 1, we can then write locally

$$\frac{d}{ds}(\psi - \psi_0) = -\frac{\ddot{\gamma}_1}{\dot{\gamma}_2} + \frac{\ddot{\gamma}_1}{\sin \psi_0} \equiv 0,$$

since it was established that the second equation in (3) namely $\dot{\gamma}_2 = \sin\psi_0$ holds for $\psi_0$. This implies the solution of (67) is locally identical to the solution of (2) as expected, and this reasoning can clearly be extended to the global assertion $\psi = \psi_0$. As implied, the global existence of the solution $\psi \in C^1(I)$ and the fact that this solution satisfies (3) may also be established along these lines.

Finally, we note the question of "consistency" for the system (67), that is for example showing the second relation $\dot{\gamma}_1\ \dot{\psi} = \ddot{\gamma}_2$ of (67) holds on an interval where the first relation $-\dot{\gamma}_2\ \dot{\psi} = \ddot{\gamma}_1$ holds and is nonsingular, is straightforward. This is in contrast to the slightly delicate argument arising in the proof of Lemma 1 in connection with the second equation in (15) for the system (2). To see this, for example, we can differentiate the relation (68) and use $-\dot{\gamma}_2\ \dot{\psi} = \ddot{\gamma}_1$ to obtain directly

$$0 = \dot{\gamma}_1\ \ddot{\gamma}_1 + \dot{\gamma}_2\ \ddot{\gamma}_2 = -\dot{\gamma}_1\ \dot{\gamma}_2\ \dot{\psi} + \dot{\gamma}_2\ \ddot{\gamma}_2$$

which implies $\ddot{\gamma}_2 = \dot{\gamma}_1\ \dot{\psi}$.

## References


1. Anna Aspley, Chang He, and John McCuan. Force profiles for parallel plates partiall immersed in a liquid. *J. Math. Fluid Mech.*, 17(1):87–102, 2015.
2. Ch. Delaunay. Sur la surface de révolution dont la courbure moyenne est constant. *Journal de Mathémathiques Pure et Appliquée*, 16:309–321, 1841.
3. Manfredo do Carmo. *Differential Geometry of Curves and Surfaces*. Prentice-Hall, 1976.
4. Jeffrey Elms, Ryan Hind, Roberto Lopez, and John McCuan. Plateau's rotating drops and rotational figures of equilibrium. *J. Math. Anal. Appl.*, 446(1):201–232, 2017.
5. Leonhard Euler. *Methodus inveniendi lineas curvas maximi minimive proprietate gaudentes, sive solutio problematis isoperimetrici lattissimo sensu accepti*. Bosquet, Lausanne, 1744.
6. Robert Finn. *Equilibrium Capillary Surfaces*. Springer, 1986.
7. Ryan Hind and John McCuan. On toroidal rotating drops. *Pacific J. Math.*, 224(2):279–289, 2006.
8. John McCuan. New geometric estimates for euler elastica. *J. Elliptic Parabol. Equ*, 1:387–402, 2015.
9. John McCuan. The stability of cylindrical pendant drops. *Mem. Amer. Math. Soc*, 250(1189):1–109, 2017.
10. John McCuan and Ray Treinen. Capillarity and archimedes' principle of flotation. *Pacific J. Math.*, 265(1):123–150, 2013.
11. Ivaïlo M. Mladenov and Miriana Hadzhilazova. *The Many Faces of Elastica*. Springer, 2013.
12. James R. Munkres. *Topology A First Course*. Prentice-Hall, 1975.
13. Michael Spivak. *A Comprehensive Introduction to Differential Geometry*, volume II. Publish or Perish, 1970.
14. J. J. Stoker. *Differential Geometry*. Wiley & Sons, 1969.
15. Henry Wente. The stability of the axially symmetric pendant drop. *Pacific J. Math.*, 88(2):421–470, 1980.
16. Henry Wente. Exotic capillary tubes. *J. Math. Fluid Mech.*, 13(3):355–370, 2011.

# Localized Waves on the Periodic Background for the Derivative Nonlinear Schrödinger Equation


**Lifei Wu, Yi Zhang, Rusuo Ye, and Jie Jin**

**Abstract** The localized waves based on the plane, periodic and double-periodic backgrounds for the derivative nonlinear Schrödinger equation are constructed in this paper. Especially, we give a determinant representation of the semi-degenerate Darboux transformation by using the Taylor expansion technique. Additionally, by changing the amplitude of seed solution and the value of the spectral parameters, energy conversion occurs between the localized waves and different backgrounds, resulting in different dynamic behaviors.

**Keywords** Periodic background · Rogue wave · Darboux transformation · Taylor expansion

## 1 Introduction

As far as we know, rogue wave and the breather are two kinds of nonlinear localized waves, which have attracted great attention in Bose–Einstein condensates, capillary wave, hydrodynamics and other fields [1–5]. Breathers, which are localized in time or space, produced by instability of small amplitude disturbances, [6–8]. The Peregrine soliton as the prototype of the rogue wave appears while the period of the breather tends to infinity [9–11]. On the one hand, compared with the breather, rogue wave is localized in time and space. On the other hand, compared with the strong stability of soliton, rogue wave is unstable and unpredictable. Based on the above facts, it is valuable to research the interaction solutions among the breathers, rogue waves and solitons [12–14].

Because of the strict integrability of the nonlinear Schrödinger (NLS) type equation, the interaction solutions for the NLS-type equation can be studied by some specific methods. Such as, the dark-bright semi-rational solitons for the higher-order coupled NLS equation have been derived by using Darboux transformation (DT)

L. Wu · Y. Zhang (✉) · R. Ye · J. Jin
Department of Mathematics, Zhejiang Normal University, Jinhua 321004, China
e-mail: zy2836@163.com



S. Manukure and W.-X. Ma (eds.), *Nonlinear and Modern Mathematical Physics*,
Springer Proceedings in Mathematics & Statistics 459,
https://doi.org/10.1007/978-3-031-59539-4_14

[15]. Based on the extended generalized DT, the hybrid rogue wave and breather for the NLS equation have been studied [16]. In addition, the variety of nonautonomous complex wave solutions for the $(2+1)$-dimensional NLS equation and the bright and dark solitons for the fifth-order NLS equation with variable coefficients have been studied by the $(G'/G)$-expansion method and the new optical solitons to the time-fractional integrable generalized $(2+1)$-dimensional NLS equation have been obtained by three different methods [17–19].

The purpose of the current research is to study the interaction solutions between different nonlinear localized waves for the derivative NLS equation (DNLS) which has been widely applied in nonlinear optics, finance and plasma physics [20–22], as follows

$$iq_t - q_{xx} + i\left(q|q|^2\right)_x = 0. \tag{1}$$

In recent years, the interaction solutions and several interesting results for (1) have been extensively studied by using DT [23–26]. The Peregrine soliton can be generated by the interaction between the phase solution and the breather solution. In addition, through numerical verification, when the modulation of the periodic wave is unstable, rogue wave can maintain the space-time localization. On the contrary, the rogue wave degenerates into the soliton and periodic wave [27].

Different parameters also have important influence on the interaction between localized waves. By adjusting shift parameters, higher-order rogue waves with different structures and the formation process of higher-order rogue waves can be obtained [28, 29]. It should be noted that the effect of spectral parameters on the interaction solutions among the breathers, rogue waves and periodic backgrounds for (1) have not been reported before.

Furthermore, by improving the interaction and degeneracy of breathers and rouge waves solutions, the semi-degenerate DT is constructed. Thus, the breather and rogue wave on the periodic background [30], the interaction solutions between different types of breathers and rogue waves can be found by using semi-degenerate DT [31]. In our present work, in order to further study the interaction solution between the rogue wave and the breather, one use Taylor expansion technique to obtain a determinant representation of the semi-degenerate DT for (1). Localized waves on different backgrounds for (1) have been given by the semi-degenerate DT. In addition, we make a detailed dynamic analysis of the important influence of spectral parameters on the interaction solution between rogue waves and the breather. It is worth noting that by changing the conditions satisfied by the spectral parameters $\lambda$, we obtain the interaction solutions of rogue waves, periodic backgrounds and breathers. As far as we know, the process of the first-order rogue wave evolving into the interaction solution of the breather solution and the rogue wave for (1) has not been obtained.

This paper is structured as follows. In Sect. 2, the semi-degenerate DT for (1) can be given by using the modified Taylor expansion technique. In Sect. 3, based on the explicit expression and the influence of different parameters, we can get the dynamics of interaction among the breather, rogue waves, and periodic backgrounds. Our conclusions are given in Sect. 4.

## 2 The DT for the DNLS Equation

Starting from KN system

$$r_t - ir_{xx} - \left(r^2 q\right)_x = 0, \tag{2}$$

$$q_t + iq_{xx} - \left(rq^2\right)_x = 0. \tag{3}$$

Equation 1 can be obtained under reduced condition $r = -q^*$ and the Lax pair can be derived by

$$\begin{aligned} \Phi_{\mathrm{x}} &= U\Phi = \left(J\lambda^2 + Q\lambda\right)\Phi, \\ \Phi_{\mathrm{t}} &= V\Phi = \left(2J\lambda^4 + 2Q\lambda^3 + V_2\lambda^2 + V_1\lambda\right)\Phi, \end{aligned} \tag{4}$$

where $\Phi = (\phi, \varphi)^T$ is a column vector, $\lambda$ is the spectral parameter and

$$J = \begin{pmatrix} i & 0 \\ 0 & -i \end{pmatrix}, Q = \begin{pmatrix} 0 & q \\ r & 0 \end{pmatrix}, V_1 = \begin{pmatrix} 0 & -iq_x + q^2 r \\ ir_x + r^2 q & 0 \end{pmatrix}, V_2 = Jqr.$$

Under the compatibility condition $U_t - V_x + [U, V] = 0$ of Lax pair (4), (2) and (3) are equivalent. According to the gauge transformation

$$\Phi^{[1]} = T\Phi, \tag{5}$$

the Lax pair (4) can be converted to

$$\Phi^{[1]}{}_x = U^{[1]}\Phi^{[1]}, U^{[1]} = \left(T_x + TU\right)T^{-1}, \tag{6}$$

$$\Phi^{[1]}{}_t = V^{[1]}\Phi^{[1]}, V^{[1]} = \left(T_x + TV\right)T^{-1}. \tag{7}$$

After detailed calculation, it can be found that once the matrix $T$ is found, $U^{[1]}$, $V^{[1]}$ and $U$, $V$ will have the same form. In this way, (6) and (7) can be invariant under the gauge transformation (5).

In fact, the $N$-fold Darboux matrix $T$ of (1) have been given in [23], as follows,

$$T_n = \sum_{l=0}^{n} F_l \lambda^l,$$

with

$$F_n = \begin{pmatrix} f_{11,n} & 0 \\ 0 & f_{22,n} \end{pmatrix} \in D, \; F_{n-1} = \begin{pmatrix} 0 & f_{12,n-1} \\ f_{21,n-1} & 0 \end{pmatrix} \in A,$$

where

$$F_l \in D = \begin{pmatrix} f_{11} & 0 \\ 0 & f_{22} \end{pmatrix} \text{ (if } l - n \text{ is even)},$$

$$F_l \in A = \begin{pmatrix} 0 & f_{12} \\ f_{21} & 0 \end{pmatrix} \text{ (if } l-n \text{ is odd)}.$$

Here $f_{11}$, $f_{12}$, $f_{21}$, $f_{22}$ are complex functions with $x$ and $t$.

Let $\Phi_j = \left(\phi_j, \varphi_j\right)^T$ be the solutions of system (4) with the spectral parameters $\lambda_j$, $j = 1, 2, \cdots, n$. Then, $q^{[n]}$ can be derived by

$$q^{[n]} = \frac{\Theta_{11}^2}{\Theta_{21}^2} q + 2i \frac{\Theta_{11}\Theta_{12}}{\Theta_{21}^2}, \tag{8}$$

with

(1) when $n = 2k$

$$\Theta_{11} = \begin{vmatrix} \lambda_1^{n-1}\varphi_1 & \lambda_1^{n-2}\phi_1 & \lambda_1^{n-3}\varphi_1 & \cdots & \lambda_1\varphi_1 & \phi_1 \\ \lambda_2^{n-1}\varphi_2 & \lambda_2^{n-2}\phi_2 & \lambda_2^{n-3}\varphi_2 & \cdots & \lambda_2\varphi_2 & \phi_2 \\ \vdots & \vdots & \vdots & \vdots & \vdots & \vdots \\ \lambda_n^{n-1}\varphi_n & \lambda_n^{n-2}\phi_n & \lambda_n^{n-3}\varphi_n & \cdots & \lambda_n\varphi_n & \phi_n \end{vmatrix},$$

$$\Theta_{12} = \begin{vmatrix} \lambda_1^{n}\phi_1 & \lambda_1^{n-2}\phi_1 & \lambda_1^{n-3}\varphi_1 & \cdots & \lambda_1\varphi_1 & \phi_1 \\ \lambda_2^{n}\phi_2 & \lambda_2^{n-2}\phi_2 & \lambda_2^{n-3}\varphi_2 & \cdots & \lambda_2\varphi_2 & \phi_2 \\ \vdots & \vdots & \vdots & \vdots & \vdots & \vdots \\ \lambda_n^{n}\phi_n & \lambda_n^{n-2}\phi_n & \lambda_n^{n-3}\varphi_n & \cdots & \lambda_n\varphi_n & \phi_n \end{vmatrix},$$

$$\Theta_{21} = \begin{vmatrix} \lambda_1^{n-1}\phi_1 & \lambda_1^{n-2}\varphi_1 & \lambda_1^{n-3}\phi_1 & \cdots & \lambda_1\phi_1 & \varphi_1 \\ \lambda_2^{n-1}\phi_2 & \lambda_2^{n-2}\varphi_2 & \lambda_2^{n-3}\phi_2 & \cdots & \lambda_2\phi_2 & \varphi_2 \\ \vdots & \vdots & \vdots & \vdots & \vdots & \vdots \\ \lambda_n^{n-1}\phi_n & \lambda_n^{n-2}\varphi_n & \lambda_n^{n-3}\phi_n & \cdots & \lambda_n\phi_n & \varphi_n \end{vmatrix},$$

(2) when $n = 2k + 1$

$$\Theta_{11} = \begin{vmatrix} \lambda_1^{n-1}\varphi_1 & \lambda_1^{n-2}\phi_1 & \lambda_1^{n-3}\varphi_1 & \cdots & \lambda_1\phi_1 & \varphi_1 \\ \lambda_2^{n-1}\varphi_2 & \lambda_2^{n-2}\phi_2 & \lambda_2^{n-3}\varphi_2 & \cdots & \lambda_2\phi_2 & \varphi_2 \\ \vdots & \vdots & \vdots & \vdots & \vdots & \vdots \\ \lambda_n^{n-1}\varphi_n & \lambda_n^{n-2}\phi_n & \lambda_n^{n-3}\varphi_n & \cdots & \lambda_n\phi_n & \varphi_n \end{vmatrix},$$

$$\Theta_{12} = \begin{vmatrix} \lambda_1^{n}\phi_1 & \lambda_1^{n-2}\phi_1 & \lambda_1^{n-3}\varphi_1 & \cdots & \lambda_1\phi_1 & \varphi_1 \\ \lambda_2^{n}\phi_2 & \lambda_2^{n-2}\phi_2 & \lambda_2^{n-3}\varphi_2 & \cdots & \lambda_2\phi_2 & \varphi_2 \\ \vdots & \vdots & \vdots & \vdots & \vdots & \vdots \\ \lambda_n^{n}\phi_n & \lambda_n^{n-2}\phi_n & \lambda_n^{n-3}\varphi_n & \cdots & \lambda_n\phi_n & \varphi_n \end{vmatrix},$$

$$\Theta_{21} = \begin{vmatrix} \lambda_1^{n-1}\phi_1 & \lambda_1^{n-2}\varphi_1 & \lambda_1^{n-3}\phi_1 & \cdots & \lambda_1\varphi_1 & \phi_1 \\ \lambda_2^{n-1}\phi_2 & \lambda_2^{n-2}\varphi_2 & \lambda_2^{n-3}\phi_2 & \cdots & \lambda_2\varphi_2 & \phi_2 \\ \vdots & \vdots & \vdots & \vdots & \vdots & \vdots \\ \lambda_n^{n-1}\phi_n & \lambda_n^{n-2}\varphi_n & \lambda_n^{n-3}\phi_n & \cdots & \lambda_n\varphi_n & \phi_n \end{vmatrix}.$$

In order to construct the determinant representation of semi-degenerate DT, we adjust the specific process of Taylor expansion. In what follows, we choose the seed solution $q = de^{i(\omega x+kt)}$, $k = -\omega d^2 + \omega^2$, and $\omega$, $d$ are two real constants.

**Theorem 1** *Assuming* $\lambda_0 = \frac{1}{2}\left(\sqrt{-d^2+2\omega} - id\right)$, *the spectral parameters satisfy the conditions* $\lambda_{2j-1} = \lambda_0 + \varepsilon^2\left(\lambda_{2j} = -\lambda_0^* + \varepsilon^2\right)$, $\varepsilon \to 0$, *for* $j = 1, 2, \cdots, l$ *and* $\lambda_m = \alpha_m + i\beta_m$, *for* $2l+1 \le m \le n$, *where* $\alpha_m$ *and* $\beta_m$ *are real numbers. The Bäcklund transformation for (1) can be given by the following formula:*

$$q_n = \frac{\delta_{11}^2}{\delta_{21}^2} q + 2i\frac{\delta_{11}\delta_{12}}{\delta_{21}^2}, \tag{9}$$

*where* $\delta_{ij}$ $(i, j = 1, 2)$ *will be presented below.*

***Proof*** When $n = 2k$, take determinant $\Theta_{11}$ for example, give the concrete process below:

(i) Set $\lambda_1 = \lambda_0 + \varepsilon^2$ $(\lambda_2 = -\lambda_0^* + \varepsilon^2)$, elements which in the first and second rows of determinant $\Theta_{11}$ are expanded by Taylor series of order 4 around $\varepsilon = 0$, and then the coefficients of $\varepsilon^2$ are extracted.

(ii) Set $\lambda_3 = \lambda_0 + \varepsilon^2$ $(\lambda_4 = -\lambda_0^* + \varepsilon^2)$, elements which in the third and fourth rows of determinant $\Theta_{11}$ are expanded by Taylor series of order 6 around $\varepsilon = 0$, and then the coefficients of $\varepsilon^4$ are extracted.

(iii) Set $\lambda_{2l-1} = \lambda_0 + \varepsilon^2$ $(\lambda_{2l} = -\lambda_0^* + \varepsilon^2)$, elements which in the $(2l-1)$th and $2l$th rows of determinant $\Theta_{11}$ are expanded by Taylor series of order $2l+2$ around $\varepsilon = 0$, and the coefficients of $\varepsilon^{2l}$ are extracted.

(iv) The $(2j+1)$th and $(2j+2)$th rows of determinant $\Theta_{11}$ is unchanged $(l \le j \le k-1)$.

Thus, $\Theta_{11}$ can be written as

$$\delta_{11} = \begin{vmatrix}
\varphi[1,n-1,1] & \phi[1,n-2,1] & \varphi[1,n-3,1] & \cdots & \varphi[1,1,1] & \phi[1,0,1] \\
\varphi[2,n-1,1] & \phi[2,n-2,1] & \varphi[2,n-3,1] & \cdots & \varphi[2,1,1] & \phi[2,0,1] \\
\varphi[1,n-1,2] & \phi[1,n-2,2] & \varphi[1,n-3,2] & \cdots & \varphi[1,1,2] & \phi[1,0,2] \\
\varphi[2,n-1,2] & \phi[2,n-2,2] & \varphi[2,n-3,2] & \cdots & \varphi[2,1,2] & \phi[2,0,2] \\
\vdots & \vdots & \vdots & \vdots & \vdots & \vdots \\
\varphi[1,n-1,l] & \phi[1,n-2,l] & \varphi[1,n-3,l] & \cdots & \varphi[1,1,l] & \phi[1,0,l] \\
\varphi[2,n-1,l] & \phi[2,n-2,l] & \varphi[2,n-3,l] & \cdots & \varphi[2,1,l] & \phi[2,0,l] \\
\lambda_{2l+1}^{n-1}\varphi_{2l+1} & \lambda_{2l+1}^{n-2}\phi_{2l+1} & \lambda_{2l+1}^{n-3}\varphi_{2l+1} & \cdots & \lambda_{2l+1}\varphi_{2l+1} & \phi_{2l+1} \\
\lambda_{2l+2}^{n-1}\varphi_{2l+2} & \lambda_{2l+2}^{n-2}\phi_{2l+2} & \lambda_{2l+2}^{n-3}\varphi_{2l+2} & \cdots & \lambda_{2l+2}\varphi_{2l+2} & \phi_{2l+2} \\
\vdots & \vdots & \vdots & \vdots & \vdots & \vdots \\
\lambda_{2k-1}^{n-1}\varphi_{2k-1} & \lambda_{2k-1}^{n-2}\phi_{2k-1} & \lambda_{2k-1}^{n-3}\varphi_{2k-1} & \cdots & \lambda_{2k-1}\varphi_{2k-1} & \phi_{2k-1} \\
\lambda_{2k}^{n-1}\varphi_{2k} & \lambda_{2k}^{n-2}\phi_{2k} & \lambda_{2k}^{n-3}\varphi_{2k} & \cdots & \lambda_{2k}\varphi_{2k} & \phi_{2k}
\end{vmatrix},$$

where the first $2l$ rows of the determinant $\delta_{11}$, constructed in steps (i–iii), are rational functions, and the remaining elements are still exponential functions. For $\Theta_{12}$ and

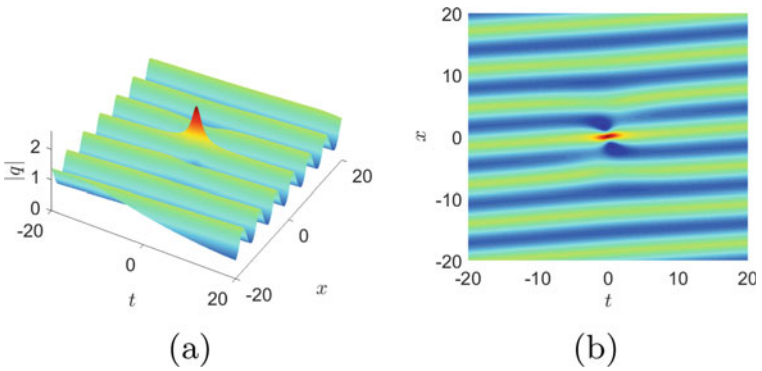


**Fig. 1** The first-order rogue wave on the periodic background by choosing: $\omega = 1, d = 1, \beta_3 = \frac{1}{5}$

$\Theta_{21}$, similar steps lead to new determinant representations of $\delta_{12}$ and $\delta_{21}$, which have similar forms to $\delta_{11}$.

Taking the similar procedure as above, one can obtain the new determinant form of $\delta_{11}$, $\delta_{12}$ and $\delta_{21}$ when $n = 2k + 1$. □

## 3 Interaction Behaviours of the Localized Waves

We obtain localized waves on different backgrounds and discuss the influence on them for different parameters in this section.

### *3.1 Localized Waves on the Periodic Background*

When $n = 3$, $\lambda_1 = \frac{\sqrt{-d^2+2\omega}-id}{2}$, $\lambda_2 = -\lambda_1^*$, and $\lambda_3 = i\beta_3$. It shows that the values of $d$, $\beta_3$ affect the interaction solution between rogue waves and periodic background. Setting $\omega = 1$, and taking $d = 1$, $\beta_3 = \frac{1}{5}$, the first-order rogue wave on the periodic background can be derived, see Fig. 1. Since the value of $\omega$ has no significant influence on the solution, here we only discuss the values of $d$ and $\beta_3$. Take it as the control group, the values of $d$ and $\beta_3$ are adjusted respectively, and other parameters remain unchanged. Thus from the following two cases to consider:

**Case 1. Adjust the value of d**

Firstly, we can see in Fig. 2a that when $d = \frac{1}{1000}$, it is a periodic wave, and the amplitude is $\frac{201}{500}$. The middle of the periodic wave begins to swell when the value of $d$ increases. When $d = \frac{1}{100}$, the amplitude of periodic wave at uplift position reaches $\frac{21}{50}$, while the other part drops to $\frac{2}{5}$ in Fig. 2b. When $d = \frac{1}{20}$, the amplitude of uplifted

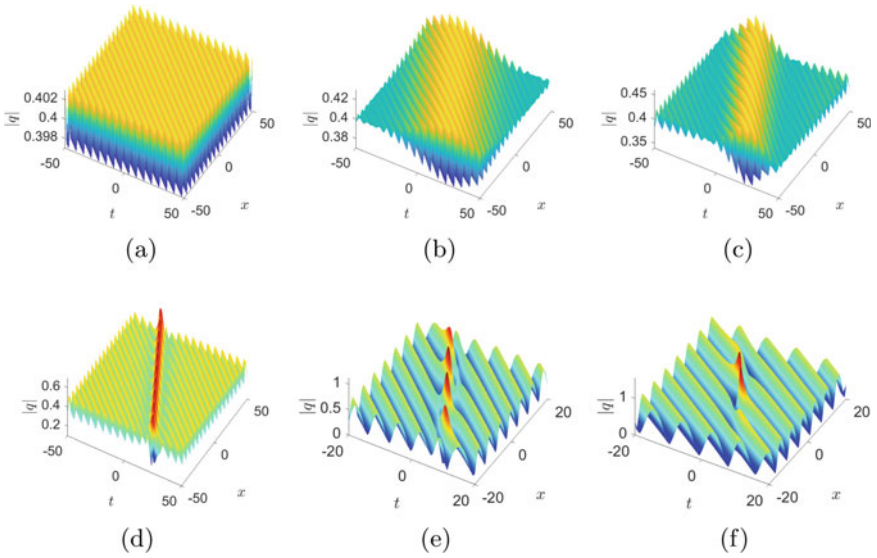


**Fig. 2** Solution for interaction among the the breather, periodic background and rogue wave by choosing: $\omega = 1$, $\beta_3 = \frac{1}{5}$, **a** $d = \frac{1}{1000}$; **b** $d = \frac{1}{100}$; **c** $d = \frac{1}{20}$; **d** $d = \frac{1}{10}$; **e** $d = \frac{1}{4}$; **f** $d = \frac{1}{2}$

periodic wave reaches $\frac{9}{20}$, and the uplift area becomes narrower than that of $d = \frac{1}{100}$, see Fig. 2c. This is a process of periodic wave energy conversion. As the value of $d$ continues to increase, the energy of the periodic wave converges, making the breather appear on the periodic background in Fig. 2d. With the value of $d$ increases from $\frac{1}{10}$ to $\frac{1}{2}$, the period and amplitude of the breather have been changed, see Fig. 2d–f. The above description shows that with the increase of $d$, the periodic wave energy converges and gradually forms the breather, which is a process of breather formation. When $d = 1$, the breather interact with the periodic wave, and the energy converge into a rogue wave, see Fig. 1.

**Case 2. Adjust the value of $\beta_3$**

With the decrease of the value of $\beta_3$, the period of the periodic background becomes larger, the amplitude changes, and wave surface fluctuation of periodic background tends to be gentle from intense. Meanwhile, the amplitude of the rogue wave also changes. It means that the value of $\beta_3$ affects the energy conversion of periodic background. As the value of $\beta_3$ increases, the energy of the periodic background is converted into a rogue wave, see Fig. 3.

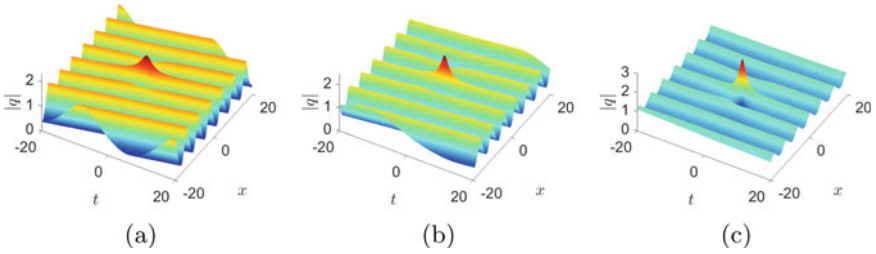


**Fig. 3** Solution for interaction between the periodic background and rogue wave by choosing: $\omega = 1$, $d = 1$, **a** $\beta_3 = \frac{1}{2}$; **b** $\beta_3 = \frac{1}{4}$, **c** $\beta_3 = \frac{1}{10}$

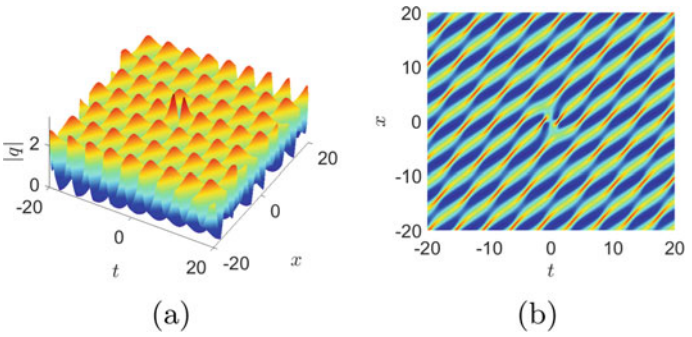


**Fig. 4** Two rogue waves on the double-periodic background: $\omega = 1$, $d = 1$, $\alpha_3 = 0$, $\beta_3 = \frac{1}{5}$, $\alpha_4 = 0$, $\beta_4 = \frac{5}{7}$

## 3.2 *Localized Waves on the Double-Periodic Background*

When $n = 4$, $\lambda_1 = \frac{\sqrt{-d^2+2\omega}-id}{2}$, $\lambda_2 = -\lambda_1^*$, and $\lambda_3 = i\beta_3$, $\lambda_4 = i\beta_4$. Different from $n = 3$, set $\omega = 1$, and take $d = 1$, $\beta_3 = \frac{1}{5}$, $\beta_4 = \frac{5}{7}$, one can obtain two rogue waves on the double-periodic background, see Fig. 4. Take it as the control group, the values of $d$, $\beta_3$ and $\beta_4$ are adjusted respectively, and other parameters remain unchanged. We also consider the following two cases:

**Case 1. Adjust the value of d**

Firstly, when the value of $d$ is very small, it is a double-periodic wave. As the parameter $d$ increases, the double-periodic wave energy converges. After that, the breather appears. The period, size and width of the breather increase with the increase of the value of $d$, and the amplitude of the double-periodic background increases, see Fig. 5. Finally, when $d = 1$, the energy, which is the interaction of the breather with the double-periodic wave, converges to form two rogue waves on the double-periodic background, see Fig. 4.

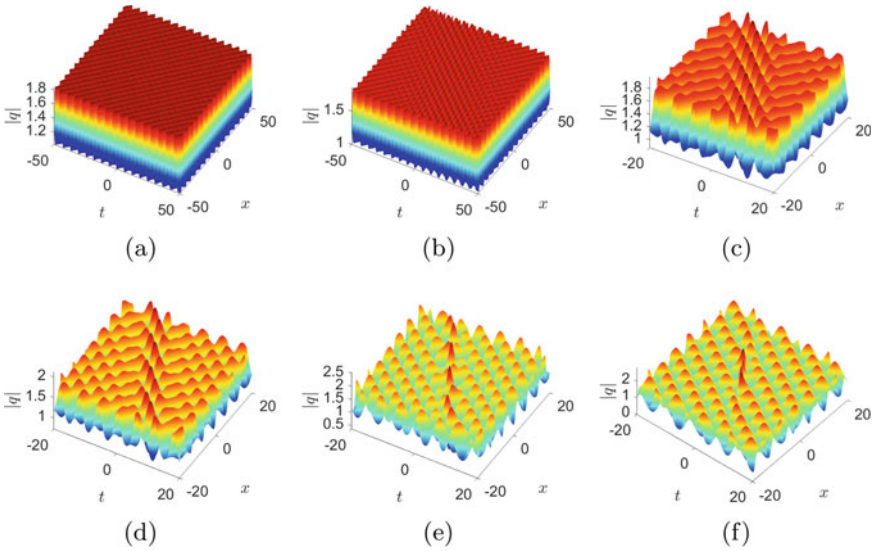


**Fig. 5** Solution for interaction among the double-periodic background, the breather and rogue waves with the parameters: $\omega = 1$, $\alpha_3 = 0$, $\beta_3 = \frac{1}{5}$, $\alpha_4 = 0$, $\beta_4 = \frac{1}{5}$, **a** $d = \frac{1}{1000}$; **b** $d = \frac{1}{50}$; **c** $d = \frac{1}{20}$; **d** $d = \frac{1}{10}$; **e** $d = \frac{1}{4}$; **f** $d = \frac{1}{2}$

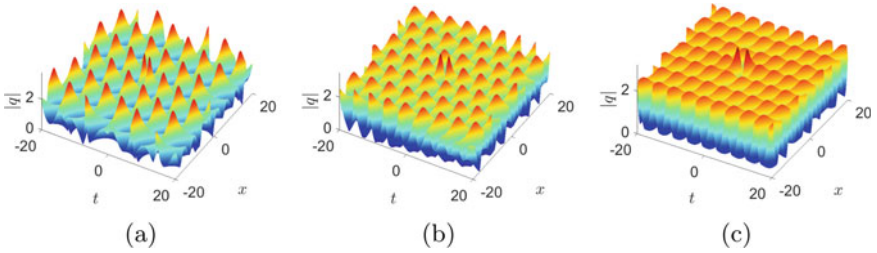


**Fig. 6** Two rogue waves on the double-periodic background by choosing: $\omega = 1$, $d = 1$, $\alpha_3 = 0$, $\alpha_4 = 0$, $\beta_4 = \frac{5}{7}$ **a** $\beta_3 = \frac{1}{2}$; **b** $\beta_3 = \frac{1}{4}$; **c** $\beta_3 = \frac{1}{10}$

**Case 2. Adjust the value of $\beta_3$**

When the value of $\beta_3$ decreases, two rogue waves interact with the double-periodic wave, simultaneous variation of amplitude of rogue wave and double-periodic wave, see Fig. 6.

## *3.3 Localized Waves on the Plane Wave Background*

For $n = 4$, $\lambda_1 = \frac{\sqrt{-d^2+2\omega}-id}{2}$, $\lambda_2 = -\lambda_1^*$, and $\lambda_3 = \alpha_3 + i\beta_3$, $\lambda_4 = -\lambda_3^*$. We can derive three types of second-order semi-rational solution by setting different spectral

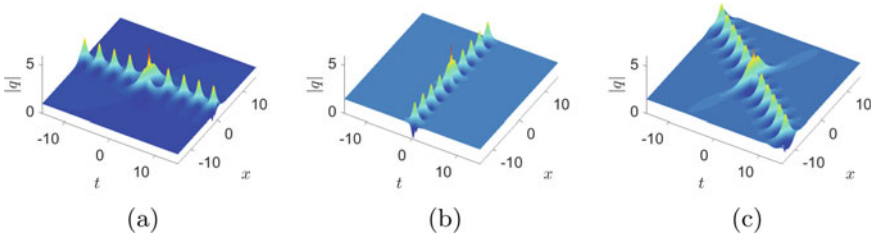


**Fig. 7** The semi-rational solutions by choosing: **a** $\omega = 1$, $d = 1$, $\lambda_1 = \frac{1}{2} - \frac{1}{2}i$, $\lambda_2 = -\frac{1}{2} - \frac{1}{2}i$, $\lambda_3 = \frac{3}{5} - \frac{3}{5}i$, $\lambda_4 = -\frac{3}{5} - \frac{3}{5}i$; **b** $\omega = 1$, $d = 1$, $\lambda_1 = \frac{3}{4} - \frac{3}{4}i$, $\lambda_2 = -\frac{3}{4} - \frac{3}{4}i$, $\lambda_3 = \frac{1}{2} - \frac{1}{2}i$, $\lambda_4 = -\frac{1}{2} - \frac{1}{2}i$; **c** $\omega = \frac{3}{2}$, $d = \frac{3}{2}$, $\lambda_1 = \frac{2}{5} - \frac{3}{4}i$, $\lambda_2 = -\frac{2}{5} - \frac{3}{4}i$, $\lambda_3 = \frac{1}{2} - \frac{3}{5}i$, $\lambda_4 = -\frac{1}{2} - \frac{3}{5}i$

parameter values in Fig. 7. Here, we should remark that, the recent paper [29] also reported the three types of second-order semi-rational solution and proposed that if Im $(\lambda_3) > 0$, one cannot derive the second-order rogue wave.

However, in our present work, one can find that the first-order rogue wave transforms to two rogue waves and a breather as the value of Im $(\lambda_3)$ increases. Firstly, when Im $(\lambda_3) = 0$, it is the first-order rogue wave. When Im $(\lambda_3) = \frac{1}{10}$, the periodic solution appears and the peak of rogue wave becomes smooth. With the increase of Im $(\lambda_3)$, the energy of periodic solution increases. When Im $(\lambda_3) = \frac{1}{5}$, there is a small amplitude of breather, and the rogue wave changes from single peak to double peak, but it is not completely separated. As the value of Im $(\lambda_3)$ increases from $\frac{3}{10}$ to $\frac{2}{5}$, the rogue wave gradually separates with the increase of the amplitude of the breather. Until Im $(\lambda_3) = 1/2$, the two peaks of the rogue wave are completely separated, generating two first-order rogue waves. At the same time, the period of the breather decreases and the amplitude increases. Obviously, Im $(\lambda_3)$ also affects the propagation direction of the breather, as shown in Fig. 8.

## 4 Conclusion

This paper presents the dynamic behavior of different types of solutions, including the first-order rogue wave on the periodic background, two rogue waves on the double-periodic background and the interaction solution between the second-order rogue wave and the breather for Eq. (1) in detail. In addition, we conclude that different parameters have different effects on the dynamic behavior of solutions. On the one hand, parameter $d$ affects the energy conversion of periodic waves. The periodic solution is generated by the energy convergence of periodic waves. With the increase of the value of $d$, the energy continues to gather, and the periodic solution is gradually transformed into the breather. The period and amplitude of breather increase with the value of $d$, and finally form the rogue wave. On the other hand, the interaction solution between the periodic wave and rogue waves is affected by the imaginary part

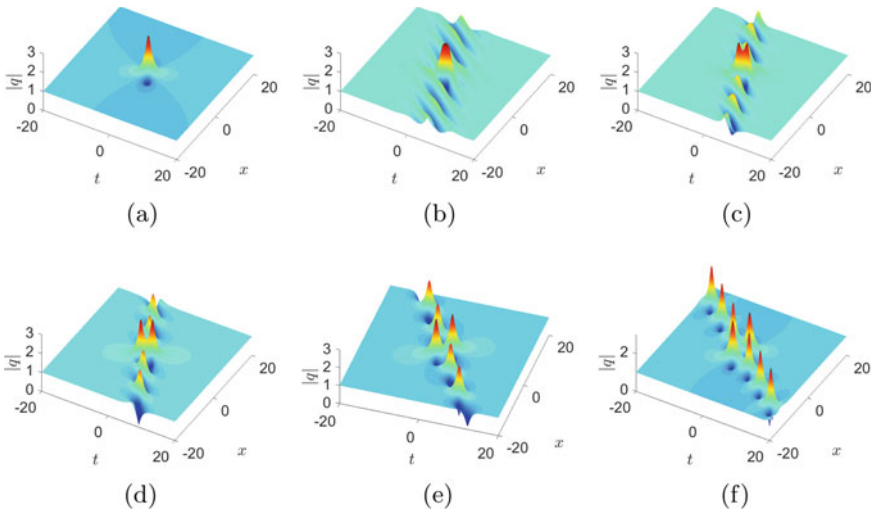


**Fig. 8** Solution for interaction between rogue waves and the breather by choosing: $\omega = 1$, $d = 1$, $\lambda_1 = \frac{1}{2} - \frac{1}{2}i$, $\lambda_2 = -\frac{1}{2} - \frac{1}{2}i$, **a** $\lambda_3 = \frac{3}{5}$, $\lambda_4 = -\frac{3}{5}$; **b** $\lambda_3 = \frac{3}{5} + \frac{1}{10}i$, $\lambda_4 = -\frac{3}{5} + \frac{1}{10}i$; **c** $\lambda_3 = \frac{3}{5} + \frac{1}{5}i$, $\lambda_4 = -\frac{3}{5} + \frac{1}{5}i$; **d** $\lambda_3 = \frac{3}{5} + \frac{3}{10}i$, $\lambda_4 = -\frac{3}{5} + \frac{3}{10}i$; **e** $\lambda_3 = \frac{3}{5} + \frac{2}{5}i$, $\lambda_4 = -\frac{3}{5} + \frac{2}{5}i$; **f** $\lambda_3 = \frac{3}{5} + \frac{1}{2}i$, $\lambda_4 = -\frac{3}{5} + \frac{1}{2}i$

of $\lambda$. Besides that, spectral parameters also affect the interaction solution between rogue waves and the breather. For instance, when $n = 4$, if the spectral parameters $\lambda_3$ and $\lambda_4$ satisfy the relation $\lambda_3 = -\lambda_3^*$ and $\lambda_4 = -\lambda_4^*$, two rogue waves are generated on the double-periodic background. If they satisfy $\lambda_4 = -\lambda_3^*$, the second-order rogue wave with the breather will be generated on the plane wave background. Particularly, if Im $(\lambda_3) > 0$, the first-order rogue wave will interact with the plane wave to form the breather, and the rogue wave will be separated into two rogue waves as the value of Im $(\lambda_3)$ increases. Meanwhile, it also changes the direction of breather propagation.

**Conflict of Interest** This work does not have any conflicts of interest.

**Acknowledgements** This work is supported by the National Natural Science Foundation of China (No.12271488 and No. 11371326).

## References

1. Bludov, Y. V., Konotop, V. V., Akhmediev, N.: Matter rogue waves. Phys. Rev. A. 80(3), 033610 (2009).
2. Shats, M., Punzmann, H., Xia, H.: Capillary rogue waves. Phys. Rev. Lett. 104(10), 104503 (2010).
3. Chabchoub, A., Hoffmann, N, P., Akhmediev, N.: Rogue wave observation in a water wave tank. Phys. Rev. Lett. 106(20), 204502 (2011).

4. Chabchoub, A., Hoffmann, N., Onorato, M., Akhmediev, N.: Super rogue waves: observation of a higher-order breather in water waves. Phys. Rev. X 2(1): 011015 (2012).
5. Chabchoub, A., Hoffmann, N., Onorato, M., Slunyaev, A., Sergeeva, A., Pelinovsky, E., Akhmediev, N.: Observation of a hierarchy of up to fifth-order rogue waves in a water tank. Phys. Rev. E 86(5), 056601 (2012).
6. Kedziora, D. J., Ankiewicz, A., Akhmediev, N.: Second-order nonlinear Schrödinger equation breather solutions in the degenerate and rogue wave limits. Phys. Rev. E 85(6), 066601 (2012).
7. Ma, Y. C.: The perturbed plane-wave solutions of the cubic Schrödinger equation. Stud. Appl. Math. 60(1), 43-58 (1979).
8. Akhmediev, N. N., Korneev, V. I.: Modulation instability and periodic solutions of the nonlinear Schrödinger equation. Theor. Math. Phys. 69(2), 1089-1093 (1986).
9. Peregrine, D. H.: Breaking waves on beaches. Annu. Rev. Fluid. Mech. 15(1), 149-178 (1983).
10. Akhmediev, N., Ankiewicz, A., Taki, M.: Waves that appear from nowhere and disappear without a trace. Phys. Lett. A 373(6), 675-678 (2009).
11. Akhmediev, N., Soto-Crespo, J. M., Ankiewicz, A.: Extreme waves that appear from nowhere: on the nature of rogue waves. Phys. Lett. A 373(25), 2137-2145 (2009).
12. Liu, JG., Osman, M.S., Zhu, WH. et al.: Different complex wave structures described by the Hirota equation with variable coefficients in inhomogeneous optical fibers. Appl. Phys. B 125, 175 (2019).
13. Liu, JG., Zhu, WH.: Multiple rogue wave, breather wave and interaction solutions of a generalized $(3 + 1)$-dimensional variable-coefficient nonlinear wave equation. Nonlinear Dyn 103, 1841–C1850 (2021).
14. Liu, JG., Zhu, WH., He, Y.: Variable-coefficient symbolic computation approach for finding multiple rogue wave solutions of nonlinear system with variable coefficients. Z. Angew. Math. Phys. 72, 154 (2021).
15. Du, Z., Tian, B., Chai, H. P., Zhao, X. H.: Dark-bright semi-rational solitons and breathers for a higher-order coupled nonlinear Schrödinger system in an optical fiber. Appl. Math. Lett. 102, 106110 (2020).
16. Li, B. Q., Ma, Y. L.: Extended generalized Darboux transformation to hybrid rogue wave and breather solutions for a nonlinear Schrödinger equation. Appl. Math. Comput. 386, 125469 (2020).
17. Liu, JG., Osman, M.S., Wazwaz, A.M.: A variety of nonautonomous complex wave solutions for the $(2 + 1)$-dimensional nonlinear Schrödinger equation with variable coefficients in nonlinear optical fibers. Optik 180, 917-923 (2019).
18. Zhu, WH., Liu, JG.: Bright and dark solitons for the fifth-order nonlinear Schrödinger equation with variable coefficients. Optik 276, 170618 (2023).
19. Zhu, WH., Raheel, M., Liu, JG.: Exploring the new optical solitons to the time-fractional integrable generalized $(2 + 1)$-dimensional nonlinear Schrödinger system via three different methods. Open Physics, 20(1), 859-874 (2022).
20. Tzoar, N., Jain, M.: Self-phase modulation in long-geometry optical waveguides. Phys. Rev. A 23(3), 1266 (1981).
21. Ruderman, M. S.: Propagation of solitons of the derivative nonlinear Schrödinger equation in a plasma with fluctuating density. Phys. Plasmas 9(7), 2940-2945 (2002).
22. MjØlhus, E.: On the modulational instability of hydromagnetic waves parallel to the magnetic field. J. Plasma Phys. 16(3), 321-334 (1976).
23. Xu, S., He, J., Wang, L.: The Darboux transformation of the derivative nonlinear Schrödinger equation. J. Phys. A-Math. Theor. 44(30), 305203 (2011).
24. Guo, B., Ling, L., Liu, Q. P.: High-order solutions and generalized Darboux transformations of derivative nonlinear Schrödinger equations. Stud. Appl. Math. 130(4), 317-344 (2013).
25. Xu, S., Wang, L., Erdlyi, R., He, J.: Degeneracy in bright-dark solitons of the derivative nonlinear Schrödinger equation. Appl. Math. Lett. 87, 64-72 (2019).
26. Xu, S., He, J., Mihalache, D.: Rogue waves generation through multiphase solutions degeneration for the derivative nonlinear Schrödinger equation. Nonlinear Dynam. 97(4), 2443-2452 (2019).

27. Chen, J., Pelinovsky, D. E.: Rogue waves on the background of periodic standing waves in the derivative nonlinear Schrödinger equation. Phy. Rev. E 103(6), 062206 (2021).
28. Zhang, Y., Guo, L., Xu, S., Wu, Z., He, J.: The hierarchy of higher order solutions of the derivative nonlinear Schrödinger equation. Commun. Nonlinear Sci. 19(6), 1706-1722 (2014).
29. Wang, L., Zhu, Y. J., Wang, Z. Z., Qi, F. H., Guo, R.: Higher-order semirational solutions and nonlinear wave interactions for a derivative nonlinear Schrödinger equation. Commun. Nonlinear Sci. 33, 218-228 (2016).
30. Xue, B., Shen, J., Geng, X.: Breathers and breather-rogue waves on a periodic background for the derivative nonlinear Schrödinger equation. Phy. Scripta 95(5), 055216 (2020).
31. Liu, W., Zhang, Y., He, J.: Rogue wave on a periodic background for Kaup-Newell equation. Rom. Rep. Phys. 70, 106 (2018).

# $l^p$ Solution to the Initial Value Problem of the Discrete Nonlinear Schrödinger Equation with Complex Potential


**Guoping Zhang and Ghder Aburamyah**

**Abstract** In this paper we study the time-dependent discrete nonlinear Schrödinger equation with complex, not necessarily bounded potential and sufficiently general nonlinearity on a multidimensional lattice with a weighted $l^p$ initial value. Under natural assumptions, we prove the global well-posedness in weighted $l^p$ spaces.

**Keywords** Discrete nonlinear Schrödinger equation · Semigroup · Initial value problem · Lipschitz continuous · Complex potential · $l^p$ solution

**2010 Mathematics Subject Classification** 37L60 · 35B41 · 35Q55

## 1 Introduction

The discrete nonlinear Schrödinger equation (DNLS) is a mathematical model that describes the dynamics of wave propagation in discrete systems, where the wave's behavior is governed by nonlinear effects. It is a discrete analog of the famous nonlinear Schrödinger equation, which describes the behavior of wave packets in continuous media.

The DNLS equation is commonly used to study various physical phenomena in a wide range of fields, including condensed matter physics, optics, and Bose-Einstein condensates. It arises in systems such as nonlinear optical waveguides, coupled oscillators, and discrete lattices.

In general the one-dimensional DNLS equation is written in the following form:

$$i\frac{d\psi_n}{dt} + \alpha\psi_n + \beta|\psi_n|^2\psi_n + \gamma(\psi_{n+1} + \psi_{n-1}) = 0,$$

G. Zhang (✉) · G. Aburamyah
Department of Mathematics, Morgan State University, Baltimore, MD 21251, USA
e-mail: guouping.zhang@morgan.edu

G. Aburamyah
e-mail: ghabu2@morgan.edu



S. Manukure and W.-X. Ma (eds.), *Nonlinear and Modern Mathematical Physics*,
Springer Proceedings in Mathematics & Statistics 459,
https://doi.org/10.1007/978-3-031-59539-4_15

where $\psi_n$ represents the complex-valued amplitude of the wave at site $n$, and $t$ is time. The coefficients $\alpha$, $\beta$, and $\gamma$ determine the properties of the system, such as the dispersion and nonlinearity. The first term on the left-hand side represents the temporal evolution of the wave, while the second term accounts for any linear potential acting on the system. The third term describes the nonlinear self-interaction of the wave, which depends on the amplitude squared $|\psi_n|^2$. The fourth term represents the coupling between neighboring sites, with $\psi_{n+1}$ and $\psi_{n-1}$ denoting the amplitudes at the adjacent sites.

Solutions of the DNLS equation can exhibit a wide range of interesting phenomena, including soliton formation, nonlinear wave propagation, and energy localization. These phenomena are a consequence of the interplay between the linear and nonlinear terms in the equation.

The DNLS equation is usually studied numerically due to its nonlinear nature. Various numerical techniques, such as finite difference methods, spectral methods, or split-step methods, are employed to simulate and analyze the dynamics of wave packets governed by the DNLS equation.

Understanding the properties and dynamics of the DNLS equation is crucial for gaining insights into the behavior of discrete wave systems and exploring nonlinear effects in different physical systems. For instance, we mention nonlinear wave transmission in discrete media, propagation of localized pulses in coupled waveguides and optical fibers, and modeling Bose-Einstein condensates (see, e.g., [6, 9, 10] and references therein).

Research activity in this area mainly focuses on the so-called "breathers," which are standing waves. The profile function of such a wave solves an appropriate stationary DNLS equation. Most works in this direction deal with (discrete) translation-invariant DNLS on a one-dimensional lattice and employ perturbation techniques, two-dimensional discrete-time dynamical systems, and numerical simulation (see, e.g., [4–6] and references therein).

On the other hand, the series of papers [2, 13–17, 20–24] applies the theory of critical points of smooth functionals to the study of breathers for DNLS with various types of nontrivial potentials. In this context, we also mention the remarkable paper [19].

In [25] we investigated the weighted $l^2$ solution of the following initial value problem for the time-dependent $d$-dimensional discrete nonlinear Schrödinger equation

$$i\dot{u} = -\Delta u + Wu - f(n,u) + b(t,n), \tag{1}$$

$$u(0,n) = u^0(n)\,, \tag{2}$$

where the potential $W = V + i\delta$ is a complex function of

$$n = (n_1, n_2, \ldots, n_d) \in \mathbb{Z}^d\,,$$

$\dot{u}$ stands for the time derivative and $-\Delta$ is the $d$-dimensional discrete Laplacian defined by

$$\begin{aligned}\Delta u(n) = {} & u(n_1 - 1, n_2, \ldots, n_m) + u(n_1, n_2 - 1, \ldots, n_d) + \cdots + u(n_1, n_2, \ldots, n_d - 1) \\ & - 2du(n_1, n_2, \ldots, n_d) \\ & + u(n_1 + 1, n_2, \ldots, n_d) + u(n_1, n_2 + 1, \ldots, n_d) + \cdots + u(n_1, n_2, \ldots, n_d + 1),\end{aligned}$$

Note that if $\delta(n)$ is negative for all $n \in \mathbb{Z}^d$, the part $\delta$ of the potential represents dissipation effects. Additionally, our Assumption $(iii)$ below allows the nonlinearity to contain a dissipative term. This DNLS (1) is the space discretization of the nonlinear Schrödinger equation in continuous media.

Only a few papers [7, 8, 11, 12] are devoted to equations of the form (1). The paper [12] focuses on the initial value problem for the DNLS with a zero potential and power nonlinearity on a one-dimensional lattice with weighted $l^2$ initial value. The main result provides global well-posedness in weighted $l^2$ spaces with power weights. In [7, 8], the authors consider the DNLS with $V = 0$ and $\delta = \text{const}$. The main results are global well-posedness in the conservative ($\delta = 0$) and dissipative ($\delta < 0$) cases, as well as the existence of attractors in weighted $l^2$ spaces in the conservative case, on one-dimensional and multidimensional lattices, respectively. In the paper [11], the well-posedness in weighted spaces is studied for the DNLS on a one-dimensional lattice in the case when $W = V$ is a general real potential and $b = 0$.

In [25], we extended those results to the multidimensional case, allowing a sufficiently general, not necessarily bounded potential $W$ with weighted $l^2$ initial value. In this paper, we will investigate the initial value problem for the DNLS with a weighted $l^p$ initial value.

To the best of our knowledge, no other mathematician has investigated the initial value problem for the DNLS with a weighted $l^p$ initial value. Since $l^p$ is no longer a Hilbert space like $l^2$ when $p \neq 2$, we cannot use the features of a Hilbert space to prove our main results on $l^p$ global solutions. Instead, we use the integral equation defining the mild solution of the DNLS in [25] to prove our major results on $l^p$ global solutions by leveraging the existing $l^2$ global solutions obtained in [25].

The organization of this paper is as follows: For readers' convenience, we provide a reminder of some preliminaries on the semigroup theory of abstract differential equations in Sect. 2. The local weighted $l^p$ well-posedness result is proved in Sect. 3. Section 4 is devoted to the existence of weighted $l^p$ global solutions.

## 2 Semigroup Theory and Abstract Initial Value Problem

We treat (1) as an abstract differential equation of the form

$$\dot{u} = Au + N(t, u) \tag{3}$$

in a complex Banach space. We always assume that $A$ is a closed operator in a Banach space $E$ with the domain $D(A)$, and $N : [0, \infty) \times E \to E$ is continuous. Let us provide a reminder of some elementary facts related to such equations.

A family $U(t),\ t \in [0, \infty)$, of bounded linear operators in $E$ is a strongly continuous *semigroup of operators* if

(1) $U(t)v$ is a continuous function on $[0, \infty)$ with values in $E$ for every $v \in E$;
(2) $U(0) = I$ is the identity operator in $E$;
(3) $U(t + s) = U(t)U(s)$ for all $t, s \in [0, \infty)$.

If the family $U(t)$ is defined for all $t \in \mathbb{R}$ and satisfies (1)–(3) above on the whole real line, we say that $U(t)$ is a strongly continuous *group of operators*.

If $U(t)$ is a strongly continuous semigroup of operators, then its *generator* $A$ is defined by

$$Av = \lim_{t \to 0^+} t^{-1}(U(t) - I)v, \tag{4}$$

where the domain $D(A)$ consists of those $v \in E$ for which the limit in (4) exists.

The following result is well known (see, e.g., [3, 18]).

**Proposition 2.1** *If $A$ is a generator of a strongly continuous semigroup in a Banach space $E$ and $B$ is a bounded linear operator in $E$, then $A + B$ is a generator of a strongly continuous semigroup.*

If $A$ is a bounded linear operator, then it generates a one-parameter group $e^{tA}$. In general, if $A$ is a generator of a strongly continuous semigroup, we still use the same exponential notation $e^{tA}$ for the semigroup generated by $A$.

Now we discuss the abstract initial value problem for Eq. (3), with initial data

$$u(0) = u^0 \in E. \tag{5}$$

If $A$ is a bounded operator, then it is sufficient to consider classical solutions, i.e. continuously differentiable functions with values in $E$ that satisfy (3) and (5). In general, when the operator $A$ is unbounded, we consider mild solutions to (3) and (5).

A continuous function $u$ on $[0, T]$ with values in $E$ is a *mild solution* of the initial value problem (3) and (5) if it satisfies the following integral equation

$$u(t) = e^{tA}u^0 + \int_0^t e^{(t-s)A}N(s, u(s))ds. \tag{6}$$

In the case when the operator $A$ is bounded, these are classical solutions.

We need the following well-known result (see. e.g., [1, 18]).

**Proposition 2.2** *Let $A$ be a generator of a strongly continuous semigroup in a Banach space $E$, and $N(t, u) : [0, \infty) \times E \to E$ be continuous in $t$ and locally Lipschitz continuous in $u$ with Lipschitz constant being bounded on bounded intervals of $t$. That is, for any $T > 0$ and $R > 0$, there exists $C = C(T, R) > 0$ such that*

$$\max_{0\le t\le T}\|N(t,w)-N(t,w')\|\le C\|w-w'\| \tag{7}$$

*whenever* $\|w\|\le R$ *and* $\|w'\|\le R$.

*(a) For every* $u^0\in E$, *there exists a unique local mild solution of the initial value problem (3) and (5) defined on the maximal interval* $[0,\tau_{max})$.

*(b) If* $\tau_{max}<\infty$, *then* $\lim_{t\nearrow\tau_{max}}\|u(t)\|=\infty$.

*(c) The solution* $u(t)$ *depends continuously on* $u^0$ *in the topology of uniform convergence on bounded closed subintervals of* $[0,\tau_{max})$.

*(d) Assume, in addition, that the map* $N:[0,\infty)\times E\to E$ *is locally Lipschitz continuous,* i.e., *for any* $T>0$ *and* $R>0$, *there exists* $C=C(T,R)>0$ *such that*

$$\|N(t,w)-N(t',w')\|\le C(|t-t'|+\|w-w'\|) \tag{8}$$

*whenever* $t\in[0,T]$, $t'\in[0,T]$, $\|w\|\le R$ *and* $\|w'\|\le R$. *If* $u^0\in D(A)$, *then the mild solution of the initial value problem (3) and (5) is a classical solution.*

**Remark 2.1** Assumption (7) implies automatically that $N$ is bounded on bounded sets.

**Remark 2.2** If $N(t,u)$ is globally Lipschitz continuous in $u$, i.e. there exists a constant $C=C(T)>0$ such that

$$\max_{0\le t\le T}\|N(t,w)-N(t,w')\|\le C\|w-w'\|,\quad \forall w,w'\in E, \tag{9}$$

then the initial value problem (3) and (5) possesses a unique global mild solution defined on $[0,\infty)$. Moreover, the solution $u(t)$ depends continuously on $u^0$ in the topology of uniform convergence on bounded closed subintervals of $[0,\infty)$.

**Remark 2.3** Let $N(t,u)$ be of the form

$$N(t,u)=N(u)+f(t)\,.$$

Then assumption (8) holds if and only if $N$ and $f$ are locally Lipschitz continuous on $E$ and $[0,\infty)$, respectively.

## 3 Local Solution to the Initial Value Problem of the DNLS Equation

In this section, we consider Eq. (1) under the following assumptions:

(i) The complex potential $W=V+i\delta$ is such that both $V$ and $\delta$ are real-valued functions on $\mathbb{Z}^d$, and

$$\overline{\delta}=\sup\{\delta(n)|n\in\mathbb{Z}^d\}<\infty\,.$$

(ii) The nonlinearity $f : \mathbb{Z}^d \times \mathbb{C} \to \mathbb{C}$ satisfies the following conditions:

(1) $f(n, 0) = 0$,
(2) $f(n, z) = o(z)$ as $z \to 0$ uniformly with respect to $n \in \mathbb{Z}^d$,
(3) $f$ is uniformly locally Lipschitz continuous, that is, for every $R > 0$, there exists a constant $C = C(R)$ independent of $n \in \mathbb{Z}^d$ such that

$$|f(n, z) - f(n, z')| \le C|z - z'|$$

for all $n \in \mathbb{Z}^d$ whenever $|z| \le R$ and $|z'| \le R$.

(iii) The nonlinearity $f(n, z)$ is of the form $f(n, z) = g(n, |z|)z$, where $g(n, r)$ is a function and its imaginary part is nonnegative. Examples of nonlinearities that satisfy Assumptions $(ii)$ and $(iii)$ are as follows.

- Power nonlinearity

$$f(n, z) = \gamma_n |z|^{p-1} z, \quad p > 1,$$

- Saturable nonlinearities such as

$$f(n, z) = \gamma_n \frac{|z|^{p-1} z}{1 + |z|^{p-1}}, \quad p > 1,$$

and

$$f(n, z) = \gamma_n (1 - e^{(-a_n |z|^2)}) z, \quad a_n > 0,$$

where $\mathrm{Im}\gamma_n \ge 0$ for all $n \in \mathbb{Z}^d$.
We are interested in finding solutions to Eq. (1) in weighted $l^p$-spaces. Let $\Theta = (\theta_n)_{n \in \mathbb{Z}^d}$ be a sequence of positive numbers (weights). The space $l^p_\Theta(\mathbb{Z}^d)$ consists of all two-sided sequences of complex numbers such that the norm

$$\|u\|_{l^p_\Theta} = \Big(\sum_{n \in \mathbb{Z}^d} |u(n)\theta_n|^p\Big)^{1/p}$$

is finite. We notice that $u \in l^p_\Theta(\mathbb{Z}^d)$ if and only if $u\Theta \in l^p(\mathbb{Z}^d)$ and

$$\|u\|_{l^p_\Theta} = \|u\Theta\|_{l^p}.$$

Therefore for $1 \le p < q \le \infty$ we have

$$\|u\|_{l^q_\Theta} \le \|u\|_{l^p_\Theta}$$

and

$$l^p_\Theta(\mathbb{Z}^d) \subset l^q_\Theta(\mathbb{Z}^d).$$

**Remark**: The weighted $l^2$ space with weight sequence $\Theta$ in [25] is the same as the space $l^2_{\Theta^{1/2}}(\mathbb{Z}^d)$ defined above with the same weight sequence $\Theta$.

We always assume that the weight $\Theta$ is *regular* in the sense that:

(iv) The sequence $\Theta$ is bounded below by a positive constant, and there exists a constant $c_0 \geq 1$ such that

$$c_0^{-1} \leq \frac{\theta_{n+e_i}}{\theta_n} \leq c_0$$

for all $n \in \mathbb{Z}^d$ and $i = 1, \ldots, d$, where $e_i \in \mathbb{Z}^d$ has 1 at the $i$-th component and 0 elsewhere.

From Assumption $(iv)$, we obtain

$$\|u\|_{l^p(\mathbb{Z}^d)} \leq C_0 \|u\|_\Theta, \tag{10}$$

which implies that $l^p_\Theta(\mathbb{Z}^d)$ is densely and continuously embedded into $l^p(\mathbb{Z}^d)$. Setting $\Theta_0$ as the constant weight with unit components, we have that

$$l^p_{\Theta_0}(\mathbb{Z}^d) = l^p(\mathbb{Z}^d)$$

From the perspective of functional analysis, Assumption $(iv)$ means that the space $l^p_\Theta(\mathbb{Z}^d)$ is translation invariant. More precisely, let $S_i$ and $T_i$ be the operators defined by

$$(S_i w)(n) = w(n - e_i), \qquad (T_i w)(n) = w(n + e_i), \quad i = 1, \cdots, d.$$

Indeed, Assumption $(iv)$ holds if and only if for all $i = 1, \ldots, d$, both $S_i$ and $T_i$ are linear bounded operators in $l^p_\Theta(\mathbb{Z}^d)$. It's worth noting that $S_i$ and $T_i$ are mutually inverse operators. However, the translation invariance of the space $l^p_\Theta(\mathbb{Z}^d)$ doesn't imply that the norm $\|\cdot\|_\Theta$ is translation invariant.

The most important examples of regular weights satisfying Assumption $(iv)$ are

- Power weight:
$$\theta_n = (1 + |n|)^\lambda, \quad \lambda > 0;$$

- Exponential weight:
$$\theta_n = e^{\alpha|n|}, \quad \alpha > 0.$$

More generally, the weight $\theta_n = e^{\alpha|n|^\beta}$, $\alpha > 0$ satisfies Assumption $(iv)$ if and only if $0 < \beta \leq 1$.

To understand the Eq. (1) in the framework of evolution equations, we can interpret it as an evolution equation of the form (3), where $A = -iH$ and $H$ is the Schrödinger operator defined as

$$H = -\Delta + W \tag{11}$$

and the operator $N$ is given by

$$N(t,u)(n) = i\ f(n,u(t,n)) - i\ b(t,n). \tag{12}$$

To establish a precise interpretation, we need to analyze certain properties of the Schrödinger operator $H$ in the space $l^p_\Theta(\mathbb{Z}^d)$. First, we observe that the operator (of multiplication by) $-iW = -iV + \delta$ is a diagonal operator. Since $V$ is real and $\delta(n) \le \overline{\delta}$ for all $n \in \mathbb{Z}^d$, the operator $-iW$ generates a strongly continuous semigroup in $l^p_\Theta(\mathbb{Z}^d)$ given by

$$(e^{-itW}u)(n) = e^{-iV(n)t}e^{\delta(n)t}u(n), \quad n \in \mathbb{Z}^d\,.$$

The domain of this operator in $l^p_\Theta(\mathbb{Z}^d)$ is defined as

$$D_\Theta = \{u \in l^p_\Theta(\mathbb{Z}^d) :\ Wu \in l^p_\Theta(\mathbb{Z}^d)\}. \tag{13}$$

where we use the notation $D$ to represent the domain of the operator $W$ in $l^p(\mathbb{Z}^d)$. It is clear that $D_\Theta \subset D$.

Next, we consider the discrete Laplacian operator $-\Delta$, which is a bounded operator in $l^p_\Theta(\mathbb{Z}^d)$. The Laplacian can be represented as

$$-\Delta = -\sum_{i=1}^{d} \nabla_i^- \nabla_i^+ = -\sum_{i=1}^{d} \nabla_i^+ \nabla_i^- = \sum_{i=1}^{d} (\nabla_i^- - \nabla_i^+),$$

where

$$\nabla_i^- u(n) = u(n) - S_i u(n), \quad \nabla_i^+ u(n) = T_i u(n) - u(n)\,, \quad i = 1, \ldots, d\,,$$

and $S_i$ and $T_i$ are the shift operators defined previously.

By Assumption $(iv)$, we can establish the boundedness of the shift operators $S_i$ and $T_i$ in $l^p_\Theta(\mathbb{Z}^d)$.

$$\|S_i u\|_{l^p_\Theta} = (\sum_{n\in\mathbb{Z}^d} |u(n-e_i)\theta_n|^p)^{1/p} = (\sum_{n\in\mathbb{Z}^d} |u(n)|^p \theta^p_{n+e_i})^{1/p} \le c_0 \|u\|_{l^p_\Theta},$$

and

$$\|T_i u\|_{l^p_\Theta} = (\sum_{n\in\mathbb{Z}^d} |u(n+e_i)\theta_n|^p)^{1/p} = (\sum_{n\in\mathbb{Z}^d} |u(n)|^p \theta^p_{n-e_i})^{1/p} \le c_0 \|u\|_{l^p_\Theta},$$

which imply

$$\|\nabla_i^+ u\|_{l^p_\Theta} \le (c_0+1)\|u\|_{l^p_\Theta}, \quad \|\nabla_i^- u\|_{l^p_\Theta} \le (c_0+1)\|u\|_{l^p_\Theta}.$$

Thus, both $\nabla_i^+$ and $\nabla_i^-$ are bounded operators in $l^p_\Theta(\mathbb{Z}^d)$, hence so is $-\Delta$. Therefore, we have the inequality:

$$\| - \Delta u\|_{l^p_\Theta} \leq 2d(c_0 + 1)\|u\|_{l^p_\Theta}. \tag{14}$$

Based on Proposition 2.1, we can derive the following lemma.

**Lemma 3.1** *The operator $A = -iH$ is a generator of strongly continuous group $e^{tA}$ in the space $l^p_\Theta(\mathbb{Z}^d)$. Moreover, there exist two constants $M \geq 1$ and $\omega$ such that for all $t \geq 0$*

$$\|e^{tA}\| \leq Me^{\omega t}. \tag{15}$$

This lemma establishes the generator property of $A$ and provides an estimate on the growth of the group $e^{tA}$ in the space $l^p_\Theta(\mathbb{Z}^d)$.

We define the operator $N(t, u)$ as follows

$$N(t, u)(n) = if(n, u(n)) - ib(t, n).$$

Then the Eq. (1) can be expressed in the form of Eq. (3). Our well-posedness result is the following.

**Theorem 3.1** *(1) Under Assumptions $(i)$, $(ii)$ and $(iv)$, if $b \in C([0, \infty), l^p_\Theta(\mathbb{Z}^d))$, then for every $u^0 \in l^p_\Theta(\mathbb{Z}^d)$, problem (1) and (2) has a unique local mild solution $u \in C([0, T], l^p_\Theta(\mathbb{Z}^d))$ for some $T > 0$.*

*(2) The mild solution $u(t) \in C([0, T], l^p_\Theta(\mathbb{Z}^d))$ of problem (1) and (2) obtained in part (1) is a classical solution if one of the following conditions holds*

*$(a)$ $u^0 \in l^p_\Theta(\mathbb{Z}^d)$ and $W$ is bounded;*

*$(b)$ $u^0 \in D(A) = D_\Theta$ and $b : [0, \infty) \to l^p_\Theta(\mathbb{Z}^d)$ is locally Lipschitz continuous.*

The basic property of the operator $N$ is given in the following lemma.

**Lemma 3.2** *Assume that assumptions (i), (ii) and (iv) are satisfied and $b \in C([0, \infty), l^p_\Theta(\mathbb{Z}^d))$. Then the operator $N(t, u) : [0, \infty) \times l^p_\Theta(\mathbb{Z}^d)) \to l^p_\Theta(\mathbb{Z}^d))$ is continuous in $t$ and locally Lipschitz continuous in $u$ with Lipschitz constant being independent of $t$. Moreover, if the nonlinearity $f(n, z)$ is uniformly globally Lipschitz continuous, i.e. there is a constant $C > 0$, independent of $n$, such that*

$$|f(n, z) - f(n, z')| \leq C|z - z'|, \quad \forall z, z' \in \mathbb{C}, \tag{16}$$

*then for all $t \geq 0$*

$$\|N(t, w) - N(t, w')\|_{l^p_\Theta} \leq C\|w - w'\|_{l^p_\Theta}, \quad \forall w, w' \in l^p_\Theta(\mathbb{Z}^d).$$

***Proof*** Suppose that $\|w\|_{l^p_\Theta} \leq R$ and $\|w'\|_{l^p_\Theta} \leq R$. Due to the continuous embedding $l^p_\Theta(\mathbb{Z}^d) \subset l^p(\mathbb{Z}^d)$, we see that $\|w\|_{l^p(\mathbb{Z}^d)} \leq R'$ and $\|w'\|_{l^p(\mathbb{Z}^d)} \leq R'$, with some $R' > 0$. By the property of $l^p(\mathbb{Z}^d)$ we have

$$\|w\|_{l^\infty(\mathbb{Z}^d)} \leq \|w\|_{l^p(\mathbb{Z}^d)}, \tag{17}$$

which implies $\|w\|_{l^\infty(\mathbb{Z}^d)} \le R'$ and $\|w'\|_{l^\infty(\mathbb{Z}^d)} \le R'$. Now assumptions (i) and (ii) imply that for all $t \ge 0$

$$\begin{aligned}\|N(t,w) - N(t,w')\|_{l^p_\Theta}^p &= \sum_{n\in\mathbb{Z}^d} |f(n,w(n)) - f(n,w'(n))|^p \theta_n^p \\ &\le C(R') \sum_{n\in\mathbb{Z}^d} |w(n) - w'(n)|^p \theta_n^p = C(R')\|w - w'\|_{l^p_\Theta}^p.\end{aligned}$$

The second statement of the lemma is trivial. □

**Remark 3.1** It is easily seen that any mild solution of (1) in $l^p_\Theta(\mathbb{Z}^d)$ is a mild solution in $l^p(\mathbb{Z}^d)$.

**Proof of Theorem** 3.1. (1) The existence of a unique local mild solution in $C([0,T], l^p_\Theta(\mathbb{Z}^d))$ for some $T > 0$ just follows from Lemmas 3.1 and 3.2 and Proposition 2.2.

(2) If $W$ is bounded, then the generator $A$ is bounded in $l^p_\Theta(\mathbb{Z}^d)$ which implies that each mild solution is actually a classical solution.

Part $(b)$ follows from Proposition 2.2 $(d)$ and Remark 2.3.

## 4 Existence of Global Solutions

To investigate the existence of global $l^p$ solutions, we consider two cases: $1 \le p < 2$ and $2 < p < \infty$.

### *4.1 Case 1:* $1 \le p < 2$

In this case, since we have the inclusion $l^p_\Theta(\mathbb{Z}^d) \subset l^2_\Theta(\mathbb{Z}^d)$, we can establish the existence of a global $l^2$ solution by applying Theorem 3.1 in [25]. Utilizing this result, we can prove the following theorem.

**Theorem 4.1** *(1) Under assumptions* $(i)$, $(ii)$, $(iii)$, *and* $(iv)$, *if* $\overline{\delta} \le 0$ *and* $b \in C([0,\infty), l^p_\Theta(\mathbb{Z}^d)) \bigcap L^1([0,\infty), l^2(\mathbb{Z}^d))$, *then for every* $u^0 \in l^p_\Theta(\mathbb{Z}^d)$, *problem (1) and (2) has a unique global mild solution* $u \in C([0,\infty), l^p_\Theta(\mathbb{Z}^d))$ *which continuously depends on* $u^0$ *in the topology of uniform convergence on bounded closed subintervals of* $[0,\infty)$. *Moreover, for any* $t \ge 0$

$$\|u(t)\|_{l^p_\Theta} \le (\|u^0\|_{l^p_\Theta} + B(\omega + CM, t))e^{(\omega+CM)t}, \tag{18}$$

*where*

$$B(\omega + CM, t) = \int_0^t e^{-(\omega+CM)s} \|b(s)\|_{l^p_\Theta} \, ds,$$

*C is the Lipschitz contant independent of t, $\omega$ and M are the constants in Lemma 3.1.*

(2) *The global mild solution $u(t) \in C([0, \infty), l^p_\Theta(\mathbb{Z}^d))$ of problem (1) and (2) obtained in* (1) *is a classical solution if one of the following conditions holds*
(a) $u^0 \in l^p_\Theta(\mathbb{Z}^d)$ *and W is bounded;*
(b) $u^0 \in D(A) = D_\Theta$ *and* $b : [0, \infty) \to l^p_\Theta(\mathbb{Z}^d)$ *is locally Lipschitz continuous.*

In order to prove Theorem 4.1 we need the following lemmas.

**Lemma 4.1** *Assume that assumptions (i), (ii) and (iii) are satisfied and $b \in C([0, \infty), l^2(\mathbb{Z}^d))$. If $u^0 \in l^2(\mathbb{Z}^d))$, then by Theorem 3.1 in [25], the global solution $u(t) \in C([0, \infty), l^2(\mathbb{Z}^d))$ satisfies*

$$\|u(t)\|_{l^2} \le \|u^0\|_{l^2} + B(t))e^{\bar{\delta}t} \tag{19}$$

*where*

$$B(t) = \int_0^t e^{-\bar{\delta}s} \|b(s)\|_{l^2} ds.$$

*Furthermore if $\bar{\delta} \le 0$ and $b \in L^1([0, \infty), l^2(\mathbb{Z}^d))$, then*

$$\|u(t)\|_{l^2} \le \|u^0\|_{l^2} + \overline{b} \equiv R \tag{20}$$

*where*

$$\overline{b} = \int_0^\infty \|b(s)\|_{l^2} ds.$$

***Proof*** Firstly we consider $u^0 \in D(A)$, by Theorem 3.1 in [25] $u(t)$ is a classical solution and satisfies

$$\begin{aligned} &i\dot{u}(t) = (-\Delta + W)u(t) - f(n, u(t)) + b(t, n) \\ &\dot{u}(t) = -i(-\Delta + W)u + if(n, u) - ib \\ &(\dot{u}(t), u(t)) = (-i(-\Delta + W))u, u) + (if(n, u), u) - (ib, u) \end{aligned}$$

$W = V + i\delta$, $-\Delta + V$ is self-adjoint on $l^2$, therefore $((-\Delta + V)u, u)$ is real

$$\begin{aligned} &RHS = -i((-\Delta + V)u, u) + (\delta u, u) + i(Re(g)u, u) - (Im(g)u, u) - i(b, u) \\ &Re(RHS) = (\delta u, u) - (Im(g)u, u) + Im(b, u) \end{aligned}$$

By assumption (i) and (iii) we obtain

$$\frac{1}{2}\frac{d}{dt}\|u(t)\|_{l^2}^2 \leq \bar{\delta}\|u(t)\|_{l^2}^2 + \|b(t)\|_{l^2}\|u(t)\|_{l^2}$$

Since $u(t)$ is a classical solution, by chain rule we have

$$\|u(t)\|_{l^2}\frac{d}{dt}\|u(t)\|_{l^2} \leq \bar{\delta}\|u(t)\|_{l^2}^2 + \|b(t)\|_{l^2}\|u(t)\|_{l^2}$$

We set

$$w(t) = \|u(t)\|_{l^2}$$

then we have

$$\frac{dw}{dt} \leq \bar{\delta}w + \|b(t)\|_{l^2}$$

By Gronwall's inequality, we obtain

$$\|u(t)\|_{l^2} \leq (\|u^0\|_{l^2} + B(t))e^{\bar{\delta}t}$$

$$B(t) = \int_0^t e^{-\bar{\delta}s}\|b(s)\|_{l^2}ds$$

If $b \in L^1([0,\infty), l^2(\mathbb{Z}^d))$, we denote

$$\bar{b} = \int_0^\infty \|b(s)\|_{l^2}ds \ < \ \infty$$

$$\|u(t)\|_{l^2} \leq \|u^0\|_{l^2} + \bar{b} \equiv R.$$

For $u^0 \in l^2$, we can choose a sequence $\{u^0_{(k)}\} \in D(A)$ which converges to $u^0$ in $l^2$. We have

$$\|u_{(k)}(t)\|_{l^2} \leq (\|u^0_{(k)}\|_{l^2} + B(t))e^{\bar{\delta}t}$$

□

Let $k \to \infty$ we obtain the estimate (19).
From the assumption (ii) we can define the optimal Lipschitz constant

$$C(r) = \sup_n \sup_{|z-z'|\leq r} \frac{|f(n,z) - f(n,z')|}{|z - z'|}.$$

Notice that $C(r)$ is a nondecreasing function of $r$ and $f(n,0)=0$ implies for any $n\in\mathbb{Z}^d$ and $|z|\le r$

$$|f(n,z)|\le C(r)|z|.$$

**Lemma 4.2** *Assume that assumptions (i), (ii), (iii) and (iv) are satisfied and* $b\in C([0,\infty),l^p_\Theta(\mathbb{Z}^d))\bigcap L^1([0,\infty),l^2(\mathbb{Z}^d))$. *If* $\overline{\delta}\le 0$, *then for any* $u^0\in l^p_\Theta(\mathbb{Z}^d)\subset l^2(\mathbb{Z}^d)$, *the global* $l^2$ *solution satisfies the following estimate: for all* $t\ge 0$

$$\|N(t,u(t))\|_{l^p_\Theta}\le C(R)\|u(t)\|_{l^p_\Theta}+\|b(t)\|_{l^p_\Theta}.$$

***Proof*** $N(t,u(t,n))=if(n,u(t,n))-ib(t,n)$. By Lemma 4.1

$$|u(t,n)|\le\|u(t)\|_{l^\infty}\le\|u(t)\|_{l^2}\le R,\quad\forall t,n.$$

which implies that

$$|f(n,u(t,n))|\le C(R)|u(t,n)|$$

and

$$\|f(n,u(t,n)\|_{l^p_\Theta}\le C(R)\|u(t)\|_{l^p_\Theta}.$$

Therefore we have

$$\|N(t,u(t))\|_{l^p_\Theta}\le C(R)\|u(t)\|_{l^p_\Theta}+\|b(t)\|_{l^p_\Theta}.$$

□

**Proof of Theorem** 4.1. (1) We define

$$B(\omega,t)=\int_0^t e^{-\omega s}\ \|b(s)\|_{l^p_\Theta}\,ds$$

From the integral equation (6) and using Lemma 3.1 we obtain

$$\|u(t)\|_{l^p_\Theta}\le Me^{\omega t}\|u^0\|_{l^p_\Theta}+M\int_0^t e^{\omega(t-s)}\|N(s,u)\|_{l^p_\Theta}ds$$

Then by Lemma 4.2 we have

$$\|N(s,u(s))\|_{l^p_\Theta}\le C(R)\|u(s)\|_{l^p_\Theta}+\|b(s)\|_{l^p_\Theta}.$$

We denote $C$ as $C(R)$ in the following calculations.

$$e^{-\omega t}\|u(t)\|_{l^p_\Theta}\le M\|u^0\|_{l^p_\Theta}+M\int_0^t e^{-\omega s}\|b(s)\|_{l^p_\Theta}\,ds+CM\int_0^t e^{-\omega s}\|u(s)\|_{l^p_\Theta}\,ds$$

We set

$$w(t) = e^{-\omega t} \|u(t)\|_{l^p_\Theta},$$

then

$$w(t) \le M\ (\|u^0\|_{l^p_\Theta} + B(\omega, t))\ + CM \int_0^t w(s)ds$$

By Gronwall's inequality, we obtain

$$\begin{aligned} w(t) &\le M\big(\|u^0\|_{l^p_\Theta} + B(\omega,t)\big) + CM^2 \int_o^t e^{CM(t-s)}(\|u^0\|_{l^p_\Theta} + B(\omega,s))ds \\ &= M\big(\|u^0\|_{l^p_\Theta} + B(\omega,t)\big) + CM^2\|u^0\|_{l^p_\Theta} \frac{e^{CM(t-s)}}{-CM}\Big|_0^t + CM^2 e^{CMt} \int_0^t e^{-CMs} B(\omega,s)ds \\ &= M\big(\|u^0\|_{l^p_\Theta} + B(\omega,t)\big) + M\ \|u^0\|_{l^p_\Theta}\ (e^{CMt} - 1) + CM^2 e^{CMt} \int_0^t e^{-CMs} B(\omega,s)ds \\ &= M\big(e^{CMt}\|u^0\|_{l^p_\Theta} + B(\omega,t)\big) + CM^2 e^{CMt} \int_0^t e^{-CMs} B(\omega,s)ds \end{aligned}$$

$$\begin{aligned} \int_0^t e^{-CMs}\ B(\omega,s)\ ds\ &=\ \int_0^t e^{-CMs} \int_0^s e^{-\omega\tau}\ \|\ b(\tau)\ \|_{l^p_\Theta}\ d\tau\ ds \\ &= \int_0^t e^{-\omega\tau}\ \|\ b(\tau)\ \|_{l^p_\Theta} \int_\tau^t e^{-CMs}\ ds \\ &= \frac{1}{CM} \int_0^t \|b(\tau)\|_{l^p_\Theta}\ e^{-\omega\tau}\ (\ e^{-CM\tau}\ -\ e^{-CMt}\ )\ d\tau \\ &= \frac{1}{CM}\ [\ \int_0^t\ e^{-(\omega+CM)\tau}\ \|b(\tau)\|_{l^p_\Theta}\ -\ e^{-CMt} \int_0^t\ e^{-\omega t}\ \|b(\tau)\|_{l^p_\Theta}\ d\tau\ ] \\ &= \frac{1}{CM}[B(\omega + CM, t)\ -\ e^{-CMt}\ B(\omega,t)\ ] \end{aligned}$$

$$\begin{aligned} e^{-\omega t}\ \|u(t)\|_{l^p_\Theta}\ &=\ w(t)\ \le\ Me^{CMt}\ [\ \|u^0\|_{l^p_\Theta}\ +\ B(\omega + CM, t)] \\ \|u(t)\|_{l^p_\Theta}\ &\le\ M\ e^{(\omega+CM)t}\ [\ \|u^0\|_{l^p_\Theta}\ + B(\omega + CM, t)\ ] \end{aligned}$$

Therefore we proved the estimate (22) from which we can conclude the existence of global weighted $l^p$ solution by a standard argument by contradiction.

(2) If $W$ is bounded, then the generator $A$ is bounded in $l^p_\Theta(\mathbb{Z}^d)$ which implies that each mild solution is actually a classical solution.

Part $(b)$ follows from Proposition 2.2 $(d)$ and Remark 2.3.

**Remark 4.1** When we take $\Theta = \Theta_0$ we obtain the regular global $l^p$ solution $u$ and moreover we have

$$u \in C([0,\infty), l^p(\mathbb{Z}^d)) \bigcap L^\infty([0,\infty), l^2(\mathbb{Z}^d))$$

## 4.2 Case 2: $2 < p < \infty$

In this case, the relationship $l^p_\Theta(\mathbb{Z}^d) \subset l^2_\Theta(\mathbb{Z}^d)$ fails, and we cannot obtain a global $l^2$ solution using Theorem 3.1 in [25]. However, for some special weight functions such as power weights and exponential weights, we can still prove the existence of global weighted $l^p$ solutions.

The following lemma supports our additional assumption on weight functions in the theorem.

**Lemma 4.3** (1) *The power weight* $\Psi^\lambda = \{(1+|n|)^\lambda : n \in \mathbb{Z}^d\}$ *is regular if and only if* $\lambda \geq 0$, *and* $\Psi^{-\lambda} \in l^q$ *if and only if* $\lambda q > d$.

(2) *The exponential weight* $\Phi^\alpha = \{e^{\alpha|n|} : n \in \mathbb{Z}^d\}$ *is regular if and only if* $\alpha \geq 0$, *and* $\Phi^{-\alpha} \in l^q$ *for any* $1 \leq q \leq \infty$ *if* $\alpha > 0$.

**Theorem 4.2** *(1) Under assumptions* $(i)$, $(ii)$, $(iii)$, *and* $(iv)$, *if* $\overline{\delta} \leq 0$, $b \in C([0,\infty), l^p_\Theta(\mathbb{Z}^d)) \bigcap L^1([0,\infty), l^2(\mathbb{Z}^d))$, *and in addition*

$$\Theta^{-1} \in l^q, \quad q = 2 + \frac{4}{p-2}, \tag{21}$$

*then for every* $u^0 \in l^p_\Theta(\mathbb{Z}^d)$, *problem (1) and (2) has a unique global mild solution* $u \in C([0,\infty), l^p_\Theta(\mathbb{Z}^d))$ *which continuously depends on* $u^0$ *in the topology of uniform convergence on bounded closed subintervals of* $[0,\infty)$. *Moreover, for any* $t \geq 0$

$$\|u(t)\|_{l^p_\Theta} \leq (\|u^0\|_{l^p_\Theta} + B(\omega + CM, t))e^{(\omega+CM)t}, \tag{22}$$

*where*

$$B(\omega + CM, t) = \int_0^t e^{-(\omega+CM)s} \|b(s)\|_{l^p_\Theta}\, ds,$$

*C is the Lipschitz contant independent of* $t$, $\omega$ *and* $M$ *are the constants in Lemma 3.1.*

(2) *The global mild solution* $u(t) \in C([0,\infty), l^p_\Theta(\mathbb{Z}^d))$ *of problem (1) and (2) obtained in* (1) *is a classical solution if one of the following conditions holds*
*(a)* $u^0 \in l^p_\Theta(\mathbb{Z}^d)$ *and* $W$ *is bounded;*
*(b)* $u^0 \in D(A) = D_\Theta$ *and* $b : [0,\infty) \to l^p_\Theta(\mathbb{Z}^d)$ *is locally Lipschitz continuous.*

***Proof*** Combining the condition (21) and Hölder inequality we obtain

$$\begin{aligned} \|u^0\|_{l^2} &\leq \|u^0\Theta\|_{l^p} \|\Theta^{-1}\|_{l^q}, \quad q = 2 + \frac{4}{p-2} \\ &= \|u_0\|_{l^p_\Theta} \|\Theta^{-1}\|_{l^q} < \infty \end{aligned}$$

which implies $u^0 \in l^2$ and Lemmas 4.1 and 4.2 hold. □

By a similar argument as in the proof of Theorem 4.1 we can prove Theorem 4.2.

**Remark 4.2** (1) When we take $\Theta = \Psi^\lambda$, by Lemma 4.3 the condition (21) becomes

$$\lambda > d(\frac{1}{2} - \frac{1}{p}).$$

(2) When we take $\Theta = \Phi^\alpha$, by Lemma 4.3 the condition (21) is automatically true if $\alpha > 0$ and no additional assumption is needed.
(3) We cannot obtain the regular global $l^p$ solution as a special case of Theorem 4.2.

## References


1. T. Cazenave and A. Haraux *An Introduction to Semilinear Evolution Equations*, Translation © Oxford University Press, 1998.
2. M. Cheng and A. Pankov, *Gap solitons in periodic nonlinear Schrödinger equations with nonlinear hopping*, Electr. J. Differential Equat., 287 (2016), 1–14.
3. K.-J. Engel and R. Nagel, *A Short Course on Operator Semigroups*, Springer, New York, 2006.
4. S. Flach and A. V. Gorbach, *Discrete breathers—advances in theory and applications*, Phys. Repts, 467 (2008), 1–116.
5. S. Flach and C. R. Willis, *Discrete breathers*, Phys. Repts, 295 (1998), 181–264.
6. D. Hennig and G. P. Tsironis, *Wave transmission in nonlinear lattices*, Physics Repts, 309 (1999), 333–432.
7. N. I. Karachalios and A. N. Yannacopoulos, *Global existence and compact attractors for the discrete nonlinear Schrödinger equations*, J. Differential Equat., 217 (2005), 88–123.
8. N. I. Karachalios and A. N. Yannacopoulos, *The existence of global attractor for the discrete nonlinear Schrödinger equation.II. Compactness without tail estimates in* $\mathbb{Z}^N$, $N \geq 1$, *lattices*, Proc. Roy. Soc. Edinburgh, 137A (2007), 63–76.
9. P. G. Kevrekidis (ed.), *The Discrete Nonlinear Schrödinger Equation: Mathematical Analysis, Numerical Computations and Physical Perspectives*, Springer, Berlin, 2009.
10. P. G. Kevrekidis, K. Ø. Rasmussen and A. R. Bishop, *The discrete nonlinear Schrödinger equation: a survey of recent results*, Intern. J. Modern. Phys. B, 15 (2001), 2833–2900.
11. G. N'Guérékata and A. Pankov, *Global well-posedness for discrete nonlinear Schrödinger equation*, Applicable Anal., 89 (2010), 1513–1521.
12. P. Pacciani V. V. Konotop and G. Perla Menzala, *On localized solutions of discrete nonlinear Schrödinger equation: an exact result*, Physica D, 204 (2005), 122–133.
13. A. Pankov, *Gap solitons in periodic discrete nonlinear Schrödinger equations*, Nonlinearity, 19 (2006), 27–40.
14. A. Pankov, *Gap solitons in periodic discrete nonlinear Schrödinger equations, II: a generalized Nehari manifold approach*, Discr. Cont. Dyn. Syst. A, 19 (2007), 419–430.
15. A. Pankov, *Gap solitons in periodic discrete nonlinear Schrödinger equations with saturable nonlinearities*, J. Math. Anal. Appl., 371 (2010), 254–265.
16. A. Pankov and V. Rothos, *Periodic and decaying solutions in discrete nonliinear Schrödinger equations with saturable nonlinearity*, Proc. Roy. Soc. A, 464 (2008), 3219–3236.
17. A. Pankov and G. Zhang, *Standing wave solutions for discrete nonlinear Schrödinger equations with unbounded potentials and saturable nonlinearities*, J. Math. Sci., 177 (2011), 71–82.
18. A. Pazy, *Semigroups of Linear Operators and Applications*, Springer, New York, 1983.

19. M. I. Weinstein, *Excitation threshold for nonlinear localized modes on lattices*, Nonlinearity, 19 (1999), 673–691.
20. G. Zhang, *Breather solutions of the discrete nonlinear Schrödinger equation with unbounded potential*, J. Math.Phys., 50 (2009), 013505.
21. G. Zhang, *Breather solutions of the discrete nonlinear Schrödinger equation with sign changing nonlinearity*, J. Math.Phys., 52 (2011), 043516.
22. G. Zhang and F. Liu, *Existence of breather solutions of the DNLS equation with unbounded potential*, Nonlin. Anal., 71 (2009), e786–e792.
23. G. Zhang and A. Pankov, *Standing waves of the discrete nonlinear Schrödinger equations with growing potentials*, Commun. Math. Analysis, 5(2)(2008), 38–49.
24. G. Zhang and A. Pankov, *Standing wave solutions for the discrete nonlinear Schrödinger equations with unbounded potentials, II*, Applicable Anal., 89 (2011), 1541–1557.
25. A. Pankov and G. Zhang, *Initial value problem of the discrete nonlinear Schrödinger equation with complex potential*, Applicable Analysis, Volume 101, Issue 16 (2022), pp. 5760-5774.

# Darboux Transformations for Bi-integrable Couplings of the AKNS System


**Yu-Juan Zhang and Wen-Xiu Ma**

**Abstract** We construct Darboux transformations for bi-integrable couplings of soliton equations. Then we apply the resulting theory to a kind of bi-integrable couplings of the AKNS systems. Particularly, we present exact one-soliton-like solutions for the bi-integrable couplings of the nonlinear Schrödinger equations.

**Keywords** Non-semisimple Lie algebra · AKNS bi-integrable couplings · Nonlinear Schrödinger equation · Soliton-like solutions

## 1 Introduction

Integrable systems usually possess linear representations, e.g., Lax representations associated with matrix loop algebras. Simple matrix loop algebras generate integrable systems, and semisimple matrix loop algebras generate separated integrable systems. Integrable couplings [1, 2] are a kind of integrable systems which are associated with non-semisimple matrix loop algebras [3]. Particularly, by enlarging semisimple matrix loop algebras to non-semisimple matrix loop algebras, we obtain Lax pairs for integrable couplings. This is based on a fact that every non-semisimple Lie algebra possesses a semi-direct sum decomposition of a semisimple Lie algebra and a solvable Lie algebra [4], i.e., let $\mathfrak{g}$ denote a non-semisimple Lie algebra.

$$\bar{\mathfrak{g}} = \mathfrak{g} \in \mathfrak{g}_c, \ \ \mathfrak{g} \text{ - semisimple}, \ \ \mathfrak{g}_c \text{ - solvable}, \tag{1}$$

where the subscript $c$ indicates a contribution to the construction of coupling systems. The notion of semi-direct sum means that the two Lie subalgebras $\mathfrak{g}$ and $\mathfrak{g}_c$ satisfy

Y.-J. Zhang (✉)
School of Mathematics and Statistics, Xidian University, Xian 710126, P. R. China
e-mail: zhangyj@xidian.edu.cn

W.-X. Ma
Department of Mathematics and Statistics, University of South Florida, Tampa, FL 33620-5700, USA



S. Manukure and W.-X. Ma (eds.), *Nonlinear and Modern Mathematical Physics*,
Springer Proceedings in Mathematics & Statistics 459,
https://doi.org/10.1007/978-3-031-59539-4_16

$$[\mathfrak{g}, \mathfrak{g}_c] \subseteq \mathfrak{g}_c, \tag{2}$$

where $[\mathfrak{g}, \mathfrak{g}_c] = \{[A, B] \mid A \in \mathfrak{g},\ B \in \mathfrak{g}_c\}$, with $[\cdot, \cdot]$ denoting the Lie bracket of $\bar{\mathfrak{g}}$. Obviously, $\mathfrak{g}_c$ is an ideal Lie sub-algebra of $\bar{\mathfrak{g}}$.

An integrable coupling of a given integrable system

$$u_t = K(u) \tag{3}$$

is a triangular integrable system of the following form [1, 5, 6]:

$$\begin{cases} u_t = K(u), \\ u_{1,t} = T(u, u_1). \end{cases} \tag{4}$$

Let $A_1$ and $A_2$ be square matrices of the same order. Then the $2 \times 2$ block matrices

$$M_1(A_1, A_2) = \begin{bmatrix} A_1 & A_2 \\ 0 & A_1 \end{bmatrix}, \tag{5}$$

define an enlarged Lie algebra $\bar{\mathfrak{g}}$ with the following semidirect sum decomposition:

$$\bar{\mathfrak{g}} = \mathfrak{g} \in \mathfrak{g}_c, \quad \mathfrak{g} = \{M_1(A_1, 0)\}, \quad \mathfrak{g}_c = \{M_1(0, A_2)\}, \tag{6}$$

which can be used to generate integrable couplings. Moreover, the variational identity is applied to construct the Hamiltonian structures of integrable couplings [5, 7].

A bi-integrable coupling [8] of a given integrable system (3) is an enlarged triangular integrable system of the following form:

$$\begin{cases} u_t = K(u), \\ u_{1,t} = T_1(u, u_1), \\ u_{2,t} = T_2(u, u_1, u_2). \end{cases} \tag{7}$$

Similarly, let $A_1$, $A_2$ and $A_3$ be square matrices of the same order. Then the $3 \times 3$ block matrices of the following type:

$$M_2(A_1, A_2, A_3) = \begin{bmatrix} A_1 & A_2 & A_3 \\ 0 & A_1 & A_2 \\ 0 & 0 & A_1 \end{bmatrix}, \tag{8}$$

define an enlarged Lie algebra $\bar{\mathfrak{g}} = \mathfrak{g} \in \mathfrak{g}_c$ with

$$\mathfrak{g} = \{M_2(A_1, 0, 0)\}, \quad \mathfrak{g}_c = \{M_2(0, A_2, A_3)\}, \tag{9}$$

which can be used to generate bi-integrable couplings.

Furthermore, a tri-integrable coupling [6, 9] is of the form:

$$\begin{cases} u_t = K(u), \\ u_{1,t} = T_1(u, u_1), \\ u_{2,t} = T_2(u, u_1, u_2), \\ u_{3,t} = T_2(u, u_1, u_2, u_3). \end{cases} \tag{10}$$

The $4 \times 4$ block matrices

$$M_3(A_1, A_2, A_3, A_4) = \begin{bmatrix} A_1 & A_2 & A_3 & A_4 \\ 0 & A_1 & A_2 & A_3 \\ 0 & 0 & A_1 & A_2 \\ 0 & 0 & 0 & A_1 \end{bmatrix}, \tag{11}$$

defining an enlarged Lie algebra $\bar{\mathfrak{g}} = \mathfrak{g} \in \mathfrak{g}_c$ with

$$\mathfrak{g} = \{M_3(A_1, 0, 0, 0)\}, \quad \mathfrak{g}_c = \{M_3(0, A_2, A_3, A_4)\},$$

produce Lax pair matrices for tri-integrable couplings.

There are many approaches for solving integrable systems, for example, the homogeneous balance method [10], the Hirota bilinear method [11], the bilinear neural network method [12–15], the transformed rational function method [16], the Darboux transformation [17–19] and the inverse scattering transformation [20]. The Darboux transformation is a pretty systematic and direct approach, and it relies on Lax pairs involving a spectral parameter.

Darboux transformations for integrable couplings have been solved in [21]. In this paper, we construct Darboux transformations for bi-integrable couplings. This paper is organized as follows: In Sect. 2, we present a procedure for constructing Darboux transformations for spectral problems associated with bi-integrable couplings, thereby giving a formula of Darboux transformations of bi-integrable couplings. In Sect. 3, we apply this formula to a kind of bi-integrable couplings of the AKNS hierarchy, and compute exact solutions for the bi-integrable coupling system of the nonlinear Schrödinger equations. At the end, we will give a concluding remark.

## 2 Darboux Transformations of Bi-integrable Couplings

To define the spectral problems of bi-integrable couplings, we denote $\bar{u} = (u^T, u_1^T, u_2^T)^T$ as the potential functions, where $u, u_1, u_2$ being $N$ dimensional column vectors. Set $\bar{U}$ and $\bar{V}^{[m]}$ being elements in a non-semisimple matrix loop algebra defined by

$$\bar{U}(\bar{u},\lambda)=\begin{bmatrix} U(u,\lambda) & U_1(u_1,\lambda) & U_2(u_2,\lambda)\\ 0 & U(u,\lambda) & U_1(u_1,\lambda)\\ 0 & 0 & U(u,\lambda)\end{bmatrix}, \tag{12}$$

$$\bar{V}^{[m]}(\bar{u},\lambda)=\begin{bmatrix} V^{[m]}(u,\lambda) & V_1^{[m]}(u,u_1,\lambda) & V_2^{[m]}(u,u_1,u_2,\lambda)\\ 0 & V^{[m]}(u,\lambda) & V_1^{[m]}(u,u_1,\lambda)\\ 0 & 0 & V^{[m]}(u,\lambda)\end{bmatrix}, \tag{13}$$

in which $U, U_1, U_2$ are $N\times N$ matrices depending on the spectral parameter $\lambda$. Set $\bar{\phi}=(\chi^T,\psi^T,\phi^T)^T$ as the enlarged eigenfunction, with $\chi,\psi,\phi$ being $N$ dimensional column vectors. Then the spectral problems of bi-integrable couplings (7) are defined as:

$$\begin{cases}\bar{\phi}_x=\bar{U}(\bar{u},\lambda)\bar{\phi},\\ \bar{\phi}_{t_m}=\bar{V}^{[m]}(\bar{u},\lambda)\bar{\phi},\end{cases} \tag{14}$$

where $m$ is a positive integer, indicating the hierarchy. Furthermore, we assume

$$U=\lambda J+P,\quad U_i=\lambda J_i+P_i,\quad i=1,2,$$

where $J$ and $J_i$ being $N\times N$ diagonal matrices, $P$ and $P_i$ being $N\times N$ matrices consisting of dependent variables, which have zero diagonal elements, $V^{[m]}$, $V_1^{[m]}$, $V_2^{[m]}$ being $N\times N$ polynomial matrices of $\lambda$:

$$V^{[m]}=\sum_{j=0}^{m}V_j\lambda^{m-j},\quad V_i^{[m]}=\sum_{j=0}^{m}V_{i,j}\lambda^{m-j},\quad i=1,2.$$

To construct a Darboux transformation for (14), we rewrite the spectral problems (14) as follows:

$$\begin{cases}\bar{\phi}_x=\bar{U}\bar{\phi}=\left(\lambda\bar{J}+\bar{P}\right)\bar{\phi},\\ \bar{\phi}_{t_m}=\bar{V}^{[m]}\bar{\phi}=\sum_{j=0}^{m}\bar{V}_j\lambda^{m-j}\bar{\phi}.\end{cases} \tag{15}$$

where

$$\bar{J}=\begin{bmatrix} J & J_1 & J_2\\ 0 & J & J_1\\ 0 & 0 & J\end{bmatrix},\quad \bar{P}=\begin{bmatrix} P & P_1 & P_2\\ 0 & P & P_1\\ 0 & 0 & P\end{bmatrix},\quad \bar{V}_j=\begin{bmatrix} V_j & V_{1,j} & V_{2,j}\\ 0 & V_j & V_{1,j}\\ 0 & 0 & V_j\end{bmatrix}. \tag{16}$$

Assume that $\bar{D}=\bar{D}(x,t,\lambda)$ is a Darboux matrix, that is to say, $\bar{\phi}'=\bar{D}\bar{\phi}$ satisfies the same form as the spectral problems (15), i.e.,

$$\begin{cases}\bar{\phi}'_x=\bar{U}'\bar{\phi}'=\left(\lambda\bar{J}+\bar{P}'\right)\bar{\phi}',\\ \bar{\phi}'_{t_m}=\bar{V}^{[m]\prime}\bar{\phi}'=\sum_{j=0}^{m}\bar{V}'_j\lambda^{m-j}\bar{\phi}',\end{cases} \tag{17}$$

where $\bar{P}'$ is the new potential matrix. Therefore $\bar{\phi} \to \bar{\phi}'$, $\bar{P} \to \bar{P}'$ form a Darboux transformation of the spectral problems (14).

In particular, we consider a Darboux matrix of the form $\bar{D}(\lambda) = \lambda\bar{I} - \bar{S}$, where $\bar{I} = diag(I, I, I)$, with $I$ being the $N \times N$ identity matrix. A similar calculation as in [21] shows that $\lambda\bar{I} - \bar{S}$ is a Darboux matrix of the enlarged spectral problems (14) if and only if $\bar{S}$ satisfies

$$\bar{S}_x = [\bar{J}\bar{S} + \bar{P}, \bar{S}], \tag{18}$$

$$\bar{S}_{t_m} = [\sum_{j=0}^{m} \bar{V}_j \bar{S}^{m-j}, \bar{S}]. \tag{19}$$

Moreover, the potentials satisfy

$$\bar{P}' = \bar{P} + [\bar{J}, \bar{S}], \tag{20}$$

where

$$\bar{S} = \begin{bmatrix} S & S_1 & S_2 \\ 0 & S & S_1 \\ 0 & 0 & S \end{bmatrix}, \quad \bar{P}' = \begin{bmatrix} P' & P_1' & P_2' \\ 0 & P' & P_1' \\ 0 & 0 & P' \end{bmatrix}. \tag{21}$$

Introduce $\bar{S} = \bar{H}\bar{\Lambda}\bar{H}^{-1}$ as in the general Darboux transformation theory [17], where

$$\bar{H} = \begin{bmatrix} H & H_1 & H_2 \\ 0 & H & H_1 \\ 0 & 0 & H \end{bmatrix}, \quad \bar{\Lambda} = \begin{bmatrix} \Lambda & 0 & 0 \\ 0 & \Lambda & 0 \\ 0 & 0 & \Lambda \end{bmatrix}, \tag{22}$$

with $\Lambda$, $H$, $H_1$, $H_2$ being all $N \times N$ matrices. Then substitute these choices into the expression of $\bar{S}$ in (21), we obtain

$$\begin{cases} S = H\Lambda H^{-1}, \\ S_1 = -H\Lambda H^{-1} H_1 H^{-1} + H_1 \Lambda H^{-1}, \\ S_2 = H\Lambda H^{-1} H_1 H^{-1} H_1 H^{-1} - H_1 \Lambda H^{-1} H_1 H^{-1} - H\Lambda H^{-1} H_2 H^{-1} + H_2 \Lambda H^{-1}, \end{cases} \tag{23}$$

i.e.,

$$\begin{cases} S = H\Lambda H^{-1}, \\ S_1 = -SH_1 H^{-1} + H_1 \Lambda H^{-1}, \\ S_2 = -S_1 H_1 H^{-1} - SH_2 H^{-1} + H_2 \Lambda H^{-1}. \end{cases} \tag{24}$$

Now let us introduce $N$ eigenvalues $\lambda_1, \cdots, \lambda_N$, and set $\Lambda = diag(\lambda_1, \cdots, \lambda_N)$. Denote the corresponding eigenfunctions by $(\bar{\phi}^{(1)}, \cdots, \bar{\phi}^{(N)})$, where $\bar{\phi}^{(i)} = (\chi^{(i)T}, \psi^{(i)T}, \phi^{(i)T})^T$, $i = 1, \cdots, N$. $\bar{\phi}^{(i)}$ satisfies the spectral problems (14), and thus

$$\begin{cases} \chi_x^{(i)} = (\lambda J + P)\chi^{(i)} + (\lambda J_1 + P_1)\psi^{(i)} + (\lambda J_2 + P_2)\phi^{(i)}, \\ \psi_x^{(i)} = (\lambda J + P)\psi^{(i)} + (\lambda J_1 + P_1)\phi^{(i)}, \\ \phi_x^{(i)} = (\lambda J + P)\phi^{(i)}, \end{cases}$$

$$\begin{cases} \chi_{t_m}^{(i)} = \sum_{j=0}^{m} V_j \lambda^{m-j}\chi^{(i)} + \sum_{j=0}^{m} V_{1,j}\lambda^{m-j}\psi^{(i)} + \sum_{j=0}^{m} V_{2,j}\lambda^{m-j}\phi^{(i)}, \\ \psi_{t_m}^{(i)} = \sum_{j=0}^{m} V_j \lambda^{m-j}\psi^{(i)} + \sum_{j=0}^{m} V_{1,j}\lambda^{m-j}\phi^{(i)}, \\ \phi_{t_m}^{(i)} = \sum_{j=0}^{m} V_j \lambda^{m-j}\phi^{(i)}, \end{cases}$$

where $i = 1, \cdots, N$. Now set

$$H = [\phi^{(1)}, \cdots, \phi^{(N)}], \quad H_1 = [\psi^{(1)}, \cdots, \psi^{(N)}], \quad H_2 = [\chi^{(1)}, \cdots, \chi^{(N)}], \tag{25}$$

where $H$, $H_1$, $H_2$ satisfy

$$\begin{cases} H_x = JH\Lambda + PH, \\ H_{1x} = JH_1\Lambda + PH_1 + J_1H\Lambda + P_1H, \\ H_{2x} = JH_2\Lambda + PH_2 + J_1H_1\Lambda + P_1H_1 + J_2H\Lambda + P_2H; \end{cases} \tag{26}$$

$$\begin{cases} H_{t_m} = \sum_{j=0}^{m} V_j H\Lambda^{m-j}, \\ H_{1t_m} = \sum_{j=0}^{m} V_j H_1\Lambda^{m-j} + \sum_{j=0}^{m} V_{1j} H\Lambda^{m-j}, \\ H_{2t_m} = \sum_{j=0}^{m} V_j H_2\Lambda^{m-j} + \sum_{j=0}^{m} V_{1j} H_1\Lambda^{m-j} + \sum_{j=0}^{m} V_{2j} H\Lambda^{m-j}. \end{cases} \tag{27}$$

Sum up the above discussions, we obtain the following theorem:

**Theorem 1** *Let $\bar{H}$ and $\bar{\Lambda}$ be defined by (22). Then $\bar{H}$ is invertible if and only if $H$ is invertible. When $H$ is invertible, then $\bar{S} = \bar{H}\bar{\Lambda}\bar{H}^{-1}$ can be represented as in (21) with $S, S_1, S_2$ defined in (23), then $\bar{D} = \lambda\bar{I} - \bar{S}$ is a Darboux matrix of the enlarged spectral problems (14), which leads to the Bäcklund transformation for the bi-integrable coupling (7):*

$$\begin{cases} P^{[1]} = P^{[0]} + [J, S], \\ P_1^{[1]} = P_1^{[0]} + [J, S_1] + [J_1, S], \\ P_2^{[1]} = P_2^{[0]} + [J, S_2] + [J_1, S_1] + [J_2, S], \end{cases} \tag{28}$$

*where $P^{[0]}$, $P_1^{[0]}$ and $P_2^{[0]}$ are a giving seed solution.*

***Proof*** As we did in the Darboux transformation for the integrable coupling case in Ref. [21], we need to prove that for this choice of $\bar{H}$, the two conditions (18) and (19) are satisfied.

First, let us prove the Eq. (18). It is equivalent to prove

$$\begin{cases} S_x = [JS + P, S], \\ S_{1x} = [JS_1 + J_1S + P_1, S] + [JS + P, S_1], \\ S_{2x} = [JS_2 + J_1S_1 + J_2S + P_2, S] + [JS_1 + J_1S + P_1, S_1] + [JS + P, S_2]. \end{cases} \tag{29}$$

From Eq. (24), we obtain

$$\begin{cases} S_x = H_x \Lambda H^{-1} - H\Lambda H^{-1} H_x H^{-1}, \\ S_{1x} = -S_x H_1 H^{-1} - S H_{1x} H^{-1} + S H_1 H^{-1} H_x H^{-1} + H_{1x} \Lambda H^{-1} \\ \quad -H_1 \Lambda H^{-1} H_x H^{-1}, \\ S_{2x} = -S_{1x} H_1 H^{-1} - S_1 H_{1x} H^{-1} + S_1 H_1 H^{-1} H_x H^{-1} - S_x H_2 H^{-1} - S H_{2x} H^{-1} \\ \quad +S H_2 H^{-1} H_x H^{-1} + H_{2x} \Lambda H^{-1} - H_2 \Lambda H^{-1} H_x H^{-1}, \end{cases} \tag{30}$$

by using (26). Then a tedious calculation can show that the right hand sides of (30) are equal to the right hand sides of (29), respectively. Thus we proved Eq. (18).

Second, let us prove Eq. (19). We compute that

$$\bar{S}^n = \begin{bmatrix} S^n & T_n & M_n \\ 0 & S^n & T_n \\ 0 & 0 & S^n \end{bmatrix}, \tag{31}$$

where

$$M_n = T_n^{(2)} + \sum_{k=1}^{n-1} T_k S_1 S^{n-1-k}, \quad T_n = T_n^{(1)} = \sum_{k=1}^{n} T_{nk}^{(1)}, \quad T_n^{(2)} = \sum_{k=1}^{n} T_{nk}^{(2)}, \tag{32}$$

$$T_{nk}^{(1)} = S^{n-k} S_1 S^{k-1}, \quad T_{nk}^{(2)} = S^{n-k} S_2 S^{k-1}, \tag{33}$$

which tell

$$T_{11}^{(1)} = S_1, \quad T_{11}^{(2)} = S_2. \tag{34}$$

Equation (19) is equivalent to

$$\bar{S}_{t_m} = \sum_{j=0}^{m} [\bar{V}_j \bar{S}^{m-j}, \bar{S}], \tag{35}$$

and thus, we need to prove

$$\begin{cases} S_{t_m} = \sum_{j=0}^{m} [V_j S^{m-j}, S], \\ S_{1t_m} = \sum_{j=0}^{m} ([V_j S^{m-j}, S_1] + [V_{1j} S^{m-j}, S] \\ +[V_j T_{m-j}, S]), \\ S_{2t_m} = \sum_{j=0}^{m} ([V_j S^{m-j}, S_2] + [V_j T_{m-j}, S_1] + [V_{1j} S^{m-j}, S_1] \\ +[V_j M^{m-j}, S] + [V_{1j} T_{m-j}, S] + [V_{2j} S^{m-j}, S]). \end{cases} \tag{36}$$

From Eq. (24), we obtain

$$\begin{cases} S_{t_m} = H_{t_m}\Lambda H^{-1} - H\Lambda H^{-1}H_{t_m}H^{-1}, \\ S_{1t_m} = -S_{t_m}H_1H^{-1} - SH_{1t_m}H^{-1} + SH_1H^{-1}H_{t_m}H^{-1} + H_{1t_m}\Lambda H^{-1} \\ \qquad -H_1\Lambda H^{-1}H_{t_m}H^{-1}, \\ S_{2t_m} = -S_{1t_m}H_1H^{-1} - S_1H_{1t_m}H^{-1} + S_1H_1H^{-1}H_{t_m}H^{-1} - S_{t_m}H_2H^{-1} \\ \qquad -SH_{2t_m}H^{-1} + SH_2H^{-1}H_{t_m}H^{-1} + H_{2t_m}\Lambda H^{-1} - H_2\Lambda H^{-1}H_{t_m}H^{-1}, \end{cases} \tag{37}$$

by using (27). Then a tedious calculation can show that the right hand sides of (37) are equal to the right hand sides of (36), respectively. Thus we proved Eq. (19).

Finally, a simple computation

$$[\bar{J}, \bar{S}] = \begin{bmatrix} [J,S] & [J,S_1]+[J_1,S] & [J,S_2]+[J_1,S_1]+[J_2,S] \\ 0 & [J,S] & [J,S_1]+[J_1,S] \\ 0 & 0 & [J,S] \end{bmatrix}.$$

Therefore, $\bar{P}'$ and $\bar{P} + [\bar{J}, \bar{S}]$ have the same matrix form, which tells the transformation (20), i.e., $\bar{P}' = \bar{P} + [\bar{J}, \bar{S}]$. The proved transformation (20) generates Bäcklund transformation presented in (28). This completes the proof. □

Specially, for the AKNS systems, we have $N = 2$, so that all the sub-matrix in (12) and (13), as well as $J$, $J_1$, $J_2$ and $P$ are $2 \times 2$ matrices. We assume $J_1 = J_2 = J$, and

$$J = \begin{bmatrix} -1 & 0 \\ 0 & 1 \end{bmatrix}, \quad P = \begin{bmatrix} 0 & q \\ r & 0 \end{bmatrix}, \quad P_1 = \begin{bmatrix} 0 & q_1 \\ r_1 & 0 \end{bmatrix}, \quad P_2 = \begin{bmatrix} 0 & q_2 \\ r_2 & 0 \end{bmatrix}, \tag{38}$$

$$\chi = (\chi_1, \chi_2)^T, \quad \psi = (\psi_1, \psi_2)^T, \quad \phi = (\phi_1, \phi_2)^T, \tag{39}$$

$$u = (q, r)^T, \quad u_1 = (q_1, r_1)^T, \quad u_2 = (q_2, r_2)^T. \tag{40}$$

Take two arbitrary constants $\lambda_1$ and $\lambda_2$, and denote $\phi_{jk} = \phi_j(\lambda_k)$, $\psi_{jk} = \psi_j(\lambda_k)$, $\chi_{jk} = \chi_j(\lambda_k)$, $j, k = 1, 2$, and set

$$\Lambda = \begin{bmatrix} \lambda_1 & 0 \\ 0 & \lambda_2 \end{bmatrix}, \quad H = \begin{bmatrix} \phi_{11} & \phi_{12} \\ \phi_{21} & \phi_{22} \end{bmatrix}, \quad H_1 = \begin{bmatrix} \psi_{11} & \psi_{12} \\ \psi_{21} & \psi_{22} \end{bmatrix}, \quad H_2 = \begin{bmatrix} \chi_{11} & \chi_{12} \\ \chi_{21} & \chi_{22} \end{bmatrix}. \tag{41}$$

Then we obtain the associated Bäcklund transformation

$$\begin{cases} q^{[1]} = P^{[1]}[1,2], & r^{[1]} = P^{[1]}[2,1], \\ q_1^{[1]} = P_1^{[1]}[1,2], & r_1^{[1]} = P_1^{[1]}[2,1], \\ q_2^{[1]} = P_2^{[1]}[1,2], & r_2^{[1]} = P_2^{[1]}[2,1]; \end{cases} \tag{42}$$

concretely,

$$\begin{cases} q^{[1]} = q^{[0]} + 2\,\frac{\phi_{11}\phi_{12}(\lambda_1-\lambda_2)}{\phi_{11}\phi_{22}-\phi_{12}\phi_{21}}, \quad r^{[1]} = r^{[0]} + 2\,\frac{\phi_{21}\phi_{22}(\lambda_1-\lambda_2)}{\phi_{11}\phi_{22}-\phi_{12}\phi_{21}}, \\ q_1^{[1]} = q_1^{[0]} + \frac{2(\lambda_1-\lambda_2)\left({\phi_{11}}^2\phi_{12}\phi_{22}-\phi_{11}{\phi_{12}}^2\psi_{22}+{\phi_{11}}^2\phi_{22}\psi_{12}-\phi_{11}{\phi_{12}}^2\phi_{21}+\phi_{11}{\phi_{12}}^2\psi_{21}-{\phi_{12}}^2\phi_{21}\psi_{11}\right)}{(\phi_{11}\phi_{22}-\phi_{12}\phi_{21})^2}, \\ r_1^{[1]} = r_1^{[0]} + \frac{2(\lambda_1-\lambda_2)\left(\phi_{11}\phi_{21}{\phi_{22}}^2+\phi_{11}{\phi_{22}}^2\psi_{21}-\phi_{12}{\phi_{21}}^2\phi_{22}-\phi_{12}{\phi_{21}}^2\psi_{22}+{\phi_{21}}^2\phi_{22}\psi_{12}-\phi_{21}{\phi_{22}}^2\psi_{11}\right)}{(\phi_{11}\phi_{22}-\phi_{12}\phi_{21})^2}, \\ q_2^{[1]} = q_2^{[0]} + \frac{2(\lambda_1-\lambda_2)\zeta_1}{(\phi_{11}\phi_{22}-\phi_{12}\phi_{21})^3}, \quad r_2^{[1]} = r_2^{[0]} + \frac{2(\lambda_1-\lambda_2)\zeta_2}{(\phi_{11}\phi_{22}-\phi_{12}\phi_{21})^3}, \end{cases} \tag{43}$$

with

$$\begin{aligned} \zeta_1 = {} & \chi_{11}\phi_{11}{\phi_{12}}^2\phi_{21}\phi_{22} - \chi_{11}\phi_{12}{\phi_{21}}^2 - \chi_{12}{\phi_{11}}^3{\phi_{22}}^2 + \chi_{12}{\phi_{11}}^2\phi_{12}\phi_{21}\phi_{22} - \chi_{21}{\phi_{11}}^2{\phi_{12}}^2\phi_{22} \\ & + \chi_{21}\phi_{11}{\phi_{12}}^3\phi_{21} + \chi_{22}{\phi_{11}}^3\phi_{12}\phi_{22} - \chi_{22}{\phi_{11}}^2{\phi_{12}}^2\phi_{21} - {\phi_{11}}^3\phi_{12}{\phi_{22}}^2 + {\phi_{11}}^3\phi_{12}\phi_{22}\psi_{22} \\ & - {\phi_{11}}^3\phi_{12}{\psi_{22}}^2 - {\phi_{11}}^3{\phi_{22}}^2\psi_{12} + {\phi_{11}}^3\phi_{22}\psi_{12}\psi_{22} + 2\,{\phi_{11}}^2{\phi_{12}}^2\phi_{21}\phi_{22} - {\phi_{11}}^2{\phi_{12}}^2\phi_{21}\psi_{22} \\ & - {\phi_{11}}^2{\phi_{12}}^2\phi_{22}\psi_{21} + 2\,{\phi_{11}}^2{\phi_{12}}^2\psi_{21}\psi_{22} + {\phi_{11}}^2\phi_{12}\phi_{21}\phi_{22}\psi_{12} + {\phi_{11}}^2\phi_{12}\phi_{21}\psi_{12}\psi_{22} \\ & - 2\,{\phi_{11}}^2\phi_{12}\phi_{22}\psi_{12}\psi_{21} - {\phi_{11}}^2\phi_{21}\phi_{22}{\psi_{12}}^2 - \phi_{11}{\phi_{12}}^3{\phi_{21}}^2 + \phi_{11}{\phi_{12}}^3\phi_{21}\psi_{21} \\ & - \phi_{11}{\phi_{12}}^3{\psi_{21}}^2 + \phi_{11}{\phi_{12}}^2\phi_{21}\phi_{22}\psi_{11} - 2\,\phi_{11}{\phi_{12}}^2\phi_{21}\psi_{11}\psi_{22} + \phi_{11}{\phi_{12}}^2\phi_{22}\psi_{11}\psi_{21} \\ & + 2\,\phi_{11}\phi_{12}\phi_{21}\phi_{22}\psi_{11}\psi_{12} - {\phi_{12}}^3{\phi_{21}}^2\psi_{11} + {\phi_{12}}^3\phi_{21}\psi_{11}\psi_{21} - {\phi_{12}}^2\phi_{21}\phi_{22}{\psi_{11}}^2, \\ \zeta_2 = {} & \chi_{11}\phi_{11}\phi_{21}{\phi_{22}}^3 - \chi_{11}\phi_{12}{\phi_{21}}^2{\phi_{22}}^2 - \chi_{12}{\phi_{11}}\phi_{21}{\phi_{22}}^2 + \chi_{12}\phi_{12}{\phi_{21}}^3\phi_{22} - \chi_{21}{\phi_{11}}^2{\phi_{22}}^3 \\ & + \chi_{21}\phi_{11}\phi_{12}\phi_{21}{\phi_{22}}^2 + \chi_{22}\phi_{11}\phi_{12}{\phi_{21}}^2\phi_{22} - \chi_{22}{\phi_{12}}^2{\phi_{21}}^3 - {\phi_{11}}^2\phi_{21}{\phi_{22}}^3 - {\phi_{11}}^2{\phi_{22}}^3\psi_{21} \\ & + 2\,\phi_{11}\phi_{12}{\phi_{21}}^2{\phi_{22}}^2 + \phi_{11}\phi_{12}{\phi_{21}}^2\phi_{22}\psi_{22} - \phi_{11}\phi_{12}{\phi_{21}}^2{\psi_{22}}^2 + \phi_{11}\phi_{12}\phi_{21}{\phi_{22}}^2\psi_{21} \\ & + 2\,\phi_{11}\phi_{12}\phi_{21}\phi_{22}\psi_{21}\psi_{22} - \phi_{11}\phi_{12}{\phi_{22}}^2{\psi_{21}}^2 - \phi_{11}{\phi_{21}}^2\phi_{22}^2\psi_{12} + \phi_{11}{\phi_{21}}^2\phi_{22}\psi_{12}\psi_{22} \\ & + \phi_{11}\phi_{21}{\phi_{22}}^3\psi_{11} - 2\,\phi_{11}\phi_{21}{\phi_{22}}^2\psi_{12}\psi_{21} + \phi_{11}{\phi_{22}}^3\psi_{11}\psi_{21} - \phi_{12}{}^2\phi_{21}{}^3\phi_{22} - \phi_{12}{}^2\phi_{21}{}^3\psi_{22} \\ & + \phi_{12}\phi_{21}{}^3\phi_{22}\psi_{12} + \phi_{12}\phi_{21}{}^3\psi_{12}\psi_{22} - \phi_{12}\phi_{21}{}^2\phi_{22}{}^2\psi_{11} - 2\,\phi_{12}\phi_{21}{}^2\phi_{22}\psi_{11}\psi_{22} \\ & + \phi_{12}\phi_{21}\phi_{22}{}^2\psi_{11}\psi_{21} - \phi_{21}{}^3\phi_{22}\psi_{12}{}^2 + 2\,\phi_{21}{}^2\phi_{22}{}^2\psi_{11}\psi_{12} - \phi_{21}\phi_{22}{}^3\psi_{11}{}^2. \end{aligned}$$

i.e.,

$$\begin{cases} q^{[1]} = q^{[0]} + \frac{2(\lambda_1-\lambda_2)}{|H|}\phi_{11}\phi_{12}, \quad r^{[1]} = r^{[0]} + \frac{2(\lambda_1-\lambda_2)}{|H|}\phi_{21}\phi_{22}, \\ q_1^{[1]} = q_1^{[0]} + \frac{2(\lambda_1-\lambda_2)}{|H|^2}\left(\zeta_{11}-\zeta_{12}\right), \quad r_1^{[1]} = r_1^{[0]} + \frac{2(\lambda_1-\lambda_2)}{|H|^2}\left(\zeta_{13}-\zeta_{14}\right), \\ q_2^{[1]} = q_2^{[0]} - \frac{2(\lambda_1-\lambda_2)}{|H|^3}\left(\zeta_{21}+\zeta_{22}+\zeta_{23}+\zeta_{24}\right), \\ r_2^{[1]} = r_2^{[0]} - \frac{2(\lambda_1-\lambda_2)}{|H|^3}\left(\zeta_{25}+\zeta_{26}+\zeta_{27}+\zeta_{28}\right), \end{cases} \tag{44}$$

with

$$\zeta_{11} = \begin{vmatrix} \phi_{11} & 0 & 0 & 0 \\ 0 & \phi_{11} & \phi_{11} & 0 \\ 0 & -\psi_{12} & \phi_{12} & \phi_{12} \\ 0 & 0 & \psi_{22} & \phi_{22} \end{vmatrix}, \qquad \zeta_{12} = \begin{vmatrix} \phi_{12} & 0 & 0 & 0 \\ 0 & \phi_{12} & \phi_{12} & 0 \\ 0 & -\psi_{11} & \phi_{11} & \phi_{11} \\ 0 & 0 & \psi_{21} & \phi_{21} \end{vmatrix},$$

$$\zeta_{13}=\begin{vmatrix}\phi_{22}&0&0&0\\0&\phi_{22}&\phi_{22}&0\\0&-\psi_{21}&\phi_{21}&\phi_{21}\\0&0&\psi_{11}&\phi_{11}\end{vmatrix},\qquad \zeta_{14}=\begin{vmatrix}\phi_{21}&0&0&0\\0&\phi_{21}&\phi_{21}&0\\0&-\psi_{22}&\phi_{22}&\phi_{22}\\0&0&\psi_{12}&\phi_{12}\end{vmatrix},$$

$$\zeta_{21}=\begin{vmatrix}\phi_{11}&0&0&0&0&0\\0&\phi_{11}&0&\psi_{21}&\phi_{21}&\phi_{21}\\0&0&\phi_{11}&\phi_{11}&0&0\\0&0&-\psi_{12}&\phi_{12}&\phi_{12}&0\\0&\phi_{12}&0&\psi_{22}&\phi_{22}&\phi_{22}\\0&0&0&\chi_{22}&\phi_{22}&\psi_{22}\end{vmatrix},\qquad \zeta_{22}=\begin{vmatrix}\phi_{11}&0&0&0&0&0\\0&\phi_{11}&\psi_{11}&0&0&0\\0&0&\phi_{12}&0&0&\phi_{22}\\0&0&\chi_{12}&\psi_{12}&0&0\\0&0&0&\phi_{11}&\phi_{21}&2\psi_{21}\\0&\phi_{12}&\psi_{12}&\phi_{12}&\phi_{22}&2\psi_{22}\end{vmatrix},$$

$$\zeta_{23}=\begin{vmatrix}\phi_{12}&0&0&0&0&0\\0&\phi_{12}&0&\psi_{22}&\phi_{22}&\phi_{22}\\0&0&\phi_{12}&\phi_{12}&0&0\\0&0&-\psi_{11}&\phi_{11}&\phi_{11}&0\\0&\phi_{11}&0&\psi_{21}&\phi_{21}&\phi_{21}\\0&0&0&\chi_{21}&\phi_{21}&\psi_{21}\end{vmatrix},\qquad \zeta_{24}=\begin{vmatrix}\phi_{12}&0&0&0&0&0\\0&\phi_{12}&\phi_{11}&0&0&0\\0&0&\phi_{11}&0&0&\phi_{21}\\0&0&\chi_{11}&\psi_{11}&0&0\\0&0&0&\phi_{12}&\phi_{22}&2\psi_{22}\\0&\psi_{12}&\psi_{11}&\phi_{11}&\phi_{21}&2\psi_{21}\end{vmatrix},$$

$$\zeta_{25}=\begin{vmatrix}\phi_{22}&0&0&0&0&0\\0&\phi_{22}&0&\psi_{12}&\phi_{12}&\phi_{12}\\0&0&\phi_{22}&\phi_{22}&0&0\\0&0&-\psi_{21}&\phi_{21}&\phi_{21}&0\\0&\phi_{21}&0&\psi_{11}&\phi_{11}&\phi_{11}\\0&0&0&\chi_{11}&\phi_{11}&\psi_{11}\end{vmatrix},\qquad \zeta_{26}=\begin{vmatrix}\phi_{22}&0&0&0&0&0\\0&\phi_{22}&\psi_{22}&0&0&0\\0&0&\phi_{21}&0&0&\phi_{11}\\0&0&\chi_{21}&\psi_{21}&0&0\\0&0&0&\phi_{22}&\phi_{12}&2\psi_{12}\\0&\phi_{21}&\psi_{21}&\phi_{21}&\phi_{11}&2\psi_{11}\end{vmatrix},$$

$$\zeta_{27}=\begin{vmatrix}\phi_{21}&0&0&0&0&0\\0&\phi_{21}&0&\psi_{11}&\phi_{11}&\phi_{11}\\0&0&\phi_{21}&\phi_{21}&0&0\\0&0&-\psi_{22}&\phi_{22}&\phi_{22}&0\\0&\phi_{22}&0&\psi_{12}&\phi_{12}&\phi_{12}\\0&0&0&\chi_{12}&\phi_{12}&\psi_{12}\end{vmatrix},\qquad \zeta_{28}=\begin{vmatrix}\phi_{21}&0&0&0&0&0\\0&\phi_{21}&\phi_{22}&0&0&0\\0&0&\phi_{22}&0&0&\phi_{12}\\0&0&\chi_{22}&\psi_{22}&0&0\\0&0&0&\phi_{21}&\phi_{11}&2\psi_{11}\\0&\psi_{21}&\psi_{22}&\phi_{22}&\phi_{12}&2\psi_{12}\end{vmatrix}.$$

To obtain the second Darboux transformation, we do this procedure again. Precisely, we derive new eigenfunctions from the first Darboux transformation:

$$\bar{\phi}^{[1]}=\bar{\phi}'=\bar{D}\bar{\phi}=(\lambda\bar{I}-\bar{S})\bar{\phi}=\begin{bmatrix}\lambda I-S&S_1&S_2\\0&\lambda I-S&S_1\\0&0&\lambda I-S\end{bmatrix}\begin{bmatrix}\chi\\\psi\\\phi\end{bmatrix}$$
$$=\begin{bmatrix}(\lambda I-S)\chi+S_1\psi+S_2\phi\\(\lambda I-S)\psi+S_1\phi\\(\lambda I-S)\phi\end{bmatrix}=\begin{bmatrix}\chi^{[1]}\\\psi^{[1]}\\\phi^{[1]}\end{bmatrix},\tag{45}$$

which is the new eigenfunction we need to use in the second Darboux transformation. Similarly, $\chi^{[1]}$, $\psi^{[1]}$, $\phi^{[1]}$ are two component vectors which we denoted by $\chi^{[1]}=(\chi_1^{[1]},\chi_2^{[1]})^T$, $\psi^{[1]}=(\psi_1^{[1]},\psi_2^{[1]})^T$, $\phi^{[1]}=(\phi_1^{[1]},\phi_2^{[1]})^T$. Assume $\lambda_3$ and $\lambda_4$ are another two arbitrary constants which are different from $\lambda_1$ and $\lambda_2$, and denote

$$\phi(\lambda_k)=\begin{pmatrix}\phi_{1k}\\ \phi_{2k}\end{pmatrix}=\begin{pmatrix}\phi_1(\lambda_k)\\ \phi_2(\lambda_k)\end{pmatrix},\quad \psi(\lambda_k)=\begin{pmatrix}\psi_{1k}\\ \psi_{2k}\end{pmatrix}=\begin{pmatrix}\psi_1(\lambda_k)\\ \psi_2(\lambda_k)\end{pmatrix},\tag{46}$$

$$\chi(\lambda_k)=\begin{pmatrix}\chi_{1k}\\ \chi_{2k}\end{pmatrix}=\begin{pmatrix}\chi_1(\lambda_k)\\ \chi_2(\lambda_k)\end{pmatrix},\quad k=3,4.\tag{47}$$

Set

$$\tilde{\Lambda}=\begin{bmatrix}\lambda_3 & 0\\ 0 & \lambda_4\end{bmatrix},\tag{48}$$

$$\begin{cases}\tilde{H}=\left(\phi^{[1]}(\lambda_3),\phi^{[1]}(\lambda_4)\right)=((\lambda_3 I-S)\phi(\lambda_3),(\lambda_4 I-S)\phi(\lambda_4)),\\ \tilde{H}_1=\left(\psi^{[1]}(\lambda_3),\psi^{[1]}(\lambda_4)\right)\\ \quad=((\lambda_3 I-S)\psi(\lambda_3)+S_1\phi(\lambda_3),(\lambda_4 I-S)\psi(\lambda_4)+S_1\phi(\lambda_4)),\\ \tilde{H}_2=\left(\chi^{[1]}(\lambda_3),\chi^{[1]}(\lambda_4)\right)\\ \quad=((\lambda_3 I-S)\chi(\lambda_3)+S_1\psi(\lambda_3)+S_2\phi(\lambda_3),(\lambda_4 I-S)\chi(\lambda_4)+S_1\psi(\lambda_4)+S_2\phi(\lambda_4)).\end{cases}$$

Then

$$\begin{cases}\tilde{S}=\tilde{H}\tilde{\Lambda}\tilde{H}^{-1},\\ \tilde{S}_1=-\tilde{H}\tilde{\Lambda}\tilde{H}^{-1}\tilde{H}_1\tilde{H}^{-1}+\tilde{H}_1\tilde{\Lambda}\tilde{H}^{-1},\\ \tilde{S}_2=\tilde{H}\tilde{\Lambda}\tilde{H}^{-1}\tilde{H}_1\tilde{H}^{-1}\tilde{H}_1\tilde{H}^{-1}-\tilde{H}_1\tilde{\Lambda}\tilde{H}^{-1}\tilde{H}_1\tilde{H}^{-1}-\tilde{H}\tilde{\Lambda}\tilde{H}^{-1}\tilde{H}_2\tilde{H}^{-1}+\tilde{H}_2\tilde{\Lambda}\tilde{H}^{-1},\end{cases}\tag{49}$$

Such that $\lambda\bar{I}-\tilde{\bar{S}}$ is the second Darboux matrix, where

$$\tilde{\bar{S}}=\begin{bmatrix}\tilde{S} & \tilde{S}_1 & \tilde{S}_2\\ 0 & \tilde{S} & \tilde{S}_1\\ 0 & 0 & \tilde{S}\end{bmatrix}.\tag{50}$$

Starting from the first DT solutions $P^{[1]}$, $P_1^{[1]}$ and $P_2^{[1]}$, we obtain the second Darboux transformation solutions:

$$P^{[2]}=P^{[1]}+[J,\tilde{S}],\quad P_1^{[2]}=P_1^{[1]}+[J,\tilde{S}_1]+[J_1,\tilde{S}],\tag{51}$$

$$P_2^{[2]}=P_2^{[1]}+[J,\tilde{S}_2]+[J_1,\tilde{S}_1]+[J_2,\tilde{S}].\tag{52}$$

## 3 Applications to Bi-integrable Couplings of the AKNS System

In this section, we construct a hierarchy of AKNS bi-integrable couplings and then apply the resulting Darboux transformation theory to the construction of the one-soliton-like solutions of the AKNS bi-integrable coupling system, particularly, we present the one-soliton-like solution of the bi-integrable couplings of the nonlinear Schrödinger equation.

### *3.1 A Hierarchy of the Bi-integrable Couplings of the AKNS System*

First, we construct a hierarchy of AKNS bi-integrable couplings. We assume that $\bar{\phi} = (\chi^T, \psi^T, \phi^T)^T = (\chi_1, \chi_2, \psi_1, \psi_2, \phi_1, \phi_2)^T$ is the eigenfunction, and $\bar{u} = (q, r, q_1, r_1, q_2, r_2)^T$ is the potential. The spatial spectral problem is defined in the first equation of (14) and the Eq. (12), with $J_2 = J_1 = J$, and

$$U(u,\lambda) = \begin{bmatrix} -\lambda & q \\ r & \lambda \end{bmatrix}, \quad U_1(u_1,\lambda) = \begin{bmatrix} -\lambda & q_1 \\ r_1 & \lambda \end{bmatrix}, \quad U_2(u_2,\lambda) = \begin{bmatrix} -\lambda & q_2 \\ r_2 & \lambda \end{bmatrix}, \tag{53}$$

where we denote $u = (q, r)^T$, $u_1 = (q_1, r_1)^T$, $u_2 = (q_2, r_2)^T$. In addition, we introduce

$$\bar{W}(\bar{u},\lambda) = \begin{bmatrix} W(u,\lambda) & W_1(u,u_1,\lambda) & W_2(u,u_1,u_2,\lambda) \\ 0 & W(u,\lambda) & W_1(u,u_1,\lambda) \\ 0 & 0 & W(u,\lambda) \end{bmatrix}, \tag{54}$$

$$W(u,\lambda) = \begin{bmatrix} a & b \\ c & -a \end{bmatrix}, \quad W_1(u,u_1,\lambda) = \begin{bmatrix} e & f \\ g & -e \end{bmatrix}, \quad W_2(\bar{u},\lambda) = \begin{bmatrix} e' & f' \\ g' & -e' \end{bmatrix}. \tag{55}$$

Then the stationary zero curvature equation $\bar{W}_x = [\bar{U}, \bar{W}]$ results in

$$W_x = [U, W], \tag{56}$$

$$W_{1x} = [U, W_1] + [U_1, W], \tag{57}$$

$$W_{2x} = [U, W_2] + [U_1, W_1] + [U_2, W]. \tag{58}$$

i.e.,

$$\begin{cases} a_x = qc - rb, \\ b_x = -2\lambda b - 2qa, \\ c_x = 2\lambda c + 2ra; \end{cases} \tag{59}$$

$$\begin{cases} e_x = qg - rf + q_1 c - r_1 b, \\ f_x = -2\lambda f - 2qe - 2\lambda b - 2q_1 a, \\ g_x = 2\lambda g + 2re + 2\lambda c + 2r_1 a; \end{cases} \tag{60}$$

$$\begin{cases} e_x^{'} = qg^{'} - rf^{'} + q_1 g - r_1 f + q_2 c - r_2 b, \\ f_x^{'} = -2\lambda f^{'} - 2qe^{'} - 2\lambda f - 2q_1 e - 2\lambda b - 2q_2 a, \\ g_x^{'} = 2\lambda g^{'} + 2re^{'} + 2\lambda g + 2r_1 e + 2\lambda c + 2r_2 a. \end{cases} \tag{61}$$

Assume that $m$ is a positive integer, and set

$$W = \sum_{i\geq 0} W_i \lambda^{-i} = \sum_{i\geq 0} \begin{bmatrix} a_i & b_i \\ c_i & -a_i \end{bmatrix} \lambda^{-i}, \tag{62}$$

$$W_1 = \sum_{i\geq 0} W_{1,i} \lambda^{-i} = \sum_{i\geq 0} \begin{bmatrix} e_i & f_i \\ g_i & -e_i \end{bmatrix} \lambda^{-i}, \tag{63}$$

$$W_2 = \sum_{i\geq 0} W_{2,i} \lambda^{-i} = \sum_{i\geq 0} \begin{bmatrix} e_i^{'} & f_i^{'} \\ g_i^{'} & -e_i^{'} \end{bmatrix} \lambda^{-i}. \tag{64}$$

Substituting them into the Eqs. (56), (57) and (58), and comparing the coefficients of $\lambda$, we obtain the recursion relations:

$$\begin{cases} a_0 = \alpha, \quad b_0 = 0, \quad c_0 = 0, \\ a_{i,x} = qc_i - rb_i, \\ b_{i+1} = -\frac{1}{2} b_{i,x} - qa_i, \\ c_{i+1} = \frac{1}{2} c_{i,x} - ra_i, \end{cases} \quad i \geq 0; \tag{65}$$

$$\begin{cases} e_0 = \beta, \quad f_0 = 0, \quad g_0 = 0, \\ e_{i,x} = qg_i - rf_i + q_1 c_i - r_1 b_i, \\ f_{i+1} = -\frac{1}{2} f_{i,x} - qe_i - q_1 a_i - b_{i+1}, \\ g_{i+1} = \frac{1}{2} g_{i,x} - re_i - r_1 a_i - c_{i+1}, \end{cases} \quad i \geq 0; \tag{66}$$

$$\begin{cases} e_0^{'} = \gamma, \quad f_0^{'} = 0, \quad g_0^{'} = 0, \\ e_{i,x}^{'} = qg_i^{'} - rf_i^{'} + q_1 g_i - r_1 f_i + q_2 c_i - r_2 b_i, \\ f_{i+1}^{'} = -\frac{1}{2} f_{i,x}^{'} - qe_i^{'} - q_1 e_i - q_2 a_i - f_{i+1} - b_{i+1}, \\ g_{i+1}^{'} = \frac{1}{2} g_{i,x}^{'} - re_i^{'} - r_1 e_i - r_2 a_i - g_{i+1} - c_{i+1}, \end{cases} \quad i \geq 0. \tag{67}$$

where $\alpha, \beta$ and $\gamma$ are arbitrary constants, real or complex numbers. In addition, choose the constants of integration to be zero:

$$a_i|_{u=0} = 0, \quad e_i|_{(u,u_1)=0} = 0, \quad e_i^{'}|_{(u,u_1,u_2)=0} = 0, \quad i \geq 1. \tag{68}$$

This way we can define $b_i, c_i, f_i, g_i, f_i^{'}, g_i^{'}$, and $a_i, e_i, e_i^{'}$ from (65), (66) and (67) uniquely.

Now, take into account the temporal spectral problem defined in the second equation of (14) and the Eq. (13), with

$$\begin{aligned}
V^{[m]} &= \begin{bmatrix} a^{[m]} & b^{[m]} \\ c^{[m]} & -a^{[m]} \end{bmatrix} = (\lambda^m W)_+ = \sum_{i=0}^{m} W_i \lambda^{m-i}, \quad m \geq 0, \\
V_1^{[m]} &= \begin{bmatrix} e^{[m]} & f^{[m]} \\ g^{[m]} & -e^{[m]} \end{bmatrix} = (\lambda^m W_1)_+ = \sum_{i=0}^{m} W_{1,i} \lambda^{m-i}, \quad m \geq 0, \\
V_2^{[m]} &= \begin{bmatrix} e^{[m]'} & f^{[m]'} \\ g^{[m]'} & -e^{[m]'} \end{bmatrix} = (\lambda^m W_2)_+ = \sum_{i=0}^{m} W_{2,i} \lambda^{m-i}, \quad m \geq 0.
\end{aligned}$$

Then the enlarged zero curvature equations: $\bar{U}_{t_m} - \bar{V}_x^{[m]} + [\bar{U}, \bar{V}^{[m]}] = 0$, i.e.,

$$U_{t_m} - V_x^{[m]} + [U, V^{[m]}] = 0, \tag{69}$$

$$U_{1t_m} - V_{1x}^{[m]} + [U, V_1^{[m]}] + [U_1, V^{[m]}] = 0, \tag{70}$$

$$U_{2t_m} - V_{2x}^{[m]} + [U, V_2^{[m]}] + [U_1, V_1^{[m]}] + [U_2, V^{[m]}] = 0, \tag{71}$$

together with the recursion relations (65), (66) and (67), generate the enlarged hierarchy of AKNS bi-integrable couplings:

$$\bar{u}_{t_m} = \begin{bmatrix} q \\ r \\ q_1 \\ r_1 \\ q_2 \\ r_2 \end{bmatrix}_{t_m} = \bar{K}_m(\bar{u}) = \begin{bmatrix} -2b_{m+1} \\ 2c_{m+1} \\ -2(f_{m+1} + b_{m+1}) \\ 2(g_{m+1} + c_{m+1}) \\ -2(f_{m+1}^{'} + f_{m+1} + b_{m+1}) \\ 2(g_{m+1}^{'} + g_{m+1} + c_{m+1}) \end{bmatrix} \tag{72}$$

$$= \bar{\Phi}^m \begin{bmatrix} -2b_1 \\ 2c_1 \\ -2(f_1 + b_1) \\ 2(g_1 + c_1) \\ -2(f_1^{'} + f_1 + b_1) \\ 2(g_1^{'} + g_1 + c_1) \end{bmatrix} = \bar{\Phi}^m \begin{bmatrix} 2\alpha q \\ -2\alpha r \\ 2(\beta q + \alpha q_1) \\ -2(\beta r + \alpha r_1) \\ 2(\gamma q + \beta q_1 + \alpha q_2) \\ -2(\gamma r + \beta r_1 + \alpha r_2) \end{bmatrix}, \tag{73}$$

where the enlarged hereditary recursion operator $\bar{\Phi}$ reads

$$\bar{\Phi} = \begin{bmatrix} \Phi & 0 & 0 \\ \Phi_1 - \Phi & \Phi & 0 \\ \Phi_2 - \Phi_1 & \Phi_1 - \Phi & \Phi \end{bmatrix}, \tag{74}$$

with $\Phi$, $\Phi_1$ and $\Phi_2$ being defined by

$$\Phi = \begin{bmatrix} -\frac{1}{2}\partial + q\partial^{-1}r & q\partial^{-1}q \\ -r\partial^{-1}r & \frac{1}{2}\partial - r\partial^{-1}q \end{bmatrix},$$
$$\Phi_1 = \begin{bmatrix} q_1\partial^{-1}r + q\partial^{-1}r_1 & q_1\partial^{-1}q + q\partial^{-1}q_1 \\ -(r_1\partial^{-1}r + r\partial^{-1}r_1) & -(r_1\partial^{-1}q + r\partial^{-1}q_1) \end{bmatrix},$$
$$\Phi_2 = \begin{bmatrix} q_2\partial^{-1}r + q_1\partial^{-1}r_1 + q\partial^{-1}r_2 & q_2\partial^{-1}q + q_1\partial^{-1}q_1 + q\partial^{-1}q_2 \\ -(r_2\partial^{-1}r + r_1\partial^{-1}r_1 + r\partial^{-1}r_2) & -(r_2\partial^{-1}q + r_1\partial^{-1}q_1 + r\partial^{-1}q_2) \end{bmatrix}.$$

The first few equations are computed as follows:

$$\bar{u}_{t_1} = \bar{K}_1(\bar{u}) = \begin{bmatrix} -\alpha q_x \\ -\alpha r_x \\ -\beta q_x - \alpha(q_{1x} - q_x) \\ -\beta r_x - \alpha(r_{1x} - r_x) \\ -\gamma q_x - \beta(q_{1x} - q_x) - \alpha(q_{2x} - q_{1x}) \\ -\gamma r_x - \beta(r_{1x} - r_x) - \alpha(r_{2x} - r_{1x}) \end{bmatrix}, \tag{75}$$

$$\bar{u}_{t_2} = \bar{K}_2(\bar{u}) = \begin{bmatrix} \alpha K_{2,1} \\ -\alpha\tilde{K}_{2,1} \\ \beta K_{2,1} + \alpha\left(K_{2,2} - 2K_{2,1}\right) \\ -\beta\tilde{K}_{2,1} - \alpha\left(\tilde{K}_{2,2} - 2\tilde{K}_{2,1}\right) \\ \gamma K_{2,1} + \beta\left(K_{2,2} - 2K_{2,1}\right) + \alpha\left(K_{2,3} - 2K_{2,2} + K_{2,1}\right) \\ -\gamma\tilde{K}_{2,1} - \beta\left(\tilde{K}_{2,2} - 2\tilde{K}_{2,1}\right) - \alpha\left(\tilde{K}_{2,3} - 2\tilde{K}_{2,2} + \tilde{K}_{2,1}\right) \end{bmatrix}, \tag{76}$$

with

$$K_{2,1} = \frac{1}{2}q_{xx} - q^2r, \quad K_{2,2} = \frac{1}{2}q_{1xx} - q^2r_1 - 2qrq_1,$$
$$K_{2,3} = \frac{1}{2}q_{2xx} - q^2r_2 - 2qrq_2 - q_1^2r - 2q_1r_1q;$$
$$\tilde{K}_{2,1} = \frac{1}{2}r_{xx} - qr^2, \quad \tilde{K}_{2,2} = \frac{1}{2}r_{1xx} - r^2q_1 - 2qrr_1,$$
$$\tilde{K}_{2,3} = \frac{1}{2}r_{2xx} - r^2q_2 - 2qrr_2 - r_1^2q - 2q_1r_1r;$$

$$\bar{u}_{t_3} = \bar{K}_3(\bar{u}) = \begin{bmatrix} \alpha K_{3,1} \\ \alpha \tilde{K}_{3,1} \\ \beta K_{3,1} + \alpha \left(K_{3,2} - 3K_{3,1}\right) \\ \beta \tilde{K}_{3,1} + \alpha \left(\tilde{K}_{3,2} - 3\tilde{K}_{3,1}\right) \\ \gamma K_{3,1} + \beta \left(K_{3,2} - 3K_{3,1}\right) + \alpha \left(K_{3,3} - 3K_{3,2} + 3K_{3,1}\right) \\ \gamma \tilde{K}_{3,1} + \beta \left(\tilde{K}_{3,2} - 3\tilde{K}_{3,1}\right) + \alpha \left(\tilde{K}_{3,3} - 3\tilde{K}_{3,2} + 3\tilde{K}_{3,1}\right) \end{bmatrix}, \quad (77)$$

with

$$\begin{aligned}
K_{3,1} &= -\frac{1}{4}q_{xxx} + \frac{3}{2}qrq_x, \quad K_{3,2} = -\frac{1}{4}q_{1xxx} + \frac{3}{2}qrq_{1x} + \frac{3}{2}(q_1r + qr_1)q_x, \\
K_{3,3} &= -\frac{1}{4}q_{2xxx} + \frac{3}{2}qrq_{2x} + \frac{3}{2}(q_2r + qr_2 + q_1r_1)q_x + \frac{3}{2}(q_1r + qr_1)q_{1x}, \\
\tilde{K}_{3,1} &= -\frac{1}{4}r_{xxx} + \frac{3}{2}qrr_x, \quad \tilde{K}_{3,2} = -\frac{1}{4}r_{1xxx} + \frac{3}{2}qrr_{1x} + \frac{3}{2}(q_1r + qr_1)r_x, \\
\tilde{K}_{3,3} &= -\frac{1}{4}r_{2xxx} + \frac{3}{2}qrr_{2x} + \frac{3}{2}(q_2r + qr_2 + q_1r_1)r_x + \frac{3}{2}(q_1r + qr_1)r_{1x}.
\end{aligned}$$

## 3.2 One-Soliton-Like Solutions to the Bi-integrable Couplings of the Nonlinear Schrödinger Equation

Let us consider the $\bar{K}_2$ system, i.e., we set $m = 2$ in the AKNS bi-integrable coupling hierarchy (73). The corresponding integrable coupling system (73) of the nonlinear Schrödingier (NLS) equations reads as follows:

$$\begin{cases}
q_t = \alpha\left(\frac{1}{2}q_{xx} - q^2r\right), \\
r_t = -\alpha\left(\frac{1}{2}r_{xx} - r^2q\right), \\
q_{1t} = \alpha\left(\frac{1}{2}q_{1xx} - q^2r_1 - 2qrq_1 - q_{xx} + 2q^2r\right) + \beta\left(\frac{1}{2}q_{xx} - q^2r\right), \\
r_{1t} = -\alpha\left(\frac{1}{2}r_{1xx} - r^2q_1 - 2qrr_1 - r_{xx} + 2qr^2\right) - \beta\left(\frac{1}{2}r_{xx} - qr^2\right), \\
q_{2t} = \alpha\left(\frac{1}{2}q_{2xx} - q^2r_2 - 2qrq_2 - q_1^2r - 2q_1r_1q - q_{1xx} + 2q^2r_1 + 4qrq_1 + \frac{1}{2}q_{xx} - q^2r\right) \\
\quad +\beta\left(\frac{1}{2}q_{1xx} - q^2r_1 - 2qrq_1 - q_{xx} + 2q^2r\right) + \gamma\left(\frac{1}{2}q_{xx} - q^2r\right). \\
r_{2t} = -\alpha\left(\frac{1}{2}r_{2xx} - r^2q_2 - 2qrr_2 - r_1^2q - 2q_1r_1r - r_{1xx} + 2r^2q_1 + 4qrr_1 + \frac{1}{2}r_{xx} - qr^2\right) \\
\quad -\beta\left(\frac{1}{2}r_{1xx} - r^2q_1 - 2qrr_1 - r_{xx} + 2qr^2\right) - \gamma\left(\frac{1}{2}r_{xx} - qr^2\right).
\end{cases} \quad (78)$$

Starting from the zero seed solution, by solving the corresponding linear systems in (14), we obtain the eigenfunctions:

$$\begin{cases} \chi_1 = \frac{1}{2}\,\lambda\,\left(\beta^2\lambda^3 t^2 - 2\beta\,\lambda^2 t x + 2\gamma\,\lambda\,t + \lambda\,x^2 - 2\,x\right)\mathrm{e}^{\lambda\,(\alpha\lambda t - x)}, \\ \chi_2 = \frac{1}{2}\,\lambda\,\left(\beta^2\lambda^3 t^2 - 2\beta\lambda^2 t x - 2\gamma\,\lambda\,t + \lambda\,x^2 + 2\,x\right)\mathrm{e}^{-\lambda\,(\alpha\lambda t - x)}, \\ \psi_1 = \lambda\,(\beta\lambda t - x)\,\mathrm{e}^{\lambda(\alpha\lambda t - x)}, \quad \psi_2 = -\lambda\,(\beta\lambda t - x)\,\mathrm{e}^{-\lambda(\alpha\lambda t - x)}, \\ \phi_1 = \mathrm{e}^{\lambda(\alpha\lambda t - x)}, \quad \phi_2 = \mathrm{e}^{-\lambda(\alpha\lambda t - x)}. \end{cases} \tag{79}$$

Substituting (79) into the associated Bäcklund transformation (43), we obtain the one-soliton-like solution of the integrable coupling system defined by (78):

$$\begin{aligned} q &= -(\lambda_1 - \lambda_2)e^{\alpha({\lambda_1}^2+{\lambda_2}^2)t-(\lambda_1+\lambda_2)x}\,\mathrm{sech}\xi, \\ r &= (\lambda_1 - \lambda_2)e^{-\alpha({\lambda_1}^2+{\lambda_2}^2)t+(\lambda_1+\lambda_2)x}\,\mathrm{sech}\xi, \\ q_1 &= -\frac{1}{2}(\lambda_1 - \lambda_2)\rho_1\,\mathrm{sech}^2\xi, \\ r_1 &= -\frac{1}{2}(\lambda_1 - \lambda_2)\rho_2\,\mathrm{sech}^2\xi, \\ q_2 &= -\frac{1}{4}(\lambda_1 - \lambda_2)\rho_3\,\mathrm{sech}^3\xi, \\ r_2 &= \frac{1}{4}(\lambda_1 - \lambda_2)\rho_4\,\mathrm{sech}^3\xi, \end{aligned}$$

where

$$\begin{aligned} \xi &= (\lambda_1 - \lambda_2)[\alpha(\lambda_1 + \lambda_2)t - x], \\ \rho_1 &= (2\beta{\lambda_2}^2 t - 2\lambda_2 x + 1)e^{2\lambda_1(\alpha\lambda_1 t - x)} + (2\beta{\lambda_1}^2 t - 2\lambda_1 x + 1)e^{2\lambda_2(\alpha\lambda_2 t - x)}, \\ \rho_2 &= (2\beta{\lambda_2}^2 t - 2\lambda_2 x - 1)e^{-2\lambda_1(\alpha\lambda_1 t - x)} + (2\beta{\lambda_1}^2 t - 2\lambda_1 x - 1)e^{-2\lambda_2(\alpha\lambda_2 t - x)}, \\ \rho_3 &= (\mu_1 + \delta_1)\,\mathrm{e}^{3\,\epsilon_2 - \epsilon_1} + (\mu_2 + \delta_2)\,\mathrm{e}^{3\,\epsilon_1 - \epsilon_2} + (\delta_1 - \mu_1 + \delta_2 - \mu_2 + 4 + 8\,\nu)\,\mathrm{e}^{\epsilon_1 + \epsilon_2}, \\ \rho_4 &= (\mu_1 - \delta_1)\,\mathrm{e}^{-3\,\epsilon_2 + \epsilon_1} + (\mu_2 - \delta_2)\,\mathrm{e}^{-(3\,\epsilon_1 - \epsilon_2)} + (-\delta_1 - \mu_1 - \delta_2 - \mu_2 + 4 + 8\,\nu) \\ &\quad \mathrm{e}^{-(\epsilon_1 + \epsilon_2)}, \end{aligned}$$

with

$$\begin{aligned} &\mu_i = 2\,\beta^2{\lambda_i}^4 t^2 - 4\,\beta{\lambda_i}^3 x t + 2\,{\lambda_i}^2 x^2 + 1, \quad \delta_i = 2\,\beta{\lambda_i}^2 t + 2\,\gamma{\lambda_i}^2 t - 4\lambda_i x, \\ &\epsilon_i = \alpha{\lambda_i}^2 t - \lambda_i x, \quad i = 1, 2, \\ &\nu = \beta^2{\lambda_1}^2{\lambda_2}^2 t^2 - \beta{\lambda_1}^2\lambda_2 x t - \beta\lambda_1{\lambda_2}^2 x t + \lambda_1\lambda_2 x^2. \end{aligned}$$

## 4 Conclusion and Comments

We have successfully constructed a kind of Darboux transformation for bi-integrable couplings. An application was made to the presented bi-integrable couplings of the AKNS system of integrable models. In particular, exact solutions were generated for the bi-integrable couplings of the nonlinear Schrödinger equations. The Darboux transformation for tri-integrable couplings can be similarly constructed. It is expected that physical applications could be presented to these integrable couplings of soliton equations in the future.

The work was supported in part by National Natural Science Foundation of China under Grant No. 61807025, and the Fundamental Research Funds for the Central Universities ZYTS23049.

## References

1. Ma, W. X., Fuchssteiner, B.: Integrable theory of the perturbation equations. Chaos, Solitons & Fractals. **7**, 1227-1250 (1996)
2. Ma, W. X.: Integrable couplings of soliton equations by perturbations I. A general theory and application to the KdV hierarchy. Methods Appl. Anal. **7**, 21-55 (2000)
3. Ma, W. X., Xu, X. X., Zhang, Y. F.: Semidirect sums of Lie algebras and discrete integrable couplings. J. Math. Phys. **47**, 053501-053521 (2006)
4. Frappat, L., Sciarrino, A., Sorba, P.: Dictionary on Lie Algebras and Superalgebras. Academic Press Inc., San Diego, CA 146 pp. (2000)
5. Ma, W. X., Chen, M.: Hamiltonian and quasi-Hamiltonian structures associated with semi-direct sums of Lie algebras. J. Phys. A: Math. Gen. **39**, 10787-10801 (2006)
6. Ma, W. X., Integrable couplings and matrix loop algebra, in: Nonlinear and Modern Mathematical Physics, pp.105-122, edited by Ma, W. X. and Kaup, D., AIP Conference Proceedings, Vol.1562 (American Institute of Physics, Melville, NY, 2013)
7. Ma, W. X.: Variational identities and Hamiltonian structures, in: Nonlinear and Modern Mathematical Physics, pp.1-27, edited by Ma, W. X., Hu, X. B., and Liu, Q. P., AIP Conference Proceedings, Vol.1212 (American Institute of Physics, Melville, NY, 2010)
8. Ma, W. X.: Loop algebras and bi-integrable couplings. Chin. Ann. Math. B **33**, 207-224 (2012)
9. Ma, W. X., Meng, J. H., Zhang, H. Q.: Tri-integrable couplings by matrix loop algebras. Int. J. Nonlinear Sci. Numer. Simul. **14**, 377-388 (2013)
10. Wang, M. L.: Exact solutions for a compound KdV-Burgers equation. Phys. Lett. A **213**, 279-287 (1996)
11. Hirota, R.: The Direct Method in Soliton Theory, Cambridge Tracts in Mathematics, Vol.155, Cambridge University Press, Cambridge (2004)
12. Zhang, R. F., Bilige, S.D.: Bilinear neural network method to obtain the exact analytical solutions of nonlinear partial differential equations and its application to p-gBKP equatuon. Nonlinear Dyn. **95**, 3041–C3048 (2019)
13. Zhang, R.F., Li, M.C., Albishari, M., Zheng, F.C., Lan, Z.Z.: Generalized lump solutions, classical lump solutions and rogue waves of the (2+1)-dimensional CaudreyCDoddCGibbonCKoteraCSawada-like equation. Appl. Math. Comput. **403**, 126201 (2021)
14. Zhang, R.F., Li, M.C., Gan, J.Y., Li, Q., Lan, Z.Z.: Novel trial functions and rogue waves of generalized breaking soliton equation via bilinear neural network method. Chaos Solitons Fractals **154**, 111692 (2022)

15. Zhang, R.F., Li, M.C., Cherraf, A., Vadyala, S. R.: The interference wave and the bright and dark soliton for two integro-differential equation by using BNNM. Nonlinear Dyn. **111**, 8637-C8646 (2023)
16. Ma, W. X., Lee, J. H.: A transformed rational function method and exact solutions to the $3 + 1$ dimensional Jimbo-Miwa equation. Chaos, Solitons & Fractals. **42**, 1356-1363 (2009)
17. Ma, W. X.: Darboux transformations for a Lax integrable system in $2n$ dimensions. Lett. Math. Phys. **39**, 33-49 (1997)
18. Zhao, D., Zhang, Y. J., Lou, W. W., Luo, H. G.: AKNS hierarchy, Darboux transformation and conservation laws of the 1-D nonautonomous nonlinear Schrödinger equations. J. Math Phys. **52**, 043502, pp.16 (2011)
19. Zhang, Y. J., Zhao, D., Luo, H. G.: Multi-soliton management by the integrable nonautonomous nonlinear integro-differential Schrödinger equation, Ann. Physics **350**, 112-123 (2014)
20. Ablowitz, M. J., Kaup, D. J., Newell A. C., Segur, H.: The inverse-scattering transform-Fourier analysis for nonlinear problems, Stud. Appl. Math. **53**, 249-253 (1974)
21. Ma, W. X., Zhang, Y. J.: Darboux transformations of integrable couplings and applications, Reviews in Mathematical Physics **30**, 185003, 26pp (2018)